Role of Life Strategies in Diatom Biodiversity: A Modelling Approach

Thesis

Role of Life Strategies in Diatom Biodiversity: a Modelling Approach

Krzysztof Franciszek Stec

Master of Science in Mathematics, AGH University of Science and Technology, Krakow, Poland

Doctor of Philosophy

November, 2015

Stazione Zoologica Anton Dohrn, Naples, Italy

The Open University, London, United Kingdom

DATE OF SUBMISSION: 30 OCTOBER 2015

DATE OF AWARD: 18 JULY 2016

ProQuest LLC.
789 East Eisenhower Parkway
P.O. Box 1346
Ann Arbor, MI 48106 – 1346

I dedicate this thesis to my grandmother Magdalena Chyclak

Abstract

A theoretical framework explaining what regulates the number of species and their temporal and spatial patterns is still lacking making plankton diversity a challenging issue in ecology. In this study the nature and relevance of some of the drivers of marine diatoms dynamics and diversity over the seasons have been investigated by coupling experimental and numerical approaches. The main focus was on the life cycle, especially important for marine diatoms and overlooked as a possible driver of diversity.

The performed laboratory experiments provided evidence of growth rate decrease occurring independently from resource availability during the sexual phase, which is a mandatory component of most diatom life cycles. The ecological and evolutionary implications of this biological mechanism have been explored with a developed *ad hoc* numerical model of seasonal plankton dynamics in the mixed layer. The model includes a detailed parametrization of the physical and chemical environments, and a set of phytoplankton species characterized by distinct physiological traits. The validation exercise demonstrated model's applicability to address questions on plankton seasonal dynamics and diversity patterns.

The modelling exercise showed that the coordinated growth rate reduction in diatoms during mating, even in presence of plentiful resources, would affect diversity patterns and functioning of the plankton community even if shared only by a subset of species.

In addition, other factors including grazers' migration and phytoplankton species immigration, as well as the role of the seasonal characteristics of the water column affecting plankton succession and species diversity were also investigated.

This suggests that the above factors impact the community structure and its time course. In particular, biological regulation in diatoms, and likely in many other protists, can be remarkably sophisticated and should be considered to improve our understanding of plankton diversity, a question made even more important by the current climate change.

Acknowledgements

I would like to thank the Open University and Stazione Zoologica Anton Dohrn for giving me the opportunity and fellowship to pursue my Ph.D.

I want to thank to Dr Daniele Iudicone, my director of studies, for teaching, helping, and supporting me during these years and to whom I owe a great debt of gratitude. I would like to express a special appreciation for my supervisors Dr. Marina Montresor, Dr Maurizio Ribera d'Alcala and Dr. Tim Wyatt for the support, discussions, patience and encouragement given to me during my PhD.

I would like to thank to all the colleagues at the Institute with whom I shared time and space. Gianluca, Ceci, Vasco, Davide, Laura Vitale and Laura Escalera, Eleonora, Shrikant, Raghu, Sneha, Chetan, Gauri, Romain, Luigi, Nico and Christophe thanks for all your kind gestures. A special note of thanks goes to my good friends Swaraj and Deepak.

I really appreciate the calm and patience shown by my family during my Ph.D tenure. The support received from my wife Joanna, mother Anna, brother Grzegorz, sisters Katarzyna and Agnieszka, and my grandmother Magdalena has always made me confident that I am on the right track in my life. They have played a big role in helping me remain composed and focused during my Ph.D period. I thank them for all the support and encouragement.

Finally, I would like to thank to all my relatives, especially to Patrycja, Lukasz, Barbara and Jerzy, Marzena, Piotr and Wiktoria for the support. A special acknowledgement goes to Hania, Julka and Tymek you may be tiny but you play a great role in my life.

Contents

List of Figures

List of Tables

Chapter 1

Introduction

The interest in micro-organisms is motivated by the recent findings of unexpected high diversity in the oceans, the potential applied use of this diversity and the challenge to explain the ecological and evolutionary role of the biodiversity (Schulze and Mooney [1994], McCann [2000], www.coml.org). Each day, phytoplankton fix more than a hundred million tons of carbon (Falkowski and Oliver [2007]; Behrenfeld et al. [2001]; Falkowski et al. [1998]) which is subsequently transferred into the marine ecosystem, supporting secondary production in all subsequent trophic levels and setting an upper limit on sustainable fishing yields (Behrenfeld et al. [2001]; Falkowski et al. [1998]; Walsh [1981]). Pathways of carbon transfer are influenced by phytoplankton community composition (Laws et al. [2000]; Michaels and Silver [1988]), therefore changes in this composition can potentially generate cascading effects on food web dynamics (Beardall and Stojkovic [2006]; Laws et al. [2000]; Irwin et al. [2006]), global primary production (Beardall and Raven [2004]) and biogeochemical cycling of several major elements (Sterner and Elser [2002]; Thingstad and Cuevas [2010]; Arrigo [2004]) in particular global carbon cycle (Falkowski et al. [1998]) and its flux from the atmosphere to the surface ocean (Falkowski and Oliver [2007], Falkowski et al. [1998]). Finally, the alterations to this system due to diversity changes can potentially have implications for the global ecosystem and world economy (De Groot et al. [2002]). Yet, the knowledge on what governs the effect of diversity on productivity in pelagic ecosystems is still scarce (Duffy et al. [2006]; Cardinale et al. [2012]; Ptacnik et al. [2008], Ptacnik et al. [2010]).

1.1 How to define diversity?

Diversity is a widely used term to refer diversity of biota in different domains and at different scales. The diversity of species may be quantified at different levels. The most frequently used measure of diversity is 'species richness', i.e. the number of species present in an selected ecosystem (Hill [1973]). It depends on the level of taxonomic identification, which - in the case of phytoplankton - is largely based on morphology and recently on genetic markers. 'Species diversity' does not account for species abundance, which affects diversity (Stirling and Wilsey [2001]; but also Whittaker [1965];

Hurlbert [1971]). The relative contributions of species to the community is captured by the 'species evenness' (or species equitability) ranging from near 0 (low evenness or dominance of a single or a few species) to 1 (maximum eveness or equal abundance of several species) (Alatalo [1981]; Smith and Wilson [1996]). The Shannon Index H (or Shannon-Weaver Index; Shannon and Weaver [1949]) combines both species richness and evenness:

$$H = -\sum_{i=1}^{n} p_i log(p_i), \quad p_i = \frac{P_i}{\sum_{k=1}^{n} P_k} \tag{1.1}$$

where P_i is the biomass or abundance for the individual phytoplankton species i ($i = 1, \ldots, n$; n -number of species).

Despite being widely used and valued as a measure of the joint effects of species richness and evenness, Shannon index is critisized as it is not intuitively related to ecological diversity (Hurlbert [1971]), it is insensitive to different species abundance distributions (May [1975]), it is descriptive (Ghilarov [1996]), and it has a small-sample bias (Stirling and Wilsey [2001], for a detailed discussion).

De Benedictis (De Benedictis [1973]) first argued that mathematical relationships constrain correlations between species richness, evenness, and Shannon index to be positive and strong. This idea was further developed by Hill (Hill [1973]) who argued that diversity is fundamentally the number of species in a community and that other diversity measures comprise a related, higher order series. Finally, under the assumption of log-normal or log-series species abundance distribution, May (May [1975]) derived positive relationships between species richness, evenness, and Shannon index. In fact, the observed patterns of species abundance frequently followed these log-normal distributions (May [1975]; Magurran and Magurran [1988]), which suggests that species richness is a common cause of variation in relative abundance and diversity. Consequently, the species richness is currently used as the sole measure of diversity in many reviews (e.g., Ricklefs et al. [1993]; Harper and Hawksworth [1994]; McKinney and Drake [2013]).

In parallel to taxonomic diversity, functional diversity is frequently considered. Functional diversity reflects the functional multiplicity within a community rather than the multiplicity of species. A simple measure of functional diversity is the number of co-

occurring functional types (Tilman [2001]Tilman [2001]; Hooper et al. [2005], Petchey and Gaston [2006], Petchey and Gaston [2006]; Longhi and Beisner [2010]; Behl et al. [2011]), analogous to species richness at the species level. The functional types are defined as 'sets of species showing similar responses to the environment and similar effects on ecosystem functioning' (Gitav and Noble [1997]). As such, functional diversity depicts the variety of effects organisms have on a particular ecosystem (Tilman [2001]; Hooper et al. [2005]). The impact of a species on the environment is determined by its traits, defined as the properties of an organism which are measurable and influence one or more essential functional processes such as growth, reproduction, nutrient acquisition, etc. Therefore, the functional diversity measures the similarity in traits of the species in a community, and thereby the range of effects on the ecosystem. In general, all traits should be easily measurable (Keddy [1992]; McIntyre et al. [1999]; Walker et al. [1999]). Therefore a key aspect of functional diversity appears to be the selection of traits to be considered in the assignment of organisms to functional types (Petchey et al. [2009]). Because it implicitly takes into account ecological mechanisms, functional diversity may be better suited for investigating changes in ecosystem functioning than taxonomic diversity measures (Petchey and Gaston [2006], Longhi and Beisner [2010], Behl et al. [2011]). This study will use the number of coexisting phytoplankton species as a simple measure for simulated diversity, due to direct representation of the various phytoplankton species dynamics.

Notably, the phytoplankton assemblage includes a vast number of taxa, many of which occur in such small quantities which may not be recorded in routine sampling, and many taxa cannot be identified to species level by routine methods such as light microscopy of preserved samples, even by a skilled taxonomist. Hence, it is impossible to asses a complete list of species in the ecosystem at any given point in time and consequently the phytoplankton biodiversity is notoriously difficult to estimate.

1.2 Global plankton diversity

There is some evidence of latitudinal diversity gradients among certain taxa of marine microbes (Currie [1991]; Hillebrand [2004]), in particular bacterioplankton (Pommier

et al. [2007], Fuhrman et al. [2008]) and coccolithophorids (Honjo and Okada [1974], Cermeño et al. [2008]), but the generality of these patterns, particularly in an open ocean remains equivocal (Cermeño et al. [2008]). The extent to which and why marine phytoplankton may follow latitudinal patterns is not yet clear, although it has been argued that the biogeography of microbes, similarly to macroorganisms, is governed by a similar set of processes including colonization, speciation (diversification) and extinction (Martiny et al. [2006]).

The analysis of data on marine plankton assemblages, in terms of species composition and biomass, demonstrated that marine phytoplankton diversity is a unimodal function of phytoplankton biomass, and highest phytoplankton diversity is observed in regimes with intermediate biomass, and thus productivity (Irigoien [2005], Rosenzweig [1995], Waide et al. [1999], Mittelbach et al. [2001], Kassen et al. [2000]). Communities with high biomass tend to be dominated by a single species, which might be able to escape the grazing pressure because of its size or defence mechanisms (Strom et al. [2001]; Hamm et al. [2003]). Light limitation through shading might further reduce diversity during intense phytoplankton blooms, as it was suggested by recent studies (Huisman et al. [1999a]; Irigoien [2005]). In low biomass communities, nutrient limitation is responsible for the co-dominance of a few small phytoplankton species (Irigoien [2005]). The dominance of small taxa may be attributed to their high surface-to-volume ratio that is more favourable for acquiring nutrients under nutrient depleted conditions (Raven [1998]).

1.3 Mechanisms of coexistence

The mechanisms maintaining the diversity of phytoplankton have long interested ecologists (Hutchinson [1961]), and the explanations for the diversity distribution patterns have been classified as historical (invoking events and changes in Earth history, such as Milankovitch cycles), evolutionary (examining the rates of speciation and extinction and their balance through time), or ecological (Fuhrman et al. [2008]; Mittelbach et al. [2007]; MacArthur and Wilson [1967]; Allen et al. [2006]).

Aquatic habitats are characterized by a large number of coexisting phytoplankton

species. This evident coexistence in the natural world was opposed by experiments, which demonstrated that species competing for a shared resource drive each other to extinction (Gause [1934]). This effect became known as the 'competitive exclusion principle' (Hardin et al. [1960]), and brought up the question of how a large number of phytoplankton species can coexist on a small number of shared resources like light and nutrients (Hutchinson [1961]). In order to resolve this "paradox of the plankton", a number of hypotheses have been formulated (Sommer and Worm [2002]; Roy and Chattopadhyay [2007]) comprising equilibrium and non-equilibrium mechanisms (top-down (Prowe et al. [2012a]) and bottom-up regulations (Huisman et al. [1999a]), non-equilibrium hypotheses (Connell [1978]), chaos and internal oscillations (Huisman et al. [2001], Benincà et al. [2008], Dakos et al. [2009]), competition in an open chaotic mixing (Károlyi et al. [2000]), and mutualistic interactions (Mougi and Kondoh [2012]). The following overview will concentrate on mechanisms affecting coexistence in the pelagic ocean.

The resource competition theory may elucidate some of the mechanisms of coexistence. Resource competition theory (Tilman [1977], Tilman et al. [1982]) provides a framework for interpreting the relationship between organisms and their resource environment. Consider a single phytoplankton species P, nourished by a single abiotic resource R (eq. 1.2), where nutrient limitation is parametrised as a Monod function with a half-saturation constant H (eq. 1.2).

$$\frac{dP}{dt} = r\frac{R}{R+H}P - mP, \tag{1.2}$$

where r, m, and H are respectively the maximum growth rate, the half-saturation concentration for nutrient uptake, and the mortality of a species. In such simple system, as the population increases, it reduces the resource concentration in its environment and thus decrease its own population growth. Eventually, it will reduce R to a level at which the population can no longer increase, and it can therefore reduce R not further. This level of R is called critical resource level, R^*, for which growth rate just balances mortality (eq. 1.3).

$$R^* = \frac{mH}{r-m} \tag{1.3}$$

The ambient concentration of the limiting resource, R^*, is determined by the physiological characteristics of the organism and hence is species-specific.

Competitive exclusion can be demonstrated by looking at two phytoplankton species, P_1 and P_2, competing for a single abiotic resource, e.g., a nutrient R, in equilibrium. For each species, P_i, the critical resource level R^*_i depends on the individual growth and loss characteristics and thus differ between the two species. In equilibrium and in the absence of other competitors, each species would draw down nutrients to its R^*. If two species compete in a well-mixed and constant environment, the species with the lower R^* can persist at a lower nutrient level, and excludes the other species by drawing down nutrients to a level at which the other species cannot compensate mortality losses. In such environments, the species with the lowest R^* always wins the competition (Stewart and Levin [1973]; Tilman [1977]).

In an equilibrium system, one resource represents one single limiting factor, and consequently allows only one species to exist (Levin [1970]). Additional limiting factors, like different nutrients, can increase the number of coexisting species. However, stable coexistence of two species on two resources in the absence of predators is possible only if each species is limited by a different resource and also consumes proportionally more of this resource than the other species (resource ratio hypothesis; Tilman [1977]). The presence of grazers (or top-down control) is another frequently invoked mechanism shaping phytoplankton species diversity. Within equilibrium systems a generalist predator can have a role analogous to a limiting resource (see Chesson [2000], and references therein). If grazing intensity is considered to be a linear function of prey concentration, the species with the highest tolerance to grazing will exclude the more susceptible species through apparent competitive exclusion. At the same time, predators may promote species coexistence. Predators specialized on individual prey species act as a limiting factor for its respective prey species and hold down its density (Vallina et al. [2014]). Alternatively, generalist predators may enable prey species to coexist if they exhibit switching behaviours, i.e., if they consume disproportionally more of the most abundant resource (Prowe et al. [2012a]). This mechanism of predator-mediated coexistence is implied by grazing functional responses which, for example, depend quadratically on prey concentration (Prowe et al. [2012a]). These bottom-up and top-down

mechanisms increase negative intraspecific interactions, i.e., between individuals of one prey type, relative to negative interspecific interactions, and are therefore considered stabilizing (Chesson [2000]). They promote systems in which intraspecific competition exceeds interspecific competition, which allows coexistence. The above mechanisms assume that an environment is at equilibrium. However, in natural communities environmental conditions can vary in space and time. Non-equilibrium conditions allow the coexistence of more species than limiting resources (Armstrong and McGehee [1980], Sommer [1985], Levin [1970]). Therefore, the other line of proposed solutions for the paradox of the plankton addresses non-equilibrium mechanisms and variable environmental conditions. A leading idea about how this variability, in form of disturbances and other environmental fluctuations, affects species diversity is the Intermediate Disturbance Hypothesis (IDH here after; Connell [1978], Sommer [1995]). The IDH states that diversity of competing species is maximized at intermediate frequencies and/or intensities of disturbance or environmental change. At low frequencies of disturbance, competitive exclusion results in low diversity. If disturbances are too frequent, few species with traits like a high maximum growth rate are selected for, again resulting in low diversity. In experimental plankton systems, nutrient pulses or artificial mixing are typically used to disturb the system by changing the relative fitness of species or the competitive hierarchy (Sommer and Worm [2002]). Specifically, pulsed supply of nutrients has been shown to increase the number of coexisting species in a phytoplankton community above the number of limiting resources in laboratory chemostat cultures (Sommer [1984]). Empirical evaluations of the IDH, however, appear mixed: the proportion of published diversity-disturbance relationships reporting the predicted peak of diversity at intermediate disturbance levels varies between less than 20% (Mackey and Currie [2001], Randall Hughes et al. [2007]) and 46% (Kershaw and Mallik [2013]). It is possible that some empirical studies failed to support the IDH because they failed to sample a sufficient range of disturbance frequencies or intensities. At the same time, published empirical studies might overstate the frequency of humped diversity-disturbance relationships because researchers tend to look for such relationships only in systems where they think they are particularly likely to find them. Notably, recent models predict various diversity-disturbance relationships, including both humped and

non-humped relationships (Miller et al. [2011]. These models therefore have the potential to explain the wide range of diversity-disturbance relationships seen in nature, and the rarity of humped relationships. Because of its vulnerability to misinterpretation and misrepresentation, Connell's IDH has been recently criticized and argued as invalid due to logical inconsequences (see Fox [2013] for detailed discussion). The IDH addresses the system's disequilibrium as a consequence of external disturbance. Disequilibrium, however, may be also caused by the internal system's processes. In the 1970s, it has been discovered that simple population models may generate complex chaotic dynamics (May 1970, 1976). Since then, a lot of attention was focused on the phytoplankton non-equilibrium dynamics generated by competition for limiting resources (Huisman et al. [1999a]), but also predator-prey interactions (Gilpin [1975], Vandermeer [1993]) and food-chain dynamics (Hastings and Powell [1991], van Nes and Scheffer [2004]). For instance, Huisman and Weissing (1999) analyzed a resource competition model and showed that competition for limiting resources may lead to complex system dynamics if multiple species compete for at least three resources. This complex dynamics, in form of oscillations and chaotic fluctuations in species abundances, was later reported for different mathematical formulations of resource competition, and over a relatively wide range of the model parameters (Huisman et al. [2001]; Huisman and Weissing [2002]; Kenitz et al. [2013]; review by Scheffer et al. [2003]). This chaotic behaviour thus was considered to be quite robust. In contrast to the overwhelming theoretical attention, convincing empirical evidence of chaos in real ecosystems is rare. Beninca etal (2008) analyzed a time series of a plankton community collected from the Baltic Sea and cultured in a laboratory mesocosm for more than eight years (Heerkloss and Klinkenberg [1998]. Despite constant external conditions, the species abundances showed strong fluctuations. The observed population dynamics was characterized by positive Lyapunov exponents of similar magnitude for each species, demonstrating that species interactions in food webs could, indeed, generate chaos. Both mathematical models (Hastings and Powell [1991]; citevandermeer1993loose; Huisman and Weissing [1999];Brose [2008];) and laboratory experiments (Benincà et al. [2008], but also Becks et al. [2005]; Graham et al. [2007]) have shown that non-equilibrium dynamics may be an intrinsic property of a multi-species communities. Hence, it is conceivable that the

oscillations generated by competition may favor the coexistence of number of phytoplankton species greatly exceeding the number of limiting resources, even in a constant and well-mixed environment. It is important to note, that the list of mechanisms presented above do not complete the broad spectrum of mechanisms which could maintain species diversity (see review by Chesson [2000]) invoking, among many other, neutrality (Hubbell [2001]) in form of absence of competitive edge among species belonging to same trophic level, contemporaneous disequilibrium and role of mixing (Richerson et al. [1970], Lévy et al. [2014]), open chaotic mixing (Károlyi et al. [2000]) and mutualistic interactions (Mougi and Kondoh [2012]). These mechanisms however will not discussed in here.

1.4 Diversity and ecosystem functioning

The pelagic ocean hosts a large diversity across trophic levels (e.g., Tittensor et al. [2010]). The functioning of the global ecosystem is mediated in large part by pelagic marine organisms through their influence on biomass production, elemental cycling, and atmospheric composition (Falkowski et al. [1998], Balmford et al. [2002], Daily [1997]). Thus, the coupling of diversity and ecosystem functioning has been a focus of research for several decades (Schulze and Mooney [1994],McCann [2000]). Theory (Tilman et al. [1997a],Yachi and Loreau [1999]) predicts that the stability and functioning of this complex system can be influenced by both the composition and the richness of taxa within its compartments (Cardinale et al. [2012]). The hypothesis that diversity of primary producers influences the functioning of ecosystems in terms of primary production, total biomass, or nutrient use, has received a considerable empirical support in recent years (Ptacnik et al. [2008], Cardinale et al. [2011]). These experiments demonstrated that, averaged over different species and habitats, species loss reduces the biomass and resource-use efficiency of the primary producers, and might reduce primary productivity (Ptacnik et al. [2008], Cardinale et al. [2011]). These responses vary, however, in strength and direction for different types of ecosystems and different indicators of ecosystem functioning such as producer biomass, nutrient concentrations, or primary production (Hooper et al. [2005]; Cardinale et al. [2011]). Phytoplankton

diversity in particular influences ecological and biogeochemical processes as it relates to the community composition which forms the basis of the pelagic food web (Duffy et al. [2006]). The composition of the phytoplankton community may affect the export of organic matter from the surface to the deep ocean, and thereby the global cycles of nitrogen, phosphorus, and carbon (Redfield [1958]; Falkowski et al. [1998]; Caron and Countway [2009]), including uptake of atmospheric CO_2 (e.g., Arrigo et al. [1999]; Finkel and Irwin [2000]; Hilligsøe et al. [2011]; Behl et al. [2011]) and Carbon sedimentation (Sieracki et al. [1993], Assmy et al. [2013]). Phytoplankton community structure may also affect zooplankton production and composition, and propagate up to fisheries and humans as end-users of the fisheries (Richardson and Schoeman [2004]; Hilligsøe et al. [2011]; Ainsworth et al. [2011]). The system biomass or primary production is frequently suggested to take form of a saturation function of species diversity (Cardinale et al. [2011]; Tilman et al. [1997a]). For such relationship, initial diversity loss from systems with high diversity has only a minimal effect on ecosystem functioning, however, at some point, further loss of diversity results in a pronounced reduction in functioning. The positive relationship between these two is repeatedly attributed to either or both of two mechanisms: (1) the selection effect can increase functioning since a more diverse community has a higher probability of containing a highly productive species, which dominates the community (Aarssen [1997]; Huston [1997]) and which affects the performance of other species via competition (Cardinale et al. [2004]; Weis et al. [2007]); (2) complementarity of species or groups through niche or resource partitioning can increase functioning in more diverse communities by increasing the resource usage efficiency (Tilman et al. [1997a]; Loreau [1998]; Cardinale et al. [2002]). In the classical understanding, niches arise from variability in ecological factors within the system, e.g., temperature or prey size, and can be identified by the degree of resource use along such gradients (Hutchinson [1957],MacArthur and Wilson [1967]; Schoener [1989]). The experimental evidence for diversity-ecosystem functioning relationships predominantly originates from terrestrial and benthic ecosystems and the underlying mechanisms were derived mostly from these data (Hooper et al. [2005]; Cardinale et al. [2011]). Experimental studies on pelagic communities are still scarce (Duffy et al. [2006];Ptacnik et al. [2010]; Cardinale et al. [2011]). Nevertheless, experi-

ments controlling phytoplankton diversity and compilations of field data from natural communities, suggest that some of the mechanisms governing spatially organised terrestrial ecosystems are applicable for the pelagic ocean (Duffy et al. [2006]). Ptacnik etal (2008) reported an increase in efficiency of nutrients usage (and decrease in its variability) related to higher species diversity in the communities across different lakes, and in the Baltic Sea. A possible explanation for this increase was suggested by Striebel et al. (Striebel et al. [2009]) and invokes correlation between high algal diversity and high pigment diversity, which results in higher carbon fixation (=net primary production) at higher diversity due to light use complementarity. Other studies however find neutral (Gamfeldt et al. [2005]) or negative (Schmidtke et al. [2010]) relationships between diversity and ecosystem functioning, or more complex temporal patterns (Weis et al. [2007]). Thus the relationship between diversity and pelagic ecosystem functioning remains equivocal.

1.5 Diversity in aquatic ecosystem models

In light of scarce empirical data on the phytoplankton diversity and distribution patterns, modelling provides an important tool for understanding them and exploring their possible response to changing climate. The models of marine ecosystems in form of NPZ or NPZD configurations in which nutrients, phytoplankton, zooplankton and detritus form the main model structure (e.g. Steele [1974]; Wroblewski et al. [1988]), continue to demonstrate their value in both regional and global modelling studies (e.g. Kawamiya et al. [2000]; Palmer and Totterdell [2001]; Anderson and Pondaven [2003]; Schartau and Oschlies [2003]). There has been a recent interest in trait-based approach in marine ecology because it holds the potential of increasing our ability to explain the organization of ecological communities and predict their reorganizations under global change (Litchman and Klausmeier [2008], Litchman et al. [2007], Finkel [2001], Armstrong [1999]). Key physiological characteristics, or traits, provide a means by which to organize the all-important trade-offs, i.e. the costs and benefits of particular physiological characteristics (e.g., Margalef [1978], Reynolds [1984]). Litchman & Klausmeier (2008) provide an excellent review of key phytoplankton traits and trade-offs, with

implications for modeling. The major ecological axes that define ecological niches of phytoplankton are physical environment, resources, and natural enemies (grazers and parasites) (Margalef [1978]; Reynolds [1984]; Tilman et al. [1982]). For each of these axes a whole hierarchy of traits exists, from the subcellular to population level, which allow phytoplankton to survive and reproduce in the environment. Traits can be classified by ecological function (reproduction, resource acquisition, and predator avoidance) and trait type (morphological, physiological, behavioral, and life history) (Litchman and Klausmeier [2008]).

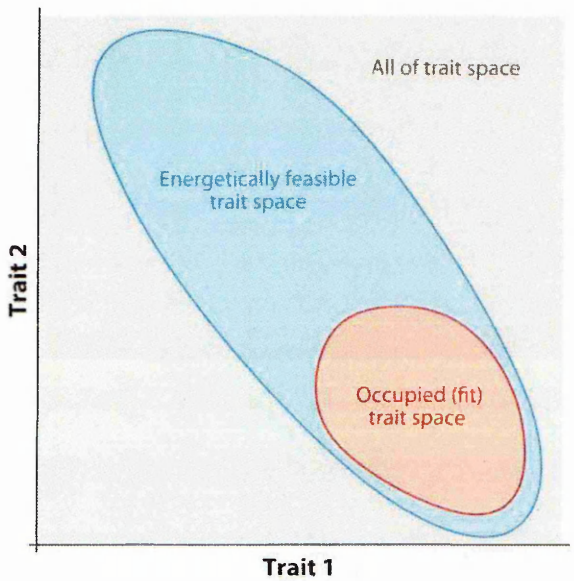

Figure 1.1: Traits and trade-offs: Schematic of a generic two-dimensional trait space that characterizes each phytoplankton's physiology. Energetic trade-offs limit the actual area that can be plausibly occupied, resulting in a correlation of traits. Such correlations have been observed in laboratory studies for, e.g., maximum nutrient-uptake rates and nutrient half-saturation constants and minimum cell quota (e.g., Litchman et al. [2007]). Of these physically reasonable trait combinations, only a subset is likely to be fit in a particular environment, and thus the observed set of trait combinations does not necessarily fill all possible areas of parameter space. In a different environment, a different subset will be fit. Figure taken from Follows and Dutkiewicz [2011])

An example of a trade-off between traits is that between K and r strategists (MacArthur and Wilson [1967], Kilham and Hecky [1988]). Gleaners, or K-strategists, are adapted to compete effectively for limited resources, hence are characterized by high nutrient affinities (low half-saturation). Opportunists, or r-strategists, are adapted to take advantage when resources are abundant and are characterized by high maximum

nutrient uptake rates (or maximum growth) (Grover [1991]). There are strong laboratory evidences justifying a trade-off between half-saturation and maximum growth (or nutrient uptake) in marine phytoplankton (Litchman et al. [2007]) that is tied, in part, to cell size but also to trade-offs between encounter rates and handling of resources (Smith et al. [2009]). Consider a two-dimensional trait space (Fig. 1.1) in which each type of phytoplankton in a modelled population must be characterized. A completely random assignment of the two traits may generate an organism anywhere in the two-dimensional trait space. The correlation between the traits, due to energy or resource trade-offs, may limit the actual area that can be plausibly occupied. Further restrictions on the physically reasonable trait combinations imposed by the particular environment and/or co-existing species, create the observed set of trait combinations (Bruggeman and Kooijman [2007]).

To date, mechanistic models and laboratory characterizations are being used to provide parametrization of the fundamental constraints for the trade-offs that regulate microbial responses (Litchman et al. [2007], Finkel [2001], Armstrong [1999]). One important constraint is represented by the organism size. It has long been recognized that microbial growth, respiration, nutrient acquisition, light harvesting, and sinking speed scale with cell volume or mass (e.g., Laws [1975], Banse [1982], Tang [1995], Litchman et al. [2007], Finkel [2001], Kooijman [2001]). Thereby, the cell size is frequently used as a key trait, which not only organizes other traits but above all allows reducing the region of possible trait space in ecosystem models (Litchman and Klausmeier [2008]). Relationships between phytoplankton cell size, abundance, respiration, and links to environmental controls can be captured by such models (e.g., Laws [1975], Irwin et al. [2006]).

The requirement of traits and trade-offs is of prime significance for selection-based models (e.g., Follows et al. [2007]), models with adaptive dynamics (e.g., Bruggeman and Kooijman [2007]), and for functional group models (PFT). In such models, the species coexistence, and hence community structure in marine ecosystems, is governed by the differences of the species traits and by trade-offs amongst them. The trait-based approach allows to investigate mechanisms of phytoplankton coexistence and consequences of diversity for simulated biogeochemical cycling.

On the global scale, the 'Darwin model' developed by Follows et al. [2007] resolves phytoplankton diversity by explicitly formulating a self-assembling community. The species are distinguished by physiological traits including sensitivity of growth to light, nutrients, and temperature. Eventhough, all the parameter values are distributed stochastically in the 'Darwin model', the size classes assigned to phytoplankton species provides some organizing trade-offs amongst them. This suite of virtual organisms was initialized in an ocean circulation and biogeochemistry model resolving nitrogen, phosphorus, iron, and silica cycles. Phytoplankton interactions with the environment determine their performance. This, in turn, organizes ecosystem structure and the feedback on the resources. As such, the community structure is not imposed but it emerges from a broader set of possibilities: it self-organises itself. As a result, many phytoplankton species with physiologies resembling real world analogs were consistently fit and populated the model ocean with plausible distributions and abundances (Follows et al. [2007]). In this complex model of phytoplankton communities, the frequency of environmental fluctuations appears to select the most successful strategy, low R^* or high maximum growth rate, in each region according to the mechanisms underlying the intermediate disturbance hypothesis. However, highest diversity culminates in hot spot regions, eg. the Gulf Stream, where species dominating different latitudinal - productivity regions are brought together by lateral advection and not at intermediate disturbance frequencies (Barton et al. [2010]). Diversity simulated by Darwin model is thus determined by the balance between replenishment of species by dispersal and exclusion rates due to environmental filtering and competitive interactions (MacArthur and Wilson [1967]; Leibold and Norberg [2004]). High dispersal rates characteristic of phytoplankton may potentially overwhelm the effect of spatial constraints and environmental determinants ('everything is everywhere'). The local communities appear to be selected by the local environment from a large number of potential species due to high dispersal rates of phytoplankton (Cermeño et al. [2010]; Ptacnik et al. [2010]). These potential species can be thought of as a regional species pool (metacommunity; Leibold and Norberg [2004]) which is selected from the global species pool by the regional environment (Ptacnik et al. [2010]). Consequently, the local diversity is controlled by both local and regional environmental factors.

Alternatively, it has been proposed to focus on the adaptive community structure (adaptive dynamics models), based on the distribution of the means and variances of traits within a group of species (Norberg et al. [2001], Savage et al. [2007]). Models developed within this theoretical framework represent diversity by describing a community using a distribution of traits and trade-offs values. Notably, the distribution of traits and their variance describe the adaptive capacity of phytoplankton community, critical for the ecosystem's ability to maintain certain processes under change in environmental forcing (Norberg [2004]). For these reasons, this approach makes explicit predictions regarding the relation between the environment, trait distributions, and ecosystem processes (Norberg [2004], Bruggeman and Kooijman [2007]). Within these models, species diversity may be sustained either by the complementarity of two traits (Savage et al. [2007]), or by processes that simulate migration or dispersal (Norberg et al. [2001], Bruggeman and Kooijman [2007]), hence indirectly recalls the paradigm of Baas-Becking (1934) - 'everything is everywhere, but environment selects'.

The current trend in marine ecosystem modelling is to divide phytoplankon into various plankton functional types (PFTs) including diatoms, coccolithophorids, nitrogen fixers, picophytoplankton, phytoflagellates and dinoflagellates, small or large zooplankton (Totterdell et al. [1993], Blackford et al. [2004]; Quere et al. [2005]). The division into PFTs is in fact an aggregation within one state variable of species with a similar role in the food web or in biogeochemical cycling (e.g., nitrogen fixation or export of organic matter). Consequently, the species aggregated within one PFT might considerably differ in their ecology or life history and thus may have significantly different traits eg., nutrient affinity or susceptibility to grazing (Anderson [2005]). Thereby, accuracy in the representation of the diversity within PFTs is required, otherwise a correct representation of phytoplankton distribution patterns cannot be achieved (Thingstad and Cuevas [2010]).

In order to illustrate the scale of the PFTs aggregation and related to it issues I present a brief description of diatom's ecology and life history.

1.6 Diatoms life history

Diatoms play an important role in the biogeochemical cycle of carbon (Smetacek [1999b]) and silica (Smetacek et al. [2004], Tréguer and De La Rocha [2013]). They are responsible for a considerable fraction of the primary production in the ocean transforming the inorganic carbon dissolved in the seawater into organic matter via the process of photosynthesis. Moreover, their capability to biomineralize silicon by transforming the silicic acid into the glass frustule, makes them the key organisms governing the silicon biogeochemical cycle. Their physiological properties including the ability to grow under dim light and high affinity for the main inorganic nutrients (Smetacek [1999b]) allows them to profit from the replete nutrients conditions and increasing day-length in the late winter / early spring period in temperate and polar regions. Moreover, silica frustules provide an extra protection against grazing (Hamm and Smetacek [2007]). Diatoms tend to dominate most algal blooms in oceans and lakes including spring bloom in temperate and polar regions. As diatoms sink along the water column at the end of bloom, they export organic carbon and silica into the ocean's deep layers. They are either dissolved and enter again the dissolved C and Si pool, or are buried on the sea floor providing food for benthic organisms. It has been estimated that about 30% of the global primary production is exported away from the photic zone, but only about 1% gets sequestered in the deep sediments in correspondence to the areas with the highest primary production (coastal areas, upwelling regions, frontal areas etc.). The largest deposit of siliceous diatom frustules is located around Antarctica and it is largely constituted by the heavily silicified diatom *Fragilariopsis kerguelensis*, together with remnants of other large and thick-shelled species that live in the area (Smetacek et al. [2004]).

Because of their ecological importance, diatoms are frequently explicitly represented in the models addressing global distribution and diversity of phytoplankton. Their representation however is greatly simplified to the processes of nutrients acquisition, growth and mortality (Sarthou et al. [2005], Litchman et al. [2006]). It has been suggested that the representation of the phytoplankton functional groups should be improved (Anderson [2005]). Due to the fact that diatoms are characterized by complex, heteromorphic life cycles (Edlund and Stoermer [1997]; Montresor et al. [2006]), which

could alter their dynamics. Notably, some mechanisms related to life cycles have been already recognized to play important role in the bloom dynamics; the bloom formation can be initiated by germination of resting stages and the resting stage formation can be seen as a signal triggering bloom end. Moreover, There is evidence that complex life cycles affect phytoplankton species diversity and community composition (Jones and Lennon [2010]), thus life cycles have the potential to impact ecosystem functioning (Schulze and Mooney [1993], McCann [2000]). Thus, it is convincing that research should focus on deciphering the dynamics of life cycle related processes and explore their impact on the diatoms population dynamics, and consequently on phytoplankton diversity-distribution patterns. The following section consists the description of the main features of the diatoms life cycles and factors regulating transitions amongst stages.

The diatoms Diatoms are autotrophic protists present in the water column of the oceans, but also in lakes and rivers, and even in the soil, if enough humidity is present. Diatoms are surrounded by a mineral theca, the frustule, made of polymerized silicic acid that is constituted by two, slightly unequal parts that fit together as the lid on a box. These two parts are called 'epi-theca and 'hypo-theca', and each of them is constituted by a valve and a series of cingular bands. Diatoms are responsible for about 1/5 of the global carbon fixation in the world ocean (Mann [1999], Smetacek [1999b]). It is estimated that diatoms include about 200,000 species varying in size from a few micrometers (e.g. *Minutocellus*), to hundreds of micrometers, as the largest species of the genera *Rhizosolenia* or *Thalassiothrix*. Several species can form more or less long colonies in which the single cells are joined together by mucous material (e.g. *Pseudo-nitzschia, Fragilariopsis*), by siliceous extrusions (e.g. *Chaetoceros*) or by chitin filaments (e.g. *Thalassiosira*). The majority of diatom species have a benthic habit and live as epilithic on sand and stones or epiphytic on the aquatic vegetation (Kooistra et al. [2007]). Marine planktonic diatoms mostly belong to the centric lineages, but there are some genera of pennate diatoms - e.g. *Pseudo-nitzschia, Fragilariopsis, Thalassiothrix, Asterionellopsis* - that have a planktonic habit and are an important component of the marine plankton.

1.6.1 Diatom life cycles

The vast majority of phytoplankton species have a complex life histories. Life cycles of phytoplankton species have been selected over a long evolutionary history. The life history of the different species can be seen as a key element, a pathway leading to understanding of plankton ecology, plankton population dynamics and, above all, ocean functioning. A microalga can alternate in its life cycle between several distinct major phases: growth, sex, quiescence and cell death (Figure 1.2, 1.3).

The dominant phase that characterizes the life history of diatoms is the vegetative phase. During this period, we observe biomass increase as a result of mitotic divisions. The vegetative growth phase of many species is infrequently interspersed with sexual events (Chepurnov et al. [2004], Edlund and Stoermer [1997], Round et al. [1990b]). The existence of resting stages can be attributed to seasonal, environmental shifts.

It is clear, that the peculiar life cycle of diatoms is characterized by a strong link with the cell size: cells can in fact undergo specific transformations only in defined size windows. Thus, key aspects of the life cycle of diatoms are controlled by cell size (Drebes [1977b]). Notably, other factors responsible for transitions between the different phases are still largely unknown but have direct impacts on the ecological role of species and on their biogeochemical function.

1.6.1.1 Vegetative division

Growth is the vegetative phase in which cells undergo asexual reproduction (Figure 1.2, 1.3). Diatoms are surrounded by a rigid silica wall (frustule) that consist two thecae, unequal in size and overlapping as a box (hypotheca) with its lid (epitheca). During vegetative, i.e. mitotic division, each daughter cell inherits one maternal theca, which becomes the large epitheca, and builds ex novo the smaller theca, which becomes the hypotheca. As a result of this peculiar cell division mechanism, a progressive cell size reduction in the population, known as the "MacDonald-Pfitzer rule" (Macdonald [1869], Pfitzer [1869]) is observed. Thus, the vegetative growth has one serious conse-

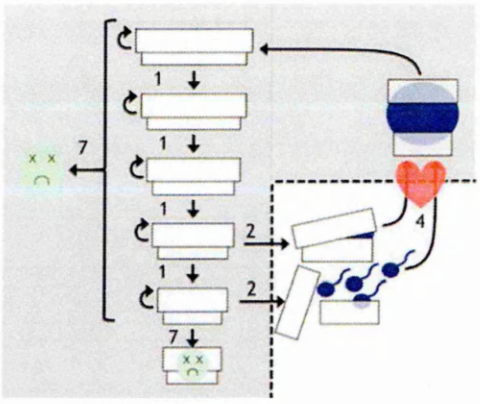

Figure 1.2: Schematic drawings illustrating the main features of the archetypal life cycles of diplontic centric diatoms. The gray shading delimits diploid stages. Arrows mark the points in the life cycle where a change of state is possible. (1) The cell can divide (growth) or enter a resting phase (quiescence). In the archetypal diatom life cycle, each cell division produces one daughter cell of the same size and one daughter cell of a smaller size than its parent; (2) the cell can undergo meiosis; (4) the gamete can find a compatible partner (syngamy, shown by the 'heart' symbol); (7) the cell death may occur, either due to external cues or to failure to restore cell size (diatoms) (shown by the "unhappy face" icon). (Figure taken from von Dassow and Montresor [2010a])

quence for diatoms; the average cell size (length in pennates and diameter in centrics) in the population decreases and the standard deviation increases (Round [1972]) as vegetative growth proceeds. Hence, the cell size of diatom species is not constant and can span considerably. For instance, *Pseudo-nitzschia multistriata* cell size span in length between 26 and 82 mm (DAlelio et al. [2009]), *Pseudo-nitzschia delicatissima* between 8 and 80 mm (Amato et al. [2005]), and *Sellaphora pupula* between 19 and 57 mm in length (Mann et al. [1999]). The continued mitotic divisions eventually lead to cells reaching critically small size and consequently cell death (Amato et al. [2005], DAlelio et al. [2009]). It has been observed that in culture cells can become considerably small and reach cell sizes that are rarely observed in the natural environment (Drebes [1977a]). The cell size reduction should be proportional to the number of divisions: the more cells divide, the smaller they become. However, the formation of shorter cells during a series of mitotic divisions in which cell much smaller than the mother cell are formed has been reported (so called 'abrupt size reduction'; Chepurnov et al. [2005]), and several studies have shown different relationships between growth rate and cell size in diatoms. For instance, *Pseudo-nitzschia delicatissima* undergoes cell size reduction over its life cycle, and cells of different size showed differences in

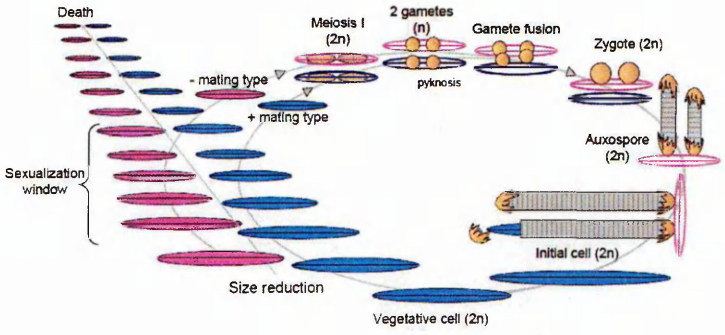

Figure 1.3: Scheme of the life cycle of a pennate diatoms belonging to the genus *Pseudo-nitzschia*. The progressive size reduction is observed during the vegetative division. Sexual reproduction in diatoms includes meiosis, gametogenesis, fertilization and formation of the auxospore within which the initial cell with the largest species-specific size is produced. The gametes of pennate diatoms are non-flagellate and have limited capacity of movement, thus the two gametangia must be positioned close enough to allow conjugation. The interaction between opposite mating types is required to start meiosis and gametogenesis. (Figure taken from Scalco [2010]).

growth rates and the amount of size reduction per cell cycle (Amato et al. [2005]). It has been showed that the average cell size reduction occurring per division was higher for larger cells, whereas the lowest values were recorded for cells whose average size was around 30% of maximal cell size. In *Thalassiosira weissflogii*, a strong positive but nonlinear relationship between growth rate and cell size was detected (Chisholm and Costello [1980], Von Dassow et al. [2006]). Over most of the size ranges of *Dityllum brightwellii, Licmophora hyalina* and *Thalassiosira nordenskioeldii*, sub-clones of smaller size grew moderately faster than larger sub-clones, but sub-clones near the minimum size grew very slowly (Paasche [1973], Durbin [1977], and Von Dassow et al. [2006]). In *Aulacoseira subarctica*, reduction in cells size up to 1 μm per division was found under unfavourable environmental conditions (Jewson [1992b]), and in *Staphanodiscus neoastrea* the largest decrease in cell diameter was observed in summer under nutrient limited conditions and in autumn under low light (Jewson [1992a]). Thus, the rate of cell size reduction in a population depends on the rate of decline in size per cell division and the division rate, and it is strongly influenced by the environmental conditions. Nevertheless, not all diatoms exhibit reduction of cell size, e.g., *Phaeodactylum tricornutum* and *Thalassiosira pseudonana*, and where it occurs such reduction is not always constant (Hildebrand et al. [2007],De Martino et al. [2007]) reviewed in Mann and Marchant [1989], Round et al. [1990b]).

1.6.1.2 The sexual phase

Sexuality is a costly and risky event (Lewis Jr [1983]). It requires more time to produce gametes and meiosis is more time and energy-consuming in comparison to mitosis. Meiosis and syngamy are complex cellular events and, consequently, they are more prone to errors. Cells undergoing gametogenesis are, in some way, lost, i.e. they cannot be used for increasing the population biomass through vegetative divisions. The energy allocated in the formation of gametes can be easily lost. Observations show that some gametangia and gametes abort. In the case of diatoms, where gametes are deprived of the siliceous frustule, gametes are also vulnerable for predation, grazing and infection. Even though it is highly risky and costly process, the benefits and advantages of sexual reproduction are remarkable and sex is reported in the vast majority of multicellular and unicellular organisms. The production of new genetic combinations through meiotic recombination provides species with long-term adaptive advantages allowing not only to survive in a changing environment but also to conquer new territories. Because of the cost and complexity, success in sexual reproduction requires a perfect timing and the right combination of the internal cues (i.e. cell size in diatoms) and the external conditions.

Sexual reproduction in diatoms includes meiosis, gametogenesis, fertilization and formation of the peculiar zygote - the auxospore - within which the initial cell with the largest species-specific size is produced (Chepurnov et al. [2004]). The auxospore is not surrounded by the siliceous frustule but by bands of organic membrane that contain only a limited amount of silica (the perizonium) and are thus capable to expand. If a population fails to restore the size, it may end up in a dead-end where cells are too small to divide and survive. The basic pattern of the sexual cycle differs between centric and pennate diatoms.

Centric diatoms It is considered, that centric diatoms are generally homothallic, though There is evidence that both homothallic and heterothallic reproduction occurs (Godhe et al. [2014]). The homotallic species are characterized by oogamous reproduction, involving the formation of uniflagellate male gametes (sperms) and larger non-motile female gametes (egg cell/s) in the same clonal culture (Figure 1.2). Within

the '-' (female) gametangium they form one or two sessile egg cell/s and within the '+' (male) gametangium, they produce numerous small uni-flagellate sperm cells. The sexual phase has been described for several centric diatoms (reviewed by Drebes [1977a], Edlund and Stoermer [1997], Chepurnov et al. [2004]). The sperm cells swim actively towards the egg cell when released, but the mechanisms of attraction and recognition between sperms and eggs are poorly known. After fertilization of the egg cell, the zygote is wrapped by an organic wall, generally covered by thin siliceous scales and becomes an auxospore which starts to expand (Chepurnov et al. [2004]). The new initial cell is synthesized inside the auxospore. The life cycle of *Leptocylindrus danicus* constitutes an exception within diatoms because the auxospore develops into a resting spore, i.e. a quiescent stage that subsequently germinates into a vegetative cell (French III and Hargraves [1985]).

Pennate diatoms Extensive investigations carried out with cultures or natural material of freshwater benthic diatoms have demonstrated that many pennates are heterothallic. Pennate diatoms produce morphologically identical but often behaviorally different gametes (Chepurnov et al. [2004], Drebes [1966], Round et al. [1990b]) (Figure 1.2, 1.3 (Figure 1.3). Only one or two gametes are produced in each gametangium - one of the two nuclei produced after the first or second meiotic divisions in fact degenerate - and the number of gametes is the same for both mating types (Chepurnov et al. [2004]Chepurnov et al. [2004], Round et al. [1990b]). A detailed description of gametogenesis has been reported for several species e.g *Amphora* sp. (Sabbe et al. [2004]), *Navicula cryptocephala* (Poulíčková and Mann [2006]), *Pseudo-nitzschia pungens* (Chepurnov et al. [2005]), *P. arenysensis* (as *P. delicatissima* Amato et al. [2005]) *P. multistriata* (DAlelio et al. [2009]), *Fragilariopsis kerguelensis* (Fuchs et al. [2013]), The gametes of pennate diatoms are non-flagellate and have limited capacity of movement, so the two gametangia must be positioned close enough to allow conjugation (Figure 1.3). In fact, interaction between opposite mating types is required to start meiosis and gametogenesis. Nevertheless a whole set of possible exceptions exist in diatom life cycles, including self-fertilization, the presence of strains that can act as both male and female, and the capability of forming polyploid auxospores. For instance,

in *Pseudo-nitzschia brasiliana* homothallic auxosporulation was found in monoclonal cultures (Quijano-Scheggia et al. [2009]), and the presence of motile gametes in the araphid pennate *Pseudostaurosira trainorii* was reported by Sato et al. (Sato et al. [2011b]). Finally, auxosporulation was at times observed in crosses between strains of the same mating type, thus suggesting the existence of bisexual strains in *P. calliantha* (Davidovich and Bates [1998b]).

Factors inducing sexual reproduction Sexual reproduction plays a crucial phase in diatom life cycle as it allows for a genetic recombination and produces large sized cells. Most of our knowledge on diatoms sexual reproduction originates from laboratory experiments carried with cultures (Chepurnov et al. [2004]). The role of different environmental cues (irradiance, photoperiod and light spectral composition, temperature, salinity, nutrient concentration) on the occurrence of sexual reproduction has been tested. Different species have different requirements for sex, and these differences might be further modulated by the environmental conditions of the sites in which they live. Because of the difficulties in data comparison across various species and experimental set-ups, the precise nature of the cues inducing sexual reproduction in diatoms remains enigmatic. It has been recognized that a specific cell size window within which gametes can be produced, is essential for sexual reproduction. This species specific size window covers typically 30-75% of the initial cells size (Chepurnov et al. [2004]). It has been reported, however, that for *P. delicatissima* the size window ranges from 20 to 85% of the initial size (Amato et al. [2005]) and for *P. mulitseries* it is 23-70% (DAlelio et al. [2009]). In the centric diatom *Thalassiosira weissflogii* spermatogenesis took place regardless the cell size range of the population (Von Dassow et al. [2006]), and an overlap in the size of initial cells and gametangia has been reported for *Coscinodiscus granii* (Nagai et al. [1995]). The cell size is closely related to the age of the clones due to the MacDonald-Pfitzer rule: cultures have to reach a certain 'age' i.e. they have to go through a certain number of vegetative divisions before undergoing the sexual phase. In fact, it has been proposed by Lewis (Lewis Jr [1984]) that diatom size reduction serves as a 'clock' to optimally set the timing of sexual reproduction. In heterothallic pennate diatoms sexual reproduction occurs when cells of compatible mating

type are cultured together (e.g. Amato et al. [2005], Chepurnov et al. [2004], DAlelio et al. [2009]). There is evidence that sexual reproduction in pennate diatoms is induced when cells in exponential growth are mixed together (Scalco et al. [2014]). Cell-cell interactions between positive and negative mating types cells determine whether or not sexual reproduction occurs. This suggests that the density of the populations plays a crucial role in inducing sexual reproduction, not only to permit the contact between cells (Bates et al. [1998]), but also to allow communication mediated by chemical compounds (pheromone-like substances; Sato et al. [2011a], Gillard et al. [2013]). Indeed, a recent study of Scalco et al. [2014] demonstrated existence of the cell concentration threshold required for successful sexualization of the pennate diatom *Pseudo-nitzschia multistriata*. A series of experiments have tested the quality and quantity of light, and temperature as cues inducing sexual phase. Drebes (Drebes [1977a]) provided evidences that increase in irradiance (from 3.7-5.6 to 37-74 $\mu mol photon / m^2 s$) led to sexual reproduction of several diatoms species, and that simultaneous increase of irradiance and temperature (from 15° to 21° C) resulted in even more intensive sexualization. Mouget et al. (Mouget et al. [2009]) demonstrated that low irradiance (60 $\mu mol photon / m^2 s$) and short photoperiod (8:16 L:D) played a key role in inducing sexualization in the marine planktonic pennate diatom Haslea ostrearia. The relationship between day length and sexual reproduction remains, however, ambiguous. A positive relationship was recorded for the planktonic *Chaetoceros curvisetus* (Furnas [1985]), and an opposite for the benthic pennate *Cocconeis scutellum* (Mizuno and Okuda [1985]). In the latter, sexual reproductions was promoted by short day-lengths, and irradiance conditions that favoured auxosporulation were suboptimal for vegetative growth. The spectral composition of light appears to be important as well. Drebes (1977)Drebes [1977b] attested lack of sexualization of *Stephanopyxis palmeriana* when cells were exposed to a mixture of white, red and far red light wavelengths. Sexual reproduction of Haslea ostrearia took place under white and red light, but not under monochromatic blue and green light (Mouget et al. [2009]). Therefore it is considered, diatom can use day-length and the spectral composition of light as cues for regulating the occurrence of sexual reproduction. Similarly to irradiance, the concentration of micro- and macronutrients might have a role in controlling sexual reproduction. Koester et al.

(Koester et al. [2007]) confirmed the requirement of nutrients for sexual reproduction in *Ditylum brightwellii* as sex did not occur under nutrient depleted conditions. Other experiments demonstrated induction of sexual reproduction as a response to the lack of manganese (Steele [1965]), silicate (Davis et al. [1973]) and nitrogen (French and Hargraves [1985]) in medium used for the experiments.

Vegetative cell enlargement and asexual auxosporulation The vast majority of diatoms restore their size solely via sexual reproduction. Some species, however, are able to restore the maximum cells size by vegetative cell enlargement or asexual auxosporulation. In both cases, a large vegetative cell is formed within an auxospore-like structure (Chepurnov et al. [2004], von Stosch [1965]). Vegetative cell enlargement is known to occur in some centric diatoms as *Coscinodiscus wailesii* (Nagai et al. [1995]); *Ditylum brighwellii* (Koester et al. [2007]), *Leptocylindrus danicus* var. *apora* (French and Hargraves [1985]) and *Skeletonema costatum* (Gallagher [1983]). Asexual auxosporulation has been reported also in pennates eg., *Achnanthes cf. subsessilis* (Sabbe et al. [2004]). In fact, in the *Achnantes* species, a whole range of reproductive system has been reported, including asexual auxosporulation in *A. cf. subsessilis* (Sabbe et al. [2004]).

1.6.1.3 Resting phase

The life cycle of many centric diatoms includes the formation of resting stages, either spores, which are morphologically differentiated from vegetative cells and have a thick wall, or resting cells, which are morphologically similar to vegetative cells, but physiologically differentiated (McQuoid and Hobson [1996]; Figure 1.2). Spores - produced by the transformation of a vegetative cell, i.e. not related to the sexual phase - are the resting stage produced by diatoms. There is only one diatom species, *Leptocylindrs danicus*, in which the auxospore transforms directly into a resting spore, i.e the formation of the spore is linked to the sexual phase. Spores can be considered as seeds that, if local conditions and time are suitable, are transformed into vegetative cells. Their metabolism rate is greatly reduced; they reduce respiration, while maintaining the ability to photosynthesize if conditions permit. Spores have undergone a noticeable

morphological and physiological differentiation and are surrounded by a resistant cell wall. A number of external factors have been found to induce spore formation. As an example, low nutrient concentration, especially nitrogen, induces spore formation in *Chaetoceros diadema*, although low temperature can positively influence the process (French III and Hargraves [1985]). In fact, the spores production of *Leptocylindrus danicus* has been detected at the end of a bloom when nutrients became depleted (Davis et al. [1980a]). The formation of resting stages may have strong impact on the population dynamics (e.g. bloom termination), number of coexisting species and their succession patterns. The huge advantages of producing resting stages suggests a high degree of plasticity of diatom life cycles and the possibility to partition the genotype in two different environments, water column and sediments at the see floor, thus contributing in the maintenance of the high diversity of unicellular organisms in a certain area. Resting stages could represent a safety mechanism for reintroduction of the species when the vegetative cell population went extinct due to unfavorable environmental conditions (McQuoid and Hobson [1996]). Some other possible advantages of the formation of resting stages are: tolerance of severe environmental conditions, such as predation and darkness. Being resistant, they can be transported at a long distance e.g. in copepod guts, in mussel shells, in ballast waters and thus colonize new environments. Germination fluxes could further contribute to enhance population density of vegetative cells during the initial phases of a bloom, but once exponential growth had started, additional germination has probably negligible effects on bloom magnitude. Spores are highly resistant stages but they are not indestructible. In nature, losses of resting stages in the sediments may be linked to germination, grazing by benthic fauna, death by parasitism and sedimentary dynamics, and may vary strongly in space and time.

1.6.1.4 Programmed cell death

Programmed cell death (PCD) has been identified in unicellular organisms such as bacteria, yeast and protozoa, thereby demonstrating that PCD might be fundamental for prokaryotic and eukaryotic microorganisms with ancient origins. Phytoplankton PCD can be seen as an endogenous biochemical pathway leading to apoptotic-like

morphological changes and, ultimately, cellular dissolution. Thus, a form of autocatalytic cell suicide. Evidence of PCD in phytoplankton was found after monitoring physiological responses to nutrient stress. Amongst the diatoms, autolysis in *Ditylum brightwellii* was an important cause of mortality in laboratory cultures that were subjected to nitrogen and phosphorus limitation (Brussaard et al. [1997]. Similarly, batch cultures of *Thalassiosira weissflogii* that are depleted of nitrogen have markedly reduced photosynthetic efficiency, selectively lose specific proteins such as ribulose-1,5-bisphosphate carboxy- lase/oxygenase (RubisCO), increased protease activity and specifically induce an unidentified protease, which was recognised as markers of apoptosis (Berges and Falkowski [1998]). Further evidences are provided by the detection of caspases, enzymes that are recognized as one of the morphological and biochemical changes consistent with PCD (Bidle and Falkowski [2004]). Indeed, five metacaspase orthologues were found in the *Thalassiosira pseudonana* genome sequences. PCD is extremely interesting, not only from the evolutionary point of view. It can be used in case of environmental stress conditions, such as famine, when suicidal cells support their neighbors by releasing nutrients. Employing PCD by cells attacked by an infection and hence preventing it from spreading around might be advantageous for the whole colony / population. This case has been reported in freshwater planktonic diatom *Asterionella formosa.* From this point of view PCD is highly altruistic. It is also a natural mechanism of eliminating a large number of individuals in the end of the growth.

1.6.2 Summary on diatoms and their representation in the models

Diatoms life cycles have been selected over a long evolutionary history, thus it is not surprising that the diversity of species is mirrored by the complexity of their life history elements. Diatom cells can alternate in their life cycle between four distinct major phases: an actively growing phase during which biomass is intrinsically increasing (in the absence of external losses), and other life phases in which cells are dormant or quiescent, undergo sexual reproduction or die (von Dassow and Montresor [2010b]). Consequently, despite being genetically identical, each population may contain indi-

viduals strongly differing in terms of their physiology, functional roles and finally fates. This implies also that a different set of descriptors, or traits, is required for each specific life cycle phase.

Morphological, physiological, behavioural and life history related traits regulate ecological functions of the cells such as resources acquisition, predators avoidance and reproduction both sexual and asexual. These traits would not only be species specific but also, most likely, population specific. as each population may be comprised of cells in various life history phases. Furthermore traits would vary on ecological time scale with respect to the ambient conditions (e.g., some diatoms species form chains under turbulent conditions which are broken in the presence of copepods) and evolutionary time scale as a mean to withstand an evolutionary arm race (e.g., Red Queen Hypothesis).

Very little is known about species-specific life cycles, and even less about factors regulating transitions among the different phases. Yet, it is clear that processes associated to the life stage transformation have direct impacts on the ecological distribution of species and on their biogeochemical function. Therefore, life cycles represent a key element for our understanding of diatoms ecology and for improving our understanding on marine ecosystem functioning.

1.7 Why further research is needed?

Ocean ecosystems are under pressure from the needs of a growing economy and from global environmental change. A co-occurrent loss of diversity observed across ecosystems raises the question of how diversity influences ecological and biogeochemical processes of ecosystems. Little is known about controls of diversity and its role in shaping ecosystem processes in the global pelagic ocean and biogeochemical cycles of nutrients and carbon. Trade-offs between traits on main ecological axes have been frequently invoked when the seasonal structure of planktonic communities was addressed. The trait-based modelling approach rarely consider biological controls deriving from specific life cycle features. The present thesis aims to extend our understanding of how life cycle related biological traits influences phytoplankton diversity in ecosystem models.

The formulated by Hutchinson (Hutchinson [1961]) "paradox of plankton" puzzled scientists for over five decades. Despite the fact that numerous mechanisms have been proposed, a unifying, accepted theoretical framework explaining what regulates the number of represented species, in space and time, is still lacking.

Much has been understood on matter and energy flow constraints in plankton communities (e.g., photosynthesis regulation). The phytoplankton functional types models, together with the selection-based models (e.g., Follows et al. [2007]), and those with adaptive dynamics (e.g., Bruggeman and Kooijman [2007]) prove to be useful when address a broad range of ecological and biogeochemical questions which, to date, have not been addressed in the context of large-scale ocean models and global climate change. The global plankton models provide the opportunity to investigate on the mechanisms shaping global patterns of phytoplankton distribution (Prowe et al. [2012a], Dutkiewicz et al. [2009]). Nonetheless, there is no model, either conceptual or numerical, able to consistently reconstruct the observed phytoplankton diversity (for a recent review of the present perspective in plankton modelling, see Hood et al. [2006]).

One of the reasons for this failure is the trait-based itself. A broad spectrum of traits has been identified for phytoplankton species including morphological, physiological, behavioral and life history traits (see review by Litchman and Klausmeier [2008]). Yet, the modelling approach frequently focuses solely on the physiological properties (e.g. ecosystem model by Litchman et al. [2006]) such as resource acquisition and physiological responses curves to various environmental forcing (Bruggeman and Kooijman [2007], Hutchinson [1957], Margalef [1974], Litchman et al. [2006]), and the resistance to grazers and disease (Litchman and Klausmeier [2008], Reynolds et al. [2006], Anderson et al. [2002]). The reason for this limited use of traits, is the limited knowledge on the life history traits of planktonic organisms which could drive their life strategies along paths more sophisticated than just those driven by the short term availability of resources.

Main attribute of most phytoplankton organisms it is that they have complex and heteromorphic life cycles including internally regulated processes such as formation of resting stages, sexual reproduction, active growth control, creation of aggregates (Edlund and Stoermer [1997]; Montresor et al. [2006]). It is reasonable to assume that those

biological traits may affect other phytoplankton traits and thus affect species dynamics independently from the constraints imposed by the abiotic factors and leading to significant changes in the community composition (Jones and Lennon [2010]). Unfortunately, studies considering life strategies in phytoplankton ecology are still considerably rare. In order to advance in our understanding of the patterns of plankton diversity and distribution, research interest ought to be focused on evaluating the impact of the biological regulation of these species-specific phases on the community dynamics over the seasonal cycle.

A growing body of research employs ocean models addressing marine biogeochemical and ecological questions including the regulations of the phytoplankton distribution and diversity patterns (Dutkiewicz et al. [2009], Prowe et al. [2012a]). Notably, the use of such models remains debatable due to theoretical and practical constraints given by limited empirical knowledge on phytoplankton biology, aggregation of diverse organisms into single state variables despite differences in life strategies, poorly understood ecology, together with unpredictable nature of the emergent dynamics of interacting equations (Anderson [2005]) and significant computational cost.

These constraints result in a considerable under-representation of phytoplankton diversity in the model ecosystems. While the phytoplankon species diversity observed in the natural environment may exceed hundreds of thousands of species, only couple of dozens are able to co-exist in the virtual ecosystems (Follows et al. [2007]). Because of that is is important to ask if a model can be used to address the issue of species diversity? The answer is: yes.

Models are abstractions of reality which are designed to focus on certain aspects of the object of study. The simplest, conceptual models take form of a verbal descriptions of systems and are communicated by diagrams that illustrate a set of components and the ways in which they interact (e.g. Margalef's Mandala). As the number of components and interactions in a diagram grows, it becomes increasingly difficult to maintain an intuitive understanding of the overall behaviour. This may be eliminated by using a mathematical description of the considered system as long as a quantitative representation of each of the interactions in the diagram is available.

Mathematical models serve as aids to ecological investigation in multiple ways.

In order to construct a mathematical model it is required to critically consider all of the mechanisms that underlie process addressed with the model. This rigorous, reflective process can reveal inconsistencies in a diagram model and highlight previously unnoticed gaps in our knowledge. Once a model has been constructed, it serves as a transparent description of the system which can be unequivocally presented.

A mathematical model is a representation of a putative descriptions of a system and its behaviour. Its analysis yields insights into why a system behaves the way it does, thus provides links between ecosystem structure and behaviour. Simulations can serve as valuable source of information as they indicate promising avenues for investigation, or reveal inconsistencies between our understanding of a system (embodied in the model) and the real world observations. In fact, the identification of such inconsistencies is a key benefit of modelling. Because of the fact that models dynamic behaviour can be thoroughly investigated, it follows that a negative result - the inability of a model to replicate experimental observations - can be taken as a falsification of the hypotheses on which the model was built. This can lead to a refinement of the biological hypotheses, and subsequently a refined model, which can then be tested again against available data.

In light of the above, there is a need for process-oriented mathematical models adopted to address specific scientific problems, in here phytoplankton species diversity observed over the seasonal cycle. These, frequently simple, models provide a platform to synthesize and quantify conceptual understanding of the processes regulating species diversity, and form basis for the exploitation of insight on the processes derived from laboratory studies and field observations. Thus, despite their limitations in reproducing the real world phytoplankton diversity mathematical models allow to organize our knowledge on processes shaping the community structure and species diversity. Mathematical models allow also to investigate the causative links between selected processes (e.g. related to complex life cycles of phytoplankton) driving population dynamics and ecosystem functioning. Furthermore they allow to identify the inconsistencies in the incorporated mechanisms underlying envisioned models' construction (e.g. perception of phytoplankton life cycles simplified only to the vegetative phase) and identify the gaps in our knowledge which needs to be filled. Because of that, the use of mathemat-

ical models, also the simple ones, ought to be considered as a tool providing general insights into the functioning and implications of explored scientific problems.

1.8 The aim of my thesis

The general aim of my thesis is to introduce new concepts in modelling plankton dynamics by gathering multidisciplinary information from biology, physics, and ecology in order to assess the nature and relevance of the drivers of that dynamics, among which the role of biological traits of planktonic organisms is considered. To be more specific, the aim is to explore factors affecting plankton succession and species diversity including grazers' migration and phytoplankton species immigration, but also to explore the role of the seasonal characteristics of the water column in shaping community structure and its time course. Finally, the aim is to inspect the impact of species-specific life cycles related traits, in particular sexual reproduction on the diversity of phytoplankton using a suitably adapted community model.

Why to focus on diatoms and their life cycle phases?

Diatoms are important components of the marine phytoplankton as the contribute significantly to the export of organic material and connect to the global silicon cycle (Smetacek [1999a], Armstrong et al. [2001]). Diatoms are characterized by a considerable phylogenetic diversity, with thousands of species with distinct biogeographic distribution and often distinct seasonal timing. They also have a complex heteromorphic life cycle (Chapter 1 Sec. 1.6). The link between population dynamics and the transition among different life cycle phases is a relevant, but still poorly explored, subject. This link extends to the geographical distribution, phenology and coexistence of diatoms species in the natural environment. The questions addressed in my thesis have been mostly focused on the transition between the vegetative growth phase and the sexual phase, and its impact on population dynamics.

Why to focus on sexual reproduction?

Because of the constraint represented by the rigid silica frustule surrounding the

cell, many diatoms experience a progressive size reduction as vegetative growth proceeds (Round et al. [1990a]). For many of them size restoration is possible only during the sexual phase (Chepurnov et al. [2005], Amato et al. [2005],Round et al. [1990a], Mann [1993]). Hence, an obligatory sexual phase is the only mean to avoid death. At the same time there is a cost associated with the sexuality (Lewis Jr [1983], Lewis Jr [1984]) which may affect its competitive abilities and consequently alter its population dynamics.

Why laboratory experiments are needed?

Ecological studies addressing plankton life strategies and their impact on ecosystem functioning are rare. Because of that, biological processes which could drive phytoplankton life strategies along paths more sophisticated than just those driven by the short term availability of resources are largely unknown. Laboratory studies phytoplankton exploring species biology, physiology, ecology and genetics offer an in-depth information on their functioning, ecological niche, interactions with other species, but also on their life cycle and mechanisms corresponding to the stage transformation. Henceforth, laboratory experiments provide an ideal set of data suitable for describing and parametrising novel mechanisms and biological traits.

Why to apply the ecological modelling approach?

Ecological models are continuously used in marine science to study ocean biogeochemistry and species diversity. Numerical models provide an excellent theoretical framework for distilling expanding knowledge base from field studies and laboratory experiments into traits of ecological and evolutionary importance. One of their potential applications is to evaluate role of processes associated with a single (or a subgroup of) species in structuring and functioning of a complex, multi-level ecosystems. In particular, a suitably adapted ecological models can address the impact of diatoms life stage transformation, here sexual reproduction, on population dynamics and further on phytoplankton community structure and ecosystem functioning.

Thesis outline The second chapter of the thesis is devoted to the description of the ecological model developed in the course of the PhD thesis. I provide a detailed description of the model components with the appropriate formulations and parametrisation. I also present model's characteristics focusing on the physical and biological processes underlining the incorporated mechanisms. I provide a rigid qualitative and quantitative validation of the model performance with respect to the field observations by comparing the predicted bulk properties of phytoplankton and nutrients with the available *in situ* data. The aim of this exercise is to establish whether or not the presented model may be considered as a valid tool for the exploration of the scientific questions stated in Chapter 1 Section 1.8.

The third chapter includes the description of the species diversity observed in the ecological model presented in Chapter 2. To be more specific, species richness and Shannon index had been used as the descriptors of the species diversity in the virtual ecosystem. Seasonal variability of species diversity is also assessed and linked with the physical conditions. I analyse the mechanisms driving species competition and shaping phytoplankton community composition on the ecological time scale. Furthermore, a structural sensitivity analysis is performed to assess model sensitivity to two selected mechanisms, namely copepods winter diapause and a phytoplankton immigration. The performed analyses are intended to illustrate how these process affect both the bulk phytoplankton properties and the species diversity, thus also the community composition. The importance and implications of the theoretical assumptions underlying the model construction is discussed in this chapter.

The forth chapter is devoted to the sensitivity study exploring the relationship between environmental forcing and functioning of a simplified ecosystem. I explored the relationship between physical forcing and the community structure. The analysis are focused on the species diversity over the seasonal cycle. The aim of this sensitivity study is to investigate how changes in the mixed layer depth, prolonged stratification and changes in the beginning and duration of spring restratification affect species community composition and species diversity in the virtual ecosystems. The results are

extrapolated into the analysis of particular environments reported in the basin of the North Atlantic and validated against the CPR data. Thus, these analyses aim at further demonstration of the model's plasticity and its applicability for various types of open ocean ecosystems.

The fifth chapter is dedicated to the description of laboratory experiments with batch cultures of marine pennate diatom *Pseudo-nitzschia multistriata.* The experiments are performed with the single mating type strains and the co-culture of opposite mating type strains, thus under conditions where sexual reproduction could not and could take place. This experimental set-up is suitable to test the hypothesis that sexual reproduction impairs population dynamics and nutrients consumption, i.e. sex is linked to a decrease in the growth rate in co-cultures as compared to the single parental strains in monoculture despite saturating nutrients concentrations.

In addition to the laboratory experiments a simple mathematical model is set-up in order to explore competition between two phytoplankton strains differing in size and their competitive abilities. The discrepancies in the phytoplankton bulk properties observed between modelling and laboratory results are subsequently used to disseminate competitive interactions from processes associated with sexual reproduction. By doing this, I intend to indicate the need for introduction of processes related to life cycles into phytoplankton competition models in order to increase their accuracy and predictive capability.

The sixth chapter includes the conceptualization and mathematical formulation of the Endogenous Growth Control mechanism (EGC) - a life cycle related, biological trait describing diatoms growth rate reduction attributed to sexual reproduction which was derived from the laboratory experiments presented in chapter 5. The impact of EGC on phytoplankton community structure and its time course is assessed with an ecological model (Chapter 2) in which a description of a some diatom species was augmented with the developed EGC formulation. The analysis presented in this chapter focus on how biological traits may restructure planktonic community and affect species diversity in the virtual ecosystem. In addition, I explore how EGC mechanism affects success rate

of sexual reproduction, henceforth I intend to evaluate how it affects species fitness. In summary, in this chapter I present some of the EGC implications considering both the ecological and evolutionary times scale.

The last, seventh, chapter includes the summary of the thesis, general conclusions and future perspectives.

In the remainder of this chapter, some background is provided on the two main fields addressed by this study, biodiversity and diatoms life cycle. The first part presents what is known specifically in relation to pelagic phytoplankton diversity, in contrast to the abundant literature on terrestrial systems. The second part discusses diatoms life cycles and factors inducing life stage transformation as a source of previously overlooked biological traits with the potential to control species diversity.

Chapter 2

Model development

2.1 Introduction

Mathematical models in marine science today are frequently used to study a broad range of subjects including ocean biogeochemistry and its response to climate change, development and potential consequences of the harmful algal blooms, or the end-to-end modelling focused on biomass transfer via trophic cascade and its socio-economical consequences. These models vary in terms of their structure, complexity, equations and parametrisation, but above all in terms of objectives and questions they address.

As presented in the Introduction, current marine ecosystem models, mainly focused on simulating biogeochemical fluxes, deal with plankton diversity, and its impact on them, by grouping plankton with similar physiology in a small number of groups (Totterdell et al. [1993], Moore et al. [2002], Gregg et al. [2003], and Anderson [2005]). The functional groups approach (PFT) necessarily eludes the problem of simulating the dynamics of real species diversity over the seasonal cycle which has been recently addressed with other approaches often complex in terms of computational requirements (Follows et al. [2007]).

Here I chose a hybrid approach, merging still simplified biological mechanisms into groups, as in other models, but with a much larger number of types, which allowed for a reasonable complexity and a better exploration of ecological implications. The biological module is coupled with a physical model inspired to the same logic, i.e., a relatively simple formulation allowing to explore the seasonal dynamics of different biomes of the global ocean. The idea behind this design is in fact to have a model that can simulate the dynamics of plankton in all the oceanic regions and seasons. Thus, to reproduce patterns and characteristics of planktonic populations observed in a mid-latitude oceanic region over the years. Thus the model has to reproduce the outcome of some relevant processes regarding seasonality, succession and interactions among planktonic species and functional groups.

The ecosystem model computes the concentration of multiple phytoplankton functional groups with their direct predators, two inorganic nutrient and detritus in the water column, hence it is a nutrients-phytoplankton-zooplankton-detritus (NPZD) type model. The ecosystem dynamics is driven by a set of bio-geochemical processes related to the environment type, while functional traits describe the planktonic community as-

sembly (eg., regulate phytoplankton species competition for resources and their relation with predation on them). The other elements of the ecosystem are greatly simplified, following a *coarse graining* approach (model zooplankton species representing a broad ensemble of real groups) or using a generic mortality (which represents, eg, viruses or higher level predation on zooplankton).

The rationale for choosing the approach described above is of having a tool well suited to analyze the processes driving biogeography, succession and diversity of plankton communities at global scale. In other words a model acceptably simple to investigate ecological hypotheses and sufficiently complex to produce new insights.

In this chapter I present the philosophy underlining the model concepts. I provide a detailed description of the model components with the appropriate formulations and parametrisation. I also present model's characteristics focusing on the physical and biological processes underlining the incorporated mechanisms. Furthermore I provide a rigid qualitative and quantitative validation of the model performance with respect to the *in situ* measurements. For this reason, the described model is set up for selected stations in the ocean using mixed layer depths from data. The predicted bulk properties of phytoplankton and nutrients are subsequently compared with the available data for this stations. The aim of this exercise it to establish whether or not the presented model may be considered as a valid tool for the exploration of the scientific questions stated at the beginning of my thesis.

2.2 Model description

2.2.1 Ecosystem model description - equations

Conceptually, this 0-D ecosystem model consists of a set of coupled differential equations (eq 2.1, 2.2, 2.3, 2.4, 2.5, 2.6) respectively resolving the concentration of nutrients: Nitrate (N) and Silicate (Si), phytoplankton (P), zoplankton (Z) and death organic matter: nitrogen detritus (D_N) and silicate detritus (D_{Si}), within and idealized formulation of seasonally changing environmental forcing. Specifically, the model equations are:

$$\frac{dN}{dt} = \frac{-q_N + w_{mix}(N_0 - N)}{H} - \sum_{i=1}^{m} \mu_i(N, Si, I)P_i + \sum_{k=1}^{n} \epsilon\,(1-e)\,(G_{P_{ik}} + G_{D_k}) + \beta D_N, \tag{2.1}$$

$$\frac{dSi}{dt} = \frac{-q_{Si} + w_{mix}\,(Si_0 - Si)}{H} - \sum_{i=1}^{m} \mu_i(N, Si, I)P_i R_i + \beta D_{Si}, \tag{2.2}$$

$$\frac{dP_i}{dt} = -\frac{q_P}{H} + \mu_i(N, Si, I)P_i - m_{Pi}P_i - \sum_{k=1}^{n} G_{P_{ik}}, \tag{2.3}$$

$$\frac{dZ_k}{dt} = -\frac{q_Z}{H} + \omega\left(\epsilon e\left(\sum_{i=1}^{m} G_{P_{ik}} + G_{D_k}\right) - m_{Zk}Z_k - m_{Z2k}Z_k^2\right), \tag{2.4}$$

$$\frac{dD_N}{dt} = -\frac{q_D}{H} + \sum_{k=1}^{n} m_{Zk}Z_k + \sum_{i=1}^{m} m_{Pi}P_i - \beta D_N - w_g\frac{D_N}{H} + \sum_{k=1}^{n}(1-\epsilon)\left(\sum_{i=1}^{m} G_{P_{ik}} + G_{D_k}\right) - \sum_{k=1}^{n} G_{D_k}, \tag{2.5}$$

$$\frac{dD_{Si}}{dt} = -\frac{q_D}{H} + \sum_{i=1}^{m} m_{Pi}P_i R_i - \beta D_N - w_g\frac{D_N}{H} + \sum_{k=1}^{n}\sum_{i=1}^{m} R_i G_{P_{ik}}, \tag{2.6}$$

The parameters' names and meanings were presented in the Tab. 2.1.

In the following the details of the model formulation are provided.

Name	Parameter	Unit
nitrate concentration	N	$mmol/m^3$
silicate concentration	Si	$mmol/m^3$
phytoplankton concentration	P	$mmol/m^3$
zooplankton concentration	Z	$mmol/m^3$
detritus nitrate concentration	D_N	$mmol/m^3$
detritus silicate concentration	D_{Si}	$mmol/m^3$
mixed layer depth	H	m
solar irradiance at time t and depth z	$I(t,z)$	$W/m^2/d$
nitrate concentration at the bottom of the MLD	N_0	$mmol/m^3$
silicate concentration at the bottom of the MLD	Si_0	$mmol/m^3$
detritus remineralisation rate	β	$1/d$
detritus sinking rate	w_g	m/d
cross-thermocline mixing	w_{mix}	$1/d$
water light attenuation	e_w	$1/m$
phytoplankton light attenuation	e_P	$m^2/mmolN$
zooplankton grazing on detritus function	G_{D_k}	
zooplankton grazing on phytoplankton function	$G_{P_{ik}}$	
phytoplankton growth rate function	$\mu_i(N,Si,I)$	
N dilution compartment due to water column deepening	q_N/H	$mmol/m^3$
Si dilution compartment due to water column deepening	q_{Si}/H	$mmol/m^3$
P dilution compartment due to water column deepening	q_P/H	$mmol/m^3$
Z dilution compartment due to water column deepening	q_Z/H	$mmol/m^3$
D_N dilution compartment due to water column deepening	q_{D_N}/H	$mmol/m^3$
D_{Si} dilution compartment due to water column deepening	$q_{D_{Si}}/H$	$mmol/m^3$
Zooplankton specific parameters (species k)		
zooplankton half-saturation for intake	H_k	$mmolNm^{-3}$
zooplankton net production efficiency	e	$-$
zooplankton absorption efficiency	ϵ	$-$
zooplankton grazing preference for P	ϕ_P	$-$
zooplankton grazing preference for D	ϕ_D	$-$
zooplankton max ingestion rate for large P	g_k	d^{-1}
zooplankton max ingestion rate for small P		
zooplankton linear mortality rate	m_Z	d^{-1}
zooplankton quadratic mortality rate	m_{Z2}	$1/(mmolNm^{-3}d)$
grazing selectivity on P_i	S_{ik}	$-$
copepods dormancy function	ω	$-$
Phytoplankton specific parameters (species i)		
growth rate	r_i	d^{-1}
half-saturation for N uptake	H_{Ni}	$mmolm^{-3}$
half-saturation for Si uptake	H_{Sii}	$mmolm^{-3}$
initial slope of P-I curve	α_i	$d^{-1}(W/m^2)^{-1}$
elemental ratios	$R_{N:Sii}$	$-$
mortality rate	m_{Pi}	d^{-1}

Table 2.1: Parameters used in the model

2.2.1.1 Species' growth rate formulation

The idealized descriptions of phytoplankton physiological processes are similar to those applied in previous studies (Evans and Parslow [1985], Fasham et al. [1990], Follows et al. [2007]). Phytoplankton growth, μ_{P_i}, was determined as a

$$\mu_{P_i} = \gamma_i^{NUT} \cdot \gamma_i^I, \tag{2.7}$$

where: γ_i^I represents the species specific photosynthetic activity, thus the sensitivity to the photon flux, and γ_i^{Nut} is the non-dimensional factors which reflect species specific sensitivity to essential nutrients, here nitrogen (N) and silicate (Si).

The effect on growth rate of nutrients availability was represented in a typical way to the NPZD-type models by a Michaelis-Menten (or Monod) function and the resources limitation of growth was determined by the most limiting one (Follows et al. [2007]):

$$\gamma_i^{Nut} = min\left\{\frac{N}{N + H_{Ni}}, \frac{Si}{Si + H_{Sii}}\right\}, \tag{2.8}$$

where: γ_i^{Nut} is the growth rate of species i as a function of nitrogen (N) and silicate (Si) availability, H_{Ni} - nitrate half-saturation of species i, H_{Sii} - silicate half-saturation of species i, N,Si - nitrate and silicate concentration respectively.

The light sensitivity of growth rate is parameterized as a function resolving both seasonal and diurnal patterns of irradiance arriving at the ocean surface (see section 2.2.4), attenuation of irradiance with depth and photosynthesis as a function of light intensity. The spectral bands were not resolved in here. The depth-average photosynthetic rate is calculated as:

$$\gamma_i^I = \frac{1}{24H}\int_0^{24}\int_0^{H} G(t,z)dzdt, \tag{2.9}$$

where: H - mixed layer depth and $G(t,z)$ is the photosynthesis-irradiance ($P-I$) curve.

The photosynthesis (2.9) was calculated using a Smith $P-I$ curve (Smith [1936],

Falkowski and Wirick [1981] for alternative formulations).

$$G(t,z) = \frac{r\alpha I(t,z)}{\sqrt{(r)^2 + (\alpha I(t,z))^2}}, \tag{2.10}$$

where: $I(t,z)$ is the local light level at time t at depth z, r is the growth rate as $I \to \infty$, and αI is the growth rate as $I \to 0$. The local light level varies with time of day but also with depth in the water column according to Beer's law

$$I(t,z) = I_0(t)e^{-(e_w + e_P P)z}, \tag{2.11}$$

where: I_0 - light intensity at the surface of the water column, e_w - water light absorption coefficient , e_P - phytoplankton light absorption coefficient, P - concentration of all phytoplankton species in the water column above depth z. Parameters e_w and e_P are often assigned values of 0.04 $[m^{-1}]$ and 0.03 $[m^2(mmolN)^{-1}]$ respectively (e.g., Fasham et al. [1990]) and were used also in here.

In fact, Evans and Parslow [1985] provide an algorithm for calculating daily depth-integrated photosynthesis while employing Smith $P - I$ curve (2.10), light extinction calculated with a single Beer's law coefficient and under an additional assumption of a triangular pattern of irradiance from sunrise to sunset

$$I(t,z) = J(t)e^{-kz}\frac{t}{\tau}, \tag{2.12}$$

where: $J(t)$ is the light level at the surface at noon (day t), $k = e_w + e_P P$ is the light attenuation coefficient accounting also for the phytoplankton self-shading, and t, measured in days, is 0 at sunrise and at sunset, and τ at noon, thus describes the triangular pattern of irradiance during the day.

Evans and Parslow [1985] claim that differences between the triangular and sinusoidal approximations ought to be negligible as long as the area under the curve is identical. The consequences of this assumption would however arise from the physical conditions such as the peak light intensity and the attenuation of light with depth, but above all from the non-linearity of the P-I curve formulation. In fact these aspects had been recently addressed by Anderson et al. [2015] - despite relatively minor

system's sensitivity to those processes it is advised to approach the light-dependent phytoplankton growth with caution and awareness of the assumed simplifications.

Following that algorithm presented by Evans and Parslow [1985], the growth rate of a phytoplankton cell averaged over a mixed layer of depth H and totalled over a day, is:

$$\gamma_i^I = \frac{2}{H}\int_0^{\tau}\int_0^{H} G(t,z)dzdt, \tag{2.13}$$

where:

$$G(t,z) = \frac{r\alpha J(t)}{\tau}\frac{e^{-kz}t}{\sqrt{r^2 + \left(\frac{\alpha J(t)}{\tau e^{kz}}\right)^2 t^2}}, \tag{2.14}$$

The transformation of vertical coordinate from depth to reciprocal light, given by: $\Psi = \frac{r\tau}{\alpha J}$ and $y = \Psi e^{kz}$ with $dz = \frac{dy}{ky}$, yields to:

$$\gamma_i^I = \frac{2r}{kH}\int_0^{\tau}\int_{\Psi}^{\Psi e^{kH}} \frac{t}{y\sqrt{y^2+t^2}}dydt, \tag{2.15}$$

where: $y = \Psi$ at $z = 0$; $y = \Psi e^{kH}$ at $z = H$.

Consequently, the phytoplankton cell photosynthetic activity rate averaged over a mixed layer of depth H and totalled over a day is given by:

$$\gamma_i^I = \frac{2r}{Hk}\left[F(\Psi e^{kH},\tau) - F(\Psi,\tau) - F(\Psi e^{kH},0) + F(\Psi,0)\right], \tag{2.16}$$

where:

$$F(y,t) = \sqrt{y^2+t^2} - t\ln\frac{t+\sqrt{y^2+t^2}}{y}. \tag{2.17}$$

It should be noted here that alternative approach to phytoplankton light-dependent growth do exist and invoke e.g. other forms of the P-I curve formulation (see Falkowski and Wirick [1981] for the details, Jassby and Platt [1976]), non-linear functions e.g., Monod equation for light capture (e.g., Litchman et al. [2006], Huisman et al. [2006]) or a product of two exponentials (Follows et al. [2007], Platt et al. [1981]). The formulation employed in here is commonly accepted in the traditional NPZD model framework (e.g., Evans and Parslow [1985], Fasham et al. [1990], Popova et al. [1997]) and demonstrate sufficiently capacity to captures the photosynthetic activity of the major functional groups.

2.2.1.2 Zooplankton grazing

Zooplankton was assumed to graze on both phytoplankton and detritus (e.g. Fasham et al. [1990]). The zooplankton growth rate was described with a basic multi-prey Holling Type III functional response (Ryabchenko et al. [1997]; Gismervik and Andersen [1997]; Koen-Alonso [2007]; Smout et al. [2010]; Gentleman et al. [2003], Prowe et al. [2012b]) with a half-saturation coefficient (H_k for zooplankton species k) regulating grazing efficiency at high prey concentrations (eq. 2.4), grazing rate (g_k described in details in section 2.2.3), selectivity coefficient of zooplankton species k for phytoplankton species i (S_{ik}), and a relative preference for detritus and phytoplankton (ϕ_D and ϕ_P respectively). Therefore the specific grazing rate of a zooplankton species k on phytoplankton species i ($i = 1 \ldots k$) was expressed by the term

$$G_{P_{ik}} = \frac{g_k \left(\phi_P S_{ik} P_i\right) P_i}{{H_k}^2 + \sum_{i=1}^{m} \left(\phi_P S_{ik} P_i\right) P_i + \left(\phi_D D\right) D} Z \tag{2.18}$$

of the equation 2.4.

In an identical manner the specific grazing rate of a zooplankton species k on detritus was expressed by

$$G_{D_k} = \frac{\left(\phi_D D\right) D}{{H_k}^2 + \sum_{i=1}^{m} \left(\phi_P S_{ik} P_i\right) P_i + \left(\phi_D D\right) D} g_k Z. \tag{2.19}$$

Zooplankton growth was described as the product of ingestion rate, absorption efficiency, ϵ and net production efficiency, e. The corollary effect of this parametrisation was a three-way fractionation of intake between zooplankton growth (ϵe), egestion ($1 - \epsilon$) and excretion ($\epsilon(1 - e)$).

The Holling Type III (or sigmoidal) response implemented in here assumes a "passive" prey type switching: as the concentration of one of the compartments (e.g., detritus) increases, the ingestion of other compartments (e.g., phytoplankton) decreases. At the same time the total ingestion always increases with an increase in total prey density.

An alternative could be provided by the "active" prey type switching (e.g., Fasham et al. [1990]) which could however lead to a decrease in the total ingestion rates despite

prey availability increase (see Gentleman et al. [2003] for the details). Such a dynamics could illustrate the sloppy feeding of copepods (Møller et al. [2003]) however this mechanism is not in the scope of this thesis.

Additional options for the grazing formulations and their in-depth analysis can be find in Gentleman et al. [2003].

The Holling Type III formulation, which is commonly used in models despite its identified flows (Gentleman et al. [2003]), has been fit to experimental data, and is known to be numerically more stable than the linear response which can give rise to large-amplitude limit cycles (see Gentleman et al. [2003] and references therein). Consequently, this formulation was implemented in here.

2.2.1.3 Phytoplankton and zooplankton mortality

The concentration of each phytoplankton group is decreased by grazing (see section 2.2.1.2) and density-independent, linear, mortality. The latter accounts for metabolic losses, sinking or "natural" (non-grazing) mortality (e.g. cell lysis). In a similar manner zooplankton concentration is a subject to various sources of mortality represented by linear and non-linear (here quadratic) mortality term (e.g., Yool et al. [2011]). The linear term represents density-independent natural mortality, whereas the quadratic term is considered to be due to predation by carnivores (as in case of phytoplankton). These formulations fall within a very vivid discussion on the sources of plankton mortality and their appropriate functional form (Steele and Henderson [1992b], Edwards and Yool [2000], Mitra et al. [2014]). A linear and quadratic form is the most common, yet in some instances a non-linear functions is also invoked(e.g. Monod equation in Fasham [1993]).

The different sources of mortality used in the model result in different fates for the above terms. Natural mortality of both phyto- and zooplankton, along with zooplankton egestion were allocated to modelled detritus. The fate of the predation-related mortality is, however, less obvious because predators' metabolic activity would result in ingested material being converted into dissolved nutrients as well as larger particulates (e.g. fecal pellets and dead material). As such, zooplankton excretion was allocated within the nutrients pool (term $\epsilon(1-e)(G_{P_{ik}}+G_{D_k})$ in eq. 2.1).

The predation-related zooplankton mortality is assumed to be immediately exported from the system e.g. due to fast-sinking detritus generated by higher predators or to higher predators' migration (e.g. Steele and Henderson [1992a]). Consequently, the predation-related zooplankton mortality represented by the quadratic term is instantly exported and thereby entirely lost from the surface mixed layer of the model.

2.2.1.4 Dissolved inorganic nutrients

The rates of change of dissolved inorganic nitrogen and silicate are given by eq. 2.1 and 2.2 respectively. Nitrogen uptake by phytoplankton is given by term $\sum_{i=1}^{m} \mu_i(N, Si, I)P_i$ in eq. 2.1. A constant ratio of silicate to nitrogen content (R_i) was assumed for the phytoplankton species (see section 2.2.2). Therefore the silicate uptake is given by $\sum_{i=1}^{m} \mu_i(N, Si, I)P_iR_i$ (eq. 2.2).

Dissolved nitrogen is regenerated in the system as a result of detritus remineralisation (βD_N) and zooplankton excretion ($\epsilon(1-e)(G_{P_{ik}} + G_{D_k})$). Furthermore the change in the surface nutrients concentration is attributed to the net transport due to mixing, thus associated with entrainment of water from deep layers ($\frac{-q_N}{H}$) and diffusion ($\frac{w_{mix}(N_0-N)}{H}$).

Dissolved silicate is regenerate in a similar manner but for the zooplankton excretion. A no silicon content in zooplankton was assumed and consequently excretion is allocated to the model detritus.

2.2.1.5 Model detritus

Nitrogen and silicate detritus (equations 2.5 and 2.6) are produced by phytoplankton and zooplankton natural mortality (linear term), and as zooplankton egestion (faecal pellet production). Additionally, in case of nitrogen detritus, zooplankton egestion contributes to detritus pool.

The loss of detritus is attributed to remineralisation (with a constant rate β) and to gravitational sinking (with a constant sinking rate w_g). Detritus loss is also due to changes in the MLD ($\frac{q_h}{H}$ term). Furthermore, zooplankton is capable to graze on nitrogen detritus which is represented by $-\sum_{k=1}^{n} G_{D_k}$ term in equation 2.5.

Parameter	Unit	Value
N_0	$mmolN/m^3$	specific profile[a]
Si_0	$mmolSi/m^3$	specific profile[a]
β	$1/d$	0.05 [b] [c]
w_g	m/d	5[b]
w_{mix}	$1/d$	0.1 [c]
e_w	$1/m$	0.04 [c]
e_p	$m^2/mmolN$	0.03 [c]

Table 2.2: Non group-specific model parameters. References: [a] - World Ocean Atlas 2013 Boyer et al. [2013], [b] - Fasham [1993],[c] - Fasham et al. [1990]

2.2.2 Phytoplankton community description

The phytoplankton community was based on the explicit representation of four functional groups of phytoplankton (Moore et al. [2002], Gregg et al. [2003],Litchman et al. [2006], Quere et al. [2005]): diatoms, coccolitophores, dinoflagellates and green algae. Each phytoplankton group was distinguished by its physiological properties, i.e., traits describing growth rate and resources requirements (Table 2.3). These traits, in form of broad ranges, were predefined on basis of extensive literature review (e.g., Litchman et al. [2006], Sarthou et al. [2005], Bagniewski et al. [2011], Signorini et al. [2012a]). The parameters describing species growth rate, nitrate half-saturation constant and initial slope of the $P-I$ curve have been generated stochastically from the predefined ranges (details below).

In case of light-dependent growth parameters, the values were chosen to represent general ranking of the modeled taxonomic groups: diatoms have the lowest light requirements, followed by dinoflagellates, green algae (prasinophytes) and coccolithophores (Brand and Guillard [1981]; Richardson et al. [1983]; Langdon [1988]).

Ecological trade-offs were imposed through highly simplified allometric constraints Follows et al. [2007]) bounding the phytoplankton physiological properties and size. In particular, all the species representing dinoflagellates, coccolitophores and green algae have been divided into large and small species with a 50:50% ratio in each group. Large phytoplankton species were distinguished by higher intrinsic maximum growth rates, higher nutrient half-saturations and were assumed to be high-light adapted due to packaging effects (Kirk [1994]; Finkel and Irwin [2000]). The values of all the parameters for each species has been randomly chosen, drawn from prescribed normal

distributions based on the median value and the 25th or 75th quartile for the small or large species respectively. Therefore, the trade-offs were implemented by randomly selecting parameter values from different (though overlapping) distributions for large and small phytoplankton.

A different approach has been implemented for the diatoms group, which are in the center of this thesis. Allometric equations bounding species physiological characteristics with the cell volume (V) have been formulated based on the experimental data. These relationships have been presented in Sarthou et al. [2005]. The size dependence of growth rate r was described by the following allometric relation:

$$r = 3.4 \cdot V^{-0.13}.$$

The parameters were based on 67 diatoms species, and the correlation coefficient was equal to 0.42. The relationship between half-saturation nutrient constant H_N and size is given by an equation:

$$H_N = 0.61 \cdot (S/V)^{-0.58},$$

where S is the surface area. The formula was based on 32 samples and the correlation coefficient was equal to 0.4.

All the diatoms species have been divided into small and large species with a 50:50% ratio. The size of each species spanning from $13\mu m^3$ to $7 \cdot 10^5 \mu m^3$ has been generated randomly with an uniform distribution. The cell size has been subsequently translated into physiological parameters with an appropriate formulas. Because of the low values of correlation coefficients of the allometric formulas, each value has been randomly increased or decreased by up to 30% of the initial value.

The distribution of the initial slope of the $P - I$ curve have been performed in an identical way as in case of the other PFTs. Thus the values of all the parameters for each species has been randomly chosen, drawn from prescribed normal distributions based on the median value and the 25th or 75thquartile for the small or large species respectively.

The set of implemented trade-offs described above reflects empirical observations, and prevent the emergence of a single model organism that can dominate all habitats

(the "Darwinian Demon").

The marine ecosystem model represents a broad spectrum of phytoplankton species representing each phytoplankton functional group. In order to overcome some difficulties attributed to limited knowledge on physiological properties of species in each functional group, a stochastic approach was applied. More specifically, each phytoplankton functional group was distinguished by the range of the parameters ruling their physiologies, namely growth rate and resources requirements. The specific values of coefficients describing each species in the community were consequently provided by random selection within these broad ranges (Tab. 2.3). The community assembly, was formed by the 40 generated species (10 in each functional group).

Nonetheless, 40 species do not reflect the astonishing phytoplankton diversity observed in marine ecosystems. Thus, to correctly consider the limitations given by the finite selection of the species, an ensemble approach (Murphy et al. [2004]) was employed. Namely, 30 phytoplankton communities were generated and treated as an ensemble set. The ensemble approach further provides the opportunity to explore the impact of the community compositions on the obtained results and their robustness.

Phytoplankton community was filled with species, though the interactions of model species with the seasonally fluctuating environment, competition with other phytoplankton, and grazing determines the composition of the phytoplankton community in a sustainable ecosystem. Because of this initial species saturation, neither community structure nor diversity were imposed, but were an emergent properties (Follows et al. [2007], Dutkiewicz et al. [2009]).

Parameter	Units	Name	Diatoms	Dinoflagellates	Coccolitophores	Green algae
r [a] *	d^{-1}	growth rate	0.76 - 1.94	0.47 - 0.77	0.91 - 1.2	1.27 - 1.59
H_N [a] *	$mmolm^{-3}$	half-saturation for N uptake	0.93 - 1.58	2.5 - 6.3	0.15 - 0.21	1.94 - 4.88
H_{Si} [b]	$mmolm^{-3}$	half-saturation for Si uptake	1	0	0	0
α *	$d^{-1}(W/m2)^{-1}$	initial slope of P-I curve	0.019 - 0.1271 [d]	0.085 - 0.115[e]	0.028-0.038[e]	0.033-0.043
$R_{N:Si}$ [b]	-	elemental ratios	1	0	0	0
m [b]	d^{-1}	mortality rate	0.1	0.033	0.1	0.1

Table 2.3: Phytoplankton group-specific model parameters. Parameters marked with * have been distributed stochastically. References: [a] Litchman et al. [2006]; [b] Follows et al. [2007]; [c] this study; [d] Sarthou et al. [2005]; [e] Signorini et al. [2012a]. In [a] case the 25th and 75th quartiles of the parameter distributions from the data compilation.

2.2.3 Zooplankton community description

The model zooplankton community includes two generalist grazers distinguished by the size. Large zooplankton (in here copepods) preferentially graze on large phytoplankton (in here diatoms and dinoflagellates), but can graze also on small phytoplankton (in here coccolitophores and green algae) and viceversa for small zooplankton (microzooplankton). This grazing selectivity expressed with a species specific selectivity coefficient (S_{ik}) was characterised similarly to Follows et al. [2007] and Dakos et al. [2009]. Consequently, the size driven grazing selectivity, resolves grazers preferences more for functional groups rather than for particular phytoplankton species. The parameters describing zooplankton physiology are not determined stochastically as it was in case of phytoplankton species.

The mesozooplanktonic population biomass in the sub-polar Atlantic region, which is the basin of interest in this study, is dominated by a copepod species *Calanus finmarchicus*. Its development involves a progression from eggs through 6 naupliar stages (N1 to N6) and 5 copepodite stages (C1 to C5) before reaching adulthood (C6). The development is arrested during copepodite moult stages C4 and C5 in the late summer and autumn and the animals then descend out of the surface waters to deep open ocean layers, typically between 500 and 1500m where they diapause (Hirche [1996]).

Diapause plays a key role in the life cycle of high latitude zooplankton. During diapause, animals avoid starving in winter by living in deep waters where metabolism is lower and met by lipid reserves. Arousal from diapause and the moult transition to copepodite stage C6 does not take place until late winter-early spring of the following year. Stage C6 copepodites migrate to the surface to begin spawning (Hirche [1996]). Low temperature, avoidance of predators, and limited parasite infection have been suggested as factors conferring high survival probability on dormant animals overwintering at depth (Kaartvedt [1996]).

While the copepods demography is not resolved in the model presented in this thesis, a simplistic representation of the copepods winter dormancy has been employed. The mechanisms replicating winter dormancy strategy was considered to be tightly connected with environmental cues (i.e. triggered by the deepening of MLD). The considered mechanism envisions a decrease of copepods' grazing and mortality rates

during winter period, hence mimics the maturation of copepodites (i.e. transformation from C5 to C6) and the diapause phase. The formulation of the winter dormancy of copepods employed in here has been inspired by Fiksen [2000], though the mathematical formulation and parametrisation has been developed *ad hoc* for the purpose of this thesis. A fixed depth of the water column has been used as a cue triggering copepods entry to a dormant stage in the late autumn/ early winter and the awakening at the end of winter/early spring.

Alternative models found in the literature considered a low local food abundance as a cue triggering diapause entry and awakening taking place whenever development reaches the point of transition from juvenile (C5 stage) to adults (C6 stage) (Hind et al. [2000]). In their study Hind *et al.* envisaged a transition from C5 to C6 stage as a continuing process taking place also during diapause albeit at a reduced rate. In fact Hind *et al.* have demonstrated that a model of *Calanus* population dynamics incorporating this awakening mechanism can be accurately synchronized to the annual cycle of temperature and chlorophyll observed in the North Atlantic as long as the production of the first generation of the year was closely tied to the start of the phytoplankton bloom.

Yet another study of *Calanus* population dynamics exploring diapause considered a low local food abundance as a cue triggering diapause entry and a photoperiod cue for awakening (Speirs et al. [2005]). Their model produced the synchronous transfer of almost all the diapausers to the surface at a fixed year day and predicted a significant abundance of diapausing individuals at depth from midsummer onwards. These results showed a considerable agreement with the *in situ* observation of *Calanus* population in the north-east Atlantic (Speirs et al. [2005]).

A dormancy function employed in this study was described by an equation:

$$\omega(t) = \frac{1}{1+e^{-s(t-t_1)}}\left(1 - \frac{1}{1+e^{-s(t-t_2)}}\right), \tag{2.20}$$

where t is time in days, s is an arbitrary shape parameter, t_1 and t_2 are the days indicating end and beginning of dormancy period. The values of $\omega(t)$ ranged from 0 to 1 and were used as a scaling factor for copepods grazing and mortality rates. Therefore

for copepods

$$g_k = \omega \hat{g}_k,$$

$$m_{Zk} = \omega \hat{m_{Zk}},$$

$$m_{Z2k} = \omega \hat{m_{Z2k}},$$

and since the life cycles were not considered for microzooplankton the parameters were as follow

$$g_k = \hat{g}_k,$$

$$m_{Zk} = \hat{m_{Zk}},$$

$$m_{Z2k} = \hat{m_{Z2k}}.$$

(note that the above was reasoned solely by the uniformity of parameters notation for copepods and microzooplankton).

The results of a sensitivity study addressing impact of threshold depth on copepods population dynamics were presented in the next chapter section 3.2.

Parameter	Units	Name	Mesozooplankton	Microzooplankton
H_k	$mmolNm^{-3}$	half-saturation for intake	0.5^e	0.5^e
e	-	net production efficiency	0.75^c	0.75^c
ϵ	-	absorption efficiency	0.69^b	0.69^b
ϕ_P	-	grazing preference for P	0.67^a	0.67^a
ϕ_D	-	grazing preference for D	0.33^a	0.33^a
$\hat{g}$	d^{-1}	max ingestion rate for large P max ingestion rate for small P	1^e 0.17^e	0.17^e 1^e
$\hat{m_Z}$	d^{-1}	linear mortality rate	0.02^e	0.02^e
$\hat{m_{Z2}}$	$(mmolNm^{-3})^{-1}d^{-1}$	quadratic mortality rate	0.1^e	0.1^e

Table 2.4: References: [a] Fasham [1993], [b] Anderson [1994], [c] Anderson and Hessen [1995], [d] inspired by Follows et al. [2007], [e] this study.

2.2.4 Environment formulation and physical forcing description

The model requires the forcing functions, here the annual cycle of solar radiation I_0, mixed layer depth (MLD) and nutrients concentration in the seasonal nutricline, to be specified.

Mixed layer depth The parametrization of the MLD (Eq. 2.21, Fig. 2.1) captures the main features of its behaviour observed in most subpolar regions of the world ocean: fast deepening during the late autumn and winter, abrupt jump in the spring, prolonged stratification in the summer, and relatively slow shallowing during the end of the summer and beginning of autumn.

The annual cycle of the MLD was considered in an idealized form described with an analytical function:

$$h(t) = \begin{cases} \text{if } \Delta_T + T_0 \leq t < S_L + \Delta_T + T1: \\ Hmin, \\ \\ \text{if } S_L + \Delta_T + T1 \leq t < T + T1: \\ -\frac{1}{2}(Hmax - Hmin)(sin(\pi \frac{t - S_L}{T - \Delta_T - S_L} + \frac{\pi}{2}) - 1) + Hmin, \\ \\ \text{if } T1 \leq t < \Delta_T + T1: \\ -\frac{1}{2}(Hmax - Hmin)(sin(\pi \frac{t - T - \Delta_T}{-\Delta_T} + \frac{3\pi}{2}) - 1) + Hmin. \end{cases} \tag{2.21}$$

where $T = 365$ and the parameters being (see also Fig. 2.1):

1. $Hmin$ - minimum MLD thickness during the year,
2. $Hmax$ - maximum MLD thickness during the year,
3. $T1$ - time point indicating end of deep winter mixing period and beginning of spring restratification,
4. ΔT - duration of spring restratification ($\Delta T = T2 - T1$),
5. S_L - length of summer stratified period ($S_L = T3 - T2$).

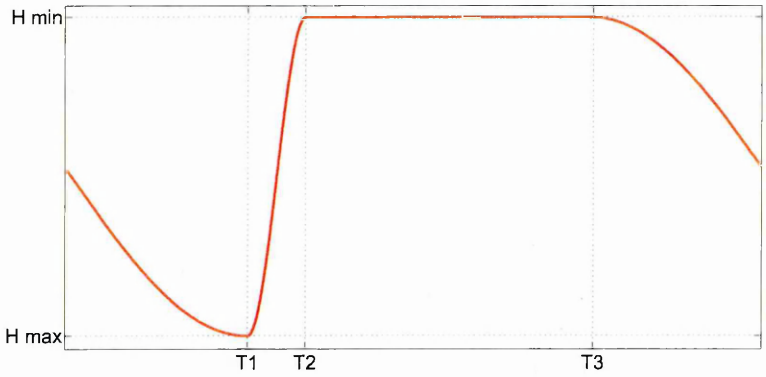

Figure 2.1: The annual cycle of mixed layer depth (MLD).

Alternatively, the seasonal mixed layer could be modeled with by a piecewise linear function (e.g. Evans and Parslow [1985], Litchman et al. [2006]), by a power sine function (e.g., Litchman et al. [2006]) or with a linear interpolation of the available data (e.g., Fasham et al. [1990]). However, the piecewise linear functions could cause numerical problems during the integration of highly non-linear systems as they are not C^1 class function (their derivative is not a continuous function or colloquially speaking because they have "sharp edges"). At the same time the power sine function does not capture well the observed dynamics of the seasonal changes in the MLD in the subpolar type environments - in particular fast deepening during the late autumn and winter, abrupt jump in the spring, prolonged stratification in the summer, and relatively slow shallowing during the end of the summer and beginning of autumn. Consequently, the linear interpolation of field data would be the most convenient alternative for our idealised MLD formulation. Yet, because of its simplicity, the analytical formulation present a broad spectrum of applications i.e. if a systems response to a climate change is to be investigated. Please note that a similar approach to seasonal MLD representation was used in Popova et al. [1997].

Nutricline gradient with depth At the end of summer as physical mixing increases, the mixed layer penetrates the deep layers, thereby providing a source of nutrients to the upper water column layers; nutrients become elevated throughout the upper water column and homogeneously distributed in the water column mixed layer. Conversely, the increase in thermal stratification deprives the upper water column of nutrients supply. The phytoplankton present in the water column consumes the avail-

able resources leading to a progressive deepening of the nutricline that consequently closely parallels the depth of the photic zone.

Because of the above, there is a gradient of nutrients with depth. Frequently, this gradient was represented with a simple linear relationships with depth, $N_0(z) = aMLD + b$, where a, b resulted from nutrient concentration vs depth linear regression (Litchman et al. [2006], Anderson et al. [2015]). In here an alternative approach has been implemented, namely autumn nutrients concentration data from World Ocean Atlas 2013 were extracted for the selected areas, linearly interpolated and used as model forcing (see details in Sec. 2.4.3 and 2.4.4). This representation captures the nutrients depletion in the photic zone during summer and emphasizes the role of the nutrients entrainment related to rapid deepening of MLD in autumn.

Surface solar irradiance The calculation of a daily photosynthesis require noon irradiance and daylength as inputs. In here a light submodel had been used to prescribe the light forcing. The equations for short-wave irradiance at the ocean surface on a clear day are those published by Shine [1984] (based on Brock [1981], Muhammad [1983]). The equation are as follow:

$$I_{clear} = \frac{I_{SC}\cos^2(z)/R_V^2}{1.2\cos(z) + e_0(1+\cos(z))/1000 + 0.0455}, \tag{2.22}$$

where: I_{SC} is the solar constant ($I_{SC} = 1368[Wm^{-2}]$: Thekaekara and Drummond [1971]), z is the solar zenith angle, e_0 is the water vapour pressure (the partial pressure of water vapour in the atmosphere; $e_0 = 12[mb]$: Josey et al. [2003]) and R_V is the Earth's radius vector (accounting for the eccentricity of the earth's orbit):

$$R_V = \frac{1}{\sqrt{1 + 0.033\cos(\frac{2\pi J}{365})}}, \tag{2.23}$$

where J is day of year (Julian day).

The equation describing solar zenith angle is given by:

$$\cos(z) = \sin(\phi)\sin(\delta) + \cos(\phi)\cos(\delta)\cos(\gamma), \tag{2.24}$$

where ϕ is latitude, δ is solar declination angle and γ time of day (where the Earth

moves 15° per hour and γ is the difference from the noon).

Solar declination angle is calculated with a formula:

$$\delta = 23.45 \sin(\frac{2\pi(284+J)}{365}. \tag{2.25}$$

Having calculated the solar irradiance at the ocean surface on a clear day it is relatively simple to compute the flux of photosynthetically active solar radiation just below the ocean surface at noon:

$$I_0 = C_{FAC} f_{PAR}(1-\phi) I_{clear}, \tag{2.26}$$

where f_{PAR} is the fraction of solar radiation of wavelength between 400 and 700 nm (PAR; typically $f_{PAR} = 0.43$, e.g. Fasham et al., 1990), ϕ is ocean albedo ($\phi = 0.04$, e.g. Fasham et al. [1990]) and C_{FAC} is the effect of clouds on atmospheric transmission. Reed [1977] proposed a simple empirical approach expressing C_{FAC} as a function of zenith angles (specified in degrees):

$$C_{FAC} = 1 - 0.0775W + 0.0019(90 - z), \tag{2.27}$$

where W is cloud fraction in oktas (in here $W = 6$ was used).

Processes attributed to the changes in mixed layer depth (MLD). The effects of changes in the ocean MLD and the corresponding entrainment process at the MLD lower boundary on the model compartments were considered by using the Evans and Parslow [1985] formulation (Eq. 2.28). With increasing mixed layer depth, h, nutrients are entrained from the underlying layer into the water column which increases their concentration. Phytoplankton and zooplankton densities become diluted as the mixed layer deepens (case (a)). Conversely, shoaling of the MLD causes loss (detrainment) of the non-motile compartments biomass (phytoplankton and small zooplankton) (case (b)) and concentrates motile compartments (copepods) (case (c)). The turbulent fluxes, q_i, at the lower boundary of the MLD are parameterized in terms of an entrainment velocity ($w_e = \frac{dH}{dt}$) in the ordinary way:

$$q_i = \begin{cases} (X_i - X_{pi})\frac{w_e}{h}, & \text{if } w_e \geq 0 \quad \text{case (a)}, \\ 0, & \text{if } w_e < 0 \text{ and and for nonmotile organisms} \quad \text{case (b)}, \\ X_i\frac{w_e}{h}, & \text{if } w_e < 0 \text{ and motile organisms} \quad \text{case (c)}, \end{cases} \tag{2.28}$$

where: h - depth of the MLD, $X_i = \{N, Si, P, Z, D_N, D_{Si}\}$ are the concentrations of the components in the resolved water column, and $X_{pi} = \{N_0, Si_0, P_0, Z_0, D_{N0}, D_{Si0}\}$ are the concentrations of the components in the seasonal nutricline which are assumed to be equal to zero for all components except for nutrients.

2.3 Simulations setup

A phytoplankton community was initialized with an identical, very low concentration ($= 10E-6[mmolN/m^3]$) in every simulated environment and the model was integrated for 10000 years, over which time a repeating annual cycle in ecosystem structure emerged. The integration was repeated 30 times, each time with a different random selection of 40 phytoplankton species. As a result an ensemble of 30 communities was created, and analysed statistically with focus on some relevant ecological metrics.

The model equations were solved in Matlab (MATLAB R2012a, The MathWorks Inc., Natick, MA, 2000) with an implicit ode15s scheme which guarantees high order of accuracy. The computation time step was dynamically determined inside the numerical routine, yet the outcome was presented with a 1 day resolution.

The source code and the scripts used for data analyses are freely available (at krzysztof.f.stec@gmail.com).

Ensemble approach Why testing 30 communities? To establish the number of communities needed to fully explore the model solutions variability, the relationship between the median number of "active" species and the number of tested communities was explored in here (Fig. 2.2). The species was considered as active if its biomass exceeded 0.1% of the total phytoplankton biomass at any given year day (e.g., Barton et al. [2010]). The annual species diversity was analysed for 50 sets of communities

$(X_i, i = 1, \ldots, 50)$ containing 1, 2, ... , or 50 phytoplankton communities, thus $\#X_i = i$. Notably $X_i \subset X_j$ if $i < j$.

The median diatoms species diversity demonstrated high variability if less than 13 communities were analysed, and tend to stabilize if higher number of communities were considered (Fig. 2.2a). Analog results were reported when diversity of species in all phytoplankton functional types (PFT) was analysed, though the amplitude of changes in case of diatoms was considerably lower and plateau in median diversity value was reached after inclusion of at least 20 communities (Fig. 2.2b). Thereby, in the following 30 communities were considered in each case to correctly assess impact of community composition on presented processes.

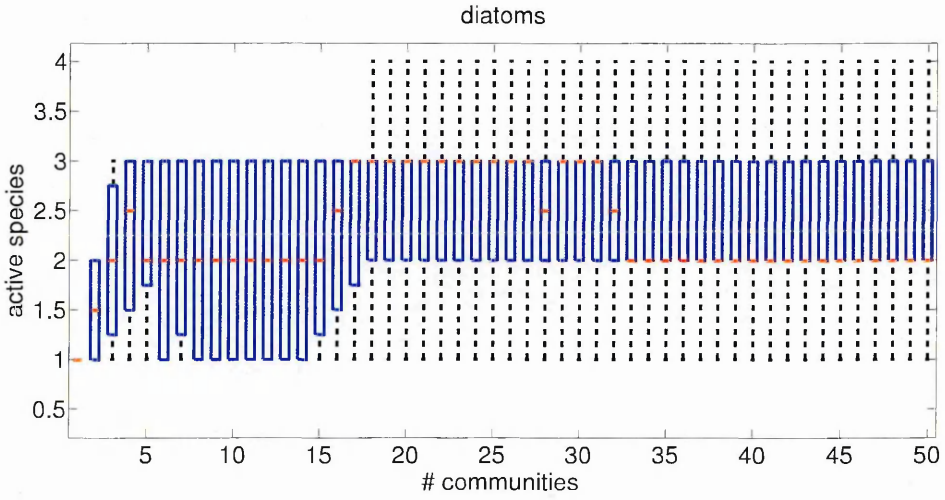

(a)

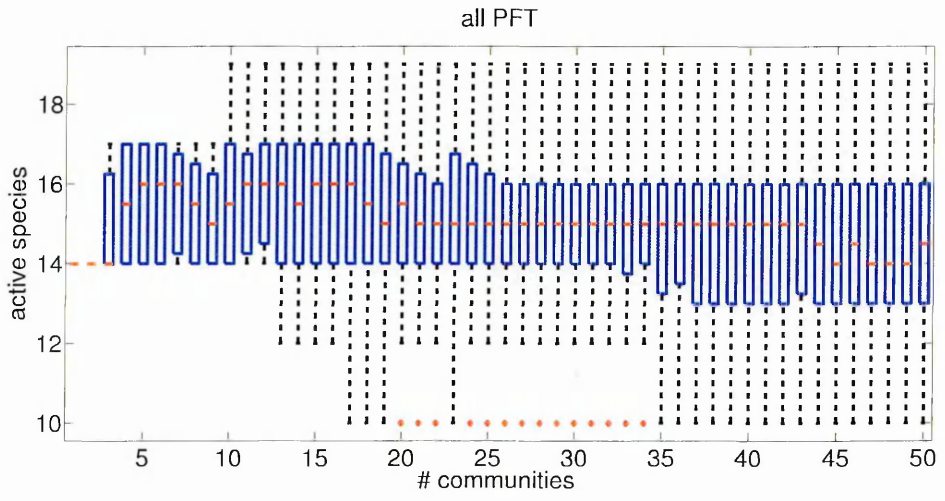

(b)

Figure 2.2: Relationship between number of considered communities (x-axis) and the distribution of the total number of active species in all the communities. These results were obtained with a model tuned for North Atlantic Bloom Experiments.

Clearly, these differences might be attributed to the community composition and to the stochasticity in the traits distribution (Sec. 2.2.2). Consequently, an ensemble approach is required to capture the main patterns in communities dynamics and multiple communities ought to be analysed for illustrative results.

2.4 Model validation

A numerical model should capture the essential bulk properties and feedbacks of the system it attempts to reproduce at the level of the data available to support it. This section was devoted to the comparison of the *in situ* data with their numerical model counterparts, i.e. to the assessment of the model skill. The goal of this verification procedure was to assess both qualitative and quantitative agreement with the data, with an emphasis on the presence or absence and relative abundance of functional groups, the pattern of seasonal succession, and the nutrient cycle.

The model results were described for two cases where the model set-up aims at replicating:

1. the dynamics of a subpolar environment in a specified location and a time window (Section 2.4.3),

2. the multi-annual average properties of a subpolar environment in a specified location (Section 2.4.4).

Both the available observational data and the model results are subject to particular uncertainties. The former arise from measurement error, inadequate sampling of a process or methodological issues, but also lack of replication. The latter originate from inaccuracies in model structure, description and parametrisation of the process, initialisation and forcing functions, etc. The process of model validation must take into account those uncertainties by balancing how well the model fits each data point (precision) and how well it reproduces the observed seasonal cycles (trends).

In here the model's precision is assessed by comparison of model results and *in situ* data in specific space and time - available for the NABE experiment performed in 1989 (Section 2.4.3). This allows to illustrate how well the model is able to reproduce the

short term, high frequency variability of the system, i.e. the phenology of the specific spring bloom, here observed in 1989 at 47°N 20°W during NABE experiment.

At the same time it is important to assess how well the model reproduces the ecosystem dynamics on a seasonal timescale. These analysis rely on the comparison of the model results with the seasonally averaged data illustrating the multiannual trends of e.g., surface chlorophyll-a and nutrients, and were performed in the Section 2.4.4. The requirement for instantaneous agreement may be relaxed here, but the model results have to match the considered data to the specified timescales. However, averaging data across multiple years to provide a climatological seasonal cycle suitable for model validation may eliminate some of their key characteristics. For instance, averaging the multiannual data of chlorophyll-a would smoothen the spring phytoplankton bloom as its magnitude and timing vary strongly between years and results in a disappearance of the characteristic spring peak. Consequently, the information provided by the validation against the average chlorophyll data would illustrate the model-data agreement of the seasonal trend but may not be illustrative for the specific observations such as spring bloom phenology observe in a particular year. For this reason the validation presented in the sections 2.4.3 and 2.4.4 should be considered as complimentary exercise generating a holistic illustration of the model's ability to reproduce the short- and long-term dynamics of the ecosystem.

In order to provide an evaluation framework for the model I rely on a combination of satellite data and field observations.

The *in situ* data originating from the North Atlantic Bloom Experiment (NABE) form an excellent base for a qualitatively estimate of model's ability to reproduce phytoplankton dynamics, in particular spring bloom formation, with the focus on processes such as nutrients consumption and phytoplankton accumulation (via chlorophyll-a concentration).

At the same time, the satellite-derived chlorophyll-a and particulate organic carbon (POC) data were used for comparison with the seasonal phytoplankton concentration generated by the model. Furthermore, satellite measurements of particulate inorganic carbon (PIC) may be used as a proxy of coccolitophores abundance (Signorini et al. [2012a]). Thus the information derived from combined PIC, POC and chlorophyll-a

concentration analysis would illustrate model ability to reproduce repetitive patterns in phytoplankton functional groups seasonal succession. These were latter compared with the Continuous Plankton Recorder (CPR) data illustrating the monthly abundance of the main phytoplankton functional groups (namely diatoms, dinoflagellates and recently coccolitophores) in the North Atlantic.

Finally, the analysis include also the degree of agreement between measured surface nutrients concentration and that generated by the model which is desired for correct representation of the biogeochemical cycle but also for the assessment of nutrients drawdown during the spring period.

2.4.1 Data sets description.

The chlorophyll-a, PIC and POC data were obtained from NASA Ocean Biology (OB). Sea-viewing Wide Field-of-view Sensor (SeaWiFS) Ocean Color Data, 2014.0 Reprocessing. NASA OB.DAAC, Greenbelt, MD, USA. doi: 10.5067/ORBVIEW-2/SEAWIFS_OC.2014.0. Accessed 2015/03/31. Maintained by NASA Ocean Biology Distibuted Active Archive Center (OB.DAAC), Goddard Space Flight Center, Greenbelt MD. The data were downloaded from their website: http://oceancolor.gsfc.nasa.gov. The multi-annual median time series of chl-a, PIC and POC were computed from data extracted for the area spanning from 45.5°N 21.5°W to 48.5°N 18.5°W. The set of extracted time series was spatially averaged and used to assess model skill in reproducing phytoplantkon concentration observed in the region of interest over multiple years (Sec. 2.4.4).

The annually averaged nutrients (N and Si) data were taken from World Ocean Atlas (WOA13) (Boyer et al. [2013]) available through the National Oceanographic Data Center (https://www.nodc.noaa.gov). The dataset, among many others, compiles roughly 50 years of ship-based profiles of nitrate and silicate into a climatology by averaging data on a 1° grid and into 33 depth levels, with a vertical bin size that varies from 5m near the surface to 25m below 100m depth. Similarly to the satellite data, a multi-annual median time series of surface nitrate and silicate were computed from data extracted for the area spanning from 45.5°N 21.5°W to 48.5°N 18.5°W, and compared with the model output.

Taxonomic data of diatoms, dinoflagellates and coccolitophores were obtained from the Continuous Plankton Recorder (CPR) from Sir Alister Hardy Foundation for Ocean Science (http://www.sahfos.ac.uk). The multi-annual monthly averaged cell concentration was extracted for the standard area E5 and E6 spaning between 45-50°N : 9-19°W, and 45-50°N : 19-31°W respectively. The size of these standard areas is relatively large, hence some spatial smoothing is to be expected.

The North Atlantic Bloom Experiment (NABE, 47°N 20°W) data were used for a comparison with the model results. These data were taken from the University Corporation for Atmospheric Research (UCAR; http:/rda.ucar.edu). The employed dataset contained *in situ* measurements of chlorophyll-a, nutrients (N and Si) concentration, and POC data obtained during the NABE cruises: Atlantis II leg 4 (1989 Apr 20 - May 10), Atlantis II leg 5 (1989 May 15 - Jun 08) and Endeavor (1989 Jun 29 - July 6).

2.4.2 Model skill assessment approach

A quantitative approach based on assessment indices and skill scores was provided to evaluate model performance. Namely, each simulation result was validated against the available observations. Normalized standard deviation $\sigma^* = \frac{\sigma_{X_M}}{\sigma_{X_D}}$, correlation coefficient (R) and root-mean-square difference of appropriate model variables (X_M) and field observation (X_D)was computed for each model simulation. The results were displayed with a Taylor diagram (Taylor [2000], see also: Jolliff et al. [2009],Signorini et al. [2012b]). The Taylor diagram is a polar coordinate diagram that assigns an angular position to the inverse cosine of R ($\cos^{-1}(R)$). Thus, a correlation of zero is 90° away from a correlation of 1. The distance from the origin ([0, 0]) is assigned to the normalized standard deviation. The reference field point (in here NABE data) is indicated for the polar coordinate ([1, 0]). The model to reference comparison points may then be gauged by how close they fall to the reference point and this distance is proportional to the normalized unbiased root-mean-square difference ($RMSD = \frac{1}{N(X_{Dmax}-X_{Dmin})}\sqrt{\sum_{i=1}^{N}(X_{Mi} - X_{Di})^2}$, where X_{Dmax}, X_{Dmin} refer to maximal and minimal value of X_D). The values of $RMSD$ span from 0 to 1, and lower values indicate lower distance between the analysed time series.

Additionally, a visual inspection of the patterns exhibited by the key model variables was performed to establish their qualitative agreement with the available observations.

2.4.3 Validation Part 1: Model validation against NABE data

2.4.3.1 NABE site simulation setup

Mixed Layer Depth. The model was forced by seasonal changes in the mixed layer depth suitably adopted to the location and period of the North Atlantic Bloom Experiment (47°N 20°W; 1989). The seasonal mixed layer was modeled with a function described in section 2.2.4 with all the parameters adjusted to reproduce the observed conditions. The *in situ* measurements obtained in the course of NABE illustrate the MLD dynamics for a period between 110 and 157 year day of 1989 (Fig. 4.4). These data are however too scarce to provide the MLD characteristics over the whole year. Hence, the remaining period description was based on average MLD measurements obtained with ARGO floats. The ARGO dataset (www.ifremer.fr/cerweb/deboyer/mld/Data.php) contains individual profiles of MLD gathered by an autonomous glider in various parts of the ocean for a period of 1998-2011. The MLD ARGO measurements used in here were based on a density difference criterion of $\Delta\rho = 0.03$ $[kg/m^3]$ from density at 10 m depth (as in de Boyer Montegut et al. [2004]). The data were extracted from the ARGO dataset for a region surrounding the NABE site, namely a squared area spanning between (45.5°N, 21.5°W) and (48.5°N, 18.5°W), and averaged over a period of 10 days forming a multi-annual average base for the MLD used in the model forcing.

As described above, the MLD reconstruction at the NABE site was fractionated into a multi-annual average signal based on ARGO data (form of a "general" solution) and a specific signal for 1989 based on *in situ* NABE measurements (form of a "particular" solution). Those two merged signals were used for fitting an analytical function (eq. 2.21) which was subsequently employed as model forcing.

The parameters used in the function formulation were provided in Tab 2.5.

Surface solar irradiance. The noon (peak daily) irradiance at the ocean surface for a 47°N latitude was calculated as described in section 2.2.4 and was depicted in

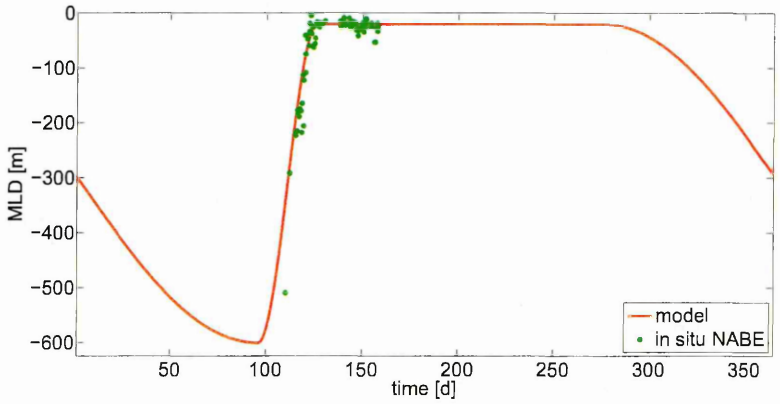

Figure 2.3: MLD recorded during the NABE 1989 (circles) and MLD used in the model for the reference simulations.

Parameter	Unit	Value
$Hmin$	m	20
$Hmax$	m	600
S_L	d	150
δT	d	30
T_{res}	yd (year day)	95

Table 2.5: Mixed layer depth characteristics used for simulations replicating North Atlantic Bloom Experiment where: $Hmax/Hmin$ - max/min value of the MLD, S_L - duration of the stratified summer period, δT - duration of the spring restratification, T_{res} - initiation of the spring restratification.

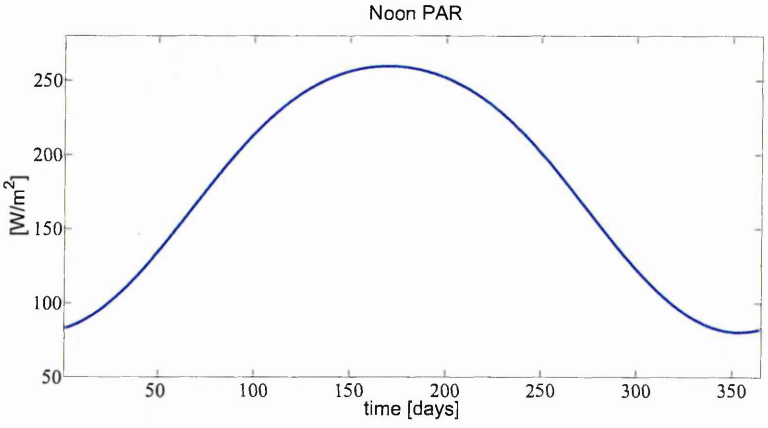

Figure 2.4: Daily noon solar irradiance at the sea surface.

Fig. 2.4.

Nutrients profiles. The nutrients gradient at the NABE site was based on the World Ocean Data 2013 (WOA13) and represented as a function of nutrients vs. depth. Both nitrate (Fig. 2.5a) and silicate (Fig. 2.5b) show strong seasonality at NABE site with considerably low concentrations during summer, increasing concentrations associated to deepening of the MLD in autumn, and maximal concentrations during winter. Following the arguments provided in section 2.2.4 linearly interpolated data from the end of summer period had been used for forcing the model simulation.

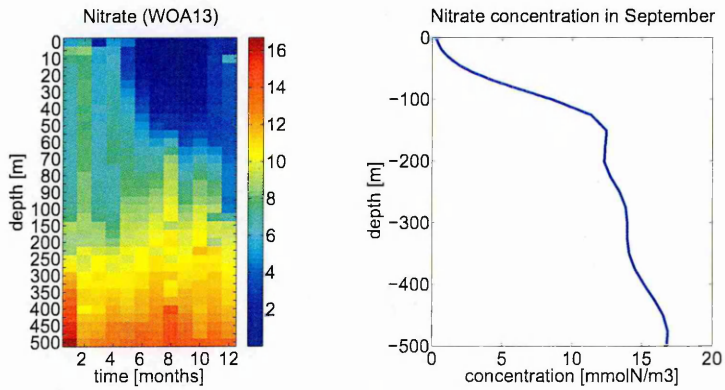

(a)

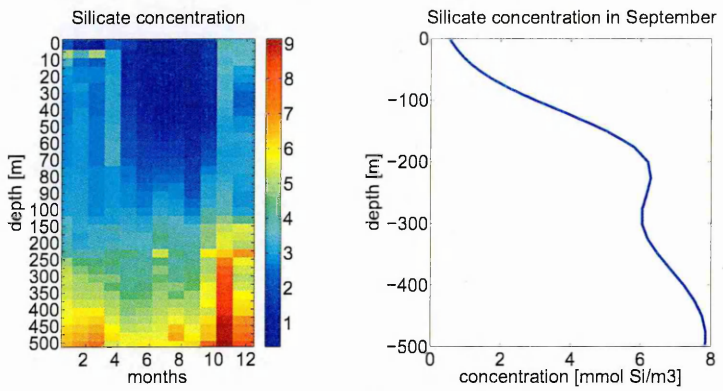

(b)

Figure 2.5: Monthly nutrients profiles with depth at the NABE site (at the 47N 20W): (a) NO_3 and (b) SiO_2. The average monthly values were depicted on left panels, while the nutrients source used in the model simulations on the right panels.

2.4.3.2 Comparison of the model results with the NABE *in situ* measurements

Despite the limitations typical of these modelling approaches (especially a low species diversity at a later time in the simulations and a too limited set of species contributing to the seasonal succession), the model successfully reproduced the wax and wane of the main functional groups over the year.

In fact a typical mid-latitude seasonal succession pattern consists of low phytoplankton abundance in winter, a spring bloom of diatoms with a subsequent bloom of non-diatom phytoplankton, often other flagellates, followed by coccolithophorids observed during stratified conditions (Painter et al. [2014], Gregg et al. [2003], Lochte et al. [1993], Broerse et al. [2000]).

The model reproduced this seasonal succession pattern with diatom bloom in spring followed by dinoflagellates,and coccolithophore dominating later in the summer together with green algae (Fig. 3.17a, 2.7).

The growth rate of all phytoplankton functional groups was considerable low during winter period. This was caused by the low surface irradiance and deep mixing reaching down to 600m, as the nutrients were well beyond species half-saturation values. Hence, all the phytoplankton species were light-limited. The increases of phytoplankton biomass in spring coincided with the water column restratification. During the stratified period, phytoplankton growth rate became quickly limited by nutrients, and the spring diatom bloom was terminated due to depletion of nutrients, and increasing grazing pressure.

Phytoplankton concentration was converted to carbon assuming a fixed Redfield C:N ratio of 6.625, and later to chlorophyll to compare the phytoplankton biomass with observations. The chlorophyll to carbon ($Chl : C$) ratios are known to vary widely in response to ambient conditions (Geider et al. [1997], Sathyendranath et al. [2009]). The analysis of the model chlorophyll computed with a mean, lower and upper range of carbon-to-chlorophyll ratios (Sathyendranath et al. [2009]; Tab 2.6) indicate that the magnitude of the bloom was in an agreement with the JGOFS data for NABE (Fig. 2.8). The model however tends to underestimate the winter and summer phytoplankton concentration which may be associated with the simplified model construction.

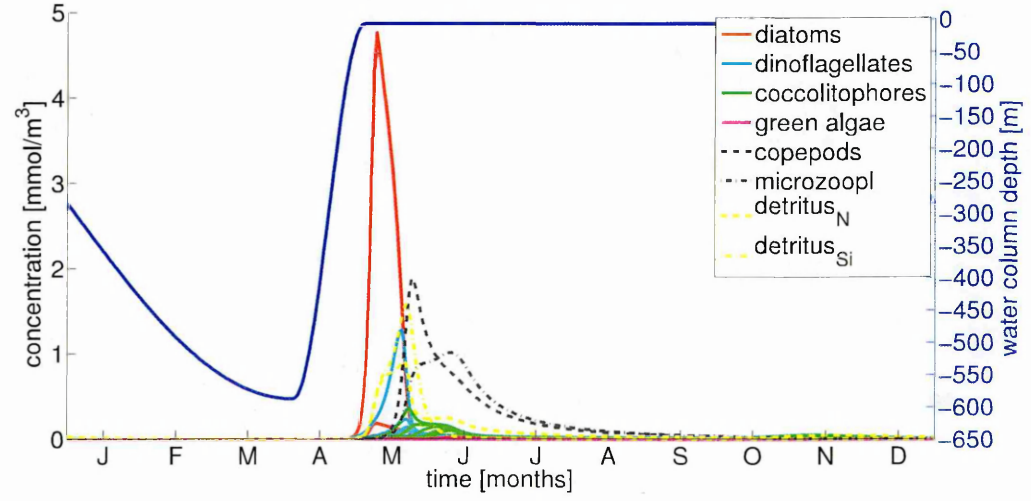

(a)

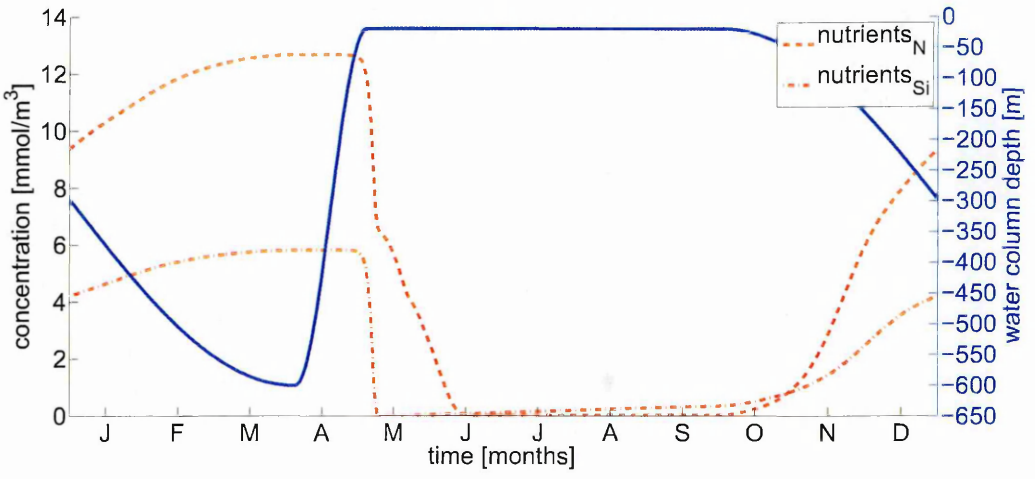

(b)

Figure 2.6: Annual cycle at NABE of modeled (a) phytoplankton species, zooplankton, and detritus concentration, and (a) nutreints concentration. Model compartments concentration plots was superimposed with a MLD on each panel.

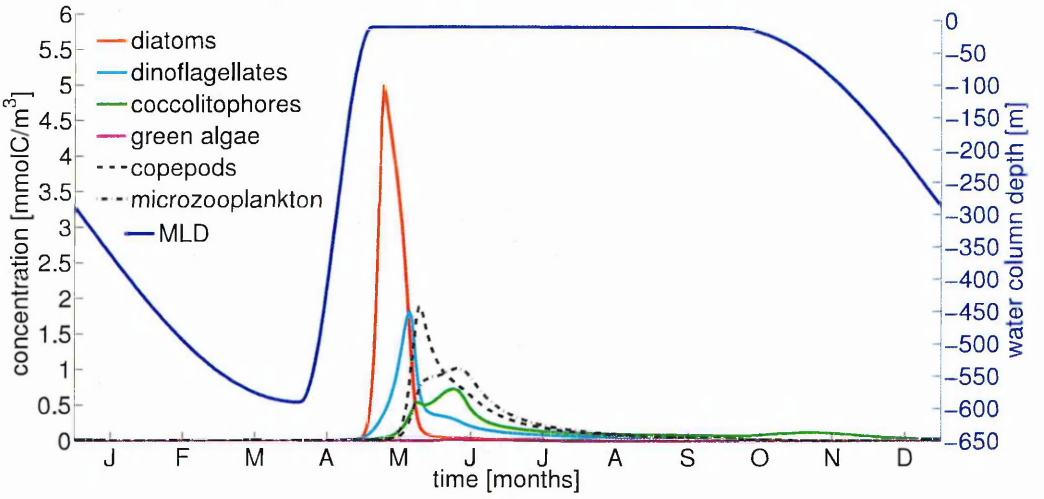

Figure 2.7: Annual cycle at NABE of modeled total phytoplankton functional groups and zooplankton. Phytoplankton PFT lines depict sum of all species' concentration belonging into one PFT.

The rate of light attenuation has been assumed to be constant with depth, yet in reality it varies with depth as a result of the changing spectral properties of the irradiance field - red light is mostly absorbed by water in the upper few meters while blue penetrates deepest. The light extinction in the upper layers of the water column is higher with respect to the lower layers. Accounting for these differences would result in a lower rate of light attenuation and in a greater penetration of light into the water column (Anderson et al. [2015]). Further more processes such as phyto-convection (Backhaus et al. [1999]) or variable rate of turbulent mixing (Huisman et al. [1999b]) which could enhance phytoplankton growth during winter have not been incorporated into the model. Finally, phytoplankton may adjust their C:Chl-a ratio in winter to mitigate the effect of the low light intensities that they experience. Change in the C:Chl-a ratio would result in higher light absorption and elevated growth rate despite deep mixing.

The water column depth during summer was restricted to the mixed layer depth which may be significantly shallower than the photic zone. As a result the growth of phytoplankton was restricted to the surface layer of the photic zone which could underestimate primary production and consequently phytoplankton concentration during summer.

Similarly to phytoplankton, zooplankton abundance was highly seasonal, with low

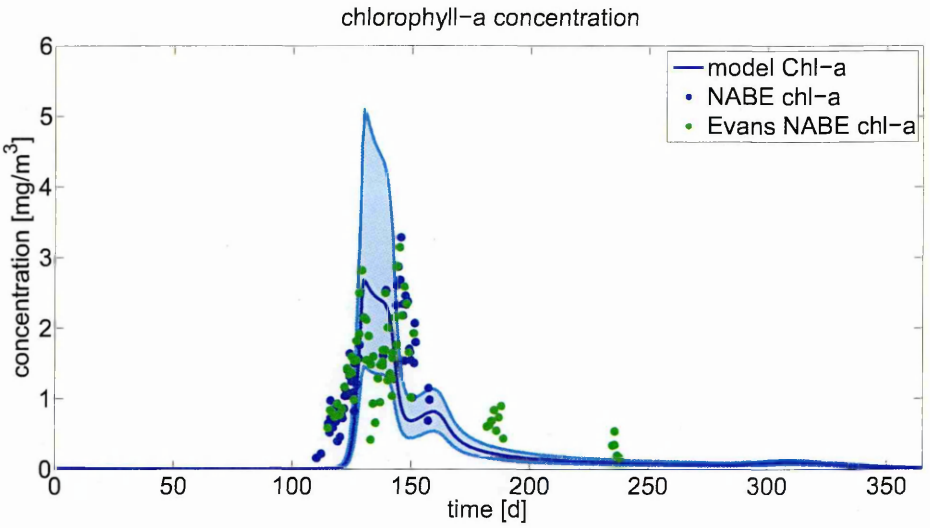

Figure 2.8: Annual cycle at NABE of modeled (lines) and observed (circles) dynamics of chlorophyll-a concentration. The blue line depicts total chlorophyll concentration computed for mean C:chl-a ratio value (Tab. 2.6). The blue-shaded area represents chlorophyll-a concentrations computed for the min and max C:chl-a ratio values.

densities during the winter and higher concentrations associated with phytoplankton blooms (Fig. 3.17a, 2.7). The peak of copepods lagged ten days behind that of diatoms, illustrating the decoupling of phytoplankton and zooplankton during the spring bloom period. Microzooplankton reached its annual concentration minimum at the end of deep mixing period and closely followed the biomass increase of phytoplankton species during and shortly after spring water column restratification. Microzooplankton peak lagged 7days behind that of coccolitophores and coincided with that of green algae. The small phytoplankton biomass (with a peak in early June) was kept under microzooplankton control.

The nutrient availability was also highly seasonal, with saturating conditions during deep mixing period and becoming depleted in the summer (Fig. 2.9).

The results presented on Fig. 3.17a were randomly selected from the explored ensemble of 30 phytoplankton communities (Section 2.2.2). The described phytoplankton functional groups seasonal succession and biomass patterns were conserved across all ensemble members. Nevertheless, variability in indices characterising simulations across all the ensemble members, ought to be expected due to differences in communities composition. Such variability was observed when species diversity was analysed. It was thus explored by considering the probability density function (pdf) of each model outcome. In fact, the analyses of the species diversity show considerable difference

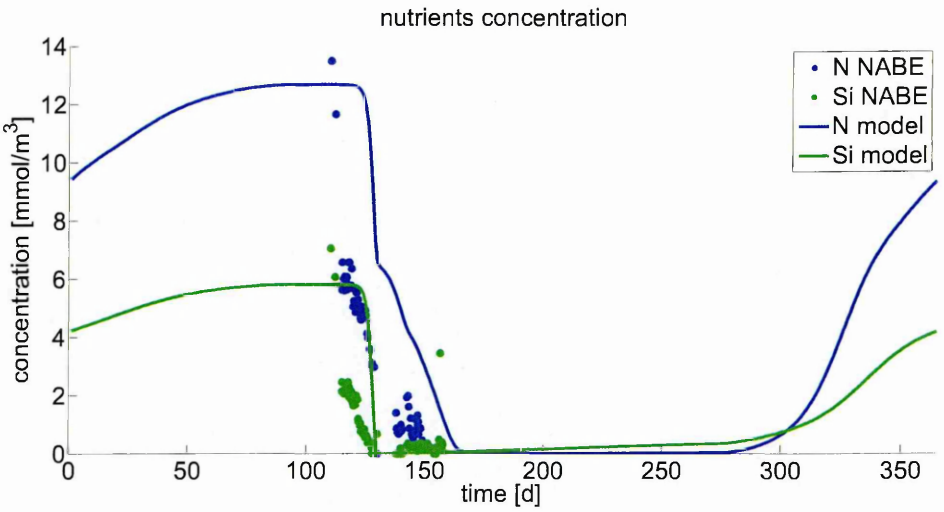

Figure 2.9: Annual cycle at NABE of modeled (lines) and observed (circles) dynamics of nitrate and silicate concentration.

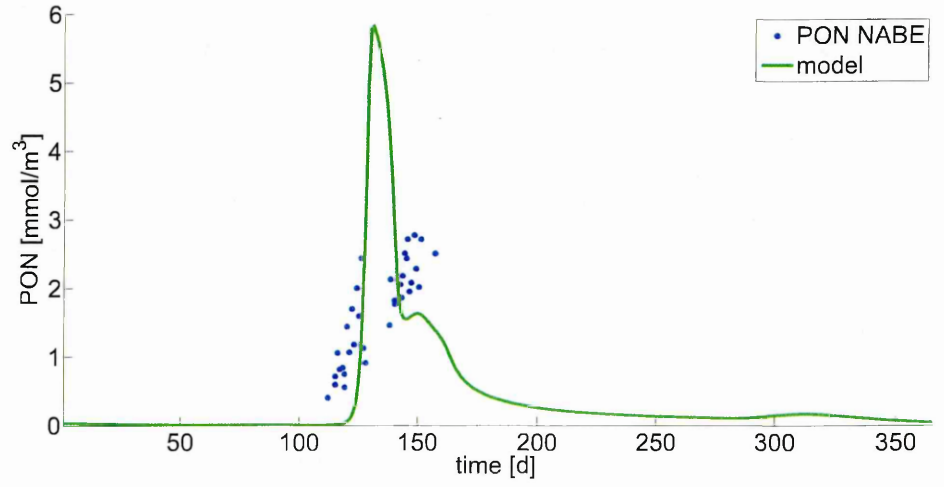

Figure 2.10: Annual cycle at NABE of modeled (lines) and observed (circles) dynamics of particulate organic nitrate (PON).

Functional group	C:Chl-a mean value	C:Chl-a observed range
Diatoms	39	21-75
Dinoflagellates	45	27-80
Green algae	99	80-126
Prymnesiophytes	65	44-82

Table 2.6: Mean and range of the carbon-to-chlorophyll ratios of different phytoplankton types Sathyendranath et al. [2009].

across all the ensemble members.

Ensemble community results Inspection of Fig. 2.12 revealed that model chlorophyll versus reference data correlation (R) ranged from 0.3 to 0.8, normalised standard deviation (σ^*) was close to 1 for the great majority of the ensemble members, and median $RMSD$ was lower than 0.35 for all the communities (Tab. 2.7). The time series analysis (Fig. 2.11) show that the seasonal patterns of phytoplankton abundance were consistent across all the tested communities despite considerable spread of correlation values. The North Atlantic Bloom Experiment was designed to capture the spring bloom dynamics. The model validation against NABE data has a strong bias towards the spring bloom period. Consequently the spread of indicator values used for model skill assessment (R, σ^* and $RMSD$) was mainly related to spring bloom phenology - its initiation, termination and intensity.

Despite having significant correlation values ($R > 0.8$) and rather low $RMSD$ values (< 0.5), the model nitrate has considerably lower normalised standard deviation with respect to the reference data (Fig. 2.13; Tab. 2.7). Time series of the observed and model nutrients (Fig. 2.9) revealed that the model reproduces well the winter nutrients concentration, yet it underestimates nitrate draw-down during the spring

Table 2.7: Comparison of the ensemble community set with the NABE in situ data. Correlation (R), normalised standard deviation (σ^*) and root-mean-square difference ($RMSD$) were computed for chlorophyll-a, NO_3 and SiO_2, and PON for all 30 communities. Presented values were: median and median absolute deviation (mad).

	Chlorophyll-a	NO_3	SiO_2	PON
R	0.49 ± 0.09	0.87 ± 0.01	0.72 ± 0.05	0.34 ± 0.07
σ^*	0.92 ± 0.09	0.38 ± 0.04	1.01 ± 0.10	0.97 ± 0.06
$RMSD$	0.29 ± 0.03	0.42 ± 0.04	0.37 ± 0.05	0.25 ± 0.03

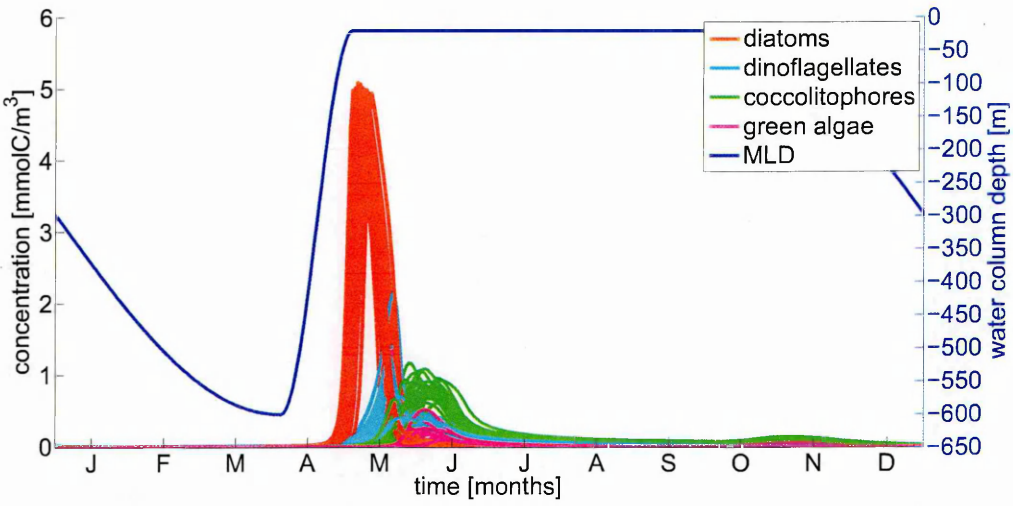

Figure 2.11: Phytoplankton functional groups concentration in all ensemble community members. Each line depicts total functional group concentration in a single community. In total 30 communities had been analysed.

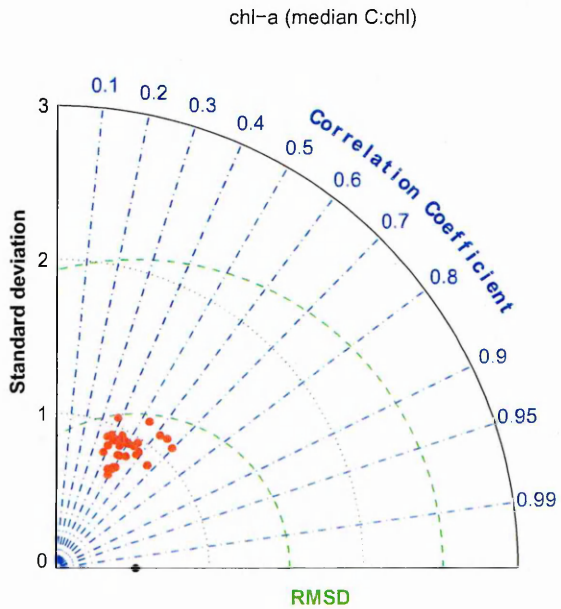

Figure 2.12: Taylor diagram depicting the ensemble set of 30 simulations results, here chlorophyll-a computed for the average C:chl-a ratio values (Tab. 2.6), compared with the NABE *in situ* data. The black dot indicates the origin of the coordinates system for the RMSD.

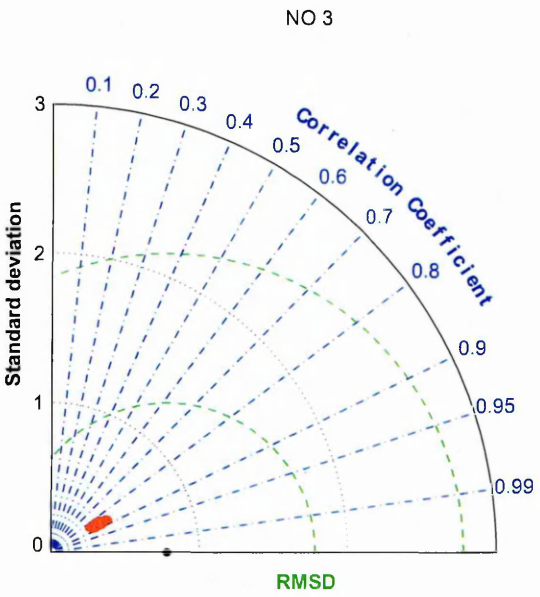

Figure 2.13: Taylor diagram depicting the ensemble set of 30 simulations results, here NO_3 concentration, compared with the NABE in situ data. The black dot indicates the origin of the coordinates system for the RMSD.

bloom. The NO_3 model concentration observed shortly after spring bloom was higher with respect to observations and consequently their standard deviation was lower. The model silicate concentration was in a good agreement with NABE measurements with R values exceeding > 0.7, σ^* close to 1 and $RMSD$ values lower than 0.4 for the vast majority of the explored communities (Fig. 2.14; Tab. 2.7).

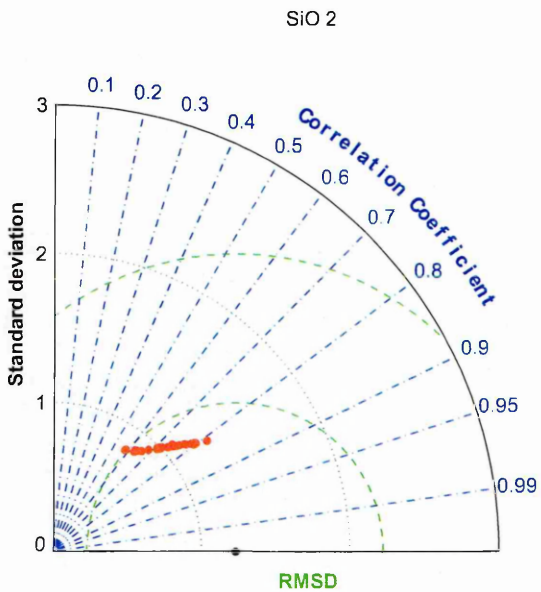

Figure 2.14: Taylor diagram depicting the ensemble set of 30 simulations results, here SiO_2 concentration, compared with the NABE in situ data. The black dot indicates the origin of the coordinates system for the RMSD.

	Median biomass	Total yearly biomass	Maximal biomass	Biomass peak time
	$[mmolN/m^2]$	$[mmolN/m^2/y]$	$[mmolN/m^2]$	$[yd]$
Phytoplankton	4.13±0.86	3276.92±433.43	102.18±12.79	128.00±15.84
Diatoms	0.44±0.33	1151.75±239.17	99.16±12.43	128.00±15.84
Dinoflagellates	1.13±0.34	569.63±169.36	9.25±3.95	140.00±17.73
Coccolitophores	1.88±0.36	1307.30±277.18	19.73±5.99	152.00±18.82
Green algae	0.01±0.20	43.92±170.82	1.74±4.33	159.00±19.87
Copepods	0.23±0.03	1064.13±132.72	29.71±4.32	140.00±17.38
Microzooplankton	0.27±0.04	846.41±110.63	24.12±3.35	159.00±19.67

Table 2.8: Phytoplankton and zooplankton maximal biomass and total yearly biomass in the ecosystem configured to mimic NABE site. The presented values are the median and median absolute deviation of the indicated variables.

2.4.4 Validation Part 2: Model validation against average NABE area data

2.4.4.1 Simulation setup

Mixed Layer Depth. The seasonal forcing used in this section was identical with that in section 2.4.3 but for the MLD. The MLD climatology was based solely on average MLD measurements obtained with ARGO floats (Fig. 2.15). The parameters used in the function formulation were provided in Tab 2.9.

2.4.4.2 Comparison of the model results with observations

The general patterns of seasonal phytoplankton and zooplankton abundance, functional groups succession, and nutrients availability (Fig. 2.17, 2.16) were similar to those observed in section 2.4.3. Some differences (e.g., lower nutrients entrainment rate and lower nutrients concentrations in winter, lower spring bloom intensity) arising from the change in MLD used as a seasonal forcing were observed. Nevertheless, the simulation results were in good agreement with the chlorophyll-a and surface nutrients data obtained from SeaWiFS and World Ocean Atlas (Sec. 2.4.1).

The analysis in this section were intended to evaluate model skill when average systems properties were taken into consideration. In order to do that multi-annual monthly means of satellite derived chlorophyll-a, POC and PIC, and surface nutrients data were compared with the monthly means of their model counterparts.

Inspection of Fig. 2.18 reveals that the great majority of the model data and the SeaWiFS chlorophyll data fall within significant R values (> 0.8) and σ^* close to 1 . The model successfully captures the general trend in the phytoplankton abundance eventhough it tends to underestimate winter chlorophyll values and overestimate spring bloom intensity (Fig. 2.19). Because of that, it may be reasonable to assume that the grazing pressure may also be underestimated. Despite these discrepancies the $RMSD$ values remain close to 0.25 (Tab. 2.10). Notably, it was demonstrated in the previous section (Sec. 2.4.3) that the model reproduces well the spring bloom magnitude.

The model ability to reproduce patterns of phytoplankton concentration throughout the year was further illustrated by the good agreement of POC and PIC (Fig. 2.23,

Parameter	Unit	Value
$Hmin$	m	20
$Hmax$	m	300
S_L	d	160
δT	d	55
T_{res}	yd (year day)	60

Table 2.9: Mixed layer depth characteristics used for simulations replicating North Atlantic Bloom Experiment where: $Hmax/Hmin$ - max/min value of the MLD, S_L - duration of the stratified summer period, δT - duration of the spring restratification, T_{res} - initiation of the spring restratification.

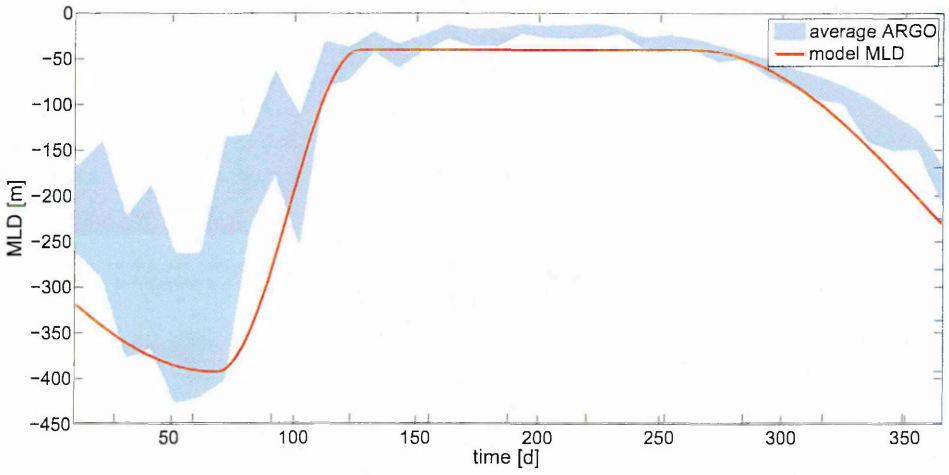

Figure 2.15: Average MLD based on the ARGO floats (blue line) and the fit (red line) used in the model simulations. The shaded area depicts the ARGO data std.

	R	σ^*	$RMSD$
chl-a	0.91 ± 0.03	1.12 ± 0.08	0.25 ± 0.015
NO_3	0.97 ± 0.0007	0.96 ± 0.01	0.19 ± 0.003
$SiO2$	0.77 ± 0.0009	1.05 ± 0.01	0.27 ± 0.0019
POC	0.90 ± 0.02	1.02 ± 0.12	0.68 ± 0.00001
PIC	0.62 ± 0.005	2.50 ± 0.16	0.44 ± 0.007

Table 2.10: Comparison of the ensemble community set with the average NABE area data. Correlation (R), normalised standard deviation (σ^*) and root-mean-square difference ($RMSD$) were computed for satellite derived chlorophyll-a, POC and PIC (SeaWiFS)and surface NO_3 and SiO_2 (WOA13) for all 30 communities. Presented values were: median and median absolute deviation (mad).

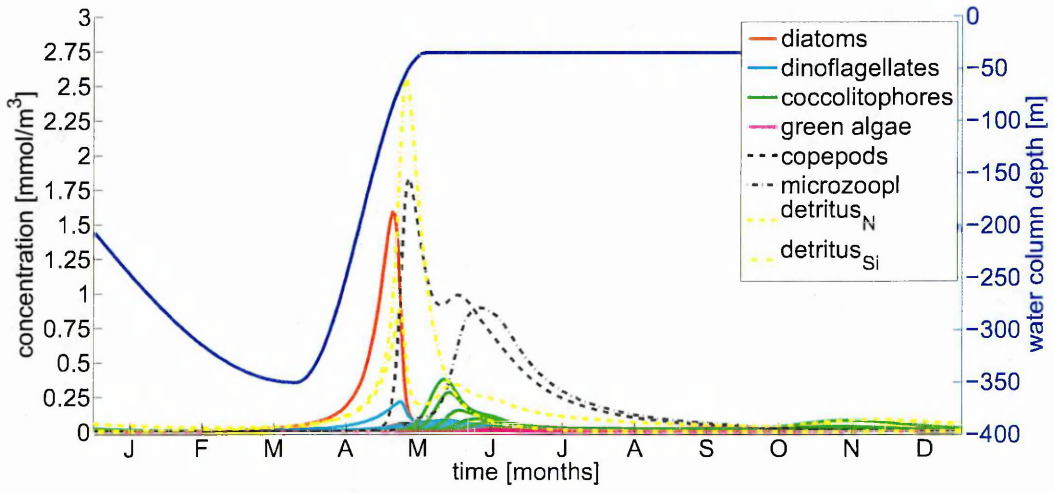

(a)

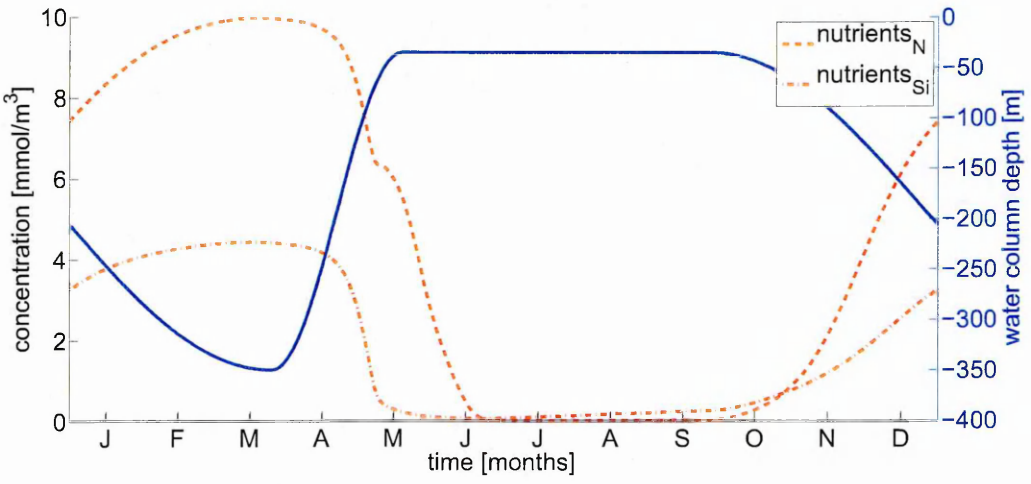

(b)

Figure 2.16: Annual cycle in an area surrounding NABE site of modeled (a) phytoplankton species, zooplankton, and detritus concentration, and (a) nutreints concentration. Model compartments concentration plots was superimposed with a MLD on each panel.

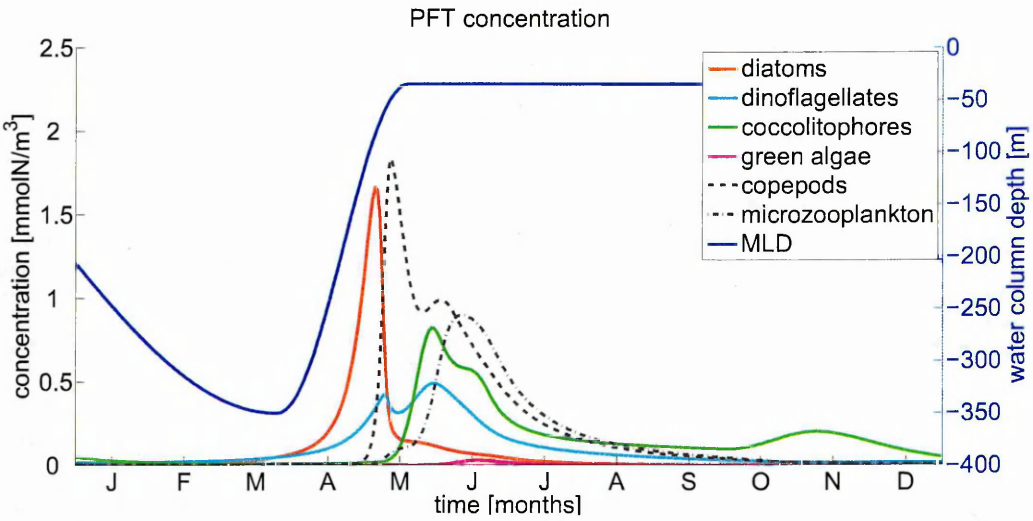

Figure 2.17: Annual cycle of modeled total phytoplankton functional groups and zooplankton in an area surrounding NABE site. Phytoplankton PFT lines depict sum of all species' concentration belonging into one PFT.

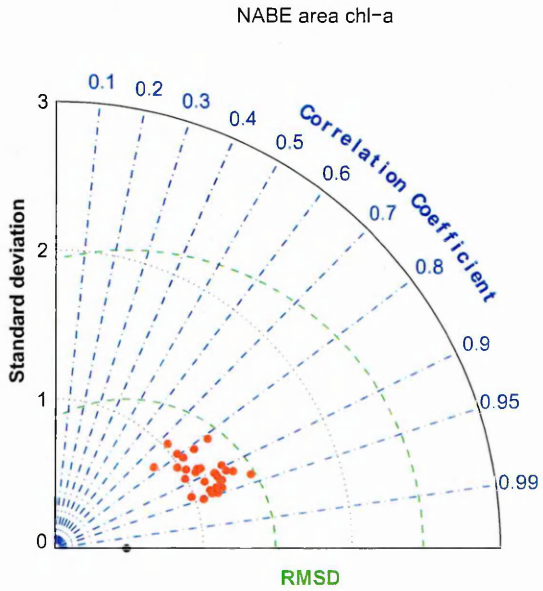

Figure 2.18: Monthly mean chlorophyll-a concentrations values from the model validated against the monthly mean surface chlorophyll-a concentration (SeaWiFS). The black dot indicates the origin of the coordinates system for the RMSD.

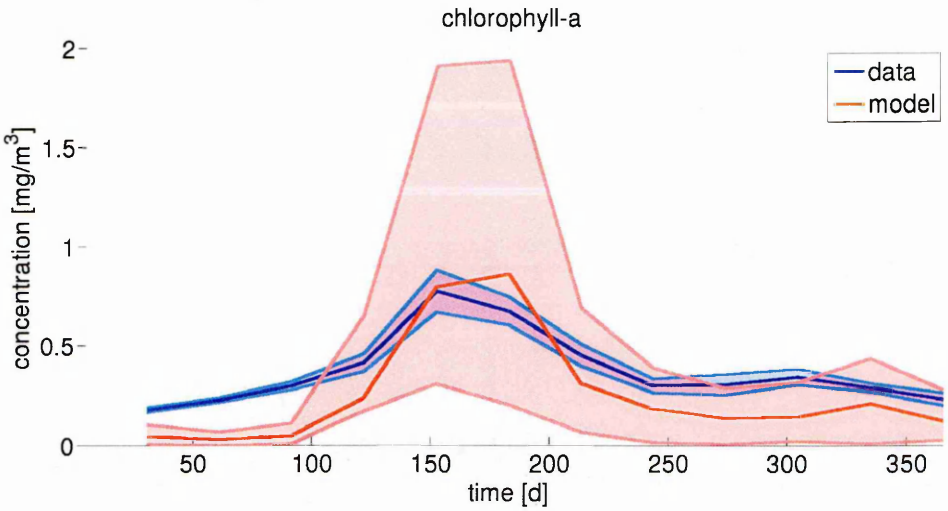

Figure 2.19: Annual cycle of the modelled chlorophyll (monthly mean) and the monthly mean surface chlorophyll-a concentrations (SeaWiFS) in an area surrounding NABE site. The shaded area depicts the standard deviation of the monthly mean chlorophyll concentrations generated by the model.

2.22; Tab. 2.10). Vast majority of the POC results fall within significant R values (> 0.8) with σ^* close to 1 and somewhat higher $RMSD$ (with median exceeding 0.65; Tab. 2.10)

The analysis of PIC show considerable correlation with the median value for all ensemble members equal to 0.62, yet $\sigma^* > 2.5$ indicate higher standard deviation in the model than in observed PIC concentrations, but the median $RMSD$ value lower than 0.44 suggest low distance between the analysed time series.

In fact, model tends to underestimate PIC and POC concentration for the most of the year in a similar matter to chlorophyll concentration.

The model versus reference nutrients comparisons fall within significant correlation values with median $R > 0.7$ for silicate and $R > 0.95$ for nitrate (Fig. 2.24 and 2.25). In both cases the normalised standard deviation was slightly higher than 1 and $RMSD$ was lower than 0.3.

The visual inspection of the surface nutrients concentration time series (Fig. 2.26) revealed that saturating conditions during deep mixing period and their depletion in the summer were well captured by the model. Some differences arose during autumn when nutrients entrainment occurred at a slower rate in the model with respect to field observations. At the same time model silicate comparison with WOA13 data show faster drawdown of the former. Despite those differences the model captures the main

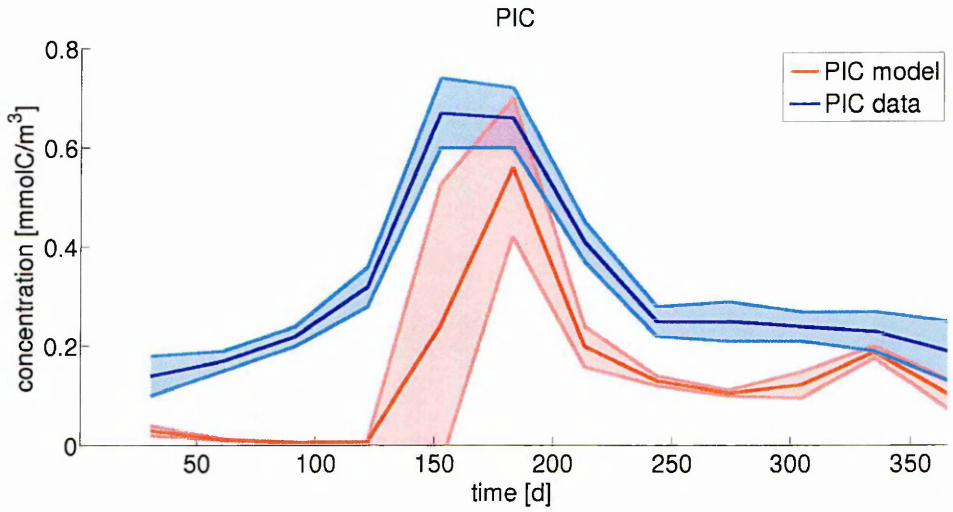

Figure 2.20: Annual cycle of the modelled PIC (monthly mean) and the monthly mean surface PIC concentrations (SeaWiFS) in an area surrounding NABE site. The shaded area depicts the standard deviation of the monthly mean PIC concentrations generated by the model.

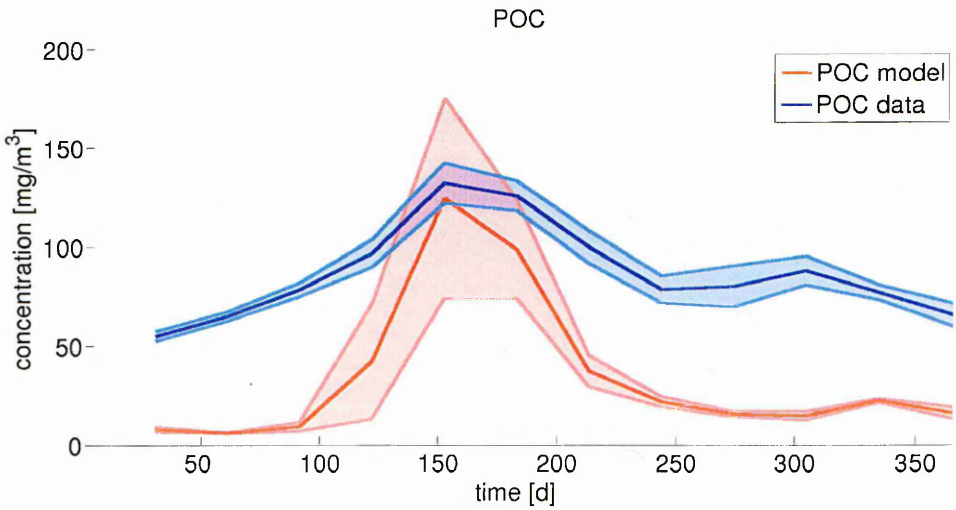

Figure 2.21: Annual cycle of the modelled POC (monthly mean) and the monthly mean surface POC concentrations (SeaWiFS) in an area surrounding NABE site. The shaded area depicts the standard deviation of the monthly mean POC concentrations generated by the model.

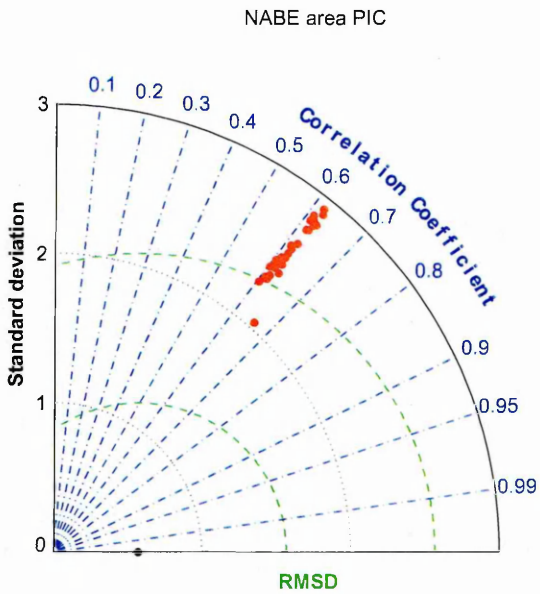

Figure 2.22: Monthly mean PIC concentrations values from the model validated against the monthly mean surface PIC concentration (SeaWiFS). The black dot indicates the origin of the coordinates system for the RMSD.

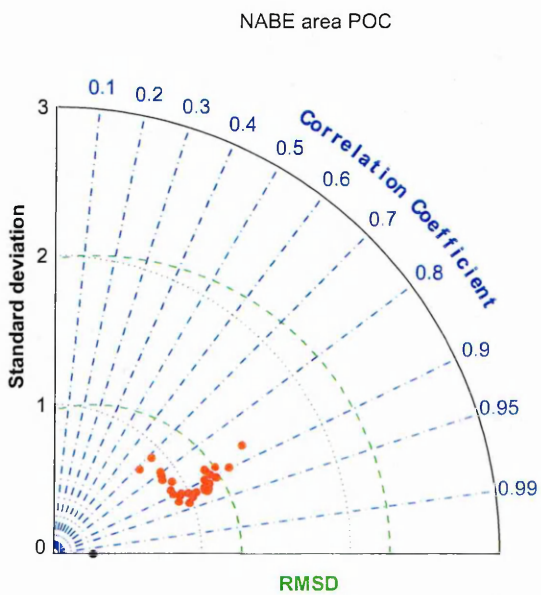

Figure 2.23: Monthly mean POC concentrations values from the model validated against the monthly mean surface POC concentration (SeaWiFS). The black dot indicates the origin of the coordinates system for the RMSD.

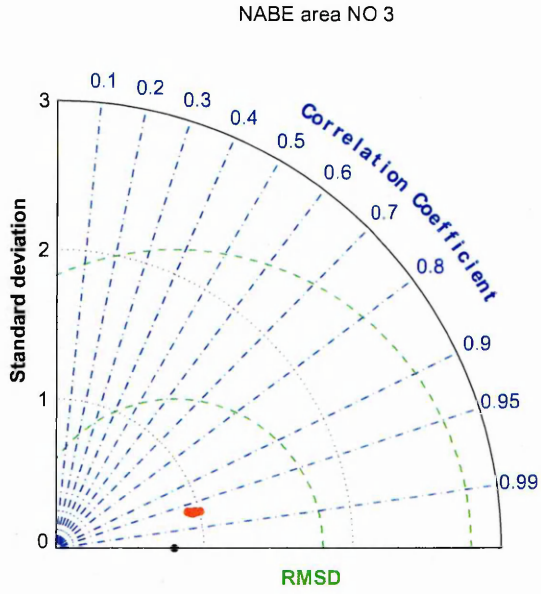

Figure 2.24: Correlation of model results with the surface nitrate concentration (WOA 2013). The black dot indicates the origin of the coordinates system for the RMSD.

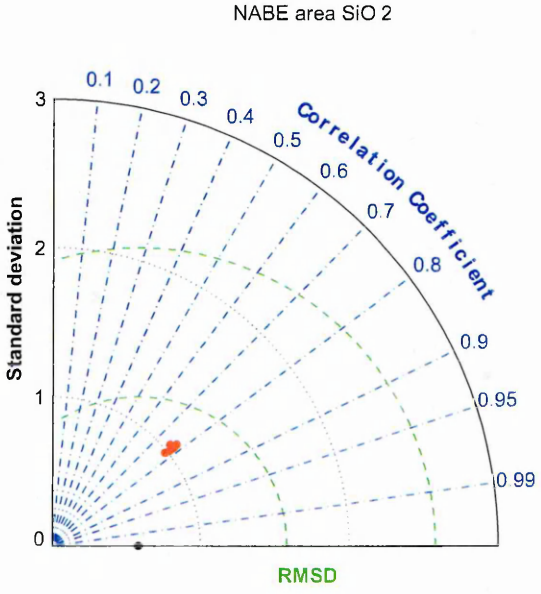

Figure 2.25: Correlation of model results with the surface silicate concentration (WOA 2013). The black dot indicates the origin of the coordinates system for the RMSD.

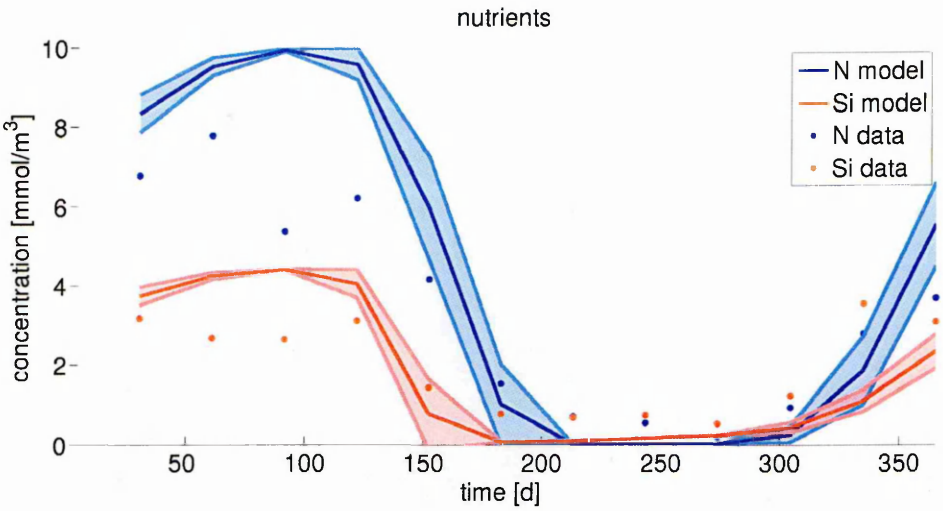

Figure 2.26: Annual cycle of model monthly median nutrients concentration (lines) and WOA13 data (circles). The shaded area represents the monthly median absolute deviation of the model nutrients.

trends in the seasonal nutrients availability considerably well.

2.4.4.3 Comparison of the model results with the Continuous Plankton Recorder Data

Taxonomic data (cell counts) were obtained from the Continuous Plankton Recorder (CPR) database (standard area E6 and E7).

The observed and model seasonal partitioning of phytoplankton functional groups (diatoms, dinoflagellates, coccolithophores and green algae) was shown in Fig. 2.27. The presented seasonality originates from the aggregated, monthly-averaged abundance of phytoplankton groups from the CPR data (cell counts) in the standard area E5 and E6, (Fig. 2.27a and 2.27b), which is compared with the monthly mean abundance (concentration) of the cumulative functional groups resolved in the model (Fig. 2.27c). The model shows (Fig. 2.27c) that diatoms are the most abundant functional group, with a large bloom in early spring. The diatom bloom is accompanied by a bloom of dinoflagellates and a subsequent bloom of coccolithophores. The model concentration of the coccolitophores was considerably higher than that observed in CPR data. The abundance of coccolithophores in the CPR data is only a fraction of what one may be expected, due to the small size of the organisms (5 μm) compared to the size of the mesh used (250 μm). The CPR data are however a relevant index of the relative annual changes and thus reveal the bloom of coccolithophores. The model concentration of

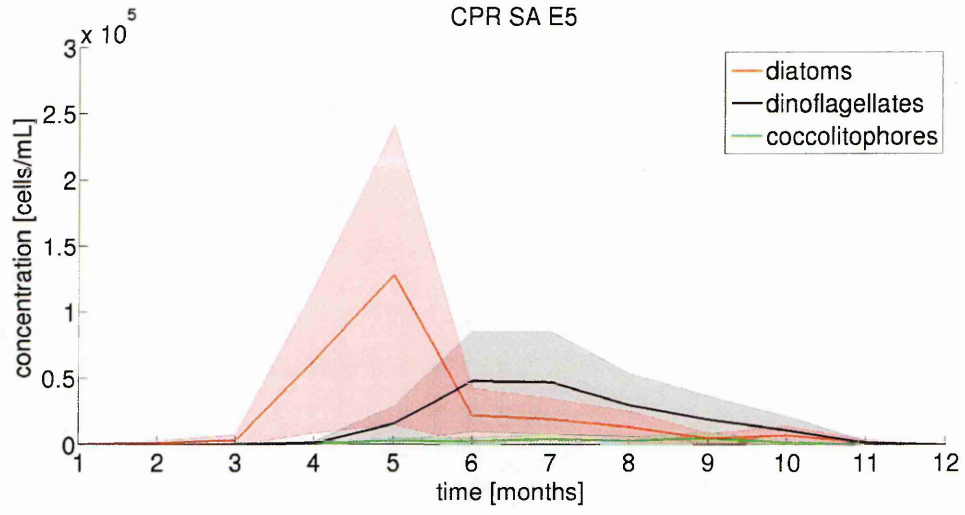

(a)

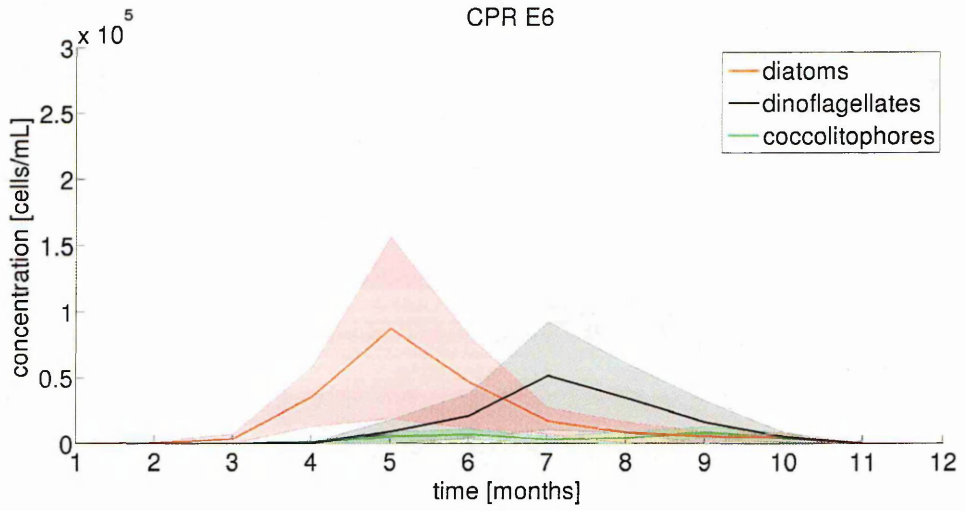

(b)

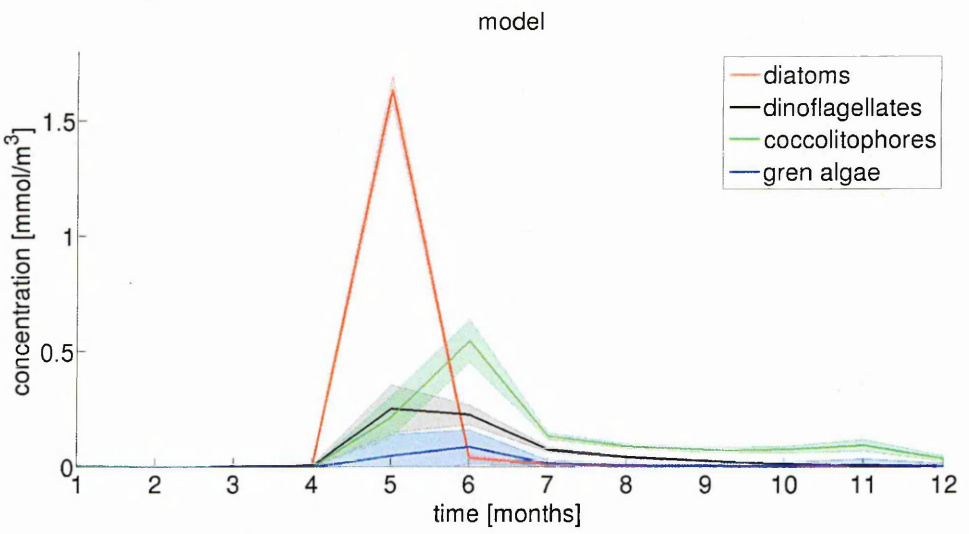

(c)

Figure 2.27: Seasonal cycles of *in situ* Continuous Plankton Recorder (CPR) cell counts for diatoms, dinoflagellates, and coccolithophores in the E5 (a) and E6 (b) standard areas, and model phytoplankton functional groups concentrations (c).

coccolithophores in the model is thus much more substantial and in line with the findings of previous field work studies in the northeast North Atlantic, reporting large concentrations of coccolithophores during the summer bloom. For example, Fernandez et al. [1993] reported a total estimated coccolithophore C biomass as large as 50% of the total phytoplankton. At the same time the model underestimates the concentration of the dinoflagellates during the summer. In fact low summer abundance of dinoflagellates is a frequent issue of most of the NPZD models. An issue that may be improved by the introduction of the mixotrophy as a characteristic mechanism of dinoflagellates (personal communication of Mick Follows)

2.5 Discussion

The ecosystem model presented above resolves the dynamics of multiple phytoplankton functional groups with their direct predators, two inorganic nutrient and detritus in the water column, hence it represents a nutrients-phytoplankton-zooplankton-detritus type models. It merged simplified biological mechanisms into groups, as in other models like Totterdell et al. [1993], Moore et al. [2002], Gregg et al. [2003], but with a much larger number of types, as in the Darwin model. This in turn allowed for a reasonable complexity and a better exploration of ecological implications.

The biological module was embedded within a traditional slab approach (Section 2.2.4). A relatively simple formulation of the physical forcing allows to explore the seasonal dynamics of different biomes of the global ocean. In particular, it enables to reproduce patterns and characteristics of planktonic populations observed in a mid-latitude oceanic region over the years.

The ecosystem dynamics is driven by a set of bio-geochemical processes related to the environment type, while functional traits describe the planktonic community assembly (eg., regulate phytoplankton species competition for resources and their relation with predation on them). Consequently, the hybrid approach developed in here allows to analyze the processes driving biogeography, succession and diversity of plankton communities at global scale.

The model construction was inspired by the Darwin model (Follows et al. [2007]).

The base construction rooted in the NPZD framework was adopted in both cases. Similarly to the Darwin model the phytoplankton community was represented by multiple, stochastically generated species (Section 2.2.2), and the zooplankton by a small and large grazer (Section 2.2.3). The physiological trade-offs used in case of dinoflagellates, coccolitophores and green algae were implemented by randomly selecting parameter values from different (though overlapping) distributions for large and small phytoplankton in a similar fashion as in the Darwin model (Section 2.2.2), thus in a similar manner to that used in the Darwin. The grazers selectivity for small and large phytoplankton cells was also inspired by the Darwin (Section 2.2.1.2). The idealized descriptions of phytoplankton physiological processes were similar to those applied by Follows *et al.*, i.e. phytoplankton growth was determined by a maximum intrinsic growth rate modulated by the availability of essential nutrients and photosynthesis, and nutrient limitation of growth was determined by the most limiting resource in both models (Section 2.2.1.1).

Nevertheless, some differences between the Follows et al. [2007] approach and the one in here were present. While Follows *et al.* used non-dimensional factors reflecting sensitivities to ambient temperature and photon flux to modulate each species' growth rates, a photosynthesis formulation based on the Smith's P-I curve was used in here and the optimal temperature windows were omitted (Section 2.2.1.1). In particular, in the absence of the optimal temperature windows species' niche may not be separated accordingly to the seasonally varying temperature, thus potentially lowers the number of co-existing species. At the same time, lack of temperature windows simplifies the overall model's construction and the description of phytoplankton species physiology. Thus simplifies the interpretation of factors affecting species co-existence addressed in this thesis.

Furthermore, given the focus on the diatoms, their physiology description was enriched with the allometric relationships forming the baseline of the considered trade-offs (Section 2.2.2). This resulted in a more accurate description of the diatoms physiology with respect to that employed in the Darwin model.

Another difference lies in the description of physiological properties of zooplankton, namely the formulation of the processes governing grazing, i.e. a Holling type III

function was used in here and Holling type II in the Darwin model (Section 2.2.1.2). Furthermore, the introduction of copepods overwintering in the presented study (Section 2.2.3) resulted in an improved biological representation of this group (See details in Chapter 3 Sec. 3.3.2).

Yet another difference was given by the number of inorganic nutrients (i.e., only Nitrate and Silicate were considered in here, while there were also Phosphorus and Iron resolved in the Darwin model) and the representation of the dead organic matter (Follows *et al.* used both particulate organic and dissolved organic matter pool, while only a single pool was resolved in here).

Finally, the physical description of the environment was simplified due to a huge computational power required to run a complex 3D model such as the Darwin on a global scale. In here a far simpler and computationally less expensive 0D approach was employed (Section 2.2.4).

Parameter tuning is inevitable in ecosystem modelling in order to ensure its agreement with the observations. The physical description of the environment has been tuned to a specific location and a characteristic time-scale of the explored scenarios (Sections 2.4.3 and 2.4.4). The solar irradiance levels and the nutrients depth profiles describing resources entrainment into the surface layer which together fuel the ecosystem have been also chosen for this particular location. Eventhough such an approach enables to adopt the model to various types of environments, its simplicity limits the number of parameters available for model adjustments.

The parameters describing phytoplankton community have been selected based on an extensive literature review, thus their values were already well known from observation and experiment. These values, in form of a broad ranges, were used to create a community of stochastically generated species. A community, which properties emerged as a result of species interactions within the virtual ecosystem. Because of that, tuning of the phytoplankton parameters would be meaningless as it would restrict the representation of the considered PFTs to a particular subgroup within a given PFT.

The model tuning was undertaken on the zooplankton parameters describing species maximal ingestion rate for large and small phytoplankton (g_k), half-saturation for

intake (H_k) and quadratic mortality term (m_{Z2}). The final values used in the model are similar to those found in the literature, e.g., $H_k = 0.5$ and $g_k = 1$ are very close to the value used by Anderson et al. [2015] or Popova et al. [1997].

The remaining model parameters have been fixed to values reported in the literature, thus originating from both experimental and modelling studies (data presented in appropriate tables of parameters with the references). Because of a satisfactory agreement between the available observations and model results, these parameters were not tuned in the model.

The modelling approach presented in here follows the guidelines of recent reviews (see Hood et al. [2006]) which strongly suggest to adapt the models to the scientific questions since there are no models able to reproduce the whole dynamics of marine ecosystems. The ecological question that stimulated the implementation of this model was to investigate the factors that determine species diversity over the seasonal cycle. The model is simultaneously acceptably simple to investigate ecological hypotheses and sufficiently complex to produce generic insights in dynamics of multi-species communities in a seasonally forced environment. This modelling approach can naturally evolve to explore the community composition and its time course in various environment types as it is discussed in the following chapters, or to explore the relations between marine ecosystems, evolution, biogeochemical cycles, and past and future climate change.

It is important to remember that there is no model addressing all the questions, however for every question there can be a model. Consequently, there are considerable differences arising from model objectives among the studies. These differences are expressed in terms of mathematical formulations, simulations' design, types of output analysis, employed mechanisms, model structure, etc. In fact, it is the *art of modelling* when it comes to shaping the overall model construction considering its *generality*, *realism* and *precision* (Levins [1966]). As it is impossible to incorporate all three characteristics, it is the choice of the modeller to sacrifice one of them in order to emphasise the remaining two and construct a suitable model (Levins [1966]). Ideally it should capture the essential properties and feedbacks of the system it intends to mimic at the level of the data available to support it. It should also produce emergent properties i.e. outcomes which are not a direct extrapolation of the processes and

switches placed in the model. Every model has artificial assumptions and therefore it is always reasonable to question the role of selected mechanisms and/or the details of the simplifying assumptions in shaping the obtained results. After all, a model is just a simplified representation of the reality - which brings up the question: How good/bad is the model?

The goal of skill assessment is to determine how well the model represents the ecosystem dynamics over a specified range of conditions. However, because of the overwhelming complexity of natural ecosystems and the knowledge limitations, observations are used as a surrogate and the model ability to mimic the ecosystem is determined in terms of how well it fits the data. Hence, skill assessment requires a set of quantitative metrics and procedures for comparing model output with observational data, and the fit is defined as the difference between the observation and the prediction. It is however important to note, as Flynn [2005] points out, that "just because a model gives a fit to a particular data set, it does not guarantee the structure is not dysfunctional". Consequently, the fit precision and the understanding of system functioning should be balanced - the mentioned *art of modelling.*

After analysing the performance of 153 biological models including plankton published from 1990 to 2002, Arhonditsis et al. [2004] concluded that the efforts to increase the level of biological detail and spatial complexity, and to explore longer simulation periods, have not led to a systematic or demonstrable improvement in model performance. They found that only 47% of the models assessed had any validation and only 30% determined some measure of goodness of fit. Interestingly, Allen et al. [2007] demonstrated lack of scientific and objective consensus as to what constitutes a "good fit" when model results and observations are visually compared. Therefore the discussion on the model fit quality should be in line with the question addressed with the model.

In Margalef's Mandala (Margalef [1978]), phytoplankton succession is viewed as traversing a phase plane defined by nutrient concentration and turbulence. The initial deep-mixing (high-turbulence and high-nutrient) environment is replaced by a stratified, nutrient depleted environment as the year progresses, creating distinct niches for different phytoplankton groups (diatoms and coccolithophorids respectively) along this

trajectory. This succession has been explained in terms of species-specific affinities for limiting nutrients, and later translated into cells morphology and size (Sournia [1982]; Aksnes and Egge [1991]; Chisholm [1992]). This mechanism was indicated by *in situ* microcosm experiments in oligotrophic environments where the phytoplankton community structure underwent considerable change as a result of nitrate addition (Carter et al. [2005]). The concept of affinity-driven succession clearly applies to the seasonal succession observable in the model results: As the bloom persists, species with low nutrient affinities (high nutrients half-saturations) are replaced by species with higher nutrient affinity (low nutrients half-saturations). Therefore, the result corroborates that, even in such simplified ecosystem model, nutrient availability and differences in nutrient affinity may control seasonal succession of phytoplankton functional groups.

The model captured the domination of biomass by large, fast growing phytoplankton, during periods when both light and nutrients are seasonally plentiful, and small phytoplankton species best able to survive on minimal resources during oligotrophic summer, when nutrients are severely limiting phytoplankton growth (Fig. 2.27c). Diatoms were characterised by high maximum growth rate and high photosynthetic efficiency (α), which represents the initial slope of the P-I curve. The combination of these traits enable them to increase ahead of other groups as light availability increases due to spring restratification (Sverdrup [1953]) and form a pronunced spring bloom. The characteristics of dinoflagellates, in particular lower inorganic nitrogen acquisition efficiency with respect to other groups, limits their persistence to late spring as they are unable to compete with the coccolitophores during summer. Prasinophytes were relatively poor nitrate competitors (Tab. 2.3) and, consequently, they can be abundant where nitrate is not depleted. Coccolitophores were characterised by low inorganic nutrients requirements and high light requirements which enabled them to dominate the ecosystem during summer stratified period when inorganic nutrients availability was limited yet cells were exposed to high irradiance levels.

The model predictions are therefore consistent with the observed patterns of the community structure in the mid-latitudes open ocean ecosystems: low phytoplankton abundance in winter, a spring bloom of diatoms and a subsequent bloom of non-diatom phytoplankton, often coccolithophorids (Lochte et al. [1993], Savidge et al.

[1995], Broerse et al. [2000]). In the introduction of Painter et al. [2014] we read: "[...] the subpolar North Atlantic is also quite distinct due to the presence of lower residual NO_3 concentrations during the summer, a pronounced phytoplankton spring bloom, prominent coccolithophore blooms and high summertime chlorophyll concentrations (Martin et al., 1993; Measures et al., 2008) [...] ". Such an agreement indicates robustness of the traits and physiological parameters distribution.

Some discrepancies between the model and the reference data need to be pointed out. Namely, the model tends to underestimate phytoplankton abundance during the deep mixing periods which is however a frequent issue of simple phytoplankton models (e.g. Litchman et al. [2006]). Too low phytoplankton concentration during deep-mixing periods would cause a delay in a spring bloom formation (Fig. 2.8) and consequently in nutrients depletion (Fig. 2.9) which in fact is observed for some communities. It is worth noting, that various physical mechanisms able to affect winter phytoplankton concentration and spring bloom initiation have been identified e.g., eddy-driven stratification (Mahadevan et al. [2012]), variability in a turbulent mixing rates (Huisman and Sommeijer [2002] and Huisman et al. [1999b], Huisman et al. [1999c]), or temporal water column restratification due to absence of storms (Stec et al. in preparation). Clearly, these mechanisms were not employed in the model construction and ought to be a subject of further investigation.

Another flow of the model could be given by summer chlorophyll concentration which may be underestimated with respect to satellite observations(Fig. 2.19).

Phytoplankton concentration is directly related to the resources availability. Nutrients supply to the stratified water column during summer is attributed to the remineralisation of detritus, zooplankton sloppy feeding and their faecal pallets, and vertical diffusion. Because of its simplified bio-chemical and physical construction the model may underestimate the supply of nutrients during summer.

During the summer months in mid-latitude ecosystems the mixed-layer remains shallow in comparison to the euphotic depth. The nutrients are drawn down to limiting levels and recycling of organic matter becomes more important during this period (Buesseler et al. [1992], Garside and Garside [1993], Schartau and Oschlies [2003]). An explicit representation of a simple microbial loop of dissolved organic nitrogen

and bacteria would improve the representation of detritus remineralisation and by including state variables for nitrate and ammonium would allow for a direct separation of new and regenerated production (e.g., Fasham et al. [1990]). Bacteria would also act as an additional food source for zooplankton and due to sloppy feeding and egestion would indirectly supply phytoplankton with viable nutrients. Introduction of microbial loop formulation could elevate the nutrients concentration during summer period and subsequently increase phytoplankton abundance.

The diffusion of resources across the thermocline in the model is controlled by the diffusion rate and the resources concentration below the mixed layer. The diffusion rate was set at 0.1 md^{-1}, which is approximately equivalent to a vertical diffusion coefficient of 0.3 cm^2s^1 across a 20 m thermocline, thus falls within the typical values observed in the North Atlantic spanning from 0.01 to 0.5 cm^2s^1 (Painter et al. [2014]). An increased diffusion rate would positively contribute to nutrients supply, however without precise values of vertical diffusion coefficient at NABE site I opted for a standard, broadly accepted parameter value (e.g., Fasham et al. [1990]).

Nutrients are being consumed in the photic zone and supplied from below it. Consequently, under stratified conditions, the shape and depth of the nutricline would be indirectly coupled with photic zone via phytoplankton activity, and the vertical profile of nutrients concentration would be non-linear (Fennel and Boss [2003]; also Omand and Mahadevan [2014]). Despite that, a linear relationship of nutrients concentration and depth is frequently considered in the 0D models (e.g.,Steele and Henderson [1993]; Fasham [1995]). Applying a linear regression to the available subthermocline NO_3 data (z ¿ 100m; data source WOA13 Boyer et al. [2013]) generates a $N_0(z) = 0.01417z+2.747$ profile with depth. If introduced into the model it imposes much higher nitrate concentration at the bottom of the summer MLD ($N_0(20) = 3.03[mmol/m^3]$) with respect to the observations (0.16 $[mmol/m^3]$ Boyer et al. [2013]), and artificially increases nutrients influx into the MLD elevating phytoplankton primary production. However, because of substantial discrepancies between the linear and observed nutrients profile I opted for the latter.

The simple two-layer physics used in here resolves a seasonally varying mixed layer containing the planktonic marine ecosystem and a deep layer that contains only nutri-

ents. Interestingly, it is the photic zone and not the MLD which frequently determines the maximal depth at which primary production takes place. When the base of the mixed layer is located above photic zone (eg., mid-summer), sufficient light exists below the mixed layer to support net growth of phytoplankton. In fact, the analysis of *in situ* vertical profiles of physical and optical data gathered by a profiling float in the North Atlantic performed by Boss and Behrenfeld (Boss and Behrenfeld [2010]) clearly indicated phytoplankton growth below the MLD. Another example of such dynamics is the deep chlorophyl maximum (DCM) which is formed in the layer in between MLD and photic zone (Fennel and Boss [2003]). In light of above, 0D models considering only MLD, hence a sublayer of the photic zone, would considerably underestimated phytoplankton concentration during the periods in which photic zone is deeper than MLD.

Coccolitophores are adapted to compete effectively for limited resources. Their high nutrient affinities (low half-saturation) allow them to increase in abundance in the late spring and peak in the beginning of summer. In fact, coccolitophores remain the most abundant phytoplankton functional group during the whole stratified period. Their biomass is controlled by the nutrients availability (bottom-up processes) and by the grazing (top-down processes). Microzooplankton is considered to be the main grazer for small phytoplankton species represented by coccolitophores and green algae. At the same time, micozooplankton is known to be grazed by copepods. This interaction has been considered in multiple ecological models (e.g., Christian et al. [2001], Leonard et al. [1999]), yet it has not been represented in here. Because of that the model may overestimate the abundance of microzooplankton during the summer and overstate top-down control on coccolitophores causing summer chlorophyll underestimation.

The photosynthetic pigments of autotrophic microorganisms are responsible for absorption of various regions of the solar light spectrum (Falkowski and Raven [2013], Falkowski et al. [2004]). Light spectrum utilization can be interpreted in terms of classical ecological theory where light offers a spectrum of resources. According to ecological theory, niche differentiation along a resource spectrum promotes species coexistence by reducing competition among them (Gause [1934], MacArthur and Levins [1967], May and Mac Arthur [1972], Rueffler et al. [2006]). The correspondence between the ab-

sorption spectra of phototrophic microorganisms and the prevailing underwater light spectrum have been reported by numerous studies (e.g., Pierson et al. [1990], Wood et al. [1998], Béja et al. [2001], Vila and Abella [2001], Rocap et al. [2003],Michael et al. [2005], Bouman et al. [2006], Sabehi et al. [2007]).

One of the model assumption is on a single coefficient characterising light attenuation in the whole water column. In reality the rate of attenuation depends on depth and light spectral composition - red light is mostly absorbed by water within first few meters of the water column while blue light penetrates deepest regions. In order to capture these spectral properties Anderson (Anderson [1993]) developed a relatively simple piece-wise approach to light attenuation with depth based on a complex treatment of submarine light (Morel [1988]). Hence, the prevailing underwater light spectrum is related to the depth and to pigment (chlorophyll) concentration. Consequently, a series of distinct niches in the underwater light spectrum could be defined while incorporating Anderson's formulation into the model. It should be expected that this model modification would lead to an increased species diversity but also to a better separation of the phytoplankton functional groups.

Clearly, the model construction is a subject to limitations typical of these modelling approaches such as the oversimplified spatial dimensions of the modelled processes and the seasonal dynamics of water column depth. Additionally, the model resolves the concentration of only two inorganic nutrients. There are compelling evidences that major taxonomic groups differ in their competitive abilities and requirements for N, P, Si, etc. Therefore, including growth dependence on other nutrients could result in better separation of different functional groups over seasonal cycle (Litchman et al. [2006]).

Possible refinements could be considered in terms of the representation of the ecosystem compartments. Additional groups, e.g., nitrogen fixers, viruses and bacteria could be represented in the model. Nitrogen fixers (cyanobacteria) could be included to apply the model to tropical and subtropical regions in the global ocean. Viruses play important yet still unquantified roles in structuring microbial communities and interrupt flows of carbon and nutrients through the microbial loop (Breitbart [2012], Lehahn et al. [2014], Short [2012], Haaber and Middelboe [2009]). Viruses can influence preda-

tor populations directly by infection and lysis or by reducing prey availability (Haaber and Middelboe [2009], Evans and Wilson [2008]). Viral-mediated cell lysis can be rapidly assimilated and remineralized by microbes causing increased bacterial growth and resulting in community restructuring. Importantly, viruses may also serve as food particles.

Furthermore, the parameter values could be modulated to mirror the diversity at the species or group level. For instance, groups/species specific C:N ratios or even flexible ratios varying with respect to ambient conditions (e.g., Talmy et al. [2014]), and species specific grazing selectivity parameters could be introduced. Similar adjustments could apply to species specific Si half-saturation values in exchange for a single value used for all considered diatoms. This would allow for a greater separation of different functional groups and species.

Additional physiological processes such as protein synthesis and toxins production together with temperature dependency of growth could also be introduced.

Moreover, the mixotrophic mode of nutrition by dinoflagellates could be implemented into the model. In fact, the introduction of mixotrophy (in form of prey ingestion and higher growth efficiency at low light) improves the dinoflagellates representation under nutrients depleted conditions during the summer period (Mick Follows personal communications; Fulton et al. [2004]).

Finally, the phytoplankton species physiological characteristics could reach over their current description restricted to the traits regulating resources acquisition efficiency and grazing resistance. In particular, life history related traits could be introduced in form of resting stage formation or sexual/asexual reproduction. In fact, in the Chapter 6 impact of sexual reproduction of the population dynamics has been explored and its impact on community composition established.

Conversely, the overall model scheme could be simplified in order to ease the assimilation of new data on microbial cell biology but also integrate information on organismal diversity, dynamics, and interactions within mathematical models. Clearly these simplifications should not hamper the essential features of the investigated problems and ought to be based on scientific question to be addressed with the model and on the current state of science (Levins [1966]).

Nonetheless, the patterns and characteristics of planktonic populations generated by the model and their qualitative and quantitative agreement with those observed in a mid-latitude oceanic region over the years suggest that the model presented in here is capable to reflect relevant properties of marine phytoplankton communities and natural interactions. Specifically, the model is able to reproduce the main properties of mid-latitude marine ecosystems such as seasonality, succession and interactions among planktonic species and functional groups. I argue that the model capability to reproduce well the macro-pattern, is due to the biological processes forming the core of its construction. In addition the simplification in the physics does not hamper the results. Thus, the model can be used for the exploration of the relevance of theoretical concepts regulating community structure and phytoplankton phenology.

Stochastic and ensemble approaches A growing number of ocean models begun resolving the community structure via the explicit representation of several phytoplankton functional groups (Totterdell et al. [1993], Moore et al. [2002]; Gregg et al. [2003], Litchman et al. [2006]), nevertheless significant challenges are still present (Anderson [2005], Hood et al. [2006]; see also Introduction). Among them a scarce knowledge on phytoplankton physiology is frequently recognised. Because of the limited quantitative information from laboratory cultures and field observations, the correct evaluation of the parameters controlling planktonic species dynamics remains problematic. Accordingly, the specification of functional groups in the vast majority of ecosystem models is subjective and somewhat arbitrary. The results generated by such models might strongly depend on the combination of parameter values, in particular those related to species physiology and community composition. Hence, it is possible that a different combination of parameters, with each of these parameters within its acceptable range may produce a different outcome despite identical physical conditions and thus decrease the results reliability.

The stochastic approach to planktonic community description allows to circumvent these obstacles, including: low species diversity imposed in most ecosystem models, difficulties in specifying the physiological rate coefficients of phytoplankton species, and prescription of dominant functional types. At the same time, the ensemble approach

(Murphy et al. [2004]) with multiple simulations performed under identical/similar conditions or theoretical assumptions, but with different planktonic communities, allows to correctly consider the limitations given by the finite selection of the species.

We still lack mechanistic models that can capture the degree of biodiversity observed in natural ecosystems. For example, because of competitive exclusion (Hardin et al. [1960]), modeled biodiversity tends to collapse over time in all ecosystem models even those explicitly resolving many different species under variable environmental forcing (Chapter 3; Bruggeman and Kooijman [2007]; Follows et al. [2007]). In the model presented in this chapter, functional diversity, expectedly, declines over time as well. Thus, in order to account for astonishing diversity of phytoplankton species it is not sufficient to initiate modelled phytoplankton communities with millions of species, as vast majority of them will perish within short period of time. Furthermore, community composition may impose some constrains on the observed results.

In order to circumvent these limitations an ensemble approach was considered in this study. The presented analyses indicate that the model outcomes are sensitive to the community composition (e.g. Fig. 2.2). Thus multi-community approach is required to properly analyse the outcomes of the model simulations and separate the variability attributed to initial community composition from that emerging due to imposed mechanisms or physical forcing. For instance the variability of total yearly phytoplankton biomass is considerably high as its median absolute deviation was equal to 12.5% of the median value computed for all ensemble members. This variability was even higher if single functional groups were considered, e.g. 21% in case of diatoms and coccolitophores, and 30% in case of dinoflagellates. Similar or even higher variability was reported if median or maximal biomass was considered. Clearly, it can be associated to the community composition as all the ensemble simulations differed only in terms of parameter values describing phytoplankton species physiology. Thus, it illustrates the intrinsic sensitivity of the multi-species community model. Consequently, the analyses of a single community could lead to a misleading conclusion by under- or overestimating observed values of the selected ecological indicators (e.g., maximal phytoplankton biomass).

This variability can be suppressed by regulating one (or many) of the model's

degrees of freedom. In fact, it is a standard modelling trick to tune the parameter values in order to increase agreement of model output with desired patterns or data (e.g., Matear, 1995). Changing the parameters affecting top-down and/or bottom-up control in each ensemble simulation would most likely result in (almost) identical seasonal phytoplankton abundance. But is it worth doing so?

It has been pointed out that for any given set of observations, it is always possible to construct many different and incompatible theories that fit the data equally well (Quine [1975]). Consequently, the chase after increasing the overall model skill could hamper its construction and result in incorrect conclusions. Thus rather than be tamed, the observed sensitivity ought to be treated as a source of valuable information on the interplay between community composition, incorporated processes and virtual ecosystem functioning.

In addition, the ensemble approach generates a dual information on explored processes: general and specific. The general information illustrates the average system response which should be expected within the assumed framework irrespectively to the community composition. The specific information on the other hand informs on how sensitive is the mechanism to additional factors, here community composition. Thus, the specific information could be interpreted in terms of mechanism plasticity

In particular, the general information is that the biogeochemical patterns of each emergent phytoplankton community in the ensemble set, were plausible with respect to observations of subpolar environment types (Sec. 2.4.3, 2.4.4). The model virtual species appear to occupy similar habitats to the real-world ecotypes. The specific information is that spring bloom phenology varies depending on the phytoplankton community composition.

Marine ecosystem models are increasingly being used to investigate how marine biota interacts with its environment and how it may respond to future climate scenarios. In turn this information is increasingly being used to guide and implement environmental policy. The presented plasticity is an intrinsic property of the models resolving phytoplankton diversity. It is embedded within its construction because of the assumed mechanisms and processes representation. Hence, it must be accounted for when results of such models are being interpreted and used to improve our under-

standing of marine ecosystem functioning.

Chapter 3

Species diversity in the model ecosystem

3.1 Introduction

A detailed description of the mathematical model developed for the purpose of this thesis had been presented in the previous chapter. The model results had been analysed in terms of the biogeochemical cycles and their agreement with several datasets. Those analysis however were far from being complete and multiple additional aspects could be considered in the continuation of this study. Among them, the issue of species diversity and community composition immediately emerges.

An overview of the phytoplankton species diversity and its interplay with ecosystem functioning had been presented in the Chapter 1. Simultaneously, the problems in species diversity representation in the ecological models had been discussed. Species diversity is a widely used term to refer diversity of biota in different domains and at different scales. The most frequently used measure of diversity is 'species richness', i.e. the number of species present in an selected ecosystem (Hill [1973]). It depends on the level of taxonomic identification, which - in the case of phytoplankton - is largely based on morphology and recently on genetic markers.

'Species diversity' quantified as richness does not account for species abundance, which affects diversity (e.g., Stirling and Wilsey [2001]; Whittaker [1965]; Hurlbert [1971]). The relative contributions of species to the community is captured by the 'species evenness' (or species equitability) typically ranging from near 0 (low evenness or dominance of a single or a few species) to 1 (maximum eveness or equal abundance of several species) (Alatalo [1981]; Smith and Wilson [1996]). The Shannon Index H (or Shannon-Weaver Index; Shannon and Weaver [1949]) measures the joint effect of species richness and evenness. It illustrates whether the species present in the ecosystem are at similar abundance (high values) or the community is dominated by a single/few species (low values).

Phytoplankton diversity affects ecological and biogeochemical processes as it relates to the community composition which forms the basis of the pelagic food web (Duffy et al. [2006]). The composition of the phytoplankton community may affect the export of organic matter from the surface to the deep ocean, and thereby the global cycles of nitrogen, phosphorus, and carbon (Redfield [1958]; Falkowski et al. [1998]; Caron and Countway [2009]), and carbon sedimentation (Sieracki et al. [1993], Assmy et al.

[2013]). Phytoplankton community structure may also affect zooplankton production and composition, affecting the functioning of the trophic cascade (Richardson and Schoeman [2004]; Hilligsøe et al. [2011]; Ainsworth et al. [2011]).

There is a need to understand the mechanisms driving phytoplankton diversity and distribution patterns, modelling provides an important tool for understanding them and exploring various mechanisms which could influence them. In here I describe the species diversity observed in the reference simulations presented in the previous chapter. For this purpose both the 'species richness' and Shannon index had been used. I further analyse the mechanisms driving species competition and shaping phytoplankton community composition.

Furthermore, a structural sensitivity analysis is performed to assess model sensitivity to two mechanisms, namely copepods winter diapause, and plankton immigration.

The former sensitivity invokes the biological mechanisms related to copepods life cycle. There is evidence that copepod *Calanus finmarchicus* undergoes a diapause during winter prior to completing its development. Assuming a fixed and cued by a single signal (mixed layer depth) winter dormancy, I analyse in here how this process affects both the bulk phytoplankton properties and the species diversity, thus also the community composition.

I also use the model to undertake analysis of model sensitivity to the presence/absence of a continuous background phytoplankton immigration. Phytoplankton immigration may be attributed to various physical and biological processes (e.g. spores germination). In here I test to what extent the continuous intrusion of phytoplankton cells at very low concentration is able to reshape the planktonic community composition and subsequently affect ecosystem functioning.

3.2 Species diversity in the model ecosystem

The results of the analysis presented in the previous chapter has been used in here to explore species diversity in a subpolar ecosystem. In particular model configuration tuned for North Atlantic Bloom Experiment in 1989 (Chapter 2, Section 4.3) has been used in here.

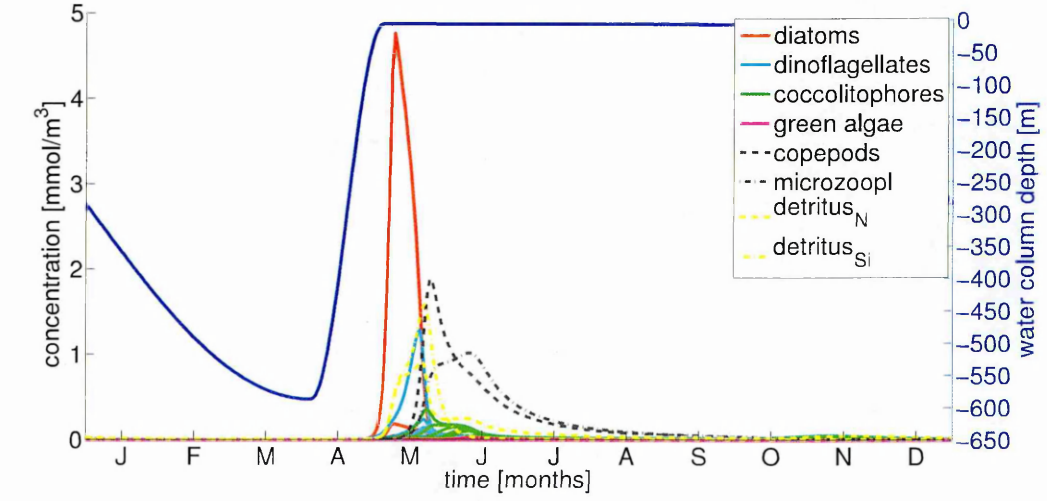

(a)

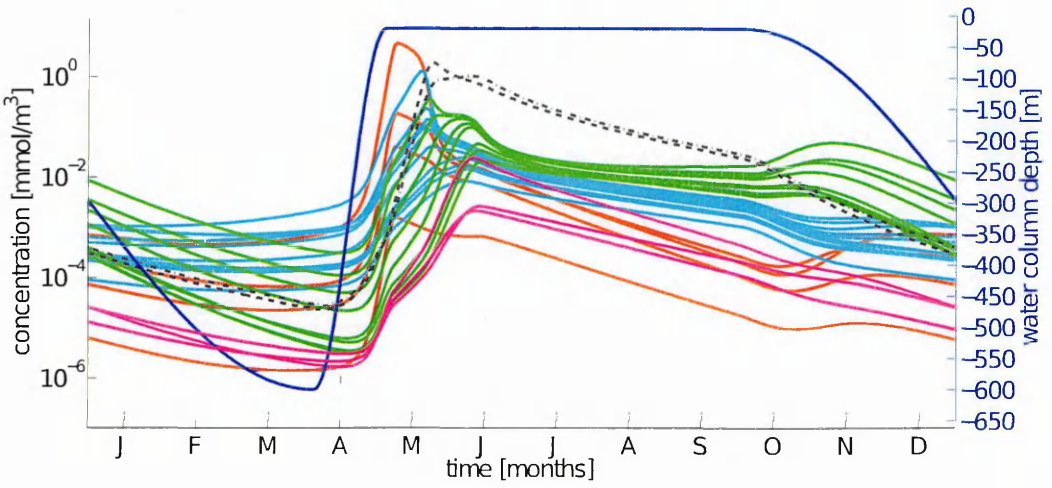

(b)

Figure 3.1: (a) Annual cycle at NABE of modeled phytoplankton functional groups (species concentration), zooplankton, nutrients and detritus, with an superimposed MLD. (b) identical as (a) but with a loged scale on Y-axis.

Each ecosystem model simulation was initialized with a relatively large number of 40 virtual phytoplankton species divided equally into 4 functional groups: diatoms, dinoflagellates, coccolitophores and green algae, whose traits were assigned stochastically from plausible ranges of possibilities (See Chapter 2 for details). The modeled phytoplankton communities "self assembled" according to the relative fitness of the phytoplankton types in the regionally and seasonally varying resource and predatory environment. The emergent phytoplankton populations captured the observed seasonal patterns in the phytoplankton biomass and community structure in subpolar type environment, including the observed spring bloom of large diatoms and dominance of small species adopted to low-nutrients conditions (here coccolitophores) during summer.

In the course of simulation, due to competition for resources and grazing pressure, most of the species declined towards extinction, yet 15 or so species on average remained active and thrived in the ecosystem. The time scale of a competitive exclusion can exceed a thousand years in environments characterised with either short (hours to days) or long (annual and longer) periodicity. On a contrary, if the environmental conditions vary on monthly time scale, competitive exclusion may occur within a period of several years or less. In fact, environmental conditions with a large amplitude variation tend to promote rapid exclusion, whereas small amplitude variations allow for extended coexistence (Barton et al. [2010])

Even though the subpolar environmental forcing employed in here was subjected to strong seasonal variations, including changes in the mixed layer depth that regulate light and nutrient availability, thus suggesting rapid species exclusion, each numerical simulation has been performed over a period of 10000 years in order to allow for a competitive exclusion also on the longer time scales. Most of the species had been competitively excluded within the first decade of simulations, thus, suggesting their maladaptation to the virtual ecosystem characteristics. At the same time species richness remained unchanged even if the period of simulations was increased by additional millennia (data not shown).

In here, the species richness was characterised as the total number of phytoplankton species which individual concentration exceeded $10^{-6}[mmolC/m^3]$ during the whole year. The overall species richness in the ecosystem ranged between 10 and 19 across

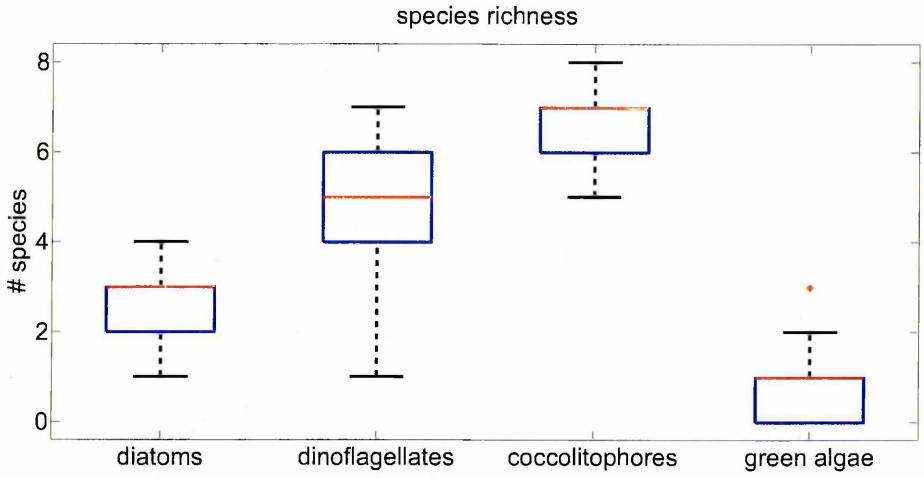

Figure 3.2: Total number of active species (species richness) in each functional group reported across all explored communities.

all ensemble communities with the median number of active species equal to 15 (STD = 2.04). Considering phytoplankton functional groups, the median number of diatoms was equal to 3 (STD=0.89), coccolitophores 7 (STD=0.81), dinoflagellates 5 (STD=1.74) and green algae 1 (STD=0.86) (Fig. 3.2). Hence, all the functional groups were represented. Despite presence of green algae their total accumulated biomass was considerably low and this group was barely visible on the annual time scale (Fig. 3.17a; also Table 8 in Chapter 2).

The number of active species varied considerably across the ensemble members (Fig. 3.2) thus justifying post hoc the need for an ensemble approach employed in here (see also Chapter 2 Section 3).

The modelling framework used in this study is clearly unable to reproduce the diversity observed in nature, but it still may be used for investigation of processes affecting species diversity and their coexistence (see chapter 1 for details).

The analysis of the daily values of Shannon diversity index show that the minimal diversity coincide with the spring diatom bloom, and the maximal Shannon diversity was observed during summer and winter (Fig. 3.3b). The subsequent autumn diversity minimum was again attributed to the autumn bloom.

In here low values of the Shannon diversity ($0.25 < H < 1.5$; Fig. 3.3b) coincided with spring bloom when the whole ecosystem was dominated by a single (or a few) diatoms species responsible for the vast majority of the biomass in that period (Fig.

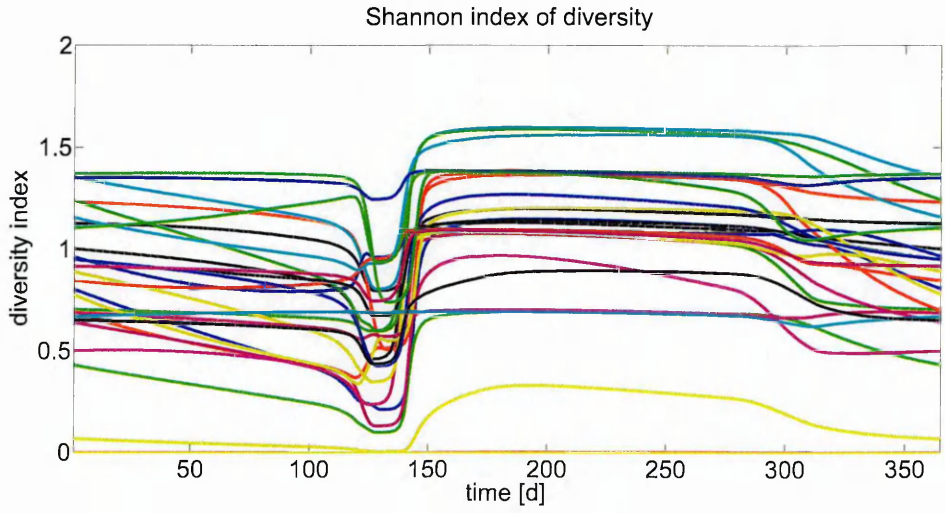

(a)

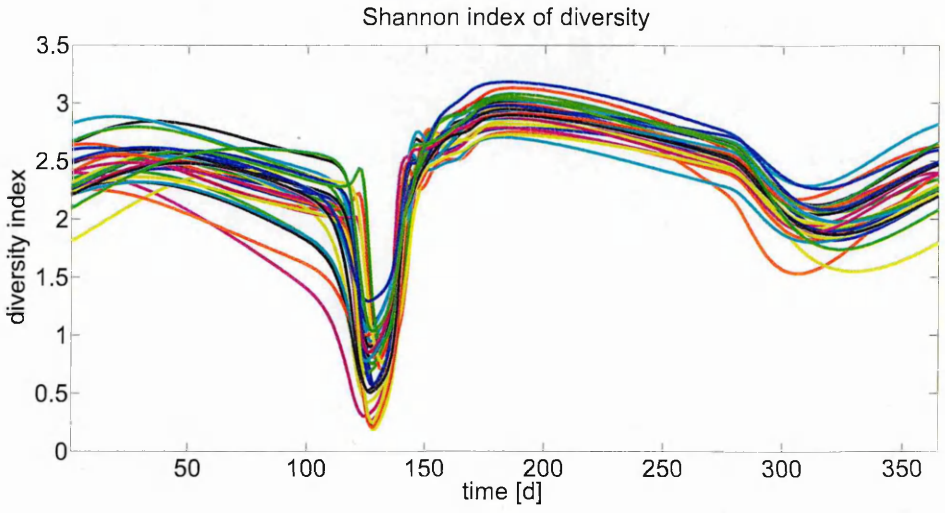

(b)

Figure 3.3: Shannon index of diversity for multiple NABE site simulations in a reference case. Each line depicts seasonal variability of Shannon diversity index value computed for: (a) diatoms and (b) all the species in a single community.

3.1b). On a contrary during summer numerous coccolitophores and dinoflagellates were observed simultaneously, and in winter the ecosystem is saturated with species representing all functional groups considered in the simulation (Fig. 3.3b), thus, the Shannon index was elevated ($H > 2$).

The slight decrease of Shannon diversity was observed during autumn, when a small autumn bloom was formed by species representing coccolitophores and diatoms and producing most of the systems biomass (Fig. 3.3b). Nonetheless the index values were still exceeding 1.5.

The observed variability of seasonal Shannon diversity patterns varied considerably across all the ensemble members (Fig. 3.3b). This variability was clearly attributed to the community composition since the physical forcing, nutrients entrainments and grazers characteristics were identical. Even stronger variability was observed if only diatoms were considered (Fig. 3.3a). It also derives from the community composition, and in particular from the total number of diatoms species co-existing in the system. It may vary from 1 to 4 out of total 10 initiated in each simulation (Fig. 3.2) and strongly affect the values of diversity indicators such as Shannon index. Thus, a single community is not sufficient to conclude on the diversity patterns produced by the ecosystem explored in here, and an ensemble approach is necessary in order to account for a community composition and its impact on diversity.

It is frequently invoked that winter 'resets' population densities. This idea of winter resetting, however seemingly intuitive and straightforward, is obviously an oversimplification. Each autumn, species enter the winter season in proportions dictated by their physiological properties and environmental forcing characteristics, i.e., the species composition from the previous autumn affects the species composition of the next spring bloom.

Indeed, the dominant diatoms species in spring were also most abundant during winter and autumn. In an identical fashion, most abundant spring dinoflagellates and summer coccolitophores and green algae, were also dominating the respective functional groups in autumn. Because of that the presence of an autumn phytoplankton bloom, which was observed in some communities under particular environmental conditions (short summer, low latitudes/high light intensity), may affect ecosystem functioning

and above all community structure by increasing autumn/winter system memory and the rate of species survival.

Traits distribution of the species in the reference simulation Within each single phytoplankton community a cluster of surviving species emerges in the course of each simulation. The species that survived in the virtual ecosystem are compatible and despite competitive interactions they do not run each other towards extinction. Each cluster was composed of all (or most of) initiated PFTs and incorporates on average 11-12 species including 2 diatoms, 4-5 coccolitophores, 5 dinoflagellates and in some cases 1 green algae. The number of surviving species varied across the explored simulations spanning from 5 to 15 species, and 1-3 diatoms, 1-6 coccolitophores, 2-8 dinoflagellates and 0-1 green algae (Fig. 3.4).

Considering the representation of the PFTs' within all the simulations, but also the species diversity within each functional group it is reasonable to state that the physiological trade-offs, imposed on phytoplankton characteristics in form of the group specific parameters and of allometric relationships, were preserved amongst the persisting species in the considered ecosystem.

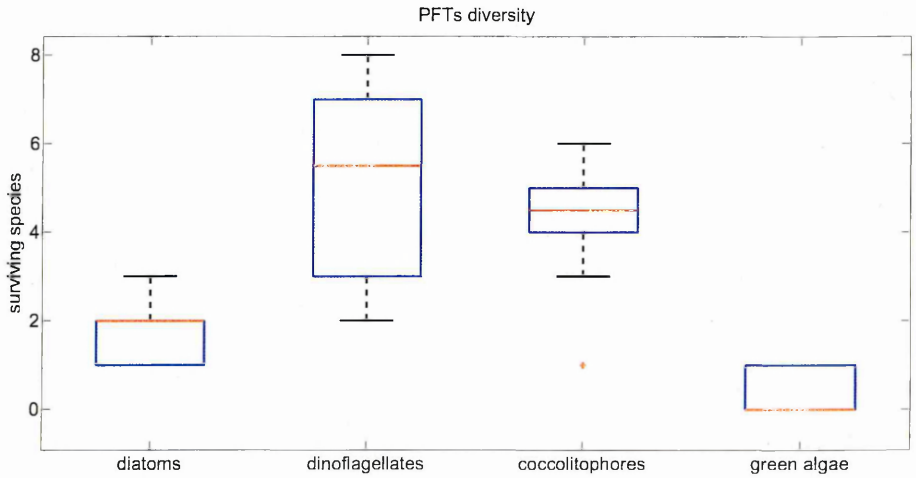

Figure 3.4: Number of species in the reference simulation.

The analysis of the maximal concentration reached by the species present in the virtual ecosystem allowed to identify regions of the physiological parameters' space which characterised the species persisting in each resolved PFT, hence the combination of trait combinations which were most successful in the ecosystem. The parameters

describing growth rate, nutrients half-saturation constant and initial slope of the P-I curve of the surviving species took values of:

1. for diatoms: $1.4 \leq r \leq 2.6$, $1 \leq H_N \leq 1.9$, $0.055 \leq \alpha \leq 0.18$ thus covering the 50%, 55% and 70% of the considered range of those parameters respectively (Fig. 3.5a, 3.6a),

2. for dinoflagellates: $0.36 \leq r \leq 0.88$, $0.48 \leq H_N \leq 9.08$, $0.039 \leq \alpha \leq 0.12$ thus covering the 70%, 91% and 89% of the considered range of those parameters respectively (Fig. 3.5b, 3.6b),

3. for coccolitophores: $1 \leq r \leq 1.3$, $0.14 \leq H_N \leq 0.28$, $0.01 \leq \alpha \leq 0.021$ thus covering the 40%, 95% and 59% of the considered range of those parameters respectively (Fig. 3.5c, 3.6c),

4. for green algae: $1.35 \leq r \leq 1.45$, $0.19 \leq H_N \leq 0.43$, $0.013 \leq \alpha \leq 0.025$ thus covering the 13%, 4% and 40% of the considered range of those parameters respectively (Fig. 3.5d, 3.6d).

The observed differences among the surviving species allowed to conclude that there are no "artificial clones" of the species, which could be expected because of the stochastic nature of the species generator. Because of that it may be concluded that the co-existence of the species within all the resolved functional groups was granted because of the discrepancies in the physiological characteristics of the persisting species.

Species characterised by a similar growth rates, half-saturation constant for nutrients acquisition and initial slopes of the P-I curve may co-exist (side-by-side) in the natural ecosystem because of the additional physiological traits differing them which could reduce the competitive edge between them and separate spatio-temporally their ecological niche. In here, however, because of the simplicity of phytoplankton physiological description such co-existence is unlikely due to the law of extinction leading some of the clones towards extinction over a long simulation time.

The stochastic approach to community description introduces some plasticity into its composition i.e. the number of PFTs is fixed yet the internal organisation of the species within the PFTs is random and it emerges from a predefined set of virtual

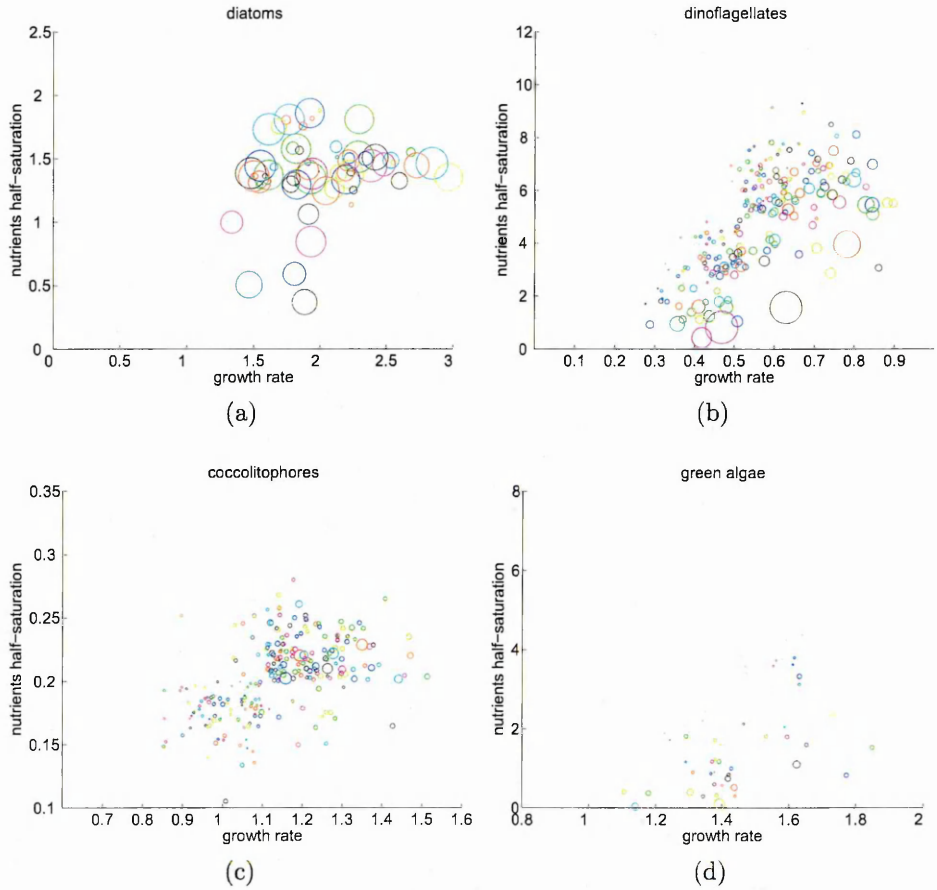

Figure 3.5: Physiological traits distribution of the species persisting in the ecosystem in the reference simulation. The plots illustrate the physiological trade-offs characterising species within the resolved phytoplankton functional groups at the steady state of the reference simulations: (a) diatoms, (b) dinoflagellates, (c) coccolitophores and (d) and green algae. Each circle depicts a single phytoplankton species. The size of the circle is proportional to the maximal concentration of the species reached during the year. The plot illustrates the characteristics of the species from all 30 ensemble communities, where the communities were distinguished by colours. The axis represents nitrate half-saturation constant and intrinsic growth rate.

species as a result of the balance between the top-down and bottom-up mechanisms driving all species dynamics. The final composition of the phytoplankton community in each case depends on the initial set of stochastically generated species with which a virtual ecosystem was seeded. This stochastic preconditioning is illustrated by the differences in the characteristics of the surviving species as indicated by the specific ecological indicators (e.g., species maximal concentration) computed for the clusters of species surviving in all considered communities (Fig. 3.5, 3.6). Clearly the species dynamics is determined by its physiological characteristics, but also by the characteristics of the species it competes with in a system of limited capacity. Each cluster covers a subset of the considered parameters space, though all the clusters considered together

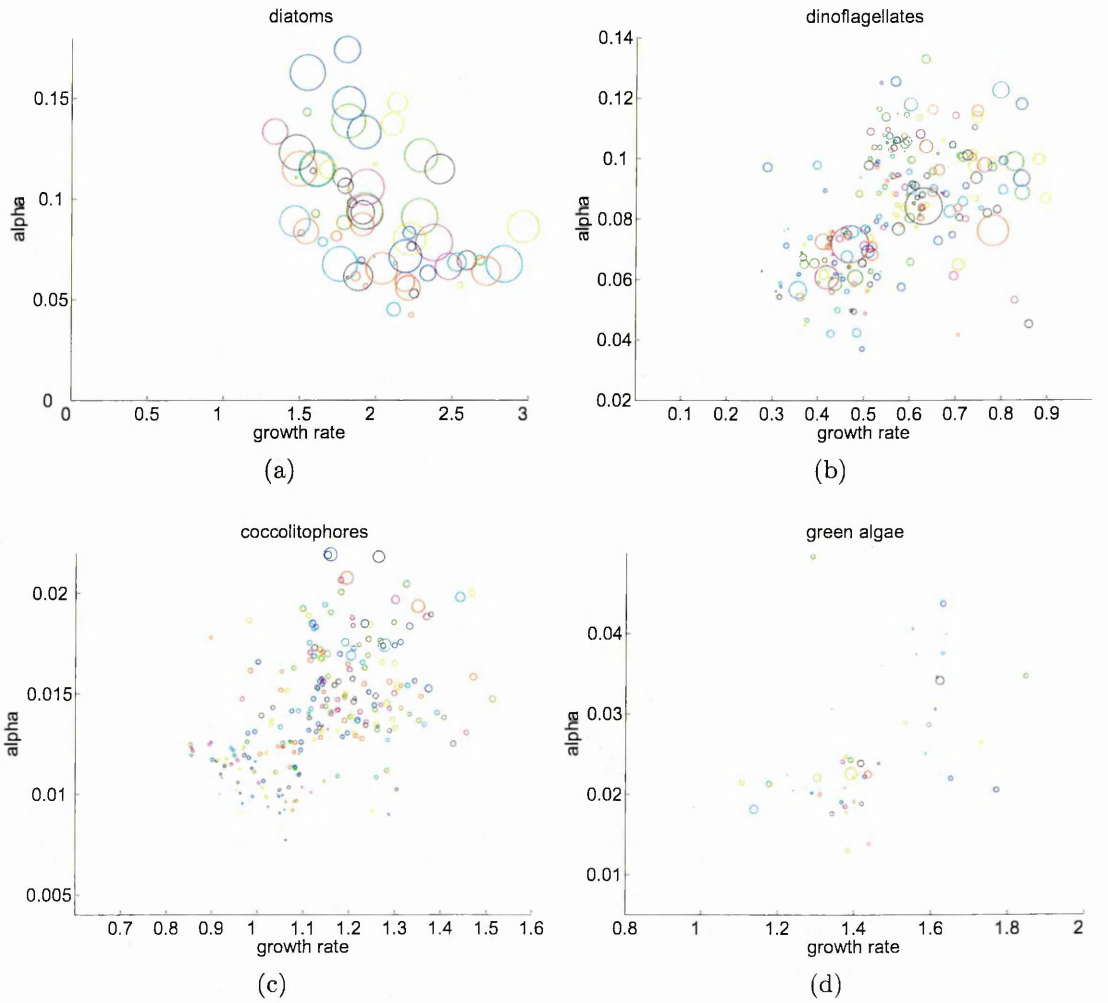

Figure 3.6: Physiological traits distribution of the species persisting in the ecosystem in the reference simulation. The plots illustrate the physiological trade-offs characterising species within the resolved phytoplankton functional groups at the steady state of the reference simulations: (a) diatoms, (b) dinoflagellates, (c) coccolitophores and (d) and green algae. Each circle depicts a single phytoplankton species. The size of the circle is proportional to the maximal concentration of the species reached during the year. The plot illustrates the characteristics of the species from all 30 ensemble communities, where the communities were distinguished by colours. The axis represents initial slope of the P-I curve and intrinsic growth rate.

cover (roughly) it whole (Fig.3.5, 3.6).

Despite the numerous possible configurations of the physiological characteristics of the surviving species' some general trends in the traits distributions were observed. Namely, surviving diatoms species were characterised by a high intrinsic growth rate ($r \geq 1.3$), while the vast majority of diatoms with low intrinsic growth rate vanished from the virtual ecosystem. Dinoflagellates species with low growth rate and high nutrients half-saturation constant were competitively excluded from the community. The clusters of surviving dinoflagellates were dominated by species relatively higher

growth and lower nutrients half-saturation constant, though a positive relationship between the intrinsic growth rate and the nutrients half-saturation constant appears to be a promising combination of the physiological traits of surviving dinoflagellates (Fig. 3.5b). Coccolitophore species observed in the virtual ecosystem appeared to be highly diversified in terms of their physiological characteristics, but the species with $r \leq 0.85$ underwent extinction in all explored communities which referred to a small fragment of the explored parameter space. On a contrary, the vast majority of the green algae species did not withstand a competition and underwent extinction in the virtual ecosystem. The most of the surviving species were characterised with a low nutrients half-saturation constant ($H_N \leq 2$, where the maximal value of H_N for green algae was approximately equal to 8), and only a few species with $H_N \geq 3$ survived.

The above observations corroborate with the broadly accepted consensus regarding the physiological characteristics of the species dominating under resources repleted/depleted condition, i.e. diatoms, considered as "opportunists", benefiting from their high growth rates and nutrients acquisition rates enabling them to rapidly increase under the nutrients and light repleted conditions, and coccolitophores, considered as "gleaners" characterised with low nutrients half-saturation constant, dominating in the ecosystems where nutrients availability is rather scarce (please see Chapter 1, section 1.5 where the "gleaners vs opportunists" strategy was discussed).

According to the resource competition theory, in a system at equilibrium, a species with a lowest resources requirements competitively excludes all the other species as it drawns down the available resources to the level at which other species are unable to balance their growth and mortality rates. The $R*$, as described in the 1st chapter, indicates the resources concentration at which specie growth rate is in balance with its mortality rate. If steady-state conditions are satisfied, species can coexist if they have the same (lowest positive) $R*$ values. This simple logic clearly expands to the balance between the population accumulation and loss rates. Then, the identical $R*$ values can be accomplished by various combinations of accumulation and loss rates, accounting also for the phytoplankton dispersal rate.

The coexistence of species in the stable subtropical environment is explained by the resources competition theory (Tilman [1981], Dutkiewicz et al. [2009], Barton et al.

[2010]). The species occupying this type of environment are characterised by low $R*$ (Chapter 1, and Tilman [1981], Dutkiewicz et al. [2009]), hence low nutrients requirements, which allows them to competitively exclude all the other species. The resources competition theory however, requires a system in an equilibrium. Thus the applications of the theory in a dynamics, subpolar environment are limited to the period of summer water column stratification Dutkiewicz et al. [2009]. It is argued, that in subpolar ecosystems, not low R^* but high growth rate, μ, determines phytoplankton community composition (Barton et al. [2010]), as it allows them to benefit from temporarily saturating resources concentrations. The distinguished role of low R^* and high μ_{max} is clearly visible when mean physiological properties of the community are analysed. Typically, phytoplankton communities inhabiting deep mixing systems benefit from substantial amounts of nutrients transported from deep water layers via wind-driven vertical mixing. These communities are dominated by species with high growth rate and nutrients half-saturation. In contrast, in stable systems, such as stratified, subtropical gyres, where the standing stock of nutrients largely depend on local recycling and diapycnal nutrient fluxes, phytoplankton communities are characterised by considerably lower growth rate and nutrients half-saturation, thus low R^*.

There are considerable differences in the physiological characteristics of the species surviving in each community, yet the seasonal dynamics of the phytoplankton community, represented by the seasonal abundance patterns of the PFTs or by the spring bloom phenology, illustrate high degree of convergence (Fig. 2.12). Despite the differences in the community composition the seasonal dynamics of the PFTs governed by the resources availability and grazing pressure is coherent with the *in situ* observation (see Sections 2.4.3 and 2.4.4). Consequently, it was possible to enrich the analysis of the ecosystem functioning performed in this thesis with the considerations of how community composition affects the ecosystem functioning or what is the spectrum of expected outcomes/interpretations of explored mechanisms with respect to the species organisations within the community (See chapter 3, 4 and 6).

Time evolution of the traits distribution in the reference simulation The virtual ecosystem was seeded with a 40 species organised into 4 functional groups. The

parameters described species physiologiacal traits were randomly selected from a parameters space predefined for each PFT (Sec. 2.2.2). The initial concentration of all phytoplankton species was equal to $= 10E - 6[mmolN/m^3]$. This approach allowed for a self-organisation of the phytoplankton community as a result of the competition for resources amongst the phytoplankton species and their interactions with the grazers. But how quickly is this self-organised pattern emerging? It is possible to answer this question by monitoring the time evolution of the traits distribution of the species surviving in the ecosystem. A maximal annual concentration was computed for each species in the community on the annual bases, which allowed for a transparent visualisation of the competitive exclusion taking place in the virtual ecosystem (Fig. 3.8, 3.9, 3.10, 3.11). The presence of all the species seeded in the system was clearly marked in the first year of the simulation (Fig. 3.8a, 3.9a, 3.10a, 3.11a), but the majority of species appeared to be maladapted and perished within the first years of the simulation, in particular:

1. 20% of the diatoms species extinct on average within the 1st year of the simulation, 70% within the 2nd and 3rd year, and the diversity stabilized after 20 years (Fig. 3.7b, 3.8),

2. 20% of the dinoflagellates species extinct on average within the first five years of the simulation and the diversity stabilized after 20 years (Fig. 3.7c, 3.9),

3. 10% of the coccolitophores species extinct on average within the first three years of the simulation and the diversity stabilized after 10 years (Fig. 3.7d, 3.10),

4. green algae population collapsed to 10% of the initial diversity after 1st year of the simulation and stabilised at this value (Fig. 3.7e, 3.11),

5. the overall species diversity decreased from 40 to 23 species in the 1st year of simulation in the majority of the communities and gradually decreased to its stable value till the 20th year of the simulation (Fig. 3.7a).

Species co-existence depend also on the interplay between the vegetative period duration and the generation time. Considering two species, out of which one is a superior competitor, when observed over a relatively short period of time with respect

to the species generation time their population dynamics might be almost identical. Only when competing over a sufficiently long period a superior species may may gain competitive advantage and out-compete the other one. This advantage may however vanish under severe environmental conditions resetting the entire ecosystem. While the species extinction may be attributed to their maladaptation to the environmental conditions or to the existence of a better competitor, the co-existence may not be so straight forward. Species may co-exist because their ecological niche is complementary, but also because the environmental conditions vary so often that the competitive exclusion may not occur.

The time scale of a competitive exclusion can exceed a thousand years in environments characterised with either short (hours to days) or long (annual and longer) periodicity. On a contrary, if the environmental conditions vary on monthly time scale, competitive exclusion may occur within a period of several years or less. In fact, environmental conditions with a large amplitude variation tend to promote rapid exclusion, whereas small amplitude variations allow for extended coexistence (Barton et al. [2010]). Indeed, such a dynamics was observed also in here, where the majority of the species were competitively excluded within the first years of the simulations and the community composition stabilised after approximately two decades (Fig. 3.7a).

Even though the subpolar environmental forcing employed in here was subjected to strong seasonal variations, including changes in the mixed layer depth that regulate light and nutrient availability, thus suggesting rapid species exclusion, each numerical simulation has been performed over a period of 10 000 years in order to allow for a competitive exclusion also on the longer time scales of the similar species which could have been created by the stochastic species generator employed in this study.. Most of the species had been competitively excluded within the first decade of simulations, thus, suggesting their maladaptation to the virtual ecosystem characteristics. At the same time species richness remained unchanged even if the period of simulations was increased by additional millennia (data not shown).

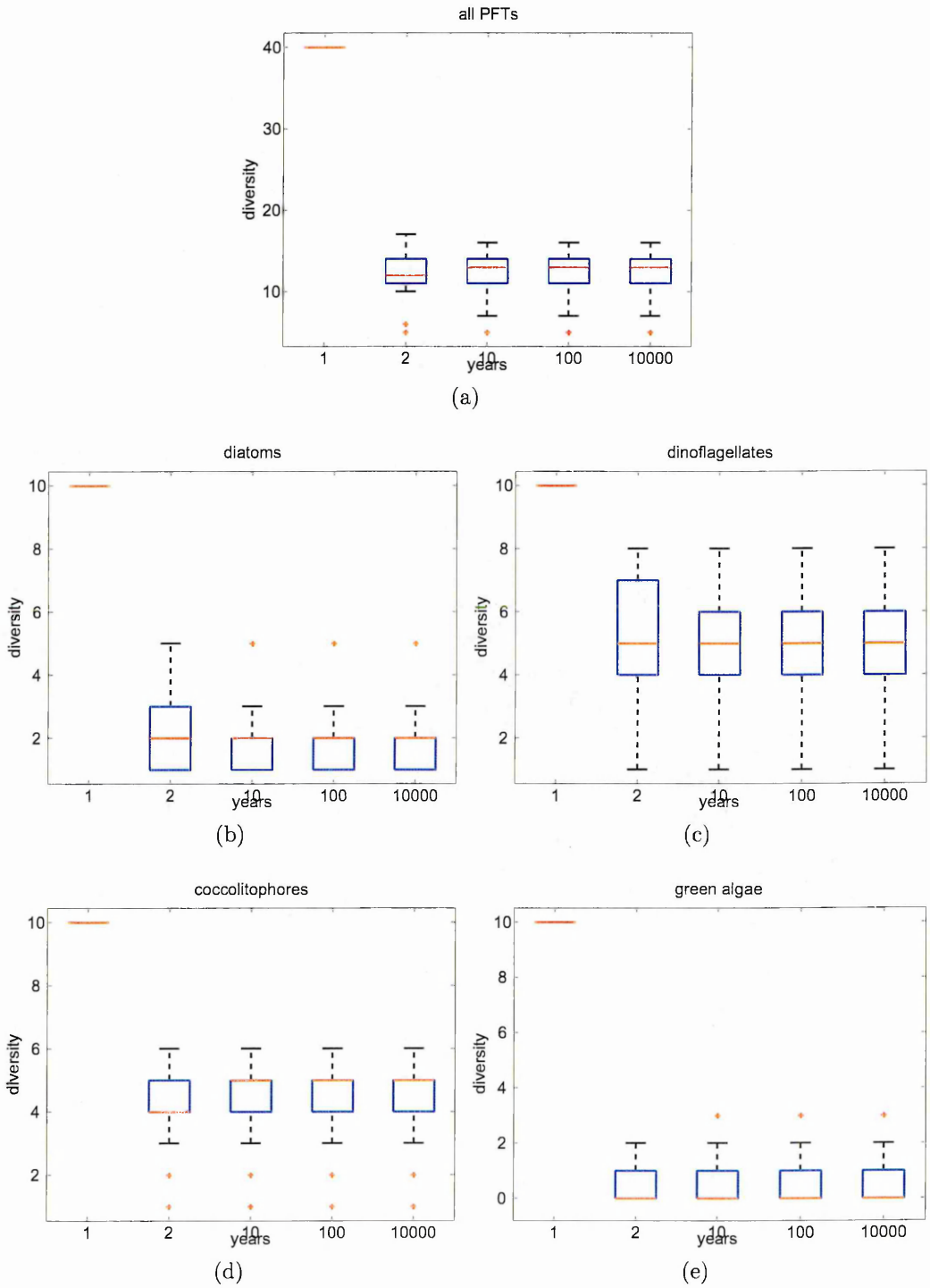

Figure 3.7: Species diversity in the community over the years: (a) all PFTs, (b) diatoms, (c) dinoflagellates, (d) coccolitophores and (e) green algae.

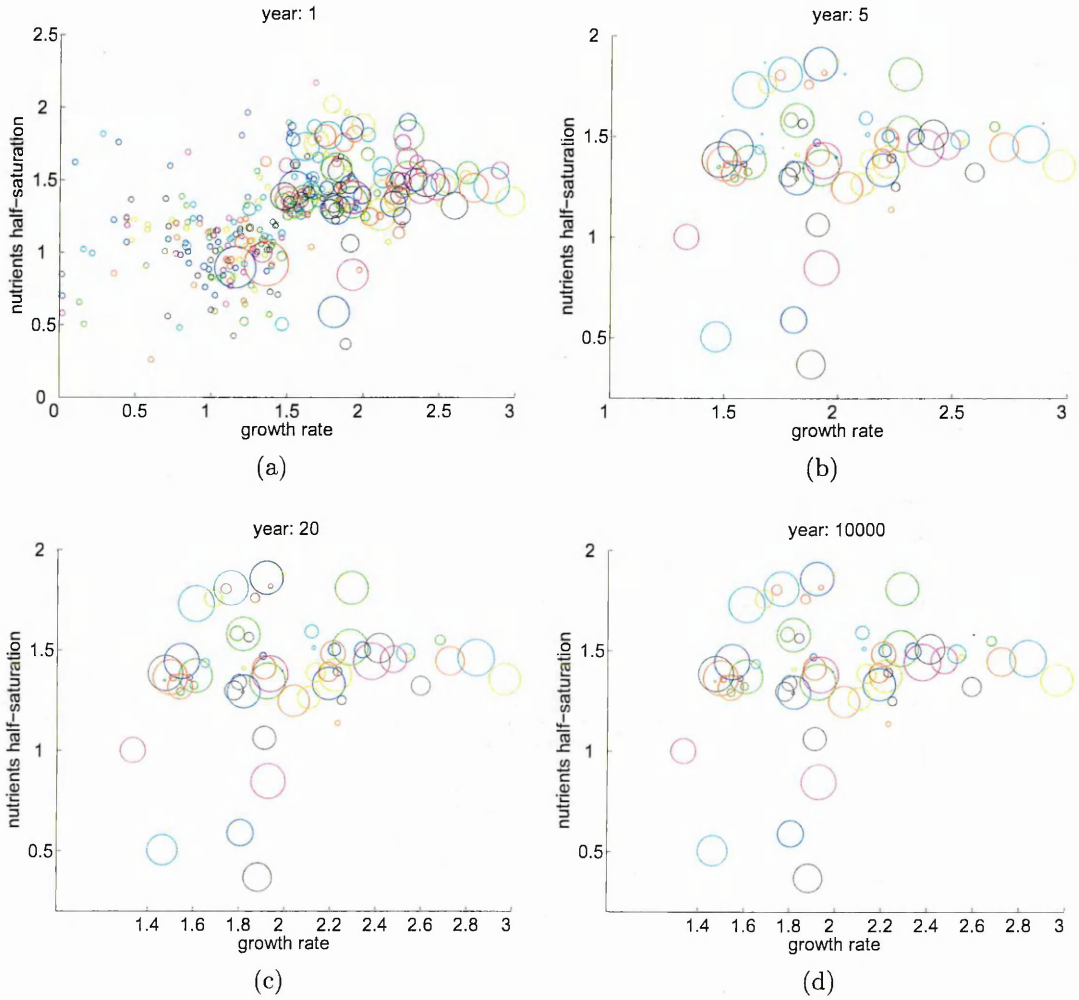

Figure 3.8: Physiological traits distribution of the diatom species enduring through time in the ecosystem in the reference simulation. The plots illustrate how the physiological trade-offs characterising species persisting in the ecosystem altered in the course of the simulation: (a) 1st year of the simulation, thus all seeded species, (b) 5th year and (c) 20th year, thus in the first years of the simulation, and (d) 10000th year of the simulation, thus at the end of the simulation at the steady state. The comparison of the figures (a) and (d) offers an insight into the physiological characteristics of the trade-offs that persisted and extinct in the time course of the reference simulations. Each circle depicts a single phytoplankton species. The size of the circle is proportional to the maximal concentration of the species reached during the year. The plot illustrates the characteristics of the species from all 30 ensemble communities, where the communities were distinguished by colours. The axis represents nitrate half-saturation constant and intrinsic growth rate.

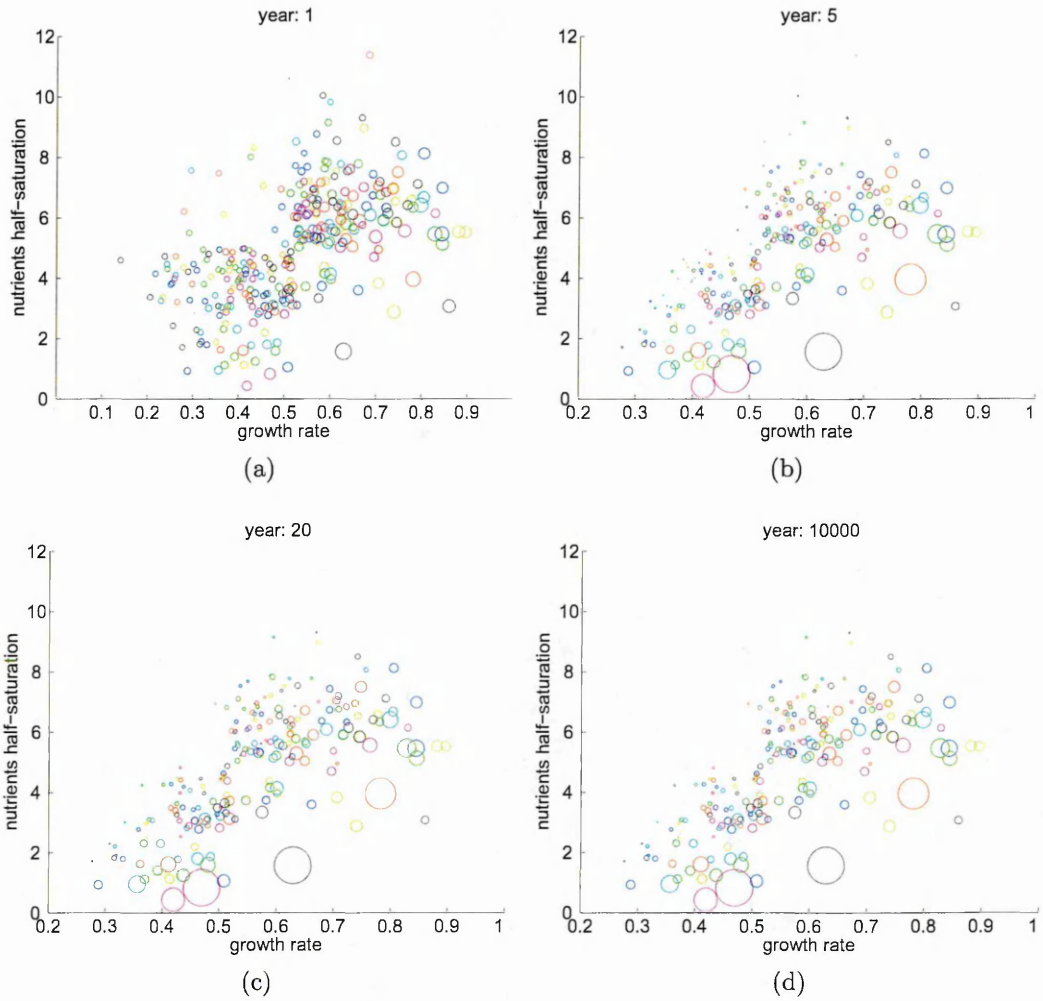

Figure 3.9: Physiological traits distribution of the dinoflagellates species enduring through time in the ecosystem in the reference simulation. The plots illustrate how the physiological trade-offs characterising species persisting in the ecosystem altered in the course of the simulation: (a) 1st year of the simulation, thus all seeded species, (b) 5th year and (c) 20th year, thus in the first years of the simulation, and (d) 10000th year of the simulation, thus at the end of the simulation at the steady state. The comparison of the figures (a) and (d) offers an insight into the physiological characteristics of the trade-offs that persisted and extinct in the time course of the reference simulations. Each circle depicts a single phytoplankton species. The size of the circle is proportional to the maximal concentration of the species reached during the year. The plot illustrates the characteristics of the species from all 30 ensemble communities, where the communities were distinguished by colours. The axis represents nitrate half-saturation constant and intrinsic growth rate.

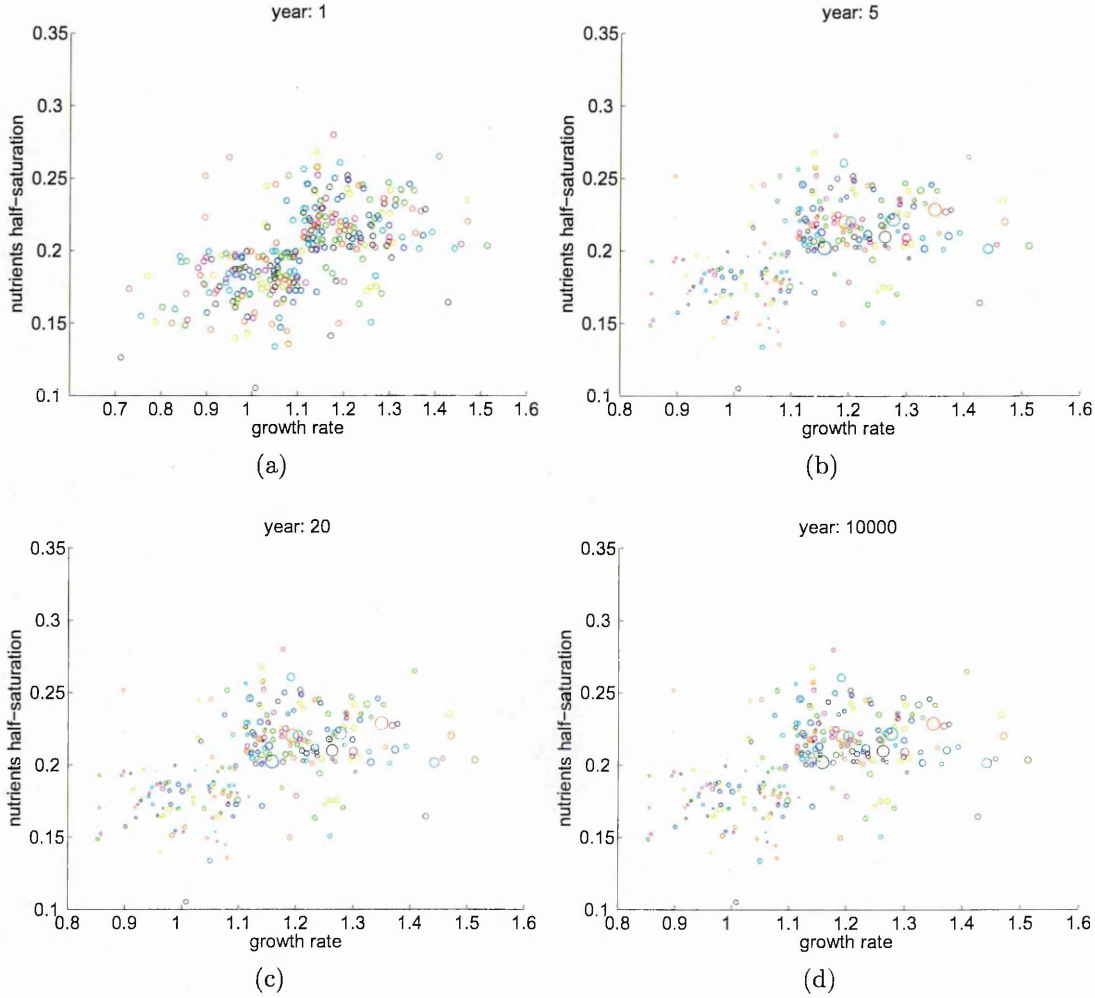

Figure 3.10: Physiological traits distribution of the coccolitophores species enduring through time in the ecosystem in the reference simulation. The plots illustrate how the physiological trade-offs characterising species persisting in the ecosystem altered in the course of the simulation: (a) 1st year of the simulation, thus all seeded species, (b) 5th year and (c) 20th year, thus in the first years of the simulation, and (d) 10000th year of the simulation, thus at the end of the simulation at the steady state. The comparison of the figures (a) and (d) offers an insight into the physiological characteristics of the trade-offs that persisted and extinct in the time course of the reference simulations. Each circle depicts a single phytoplankton species. The size of the circle is proportional to the maximal concentration of the species reached during the year. The plot illustrates the characteristics of the species from all 30 ensemble communities, where the communities were distinguished by colours. The axis represents nitrate half-saturation constant and intrinsic growth rate.

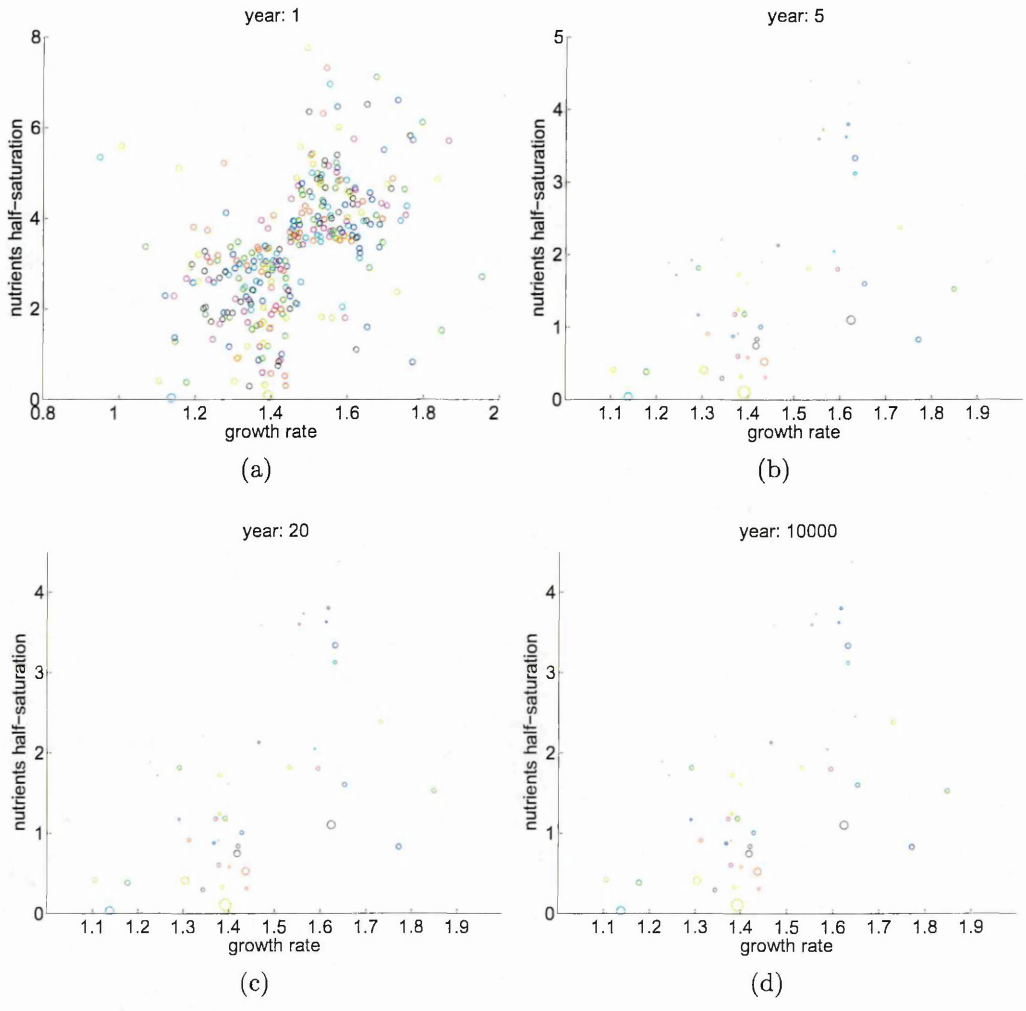

Figure 3.11: Physiological traits distribution of the green algae species enduring through time in the ecosystem in the reference simulation. The plots illustrate how the physiological trade-offs characterising species persisting in the ecosystem altered in the course of the simulation: (a) 1st year of the simulation, thus all seeded species, (b) 5th year and (c) 20th year, thus in the first years of the simulation, and (d) 10000th year of the simulation, thus at the end of the simulation at the steady state. The comparison of the figures (a) and (d) offers an insight into the physiological characteristics of the trade-offs that persisted and extinct in the time course of the reference simulations. Each circle depicts a single phytoplankton species. The size of the circle is proportional to the maximal concentration of the species reached during the year. The plot illustrates the characteristics of the species from all 30 ensemble communities, where the communities were distinguished by colours. The axis represents nitrate half-saturation constant and intrinsic growth rate.

Is the number of initiated species sufficiently high? The number of species decreases rapidly in the first years of the simulations and reaches a steady state after approximately 20years. The emerging patterns of the PFT seasonal abundance are consistent amongst all explored communities, though the species diversity varies as a result of the physiological differences of the seeded and surviving species. Because of that a question on the number of initiated species emerges. Is it sufficient to seed the virtual ecosystem with 40 species? Do those 40 species generate a sufficiently dense coverage of the considered parameter space? In order to establish that, numerical simulations exploring higher number of species (i.e., 100, 400 and 1000) occupying the ecosystem were performed. The initial concentration of all phytoplankton species was equal to $= 10E-6[mmolN/m^3]$. In each explored case the total number of species was equally divided between the considered PFTs, i.e. 25% of the species in each community were diatoms, 25% dinoflagellates, 25% of coccolitophores and 25% of green algae.

The increase in the initial number of species resulted in a slight increase of the median number of the surviving species from 11.5 in the reference case to 14, 13 and 16 in scenarios with 100, 400 and 1000 species respectively (Fig. 3.12). The most considerable change was reported for the minimal number of the species surviving in all the ecosystems which increased from 6 in the reference case to 9 in the scenario with 100 species and 11 in the other two scenarios. The maximal number of the species in all considered communities also increased: from 15 in the reference case to 15 and 16 in the case of 400 and 1000 species, and a staggering number of 22 in the case with a 100 species.

The median number of diatoms surviving in each scenario did not change and was equal to 2 (Fig. 3.12. The median number of green algae remained unchanged in the scenario exploring 100 species, and increased from 0 to 0.5 and 1 in the scenario exploring 400 and 1000 species. The median number of dinoflagellates increased from 5.5 in the reference case to 6.5 and 8 in the scenarios of 100 and 1000 species, but decreased to 5 in the case of 400 species. The median number of coccolitophores increased from 4.5 to 6 and 5 in the scenarios with 100 and 400 species, but decreased to 3.5 in the scenario with 1000 species.

Overall, the general patterns of the diversity expressed in terms of the number of

surviving species were similar in all the explored cases. If the coverage of the parameters space was insufficient when only 40 species were seeded in the virtual ecosystem, a marked change in the diversity patterns should be expected when higher number of species were used in the simulations. In fact, what could be expected is 1) an increase in the diversity or 2) a decrease in the diversity. The former would result from a stronger differentiation of the species and co-occurence of species (or groups of species) complementary in terms of niche or resource partitioning. The latter would originate from a creation of competitively superior species able to exclude all the other species and dominate in the ecosystem.

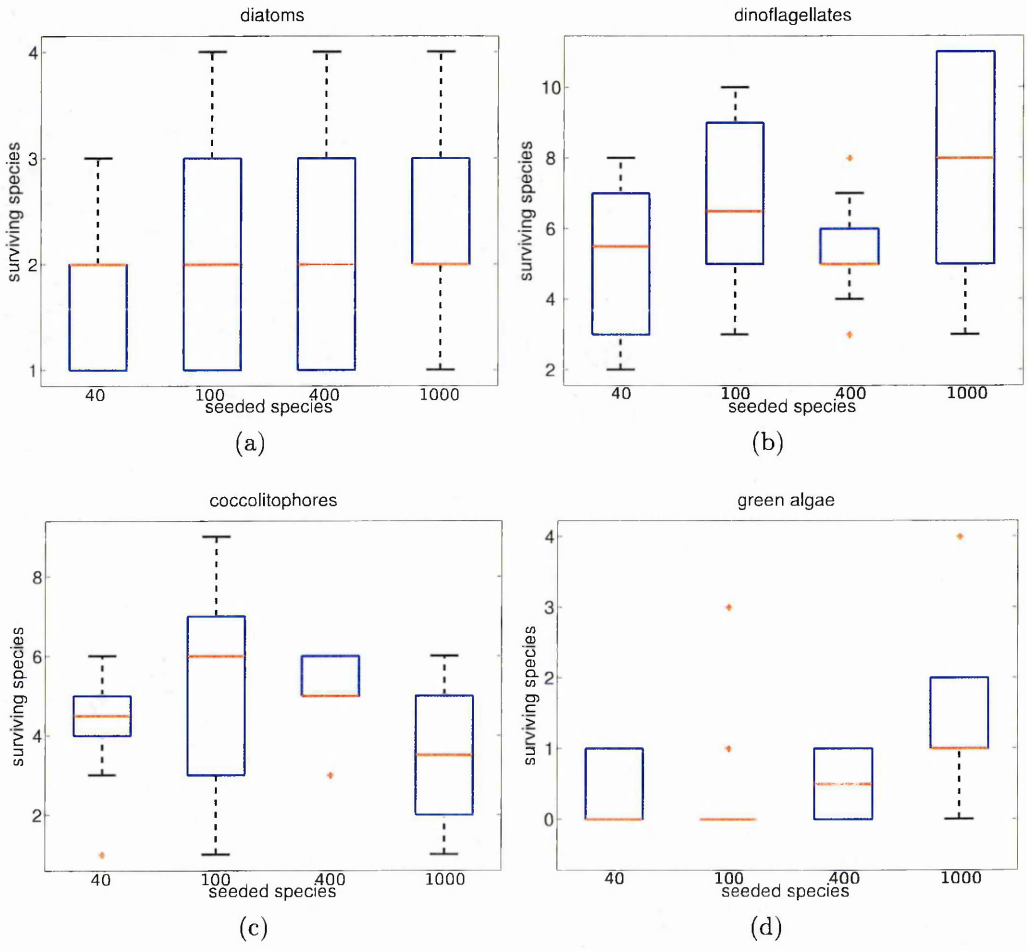

Figure 3.12: Species diversity in the scenarios exploring the number of species seeded in the virtual ecosystem: (a) diatoms, (b) dinoflagellates, (c) coccolitophores and (d) and green algae.

Since neither 1) nor 2) were observed it is reasonable to conclude that the 40 species used in the reference simulation may be considered as sufficient in terms of the parameters space coverage and of the initial resolved diversity, but also that the imposed set of traits and trade-offs unables the creation of the 'super species' (Chapter

2 Section 2.2.2).

The analysis of the traits distribution in the scenarios exploring how number of seeded species may affect community composition and diversity showed that similar species were present in the virtual ecosystems in all cases (Fig. 3.13, 3.14d, 3.15, 3.16). The variability and spread of the physiological traits of the species surviving in all considered scenarios was comparable, as well as the range of parameters characterising the species, i.e. diatoms' species characterised with a similar nutrients half-saturation constant and growth rate were reported (Fig. 3.13). This further confirms that both the number of species with which the ecosystem is seeded and the trade-offs among the physiological traits describing those species are well designed and sufficient to explore questions related to the species diversity.

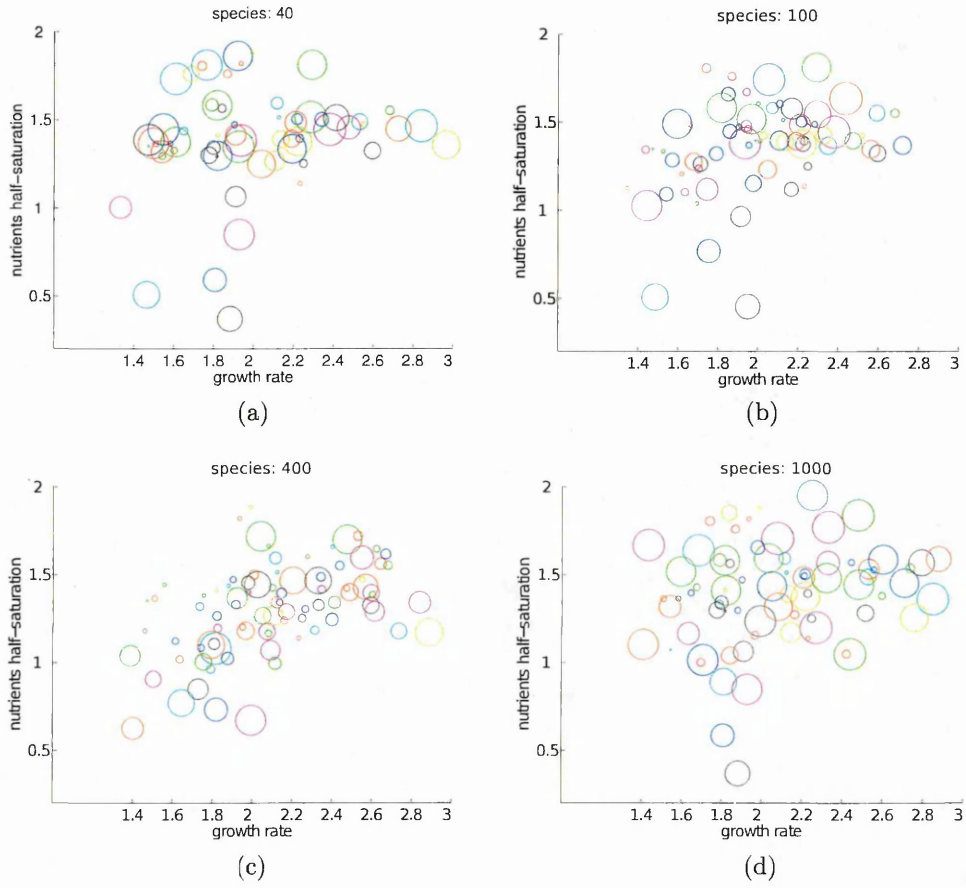

Figure 3.13: Distribution of the physiological trade-offs of the species persisting in the ecosystem distinguished in terms of the number of seeded species. The initial number of the species seeded in the ecosystem was equal to (a) 40, (b) 100, (c) 400 and (d) 1000 species. This number of species was evenly distributed among all the considered PFTs. Each circle depicts a single phytoplankton species. The size of the circle is proportional to the maximal concentration of the species reached during the year. The plot illustrates the characteristics of the species from all 30 ensemble communities, where the communities were distinguished by colours. The axis represents nitrate half-saturation constant and intrinsic growth rate.

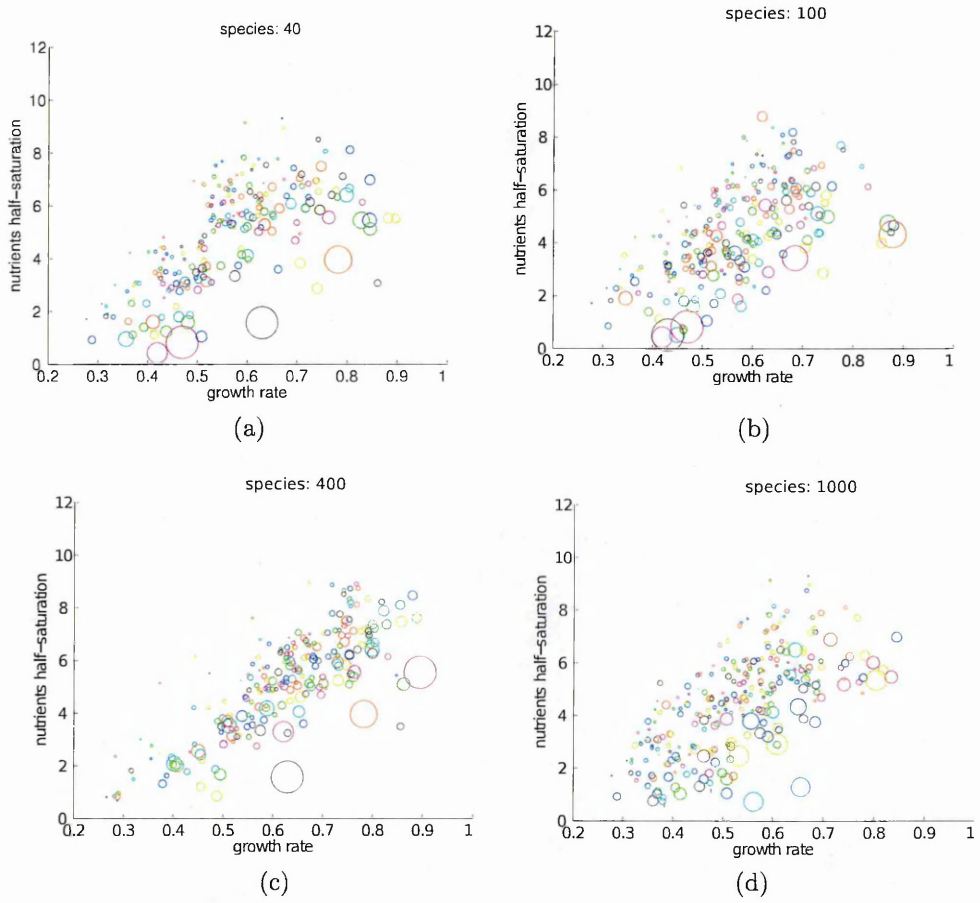

Figure 3.14: Distribution of the physiological trade-offs of the species persisting in the ecosystem distinguished in terms of the number of seeded species. The initial number of the species seeded in the ecosystem was equal to (a) 40, (b) 100, (c) 400 and (d) 1000 species. Each circle depicts a single phytoplankton species. The size of the circle is proportional to the maximal concentration of the species reached during the year. The plot illustrates the characteristics of the species from all 30 ensemble communities, where the communities were distinguished by colours. The axis represents nitrate half-saturation constant and intrinsic growth rate.

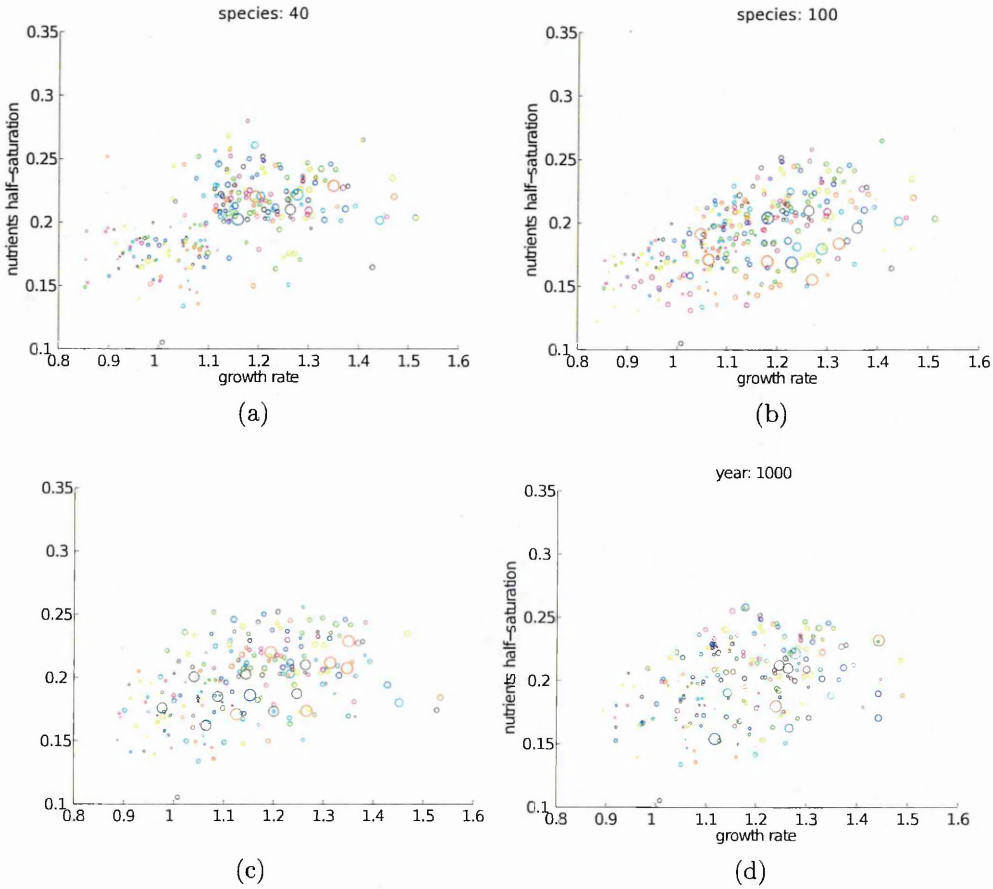

Figure 3.15: Distribution of the physiological trade-offs of the species persisting in the ecosystem distinguished in terms of the number of seeded species. The initial number of the species seeded in the ecosystem was equal to (a) 40, (b) 100, (c) 400 and (d) 1000 species. This number of species was evenly distributed among all the considered PFTs. Each circle depicts a single phytoplankton species. The size of the circle is proportional to the maximal concentration of the species reached during the year. The plot illustrates the characteristics of the species from all 30 ensemble communities, where the communities were distinguished by colours. The axis represents nitrate half-saturation constant and intrinsic growth rate.

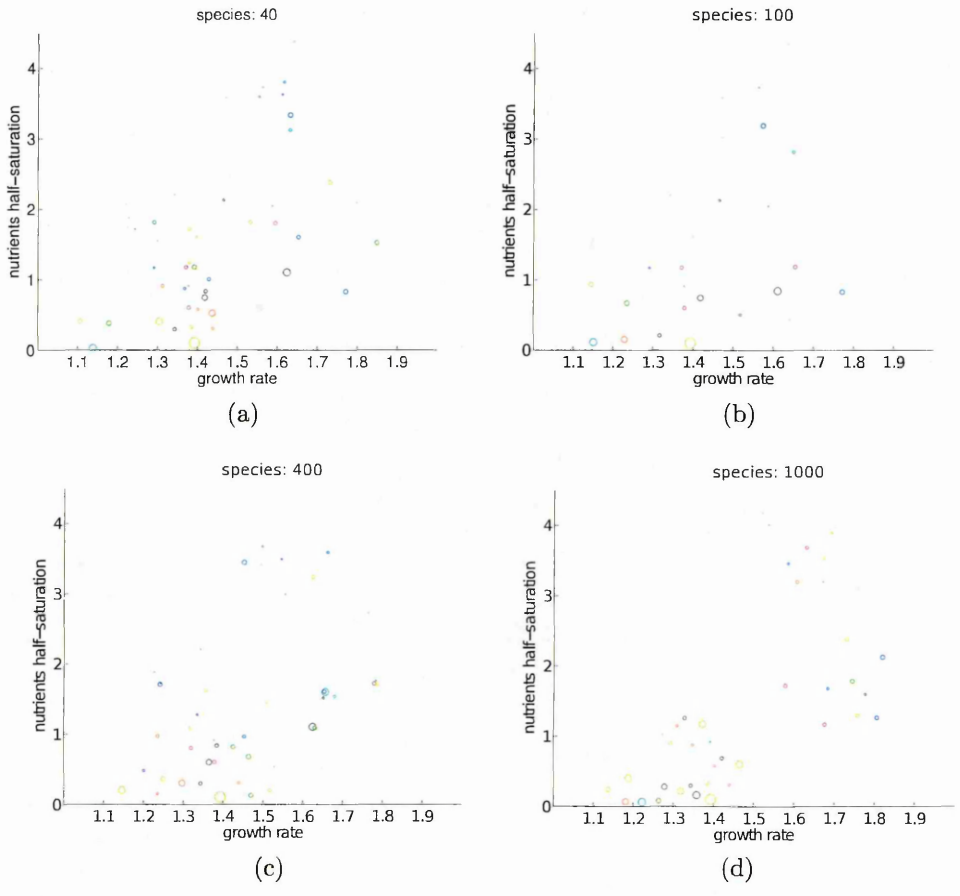

Figure 3.16: Distribution of the physiological trade-offs of the species persisting in the ecosystem distinguished in terms of the number of seeded species. The initial number of the species seeded in the ecosystem was equal to (a) 40, (b) 100, (c) 400 and (d) 1000 species. This number of species was evenly distributed among all the considered PFTs. Each circle depicts a single phytoplankton species. The size of the circle is proportional to the maximal concentration of the species reached during the year. The plot illustrates the characteristics of the species from all 30 ensemble communities, where the communities were distinguished by colours. The axis represents nitrate half-saturation constant and intrinsic growth rate.

3.3 Sensitivity study of the ecosystem to selected processes

The simplicity of the ecosystem model allowed to introduce multiple biological processes into its construction. In the following, the sensitivity to some of these processes is investigated.

3.3.1 "Everything is everywhere" principle

Migration play a major role in aquatic ecosystems: "[we conceive] the pelagic as an open system where communities are continually reshaped by species immigration" (Cloern and Dufford [2005]). Therefore in this subsection, the model includes a constant plankton immigration of trace quantities of every possible species from a predefined, infinite reservoir. This reservoir is not explicitly resolved, but may reflect phytoplankton dispersal linked to water transports and/or turbulent diffusion, thus immigration from neighbouring environments as described by Levy et al. (Lévy et al. [2014]) or featured in metapopulation theory (Hanski and Hanski [1999]; Leibold and Norberg [2004]). Alternatively it may represent permanent background concentrations of dormant life stages (e.g., spores, eggs) capable of waking up in viable environments (Anderson and Rengefors [2006]).

The fate of immigrating species is uncertain - most of them perish (local extinction), but small subsets of species will at times find a niche and either outcompete existing species or coexist with them. Thus, constant supply of individuals may saturates the community with phytoplankton species and affects its self-organisation (Section 2.2).

The net result is reminiscent of a century-old concept from microbiology: "everything is everywhere, but the environment selects." (Beijerinck [1913]; Becking [1934]).

Additionally, this constant immigration further reduces the probability of heteroclinic cycles connecting unstable equilibria. An example of such cycle moves from the monoculture equilibrium of species 1, to the monoculture equilibrium of species 2, to the monoculture equilibrium of species 3, back to species 1 and so on. Heteroclinic cycles are considered to be mostly biologically irrealistic, since species reach extremely low population abundances during these cycles without becoming extinct (May and

Leonard [1975]).

In here the impact of immigration on population dynamics was assessed.

The parametrisation and the intensity of the immigration was taken from Dakos et al. [2009]. The immigration was considered in a static form where the influx of the cells into the system took place from a predefined set. Namely, no new traits combinations were introduced by immigration. Hence, the immigrating cells were representing only the species that were present in the virtual ecosystem in each ensemble community.

The introduction of the immigration required a change in the model equations. Namely a parameter u was introduced into the equations describing change of phytoplankton (Eq. 2.3) and zooplankton (Eq. 2.4) concentration:

$$\frac{dP_i}{dt} = -\frac{q_P}{H} + \mu_i(N, Si, I)P_i - m_{Pi}P_i - \sum_{k=1}^{n} G_{P_{ik}} + u, \tag{3.1}$$

$$\frac{dZ_k}{dt} = -\frac{q_Z}{H} + \omega\left(\epsilon e(\sum_{i=1}^{m} G_{P_{ik}} + G_{D_k}) - m_{Zk}Z_k - m_{Z2k}Z_k^2\right) + u, \tag{3.2}$$

where $u = 1E-6$.

Additional analysis ought to be considered in order to explore how the community composition is to evolve in case of introduction of the new combinations of traits. In fact such simulations and analysis are considered as the continuation of this study.

The introduction of a continuous, constant immigration into the system altered the functional groups seasonal succession pattern - in the presence of immigration green algae emerged as a relevant compartment co-occuring with coccolitophores (Fig. 3.17). Immigration resulted also in a decrease of dinoflagellates abundance and a corresponding decrease in grazers abundance. As a result, the annual bio-geochemical cycle and a trophic cascade were altered. The former due to functional and physiological differences between those phytoplankton functional groups, and the latter due to the decrease in prey abundance.

The introduction of an immigration resulted also in a 17% increase of a median annual value of Shannon index of species diversity and 50% increase if only diatoms were considered (Fig. 3.18). The analysis of a daily Shannon index values indicate that the diversity was elevated throughout the whole year (Fig. 3.19).

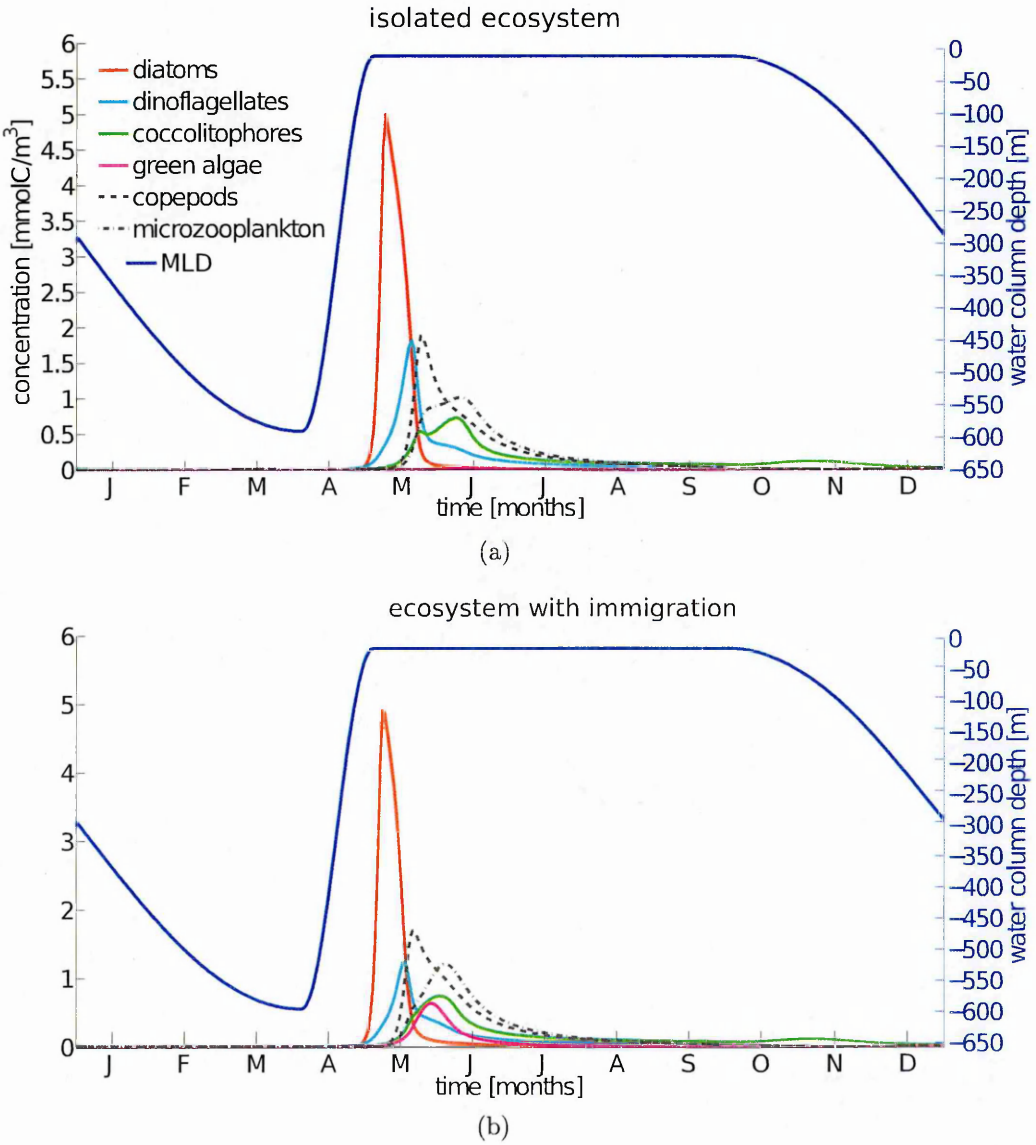

Figure 3.17: Annual cycle at NABE site of modeled phytoplankton functional groups and zooplankton, with an superimposed MLD in (a) reference case and (b) in the presence of a constant background immigration.

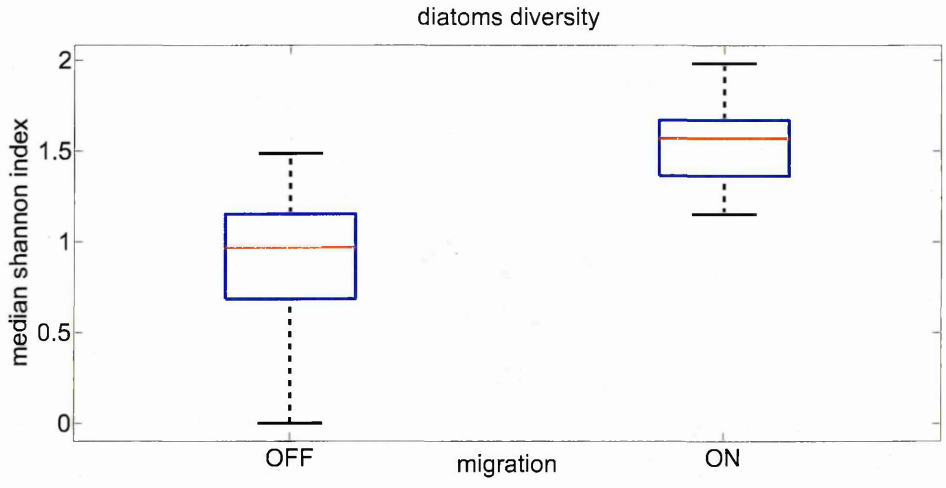

(a)

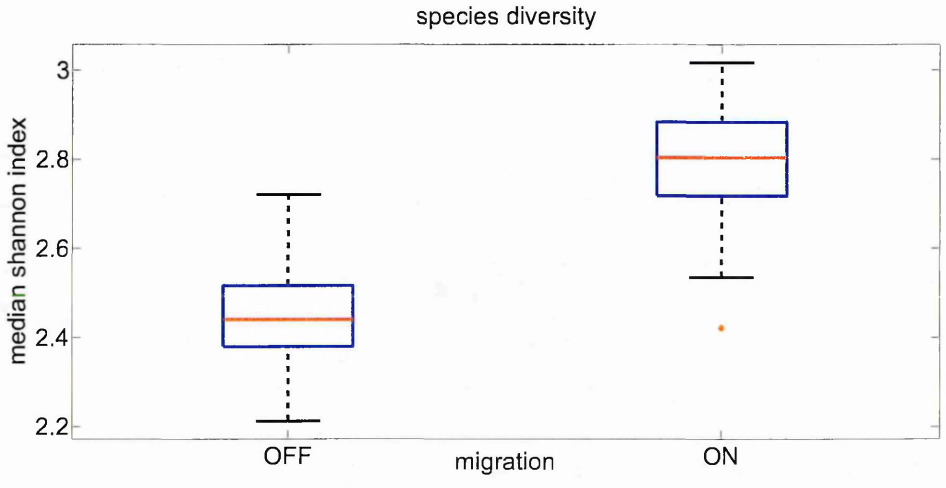

(b)

Figure 3.18: Median Shannon index of diversity for multiple NABE site simulations in case with and without immigration. The median Shannon diversity index values were computed for: (a) diatoms and (b) all the species in for all ensemble community members.

Similarly to the simulations without the immigration (Fig. 3.3b), the minimal diversity coincide with the spring diatom bloom, and the maximal diversity was observed during summer and winter (Fig. 3.19). The subsequent autumn diversity minimum has to be again attributed to the autumn bloom.

At the same time the variability of the diatoms diversity seasonal patterns observed in the absence of immigration (Fig. 3.3a) appeared to stabilise after immigration was introduced and demonstrated considerable convergence across all the ensemble communities (Fig. 3.19a).

The continuous background immigration affected the species richness in the ecosys-

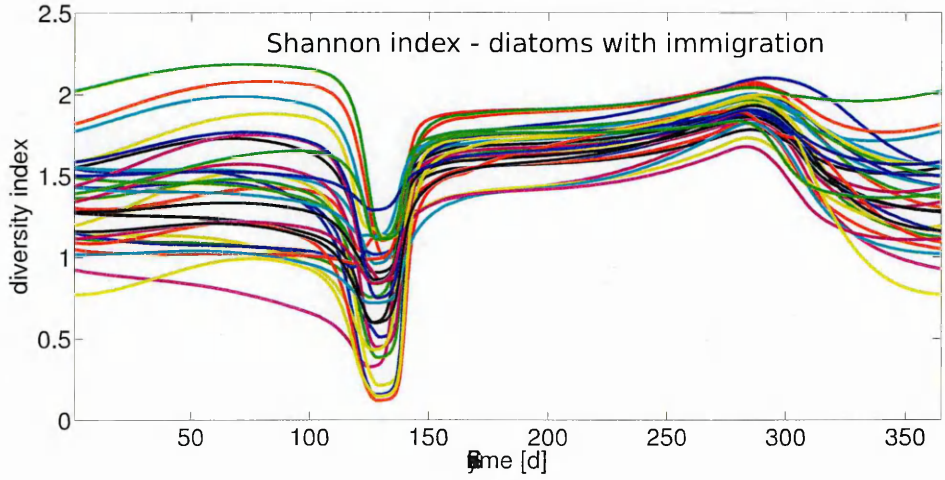

(a)

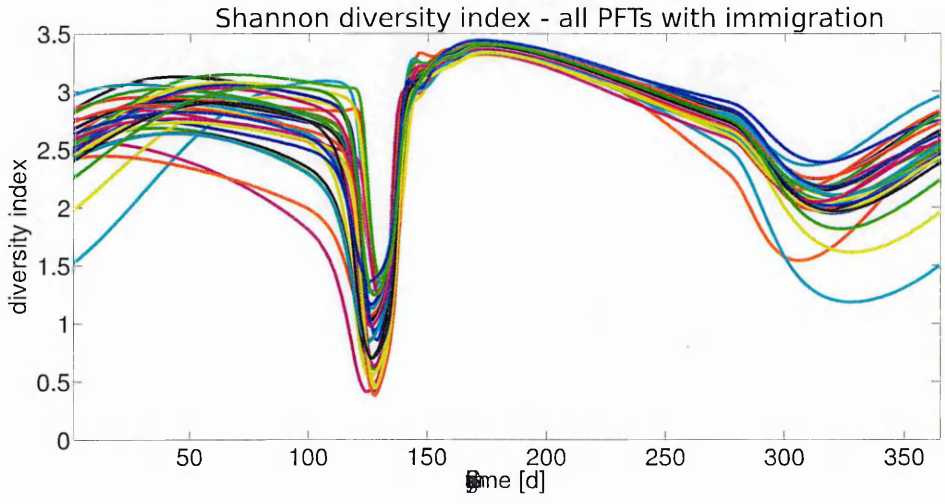

(b)

Figure 3.19: Shannon index of diversity for multiple NABE site simulations in a case considering immigration. Each line depicts seasonal variability of Shannon diversity index value computed for: (a) diatoms and (b) all the species in a single community.

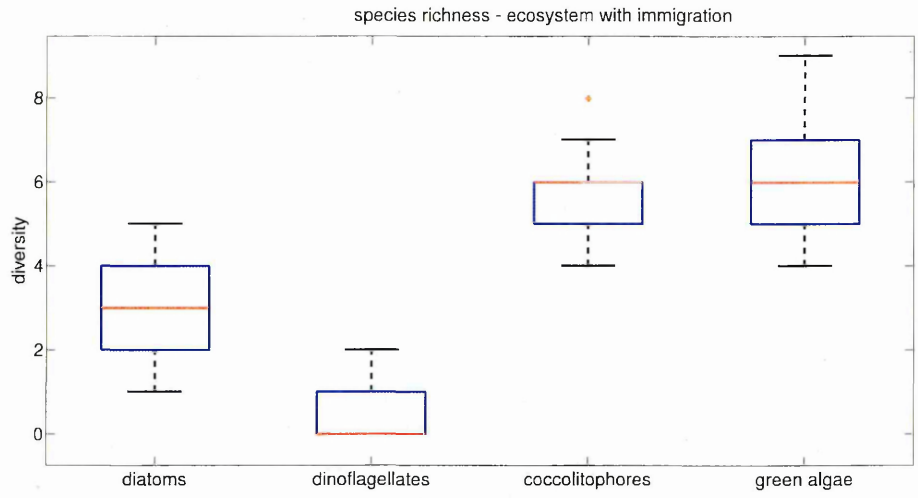

Figure 3.20: Total number of active species (species richness) in each functional group reported across all explored communities in the simulations with a constant background immigration.

tem in all of the resolved functional groups (Fig. 3.20). The median number of active diatoms increased from 2 in the reference case to 3, the median number of coccolitophores increased from 5 to 6, and green algae from 0 to 6, and the median number of active dinoflagellates decreased dramatically from 5.5 to 0 (Fig. 3.2).

The immigration of the cells into the system affected not only the species diversity but also the community composition in all the functional groups. Several relatively slow growing coccolitophores ($0.85 \leq \mu \leq 0.9$) were able to sustain in the ecosystem (Fig. 3.21c), and higher number of relatively less abundant diatoms were observed in the system (Fig. 3.21a). Notably, the physiological characteristics of the active diatoms and coccolitophores in the system with and without immigration were largely identical, though the relative abundance of the species was altered. An extinction of diatoms on a mass scale was observed in the system with a constant immigration, which was represented by a dramatic decrease in the median number of active species (by 5 species). The surviving species were characterised by a low nutrients half-saturation and intermediate growth rate ($0.4 \leq \mu \leq 0.65$, $H_N \leq 2$) or by a relatively high growth rate and intermediate nutrients half-saturation ($0.65 \leq \mu$, $2 \leq H_N \leq 6$) (Fig. 3.21b). Thus, covered only a fraction of the phase space from the reference case. The green algae increased in the abundance and diversity, in fact as a result of the boosted population accumulation rate most of the green algae species were able to sustain the

ecosystem (Fig. 3.21d).

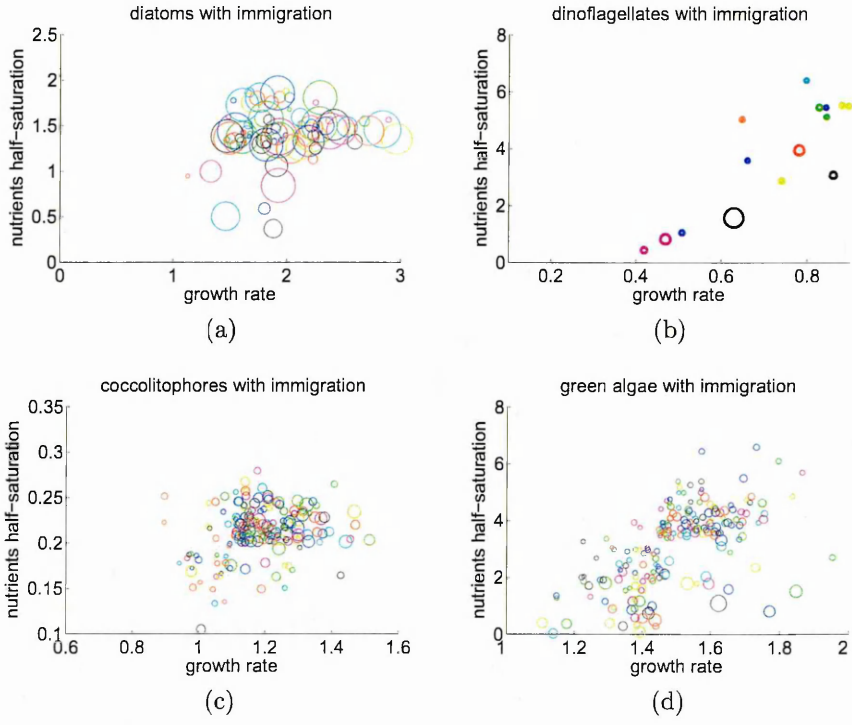

Figure 3.21: Distribution of the physiological trade-offs of the species persisting in each resolved PFT in the ecosystem perturbed with a continuous phytoplankton immigration: (a) diatoms, (b) dinoflagellates, (c) coccolitophores and (d) green algae. Each circle depicts a single phytoplankton species. The size of the circle is proportional to the maximal concentration of the species reached during the year. The plot illustrates the characteristics of the species from all 30 ensemble communities, where the communities were distinguished by colours. The axis represents nitrate half-saturation constant and intrinsic growth rate.

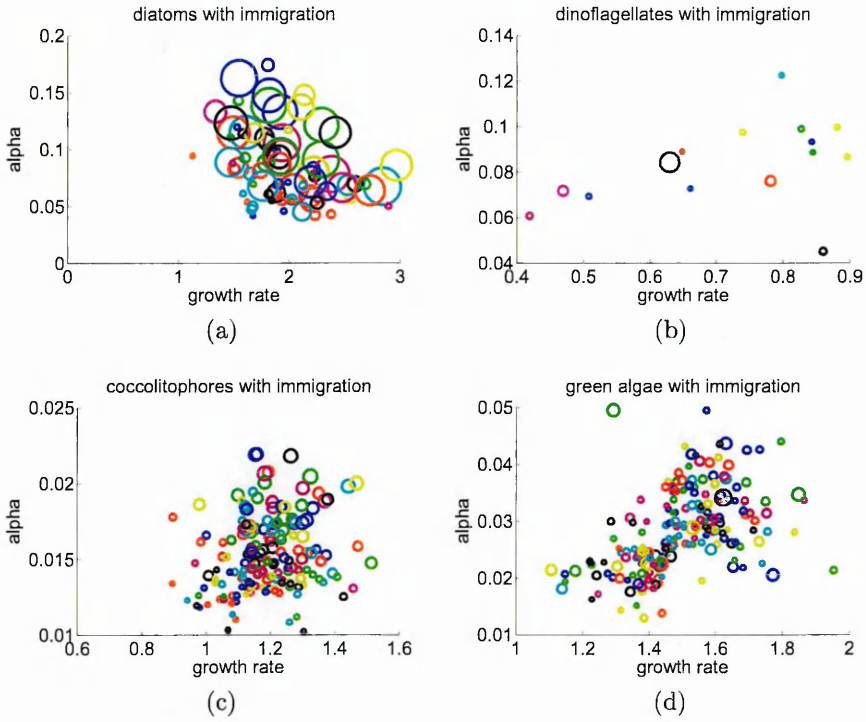

Figure 3.22: Distribution of the physiological trade-offs of the species persisting in each resolved PFT in the ecosystem perturbed with a continuous phytoplankton immigration: (a) diatoms, (b) dinoflagellates, (c) coccolitophores and (d) green algae. Each circle depicts a single phytoplankton species. The size of the circle is proportional to the maximal concentration of the species reached during the year. The plot illustrates the characteristics of the species from all 30 ensemble communities, where the communities were distinguished by colours. The axis represents initial slope of the P-I curve and intrinsic growth rate.

3.3.2 Copepods dormancy

Because of the model equations non-linearities, a controlled 'decrease' of its complexity (by eliminating the assumption one at a time) was far more illustrative, than most basic model formulation and building up the complexity with additional mechanisms and processes. The full model formulation was thus treated as a reference case, the indicated model assumptions were relaxed and the results were presented. In particular, the model formulation consisted a formulation describing copepods dormancy. The below analysis explore scenarios differing in terms of the dormancy duration (from 40 to 135 days in scenarios $th_{OD} = 550m$ and $th_{OD} = 200m$ respectively) but also a scenario in which there was no dormancy ($th_{OD} = 600m$).

Copepods winter dormancy was incorporated into the model as one of the default mechanisms (Chapter 2). The transition from active to dormant state and vice versa was associated to a certain MLD value. Namely, when mixing exceeds a critical depth,

th_{OD}, a state transformation takes place. In this section ecosystems sensitivity to th_{OD} value was explored. Specifically, the th_{OD} value was altered from 200 to 600m with a 50m step and the simulations have been repeated for all the ensemble members. The simulation set-up was identical with that presented in Chapter 2 Section 3. These values of overwintering depth translate into different time spans of dormancy periods ranging from 40 days (for $th_{OD} = 550m$) to 135days (for $th_{OD} = 200m$), and coincided with the deepest mixing period. Notably, $th_{OD} = 600m$ indicates a scenario with no copepods dormancy. The rate of the active-dormant-active transition, parameter s (Chapter 3, Section 2.3, Eq. 20) , was identical for all the investigated depths.

Copepods dormancy affects both their grazing and mortality rates. As it coincides with the deepest mixing periods, in which phytoplankton abundance reaches an annual minimum, dormancy mostly affects copepods mortality rates. By decreasing winter loss rates, copepods enter spring period at slightly higher concentration with respect to simulations without dormancy. Consequently it would result in a shift in phytoplankton seasonal abundance (Fig. 3.23). The strongest impact was observed in case of coccolitophores and dinoflagellates. The concentration of the former increased by 44% (median value for all the communities; Tab. 3.3) and the peak was advanced by 6 days (median value for all the communities; Tab. 3.2). A delay of 2.5 days of the peak concentration and a 41% decrease in its value was reported for the latter. The peak concentration of copepods increased by 13% with respect to the case without overwintering (median value for all the communities; Tab. 3.3) and took place 6 days earlier. Overwintering had very little impact on green algae and microzooplankton dynamics. Overall, copepods dormancy had a negligible effect on diatoms communities and consequently on spring bloom formation which was initiated on average on 123[yd] and peaked at approximately 4.96±0.4 $[mmolC/m^3]$ irrespectively to the overwintering depth value (Fig. 3.23; Tab. 3.2, 3.3). Furthermore, copepods overwintering affected in a limited form species diversity. Namely, the annual median value of Shannon diversity index computed for diatoms increased by 10% in a scenario considering dormancy, and the annual median value of Shannon diversity index computed for all species decreased by 2% (median value for all the communities; Tab. 3.1). The number of active species remained insensitive for presence or absence of dormancy, but also for the changes in

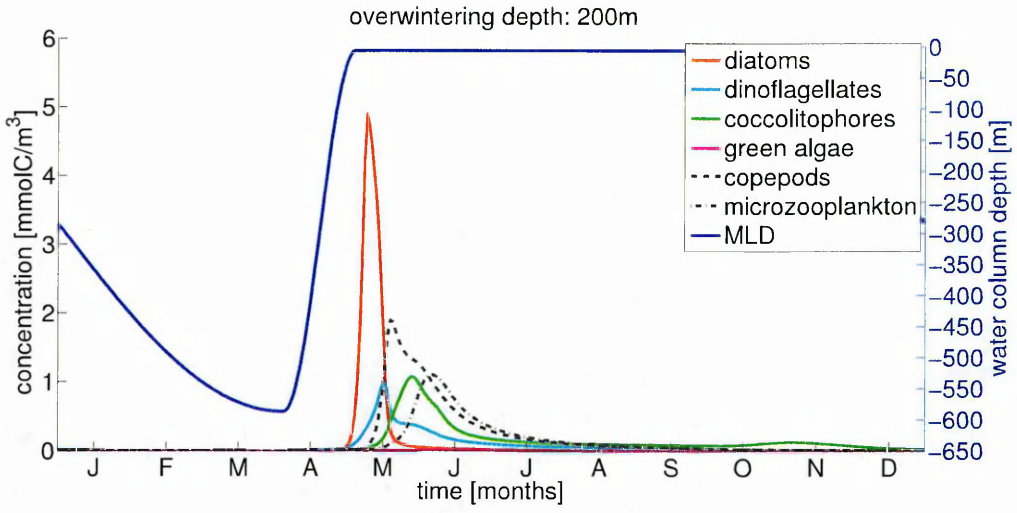

(a)

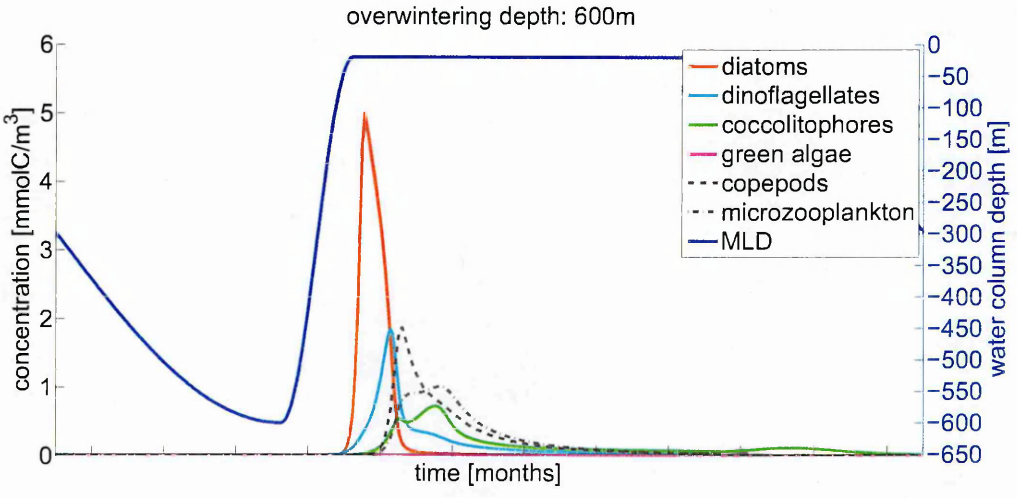

(b)

Figure 3.23: Copepods dormancy impact on functional groups seasonal abundance. Functional groups abundance (a) with and (b) without copepods winter dormancy.

overwintering depth (Tab. 3.1).

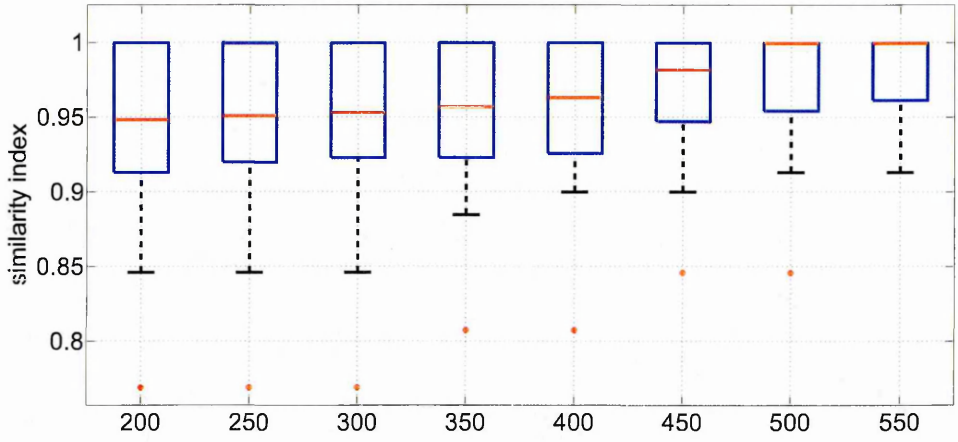

Figure 3.24: Community similarity index for various values of the copepods dormancy depth threshold. The similarity index was computed with respect to the simulations in which the copepods dormancy was absent. The value of 600m represents a case without copepods dormancy.

Overwintering depth	200	250	300	350	400	450	500	550	600
Species richness	15	15	15	15	15	15	15	15	15
Shannon index for diatoms	1.07	1.04	1.02	1.05	1.02	0.98	1.01	0.97	0.97
Shannon index for all PFT	2.39	2.40	2.41	2.40	2.41	2.42	2.43	2.42	2.43

Table 3.1: Species richness and median Shannon diversity index of diatoms and all PFTs computed for various overwintering depths. The values were computed for al ensemble community members to account for differences in community composition. The value of 600m represents a case without copepods dormancy.

Overwintering depth	200	250	300	350	400	450	500	550	600
Time of the peak									
Diatoms	128.0	128.0	128.0	128.0	128.0	128.0	128.0	128.0	128.0
Dinoflagellates	145.0	141.5	141.0	141.0	140.0	140.5	141.0	141.0	142.5
Coccolitophores	151.0	151.0	152.0	152.0	152.0	153.0	153.0	154.0	157.0
Green algae	158.5	158.5	159.5	159.5	159.5	160.5	160.5	161.0	162.0
Copepods	138.0	139.0	139.0	140.0	140.0	141.0	141.5	142.0	144.0
Microzooplankton	158.0	158.0	159.0	159.0	160.0	160.0	160.5	161.0	162.5
Bloom initiation	123.0	123.0	123.0	123.0	123.0	123.0	123.0	123.0	123.0

Table 3.2: Median values of the functional groups peak concentration timing [year day] in simulations with various values of copepods overwintering depth. Additionally, the last raw informs on the median time point of spring bloom initiation. The values were computed for all ensemble community members to account for differences in community composition. The value of 600m represents a case without copepods dormancy.

Overwintering depth	200	250	300	350	400	450	500	550	600
Maximum concentration									
Diatoms	4.92	4.94	4.95	4.96	4.97	4.98	4.98	4.99	5.00
Dinoflagellates	0.43	0.45	0.46	0.47	0.49	0.52	0.56	0.61	0.73
Coccolitophores	1.15	1.09	1.05	1.01	0.96	0.92	0.87	0.85	0.80
Green algae	0.11	0.11	0.11	0.11	0.11	0.11	0.11	0.12	0.12
Copepods	1.55	1.52	1.51	1.49	1.48	1.46	1.45	1.43	1.37
Microzooplankton	1.23	1.23	1.22	1.22	1.22	1.21	1.21	1.19	1.18

Table 3.3: Median values of the functional groups peak concentration $[mmolC/m^3]$ in simulations with various values of copepods overwintering depth. The value of 600m represents a case without copepods dormancy. The values were computed for all ensemble community members to account for differences in community composition.

3.4 Discussion

The hypothesis that phytoplankton diversity affects the ecosystem functioning has received a considerable empirical support in recent years (Ptacnik et al. [2008], Cardinale et al. [2011]). It has been demonstrated that, averaged over different species and habitats, diversity decrease impacts the biomass and resource-use efficiency of the primary producers, and might affect primary productivity (Ptacnik et al. [2008], Cardinale et al. [2011]). These responses vary, however, in strength and direction for different types of ecosystems and different indicators of ecosystem functioning such as producer biomass, nutrient concentrations, or primary production (Hooper et al. [2005]; Cardinale et al. [2011]).

Phytoplankton diversity influences ecological and biogeochemical processes as it relates to the community composition which forms the basis of the pelagic food web (Duffy et al. [2006]). The composition of the phytoplankton community may have impact on biomass production, elemental cycling, and atmospheric composition (Falkowski et al. [1998], Balmford et al. [2002], Daily [1997]). Yet, the role of diversity in controlling marine pelagic ecosystems functioning remain not well understood partially because of scarce experimental observations (Duffy et al. [2006], Ptacnik et al. [2010]).

Because of the anticipated change in the structure of the marine phytoplankton community (Morán et al. [2010], Boyd and Doney [2002], Worm et al. [2002], Cardinale et al. [2006]) and its effects on ecosystem structure and functioning (Bopp et al. [2005], Manizza et al. [2010]), the nature of processes driving marine phytoplankton diversity is becoming one of the central scientific question.

A growing number of ocean models begun resolving the community structure via the explicit representation of several phytoplankton functional groups (Totterdell et al. [1993], Moore et al. [2002]; Gregg et al. [2003], Litchman et al. [2006]), nevertheless significant challenges are still present (Chapter 1, Anderson [2005], Hood et al. [2006]). Among them a scarce knowledge on phytoplankton physiology is frequently recognised. Because of the limited quantitative information from laboratory cultures and field observations, the correct evaluation of the parameters controlling planktonic species dy-

namics remains problematic. Accordingly, the specification of functional groups in the vast majority of ecosystem models is subjective and somewhat arbitrary. The results generated by such models might strongly depend on the combination of parameter values, in particular those related to species physiology and community composition. Hence, it is possible that a different combination of parameters, with each of these parameters within its acceptable range may produce a different outcome despite identical physical conditions and thus decrease the results reliability.

Even though there are no mechanistic models able to capture the degree of biodiversity observed in natural ecosystems, modelling approach provides an important framework for broadening our knowledge on phytoplankton diversity and distribution patterns in the global ocean. The NPZD marine ecosystem models in which nutrients, phytoplankton, zooplankton and detritus form the main model structure (e.g. Steele [1974]; Wroblewski et al. [1988]), continue to demonstrate their value in both regional and global modelling studies (e.g. Kawamiya et al. [2000]; Palmer and Totterdell [2001]; Anderson and Pondaven [2003]; Schartau and Oschlies [2003]). The approach employed in here considered such a traditional NPZD model augmented with an explicit representation of phytoplankton species diversity (Chapter 2). Phytoplankton community was formed by four functional groups of phytoplankton (Moore et al. [2002], Gregg et al. [2003],Litchman et al. [2006], Quere et al. [2005]): diatoms, coccolitophores, dinoflagellates and green algae, where each functional group consisted of a relatively large number (here 10) of phytoplankton species differing randomly in physiology.

The approach was inspired by the "Darwin" ecosystem module embedded within the Massachusetts Institute of Technology general circulation model (Follows et al. [2007]). It allows for a direct and transparent interpretation of processes affecting bulk properties of the planktonic community but above all community composition and species diversity. Despite advantages it offers, an explicit diversity representation is seldom considered in the 0D models and by far remains a domain of the global 3D models.

The simplified description of phytoplankton physiology incorporated traits regulating species light and nutrients affinity, growth rate, and resilience to grazing, bounded through the allometric relationships (Chapter 2). The community structure was im-

posed only initially, and "self assembled" itself according to the relative fitness of the phytoplankton types in the seasonally varying resource and predatory environment. Because of that the final community structure emerged because of the top-down and bottom-up processes and gave rise to the seasonal succession of the functional groups observed in the course of simulations.

Environmental conditions in the subpolar environment change over the year. The transition from high-turbulence, high-nutrient environment (winter) to a stratified depleted environment (summer) creates niches occupied by different phytoplankton groups, namely diatoms, coccolithophores and dinoflagellates. Phytoplankton functional groups seasonal succession can be explained by differences amongst group-specific affinities for limiting nutrients (Margalef's Mandala Margalef [1978] discussed also in Chapter 2). The concept of affinity-driven species succession is applicable also to seasonal succession observed in the model results. Diatom species characterised with low nutrient affinities drawdown nutrients while blooming and are replaced by coccolitophores characterised with higher nutrient affinity.

Margalef's Mandala explains seasonal succession in terms of bottom-up processes. Discussed above nutrients affinities are connected with cells size and morphology (Chisholm [1992], Aksnes and Egge [1991],Sournia [1982]). Size is considered as a key trait for both phyto- and zooplankton. Larger grazers can successfully consume larger phytoplankton better than smaller grazers can (Reynolds et al. [2006], Sterner [1989]). Thus, grazing pressure is a function of phytoplankton and zooplankton size (Armstrong [1999]) but also the seasonal abundance of different grazers contribute to the seasonal succession of phytoplankton functional groups (Sterner [1989]). In the model simulations, increasing copepods grazing pressure contributes to the spring bloom termination, and microzooplankton controls abundance of small phytoplankton species during summer.

Phytoplankton functional groups succession can be explained in terms of seasonal fluctuations in resources availability and grazing pressure. In fact, bottom-up and top-down processes are frequently invoked also when species co-existence is discussed (Chapter 1; (Gause [1934], Armstrong and McGehee [1980], Stewart and Levin [1973], Tilman [1977], Chesson [2000], Prowe et al. [2012a]).

In the previous chapter bulk properties of the phytoplankton community have been

discussed and validated against appropriate *in situ* measurements. The validation of the diversity patterns discussed in here appears to be problematic, as there are no data available on the community composition in the subpolar ecosystems throughout the year. Species diversity in the mid-latitude ecosystems represents a grey area spanning from few species to maybe dozens, hundreds, thousands of species. Indeed it is not known how many species are present in there.

Phytoplankton diversity remains ambiguous for the vast majority of the marine ecosystems. Except for several ecological stations our knowledge on planktonic community composition and how it changes over the seasons is vague if not null. It is clear that numerous phytoplankton species do coexist in natural environments. For instance, over 400 phytoplankton species have been reported at the long-term ecological research station MareChiara (LTER-MC) in the Gulf of Naples (Mediterranean Sea). Hopefully similar data will be available in the near future also for the North Atlantic thanks to autonomous devices such as automated buoy system capable of assessing species diversity (personal communication of Lisa Campbell, Department of Oceanography, Texas A& M University).

It is clear that the diversity in the virtual ecosystem underestimates that observed in the nature (see also Chapter 1). Since it is impossible to reproduce the (unknown?) community composition in the subpolar ecosystems, the discussion on the species richness observed in the model can only be limited to the broad, general information regarding its seasonal variability and nature of processes affecting it.

As described in Chapter 2, each ensemble phytoplankton community was seeded with 40 stochastically generated species representing 4 different functional groups. Most of these species were excluded from the system within first years of simulations because of the competitive interactions and grazing pressure. Thus the remaining 15 or so species thriving to survive in the virtual ecosystem represented only a fraction of the original phytoplankton community. The number of species in each ensemble community ranged from 10 to 19 species, with the median value of 15. The number of species within functional groups varied as well, i.e., diatoms from 1 to 4, dinoflagellates from 1 to 7, coccolitophores from 5 to 8 and green algae from 0 to 2, with the median values of 3,5,7 and 1 for each group respectively.

Species physiology was randomly generated, as the coefficients describing species growth rate, nutrients and light affinities were provided by random selection within broad ranges defined for each functional group (Chapter 2). The differences in the diversity observed among the explored communities can be attributed to the traits distribution. These differences suggest that some combinations of traits were complimentary and allowed for coexistence of higher number of species leading to elevated diversity within functional groups. A systematic analysis of the traits distribution and observed diversity will be a subject of the analysis in the continuation of this study.

The stochastic approach imposed a risk that some of the species might be similar or even identical in terms of their growth rate and resources requirement, hence also in terms of their competitive abilities. Competitive exclusion (Hardin et al. [1960]) may operate on time scales of thousand years in environments characterised with either short (hours to days) or long (annual and longer), as well as on a time scale of several years or less if the environmental conditions vary on monthly time scale. It has been suggested that the competitive exclusion in subpolar environment operates on a relatively short time scale (years) because of strong seasonal variability in mixing and nutrients availability (Barton et al. [2010]). In order to assure that sufficient time has been provided for competitive exclusion to take place, each simulation has been performed over a 10000 years period. Indeed, most of the species declined towards extinction within first years of the simulations, and no indications of extinction were observed afterwards. Because of that the assembled community in each simulation was composed of physiologically distinct species which co-existence was stable over short and long periods of time.

The biogeochemical cycle, as discussed in Chapter 2, were preserved across all ensemble communities regardless of the community composition and species diversity. Hence, these communities could be considered as ecological analogs, but it would be an oversimplification to assume that. Indeed, the bulk properties of all considered community are similar and show good agreement with *in situ* in terms of seasonal concentration of chlorophyll-a, particulate organic carbon, etc. But at the same time the observed differences in community composition and species diversity make them vastly different in terms of their response to e.g., changes in physical forcing characteristics.

Anticipating the results presented in the next chapter, community composition may have a dramatic impact on ecosystem response to e.g., shoaling of the mixed layer depth. The analyses of a single community could overestimate or underestimate effect of maximal MLD change on the species diversity, community composition, phytoplankton productivity, trophic cascade efficiency, etc. Because of that the consideration of multiple phytoplankton communities is required to properly account for differences in community composition and phytoplankton diversity strongly underestimated in the current plankton models.

In light of above, despite its simplicity, the presented modelling approach demonstrates to be useful for investigation of the relationship between diversity and ecosystem functioning

The enormous increase in the computational power of modern computers revolutionized the marine ecosystem modelling studies - it has made it possible to investigate biogeochemical cycles at the global scale (Moore et al. [2002], Gregg et al. [2003], Quere et al. [2005], Follows et al. [2007]). The gradual introduction of relevant, novel mechanisms into the existing models was expected to increase their skill and improve our understanding of ecosystems functioning. Complexity in nature was mirrored by complexity in models. It is important however that model's complexity should be built up gradually making it possible to recognise what is important and what is not. Building up model complexity does not necessarily guarantee improved predictions unless key processes associated with system feedbacks are represented (Doney [1999], Pomeroy [2001], Dearman et al. [2003]) and accompanied by a sufficiently accurate and robust parametrization (Anderson [2005]). As such the development of new and/or improved ecosystem model formulations allowing for more realistic representation of model's compartments ought to be a priority. Clearly, these formulations ought to be first tested before inclusion in site-specific and local/global models.

I have presented such test study below. Namely I have explored two mechanisms, immigration and copapods dormancy, and their impact on ecosystem functioning. I investigated how these processes affected biogeochemical cycles and trophic cascade, but also if and how they altered species diversity.

The role of immigration The selection pressure applied to assemblages of different species leads to a change in its (community) structure (Levin [1998]; Leibold and Norberg [2004]). It has been recognised, that the rate at which the community responds to selection pressure is tightly linked with the diversity (Wirtz and Eckhardt [1996]; Norberg et al. [2001]) and consequently the diversity plays a major role in models, describing the adaptive behavior of communities. The presence and persistence of biodiversity is often linked to spatio-temporal heterogeneity (Tilman et al. [1982], Tilman and Kareiva [1997]; Chesson [2000]). In the model presented in this chapter, temporal heterogeneity was produced via seasonally fluctuations of light intensity and MLD. Despite the explicit planktonic community structure, these fluctuations proved capable of inducing seasonal changes in community structure.

The studies addressing species diversity often rely on a continuous species immigration (Norberg et al. [2001], Bruggeman and Kooijman [2007], Dakos et al. [2009]). Not surprisingly, the rate of immigration is crucial: a weak input remains negligible, whereas a strong input keeps the community close to its reference state and prevents it from adapting to changing physical conditions.

The basic model configuration used in this study does not include immigration, however its impact on population dynamics and species phenology had been addressed (Sec. 3.3.1).

Stochastic approach to species description (Chapter 3 Section 2.2) resulted in multiple phytoplankton species introduced into a specified environment. In the course of simulation, the competition for resources and grazing pressure led maladapted species to extinction. Consequently, most of the initial species diversity was lost within couple of seasons in the reference scenario representing an isolated ecosystem. Notably, isolated marine ecosystems do not exist in nature, hence introducing immigrations into ecological models represent a simple step towards realism.

Ocean dynamics (e.g., lateral advection and stirring due to planetary waves) mix organisms from different habitats which may maintain coexistence of multiple phytoplankton types (Richerson et al. [1970], and Sec. 3.3.1). An example of such dynamics is observed in the Gulf Stream region where the boundary current transports away the subtropical communities, which are subsequently mixed with locally adapted or-

ganisms and eventually outcompeted. Due to the fact that the exclusion time scale is relatively long when compared to the advective time scale the transported population contributes to the local diversity (Barton et al. [2010]), hence, forming a region of an elevated phytoplankton diversity ("hot spot"). The role of oceanic dispersal in setting patterns of phytoplankton diversity was a subject of a detailed analysis by Levy et al. (Lévy et al. [2014]). The results presented by Levy et al. suggest that dispersal increased the ability for coexistence at the local scale and changed the community structure. A continuous and constant immigration introduced into the model (Sec. 3.3.1) may reflect dispersal in its simplest form. Thus, the model results (Sec. 3.3.1) are in line with hypotheses from theoretical ecological studies (e.g., Mouquet and Loreau [2003]) and a meta-analysis of observations from terrestrial ecosystem (Cadotte [2006]) suggesting increase of local diversity with dispersal, but also with the insights derived from far more complex models e.g. with Darwin models (Barton et al. [2010], Lévy et al. [2014]).

According to the resource competition theory, in a system at equilibrium, a species with a lowest resources requirements competitively excludes all the other species as it drawns down the available resources to the level at which other species are unable to balance their growth and mortality rates. The $R*$, as described in the 1st chapter, indicates the resources concentration at which specie growth rate is in balance with its mortality rate. If steady-state conditions are satisfied, species can coexist if they have the same (lowest positive) $R*$ values. This simple logic clearly expands to the balance between the population accumulation and loss rates. Then, the identical $R*$ values can be accomplished by various combinations of accumulation and loss rates, accounting also for the phytoplankton dispersal rate. A consideration of a continuous background immigration introduces an additional degree of freedom into the $R*$ formulation and allows for a co-existence of a wider set of species. The $R*$ scenario is relevant when the system is close to statistical steady-state equilibrium, that is, all year long in the subtropical ocean and during summer in the subpolar ocean, as shown by Dutkiewicz et al. [2009]. Thus the resources competition theory and $R*$ accounting for immigration offers a compelling explanation of the increased species diversity observed in the ecosystems explored in here.

Immigration may also reflect formation of resting stages and consequent encystment and excystment. As described in Chapter 1, the formation of resting stages could represent a safety mechanism for reintroduction of the species when the vegetative cell population went extinct due to unfavourable conditions (McQuoid and Hobson [1996]). Resting stages tolerance to harsh environmental conditions such as darkness and nutrients depletion, and grazing have a positive effect on the species survival. Thus, the resting stage formation would have a positive effect on the system memory. In fact, the spores production of *Leptocylindrus danicus* has been detected when nutrients became depleted, which coincided with the end of a bloom (Davis et al. [1980a]). Moreover, the spores capability to germinate even after long dormancy periods (Davis et al. [1980a]) would be sufficient to survive both severe nutrients depletion and high grazing pressure observed in the model ecosystem during summer period. Additional germination fluxes could further contribute to enhance population density of vegetative cells during the initial phases of a bloom. Consequently, the formation of resting stages would have a strong impact on the population dynamics (e.g. bloom development and termination), and thus to affect the phytoplankton succession patterns and potentially increase the number of coexisting species.

Because of that the role of immigration and emigration should be a subject of a detailed analysis in the continuation of this study. In particular its intensity and time periods in which it takes place should be explored.

Copepods dormancy The model, despite its simplicity, successfully captures the bloom dynamics in a subpolar environments. During the winter period phytoplankton experience low light levels, due to low solar radiation as well as strong mixing. As a result, light limits phytoplankton growth to such extent that species concentrations are nearly negligible, while the nutrient concentration remains high. The individuals able to survive in such conditions are characterised by their light affinity rather than their nutrient affinity. Consequently, at the onset of the bloom the water column is dominated by diatom species adapted to low light conditions and high nutrient concentrations. The increase of phytoplankton species concentration and bloom formation is possible when light-limited growth rate exceeds mortality and grazing (Figure 3.17a).

The Critical Depth Hypothesis (Sverdrup [1953]) states that phytoplankton blooms occur when surface mixing shoals to a depth shallower than a critical depth - depth where phytoplankton growth exceeds losses. It reflects the assumption that blooms are caused by, and not simply correlated with, enhanced accumulation rates in response to improved light, temperature, and stratification conditions. The Dilution-Recoupling Hypothesis (Behrenfeld [2010]) can be treated as a refinement of Sverdrup's critical depth. It focuses on the balance between phytoplankton growth and grazing, and the seasonally varying physical processes influencing this balance. Behrenfeld argues that the occurrence of optimum growth conditions allows for both the growth of predator and prey, which results in increased interactions between the two (predator-prey interactions recoupling). In the winter period, this relationship is diluted as a result of deep mixing. In here even stronger decoupling was imposed by assuming copepods dormancy phase. During this phase, which may involve a true diapause (Hirche [1996]), the copepod normally descends to great depth where it resides until late winter or spring.

The dormancy impacts the encounter rate between phyto- and zooplankton; because of the copepods dormancy the encounter rate is equal to 0, and increases as the copepods exit diapause phase and concentrate in the water column active layer. Thus, in a very simplified form address a key point not considered in the Dilution-Recoupling hypothesis.

The results of the simulations (Sec. 3.3.2) suggest that copepods winter dormancy affecting their concentration during MLD shoaling did not have a strong impact on the spring bloom onset. In the tested scenario, invoking sensitivity to the depth triggering winter dormancy, the onset of spring bloom occurred at the same year day for the vast majority of cases (here 'case' refer to different communities but also to the tested overwintering depth).

These results suggest that the resources limitations imposed on the phytoplankton growth rate (light limitations), rather than balance between growth and grazing rates, regulates the bloom onset. It has to be considered though, that the simple model construction, does not refute all the key points of the Dilution-Recoupling Hypothesis; i.e. net positive growth rate of some phytoplankton species was observed during the

deep-mixing period. Moreover, the model assumes constant deep mixing during winter, while there are evidences of calm periods and temporal water column restratification, which could potentially boost phytoplankton growth and allow for biomass accumulation (Stec et al. in preparations). In this case the role of copepods dormancy in shaping phytoplankton and zooplankton dynamics could be vastly different and needs to be explored.

The results obtained in the section 3.3.2 show that the model assumptions regulating copepods dormancy did not affect significantly their population dynamics, nor the phytoplankton functional groups seasonal succession. Nonetheless, copepods are known for their dormancy and life stage transformation during which they do not graze - considering them as active in those periods could be considered as a misrepresentation of this group. Thus, it is argued, that presence of dormancy - a particular biological process characteristic for copapods in the subpolar environments- improved the biological representation of this functional group resulting in an improved realism of the model. This qualitative improvement was obtained by increasing the resemblance of abundance patterns observed in the model simulations to the patterns observed in nature (e.g., at North Atlantic; Joint et al. [1993]).

There is a need to develop new and improved ecosystem model formulations focused on the details of considered processes (Anderson [2005]). Considering the above, should copepods dormancy be incorporated in all the models mimicking dynamics of the subpolar ecosystems? The answer is not straightforward and relies on the balance between the cost of such model augmentation and the scientific weight of the results it generates.

It is important to note that every new process introduced into the model increase the computational effort required for the numerical simulations. Despite the simplicity of the mathematical formula describing active-dormant state transition employed in this study resulted in a 2-4% increase in the duration of each performed simulation. This cost is likely to further increase if more complex formulations were considered and if the formulations was introduced into a global 3D model. Under certain conditions such an additional cost may not be ignored. Additionally, while novel processes are introduced into the models, the uncertainties associated with those processes are being

introduced as well. These uncertainties originate from the limitations of the available information on the process itself and our understanding of the process dynamics. These uncertainties may affect the quality of the data generated by the model, hence should be considered.

It is again the *art of modelling* to balance *generality*, *realism* and *precision* of the approach and to develop a model configuration suitable to address a specific scientific question (Levins [1966]). Clearly in some instances introduction of the copepods dormancy could be omitted due to its rather insignificant impact on seasonal abundance patterns of phytoplankton and copepods, and due to the additional computational cost.

However, if the scientific question is focused on the copepods population dynamics then the dormancy might be considered. For instance, Backhaus et al. [1994] proposed that the seasonal vertical migration of *Calanus finmarchicus* in the Northeastern Atlantic maintains its spatial persistence in the face of a strongly advective system. In this hypothesis, the over-winter stock would form the epicentre of the regional population, and its location should be tied to large-scale circulation features. New generations produced during spring and summer would possibly populate broad areas (i.e. due to diffusion) with a scope for return to an over-wintering epicentre. The exploration of such a hypothesis would possibly require a formulation of the winter copepods diapause which should be approach with caution and which ought to be tested thoroughly.

Chapter 4

Model sensitivity to physical forcing

4.1 Introduction

The variability in environmental conditions has long been recognised to shape the properties of the phytoplankton seasonal succession and community composition (Margalef [1968],Tozzi et al. [2004]). The physical forcing acting on the ocean is highly variable both at global and at basin scale. This impacts on the mixed layer depth and its variation along the year (Sprintall and Roemmich [1999], Monterey and S [1997],de Boyer Montegut et al. [2004]). Considering the subpolar North Atlantic Ocean, which is the basin chosen as a reference (Chapter 2), the maximal MLD varies from less than 100 m (e.g. south-eastern region) and more than 500 m during winter months (e.g., Labrador Sea) (Fig. 4.1, 4.2 and 4.3). These data were analysed here in order to derive an appropriate parametrisation of the physical forcing used in the model, focusing on the variability of maximal MLD value, beginning of spring restratification and duration of summer stratification. Clearly, these parameters demonstrate a high spatial variability.

The analysis also show that the physical forcing in the area surrounding the North Atlantic Bloom Experiment exhibit strong inter-annual variability (Fig. 4.4). The multi-annual median value of the maximal winter MLD oscillates around 300m though there are observation of MLD shallower than 300m as well as deeper than 500m during winter months. Variability in the spring water column restratification characteristics is also observed. Namely, the restratification may occur between 75th and 115th year day, where both the restratification initiation and its duration are likely to change over consecutive years. The duration of summer stratification and initiation of autumn water column deepening, as well as nutrients entrainment attributed to the latter, also varies on the multi-annual time scale. For instance, despite the average MLD in November and December exceeding 100-150m, there are several observations of MLD=50m in December. In a similar fashion, the autumn water column deepening may be advanced with respect to the multi-annual average.

What Fig. 4.1, 4.2, 4.3 and 4.4 show is likely going to change in the following years because of a future increase in atmospheric greenhouse gases. Climate models predict that global warming will increase the stability of the vertical stratification, and reduce vertical mixing in large parts of the oceans (Sarmiento et al. [1998], Bopp et al.

[2001], Sarmiento et al. [2004], Schmittner et al. [2005], Schmittner et al. [2008]). In particular a shift in the beginning of spring water column restratification (anticipation in the Pacific Ocean and delay at North Atlantic; Russell et al. [1995]), a lengthening of summer stratification and a decrease of vertical mixing (Manabe et al. [1991]; Sarmiento et al. [1998]) is expected. The nutrient concentrations and fluxes, as determined by the MLD and local uptake and the light availability are the abiotic factors driving the phytoplankton growth and accumulation (see Chapter 3) and consequently affect the community composition (Margalef [1978], Iglesias-Rodríguez et al. [2002]). It has been demonstrated that the availability of inorganic nutrients exerts a major control on phytoplankton biomass, primary productivity, and community structure Longhurst et al. [1995]. Previous studies addressing phytoplankton community composition in the Atlantic Ocean have shown that patterns of the diatoms and coccolithophorids distribution are correlated with the nutricline depth and thus with the rate of nutrient supply to the upper mixed layer of the ocean (Cermeño et al. [2008]). Moreover, variability of turbulence or vertical motion in the mixed layer could favour smaller cells in summer and larger cells in winter by affecting sinking and swimming velocities (Kiørboe [1993]).

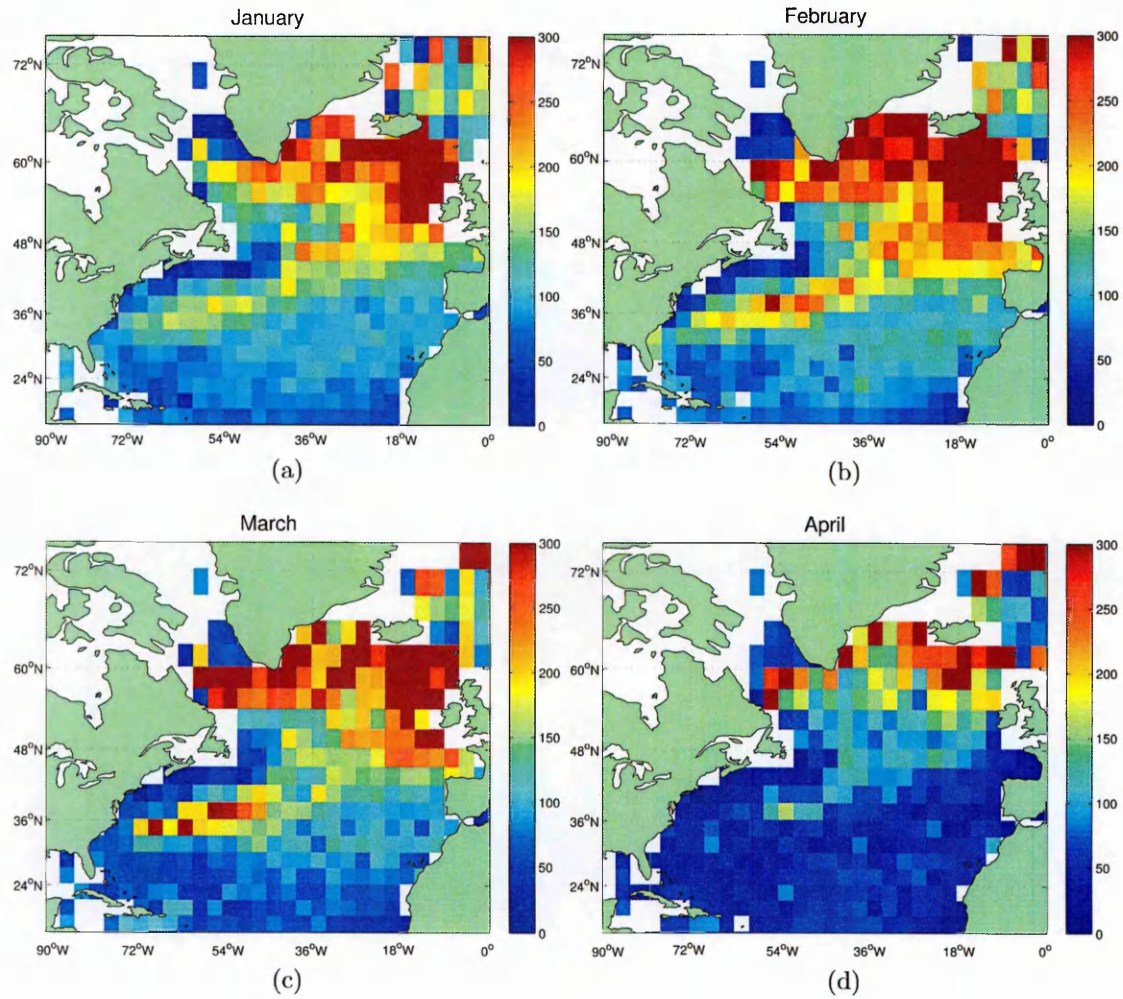

Figure 4.1: Monthly (January-April) values of the median mixed layer depth in the different areas as derived from the ARGO (1998-2011) data (http://www.ifremer.fr/cerweb/deboyer/mld/Data.php). The MLD climatology was estimated from individual profiles, with a density difference criterion of $\Delta\rho = 0.03$ $[kg/m^3]$ from density at 10 m depth (as in de Boyer Montegut et al. [2004]). Data reduction was performed by taking the median of the MLDs on each 3° grid box. White pixels indicate lack of data for a given region.

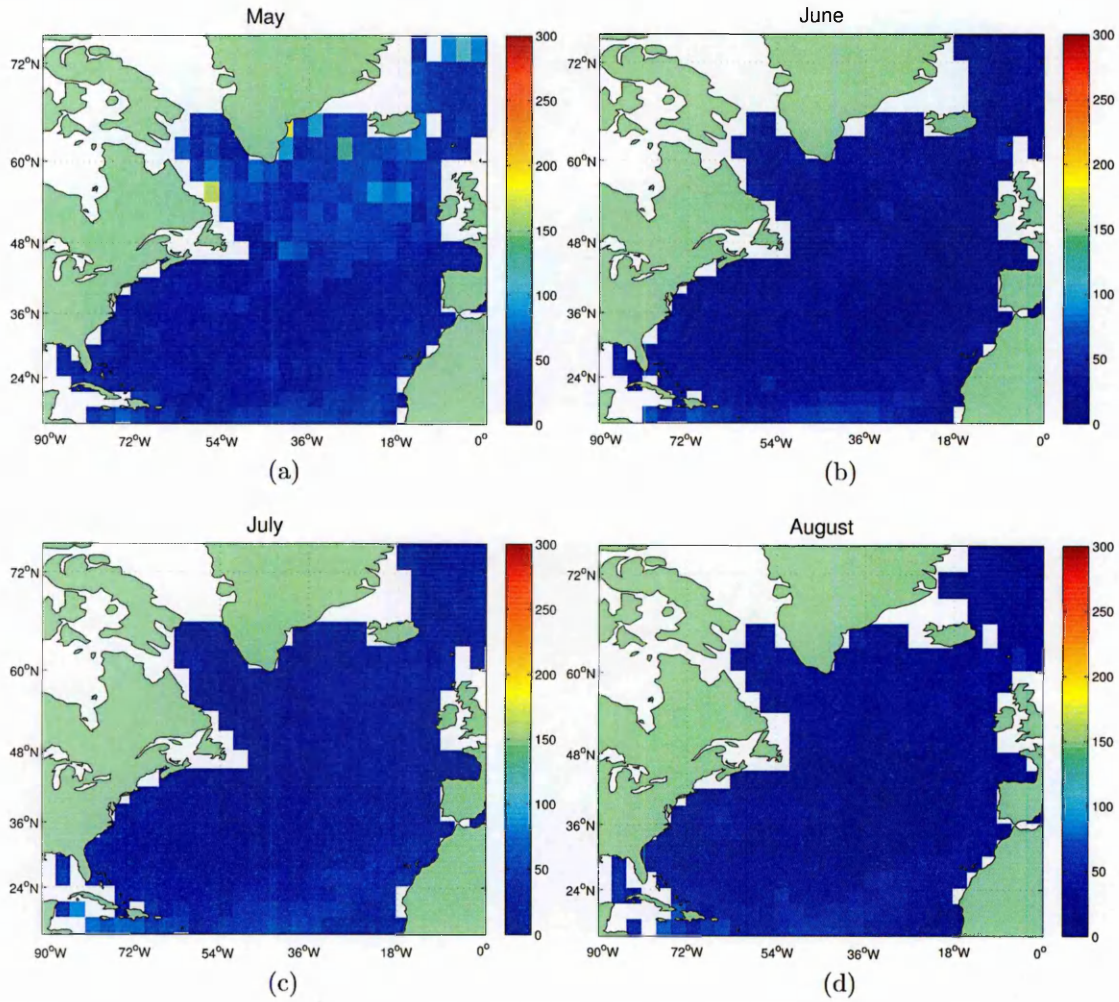

Figure 4.2: Monthly (May-August) values of the median mixed layer depth in the different areas as derived from the ARGO (1998-2011) data (http://www.ifremer.fr/cerweb/deboyer/mld/Data.php). The MLD climatology was estimated from individual profiles, with a density difference criterion of $\Delta\rho = 0.03$ $[kg/m^3]$ from density at 10 m depth (as in de Boyer Montegut et al. [2004]). Data reduction was performed by taking the median of the MLDs on each 3° grid box. White pixels indicate lack of data for a given region.

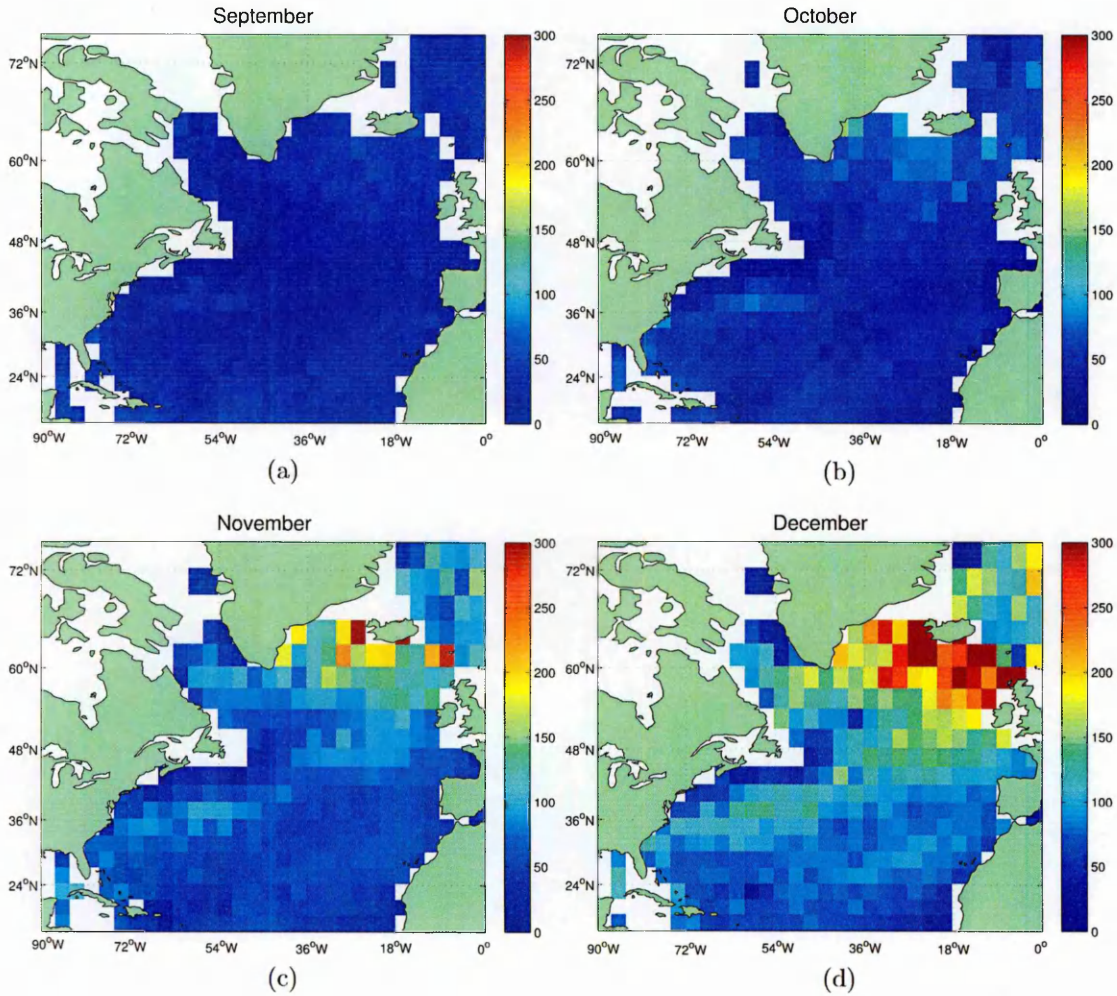

Figure 4.3: Monthly (September-December) values of the median mixed layer depth in the different areas as derived from the ARGO (1998-2011) data (http://www.ifremer.fr/cerweb/deboyer/mld/Data.php). The MLD climatology was estimated from individual profiles, with a density difference criterion of $\Delta\rho = 0.03$ $[kg/m^3]$ from density at 10 m depth (as in de Boyer Montegut et al. [2004]). Data reduction was performed by taking the median of the MLDs on each 3° grid box. White pixels indicate lack of data for a given region.

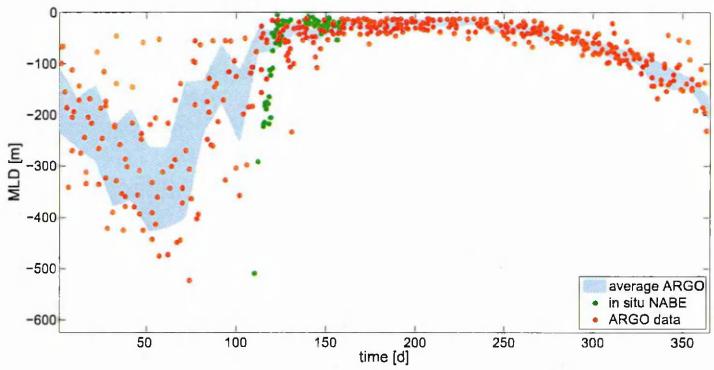

Figure 4.4: Multiannual variability of the mixed layer in the area surrounding NABE. The green dots represent the *in situ* measurements of the MLD during the North Atlantic Bloom Experiment in 1989. The red dots represent the ARGO measurements (1998-2011) based on a density difference criterion of $\Delta\rho = 0.03$ $[kg/m^3]$ (as in de Boyer Montegut et al. [2004]) in the region surrounding the NABE site (45.5°N, 21.5°W) and (48.5°N, 18.5°W). These ARGO measurements were averaged over a period of 10 days forming a multi-annual mean signal depicted here as the blue area.

The MLD ARGO measurements used in here were based on a density difference criterion of $\Delta\rho = 0.03$ $[kg/m^3]$ from density at 10 m depth (as in de Boyer Montegut et al. [2004]). The data were extracted from the ARGO dataset for a region surrounding the NABE site, namely a squared area spanning between (45.5°N, 21.5°W) and (48.5°N, 18.5°W), and averaged over a period of 10 days forming a multi-annual average

As illustrated above, there is evidence that physical forcing exhibit strong spatial and temporal variability. Such a variability in the maximal MLD, spring restratification characteristics and summer stratification is observed in the whole North Atlantic basin if the multi-annual average is considered (Fig. 4.1, 4.2, 4.3) but also on the local scale in form of a inter-annual variability (Fig. 4.4).

The seasonal forcing characteristics employed in the previous chapters covers only a fraction of what is observed in the mid-latitude environments. Thus, in this chapter I explore the relationship between physical forcing and the community structure. The analysis are focused on the species diversity over the seasonal cycle. The aim of this sensitivity study is to investigate how changes in the mixed layer depth, prolonged stratification and changes in the beginning and duration of spring restratification affect species community composition and species diversity in the virtual ecosystem.

The sensitivity study presented in here ought to be considered as a theoretical exercise exploring the relationship between environmental forcing and functioning of

a simplified ecosystem. Nonetheless, the presented sensitivity study is used also to ensure credibility of the model employed in this thesis. The results are extrapolated into the analysis of particular environments reported in the basin of the North Atlantic and qualitatively compared with the CPR data.

4.2 Methods

In the Chapter 3, the physical forcing used in the model was described. In here a more detailed description is provided.

To mimic the variation of MLD in different areas, while keeping the formulation reasonably simple, an analytical function presented in Chapter 2 (Eq. 21) has been used. Though idealised, the model forcing captures the main features of the mixed layers behaviour observed in subpolar regions of the world ocean, i.e. fast deepening during the autumn and winter, abrupt jump in the spring, and prolonged stratification during the end of spring and summer (Fig. 1) in Chapter 2).

The other terms of physical forcing that has been considered are the solar irradiance, as the source of energy for plankton photosynthesis, computed for a given latitude as a photosynthetically active radiation, and the nutricline depth (see Chapter 3 Section 2.2)

The impact of environmental forcing on community composition and its time course was explored with the model presented in the previous chapter. Similarly to numerical simulations in Chapter 3, 40 phytoplankton species were generated stochastically (Section 2.4 Chapter 3) and initialized with a low concentration ($= 10^{-6}$ $[mmolC/m^3]$) in the system. The model was integrated for 100 years, over which time a repeating annual cycle in ecosystem structure emerged. Out of the 10000 years of simulation, the last 30 years were analysed. The simulations were repeated 30 times, each time with a different random selection of phytoplankton species physiologies, forming an ensemble of 30 members. The results of the ensemble set of simulations were analysed and compared across systems where physical forcing was varied.

The impact of seasonal forcing characteristics on the phytoplankton dynamics with the special focus on the maximal MLD value, beginning of spring restratification and

its duration, and duration of summer stratification (Table 4.1). As descriptors of this dynamics, abundance patterns of phyto- and zooplankton, and the median species diversity were used. The species diversity was measured as a total number of species when: 1) median biomass over the seasonal cycle or 2) maximal concentration throughout the whole year exceeded a specified threshold: 0.004 $[mmolC]$ or 0.05 $[mmolC/m^3]$, respectively. The diversity index based on the maximal concentration accounts for the species which at least once during the seasonal cycle are able to cross a predefined threshold, i.e., they mainly are the "bloom forming" species. Notably, not all the species form a conspicuous bloom (Assmy and Smetacek [2009]). In fact, most of the species does not form bloom, and many of them may be present in low concentrations throughout the whole seasonal cycle - these species are accounted for with the biomass based diversity index.

The mathematical formulation of the MLD seasonal dynamics considers several parameters which can be modulated in order to adjust it to the specific local conditions (see also Chapter 3 sec. 2.4 for the details). In particular such adjustments had been made to represent both the specific physical forcing observed during the North Atlantic Bloom Experiment in the 1989 (Chapter 2 sec. 4.1) and the multi-annual average observed in the surrounding NABE area (Chapter 2 sec. 4.2). The variability of the parameter values (Tab. 4.1) considered in this exercise reflect the variability of the physical forcing observed in the NABE area over multiple years. To some extent it reflects also the variability of the average seasonal forcing observed in the whole North Atlantic basin.

The subpolar type environment (Chapter 2) was considered as a reference case, and only one parameter (Tab. 4.1) was varied at a time. Thus, for instance, when exploring the impact of T_0, all other parameters were fixed to the values in the reference case - namely: $h_{min} = 20m$, $h_{max} = 600m$, $\Delta_T = 30d$, $S_L = 150d$ and $T_0 = 85yd$.

In the following paragraphs the impact of the parameters on each of the descriptors is described in details. The data are presented in two parts: first is dedicated to the analysis of the species diversity, while the second focuses on the change in abundance patterns.

Parameter	Meaning	Minimal value	Step	Maximal value
h_{max} $[m]$	maximum MLD	200	100	600
T_0 $[yd]$	restratification initiation	75	10	115
δt $[yd]$	restratification duration	20	10	60
S_L $[d]$	summer stratification duration	135	15	195

Table 4.1: Parameters set explored in the sensitivity study of the environmental forcing parametrisation. Ecosystems sensitivity to each indicated parameter was evaluated by generating an ensemble set of 30 simulations for all possible parameter values and comparing them with the reference case.

4.3 Phytoplankton response to various physical forcing.

4.3.1 Change in species diversity related to the physical forcing.

Maximal mixed layer depth. A decrease in the maximal value of the MLD from 600m to 200m resulted in a slight decrease of the median species diversity whether either median biomass or max concentration was considered (from 20 to 19 for biomass Fig. 4.10a; and from 13 to 11 for concentration Fig. 4.10b). Though a slight increase in median species richness by 1 species was observed in a system with 200m maximal MLD if maximal concnetration was considered as the determinant. At the same time the statistical spread (in terms of quartiles distance) of biomass based diversity was much broader for depths 500 and 600m in comparison with systems with shallower maximal MLD (Fig. 4.10).

The deepening of the water column leads to nutrients entrainments into the upper water column layer. The entrainment rate is directly related to the change in the MLD and the nutrients concentration directly below. There is a gradient with depth in nutrients concentration, thus the absolute value of the nutrients introduced into the system increases with depth. For instance the entrainment from 200m is lower than from 400m or 600m as the nutrients concentration at 400 and 600m is higher. Because of that the absolute value of the nutrients entrained into the system where maximal MLD value is equal to 200m is lower than in case of 600m. Consequently, the standing stock of nutrients towards the end of winter shows a decreasing trend corresponding to

the decreasing maximal MLD value.

At the same time there is a higher grazing pressure imposed on phytoplantkon by grazers (i.e., copepods and microzooplankton) at the beginning of spring water column restratification in the systems with lower maximal MLD (Fig. 4.25). Despite the fact that the overall grazing pressure is higher in the ecosystems with higher maximal MLD, the top-down control is stronger in the shallower ecosystems during the initial phase of spring bloom (Fig. 4.25).

Lower maximal nutrients concentration in the end of winter observed in the systems with shallower maximal MLD together with a higher grazing pressure resulted in an overall decrease of the maximal concentration of the species which concentration peak corresponds to the spring period i.e. diatoms (Fig. 4.6) and dinoflagellates (Fig. 4.7). In general, the maximal concentration of coccolitophores and green algae did not change (Fig. 4.8, 4.9).

The change in the nutrients supply and in the grazing pressure restructured the phytoplankton community and resulted in an extinction of some species, while others emerged. That was illustrated by a slight increase of the diatoms diversity in the ecosystems characterised with maximal MLD shallower than 400m which was indicated by the change of the shape of diversity PDF (Fig. 4.5a). The median diversity of dinoflagelates decreased to 4 and 3 species in the ecosystem characterised with maximal MLD equal to 300m and 200m respectively (Fig. 4.5b). The diversity of coccolitophores increased slightly which was illustrated by a change of diversity distribution, i.e. 75th quartile in ecosystems with MLD shallower than 500m (Fig. 4.5c).

community #	200	300	400	500	600
12	9	8	8	9	10
10	12	14	13	15	19
median	12	11	12	12	13

Table 4.2: Concentration based species richness in two selected communities (12th and 10th) under different environmental forcing characteristics. The seasonal dynamics of the MLD varied in terms of its maximal value.

Notably, high variability was reported in the species diversity among all 30 tested communities even under identical physical forcing conditions (Fig. 4.10; Tab. 4.2). Moreover in multiple cases variability in diversity in between communities under iden-

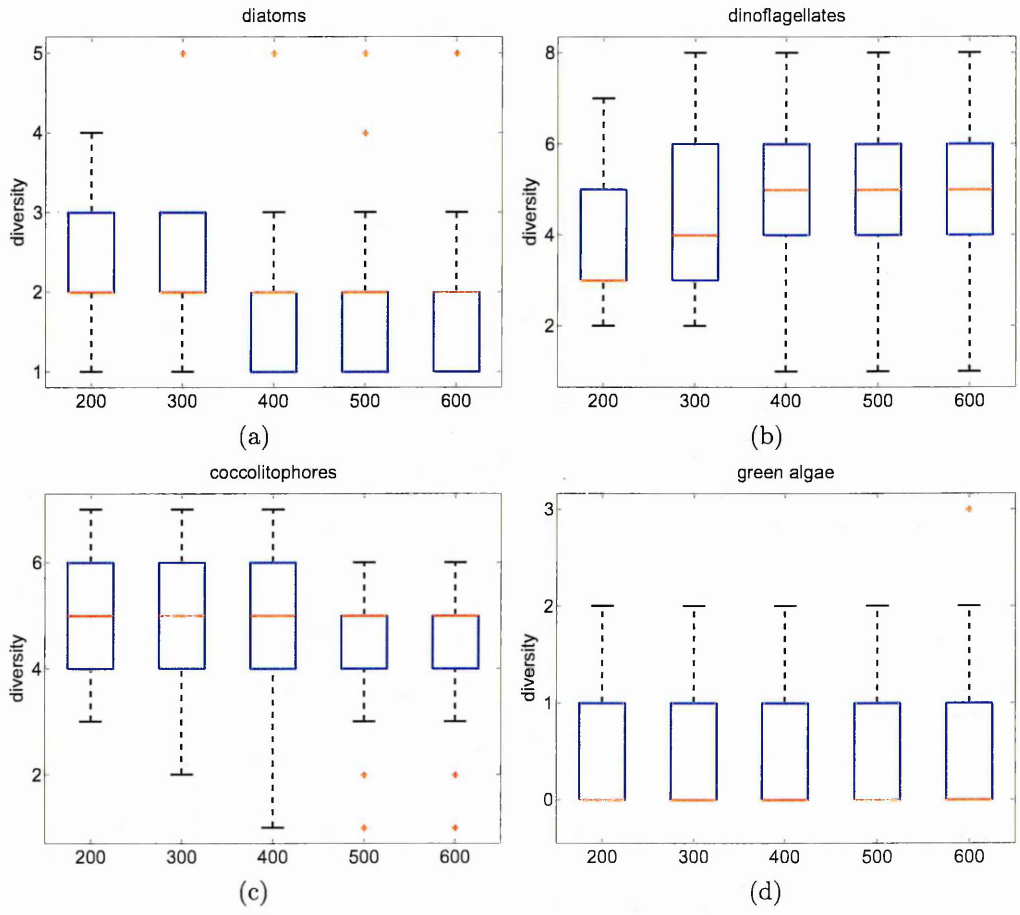

Figure 4.5: Sensitivity of the PFTs' diversity to the changes in the maximal MLD: (a) diatoms, (b) dinoflagellates, (c) coccolitophores, (d) green algae.

tical forcing was comparable (or even higher) with the variability of diversity in one selected community under different physical forcing (Fig. 4.11). For instance the change in the MLD only slightly affected species diversity in the community #12, while strong increase was observed in communities #10. Importantly, all these communities showed considerably different dynamics from the median trend derived for all the tested communities. This strongly demonstrates systems sensitivity to the parameterisation, here the physiological characteristics of the coexisting species, which can be explored with the ensemble approach.

The change in maximal MLD values affected the community composition which was represented by a change in values of the community similarity index (Fig. 4.12). The similarity index decreased in accord with the decrease of maximal MLD both if the maximal concentration and median biomass was used for determining species richness. The median community similarity decreased down to 80% and 91% (for max concentration and median biomass respectively) with respect to the scenario with maximal

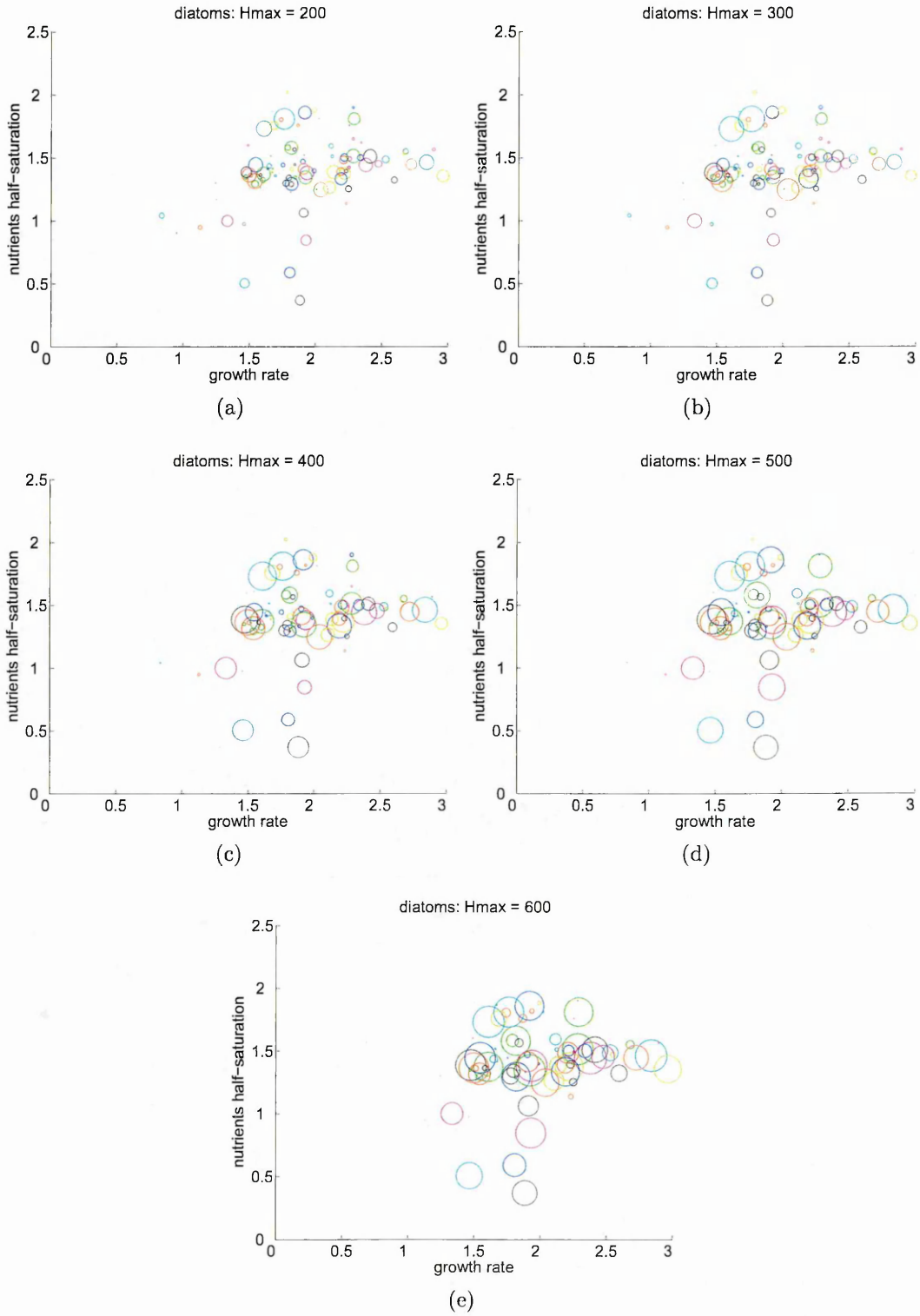

Figure 4.6: Distribution of the physiological trade-offs of the diatom species persisting in the ecosystem distinguished solely with the maximal mixed layer depth during winter: (a)200m, (b)300m, (c)400m, (d)500m, (e)600m. Each circle depicts a single phytoplankton species. The size of the circle is proportional to the maximal concentration of the species reached during the year. The plot illustrates the characteristics of the species from all 30 ensemble communities, where the communities were distinguished by colours. The axis represents nitrate half-saturation constant and intrinsic growth rate.

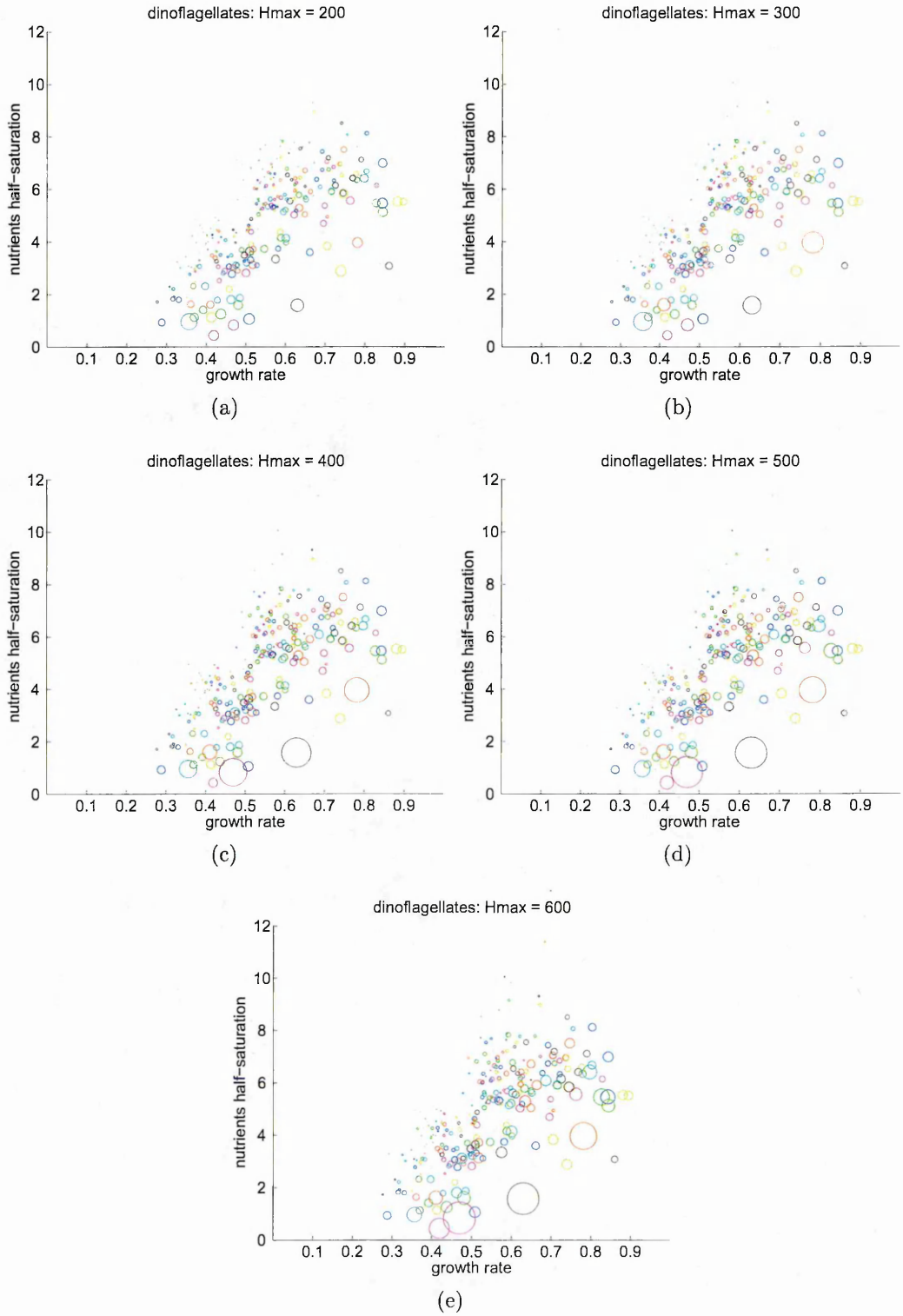

Figure 4.7: Distribution of the physiological trade-offs of the dinoflagellates species persisting in the ecosystem distinguished solely with the maximal mixed layer depth during winter: (a)200m, (b)300m, (c)400m, (d)500m, (e)600m. Each circle depicts a single phytoplankton species. The size of the circle is proportional to the maximal concentration of the species reached during the year. The plot illustrates the characteristics of the species from all 30 ensemble communities, where the communities were distinguished by colours. The axis represents nitrate half-saturation constant and intrinsic growth rate.

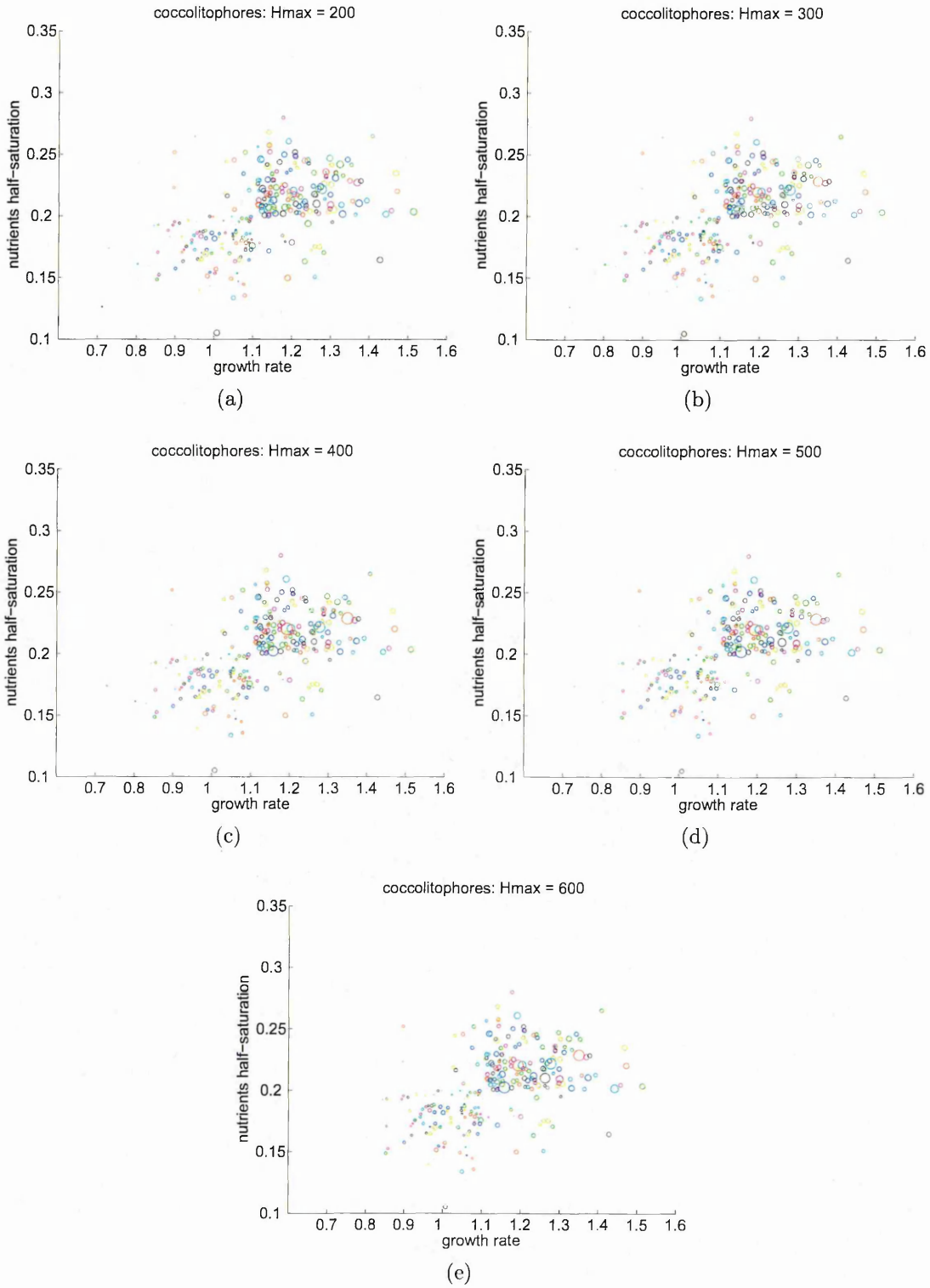

Figure 4.8: Distribution of the physiological trade-offs of the coccolitophores species persisting in the ecosystem distinguished solely with the maximal mixed layer depth during winter: (a)200m, (b)300m, (c)400m, (d)500m, (e)600m. Each circle depicts a single phytoplankton species. The size of the circle is proportional to the maximal concentration of the species reached during the year. The plot illustrates the characteristics of the species from all 30 ensemble communities, where the communities were distinguished by colours. The axis represents nitrate half-saturation constant and intrinsic growth rate.

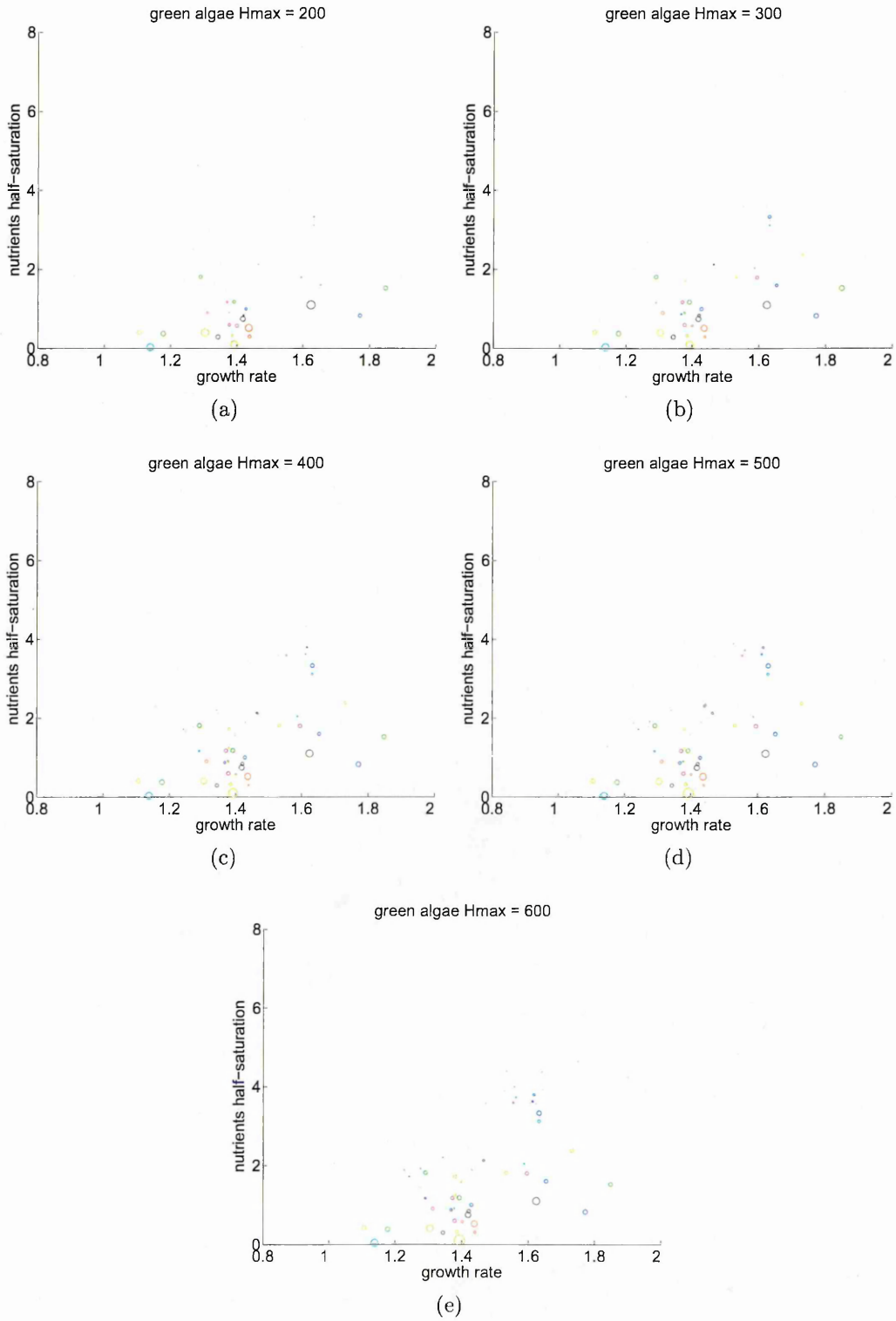

Figure 4.9: Distribution of the physiological trade-offs of the green algae species persisting in the ecosystem distinguished solely with the maximal mixed layer depth during winter: (a)200m, (b)300m, (c)400m, (d)500m, (e)600m. Each circle depicts a single phytoplankton species. The size of the circle is proportional to the maximal concentration of the species reached during the year. The plot illustrates the characteristics of the species from all 30 ensemble communities, where the communities were distinguished by colours. The axis represents nitrate half-saturation constant and intrinsic growth rate.

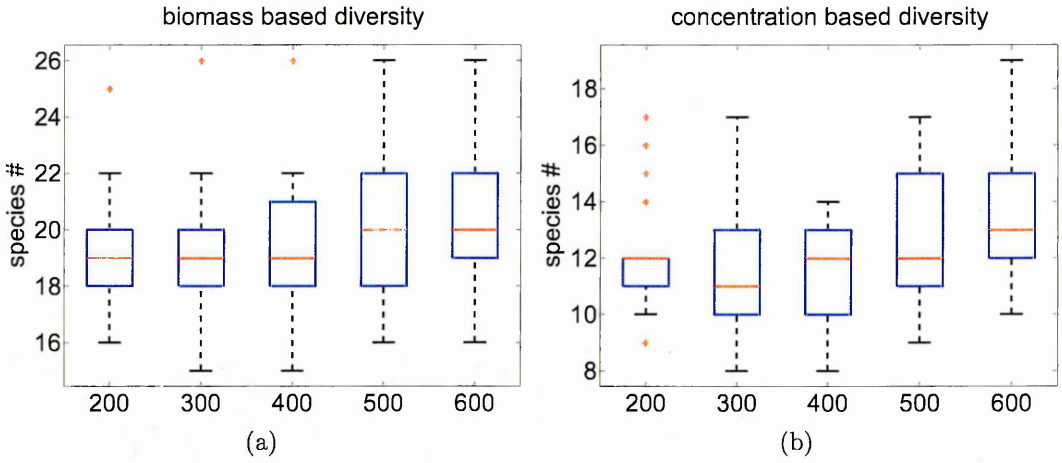

Figure 4.10: Species diversity in the systems distinguished solely by the maximal MLD value. The estimate of species diversity was based on each species (a) median biomass or (b) maximal concentration. The presented boxplots refer to species diversity observed in all ensemble communities.

MLD equal to 600m, though these values varied strongly among the communities. For instance, when considering the scenarios with 400 and 600m maximal MLD, the similarity index ranged from 68% to 100% in case of maximal concentration, and from 83% to 100% in case of median biomass (Fig. 4.12).

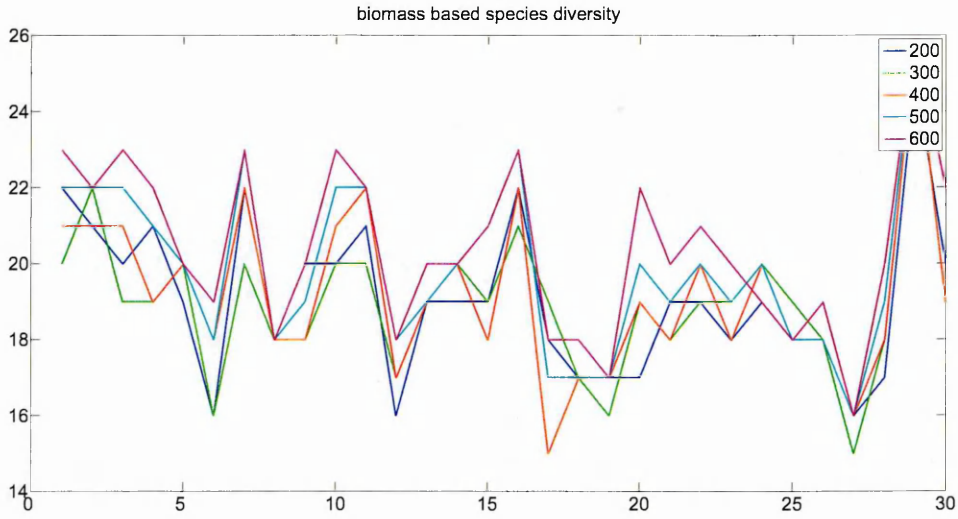

(a)

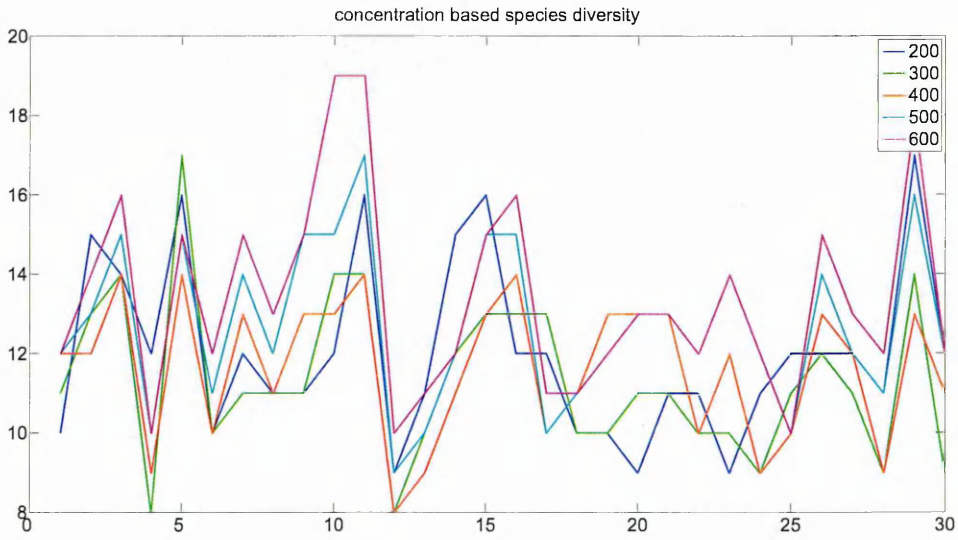

(b)

Figure 4.11: Species richness in the systems distinguished solely by the maximal MLD value. The estimate of species diversity was based on each species (a) median biomass or (b) maximal concentration. Each line depicts change of the species richness observed across all explored environmental scenarios.

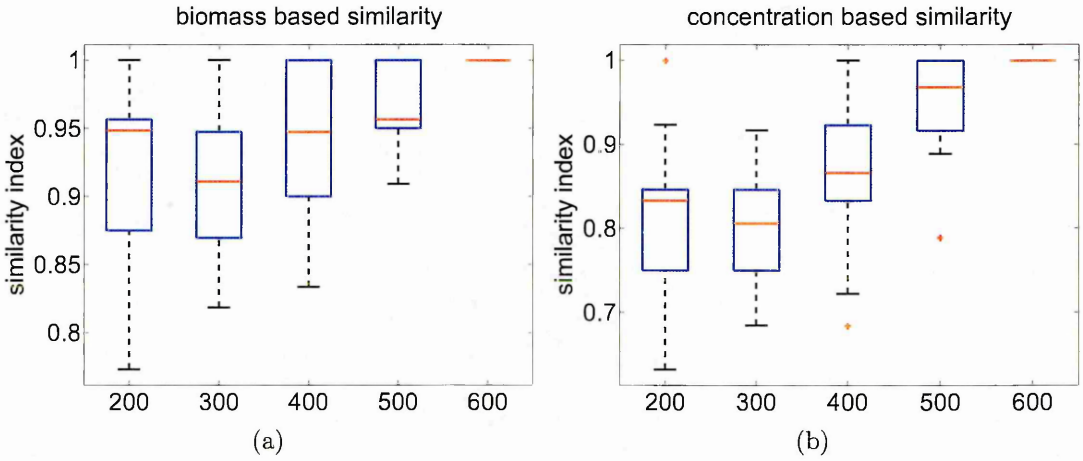

Figure 4.12: Community similarity index in environments distinguished with the maximal MLD value. Every single community was analysed in terms of its phytoplankton species composition across all explored environmental scenarios and based on this information a community similarity index was calculated. Community composition was evaluated with a (a) species median biomass or (b) its maximal concentration. The environment with a 600m maximal MLD was used as a reference case for the computations.

Beginning of spring restratification The shift in the beginning of the spring restratification from 85 [yd] used in the reference case (see Chapter 2) had a little impact on the median species diversity - an increase by 1 species was observed only in case of a 30 days advance in the restratification initiation for the indicators based on both concentration and biomass (Fig. 4.13). Nonetheless, there were multiple communities in which the number of active species decreased by 1 with the change of restratification initiation, as well as there were multiple communities in which the number of species increased with that change by 2 or more species (Fig. 4.13).

The change in the begining of spring water column restratification altered the shape of diatoms diversity distribution by elevating the 75th quartile from 3 to 5 (Fig. 4.14a). The median coccolitophores diversity remained unchanged if the beginning of restratification was advanced or retarder by 10 days, and decreased if retarded by 20 and 30 days (Fig. 4.14c). The median green algae diversity increased to 1 in case of restratification initiating at 75th yd and decreased if taking place after 95th yd (Fig. 4.14d).

The distribution of the species' physiological traits in all the cases resolved in this scenario were indistinguishable with the reference case (Fig. 3.5).

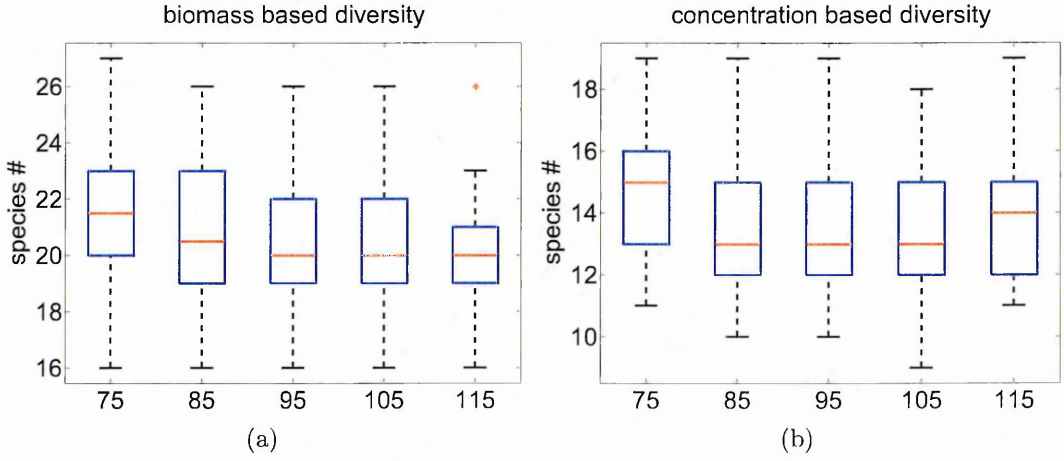

Figure 4.13: Species diversity in the systems distinguished solely by the spring water column restratification initiation. The estimate of species diversity was based on each species (a) median biomass or (b) maximal concentration. The presented boxplots refer to species diversity observed in all ensemble communities.

The shift in restratification initiation affected also the community composition (Fig. 4.13). Both the advance and the delay in the beginning of spring, indicated by water column restratification, resulted in the decrease of similarity index values, with the

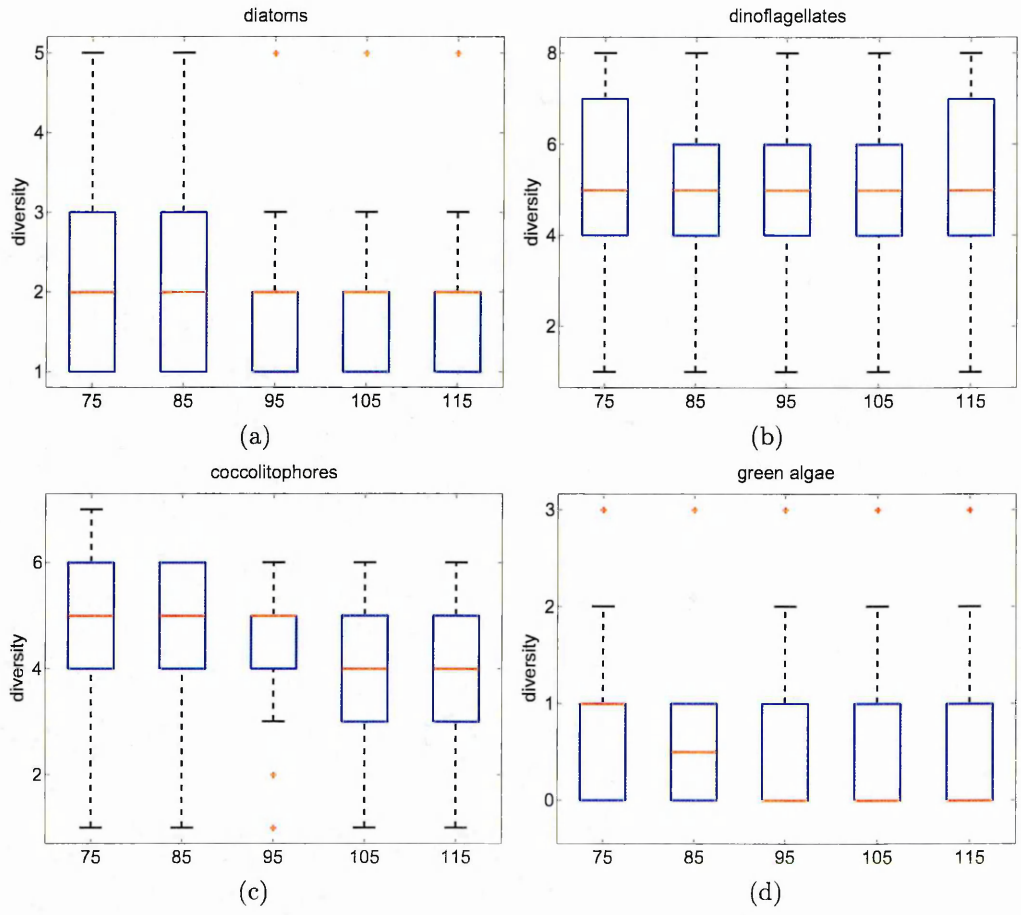

Figure 4.14: Sensitivity of the PFTs' diversity to the changes in the maximal MLD: (a) diatoms, (b) dinoflagellates, (c) coccolitophores, (d) green algae.

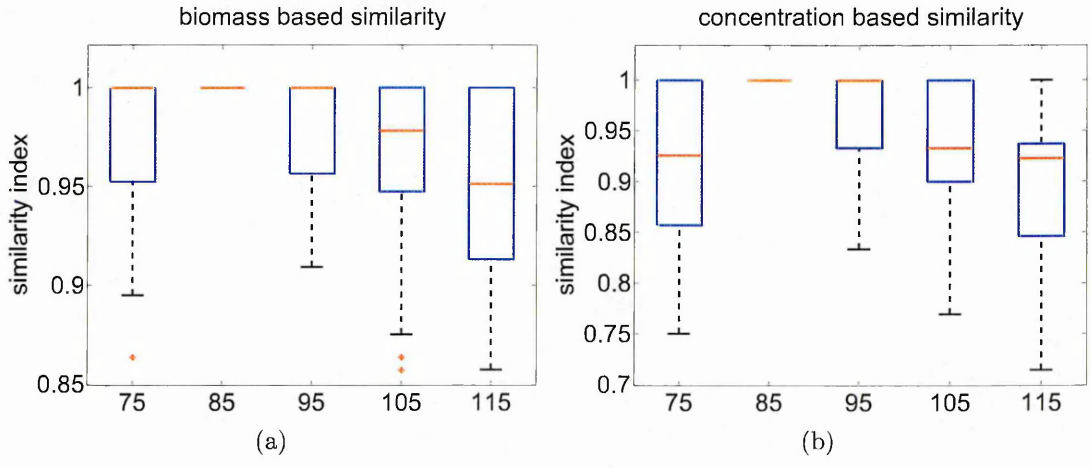

Figure 4.15: Community similarity index in environments distinguished with the spring water column restratification initiation. Every single community was analysed in terms of its phytoplankton species composition across all explored environmental scenarios and based on this information a community similarity index was calculated. Community composition was evaluated with a (a) species median biomass or (b) its maximal concentration. The environment with a spring water column restratification initiating on 85 [yd] was used as a reference case for the computations.

higher discrepancies attributed to the larger time difference between the considered and the reference case (Fig. 4.15). The stronger differences, spanning over 25% of the nominal value were reported for the index based on the maximal concentrations (Fig. 4.15b), while in case of median biomass the vast majority of similarity index values did not decrease below 89% (Fig. 4.15a).

Duration of spring restratification Similarly to the change in the initiation of spring water column restratification the change in the duration of the spring restratification had a little impact on the median species diversity (Fig. 4.16). On average the species richness was comparable in all explored cases with a small increase in case of the restratification lasting for 50 and 60 days (Fig. 4.16). In the former the median species richness increased from 13 to 14, though considering specific communities, the number of species could either decrease by 2 or increase by up to 5 species (Fig. 4.16). In the latter case, the number of species decreased on average (decrease of the median value by 1), though again the change in species richness depended on the community composition and could decrease (by up to 2) or increase (by 1) (Fig. 4.16).

The change in the duration of water column restratification did not affected the median diversity of diatoms, though it did altered the shape of the diversity distribution in a scenario exploring a rapid restratification lasting for only 20days increasing the value of the 75th quartile from 3 to 5 (Fig. 4.17a). A rapid restratification, lasting for 20 or 30 days, resulted in an elevated by 1 coccolitophores diversity (Fig. 4.17c). Conversely, the prolonged restratification, lasting for 60days, resulted in an increase of median dinoflagellates diversity (Fig. 4.17b). Green algae diversity remained almost unchanged with only exception for an increase of its median value by 0.5 in case of restratification taking place within 20 days (Fig. 4.17d).

The change in duration of spring water column restratification affected the bottom-up processes regulating species competition and led to community restructuring. Both the shortening and the elongation of the restratification period, resulted in the decrease of similarity index values, with the higher discrepancies attributed to the longest duration of this process (Fig. 4.18). The stronger differences, spanning over almost 30% of the nominal value were reported for the index based on the maximal concentrations

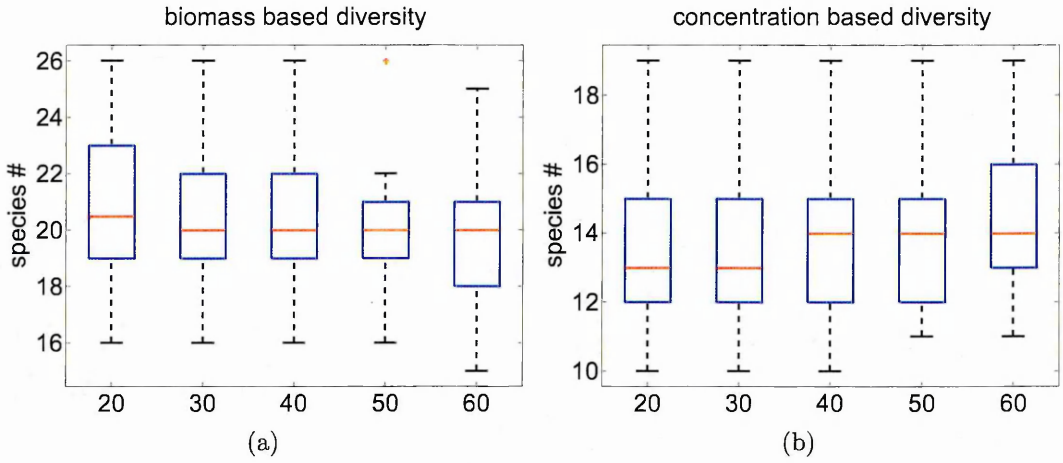

Figure 4.16: Species diversity in the systems distinguished solely by the spring water column restratification duration. The estimate of species diversity was based on each species (a) median biomass or (b) maximal concentration. The presented boxplots refer to species diversity observed in all ensemble communities.

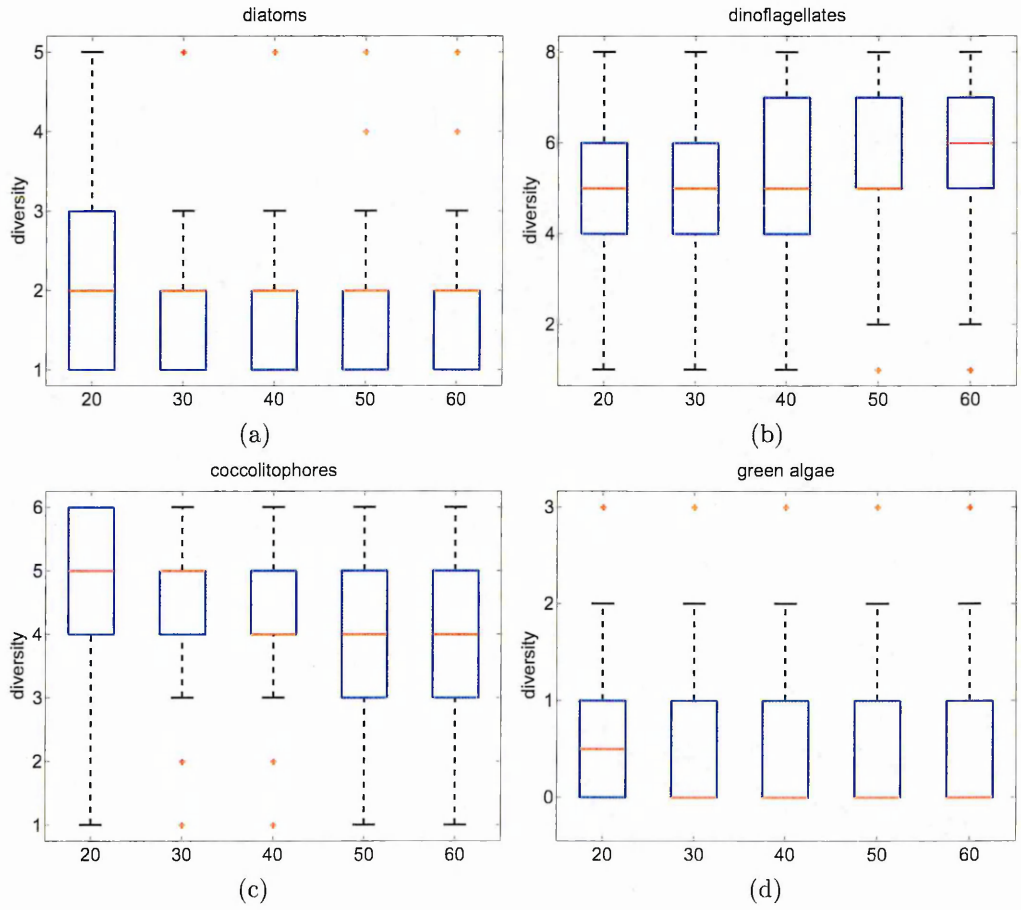

Figure 4.17: Sensitivity of the PFTs' diversity to the changes of the duration of water column restratification: (a) diatoms, (b) dinoflagellates, (c) coccolitophores, (d) green algae.

(Fig. 4.18b), while in case of median biomass the vast majority of similarity index values were confined between 90% and 100% of the nominal values in all the considered

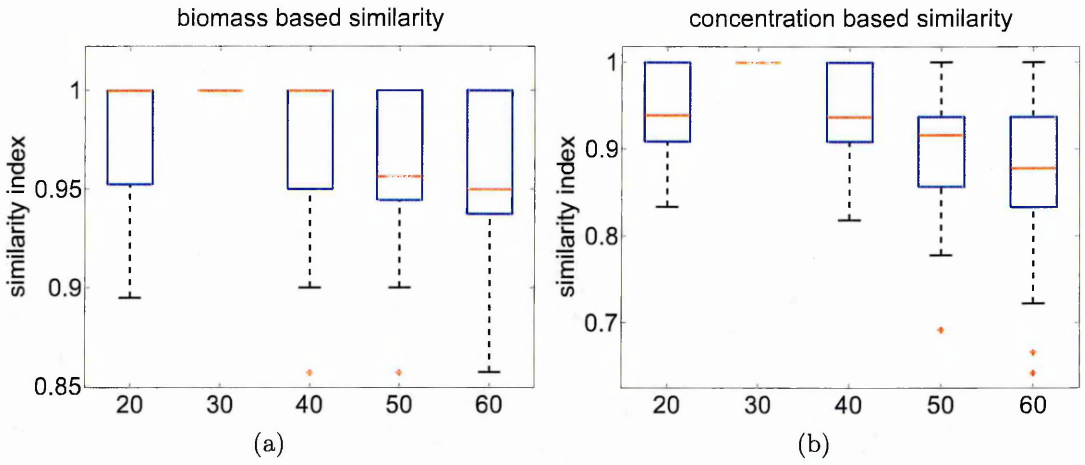

Figure 4.18: Community similarity index in environments distinguished with the spring water column restratification duration. Every single community was analysed in terms of its phytoplankton species composition across all explored environmental scenarios and based on this information a community similarity index was calculated. Community composition was evaluated with a (a) species median biomass or (b) its maximal concentration. The environment with a spring water column restratification lasting for 30d was used as a reference case for the computations.

cases (Fig. 4.18a).

The distribution of the species' physiological traits in all the cases resolved in this scenario were indistinguishable with the reference case (Fig. 3.5).

Duration of summer stratification The increase of the duration of summer stratification from 150 days up to 180 had almost neutral effect on the species richness based on maximal concentration, and only an increase in its duration up to 195 days resulted in median species richness decrease by 1 (Fig. 4.19b). On a contrary, shorter summer length led to an increase of species richness (median increase by 1 species) as presented on Fig. 4.19b.

Considering the median annual biomass as an indicator of the diversity a decreasing trend in species richness vs duration of summer stratification could be noted. Eventhough the median value decreased only by 1, the analysis of individual communities show a considerable decrease in species richness with the increase of summer duration reaching up to 5 species (Fig. 4.19a).

Considering the diversity within the functional groups, a change of the duration of summer stratification affected the shape of diversity distribution of all PFTs but green algae (Fig. 4.20). There was an increase in the diatoms diversity in case of summer

lasting for 195days which was illustrated by an increase in the 75th quartile of the diversity PDF (Fig. 4.20a), while dinoflagellates diversity decreased in that scenario (Fig. 4.20b). There was a decrease of coccolitophores diversity in scenarios considering summer lasting for 135 and 150 days (Fig. 4.20c). The green algae diversity changed only in scenario with summer length equal to 135 days, where the median diversity increase to value of 1 (Fig. 4.20d).

As in the previously paragraphs, the change in species richness clearly depended on the initial community composition thus conclusions on how duration of summer affect species richness ought to be make with care (Fig. 4.19).

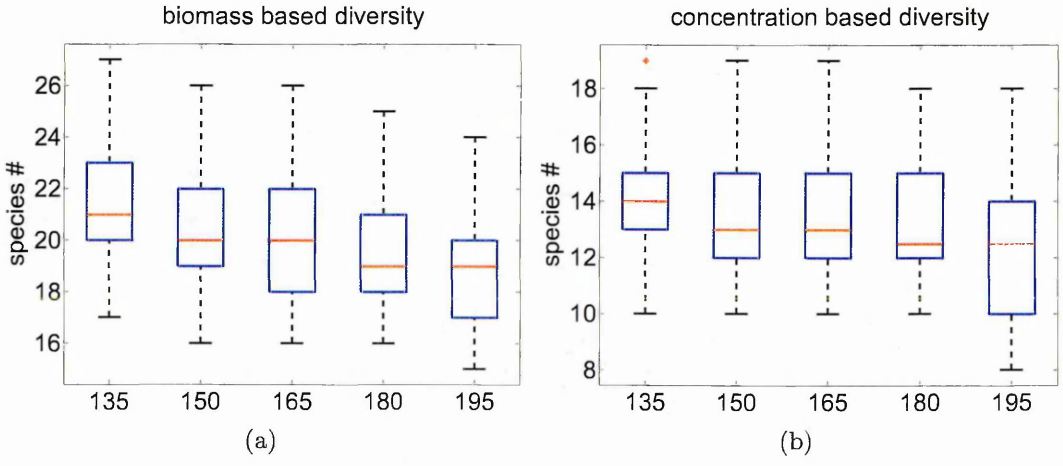

Figure 4.19: Species diversity in the systems distinguished solely by the duration of summer stratification. The estimate of species diversity was based on each species (a) median biomass or (b) maximal concentration. The presented boxplots refer to species diversity observed in all ensemble communities.

The change in duration of summer stratification affected time point of nutrients entrainment related to autumn water column deepening and consequently the bottom-up processes regulating species competition. Subsequently it led to community restructuring. Both the shortening and the elongation of the restratification period, resulted in the decrease of similarity index values, with the higher discrepancies attributed to the longest duration of summer restratification (Fig. 4.21). Notably, similar differences spanning over almost 25% of the nominal value were observed for the index based on both the maximal concentrations (Fig. 4.21b), median biomass (Fig. 4.21a).

The distribution of the species' physiological traits in all the cases resolved in this scenario were indistinguishable with the reference case (Fig. 3.5).

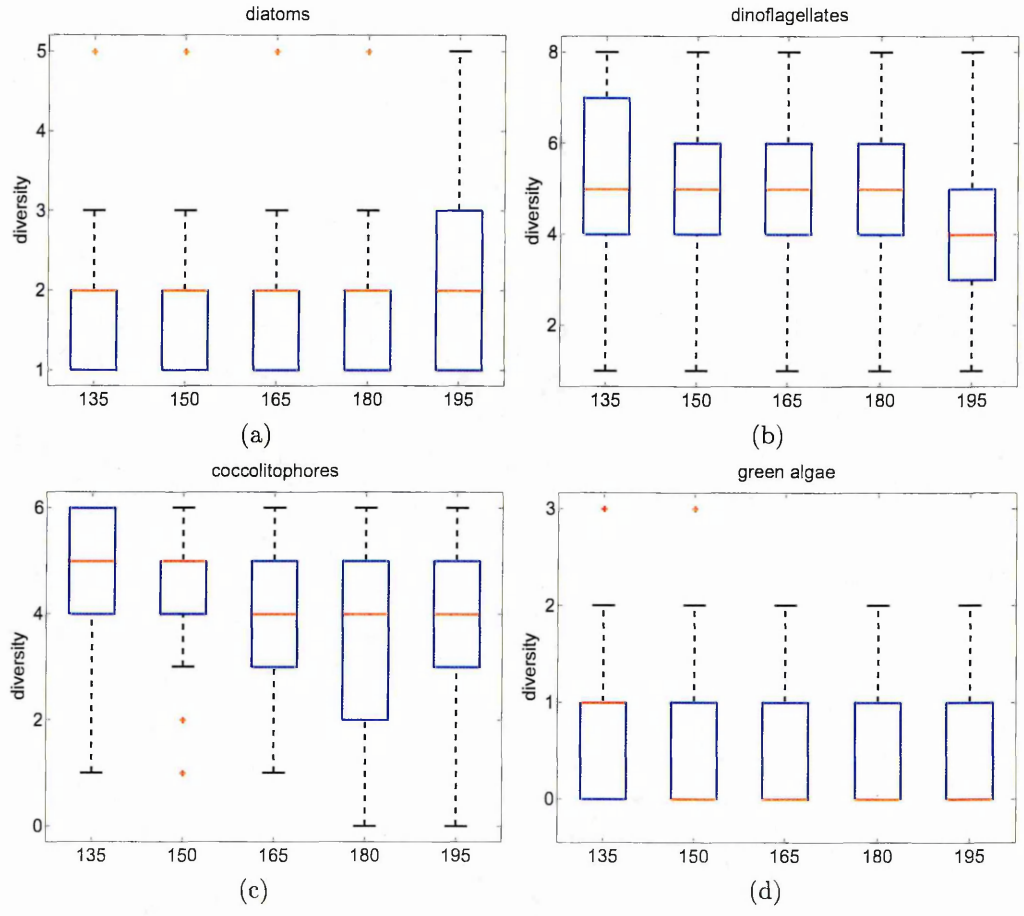

Figure 4.20: Sensitivity of the PFTs' diversity to the changes in the summer length duration: (a) diatoms, (b) dinoflagellates, (c) coccolitophores, (d) green algae.

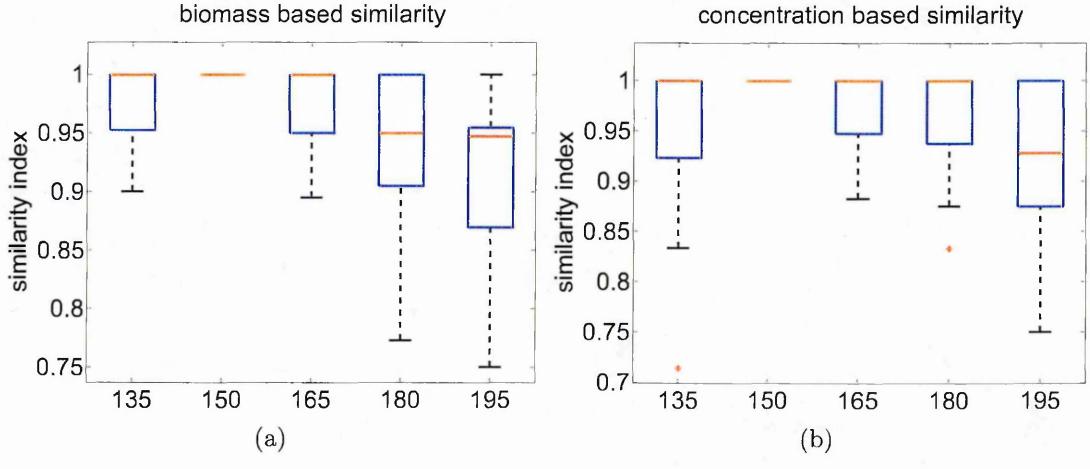

Figure 4.21: Community similarity index in environments distinguished with the duration of summer stratification. Every single community was analysed in terms of its phytoplankton species composition across all explored environmental scenarios and based on this information a community similarity index was calculated. Community composition was evaluated with a (a) species median biomass or (b) its maximal concentration. The environment with a summer stratification lasting for 150d was used as a reference case for the computations.

4.3.2 Change in the community at the functional groups level related to the physical forcing.

Change in the maximal MLD An increasing trend in the total phytoplankton yearly biomass was observed as the maximal MLD decreased from 600m to 200m (Fig. 4.22; Tab. 4.3). The median total yearly phytoplankton biomass increased by almost 4, 18 and 67% for maximal MLD equal to 500, 400 and 300m respectively, and doubled in case of 200m. This change was followed by an increase in the median total yearly biomass of diatoms (up to 4.5 folds), dinoflagellates (up to 65%), coccolitophores (68%), while the green algae decreased (by up to 95%) (Fig. 4.22; Tab. 4.3).

The change in the maximal MLD had a negative effect on total yearly copepods biomass, where its biomass decreased by up to 53.5% in case of environment with 200m maximal MLD and 13.5% in case of 300m (Fig. 4.23; Tab. 4.3). The shift from 600m to 500 or 400m had a negligible impact on copepods total yearly biomass.

Similarly to copepods, the median total yearly microzooplankton biomass decreased with the decrease of maximal MLD. In particular the shift from 600m maximal MLD to 500, 400 and 300m resulted in a median decrease of microzooplankton biomass by 6.5, 15.5 and 16.8% (Fig. 4.23; Tab. 4.3). Further decrease in the maximal MLD to 200m, however, led to an median increase of microzooplankton biomass by 53% (Fig. 4.23; Tab. 4.3). Simultaneously, statistical spread of the median copepods and microzooplankton biomass was considerably broad in an ecosystem with 200m maximal MLD, spanning over 73 and over 300% of the nominal value (Fig. 4.23; Tab. 4.3).

The performed sensitivity study revealed that the maximal MLD value had a very strong impact on the spring bloom phenology, as both its timing and magnitude were considerably affected (Fig. 4.24; Tab. 4.3). The shallower water column depth during the winter months caused lower nutrients entrainment and led to lower diatoms concentration. At the same time the average light availability increased leading to earlier spring bloom formation and consequently to higher maximal biomass (Fig. 4.24; Tab. 4.3).

Parameter	Units	200	300	400	500	600
Phytoplankton	$mmolC/m^2$	9769.06 ± 2048.54	5554.99 ± 1229.24	3829.70 ± 404.46	3441.90 ± 212.35	3308.57 ± 130.57
Diatoms	$mmolC/m^2$	5815.96 ± 2240.45	2734.83 ± 1540.33	1476.92 ± 484.82	1227.80 ± 197.20	1170.07 ± 118.09
Dinoflagellates	$mmolC/m^2$	1045.24 ± 340.51	693.78 ± 207.92	588.38 ± 147.69	599.65 ± 129.46	603.04 ± 110.41
Coccolitophores	$mmolC/m^2$	2214.76 ± 421.79	1738.63 ± 254.57	1509.93 ± 206.77	1399.68 ± 164.73	1324.75 ± 142.18
Gren algae	$mmolC/m^2$	1.44 ± 1.44	1.19 ± 1.19	13.70 ± 13.70	38.84 ± 38.80	63.31 ± 54.76
Zooplankton	$mmolC/m^2$	1832.26 ± 257.79	1641.77 ± 62.19	1712.62 ± 26.58	1832.09 ± 17.29	1922.91 ± 18.63
Copepods	$mmolC/m^2$	510.35 ± 154.59	916.65 ± 43.83	989.38 ± 21.03	1032.27 ± 21.41	1065.71 ± 21.15
Microzooplankton	$mmolC/m^2$	1265.75 ± 393.41	719.62 ± 73.30	728.02 ± 36.17	799.66 ± 29.43	853.79 ± 32.98
Maximum diatoms biomass	$mmolC/m^2$	177.04 ± 44.75	105.36 ± 25.63	85.32 ± 4.56	91.72 ± 0.70	99.20 ± 0.49
$T_{biommax}$	yd	103.00 ± 7.00	119.00 ± 3.50	123.50 ± 1.50	126.00 ± 1.00	128.00 ± 1.00
Maximum diatoms concentration	$mmolC/m^3$	1.42 ± 0.25	2.92 ± 0.28	3.90 ± 0.14	4.57 ± 0.04	4.96 ± 0.02
$T_{concmax}$	yd	113.00 ± 5.00	121.50 ± 1.50	124.00 ± 1.00	126.00 ± 1.00	128.00 ± 1.00
Spring bloom initiation	$mmolC/m^3$	54.50 ± 13.00	63.50 ± 15.00	80.00 ± 21.50	117.00 ± 7.00	122.00 ± 2.50

Table 4.3: Ecosystem properties sensitivity to the maximal MLD value. The presented values indicate total yearly biomass of the indicated groups (phytoplankton, diatoms, dinoflagellates, coccolitophores, green algae, zooplankton, copepods and microzooplankton), maximal diatoms biomass and concentration, but also the time point when the peak of diatoms biomass and concentration was observed, and the spring bloom initiation.

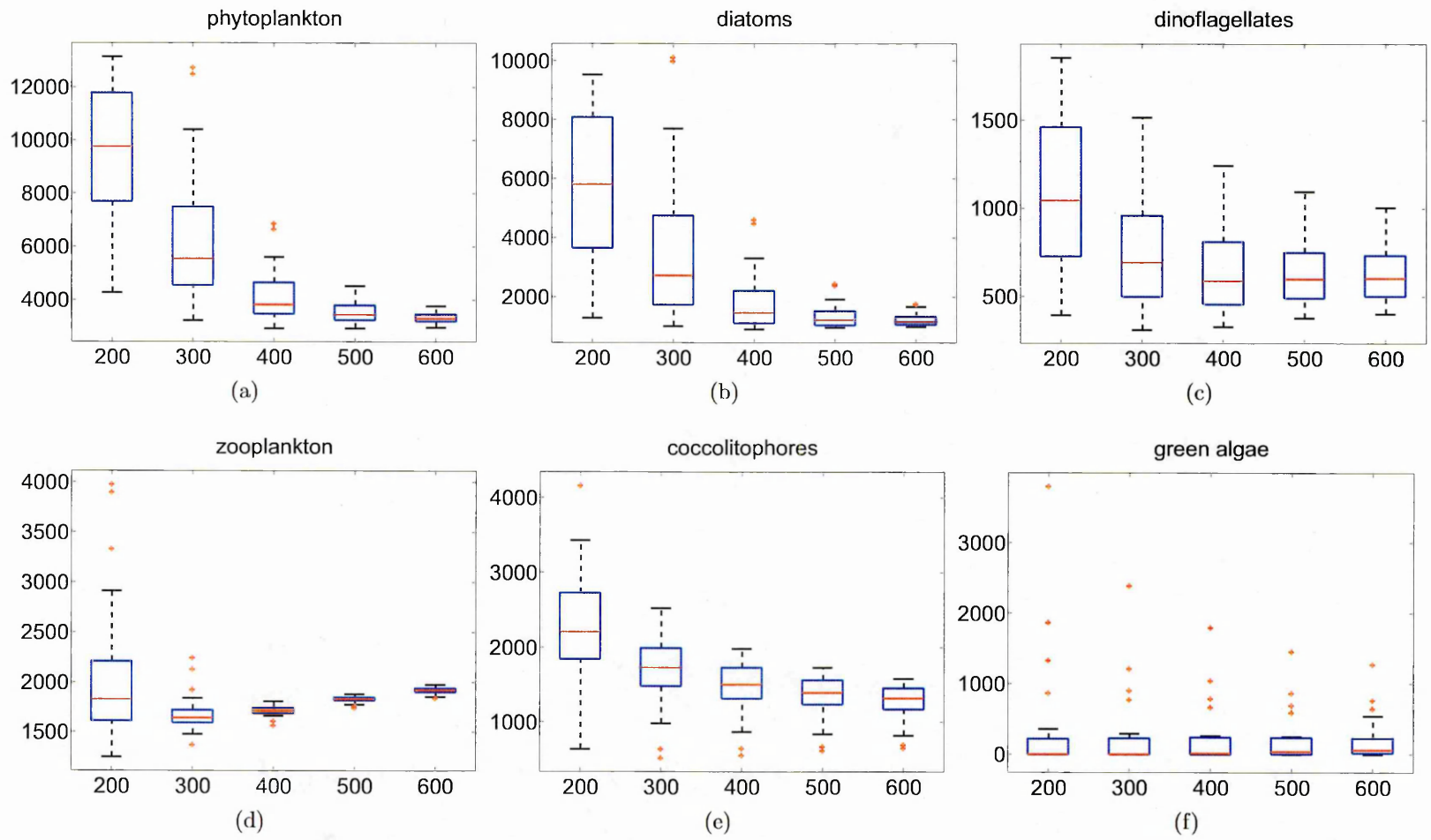

Figure 4.22: Main groups sensitivity to the maximal MLD. The panels represent total yearly biomass of: (a) phytoplankton, (b) diatoms, (c) dinoflagellates, (d) zooplankton, (e) coccolitophores and (f) green algae in all ensemble communities in ecosystems distinguished solely in terms of the maximal MLD value.

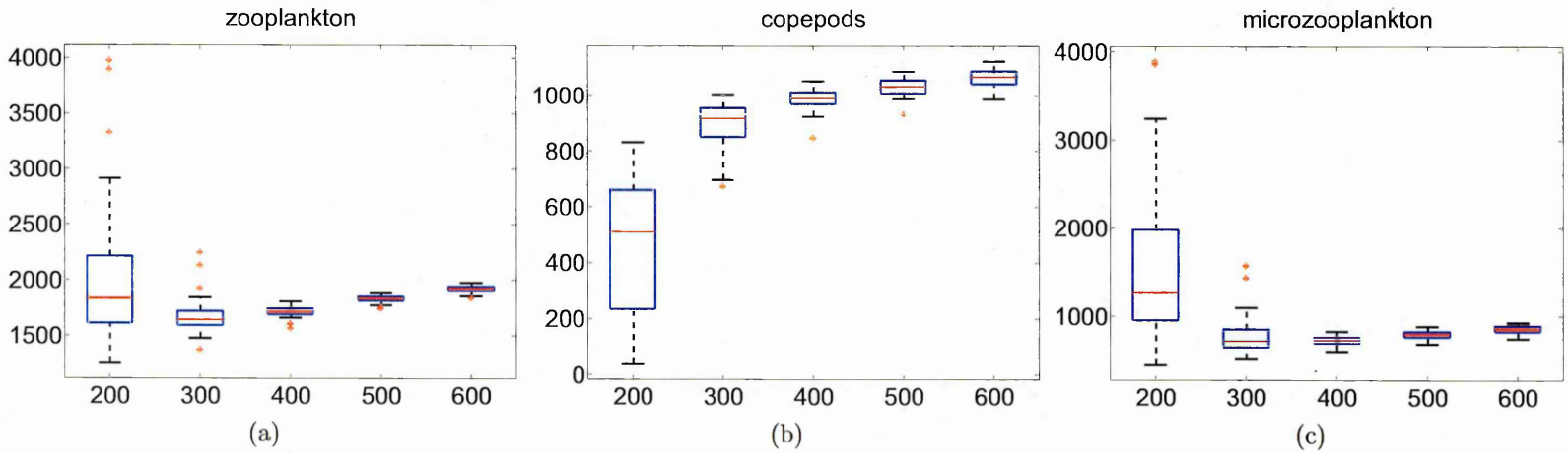

Figure 4.23: Main groups sensitivity to the maximal MLD. The panels represent total yearly biomass of: (a) zooplankton, (b) copepods and (c) microzooplankton in all ensemble communities in ecosystems distinguished solely in terms of the maximal MLD value.

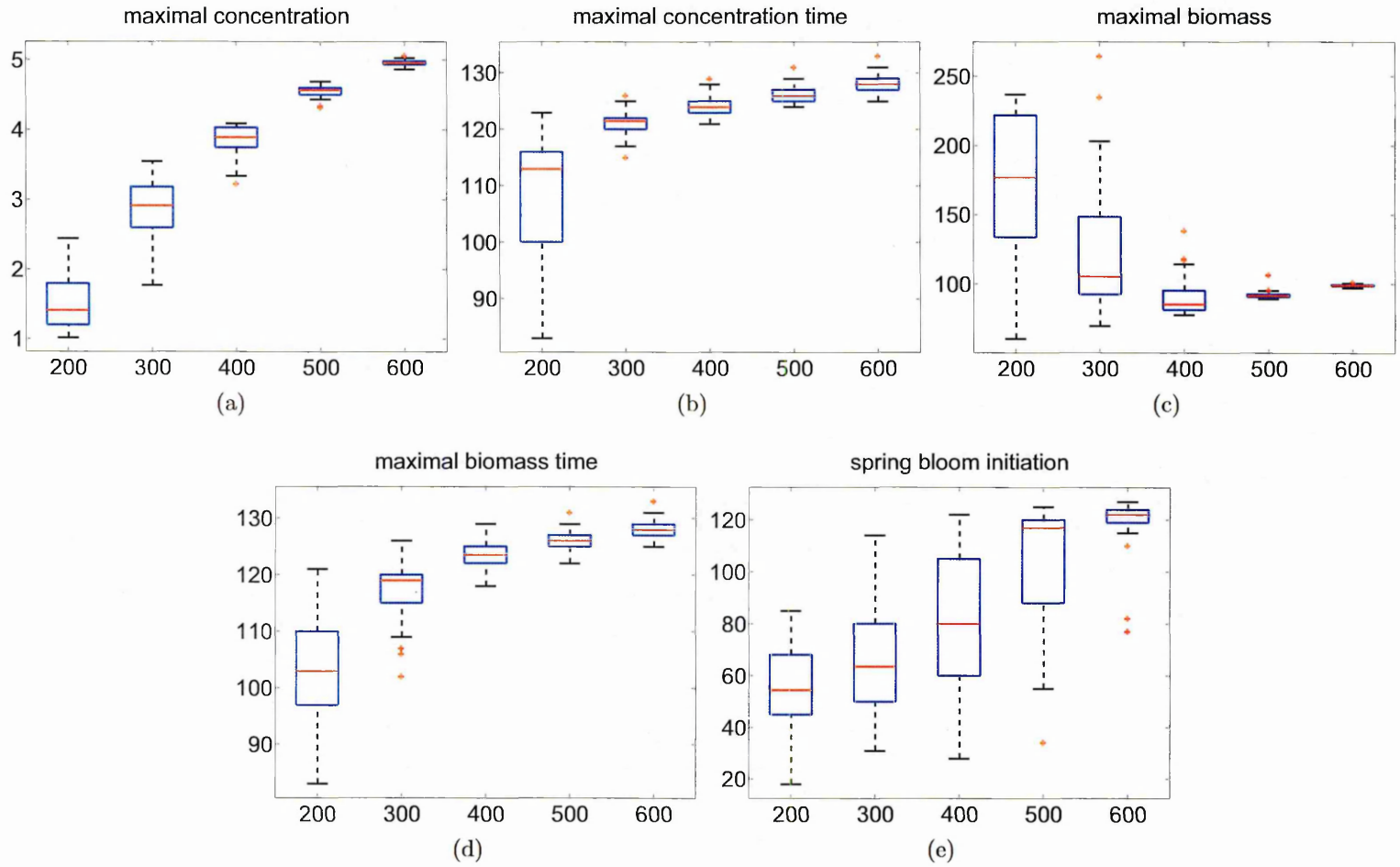

Figure 4.24: Spring bloom sensitivity to the maximal MLD. The panels represent: (a) maximal diatoms concentration, (b) year day when the maximal concentration was observed, (c) maximal diatoms biomass, (d) year day when the maximal biomass was observed and (e) initiation of the spring bloom formation in all ensemble communities in ecosystems distinguished solely in terms of the maximal MLD value.

The grazing pressure imposed on each phytoplankton species altered amongst the scenarios considering the change in the maximal MLD value. The maximal values of the cumulative grazing rate by copepods and microzooplankton observed over the year appeared to decrease in the ecosystems with the lower values of the maximal MLD depth by 2 folds (Fig. 4.25). This corresponds to an overall decrease in the grazers abundance (Fig. 4.22d) and a decrease in the maximal phytoplankton concentration during spring bloom (Fig. 4.24a) observed in the systems with lower maximal MLD. At the same time the peak in the grazing pressure is advanced in time in the systems with lower maximal MLD by up to 29 days if scenarios with 600m and 200m were considered (Fig. 4.25a, 4.25e; note that the water column restratification was initiating at 85th year day in all the explored cases). This in turn illustrates an increased grazing pressure imposed on the phytoplankton species shortly after spring water column restratification in the system with maximal MLD equal to 200m. It indicated also a tighter coupling between zooplankton and phytoplankon in the period between 85th and 120th yd. Consequently, the spring bloom of diatoms was under stronger top-down control during its initial phase which could have resulted in a lower concentration peak observed in this system (Fig. 4.24a).

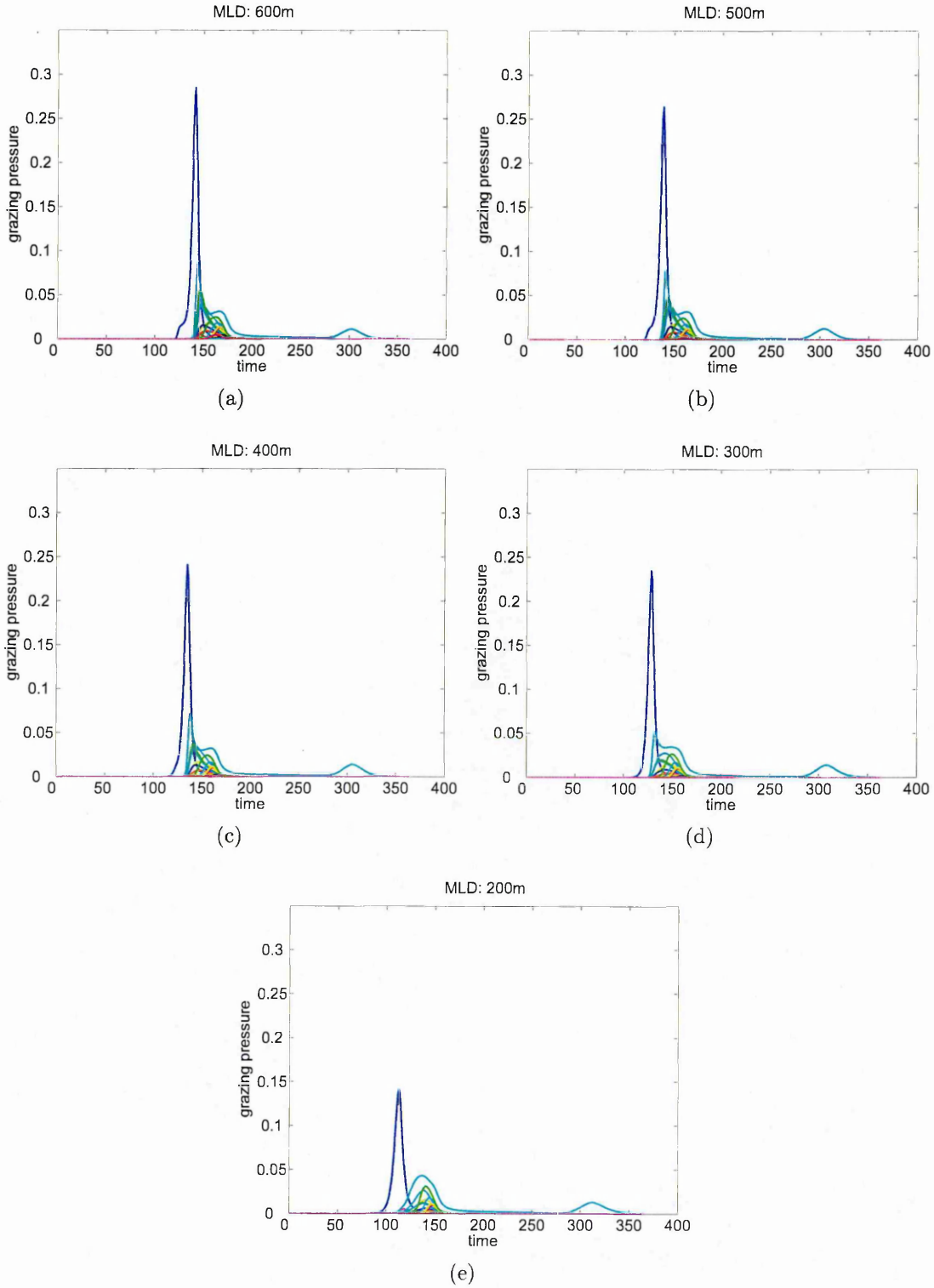

Figure 4.25: Cumulative grazing pressure imposed by copepods and microzooplakton on phytoplankton species in ecosystems distinguished with the maximal MLD value: (a) 600m, (b) 500m, (c) 400m, (d) 300m and (e) 200m. Each line depicts the grazing pressure imposed on a single species. Results have been presented for a single, randomly selected community.

Change in the beginning of spring water column restratification The gradual delay in the initiation of the spring water column retratification from 75 to 115 [yd]

resulted in a decrease of total yearly phytoplankton biomass (Fig. 4.26; Tab. 4.4). The initiation of the restratification in the reference scenario (see simulation in the Chapter 2) was assumed to occur on 85yd, thus the below comparison refer to this specific value.

The 10 days advance in the restratification resulted in approximately 25% higher total yearly phytoplankton biomass, which coincided with a similar increase of functional groups biomass: 23% diatoms, 17% dinoflagellates, 31% coccolitophores and 35% green algae (Fig. 4.26; Tab. 4.4). The zooplankton biomass increased as well (by 4%) which was associated with a 21% increase of microzooplankton as the copepods total yearly biomass decreased by 9.5% with respect to the reference scenario (Fig. 4.27; Tab. 4.4).

The delay in the water column restratification led to up to a 16% decrease of total yearly phytoplankton biomass (Fig. 4.26) together with a 44% decrease in coccolitophores and 11% coccolitophores biomass. On a contrary, the total yearly diatoms and dinoflagellates biomass showed an increasing trend with up to 4.5% median increase of the former and 13% of the latter (Fig. 4.26). This dynamics was followed by the grazers biomass, where the total yearly biomass of microzooplankton decreased by up to 9.5% and the copepods increased by 2% (Fig. 4.27; Tab. 4.4), thus reflecting the grazing preferences and pray dynamics.

The shift in the restratification initiation influenced only slightly the magnitude of the spring diatom bloom as the change in maximal concentration and biomass did not exceed 2% difference (Fig. 4.28). Furthermore, the shift in spring initiation clearly affected the timing of the spring bloom initiation and biomass maximum, yet it the observed change was simply reflecting the imposed shift in the restratification initiation (Fig. 4.28; Tab. 4.4).

Parameter	Units	75	85	95	105	115
Phytoplankton	$mmolC/m^2$	4598.80 ± 276.94	3670.52 ± 178.43	3308.57 ± 130.57	3072.91 ± 107.27	3034.40 ± 145.30
Diatoms	$mmolC/m^2$	1441.41 ± 272.47	1172.75 ± 121.23	1170.07 ± 118.09	1185.40 ± 119.52	1223.01 ± 142.24
Dinoflagellates	$mmolC/m^2$	707.59 ± 109.45	599.06 ± 114.76	603.04 ± 110.41	626.22 ± 113.02	670.90 ± 119.37
Coccolitophores	$mmolC/m^2$	2214.22 ± 284.76	1700.25 ± 203.75	1324.75 ± 142.18	1086.79 ± 93.92	948.28 ± 74.23
Gren algae	$mmolC/m^2$	77.18 ± 49.65	63.89 ± 53.80	63.31 ± 54.76	65.10 ± 56.47	66.50 ± 57.54
Zooplankton	$mmolC/m^2$	2034.35 ± 30.57	1964.88 ± 17.00	1922.91 ± 18.63	1903.97 ± 18.37	1895.86 ± 16.68
Copepods	$mmolC/m^2$	952.60 ± 37.93	1056.15 ± 22.33	1065.71 ± 21.15	1072.48 ± 21.90	1081.67 ± 21.30
Microzooplankton	$mmolC/m^2$	1091.25 ± 77.28	899.68 ± 33.86	853.79 ± 32.98	830.40 ± 30.64	814.18 ± 32.38
Maximum diatoms biomass	$mmolC/m^2$	98.89 ± 0.45	98.69 ± 0.70	99.20 ± 0.49	99.89 ± 0.48	100.20 ± 0.60
$T_{biommax}$	yd	110.00 ± 2.00	119.00 ± 1.00	128.00 ± 1.00	137.50 ± 1.50	147.00 ± 1.00
Maximum diatoms concentration	$mmolC/m^3$	4.94 ± 0.02	4.93 ± 0.04	4.96 ± 0.02	4.99 ± 0.02	5.01 ± 0.03
$T_{concmax}$	yd	110.00 ± 2.00	119.00 ± 1.00	128.00 ± 1.00	137.50 ± 1.50	147.00 ± 1.00
Spring bloom initiation	$mmolC/m^3$	103.50 ± 2.50	113.00 ± 2.00	122.00 ± 2.50	131.00 ± 3.00	140.00 ± 4.00

Table 4.4: Ecosystem properties sensitivity to the initiation of spring water column restratification. The presented values indicate total yearly biomass of the indicated groups (phytoplankton, diatoms, dinoflagellates, coccolitophores, green algae, zooplankton, copepods and microzooplankton), maximal diatoms biomass and concentration, but also the time point when the peak of diatoms biomass and concentration was observed, and the spring bloom initiation.

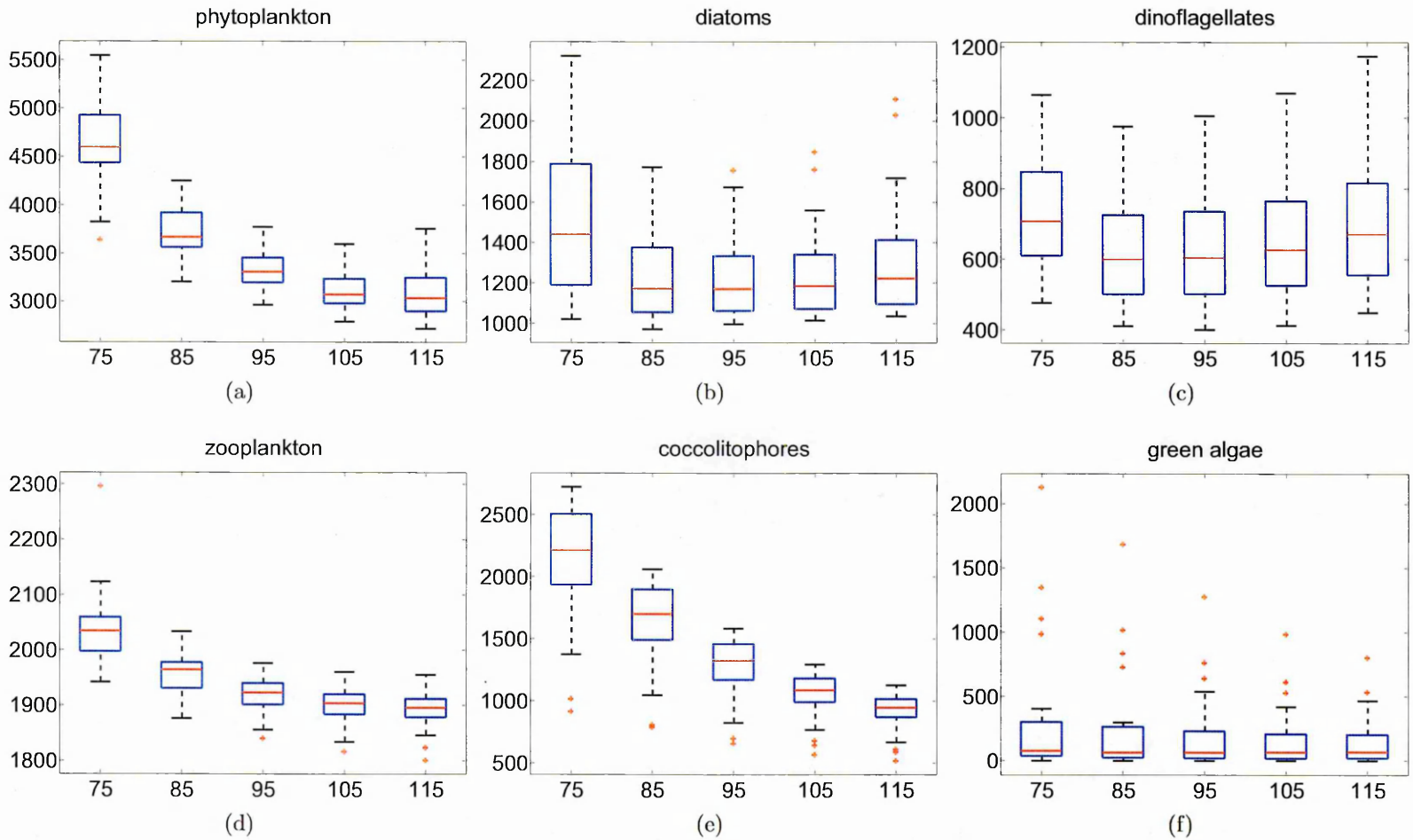

Figure 4.26: Main groups sensitivity to the spring water column restratification initiation. The panels represent total yearly biomass of: (a) phytoplankton, (b) diatoms, (c) dinoflagellates, (d) zooplankton, (e) coccolitophores and (f) green algae in all ensemble communities in ecosystems distinguished solely in terms of the beginning of spring water column restratification.

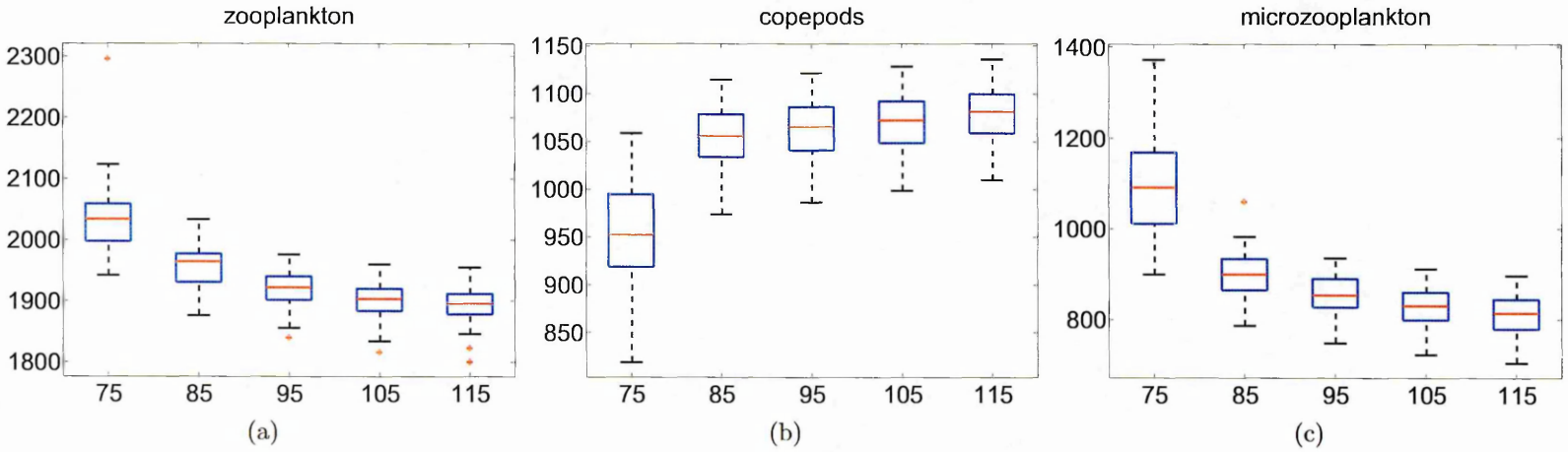

Figure 4.27: Main groups sensitivity to the spring water column restratification initiation. The panels represent total yearly biomass of: (a) zooplankton, (b) copepods and (c) microzooplankton in all ensemble communities in ecosystems distinguished solely in terms of the beginning of spring water column restratification.

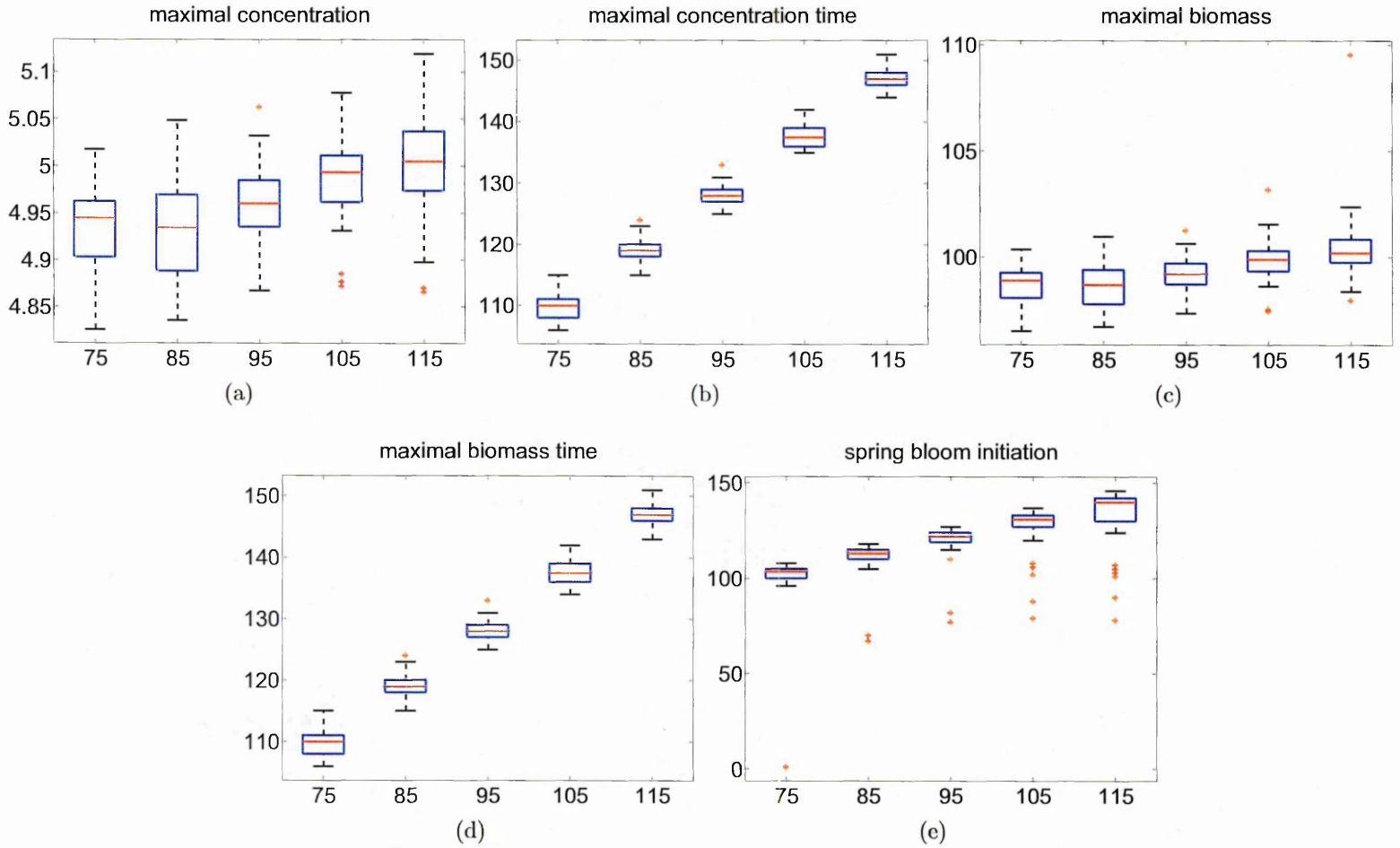

Figure 4.28: Spring bloom sensitivity to the spring water column restratification initiation. The panels represent: (a) maximal diatoms concentration, (b) year day when the maximal concentration was observed, (c) maximal diatoms biomass, (d) year day when the maximal biomass was observed and (e) initiation of the spring bloom formation in all ensemble communities in ecosystems distinguished solely in terms of the beginning of spring water column restratification.

Change in the duration of spring water column restratification The change in the length of the period over which the spring water column restratifies, δt, from 20 to 60 days resulted in a decrease of total yearly phytoplankton biomass (Fig. 4.29; Tab. 4.5). The spring restratification in the reference scenario (see simulation in the Chapter 2) was assumed to take place within 30 days, thus, similarly to the above paragraph, the below comparison refer to this specific value.

The most rapid stratification, occuring within 20 days, resulted in a 14.5% higher total yearly phytoplankton biomass, which was reflected by the increase of small in size functional groups total yearly biomass (Fig. 4.29; Tab. 4.5). The highest median increase was observed within the representatives of coccolitophores (31% increase) and green algae (13.5% increase). Diatoms total yearly biomass increased only by 2%, and dinoflagellates biomass decreased on average by 0.5% (Fig. 4.29; Tab. 4.5).

The increase in the duration of spring restratification led to a decrease in the median total yearly phytoplankton biomass by up to 9% (Fig. 4.29; Tab. 4.5). Similar dynamics was reported when green algae and coccolitophores dynamics were considered, though to a different extent (Fig. 4.29; Tab. 4.5). Namely green algae decreased by up to 6% while coccolitophores by up to 37%. Conversely, the diatoms and dinoflagellates appeared to benefit from a longer stratification and their total yearly biomass increased by 24% and 9% respectively. Interestingly though, the statistical spread of total yearly biomass of all phytoplankton community and specifically diatoms and dinoflagellates increased significantly with an increase of restratification duration spanning over 15%, 36% and 25% of the nominal value observed in the reference case.

The median total zooplankton yearly biomass varied slightly in this sensitivity study as the rate of change spanned from 1% decrease in case of $\delta t = 20$d to 2% increase in case of $\delta t = 50$d. The increase of δt from 20 to 60 with a 10days step correlated with an increasing trend in large zooplantkon total yearly biomass and a decreasing trend in small zooplankton species. The former increased by up to 10% though the median value only up to 6.5%, and the latter decreased by up to 16.5% with a median decrease of 12.3% (Fig. 4.30; Tab. 4.5).

A considerably low differences in the spring bloom intensity were observed for $20 \leq \delta t \leq 40$, namely the maximal biomass altered by $\pm 2\%$ and maximal concentration by

$\pm 3\%$ for all ensemble communities (Tab. 4.5). Nonetheless the bloom initiation and maturation reflected the change in the physical forcing characteristics as the bloom initiation shifted from 116yd to 128yd, and the timing of maximal concentration from 121yd to 136yd for $\delta t = 20$ and $\delta t = 40$ respectively (Fig. 4.31; Tab. 4.5). In fact an approximately 7days shift in the timing of bloom initiation and maximal diatoms concentration was observed per each 10days shift in δt (Fig. 4.31; Tab. 4.5).

A 2% and 5% decrease in the maximal diatoms concentration was observed in scenarios with $\delta t = 50$ and $\delta t = 60$ respectively. A community composition had a considerable impact on the rate of change which was reflected by a statistical spread of the maximal diatoms concentration in each ensemble community. These differences combined with the varioue year days at which the maximal concentration in each community was observed resulted in considerable discrepancies in maximal diatoms biomass across all ensemble community members (Fig. 4.31; Tab. 4.5). Notably, a 9.5% and almost 35% increase of maximal diatoms biomass was reported for $\delta t = 50$ and $\delta t = 60$ respectively, though the increase could reach up to almost 39% and 70% respectively (Fig. 4.31; Tab. 4.5).

Parameter	Units	20	30	40	50	60
Phytoplankton	$mmolC/m^2$	3749.54 ± 192.74	3308.57 ± 130.57	3033.09 ± 105.74	2997.14 ± 153.38	3103.94 ± 198.39
Diatoms	$mmolC/m^2$	1187.48 ± 133.50	1170.07 ± 118.09	1191.76 ± 126.88	1277.09 ± 161.38	1462.33 ± 225.46
Dinoflagellates	$mmolC/m^2$	601.68 ± 126.81	603.04 ± 110.41	619.97 ± 109.60	651.89 ± 119.13	690.48 ± 126.80
Coccolitophores	$mmolC/m^2$	1745.72 ± 214.29	1324.75 ± 142.18	1065.21 ± 89.61	919.31 ± 67.21	838.57 ± 69.76
Gren algae	$mmolC/m^2$	63.71 ± 53.60	63.31 ± 54.76	63.68 ± 56.14	62.34 ± 55.30	64.06 ± 57.02
Zooplankton	$mmolC/m^2$	1965.52 ± 17.99	1922.91 ± 18.63	1905.74 ± 18.50	1900.04 ± 16.45	1917.55 ± 19.20
Copepods	$mmolC/m^2$	1050.09 ± 23.02	1065.71 ± 21.15	1080.77 ± 21.22	1099.57 ± 21.50	1117.77 ± 21.50
Microzooplankton	$mmolC/m^2$	904.83 ± 33.60	853.79 ± 32.98	823.30 ± 32.09	803.47 ± 33.22	800.81 ± 37.37
Maximum diatoms biomass	$mmolC/m^2$	98.92 ± 0.62	99.20 ± 0.49	99.72 ± 0.59	109.34 ± 9.17	133.53 ± 11.57
$T_{biommax}$	yd	121.00 ± 1.00	128.00 ± 1.00	136.00 ± 1.00	143.00 ± 1.00	150.00 ± 1.00
Maximum diatoms concentration	$mmolC/m^3$	4.95 ± 0.03	4.96 ± 0.02	4.96 ± 0.03	4.86 ± 0.07	4.71 ± 0.07
$T_{concmax}$	yd	121.00 ± 1.00	128.00 ± 1.00	136.00 ± 1.00	143.00 ± 1.00	151.00 ± 1.00
Spring bloom initiation	$mmolC/m^3$	116.00 ± 1.50	122.00 ± 2.50	128.00 ± 3.00	134.50 ± 3.00	140.50 ± 3.00

Table 4.5: Ecosystem properties sensitivity to the duration of spring water column restratification. The presented values indicate total yearly biomass of the indicated groups (phytoplankton, diatoms, dinoflagellates, coccolitophores, green algae, zooplankton, copepods and microzooplankton), maximal diatoms biomass and concentration, but also the time point when the peak of diatoms biomass and concentration was observed, and the spring bloom initiation.

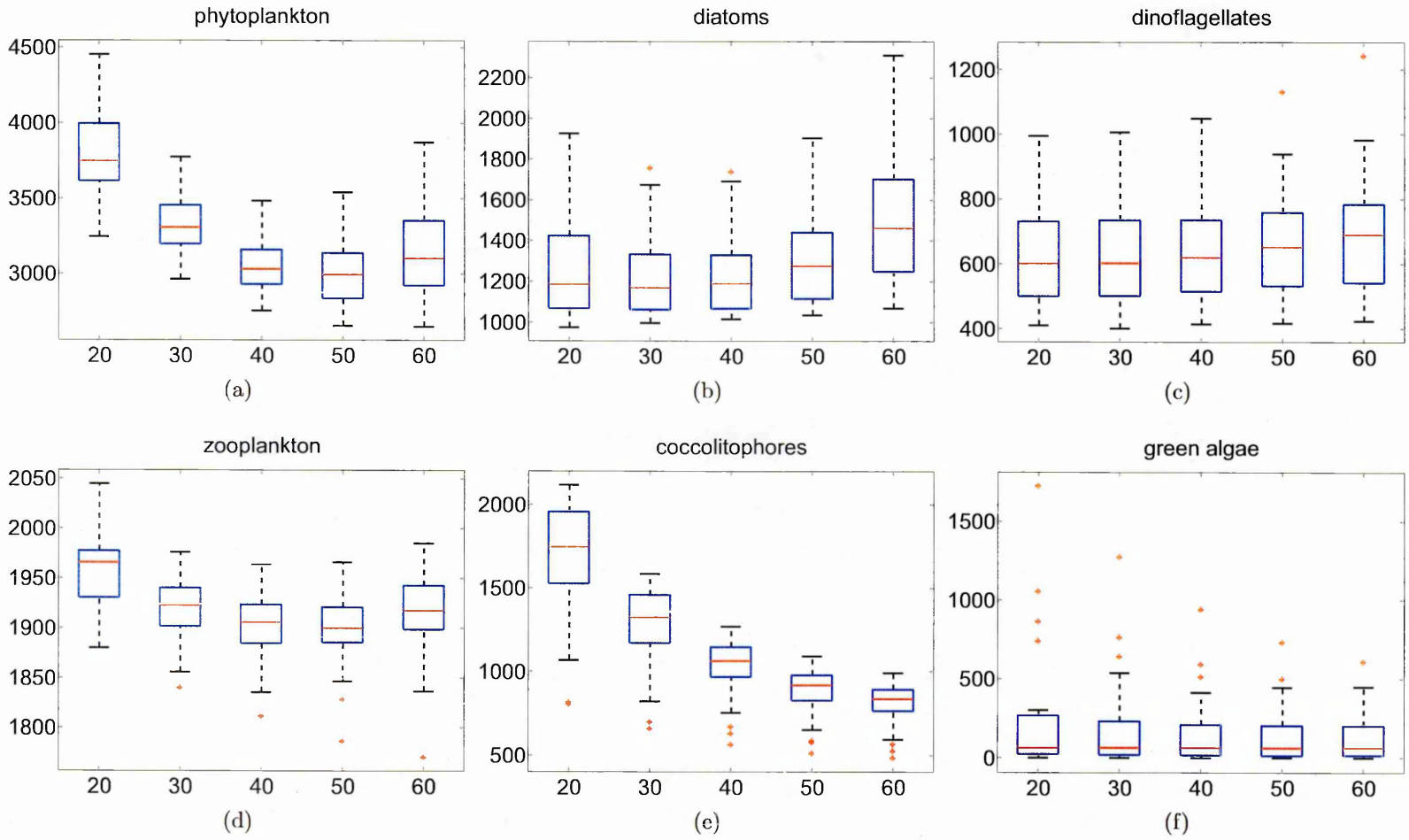

Figure 4.29: Main groups sensitivity to the spring water column restratification duration. The panels represent total yearly biomass of: (a) phytoplankton, (b) diatoms, (c) dinoflagellates, (d) zooplankton, (e) coccolitophores and (f) green algae in all ensemble communities in ecosystems distinguished solely in terms of the duration of spring water column restratification.

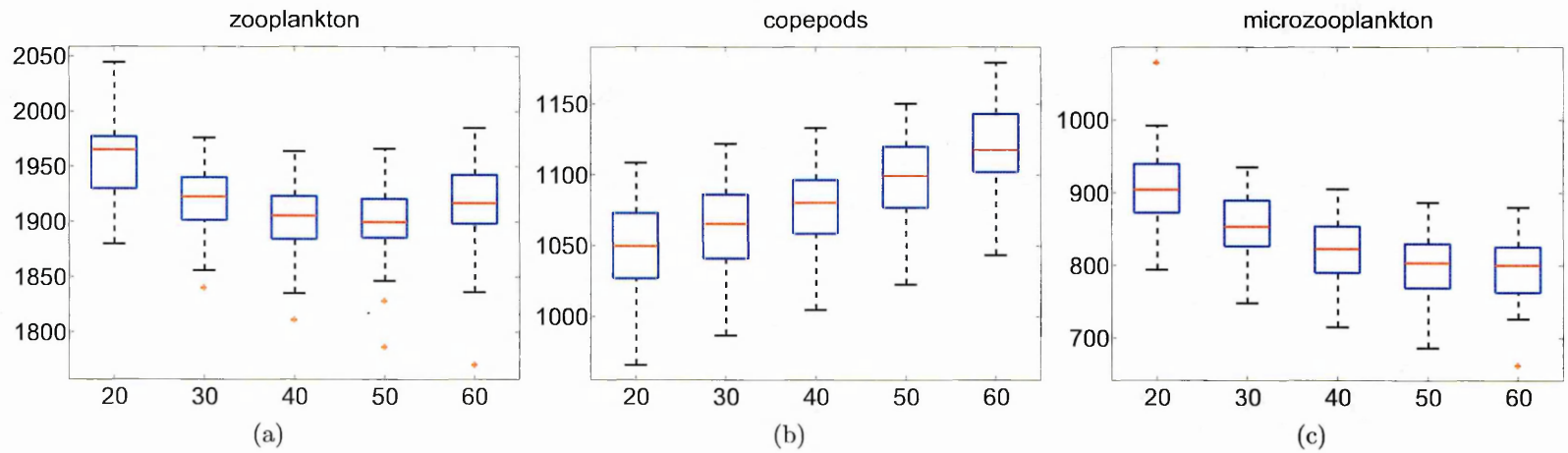

Figure 4.30: Main groups sensitivity to the spring water column restratification duration. The panels represent total yearly biomass of: (a) zooplankton, (b) copepods and (c) microzooplankton in all ensemble communities in ecosystems distinguished solely in terms of the duration of spring water column restratification.

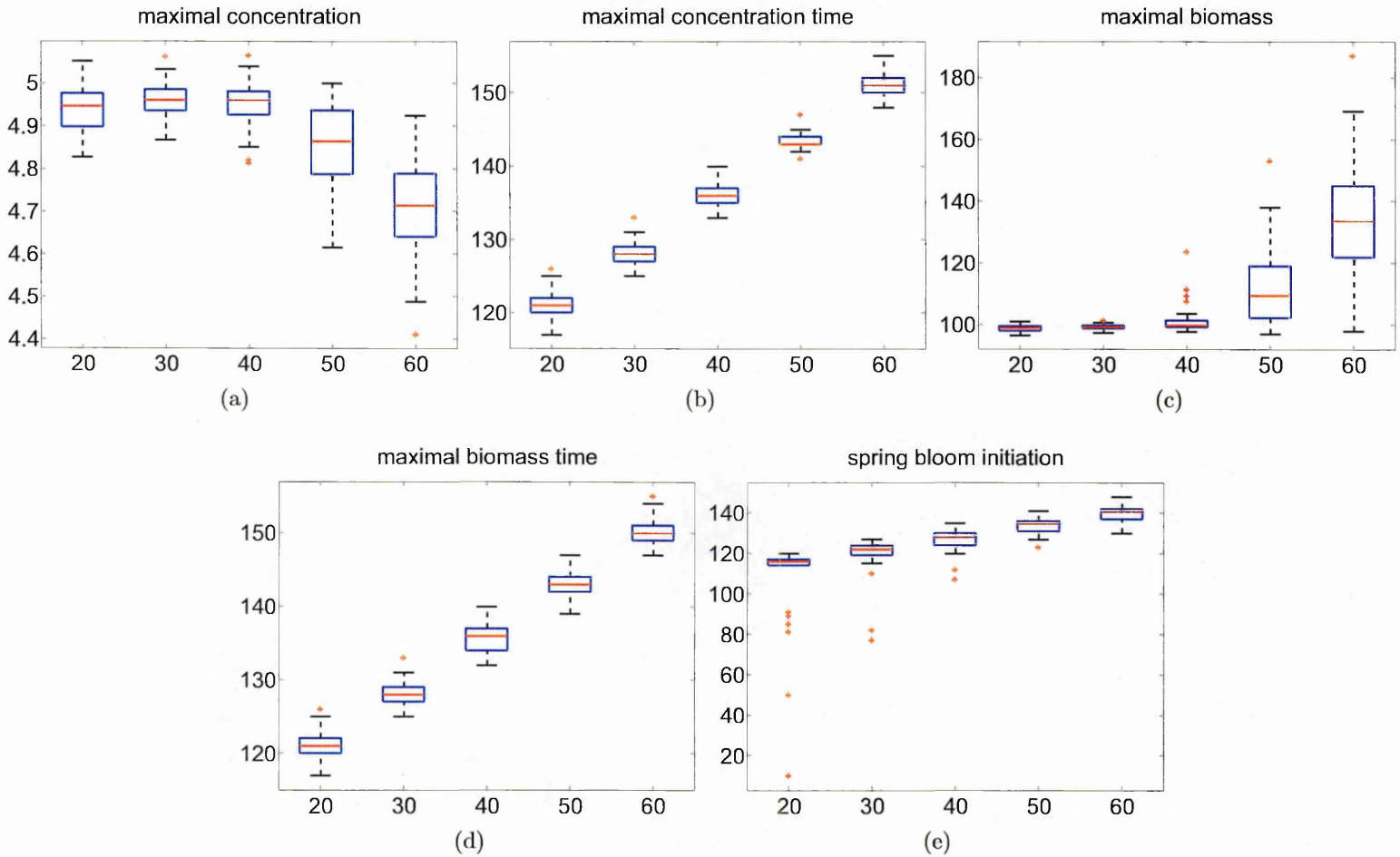

Figure 4.31: Spring bloom sensitivity to the spring water column restratification duration. The panels represent: (a) maximal diatoms concentration, (b) year day when the maximal concentration was observed, (c) maximal diatoms biomass, (d) year day when the maximal biomass was observed and (e) initiation of the spring bloom formation in all ensemble communities in ecosystems distinguished solely in terms of the duration of spring water column restratification.

Change in the duration of summer stratification A decreasing trend in the total phytoplankton yearly biomass was observed as the summer stratification period, S_L, elongated from 150 to 195 days (Fig. 4.32; Tab. 4.6). The median total yearly phytoplankton biomass decrease by 15, 22.5 and 25.5% for S_L equal to 165, 180 and 195 days respectively. This change was followed by a decrease in the median total yearly biomass of diatoms (6, 8 and 9%), dinoflagellates (14, 25 and 34%), coccolitophores (22, 31 and 33%) and green algae (7.6, 14 and 20%, for S_L equal to 165, 180 and 195 days respectively) (Fig. 4.32; Tab. 4.6).

A 30% higher total yearly phytoplankton biomass was observed in a system with a 15days duration of summer stratification with respect to the reference case (Fig. 4.32; Tab. 4.6). In fact all functional groups were on average more abundant in this type of system, namely an increase in the median total yearly biomass of diatoms (by 15%), dinoflagellaes (by 18.5%), coccolitophores (by 48.5%) and green algae (by 27.5%) was observed (Fig. 4.32; Tab. 4.6).

The change in the duration of summer restratification had a negligible effect on total yearly copepods biomass, where its change did not exceed 3% for all explored values of S_L and all ensemble communities (Fig. 4.33; Tab. 4.6). Similarly to copepods, the median total yearly microzooplankton biomass change almost imperceptibly (by 1.5%), though the statistical spread spanned from a 6.5% decrease to almost 3% increase (Fig. 4.33;Tab. 4.6). On a contrary, the shorter summer stratification caused its 6.5% median increase (Fig. 4.33) associated with an increase of small phytoplankton types abundance (Fig. 4.32;Tab. 4.6).

The performed sensitivity study revealed that the duration of summer stratification had a very little effect on the spring bloom phenology, as both its timing and magnitude caused only up to 4% change in the characteristic indicators (Fig. 4.34; Tab. 4.6). The only exception was reported for the spring bloom initiation for $S_L = 135$ days for which there was a significant increase in the statistical spread of the distribution, thus showing that in case of 25% of communities the spring bloom formation initiated on 90th yd (with the median on 120th yd; Fig. 4.34; Tab. 4.6).

Parameter	Units	135	150	165	180	195
Phytoplankton	$mmolC/m^2$	4300.45 ± 246.45	3308.57 ± 130.57	2788.43 ± 78.74	2567.24 ± 50.56	2444.05 ± 49.52
Diatoms	$mmolC/m^2$	1348.34 ± 247.90	1170.07 ± 118.09	1107.53 ± 74.20	1080.53 ± 36.86	1072.57 ± 25.77
Dinoflagellates	$mmolC/m^2$	709.62 ± 143.58	603.04 ± 110.41	520.30 ± 91.22	454.96 ± 79.37	398.11 ± 71.62
Coccolitophores	$mmolC/m^2$	1975.05 ± 248.04	1324.75 ± 142.18	1030.82 ± 71.98	920.76 ± 60.99	897.54 ± 58.82
Gren algae	$mmolC/m^2$	67.36 ± 55.56	63.31 ± 54.76	63.16 ± 54.62	60.57 ± 54.02	54.93 ± 51.23
Zooplankton	$mmolC/m^2$	1981.50 ± 23.93	1922.91 ± 18.63	1900.96 ± 21.57	1896.95 ± 18.31	1887.28 ± 17.04
Copepods	$mmolC/m^2$	1068.21 ± 22.27	1065.71 ± 21.15	1061.63 ± 20.37	1054.39 ± 19.65	1044.72 ± 18.90
Microzooplankton	$mmolC/m^2$	909.64 ± 33.15	853.79 ± 32.98	843.88 ± 26.98	839.47 ± 30.75	840.93 ± 31.63
Maximum diatoms biomass	$mmolC/m^2$	98.27 ± 0.53	99.20 ± 0.49	99.57 ± 0.60	99.89 ± 0.53	100.27 ± 0.54
$T_{biommax}$	yd	127.00 ± 1.00	128.00 ± 1.00	129.00 ± 1.00	130.00 ± 1.00	131.00 ± 2.00
Maximum diatoms concentration	$mmolC/m^3$	4.91 ± 0.03	4.96 ± 0.02	4.98 ± 0.03	4.99 ± 0.03	5.01 ± 0.03
$T_{concmax}$	yd	127.00 ± 1.00	128.00 ± 1.00	129.00 ± 1.00	130.00 ± 1.00	131.00 ± 2.00
Spring bloom initiation	$mmolC/m^3$	120.00 ± 4.00	122.00 ± 2.50	124.00 ± 2.00	125.00 ± 1.50	126.00 ± 1.50

Table 4.6: Ecosystem properties sensitivity to the duration of summer stratification. The presented values indicate total yearly biomass of the indicated groups (phytoplankton, diatoms, dinoflagellates, coccolitophores, green algae, zooplankton, copepods and microzooplankton), maximal diatoms biomass and concentration, but also the time point when the peak of diatoms biomass and concentration was observed, and the spring bloom initiation.

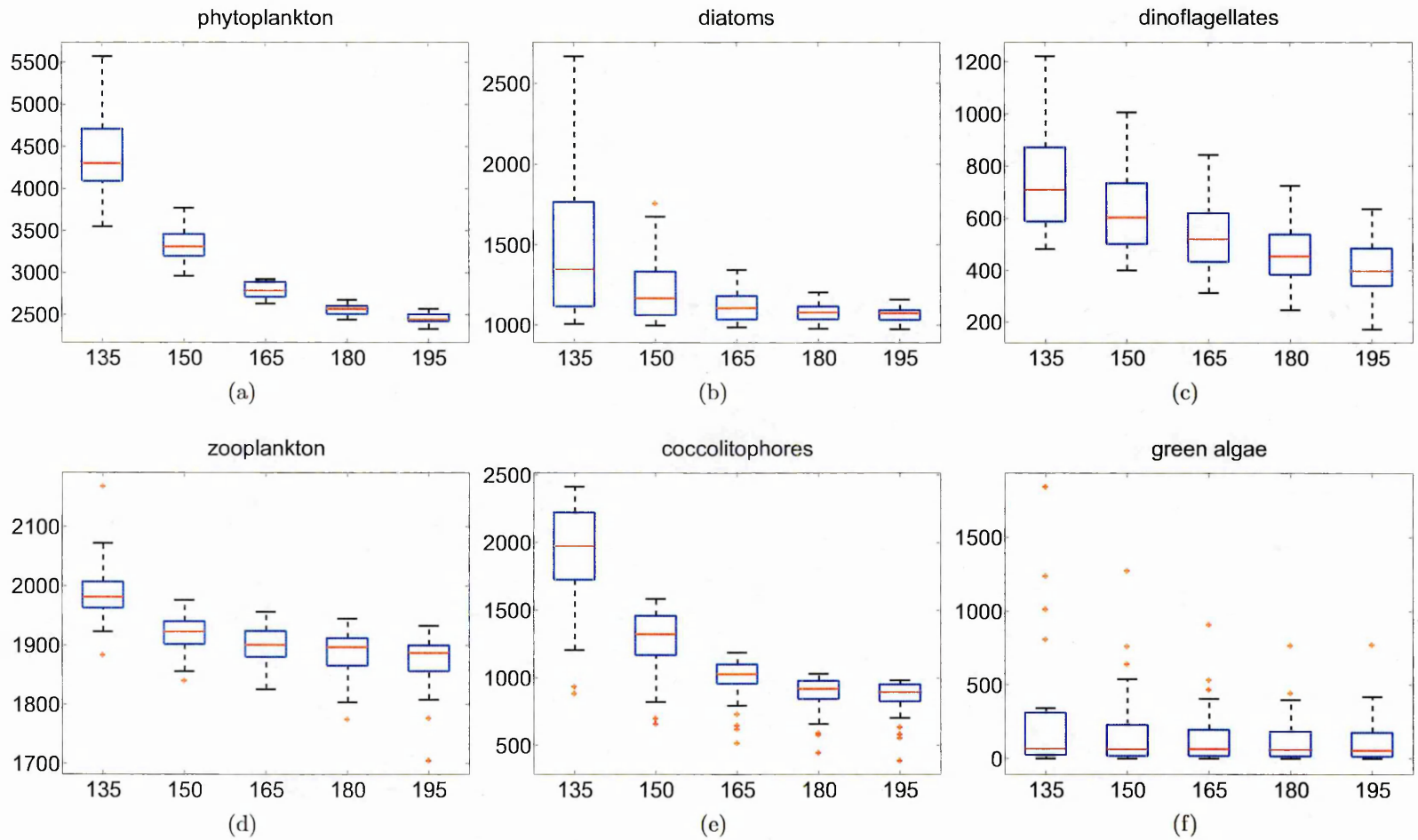

Figure 4.32: Main groups sensitivity to the duration of summer stratification. The panels represent total yearly biomass of: (a) phytoplankton, (b) diatoms, (c) dinoflagellates, (d) zooplankton, (e) coccolitophores and (f) green algae in all ensemble communities in ecosystems distinguished solely in terms of the duration of summer stratification.

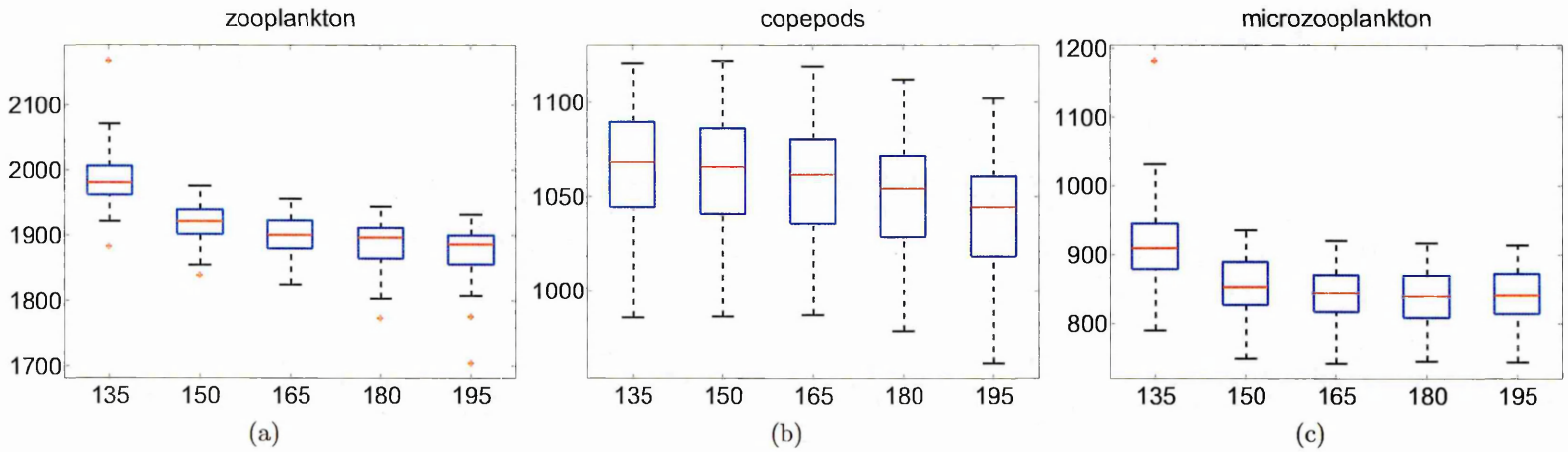

Figure 4.33: Main groups sensitivity to the duration of summer stratification. The panels represent total yearly biomass of: (a) zooplankton, (b) copepods and (c) microzooplankton in all ensemble communities in ecosystems distinguished solely in terms of the duration of summer stratification.

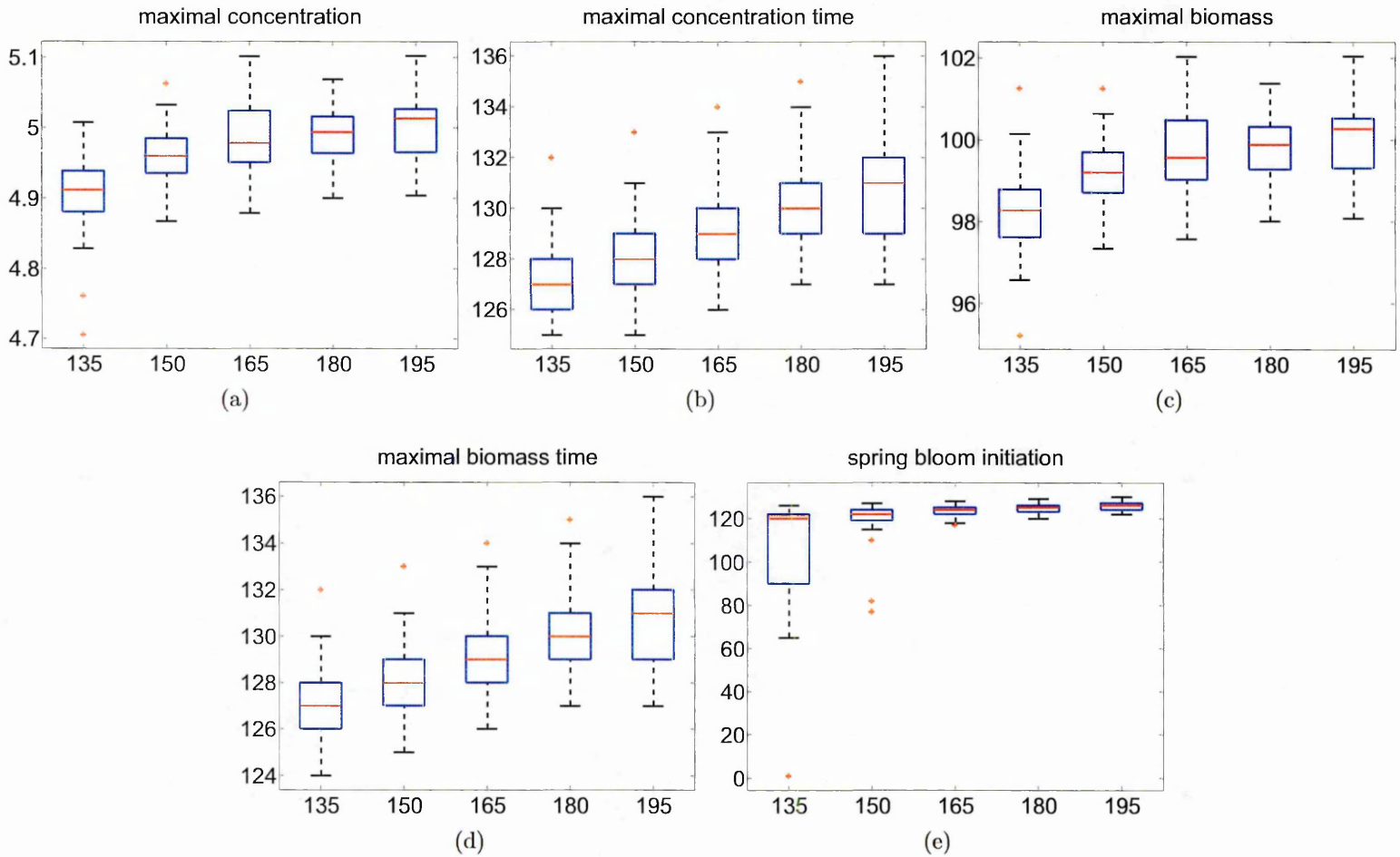

Figure 4.34: Spring bloom sensitivity to the duration of summer stratification. The panels represent: (a) maximal diatoms concentration, (b) year day when the maximal concentration was observed, (c) maximal diatoms biomass, (d) year day when the maximal biomass was observed and (e) initiation of the spring bloom formation in all ensemble communities in ecosystems distinguished solely in terms of the duration of summer stratification.

4.4 Comparison of model results with the Continuous Plankton Recorder data

In this section I present a qualitative comparison of the phytoplankton functional groups seasonal abundance data from several Continuous Plankton Recorder (CPR) standard areas with results of an ecological model tuned for a specific physical forcing characteristic for those standard areas. The idea standing behind this comparative study was to validate the information originating from the above sensitivity study against the *in situ* measurements of phytoplankton abundance.

4.4.1 Data sets

Taxonomic data of diatoms, dinoflagellates and coccolitophores were obtained from the Continuous Plankton Recorder (CPR) from Sir Alister Hardy Foundation for Ocean Science (http://www.sahfos.ac.uk). The multi-annual monthly averaged cell concentration was extracted for the standard area B6 (59-63°N : 19-31°W), C6 (54-59°N : 19-31°W), D6 (50-54°N : 19-31°W) and E6 (45-50°N : 19-31°W). The CPR data were available from 1958 to 2013 for diatoms and dinoflagellates, and from 1993 to 2013 for coccolitophores. The size of these standard areas is relatively large, hence some spatial smoothing is to be expected.

Seasonal dynamics of the mixed layer depth used in the model simulations was based on the *in situ* measurements of the MLD performed with an autonomous ARGO floats. The data were collected between 1997 and 2010 in the North Atlantic basin. The appropriate data were extracted for each selected CPR standard areas from which a monthly average was computed. An analytical function has been subsequently fit to the observed monthly signal and used as a forcing function for the simulations (see Chapter 2 Section 2.4 for the details). The estimated parameters values were presented in Table 4.7.

Light vector was calculated separately for each CPR standard area. Namely, a latitude of the central point of each standard area was used as a parameter determining the seasonal irradiance intensity (see Chapter 2 Section 2.4 for the details).

The nutricline shape and depth had been established for each CPR standard area

based on the WOA13 (see Chapter 2 Section 2.4 for the details).

	h_{max} $[m]$	T_0 $[yd]$	δt $[yd]$	S_L $[d]$
B6	418	66	81	97
C6	318	50	94	132
D6	226	69	76	112
E6	268	58	72	148

Table 4.7: Values of the parameters used for MLD characteristics in the considered CPR standard areas.

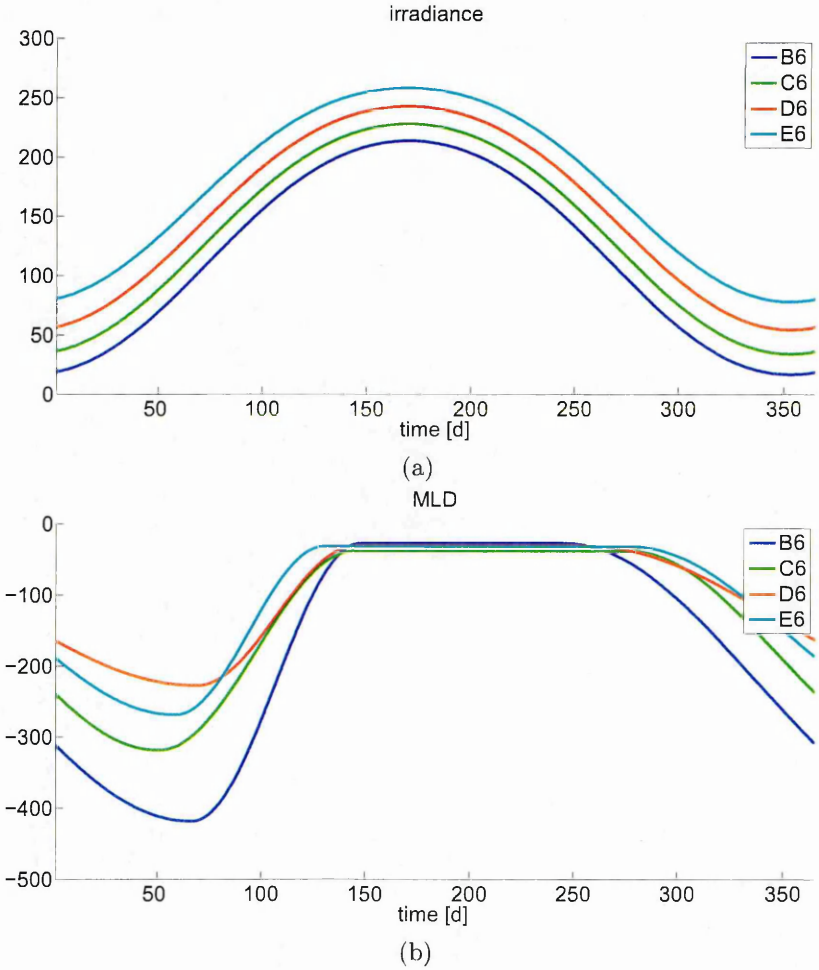

Figure 4.35: Physical conditions in the CPR B6-E6 standard areas. The panels depict: (a) seasonal surface solar irradiance and (b) seasonal dynamics of the mixed layer depth.

4.4.2 Results

The physical forcing used in the simulations aimed to replicate ecosystem dynamics in each considered CPR standard area show considerable differences in its seasonal patterns. Namely, the MLD seasonal signal varies in terms of the minimal and maximal

MLD (from 27 to 38, and from 226 to 418 respectively), duration and initiation of spring water column restratification (from 72 to 94, and from 50 to 69 yd respectively) and duration o summer stratification (from 97 to 148) (Fig. 4.35). The depth and shape of the NO_3 and SiO_2 nutricline varied as well in all considered regions. The seasonal surface light intensity decreased poleward (Fig. 4.35)

The discrepancies in the physical forcing seasonal dynamics resulted in the discrepancies in the seasonal availability of the resources. This change in the abiotic factors altered the competition among the phytoplankton species and led to community composition restructuring. The change in the bottom-up processes resulted in a considerable changes in the phytoplankton seasonal abundance patterns. For instance the maximal diatoms concentration varies from 1 to 2.2 $[mmolC/m^3]$ among considered scenarios (Fig. 4.35). The differences in the relative functional groups abundance could alter the biogeochemical cycle due to the differences in their physiological characteristics. The P:Z ratio was also altered which affected the efficiency of biomass transfer through the trophic cascade.

Furthermore, due to the differences in the spring water column restratification and the maximal MLD value, the spring bloom phenology was altered. In particular spring bloom formation in E6 was initiated early in January, thus even before water column restratification, while in other sectors it is being formed in March or April. Clearly the advance in the spring bloom formation observed in E6 can be attributed to the increased light availability during winter months. As presented in the previous section, due to lower maximal MLD and smaller nutrients standing stock, the maximal concentration observed during the spring bloom intensity in E6 was much lower with respect to other considered sectors, yet the biomass was considerably higher.

Additionally, a pronounced autumn diatom bloom was observed in sector B6. Its formation was related to a considerably short summer stratification, as the nutrients entrainment into the system due to the water column deepening is strongly coupled with still sufficiently high solar irradiance. Such conditions were not observed in other explored ecosystems.

The observed and model seasonal partitioning of phytoplankton functional groups (diatoms, dinoflagellates, coccolithophores and green algae) in all four selected CPR

standard areas were shown in Figs. 4.36b, 4.37b, 4.38b and 4.39b. The presented seasonality originates from the aggregated, monthly-averaged abundance of phytoplankton groups from the CPR data (cell counts) in the standard area B6, C6, D6 and E6 respectively, which was compared with the monthly mean abundance (concentration) of the cumulative functional groups resolved in the model (Fig. 4.36d, 4.37d, 4.38d and 4.39d). The model shows that diatoms were the most abundant functional group in all considered cases, with a large bloom in early spring. The diatom bloom was accompanied by a peak of dinoflagellates. These two functional groups were subsequently followed by coccolithophores and less abundant green algae.

In all considered scenarios, the spring diatom bloom appear to occur later than indicated by the CPR data. The initiation of the spring bloom, however, coincides with the water column restratification, and may be attributed to the overall low winter phytoplankton concentration (as explained in the Chapter 2). Nonetheless, diatoms tend to dominate the both the virtual and real ecosystem during the spring months in all explored spatial scenarios (Figs. 4.36, 4.37, 4.38 and 4.39).

Additionally, as indicated in the Chapter 2, the model tend to underestimate the dinoflagellates seasonal abundance patterns. It is worth recalling that mixotrophy, a characteristic trait for multiple dinoflagellates species, has not been considered in the model which could explain their low concentration during stratified periods. Furthermore, the CPR data were presented in $[cells/m^3]$ while the model data were in $[mmolC/m^3]$. Hence, the comparison should account for the size discrepancies between diatoms and far larger dinoflagellates cells.

The model concentration of coccolitophores was considerably higher than that observed in CPR data. One of the CPR data set limitation is that the abundance of coccolithophores in the CPR data is only a fraction of what one may be expected, due to the small size of the organisms (5 μm) compared to the size of the mesh used (250 μm). The CPR data are however a relevant index of the relative annual changes and thus reveal the bloom of coccolithophores. The model concentration of coccolithophores in the model is thus much more substantial and in line with the findings of previous field work studies in the northeast North Atlantic, reporting large concentrations of coccolithophores during the summer bloom. For example, Fernandez et al.

[1993] reported a total estimated coccolithophore C biomass as large as 50% of the total phytoplankton.

Yet another limitation of the CPR dataset is the lack of explicit representation of the green algae functional groups. Thus it was impossible to validate green algae seasonal abundance patterns against CPR dataset.

Despite all the above limitations, the qualitative resemblance of seasonal phytoplankton functional groups abundance and their succession patterns in the explored regions is uncanny. The virtual phytoplankton functional groups assemble accordingly to the imposed physical forcing characteristic for explored areas.

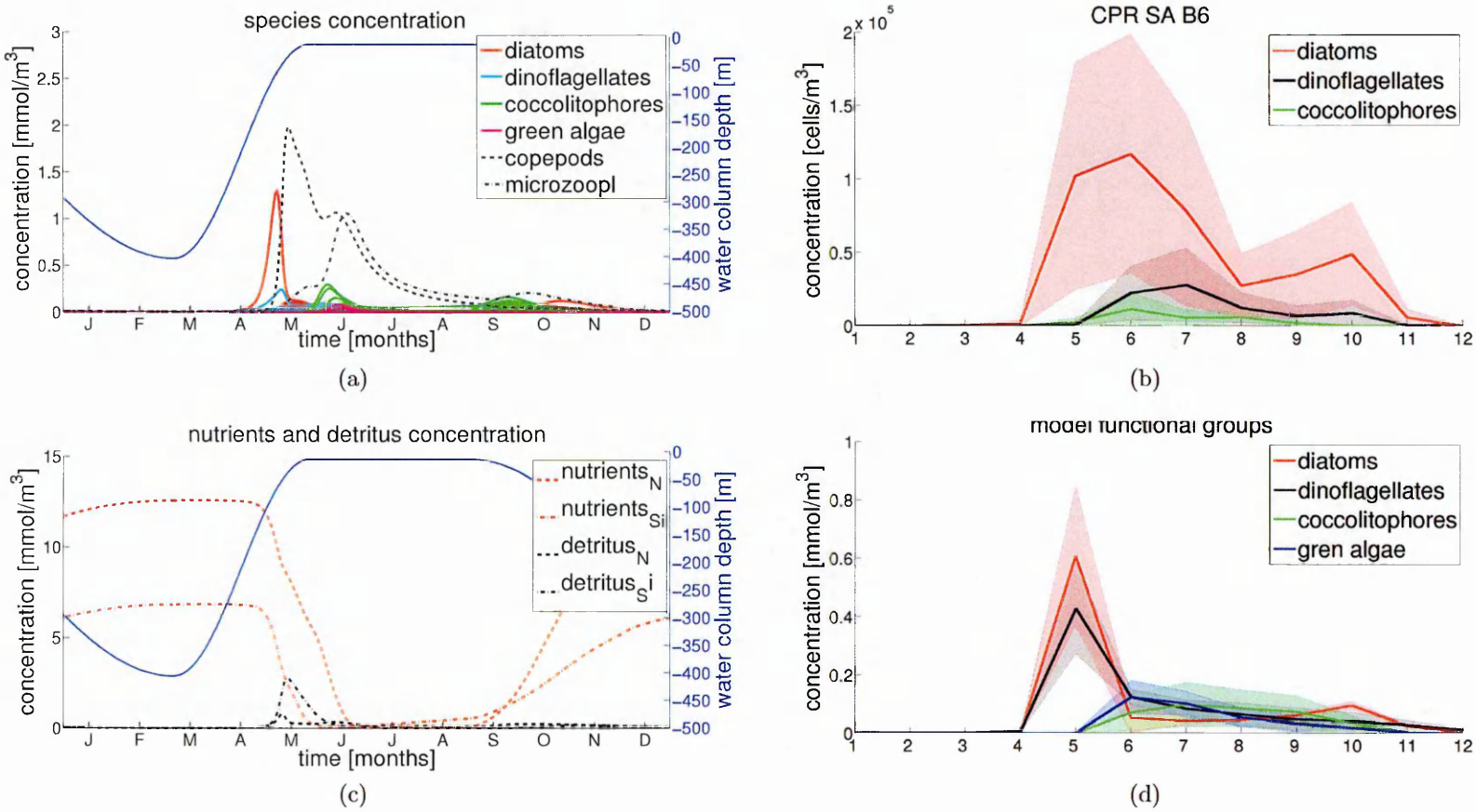

Figure 4.36: Comparison of the model and *in situ* data on phytoplankton seasonal abundance. The panels depict: (a) model phytoplankton and zooplankton species concentration, (b) monthly phytoplankton functional groups cell concentration from CPR data in a B6 standard area, (c) model nutrients and detritus concentration, (d) monthly phytoplankton functional groups concentration patterns generated by the model. The model configuration aimed to reproduce the physical forcing reported in the B6 CPR standard area.

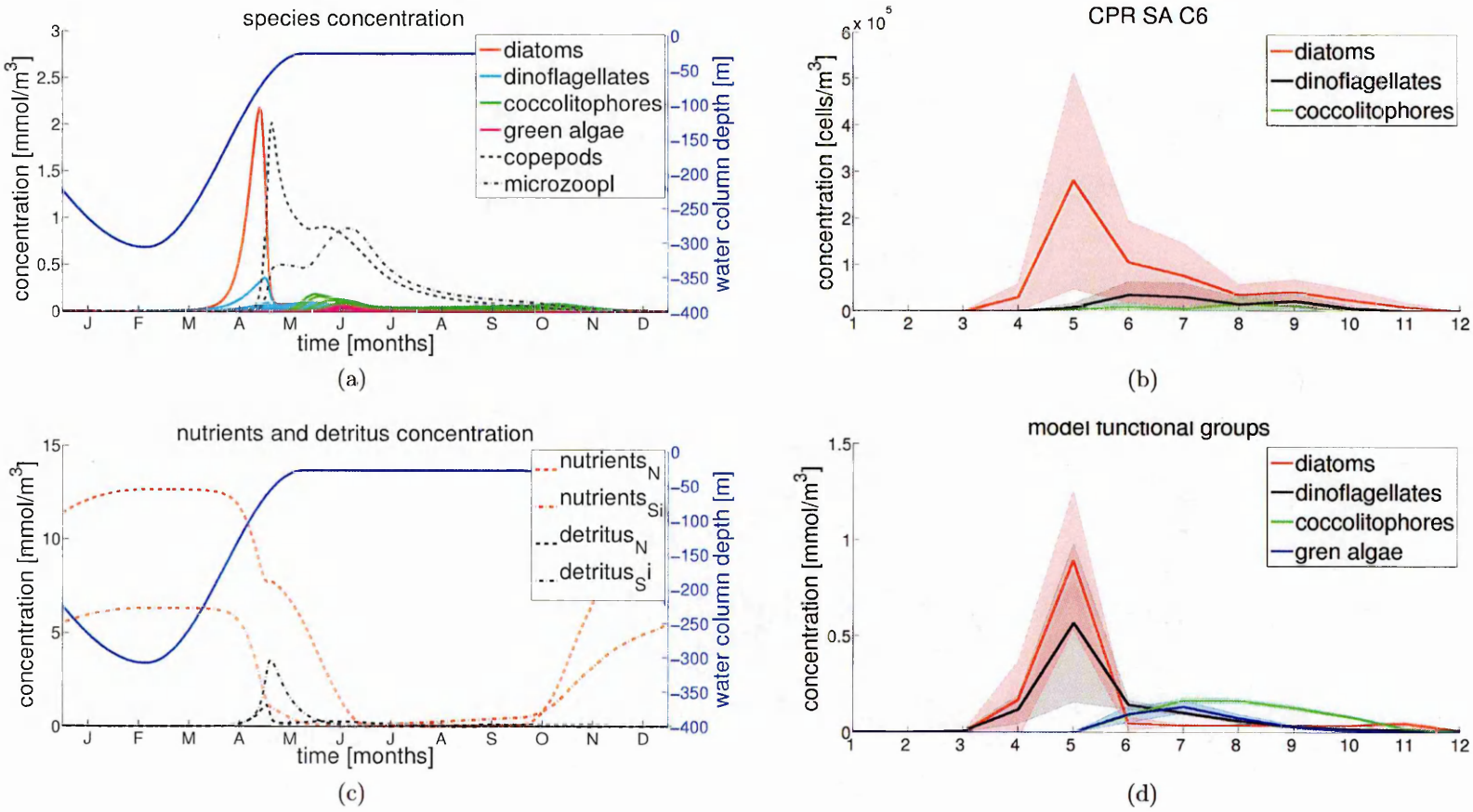

Figure 4.37: Comparison of the model and *in situ* data on phytoplankton seasonal abundance. The panels depict: (a) model phytoplankton and zooplankton species concentration, (b) monthly phytoplankton functional groups cell concentration from CPR data in a C6 standard area, (c) model nutrients and detritus concentration, (d) monthly phytoplankton functional groups concentration patterns generated by the model. The model configuration aimed to reproduce the physical forcing reported in the C6 CPR standard area.

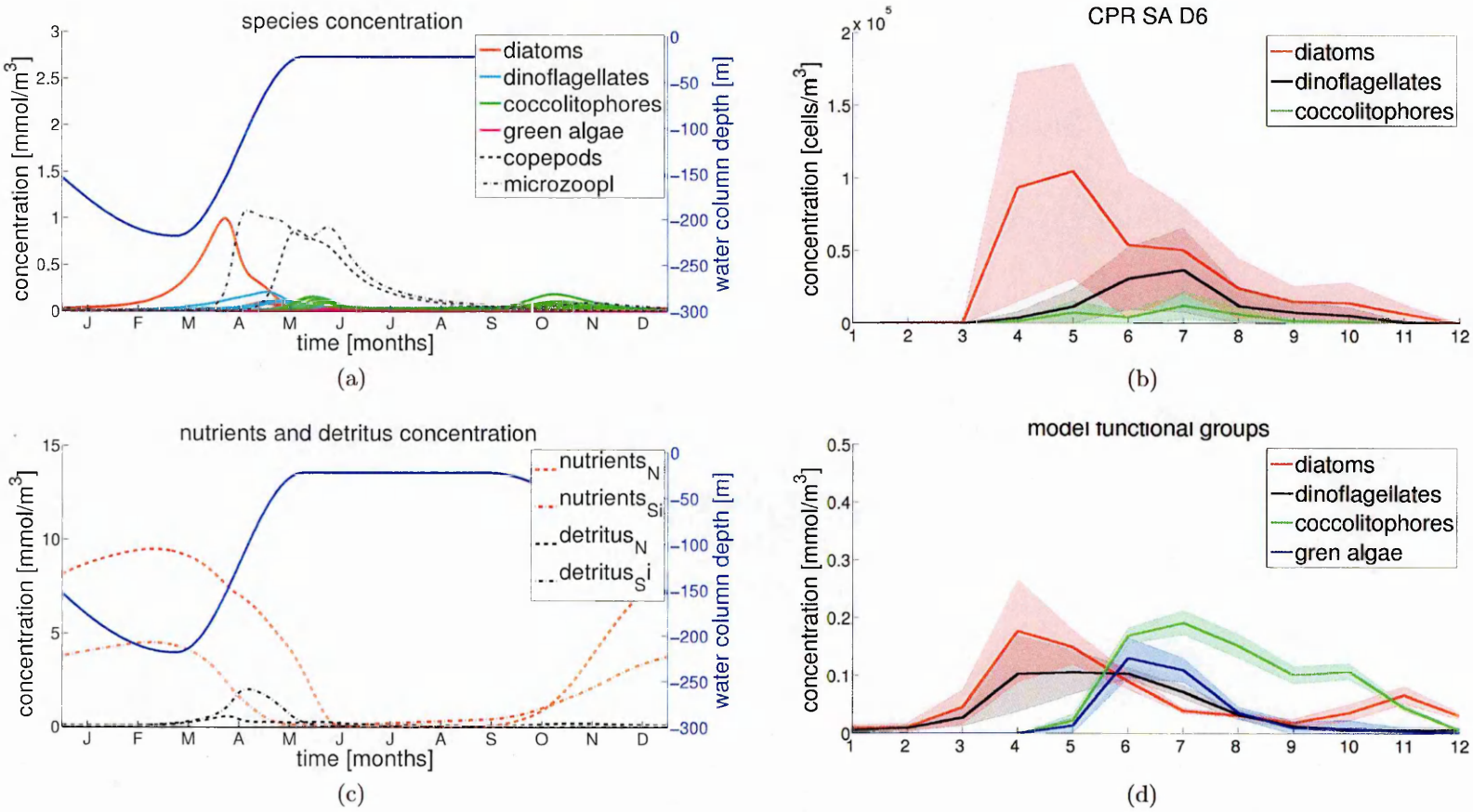

Figure 4.38: Comparison of the model and *in situ* data on phytoplankton seasonal abundance. The panels depict: (a) model phytoplankton and zooplankton species concentration, (b) monthly phytoplankton functional groups cell concentration from CPR data in a D6 standard area, (c) model nutrients and detritus concentration, (d) monthly phytoplankton functional groups concentration patterns generated by the model. The model configuration aimed to reproduce the physical forcing reported in the D6 CPR standard area.

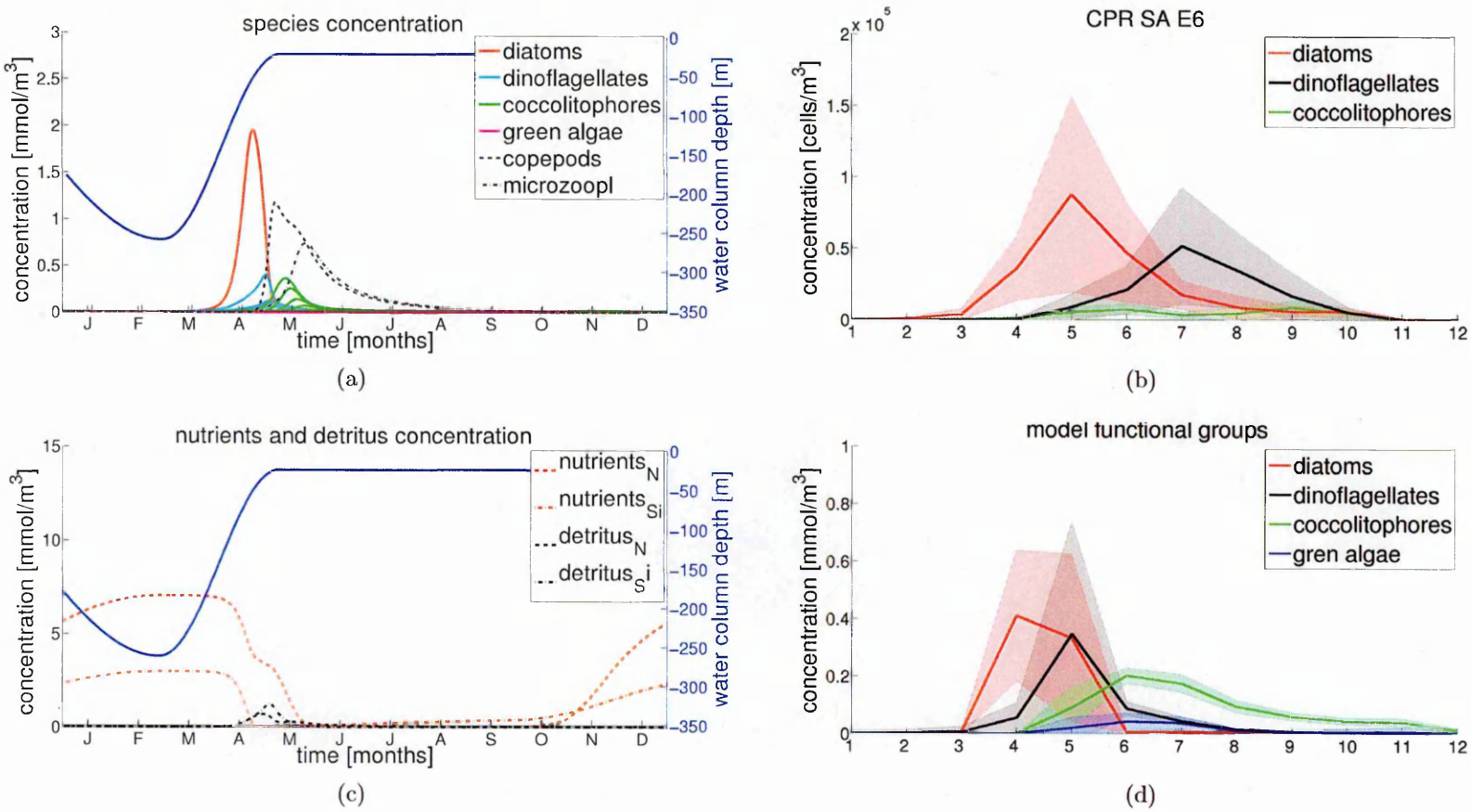

Figure 4.39: Comparison of the model and *in situ* data on phytoplankton seasonal abundance. The panels depict: (a) model phytoplankton and zooplankton species concentration, (b) monthly phytoplankton functional groups cell concentration from CPR data in a E6 standard area, (c) model nutrients and detritus concentration, (d) monthly phytoplankton functional groups concentration patterns generated by the model. The model configuration aimed to reproduce the physical forcing reported in the E6 CPR standard area.

Discussion

The mechanistic phytoplankton community model developed for the purpose of this thesis captures the principal characteristics of phytoplankton dynamics over the annual cycle and successfully reproduces the main patterns of abundance and succession observed in subpolar ecosystems (see Chapter 2). Although simplified, the analytical formulation of the physical forcing allows to mimic a broad spectrum of environment types distinguished in terms of maximal MLD, beginning and duration of spring restratification, as well as the duration of summer stratification.

The explored scenarios demonstrates that despite its simplicity, the model is able to reconstruct even subtle differences in community dynamics caused by alternation in environmental forcing. The analysis of the dynamical patterns of all the tested communities show that the bio-geochemical and community composition patterns were robust and consistent among all ensemble communities. Yet, the results were significantly different among environments with different physical forcing characteristics (e.g., Section 4.4).

The analysis of the impact of changing physical forcing conditions on the phytoplankton abundance time course appeared in multiple studies (Fasham et al. [1990], Popova et al. [1997], Peeters et al. [2012], Waniek [2003]). In here these analysis were enriched with the observations regarding species composition and diversity.

The species diversity was measured as a number of species when showing 1) maximal species concentration or 2) median species biomass exceeding a specified threshold - 0.05 $[mmolC/m^3]$ or 0.004 $[mmolC]$ respectively. The values allow to distinguish between maladapted species present in the system, and those surviving at constantly low concentrations. Notably, a bloom forming species which survival strategy relies on staying at low concentration throughout the most of the season, may be considered as inactive (extinct) based on biomass criterion, but its presence will be accounted for with the concentration criterion.

The seasonal abundance patterns showed a considerable sensitivity to the parameters regulating water column stratification: beginning of the spring restratification and duration of summer stratification. The total system biomass, including cumulative phytoplankton and zooplankton biomass, varied significantly in all tested conditions.

Furthermore the relative functional groups biomass altered in all the explored cases. Prolonged summer stratification altered the process of nutrients entrainment during the late summer / early autumn period. The difference was observed in terms of the autumn and winter biomass. Hence, the length of summer stratification may significantly impact autumn bloom formation in the regions where it was formed.

The numerical results indicated that changes in the mixed layer dynamics had the most profound effect on the functioning of the tested ecosystems. The shoaling of the max MLD value, reduced light limitations during the deep mixing period and lead to an advance in the spring bloom formation and bloom peak timing. At the same time reduced mixing decreased the nutrients supply to the water column. The nutrients standing stock at the end of the winter mixing was significantly lower in the systems with shallower mixing which resulted in a lower bloom intensity. The change in nutrients supply could affected also the balance between the dominant phytoplankton functional groups illustrated by the change in opportunists to gleaners biomass ratio.

The change in the maximal MLD affected also the coupling between the phytoplankton and zooplankton. There was an increasing trend of the total yearly phytoplankton biomass and a decreasing trend of the total yearly zooplankton biomass corresponding to a decrease of the maximal MLD value. This results in a decreasing trend in the Z:P ratio in the systems which illustrates the zooplankton and phytoplankton encounter rate and consequently illustrates the grazing pressure imposed on the phytoplankton.

The changes in the seasonal forcing had a direct impact on the bottom-up processes regulating phytoplankton dynamics: the alternations in maximal MLD value, duration of summer stratification affected nutrients supply into the system, while beginning and duration of the spring restratification affected synchronisation of MLD with the photic zone, thus the coupling of light and nutrients availability. The coupling of MLD and photic zone regulates the light, nutrients or light-nutrients limitations imposed on species' growth rates. The results show that seasonal forcing enables temporal organization of the species via bottom-up regulations, as the species become dominant during the specific periods in the year that match their highest growth potential. In this sense, seasonality generates recurrent patterns in species composition. Consequently, any change in the seasonal forcing may lead to the community restructuring and above

all affect species diversity over seasonal cycle.

A growing number of models address the impact of changing climate on the community composition and functioning of the planktonic ecosystem (e.g., Litchman et al. [2006]). Predicting phytoplankton community patterns under future scenarios has been recognised as uncertain since it might be affected by model structure and parameter combinations. The ecosystem functioning and diversity are interconnected. The most frequently suggested shape of the relationship between diversity and a measure of ecosystem functioning, such as biomass or primary production, is a saturating curve (Cardinale et al. [2012]; Tilman et al. [1997b]). For this kind of relationship, initial diversity loss from systems with high diversity has only a minimal effect on ecosystem functioning. At some point, however, further loss of diversity results in a pronounced reduction in functioning.

Very few models resolve species diversity (Follows et al. [2007], Bruggeman and Kooijman [2007]), and consequently in the studies specifically addressing community composition under climate change, role of species diversity is constantly underestimated and variability in initial community composition is not accounted for. Consequently, the general patterns in diversity or ecosystem functioning caused by climate change predicted by these model cannot be considered as robust since they do not consider the variability of the main model compartment - variability in phytoplankton species diversity.

Species diversity in the various scenarios Reduced turbulent mixing suppress upward transport of nutrients to the euphotic zone, which can have a major impact on phytoplankton productivity and species composition in nutrient-limited waters (Mann and Lazier [2009], Longhurst and Dandonneau [1999]). Clear examples supporting this statement may be found in coastal upwelling regions along the Pacific coasts of North and South America. The turbulent mixing of nutrients over the thermocline in these regions is greatly reduced during El Nino years, with major effects cascading from the phytoplankton level up to the higher trophic levels (Chavez et al. [2003], Stenseth et al. [2002]).

In the simplified physical representation of the ocean imposed in here (so called slab

physics) the virtual ecosystem formed by nutrients, phytoplankton, zooplenkton and detritus, is confined within the upper layer , while the lower layer contains only nutrients. In particular, it is considered that bottom layer nutrients concentration increases with depth. This gradient was based on World Ocean Atlas 2013 and presented in Chapter 2 Section 2.4. The depth of the upper layer is given by the seasonal dynamics of the mixed layer depth. As the mixed layer deepens the nutrients are entrained into the upper layer from the bottom layer. The entrainment rate is directly related to the change in the MLD (its first derivative) and the nutrients concentration directly below. Because of the imposed gradient with depth in nutrients concentration, the absolute value of the nutrients introduced into the system increases with depth (e.g., from 300m is lower than from 600m as the nutrients concentration at 600m is higher).

Because of the above, the reduced mixing intensity, represented in the model as the decrease in the maximal MLD value, caused a decrease in nutrients supply into the system. This coincided with a higher grazing pressure imposed on phytoplankton by grazers (i.e., copepods and microzooplankton) at the beginning of spring water column restratification. Lower maximal nutrients concentration in the end of winter observed in the systems with shallower maximal MLD together with a higher grazing pressure resulted in a strong decrease in the phytoplankton concentration. This decrease was particularly illustrated by a reduced spring bloom intensity. A decrease in concentration was accompanied by a decrease in species diversity. The lower species diversity in the system was attributed to the combination of the bottom-up (lower nutrients availability) and top-down (grazing pressure) factors. It is argued that high growth rate is the proxy of species success under nutrients replete conditions (Barton et al. [2010]). Lower nutrients concentration in the environment with shallow maximal MLD, intensified competition among diatoms species. Higher zooplankton-phytoplankton encounter rate and the overall higher grazing pressure during water column restratification further decreased net phytoplankton growth rate and caused extinction of species with low competitive abilities.

The averaged integrated light availability in the mixed layer depth increases with the decrease of maximal MLD value. Hence, the reduced mixing increases the average light availability in the winter water column and results in higher overall phytoplankton

biomass during deep mixing periods. The reduced light limitations resulted also in an advanced spring bloom formation, and as it is formed in a deeper water column the accumulated biomass is higher. Additionally, species adapted to high-light conditions e.g., coccolitophores, with highest winter concentration gain competitive advantage in the system after the bloom due to differences in initial inoculum. These species tend to dominate throughout summer, but above all competitively exclude species with higher resources requirements. Moreover, it has been recognised that reduced vertical mixing may further reduce species diversity by promoting dense blooms limiting light availability via self-shading (Huisman et al. [2004]).

In summary, the model simulations indicated change in the light and nutrients availability and the grazing pressure imposed on phytoplantkon in the systems differing in terms of the maximal MLD. Therefore, change in physical forcing altered the bottom-up and top-down factors regulating phytoplantkon dynamics, and subsequently reshaped the community. The increase in the duration of summer stratification resulted in a prolonged nutrients limitations imposed on species and caused overall decrease in their median biomass. Consequently a decreasing trend in species diversity based on biomass criterion was observed. At the same time the prolonged stratification had very little effect on spring bloom formation, hence the diversity index based on max species concentration varied only slightly. This variability can be attributed to the autumn bloom formation. In the model ecosystem the autumn bloom is not very pronounced. A longer summer stratification causes a delay in autumn nutrients entrainment, leads to a decrease in autumn/winter species biomass and consequently has a negative effect on system's memory.

The performed simulations addressing alternations in the duration and initiation of the spring water column restratification, under the assumption of constant duration of summer stratification, demonstrate its rather low impact on maximum species concentration. Shifts in the beginning in restratification impacts coupling of MLD and photic zone, thus, in case of advanced restratification solar radiation may be slightly lower with respect to corresponding cases with later restratification. Despite these differences, the concentration of species in all functional groups remained at comparable levels in all tested cases resulting in a similar species diversity and a rather high com-

munity similarity index value. The spring diatoms bloom shifted accordingly to the water column restratification initiation. The peak in copepods abundance was shifted as well. Despite the fact that the zooplankton and phytoplankton biomass was following identical trends, a small uncoupling was observed in case of spring water column restratification occuring earlier with respect to the reference case - the total yearly zooplankton biomass increased at a slower rate than phytoplankton - which was likely attributed to the copepods overwintering. Because of the lower top-down pressure, the median species biomass measured over the whole seasonal cycle increased and caused increase in the biomass based diversity index.

The results interpretation presented above refers to the median species diversity observed in all environment types. It is important to note that a high degree of variability in species diversity was observed in all communities, even under identical physical forcing; namely the species diversity index based on biomass varied between 11 and 13 in the scenario addressing changes in the maximal MLD value(Figure 4.11a, 4.2). The differences in the species composition and consecutive process of community self-organisation affected communities response to changes in the environmental factors. For instance, the analysis of species diversity in a single communities show: an increase (community #10) or a neutral effect (community #12) of increasing maximal MLD values (Table 4.2). Thus the analysis of a single community dynamics could be vastly different from the median patterns derived from the analysis of multiple communities and it could result in deriving the wrong conclusions. The ensemble approach employed in here depicts how the variability in community composition, namely the diversity of phytoplankton physiologies, may affect the ecosystem response to the environmental change. Consequently these single community analysis may over- or underestimate the importance of the explored processes in shaping phytoplankton community composition. The broad distribution of species diversity observed across all tested communities further justifies the use of an ensemble approach.

Model invalidation Thus rather than be tamed, the observed sensitivity ought to be treated as a source of valuable information on the interplay between community composition, incorporated processes and virtual ecosystem functioning.

The physical forcing used in the model has been adjusted to reflect that observed in the CPR standard areas B6 - E6 (Section 4.4). In particular the seasonal characteristics of the mixed layer, surface irradiance and nutricline shape had been altered to fit the observations specific to those areas. The model adjustments did not consider any changes in the biological model compartments, namely, the phytoplankton and zooplankton community was identical with that used in the reference scenario (see Chapter 2 sec 4.1).

The values of the parameters used in the model could be changed in order to reproduce the observed data. Such an extensive exercise had been performed by Anderson et al (Anderson et al. [2015]). Anderson at al had illustrated not only how to validate an ecological model but also had presented how plastic the models are. In particular, by altering the physical forcing and the parameter's values of a simple NPZD model, they had adjusted it to four different stations situated in the North Atlantic and South Pacific. Their illustrative study, however, had a vastly different goal than that presented in here. My approach is based on the idea that the model's simplified construction is sufficient to investigate ecological hypotheses yet it is complex enough to produce new insights. By adjusting the physical forcing and assuming a fine representation of the planktonic community, the observed differences between model and observed seasonal phytoplankton abundance can be attributed to the lacking processes and/or model's oversimplifications. As such the observed discrepancies could be used to identify relevant mechanisms driving species abundance and diversity, and seasonal succession of the phytoplankton functional groups.

Some of the discrepancies can be attributed to the physical forcing simplicity. A two-layer SLAB physics in which the ecosystem is confined within the upper layer and a lower layer that contained only nutrient in fixed concentration, with a seasonaly varying mixed layer depth is not able to reproduce the observed spatial ecosystem heterogeneity. Furthermore, it does not account for processes such as, e.g., phytoconvection which focusses on the influence of convection on primary production (Backhaus et al. [1999]) and may affect phytoplankton concentration during deep mixing periods (Große et al. [2015]).

The model formulation included two nutrients, N and Si, that can limit phyto-

plankton growth. Silicate has been used as it drives diatom growth and diatoms are the main focus of the thesis. There are compelling reasons to include additional nutrients into the models of marine phytoplankton. Litchman et al (Litchman et al. [2006]) data compilation depicted strong differences in major taxonomic groups competitive abilities not only for nitrogen, but also for iron and phosphate. Therefore, including growth dependence on Fe and P could allow for a better seasonal separation of the phytoplankton functional groups. Notably, some regions of the ocean are known to be P-limited and/or Fe-limited (Ammerman et al. [2003]). Hence, direct representation of phosphorus and iron could improve functional groups representation in those areas.

The community composition and functional groups seasonal succession are subject not only to the bottom-up processes but to the top-down processes as well. Models resolving phytoplankton diversity are likely to be more sensitive to grazing parametrisation than models considering only bulk phytoplankton properties like the total chlorophyll or biomass. In fact high sensitivity to grazing parameters and formulation has been reported in ecosystem models (Prowe et al. [2012b], Prowe et al. [2012a]). Therefore it is important to properly assess and quantify grazer impact on community structure. A simple sensitivity study exploring a particular case of grazing formulation has been presented in the 3rd Chapter of this thesis. Namely, a sensitivity to the duration of copepods dormancy has been explored. The obtained results demonstrated rather insignificant model's sensitivity to the considered formulation. Nevertheless, only a single formulation of grazing and the dormancy have been considered in there and future studies should explore how sensitive is the model to the grazing but also to the dormancy formulations.

Phytoplankton and zooplankton dynamics can be affected also by the temperature. The comprehensive compilation of planktonic protists growth rates data made by Rose and Caron [2007] supports this statement. The temperature dependence of heterotrophic protists growth rate is much stronger than that of autotrophic protists. Consequently, zooplankton's growth rate would be much lower than phytoplankton's under low water temperatures. The growth formulation accounting for the temperature dependence could affect the grazing pressure during winter and early spring months,

and lead to a change in the seasonal phytoplankton abundance but also affect the spring diatom bloom phenology. These temperature curves are to be introduced into the model in the continuation of this study. Their impact on spring bloom initiation will be evaluated as the results obtained with an augmented model's version are to be compared with the appropriate CPR time series and old model's version (as in section 4.4). Hence, all observed changes in phytoplankton and zooplankton abundance will be attributed to the newly added temperature dependencies.

The model representatives of dinoflagellates tend to peak simultaneously with or shortly after diatoms. Their presence during oligotrophic summer months is mostly limited to considerably low concentrations as they are unable to successfully compete with coccolitophores and green algae under nutrients depleted conditions. Multiple dinoflagellate species are known for their mixotrophic mode of nutrition -they are able to combine both autotrophic and heterotrophic nutrition. Mixotrophy broadens the pool of available resources (Tittel et al. [2003]), but this advantage is associated with particular physiological trade-offs. Dinoflagellates' maximum specific growth rates as well as their affinity for inorganic nutrients are typically lower in comparison with photoautotrophs such as diatoms (Edwards et al. [2012]). Similarly, their growth and grazing rates are considered to be slower than in similar heterotrophic specialists (Jeong et al. [2010]).

It has been demonstrated that the presence of mixotrophs increase the efficiency of nutrient drawdown in aquatic ecosystems (Tittel et al. [2003]) and improves dinoflagellates representation over seasonal cycle (Mick Follows personal communications; Fulton et al. [2004]). In oligotrophic environments, where resources are scarce, mixotrophs gain competitive advantage as they are able to take advantage of both inorganic and organic resource encounters (Ward et al. [2011], Havskum and Riemann [1996], Zubkov and Tarran [2008]).

Because of the above, it may be convenient to incorporate mixotrophy as a relevant trait in dinoflagellates description and consequently improve the phytoplankton functional groups seasonal succession. Additionally, this trait would be o interest if the model was used to investigate phytoplankton seasonal abundance patterns under

the climate change. It is considered that due to increasing stratification and increasing nutrients entrainment into the photic zone, the oligotrophic niche for mixotrophs may expand poleward (Sarmiento et al. [2004]).

Phytoplankton dispersal due to oceanic transport processes play an important role in shaping the structure of planktonic communities. It may be attributed to processes operating on various scales of motions e.g., the mean currents (Barton et al. [2010], Clayton et al. [2013]); mesoscale eddies and frontal dynamics (i.e., mesoscale turbulence; Bracco et al. [2000], Perruche et al. [2011]); and convective mixing (i.e., vertical diffusion; Perruche et al. [2010]). Phytoplankon dispersal may reshape phytoplanktonic assemblages by affecting the observed species diversity e.g., increases phytoplankton diversity at the local scale (of 10's-100's of km) and decreases at the regional scale (of 1000's of km) as the water mass mixing extends the range of many phytoplankton types and decreases the ability of rare types to persist in isolated areas (Lévy et al. [2014]). Consequently, phytoplankton migration leads to a complex pattern of diversity of phytoplankton types in the ocean. In fact impact of species immigration on community structure has been explored in the previous chapter and its impact on seasonal phytoplankton abundance had been assessed. As the CPR standard areas are not isolated regions, the immigration may play an important role in the dynamics of the communities occupying them.

It might be informative to adjusted ecological models to certain CPR standard areas and couple them by a simple formulation of immigration accounting for the emergent phytoplankton communities structure and their possible dispersal. With this simple approach it would be possible to address the role of immigration in structuring regional interconnected communities. This exercise is planned as a continuation of this study.

The rate of the nutrients drawdown in the photic zone is directly related to phytoplankton biomass increase. Water column shoaling relaxes the light limitations imposed on phytoplankton. Water column restratification gradually increases the average light availability in the water column. Diatoms are accustomed to low light conditions and due to their high intrinsic growth rate tend to dominate the ecosystem under nutrients

replete conditions. These traits enable them to increase ahead of other groups during the winter-spring transition as irradiance increases due to spring increase in solar declination and shoaling of the mixed layer (Sverdrup [1953]).

A slow water column restratification promotes phytoplankton species adopted to low light conditions. The extend to which these species are able to profit from saturating nutrients conditions and sufficient levels of irradiance would depend on their growth rate - the higher their growth rate the more they can increase in abundance. Under such conditions diatoms profit at most. The more prolonged water column restratification, the more competitive advantage diatoms gain, which was clearly indicated by the relative increase of diatoms biomass with respect to other functional groups in the scenarios exploring increasing duration of restratification. Conversely, a rapid water restratification exposes all phytoplankton species to high levels of irradiance and nutrients concentration saturating their growth rate. Consequently it allows all species to benefit from ambient conditions, but also diminishes competitive advantage of species adopted to low light conditions and elongates vegetative period of species adopted to high light conditions. Because of that median and total annual biomass of both coccolitophores and green algae increase in the scenarios investigating shorter duration of water column restratification.

Elevated levels of average light availability were observed also in scenarios with a shallower maximal mixed layer depth. These conditions allowed diatoms to further benefit from the saturating nutrients concentrations and accumulate biomass even before water column restratification. This was illustrated by the advance in spring bloom initiation and biomass/concentration peak occurrence. Competitive advantage of diatoms was further indicated by an increase of the maximal biomass, especially in terms of the relative functional groups maximal biomass change.

Because of the increasing nutrients concentration with depth, the average nutrients limitations increased with the decrease of maximal MLD value. Diatoms are considered as poor nutrients competitors, hence decrease of the average nutrients availability diminished their competitive advantage. As a result the median annual biomass of diatoms decreased by up to 46%. Conversely, the median coccolitophores biomass increase over the year by 224%. Clearly, this increase may be attributed to the physi-

ological properties of this group, as coccolitophores are accustomed to high light - low nutrients conditions.

Coccolitophores having higher half-saturation constants for light-dependent growth, are likely to increase in scenarios which higher (average) light availability. Stimulation of coccolitophores by prolonged stratification has been observed in the Bering Sea, where because of an unusually long water column stratification massive coccolithophore blooms were observed in 1997 and 1998 (Napp and Hunt, 2001; Iida et al., 2002). The analysis of the global satellite data showed strong association of coccolithophore blooms with highly stratified conditions (Iglesias-Rodríguez et al. [2002]). In the scenarios considering change in summer stratification relative biomass of coccolitophores increased with respect to other functional groups. Notably, all PFTs decreased in median annual biomass because of increased nutrients limitations, but the decrease of coccolitophores was at the lowest level.

Green algae are relatively poor nitrate competitors and, consequently, they can be abundant where nitrate is not depleted (HNLC regions). For example, at Ocean Station Papa (HNLC region) high prasinophyte abundance is observed (Varela and Harrison, 1999). Considered scenarios do not account for a creation of such regions, hence no significant increase of green algae was reported. An example of environmental conditions apparently promoting green algae was given by a scenario with shallower MLD led to an average decrease of light limitations. Additionally, a scenario considering rapid spring water column restratification allowed for a temporal co-occurrence of high light conditions and high nutrients concentration, as diatoms were not able to drawdown nutrients to the concentrations limiting green algae growth. Such conditions allowed green algae increase in their biomass with respect to coccolitophores and dinoflagellates.

Dinoflagellates have parameter combinations that result in a less efficient acquisition of inorganic nitrogen and phosphate, compared to other groups. These characteristics do not allow for their persistence under limitation by those nutrients. As discussed before, mixotrophy may improve representation of their seasonal abundance.

The seasonal characteristics of the water column mixed layer are likely to change in

the near future as a result of the global climate change. A change of the ratio of mixed and stratified periods duration is expected to occur in accord with the change of occurrence and duration of spring restratification. In the modelling framework considered in this thesis (Chapter 2) the change in the mixed to stratified periods duration ratio is represented by the duration of summer stratification (S_L), while the change in the storm track and the intensity of storms affecting spring water column restratification are represented by δt and t_0.

The sensitivity study presented in section 4.3 may be considered as an attempt to dissect the predicted change in physical conditions. A single complex process is decomposed into multiple simple factors spawning a resultant vector, and the prediction regarding the system's response to the former is composed with a partial information originating from the latter.

Considering an ecosystem in which the MLD is described with parameters

$$[H_{max}, \delta t, t_0, S_L] = [600m, 30d, 85yd, 150d]$$

and an expected change in the duration of summer stratification (increase by 30 days) and in the initiation of spring restratification (delayed by 20 days) attributed to the climate, it may be expected that the overall phytoplantkon and zooplankton biomass is likely to decrease as a decrease is expected for each factor separately i.e. a 22% decrease in phytoplankton total yearly biomass because of the increase in the duration of summer stratification and 16% decrease because of the delay in spring water restratification; a 1.5% decrease in zoopalnkton total yearly biomass because of the increase in the duration of summer stratification and a 2.9 % decrease because of the delay in spring water column restratification. The decrease of PFTs' total yearly biomass is also expected, e.g., a 31 and 36% decrease is expected in total yearly biomass of coccolitophores in each case, thus an overall decrease may be expected also under the new conditions; a 25% decrease and a 5% increase is expected because of each factor in case of dinoflagellates, thus an overall decrease should be expected under the changed conditions.

Such a theoretical analysis could be continued for other ecological indicators ex-

plored in the section 4.3, and could be completed for a various combination of factors explored in this chapter. It is important to note that the underlying assumption of this analysis is that the system behaves in a linear way. As in the case of dinoflagellates' total yearly biomass: a decrease of 25% because of the duration of summer stratification may cancel the 5% increase attributed to the delay in spring restratification. The system however is not linear and additional analysis are required in order to properly asses the impact of the simultaneous change in multiple parameters on ecosystem functioning as they may either cancel or amplify each other.

Conclusions Although the model presented here was a simplified system, the emergent patterns of diversity show features generally consistent with the sparse observations of marine microbial diversity. The model's diversity patterns were mediated by the the balance between top-down and bottom-up regulations, with the latter modulated by environmental variability. By employing the ensemble approach and analysing numerous phytoplankton communities, this study explored also how variability in species composition affect the observed diversity patterns. Clearly, this modelling approach might be extended to explicitly reflect a broader spectrum of marine organisms, such as heterotrophic microbes and zooplankton, hence, enable comparison with more observational data sets. Furthermore, the roles of other processes, including speciation and climate change, shaping planktonic community composition could also be explored after a proper model modification.

Chapter 5

Laboratory experiments

5.1 Introduction

It is well documented that the shift among different life stages may profoundly affect the population dynamics (Mullin and Brooks [1967], Dahms [1995], Blackburn and Parker [2005], Wyatt and Jenkinson [1997]). Life stage transition may also play an important role in shaping species diversity and community composition ([Jones2010]). For example, an alternation of growth rates, dependent on shifts among life stages, has been reported for many organisms ranging from multicellular ones e.g., brown bears (*Ursus arctos*) and raccoon dogs (Nyctereutes procyonoides) in form of winter dormancy, to macroalgae that present heteromorphic life cycles with microscopic life forms during the adverse season ([Graham, L.E., Wilcox, L.W. (2000): Algae. Prentice-Hall, Upper Saddle River.]), to unicellular fungi where a cell cycle arrest was related to the production of sex pheromones (Bardwell [2005], Côte and Whiteway [2008]). Since there are evidences that also phytoplankton species display complex, species-specific life cycles traits (von Dassow and Montresor [2010a], Chepurnov et al. [2005],Montresor et al. [2006]), it is reasonable to assume that those traits may drive species dynamics along paths more sophisticated than just those driven by the short term availability of resources and may affect their growth rate independently from the constraints imposed by the abiotic factors. For instance, the formation and germination of cysts play an important role in population dynamics of many phytoplankton species (see reviews by Montresor et al. [2006], von Dassow and Montresor [2010a], and Marcus [1998])

Among phytoplankton species, diatoms have a distinctive life cycle characterized by a progressive cell size reduction as vegetative division proceeds (Chepurnov et al. [2004], Edlund and Stoermer [1997], Round et al. [1990a]; Chapter 2). Sexual reproduction represents a fundamental phase in the life cycle of diatoms, providing genotypic diversity through meiotic recombination occurring when gametes are produced (Tesson et al. [2013]), and restoring the maximum size through the formation auxospore (Chepurnov et al. [2004]; Chapter 2). The vast majority of pennate diatoms have a heterothallic life cycle, thus strains of opposite mating type have to be co-cultured to induce the sexual phase. The sexual phase can be induced only in cells below a species-specific cell size threshold (Chepurnov et al. [2004]). However, the fact that cells are in the proper size window does not guarantee induction of sexual reproduction. The

ecological and environmental conditions that favour the occurrence of sexual reproduction in diatoms are not fully understood (see Chapter 2). Changes in salinity, light quantity and quality, or shifts in the composition of the growth medium, have been shown to induce sexualisation in centric diatoms (e.g. Godhe et al. [2014], Schultz and Trainor [1968], Schmid [1995]). At the same time there are evidences that mixing of two sexually compatible strains appears to be sufficient for the induction of sexuality in heterothallic pennate diatoms (e.g.Davidovich and Bates [1998a], Amato et al. [2005], Mann and Poulíčková [2010], Fuchs et al. [2013]).

Sexual reproduction has been a subject of a evolutionary cost-benefit analysis (Williams [1975], Maynard-Smith [1978]). Notably, sexual reproduction is a costly event (Lewis Jr [1984], Lewis Jr [1983]), which may impair growth dynamics of the population. This should be particularly relevant in unicellular organisms, where a fraction of the cell population can transform into gametes. Therefore, sexual reproduction, its frequency and success, together with the environmental conditions that might regulate the occurrence of sex are important factors to consider for explaining, and eventually modelling, population dynamics, genetic structure and persistence of diatom species in the natural environment. A recent study of Scalco et al. (Scalco et al. [2014]) provided additional evidences on the dynamics of sexual reproduction of heterothallic pennate diatom Pseudo-nitzschia multistriata. It has been demonstrated that cell density plays a crucial role in inducing sexual reproduction and, above all, a different population dynamics has been detected in cultures where sexual reproduction did and did not occur.

In this chapter, I present the results of additional laboratory experiments addressing population dynamics of *P. multistriata*. The experiment was aimed at testing differences in the growth rate and nutrients consumption rate between the monoclonal parental strains and the co-cultures in which sex was occurring. The hypothesis was that sexual reproduction impairs phytoplankton growth and nutrients consumption rate, thus affecting population dynamics and leading to a decrease in biomass accumulation. Numerical simulations had been performed in parallel to the laboratory experiments in order to access if the differences observed between the dynamics of monoclonal and cross cultures can be attributed to competition between the strains

and their size differences, or if sexual reproduction is required to explain them.Finally, I discuss the need for introducing processes related to life cycles into phytoplankton competition models in order to increase their accuracy and predictive capability.

5.2 Materials and methods

5.2.1 Laboratory experiments

5.2.1.1 Experiments design

Experiment 1 and 2 In these experiments, two pairs of parental strains, Pm+ (male) and Pm- (female), differing in cell size, so to be able to estimate the growth rate of the individual strains (Table 5.1), were used to investigate the formation of sexual stages under different conditions. Strains were grown in culture flasks incubated on a rotating wheel that keeps them gently mixed and on a shelf that favours sinking of the cells. The maximum growth rate of the individual parental strains in monoculture and of the parental strains in co-culture was determined as well. Parental strains differing in average cell size were used in order to monitor the growth rate of the individual Pm+ (male) and Pm- (female) strains. The results of the first experiment have been included in the publication Scalco et al. [2014] which I have co-authored, furthermore they were included in the Scalco's PhD Thesis (Scalco [2010]).

Two 500 ml flasks, one for each parental strain, were filled with 240 ml of f/2 medium and inoculated with cells at final concentration of about 3000 $[\frac{cells}{ml}]$. Aliquots of 30 ml were dispensed, after gentle mixing, in eight 70 ml culture flasks (mono-culture of parental strains). The stock co-culture of the two parental strains was prepared in a flask filled with 800 ml of f/2 filtered medium and inoculated with cells at final concentration of about 1500 $[\frac{cells}{ml}]$ for each parental strain (3000 $[\frac{cells}{ml}]$ in total). Aliquots of 35 ml were dispensed, after careful mixing, in 26 70 ml flasks. For each parental strain and for the crosses, half of the flasks were placed on a rotating wheel (RW) and the other half were placed on a shelf (SH). The rotating wheel and the shelf were located in a walk-in climatic chamber at a temperature of 18C and a photoperiod of 12L:12D h. The integrated irradiance at which cultures were exposed on the rotating wheel

was 60 $[\frac{\mu molphoton}{m^2\,s}]$ (110 $[\frac{\mu molphoton}{m^2\,s}]$ at the top; 35 $[\frac{\mu molphoton}{m^2\,s}]$ at the bottom), which was the same as the one on the shelf. The rotating wheel was set at a 0.1 rpm; this rotation velocity caused a gentle and constant mixing of the cultures, hence preventing cell accumulation at the bottom of the flasks. Two RW and two SH experiments were performed (Table 5.1).

Experiment 3 In this experiment, four parental strains (Table 5.1) were used to follow the growth and formation of sexual stages of the co-culture of a single mating type strains and the co-cultures of strains of opposite mating type. The strains were pre-acclimated before the experiment. Two 2l flasks, one for each mating type, were filled with 1.5 L of f/2 medium and inoculated with two strains of the same mating type at final concentration of about 6000 $[\frac{cells}{ml}]$ (3000 $[\frac{cells}{ml}]$ of each strain). The stock co-culture of the four parental strains was prepared in a similar way and was inoculated with cells at final concentration of about 1500 $[\frac{cells}{ml}]$ for each parental strain (6000 $[\frac{cells}{ml}]$ in total). Each flask was connected to an aerator that produced a gentle bubbling, and placed in a growth chamber at 18C with a 12L:12D h photoperiod with light intensity 110 $[\frac{\mu molphoton}{m^2\,s}]$.

5.2.1.2 Sampling and identification of life stages

Samples of 35 ml of culture were collected for the parental strains and the sexualized co-cultures with the frequency specified in Table 5.3. In case of Experiments 1 and 2 (RW/SH), the content of the whole flask flask was used, while in Experiment 3 (bubbling) samples were taken from the middle portion of the bottle. From this sample volume, 7 ml were fixed with formaldehyde solution at a final concentration of 1.6 % and stored in a fridge at 4C for cell counts (duplicate counts were performed). One ml of this fixed sample was used to fill a Sedgewick Rafter counting slide and cells were enumerated at the Zeiss Axiophot light microscope. The following stages were enumerated: live vegetative cells (cells with cytoplasm content), gametes/zygotes, auxospores, initial cells, and large F1 generation cells. The counts of the co-cultures of Experiments 1 and 2 had been carried out by Eleonora Scalco (IME, Stazione Zoologica Anton Dohrn), while the counts of the monoclonal cultures and all counts of

Experiment 3 were carried out by myself.

The remaining 28ml of the sample were filtered through a MILLEX-GS filter unit with a 0.22 μm pore size using a 60 ml syringe. High density polyethylene vials were used for storing the filtered samples. The filters, vials, and syringes were washed with bi-distilled water (DDW) prior the filtration. Additionally, the vials were rinsed with the filtered sample before filling them. The filtered samples were placed at -20C till the analysis. The samples were analysed for silicate SiO_2) using a FlowSys Systea Autoanalyzer, equipped with five continuous flux channels, following Hansen and Grasshoff [1983]. The analyses had been carried out by Augusto Passarelli and Francesca Margiotta (MODA, Stazione Zoologica Anton Dohrn).

5.2.2 Growth rate calculation

The cell concentration data was plotted and the exponential growth phase was identified. During the exponential phase microbial population multiply at rates that are, overall, assumed to be constant. Hence, even though there may be a spread of individual generation times, a number of organisms (X_0) will give rise to $2X_0$ progeny and these to (2^2X_0) progeny, and so on, with an overall doubling time, t_d, that is constant. It follows therefore that the number of individual organisms in the culture after incubation time t will be related to the initial population by $X_t = X_0 2^{t/t_d}$ (Guillard [1980]).

The growth rate during the vegetative phase was estimated calculating the least-squares regression of the log (base2) cell concentration data over the exponential portion of the growth curve. The slope of the linear regression provides an estimate of the maximum division rate (Guillard [1980]).

The increase in population size is associated with the consumption rate of a certain resource. I have also estimated growth rate by an independent method, i.e. the consumption rate of silicates that is needed by diatoms to synthesize the sicila frustule The growth rate of parental strains and co-cultures was thus estimated by applying a least-square regression to the log (base2) data of silicate concentration.

experiment	strain code	mating type
Experiment 1	$Sy799$	female
	$Sy793$	male
Experiment 2	$A4$	female
	710	male
Experiment 3	$GM50B$, $MVR1041.4$	female
	$VF235$, $SP3$	male

Table 5.1: *Pseudo-nitzschia multistriata* strain used for the experiments illustrated in this chapter. For each strain the LTER-MC sample code and mating type is reported.

5.2.3 Model reproducing competition experiments

A numerical simulation was run to reproduce population dynamics observed in the laboratory experiments. A simple nutrients-phytoplankton (NP) model was used, where either one or two strains of the same phytoplankton species were present:

$$\frac{dN}{dt} = -\frac{r_F N}{N + H_F} P_F - \frac{r_M N}{N + H_M} P_M, \tag{5.1}$$

$$\frac{dP_F}{dt} = \frac{r_F N}{N + H_F} P_F - m P_F, \tag{5.2}$$

$$\frac{dP_M}{dt} = \frac{r_M N}{N + H_M} P_M - m P_M, \tag{5.3}$$

where: N- nutrients concentration, P_F, P_M - concentration of female and male respectively, r_F,r_M - growth rate respectively for female and male, H_F,H_M - nutrients half-saturation value respectively for female and male, m - mortality rate.

The results of the experiments showed that the female strains had higher growth rate. It was however impossible to asses the values of nutrient half-saturation and mortality rates from the experimental results. Because of that, an identical values of those parameters were attributed to both male and female strains (Table 5.2).

The presented model ought to be considered as a simplistic representation of the laboratory experiments set-up. Eventhough phytoplankton strains were described with the growth rate, nutrient half-saturation and mortality rate, they are in fact distin-

guished solely with their growth rate. In a similar fashion there is only one virtual nutrient considered in the model which may represent silicate as well as nitrate, phosphate, etc.

Moreover, the model presented above may be considered as a stripped-down version of the model described in the 2nd chapter of this thesis. Indeed, the laboratory experiments were focused on the dynamics of a single species under controlled environmental conditions. Thus in order to mimic such a simplified case multiple model elements had to be omitted. In particular, the number of considered species needed to reflect the experimental cases, i.e. only a single species in form of one or two strains was resolved in the model configuration. The variables describing zooplankton and detritus were eliminated as the zooplankton was absent during the experiment and the experimental time-scale did not allow for the detritus remineralisation. Furthermore, due to the controlled environmental conditions the physical processes related to the changes in the MLD have been omitted as well. Finally, the number of nutrients was also decreased as the consideration of multiple nutrients would be meaningless without differentiating of the species in terms of nutrients uptake.

The model has been used to perform simulations addressing dynamics of:

1. monoclonal male strain,

2. monoclonal female strain,

3. co-culture of male and female strains.

These scenarios intend to mimic population dynamics observed in the monoclonal cultures, but above all to reproduce the dynamics of the parental strains of opposite mating types observed in the course of the experiments. The underlying assumption of the modelling scenario considering the co-culture of the parental strains is that there are solely competitive interactions among them, hence sexual reproduction does not take place.

It is intended to illustrate that the model is able to capture the dynamics observed in the experiments with the monoclonal strains but fail to reproduce the dynamics of the co-cultured parental strains. Hence, the goal is to demonstrate that processes linked to sexual reproduction must be incorporated into the modelling framework in

parameter	value
$r_F[d^{-1}]$	1
$r_M[d^{-1}]$	0.8
H_F,H_M $[\frac{\mu mol\,C}{m^3}]$	0.9
m $[d^{-1}]$	0.1

Table 5.2: Parameter values used in the model mimicking competition between strains of opposite mating type. Each strain is described with a growth rate (r_F,r_M - female and male respectively), nutrients half-saturation constant (H_F, H_M - female and male respectively) and mortality rate (m).

order to properly reproduce the dynamics of phytoplankton cultures consisting multiple strains (here 2) during the vegetative phase but also during sexual reproduction.

The analysis focused on the biomass accumulation and nutrients consumption rates in each simulation.

5.3 Results

5.3.1 Laboratory experiments

5.3.1.1 Experiment 1

Growth dynamics of the individual parental strains on RW1 and SH1 The growth dynamics of the parental strains grown in monoculture in SH1 and RW1 experiments was described in terms of observed growth rates and maximum cell concentration reached within the (Table 5.3; Figures 5.1, 5.2). The male strain reached the maximal cell concentration on day 8 (52×10^3 $[\frac{cells}{ml}]$ and 172.6×10^3 $[\frac{cells}{ml}]$ on RW1 and SH1), while the female strain on day 4 in both experiments (227×10^3 $[\frac{cells}{ml}]$ on RW1 and 529.5×10^3 $[\frac{cells}{ml}]$ on SH1). Therefore the exponential phase was significantly shorter in case of female strain. Simultaneously, the female growth rate (1.69 $[\frac{div}{d}]$ on RW1 and 1.99 on SH1) was higher than male growth rate under identical conditions (0.89 $[\frac{div}{d}]$ on RW1 and 0.79 on SH1). In all the cases, the exponential growth phase was followed by a short stationary phase followed by a rapid decline of vegetative cell concentration.

The concentration of silicate reached undetectable values on day 12, with the exception of the female culture on RW1 (Figure 5.1). The depletion of silicate could however occur earlier, considering that the sampling took place every 4 days (Figure 5.2). The

maximal division rate estimated with the SiO_2 consumption was identical for male and female culture in both experimental set-ups as it reached the value of 0.87 $[\frac{div}{d}]$. The only, slight, difference was observed in case of female strain in SH1 experiment in which case it was higher by 0.02. It is important to note that this estimation is considerably crude because of low resolution of nutrients measurements (Table 5.3).

Growth dynamics and sexual reproduction of the co-cultures of the two parental strains on RW1 and SH1 The cell concentration patterns observed in the co-cultures of RW1 and SH1 experiments differed considerably (Figure 1, 2). In both experiments, a lag-phase was observed that, in the case of the SH, corresponded to a decrease in cell concentration. The exponential phase lasted till day 10 (1.27 $[\frac{div}{d}]$) and 14 (0.57 $[\frac{div}{d}]$) on RW1 and SH1, respectively. The maximum density of the vegetative cells was 558×10^3 $[\frac{cells}{ml}]$ on RW1 and 329.6×10^3 $[\frac{cells}{ml}]$ on SH1.

Sexual reproduction occurred on both RW1 and the SH1. In the SH, gametes and auxospores were found starting from the 2nd day, while initial cells were observed from day 3 until day 6. Large F1 generation cells were recorded on the 3rd day of the experiment and were growing exponentially till 7th day (with a maximum growth rate of 1.81 $[\frac{div}{d}]$). The time at which sexual reproduction started corresponds to the observed decrease of the total cell biomass observed in the first days in cross cultures (Fig. 5.2).

On the rotating wheel experiment (RW1), gametes and auxospores were found from the 2nd day, while initial cells were observed on day 4 and 5. Sexual stages were very rare as their maximal concentration was equal to 21 $\frac{cells}{ml}]$. Large F1 generation cells were recorded after a few days from the appearance of gametes and their abundance trend paralleled that of parental strains. Their maximum growth rate was 1.44 $[\frac{div}{d}]$.

Silicate concentration varied slightly till day 6 on RW and 11 on SH, and rapidly decreased afterwards reaching undetectable values within about 5 days (Figure 5.1, 5.2). The maximal division rate of the co-culture estimated with the SiO_2 consumption was equal to 0.6 and 0.39 $[\frac{div}{d}]$ on the RW1 and SH1 respectively (Table 5.3).

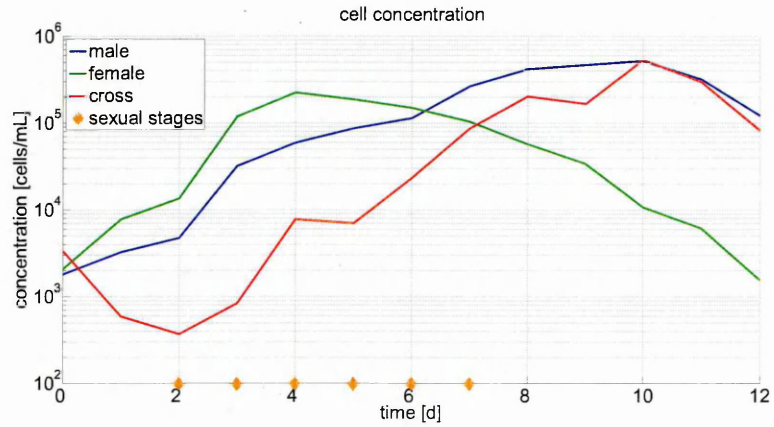

(a)

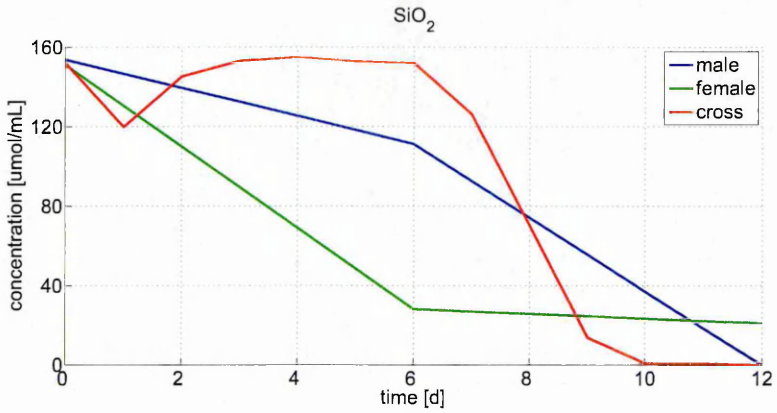

(b)

Figure 5.1: Results of Experiment 1, rotating wheel (RW1). The panels represent concentration of: (a) cells, including vegetative cells of the parental strains, sexual stages and large cells of the F1 generation (b) SiO_2 measured in the monoclonal (female and male) and co-culture (cross) experiments. The 'diamond' marks indicate days when sexual stages were observed.

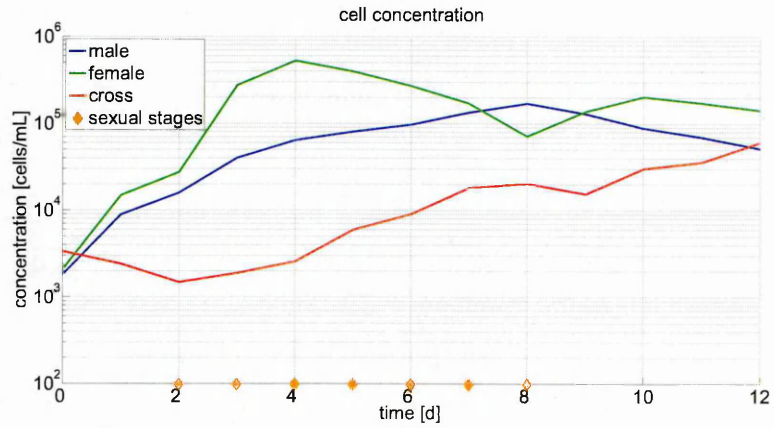

(a)

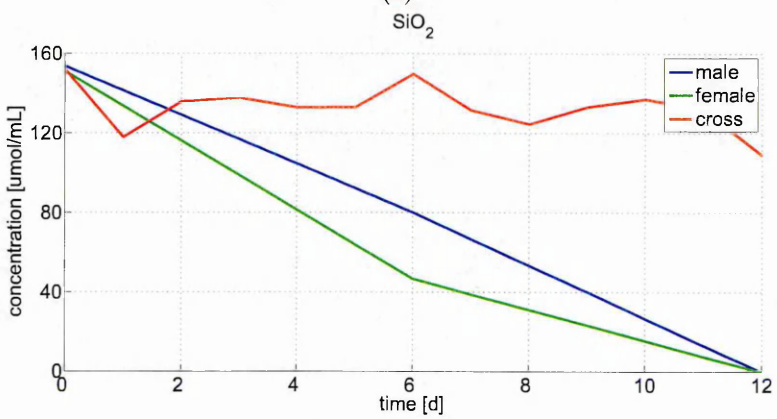

(b)

Figure 5.2: Results of Experiment 1, shelf (SH1). The panels represent concentration of: (a) cells, including vegetative cells of the parental strains, sexual stages and large cells of the F1 generation (b) SiO_2 measured in the monoclonal (female and male) and co-culture (cross) experiments. The 'diamond' marks indicate days when sexual stages were observed.

5.3.1.2 Experiment 2

Growth dynamics of the individual parental strains on RW2 and SH2 The growth dynamics of the parental strains in monocultures in SH2 and RW2 experiments varied considerably (Table 5.3; Figure 5.3, 5.4). The male strain reached the maximal cell concentration on day 6 ($108\times10^3\,[\frac{cells}{ml}]$) and day 3 ($81\times10^3\,[\frac{cells}{ml}]$) on RW2 and SH2, respectively, while the female strain on day 5 in both experiments ($84\times10^3\,[\frac{cells}{ml}]$ on RW2 and $182\times10^3\,[\frac{cells}{ml}]$ on SH2). Thus, the duration of exponential phase was comparable, though slightly shorter in case of male monoclonal culture in SH2 experiment. The female growth rate ($1.87[\frac{div}{d}]$ on RW2 and 1.45 on SH2) was higher than male growth rate ($1.1\,[\frac{div}{d}]$ on RW2 and 1.4 on SH2).

The concentration of silicate reached undetectable values on day 10 in both RW2 experiments, while on day 5 and 8 in case of female and male in SH2 experiment respectively (Figure 5.3, 5.4).

The maximal division rate of the male and female culture estimated with the SiO_2 consumption reached comparable values in the RW1 experiment (0.55 and 0.59 $[\frac{div}{d}]$ respectively). Conversely, considerable discrepancies were observed in the SH1 experiment as the division rates of the male strain ($0.82\,[\frac{div}{d}]$) was 27% lower than that of the female strain ($1.12\,[\frac{div}{d}]$; Table 5.3).

Growth dynamics and sexual reproduction of the co-cultures of the two parental strains on RW2 and SH2 The abundance patterns observed in the co-culture RW2 and SH2 experiments varied considerably in terms of growth rates but above cells concentrations (Figure 5.3, 5.4). In both experiments, a lag-phase was observed. The exponential phase lasted till day 11 (RW2 $0.53\,[\frac{div}{d}]$) and 12 ($0.82\,[\frac{div}{d}]$) on RW2 and SH2, respectively. The maximum density of the vegetative cells of both mating types was equal to $89\times10^3\,[\frac{cells}{ml}]$ on RW2 and $371\times10^3\,[\frac{cells}{ml}]$ on SH2. In the RW2 experiment gametes were observed from the 3rd day until 7th, and in SH2 from the 2nd day until 5th. Neither auxospores nor F1 generation cells were observed in these experiments.

Silicate concentration varied slightly till day 6 on SH2, and rapidly decreased afterwards reaching undetectable values within about 5 days (Figure 5.4). The depletion of

silicate on the RW2 was observed at the end of experiment (Figure 5.3). The maximal division rate estimated with the silicate consumption of the co-culture on the rotating wheel reached 0.24 $[\frac{div}{d}]$ while on the shelf it was equal to 0.47 $[\frac{div}{d}]$ (Table 5.3).

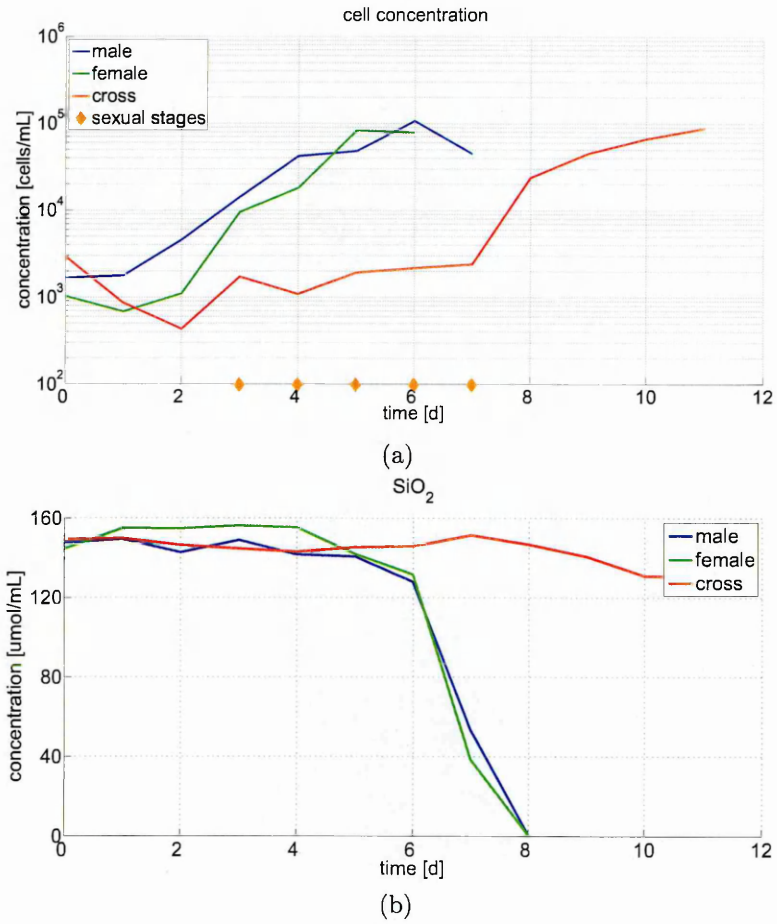

Figure 5.3: Results of Experiment 2, rotating wheel (RW2). The panels represent concentration of: (a) cells, including vegetative cells of the parental strains, sexual stages and large cells of the F1 generation (b) SiO_2 measured in the monoclonal (female and male) and co-culture (cross) experiments. The 'diamond' marks indicate days when sexual stages were observed.

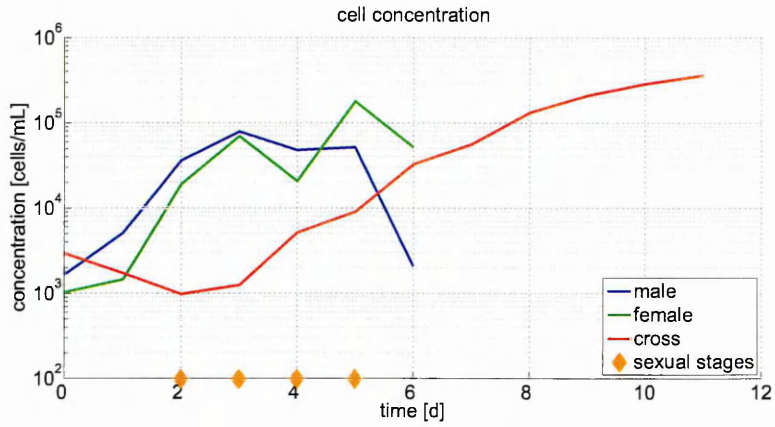

(a)

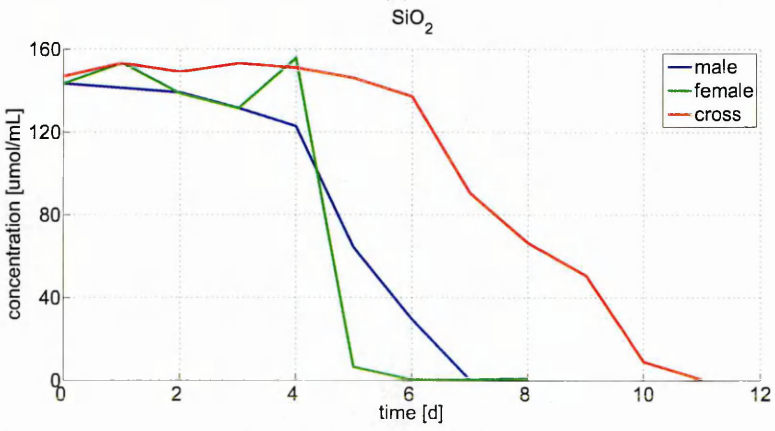

(b)

Figure 5.4: Results of Experiment 2, shelf (SH2). The panels represent concentration of: (a) cells, including vegetative cells of the parental strains, sexual stages and large cells of the F1 generation (b) SiO_2 measured in the monoclonal (female and male) and co-culture (cross) experiments. The 'diamond' marks indicate days when sexual stages were observed.

5.3.1.3 Experiment 3

Growth dynamics of the co-cultured single mating-type strains The exponential growth phase was observed for 4 and 6 days in female- and male-cultures, respectively, thus it was comparable (Figure 5.5). Similar maximal cells concentrations were recorded in both cases (1440 and 1496×10^3 $[\frac{cells}{ml}]$ in females and males, respectively) on the 6th day of the experiment. Though the strains grew with a different maximum growth rates: females - 2.36 $[\frac{div}{d}]$ and males - 1.46 $[\frac{div}{d}]$.

Silicate concentration showed a continuous decreasing trend and reached undetectable values within about 4 and 7 days (Figure 5.5). The maximal division rate estimated with the silicate consumption of the female strains reached 1.97 $[\frac{div}{d}]$ while that of the male strains was equal to 1.19 $[\frac{div}{d}]$ (Table 5.3).

Growth dynamics and sexual reproduction of the co-cultures of the four parental strains The total number of *P. multistriata* cells (parental cells of all four parental strains), i.e. the total biomass that developed in the flask, showed similar dynamics to that of the males, though the maximal cells concentrations reached on the 5th day was more than two times lower than in case of the co-cultured of strains with identical mating-type (615 $\times 10^3$ $[\frac{cells}{ml}]$). The exponential growth phase was observed during first 5 days of the experiment (Figure 5.5). The observed growth rate was equal to 1.47 $[\frac{div}{d}]$. Contrary to Experiments 1 and 2, a lag-phase was not observed in the co-cultures of strain of opposite mating type. Gametes were observed from the 2nd day until 5th, but neither auxospores nor F1 generation cells were observed.

Silicate concentration showed a continuous decreasing trend reached undetectable values within about 5 days (Figure 5.5). The maximal division rate estimated with the silicate consumption of the four co-cultured strains reached 1.29 $[\frac{div}{d}]$ (Table 5.3).

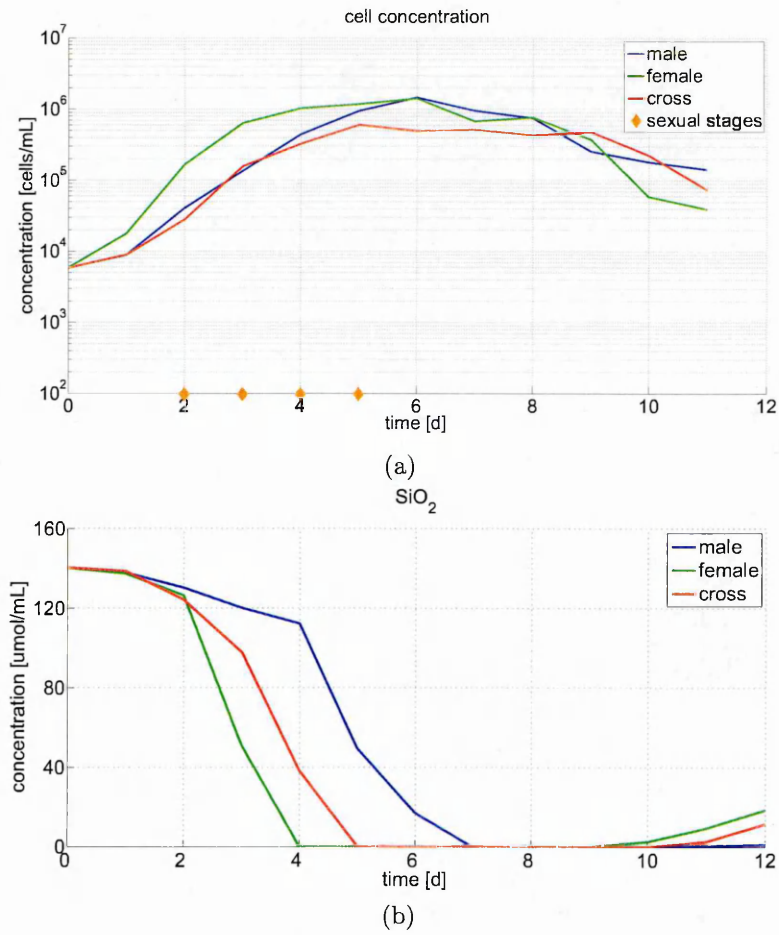

Figure 5.5: Results of the Experiment 3: Bubbling. The panels represent concentration of: (a) cells and (b) SiO_2 measured in the monoclonal and co-cultured experiments. The 'diamond' marks indicate days when sexual stages were observed.

	T_C	T_N	*Exp phase*	div_{cells}	div_{SiO_2}	C_{max} [$\times 10^3$]	SiO_{2lim}
Experiment 1 (RW/SH)							
female (-)	[0,2,4,...,12]	[0,6,12]	4 / 4	1.69 / 1.99	0.87 / 0.89	227 / 529	$\leq$12
male (+)			8 / 8	1.01 / 0.79	0.87 / 0.87	526 / 172	$\leq$12
cross	[0,1,2,...,12]	[0,1,2,...,12]	10 / >12	1.27 / 0.57 (F1) 1.44 / 1.81	0.60 / 0.39	544 / 258	11 />12
Experiment 2 (RW/SH)							
female (-)	[0,1,2,3,4,...	[0,1,2,3,4,...	5 / 5	1.87 / 1.45	0.59 / 1.12	84 / 182	10 / 5
male (+)	5,6,8,10]	5,6,8,10]	6 / 3	1.1 / 1.4	0.55 / 0.82	108 / 81	10 / 8
cross	[0,1,2,...,12]	[0,1,2,...,12]	11 / >12	0.53 / 0.82	0.24 / 0.47	89 / 371	>12 / 11
Experiment 3							
females (-)	[0,1,2,...,12]	[0,1,2,...,12]	4	2.36	1.97	1 440	4
males (+)			6	1.46	1.19	1 496	7
cross	[0,1,2,...,12]	[0,1,2,...,12]	5	1.47	1.29	615	5

Table 5.3: Sampling schedule and results of the laboratory experiments: sampling days for cell (T_C) and nutrients (T_N) concentration measurements, duration of the exponential phase in [days] (*Expphase*), maximal division rate based on cells concentration in [1/d] (div_{cells}), maximal division rate based on silicate consumption in [1/d] (div_{SiO_2}), maximal concentration reached in [cells/ml] (C_{max}), SiO_2 depletion day [day of the experiment] (SiO_{2lim}).

5.3.1.4 Experiments summary

In Table 5.3 and in Figure 6, a summary of the results obtained in the different experiment is presented. The exponential growth phase was longer in the co- cultures of strains of opposite mating type, where sex occurred (Table 5.3). The maximum growth rate of the parental strains in monoclonal cultures was higher than in the co-cultures in all experiments (Fig. 6). Sexual reproduction was observed within 2 or 3 days from the beginning of the experiments and lasted approximately 3-4 days (till day 6-7). The number of sexual stages observed in the experiment varied between 1% and 10% of the total parental cells, hence only a subset of a population underwent sexual reproduction. The period during which reduced growth rate of the parental strains was observed lasted approximately till the end of the experiments. Thus, it was observed on a time scale longer than the one in which mating was observed.

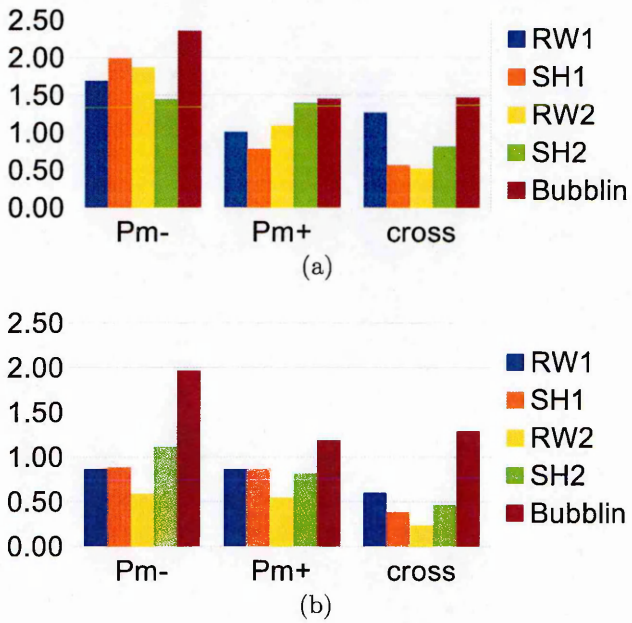

Figure 5.6: *Pseudo-nitzschia multistriata* strains (a) division rate and (b) growth rate reported in all performed laboratory experiments. The division rate was estimated directly from cell counts, while the growth rate was based on the nutrients (SiO_2) removal.

5.3.2 Model mimicking competition experiments with diatoms batch cultures

In a scenario where the growth dynamics of a single strain was simulated, the nutrients were quickly depleted and the population collapsed afterwards (on day 8 and 10 for

the female and the male strains, respectively; Fig. 5.7a, 5.7b). Similar dynamics was observed in case of two strains of the same mating type grown together. The strain with the higher growth rate (the female in the simulation) quickly dominated the population and removed all the nutrients from the system causing the collapse of the community after some days (on day 8; Fig. 5.7a, 5.7b). This dynamic arises from the competitive superiority of the faster growing (larger) strain, as higher growth rate allows for faster biomass accumulation.

The model results contrast to what was observed in the laboratory experiments, where the abundance patterns in the cross- and monoclonal cultures were vastly different, and the co-cultures of parental strains demonstrated growth rate reduction. These results illustrate that the abundance patterns of two competing phytoplankton strains is very similar to a monoclonal population. Thus, in the absence of sexual reproduction, the strains co-culture show identical dynamics as a monoclonal culture (Fig. 5.7c).

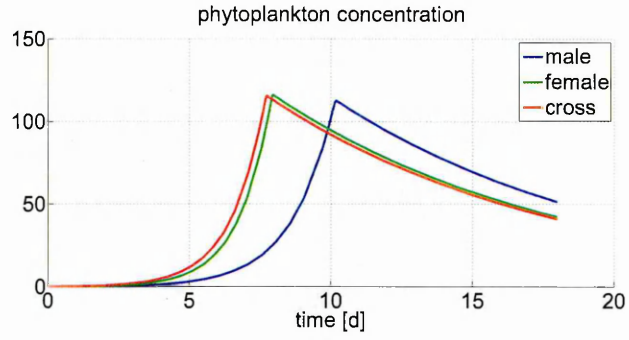

(a)

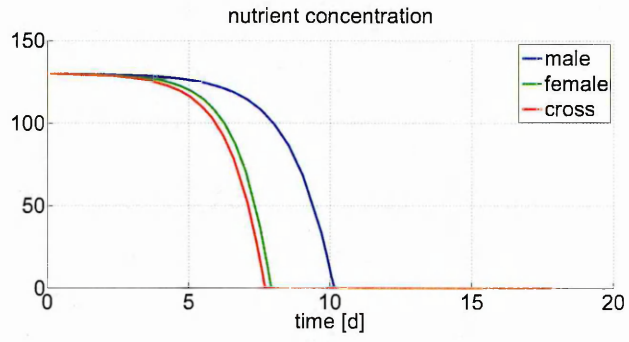

(b)

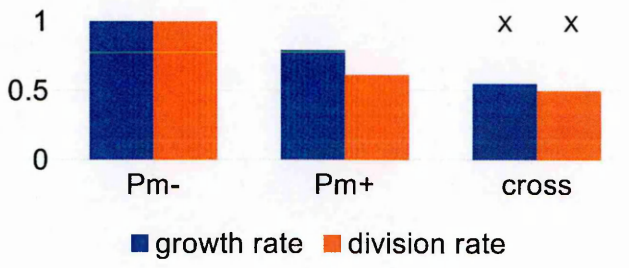

(c)

Figure 5.7: Results of the numerical simulations mimicking phytoplankton competition experiments. Plots illustrate dynamics of (a) phytoplankton and (b) nutrients concentration in monoclonal and cross experiments. The results were obtained with a simple Nutrients-Phytoplankton competition model (sec. 5.2.1). (c) the average values of the growth rate based on SiO_2 consumption (blue) and the division rate based on cell concentration (red) observed in all the laboratory experiments with monoclonal and co-cultures of *p. multistriata*. Growth rates reported in the male monoclonal cultures and co-cultures were normalised with respect to the growth rate values reported in the female monoclonal culture in each experiment and averaged. The 'X' marks represent phytoplankton growth rate in the virtual co-culture when sexual reproduction did not take place - the 'X' marks represent results obtained with a competition model (sec. 5.2.3).

5.4 Discussion

Sexual reproduction of *Pseudo-nitzschia* species was observed in the natural environment in the north-west Pacific coast (Holtermann et al. [2010]) and in the Gulf of Naples, Mediterranean Sea (Sarno et al. [2010]). The sexual reproduction occurred

during a bloom, yet the reported cells concentration varied considerably between the two cases. The concentration in the former case reached hundreds of thousands of cells ranging from 187 10^3 to 929 10^3 cells per litre of the simultaneously blooming *P. australis* and *P. pungens* species. In the latter case concentration of the blooming species reached hundreds of thousands (7 10^5 cells per litre of *P. cf. calliantha*) and millions of cells per litre (9.1 10^6 cells per litre of *P. cf. pseudodelicatissima*). Henceforth, only in the latter case the cell density was comparable with values of 2-10 10^6 cells per litre at which sexual reproduction occurred under controlled laboratory conditions as reported by Scalco [2010] and Scalco et al. [2014].

Because of this apparent mismatch between field and laboratory conditions it is considered that the physical structure of the water column, in particular so called Thin Layers (TL), may facilitate cells aggregation (Durham and Stocker [2012]). The formation of TLs may be associated with various mechanisms. Among them accumulation due to physical processes (e.g. vertical gradients of horizontal velocity due to shear, advection) and active buoyancy regulation (as in the case of aggregates of the large diatoms *Rhizosolenia* Villareal et al. [1999]) are frequently invoked. In addition, active *in situ* growth under optimal light or nutrient conditions coupled with vertical density gradients may lead to an increased cells concentration within the TL.

These structures may extend horizontally for kilometres and persist for days, yet, may be easily destroyed by wind induced turbulence and/or to changes in water density. Due to their instability, but also to their vertical thickness spanning from centimetres up to a few meters (¡5 m), it is rather difficult to detect them with conventional profiling instruments (McManus et al. [2007]).

There is evidence of phytoplankton reaching considerably higher cell concentration within the TL than in the water immediately above or beneath it (Rines et al. [2002], Velo-Suárez et al. [2008]). In fact, species belonging to the *Pseudo-nitzschia* genus were frequently recorded in TLs with cells density comprised between 5 10^4 and 3.3 10^6 cells per litre. Hence not only 2.8 - 3.3 times higher than outside of the TLs (McManus et al. [2007], Rines et al. [2002], Ryan et al. [2005], Sullivan et al. [2005], Velo-Suárez et al. [2008]) but also at the densities far more similar to those observed in laboratory studies. Consequently, phytoplankton cell aggregation in TLs may increase

the encounter rate and decrease the inter-cellular distance leading to an increased mating success probability (Lelong et al. [2012]). Alternatively, co-present species might provide the substrate on which cells can migrate towards the opposite mating types, as for instance, solitary cells and colonies of *P. cf. pseudodelicatissima* were observed together with colonies of *Chaetoceros socialis* (Rines et al. [2002], Velo-Suárez et al. [2008]) and this peculiar co-occurrence persisted for 3 weeks (Rines et al. [2002])

As illustrated in Chapter 1, very little is known about the mechanisms of diatoms sexual reproduction and the conditions in which it can occur. In this chapter I have presented the results of five intra-specific competition experiments with strains of arine pennate diatom Pseudo-nitzschia multistriata that could potentially undergo sexual reproduction (results partially published Scalco et al. [2014]). The aim of the experiments was to quantify the differences in the growth rate among two different algal suspensions, monoclonal cultures or the co-culture of strains of opposite mating type, which is the required condition for the induction of the sexual phase. It is important recalling that in heterothallic species, such as *P. multistriata*, multiple strains coexist in the natural environment and the interaction between male (mating type +) and female (mating type -) mating types is required for sexual reproduction to occur (Chepurnov et al. [2005]).

The positive and negative diatom strains were grown in mono- and co-cultures, thus under conditions where, respectively, sexual reproduction could not and could take place. In addition, the impact of different physical conditions, mixing and still conditions, was also tested. The growth rate was estimated directly from cell counts and indirectly from the nutrients removal. Both independent estimates were used since the division rate does not properly quantify the real biomass increase due to diatoms internal storage and size variations.

The growth curves in all the experiments were considerably different in terms of growth rates, maximal concentrations and duration of the exponential phase. The exponential phase duration was regulated by the nutrients availability, as its end mainly coincided with the depletion of Si. However in some cases, e.g., male strains in the RW1 and SH1 experiments, a decrease in the growth rate and vegetative cells decline was observed before Si depletion. It may be caused by a depletion of some macro- and

micro-nutrients, which were not analysed here. Thus, the mechanisms responsible for this decline remain speculative.

The differences in the growth rates observed in the monoclonal cultures can be attributed to size differences among the strains (Sarthou et al. [2005]). However, the growth dynamics observed in monocultures of single strains and in co-cultures of strains of opposite mating type, was considerably different. The co-cultures of opposite mating type grew considerably slower with respect to monoclonal cultures. Reduced growth rate in the former conditions was reported when both cell concentration and nutrients removal rate were calculated. Thus both division rate and biomass accumulation were considerably lower in cultures where sexual reproduction took place. This was evident in all experiments when comparing the growth dynamics of monocultures of the individual parental strains and the crosses. This growth rate reduction cannot be attributed to nutrients depletion, as the measurements indicate nutrient concentrations exceeding values of nutrients half-saturation constants for diatoms (Sarthou et al. [2005]). Thus, the growth rate reduction observed in co-cultures was directly related to sexual reproduction. Notably, it was observed on a time-scale longer than the time required for mating and gametes production (gametes production took place in days 2-3, and the decreased growth rate was observed all over the experiment). Consequently, the link between the onset of the sexual phase and the reduction of growth might further amplify the 'cost of sex' for these unicellular microalgae (Lewis Jr [1984], Lewis Jr [1983])., The cost of sex would not only be due to the investment of biomass into gamete formation and the risk of finding the partner, but it would also have the counter-effect of impacting the growth of vegetative parental cells. Hence, the experimental results indicate a life-cycle related mechanisms capable to control species growth rate independently from proximal factors such as physical forcing or resources availability.

Additional evidences on sexual reproduction interfering with population dynamics of *P. multistriata* have been provided also by additional laboratory experiments carried out in batch cultures (Scalco et al. [2014]). Also in these experiments, the growth dynamics of monoclonal strains different considerably from that of co-cultures undergoing sex (see Fig. 3 in Scalco et al 2014 Scalco et al. [2014]). It has also be shown

that a threshold cell density is required for the induction of sexual reproduction. The fact that a threshold cell concentration has to be reached for sex to occur supports the hypothesis that chemical cues are responsible for the induction of sexuality, as recently reported for two benthic diatoms (Sato et al. [2011a], Gillard et al. [2013]).

The observed mechanism of growth rate reduction related to sexual reproduction, raises a question: can the outcomes of the competition for resources between multiple strains during obligatory sexual phase be predicted on basis of the monoclonal experiments? As depicted on Figure 5.6, the answer is: No. The growth rate and nutrient consumption in the co-culture experiment was 50% lower than that estimated with a simple nutrients-phytoplankton competition model parametrized using the rates of monoclonal suspensions. Consequently, the endogenous control of cell growth linked to the interaction of cells of different mating type might impair population dynamics and cause a change in ecosystem functioning.

Phytoplankton are responsible for a great part of the oxygen present in our atmosphere and their cumulative energy fixation in carbon compounds is the basis for the vast majority of oceanic and fresh water food webs. Plankton play a crucial role in global biogeochemical cycles but the mechanisms that rule its dynamics at population level are not well understood. Therefore, deciphering them is of great interest. Trait-based approach is frequently invoked when the seasonal structure of planktonic communities is addressed (See Chapter 1). Traits are often used to define major phytoplankton functional groups (Litchman and Klausmeier [2008]. Phytoplankton traits can be categorised according to their ecological function (e.g., reproduction, resource acquisition, predator avoidance) or their type (e.g., morphological, physiological, behavioral, life history). Yet, the trait-based approach is mostly focused on factors regulating the ability to compete for resources and does not consider biological controls on net growth rates that may derive from chemical signalling among the cells or from specific life cycle features. Notably, the paradigm of diatoms as the competition winners in nutrient replete conditions is based on experiments made with monoclonal cultures.

In this Chapter I have provided evidence that growth rate, even in culture, may change independently from resources, in different phases of the life history of a diatom. Presented data suggest that biological processes other than resource acquisition do

participate in the definition of the species ecological niches. Consequently, in order to advance in our understanding of the plankton biodiversity and improve the skill of the biogeochemical models exploring impact of climate changes on the ecosystems, it is necessary to evaluate the impact of the biological regulation of these species-specific phases on the community dynamics over the seasonal cycle.

I thus propose that biological traits, such as life cycles, must be included in the conceptual models of plankton succession. The potential implications of such traits, namely the endogenous growth control, on phytoplankton community structure and its time course are explored in the next chapter.

5.5 Acknowledgements

Part of the laboratory work described in here, namely Experiment 1 and 2, has been performed in collaboration with Eleonora Scalco, PhD. The results of the Experiment 1 presented in this chapter have been presented in the Open University PhD thesis of E. Scalco (Scalco [2010]), and have been subsequently published as an article Scalco et al. (Scalco et al. [2014]), which I have co-authored.

Together with E. Scalco, and in collaboration with our PhD advisers, we developed the experimental protocol, prepared and run the experiments, and analysed the results of Experiments 1 and 2. The analyses of nutrient concentration were carried out by Augusto Passarelli and Francesca Margiotta (Technological Research Unit MODA, SZN).

I have conceptualised and developed the mathematical formulation of the growth rate reduction. I also developed the model for testing competition between the parental strains and bound it with the laboratory results. Finally, I have implemented the ecological model and developed the conceptual framework for testing the implications of the cell growth arrest on population dynamics.

It is impossible to decompose the intellectual investment devoted to the performed experiments as it was considered from the very beginning as a collective project addressing broad spectrum of mechanisms related to population dynamics.

Chapter 6

Endogenous growth control

6.1 Introduction

The processes and mechanisms driving species coexistence, alternation, and succession in plankton communities constitute a recurrent theme of discussion in aquatic ecology (e.g., Hutchinson [1961]; Margalef [1978],Wyatt [2014]). In a seminal paper Hutchinson Hutchinson [1961] presented a synthetic conceptual analysis on the processes that could explain the plankton paradox, i.e., the coexistence of many species competing for a very limited number of resources in an 'isotropic and unstructured environment'. He provided a list of possible scenarios among which: non-equilibrium, spatial heterogeneity, mutualistic interactions, differential predation. Additional explanations, such as absence of competitive edge among species belonging to same trophic level (Hubbell [2001]), and chaos (Huisman and Weissing [2001]) have been put forward by other authors. It has been also postulated that plankton follows the rule of a dynamic oscillating system with the insurgence of chaos and the compresence of a high number of species Benincà et al. [2008], Dakos et al. [2009]), and that the planktonic system has a chaotic dynamics induced by open chaotic mixing (Károlyi et al. [2000]). The common ground of all the above explanations is the prevalent, if not exclusive, attention to the proximate external factors.

This view is directly reflected in most of the models aimed at simulating the occurrence and succession of phytoplankton. The relevant physiological processes generally considered are species-specific uptake rates of a handful of resources (light, macro- and micro-nutrients), which, together with other environmental factors, as temperature and mixing (Hutchinson [1957], Margalef [1974]), would ultimately determine the gross growth rate of the species. Their relative weight in the community is then derived considering a mortality term, with some modulating factors, e.g., resistance to grazers and diseases (Litchman and Klausmeier [2008],Reynolds et al. [2006],Anderson et al. [2002]).

It is only recently that other phytoplankton functional traits, beyond the basic physiological ones, e.g., morphology, behavior and life histories have been suggested (Litchman and Klausmeier [2008]). These traits are weakly or not at all linked to proximate conditions and are therefore called ultimate. Because of this, they have entered the arena of potentially important components in plankton modelling (Chase

and Leibold [2003], Litchman et al. [2012]).

Despite this, physiological response curves to environmental variations (Bruggeman and Kooijman [2007], Litchman et al. [2007], Giovagnetti et al. [2012]), are, in general, the only backbone of plankton models, so far. This is likely one of the reasons why they experience so many difficulties in reproducing the diversity observed in nature. Among those ultimate factors, the life history of the species, with transitions among different stages and phases, plays an important role in population dynamics. Life history traits have been selected over the evolutionary history and determine its fitness in terms of survival and reproduction success in the face of environmental constrains.

Also phytoplankton species have complex, heteromorphic life cycles (von Dassow et al. [2015];Chapter 1), characterized by an alternation of growth and resting phases (Lennon and Jones [2011]), by phases of different ploidy and function (von Dassow et al. [2015], Frada et al. [2008]), or phases of different size and morphology (e.g. Hamm et al. [1999]) and often including a sexual phase (Chepurnov et al. [2005]). It is reasonable to assume that they may drive species dynamics along paths more sophisticated than just those regulated by the proximate factors and may affect their growth rate independently from the constraints imposed by the latter.

I here focus on the sexual phase of diatoms (Chapter 1). Because of the constraint represented by the rigid silica frustule surrounding the cell, diatoms experience a progressive cell size reduction as vegetative growth proceeds and for many of them size restoration is possible only during the sexual phase (Chepurnov et al. [2005]). This phase includes the differentiation of cells into gametangia, the stage in which meiosis and gametogenesis take place, the conjugation of gametes to form the zygote and its development into a particular stage, the auxospore, within which cells of the maximum species-specific size are produced. Centric diatoms are generally homothallic, i.e. they can interbreed within a monoclonal culture, while the vast majority of pennate diatoms are heterothallic, i.e. sex is induced only when strains of opposite mating types are present. In the Chapter 5 I have provided definitive evidence that 'male and 'female co-cultures of the planktonic diatom *Pseudo-nitzschia multistriata* engaged in sex show a marked reduction in growth as compared to the monocultures of parental strains or to co-cultures of the same mating type (Scalco et al. [2014]). Most importantly, this

endogenous regulation of growth occurs under nutrient replete conditions, thus providing experimental evidence for the capability of a microalga to regulate its growth independently from resource availability.

In this chapter I intend to carry out an in depth exploration on the concurring evidences of growth rate changes during sexual reproduction and analyse which are the ecological, in terms of species coexistence and succession in nature, and evolutionary, in terms of adaptive gains and constraints, of that trait. To this aim, I fully exploit an integrative approach, merging the information derived by focused laboratory experiments and the scenarios employing a suitably adopted mathematical model of the plankton communities in marine ecosystems.

In particular, building upon the results presented in chapter 5, I conceptualize and develop the mathematical formula describing the Endogenous Growth Control mechanism (EGC) - a life cycle related, biological trait describing the growth rate reduction of the vegetative stage attributed to sexual reproduction representing the next stage in diatoms population dynamics.

The link between the change in diatoms population dynamics attributed to the EGC mechanism and the ecosystem functioning is established with an ecological model presented in chapter 2. Namely, the impact of EGC on phytoplankton community composition and its time course is going to be assessed by comparing seasonal phytoplankton abundance, phytoplankton functional groups seasonal succession and species diversity across the ecological scenarios considering presence and absence of diatoms species which description was augmented with the developed EGC formulation.

In addition, with the scenarios built by an ad-hoc mathematical models, I explore how EGC mechanism may affect species competitive abilities and success rate of sexual reproduction. Henceforth I intend to evaluate how it may affect species fitness on the evolutionary time scale.

6.2 Further model development

6.2.1 Endogenous growth control mechanism formulation and ecological scenarios

The laboratory results presented in the previous chapter unequivocally showed that sexual reproduction affects diatoms population dynamics, independently from the resources availability. Evidence was provided for the fact that the onset of sexual phase was coupled to a marked reduction of growth of the vegetative parental cells. In a complementary set of experiments I have participated to it was further demonstrated that sexual reproduction is a density-dependent event and requires a threshold cell concentration to start(Scalco et al. [2014]). Specifically, the performed experiments indicate that *Pseudo-nitzschia multistriata* undergoes sexual reproduction at concentration approximately equal to 5000 [cells/ml].

To investigate the potential impact of such a mechanism on the composition and succession of marine phytoplankton community a formulation of the endogenous growth control mechanism (hereafter EGC) was developed and incorporated into a mathematical model of the plankton seasonal succession at mid-latitudes presented in Chapter 2.

Regarding the specific EGC formulation, it merges two aspects:

1. a successful sexual reproduction starts at a species-specific concentration threshold C_{th} (Scalco et al. [2014]),

2. passing the threshold activates the EGC mechanism,

i.e., the growth rate decreases by R independently from the resources availability (Figure 6.1):

$$\mu(N, I, P) = \left(1 - 2 \cdot R \cdot \frac{P}{P + P_{th}}\right) \cdot \hat{\mu}(N, I), \tag{6.1}$$

where $\hat{\mu}(N, I)$ - species specific growth rate dependent on the resources (N - nutrients, I - light) availability, P - phytoplankton concentration, P_{th} - phytoplankton concentration threshold required for sexual reproduction and above which the growth rate decrease is observed, R - value of the growth rate decrease.

The illustration of EGC mechanism (Eq. 6.1) functioning was presented in Fig. 6.1. The formulation of the EGC considered a temporal decrease of the species growth rate which corresponds to a sexual reproduction. Namely, a population increases as its maximal potential rate till it reaches a specific concentration threshold, P_{th}. The growth rate is decreased by R during the sexual reproduction, which was considered to last as long as the population concentration exceeds P_{th}. The growth rate increases after sexual reproduction was finished, thus when the population concentration decreased below P_{th}.

Notably, the simplified parametrisation of the EGC focuses only on the cost of sexual reproduction and its benefits are not considered in here. Future studies should address this mechanism in a balance way discussing the costs and the benefits of the sexual reproduction in the context of species diversity.

Marine diatoms span almost 6 orders of magnitude in cell volume, with the largest species reaching $\geq 10^6[\mu m^3]$ (Sarthou et al. [2005], but also Litchman and Klausmeier [2008]) and so does their carbon content per cell (Menden-Deuer and Lessard [2000]). Consequently, the 5000 [cells/ml] concentration threshold for *Pseudo-nitzschia multistriata* reported by Scalco et al (Scalco et al. [2014]) translated into carbon per m^3 would span from $1[\mu molC/m^3]$ to over 9 $[mmolC/m^3]$ if applied to all the diatom species. In particular it would be equal to 0.1 $[mmolC/m^3]$ for *Pseudo-nitzschia multistriata.*

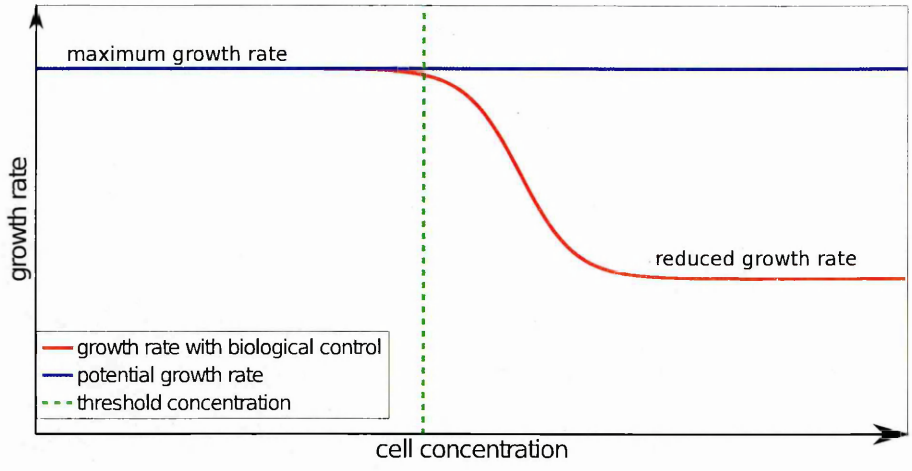

Figure 6.1: Conceptualized endogenous growth control mechanism (EGC) inspired by the laboratory experiments results. The growth rate of a species which characteristics include the EGC mechanism (red line) is reduced when a species specific concentration threshold is reached. The blue line depicts the growth rate of a species which characteristics does not include EGC mechanism. The concentration threshold (dashed green line) is associated with a sexual reproduction in this framework. The EGC mechanism is described with two parameters: concentration threshold and value of the growth rate decrease.

Scenario name	Number of species undergoing sexual reproduction
reference	0
single	1
multiple	2-4
all	all diatoms (here 10)

Table 6.1: Ecological scenarios used for exploration of the EGC impact on the community composition and its time course. The scenarios are distinguished by the number of diatom species which physiological description was enriched with the EGC mechanism.

The EGC formulation (eq. 6.1) was included in the description of diatoms species behavior accordingly to the investigated scenarios. In fact, four ecological scenarios were considered by using in each case growth rate decrease $R = 0.5$ and concentration threshold values $P_{th} = 0.1[mmolC/m^3]$, and attributing the EGC to a single species, multiple species or to all diatoms. The scenarios are:

1. *reference* - reference scenario where no EGC was used,

2. *single* - only a single diatom species description was augmented with the EGC; for each community, this selected species was the most abundant species from all those capable to cross a selected concentration thresholds in the *reference* scenario,

3. *multiple* - multiple diatom species description were augmented with the EGC; for each community, these were all the species species capable to cross a selected concentration thresholds in the *reference* scenario,

4. *all* - the description of all diatoms species was augmented with the EGC formulation.

All the numerical simulations included in this section were performed with the model described in chapter 2. The ensemble set of simulations described in Chapter 2 section 4.1 was used a *reference* scenario and further analysed in scenarios *single, multiple*, and *all* in this chapter. The physical forcing characteristics was tuned for the NABE (Sec. 4.3 Chapter 2). The results of these analysis were presented in section 6.3.1

6.2.2 Ecological niche of diatoms which life cycles include sexual reproduction

In here it was investigated if the endogenous growth control strategy was evolutionary stable, in the sense that strains reducing their growth after sexual reproduction may be competitively excluded by strains which undergo sexual reproduction, but did not decrease their growth rate afterwards.

The attention was focused on a *test* species represented by 10 strains, out of which 1 did not decrease its growth rate in accordance to sexual reproduction and 9 which did decrease it by 10, 20, 30, ..., 80, 90, 100% respectively. The *test* species were distinguished in terms of their physiological characteristics, namely intrinsic growth rate, and nutrients and light half-saturations. Each *test* species, in form of its two strains out of which one never reduces its growth rate, was seeded in an ecosystem in a steady state, and integrated for 100 years in which either a repetitive abundance pattern occurred, or the species (or its strains) underwent extinction. The explored scenarios considered ecosystem configurations invoking presence and absence of other phytoplankton species representing also non-diatoms functional groups, thus the scenarios were as follow:

1. isolated - in which the phytoplankton community was formed only by the *test* species,

2. with competitors - in which the phytoplankton community was formed by the *test* species and other phytoplankton species representing also non-diatoms functional groups,

in a subpolar environment.

The analysis further connects species physiological characteristics with sexual reproduction success rate, by incorporating EGC strategy in its description and analysing its survival rate in a given ecosystem.

All the numerical simulations included in this section were performed with a model described in chapter 2. The results of these analysis were presented in section: 6.3.2.

6.2.3 F1 generation dynamics

The endogenous growth control impairs population dynamics and in particular decreases the nutrients consumption rate, which may further affect the dynamics of the F1 generation cells. A set of simple numerical simulation was performed with the aim to investigate the competitive interactions between the F1 and the parental strains. The analysis focused on the success rate of the F1 generation cells, where as measure of success, the maximal concentration of the cells during the whole simulation was

considered. The maximal concentration of the cells is directly linked to the inoculum, thus to the strains survival rate. The model used for the simulations assumed a linear phytoplankton growth dependency on nutrients availability, thus strains were distinguished solely by their intrinsic growth rates. The model equations were:

$$\frac{dN}{dt} = -r_P N P_P - r_{F1} N P_{F1}, \tag{6.2}$$

$$\frac{dP_{F1}}{dt} = r_{F1} N P_{F1} - m P_{F1}, \tag{6.3}$$

$$\frac{dP_P}{dt} = r_P N P_P - m P_P, \tag{6.4}$$

where: N- nutrients concentration, P_{F1}, P_P - concentration of F1 and parental strains respectively, r_{F1},r_P - growth rate, respectively, for F1 and parental strains, m - mortality rate.

The competitive abilities of the parental strains and the F1 generation were given by their growth rates and assumed to take values: $r_P = 1$ and $r_{F1} \in [0.1, 6]$. Furthermore, various initial concentrations of the F1 generation cells, $\alpha \in [1\%, 30\%]$ of the initial phytoplankton concentration, were considered.

The results of these simulations were presented in the section 6.3.3

6.3 Results

6.3.1 Impact of diatom's sexual reproduction on community composition and its time course - numerical simulations

As presented in Chapter 2 the mathematical model used also in this chapter is a 0-D nutrient-phytoplankton-zooplankton-detritus (NPZD) model with two resources (N and Si), 40 phytoplankton (P) species divided into four phytoplankton functional groups (diatoms, dinoflagellates, cocolitophores and green algae), two zooplankton (Z)

species (micro- and meso-) and detritus (D_N and D_{Si}) (Moore et al. [2002],Gregg et al. [2003], Litchman et al. [2006],Quere et al. [2005]). Functional groups in phytoplankton were defined as groups of "organisms related through common bio-geochemical processes" not necessarily related phylogenetically (Iglesias-Rodríguez et al. [2002]). The phytoplankton species had different intrinsic growth rate and resources (light and nutrient) acquisition rates. The values of the coefficients describing their physiology were stochastically distributed within an assigned, broad range defined separately for each phytoplankton functional group. Therefore, the structure of the microbial community was not imposed but emerges from a wider set of predefined possibilities (Follows et al. [2007]).

Despite the limitations typical of these modelling approaches (especially a low species diversity at a later time in the simulations and a too limited set of species contributing to the seasonal succession), the model successfully reproduces the wax and wane of the main functional groups over the year. Therefore presents a suitable framework to test the broad ecological implications of the Endogenous Growth Control mechanism.

6.3.1.1 Change in the biogeochemistry

The effect of EGC is a change in seasonal patterns of phytoplankton leading to a reorganization of the community (Fig. 6.2 and 6.4) in all the considered scenarios.

The introduction of the EGC mechanism had a very little effect on the total yearly phytoplankton biomass, as its value decreased only by up to 2% in all considered scenarios (Tab. 6.2). Diatoms and dinoflagellates median total yearly biomass also decreased slightly in the scenarios in *multiple* and *all*, and the overall decrease considering all explored communities did not exceed 5 and 9% for the former and the latter group respectively. Coccolitophores increased slightly in abundance as their median total yearly biomass increased by up to 2%. A considerable decrease in the total yearly biomass was observed in case of green algae - its median value decreased by more than 40% (up to 46%) in all considered scenarios.

The median absolute deviation of the most abundant phytoplankton functional groups total yearly biomass remained at a comparable level across all considered sce-

narios, namely 20% for diatoms and coccolitophores, and 30% for dinoflagellates (these values represent value of the median absolute deviation with respect to the median data value; Tab. 6.2). High median absolute deviation of total yearly green algae biomass exceeding 100% of the nominal median value indicates strong sensitivity of those results to community composition. In particular, there were communities among all ensemble members for which green algae total yearly biomass decreased almost by 100%, while for other communities it increased by more than 100% with respect to the reference scenario (Tab. 6.2).

The median value of the median phytoplankton biomass computed over the whole year decreased by 4-6% in the scenarios exploring EGC mechanism (Tab. 6.2), though the decrease could reach up to 12% of the values observed in the *ref* scenario. The median value of the median diatoms biomass remained almost unchanged, as it oscillated within $\pm$ 1% of the reference values. However the rate of change spanned from -10% to 10% in the *single*, from -18% to 15% in the *multiple* and from -11% to 25% in the *all* scenarios if particular communities were considered. The median dinoflagellates median biomass decreased in all scenarios incorporating EGC mechanism. The median value decreased by 8% in the *single* scenario and by 11% in the *multiple* and *all*. In all cases the biomass decrease could reach up to 20%, but only in the scenario *single* a slight increase (by 1%) was reported. Median annual biomass of coccolitophores was only slightly altered - on average it decreased in all scenarios, yet the rate of decrease did not exceed 2-3%. Similarly to the total yearly biomass, the median green algae biomass was considerably altered in the EGC scenarios. The median value decreased by 12% in scenario *single* and by 22% in *multiple* and *all*. As reported above, in each scenario there were communities for which green algae median annual biomass decreased by 100%. Interestingly, the median green algae biomass could increase by up to 80% depending on the community composition in scenario *single* (Tab. 6.2).

The introduction of EGC reshaped also the spring phytoplankton bloom (Fig. 6.2; Tab. 6.2). A decrease in its intensity (down by up to 30% considering all phytoplankton functional groups) and a delay in the day of the max biomass (biomass peak) (up to 9 days) was observed. Specifically, the introduction of the EGC into the diatom's physiological characteristics had a direct impact on their maximal biomass. There

was a 5% decrease in the biomass peak intensity and a 2 days shift in its timing in the scenario *single*, though the decrease could reach up to 40% with a 8 days shift. A 20% of a median decrease and 5 days shift was reported if EGC mechanisms was attributed to a subset of diatoms or to all of them, hence in the scenarios *multiple* and *all* respectively. The range of change spanned from more than 10% to almost 45% decrease in case of maximal biomass, and from 3 to 8 days shift in case of biomass peak timing. Dinoflagellates maximal biomass increased on average in all explored scenarios: the median value computed for the whole ensemble community set increased by 20% if a single, 38% if multiple and 41% if all diatom species expressed growth rate reduction. The rate of biomass peak change spanned from approximately 10% decrease to 80% increase. The time of the biomass peak was delayed by 1 day on average, though in numerous cases it could be anticipated by up to 12 days (Tab. 6.2). The median value of the coccolitophore maximal biomass increased by 5% in the *single* and almost 10% in the *multiple* and *all*. The decrease of 11 and 20% was observed only in case of two communities in scenarios *multiple* and *all*, but a decrease reaching up to 12% appeared to be quite common in a *single* scenario as it is covered by the 1st quartile of the biomass peak probability distribution. The green algae biomass peak decreased on average 20% (*single*) and 40% (*multiple* and *all*), though similarly to other biomass indicators presented above, the rate of change spanned from 100% decrease to 80% increase in all scenarios. On average, the biomass peak of coccolitophores and green algae was anticipated in all scenarios, however the median value altered only slightly in case of green algae and remained unchanged in case of coccolitophores (Tab. 6.2).

The vegetative period duration was altered as well. The signatures of silicate limitations were postponed by up to 12 days and of nitrate limitations advanced by up to 4 days (Fig. 6.15; Tab. 6.2).

The change in phytoplankton community composition and functional groups biomass propagated upwards in the food chain. The microzooplankton total yearly biomass decreased by up to 23% with the median decrease of 10, 14 and 14% in scenarios *single*, *multiple* and *all*. Conversly, copepods total yearly biomass increased on average. However since the range of increase did not exceed 3% on average in all scenarios, and the maximal increase was lower than 5%, the increase may be considered as negligible.

Median annual copepods biomass decreased in all considered scenarios. The median value computed for all communities decreased by 4-5%, but the median biomass decrease could reach up to 10% (Tab. 6.2). Similar, yet somewhat stronger response was reported in case of microzooplankton. The median value decreased on average by 6-8%, with the maximal decrease reaching up to 16%. Copepods maximal biomass increased in all scenarios. The median value increased by 6, 16 and 17.5% in scenarios *single*, *multiple* and *all* respectively. The maximal rate of increase reported in each scenario reached 50% of the reference values. The increase in the peak intensity was accompanied by a 3-4 day shift in its occurrence. Microzooplankton biomass peak decreased on average as indicated by the 4-8% decrease in its median value and maximal decrease reaching up to 20% in all scenarios.

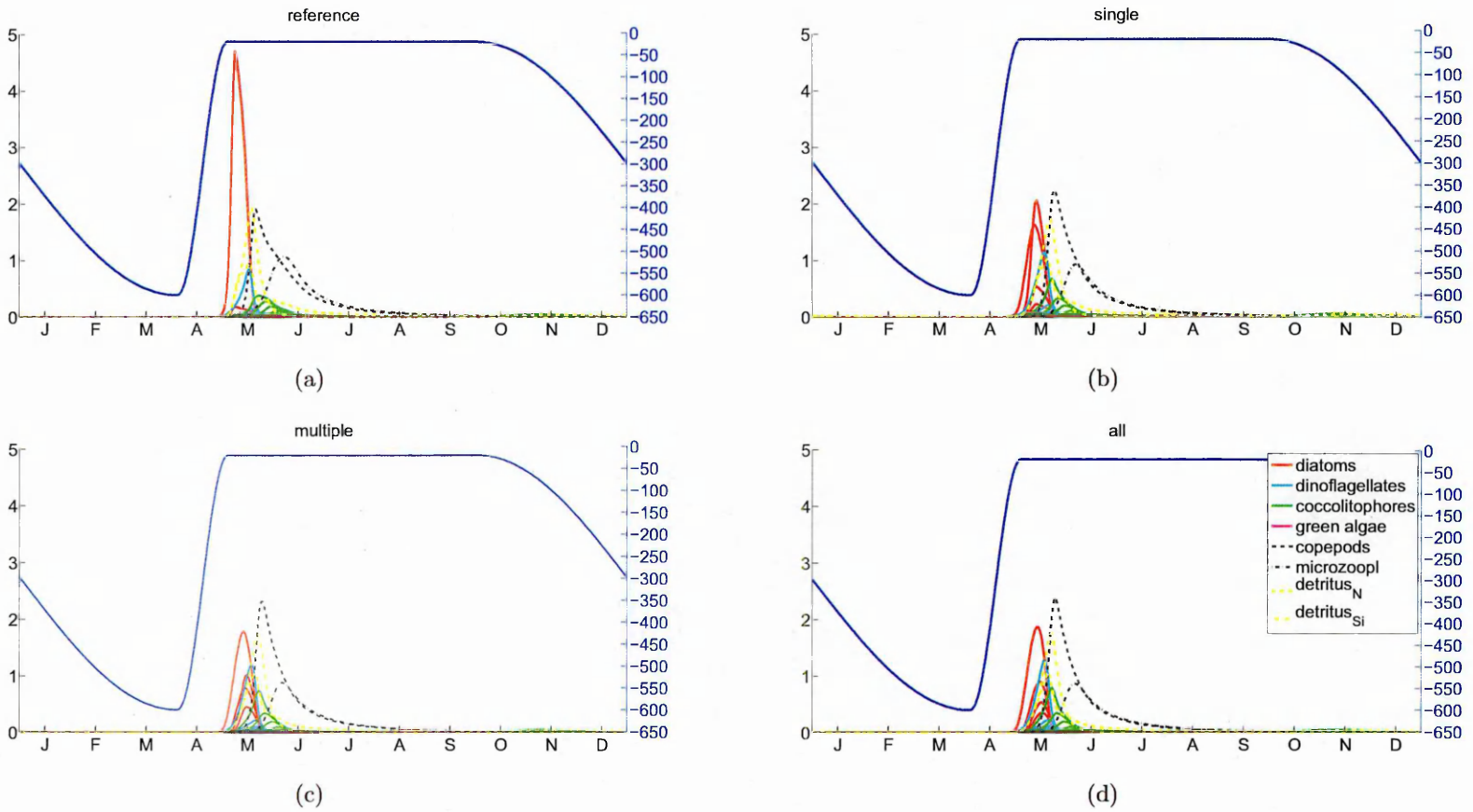

Figure 6.2: Model compartments concentrations in the (a) *reference*, (b) *single*, (c) *multiple* and (d) *all* scenario. Phytoplankton species were color-grouped according to the PFT, yet each line depicts single species concentration. In all the scenarios the last year of a simulation for the same planktonic community was depicted. Parameters used for the EGC: concentration threshold - 0.1 $[mmolC/l]$, growth rate decrease 50%)

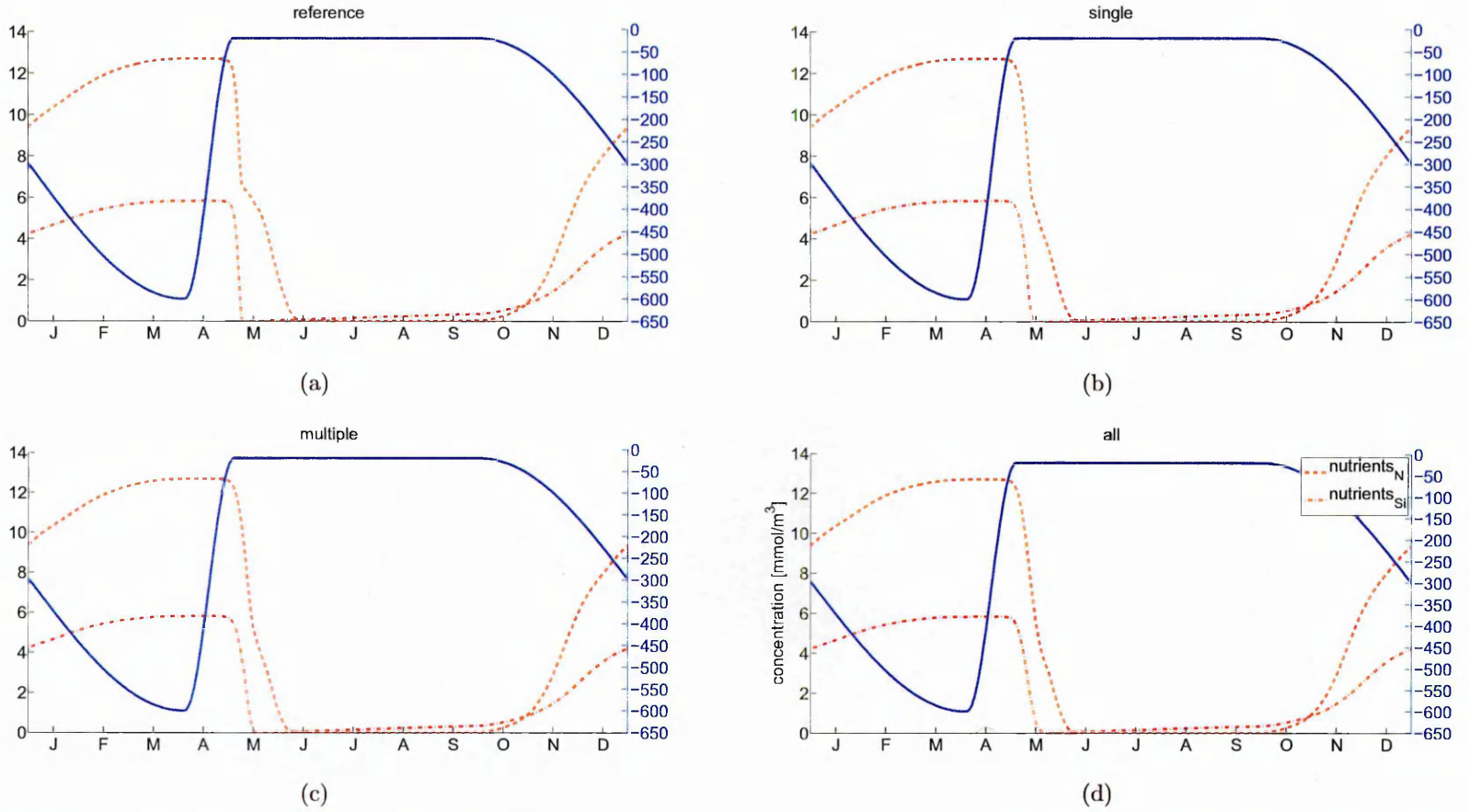

Figure 6.3: Model nutrients concentrations in the (a) *reference*, (b) *single*, (c) *multiple* and (d) *all* scenario. In all the scenarios the last year of a simulation for the same planktonic community was depicted. Parameters used for the EGC: concentration threshold - 0.1 $[mmolC/l]$, growth rate decrease 50%)

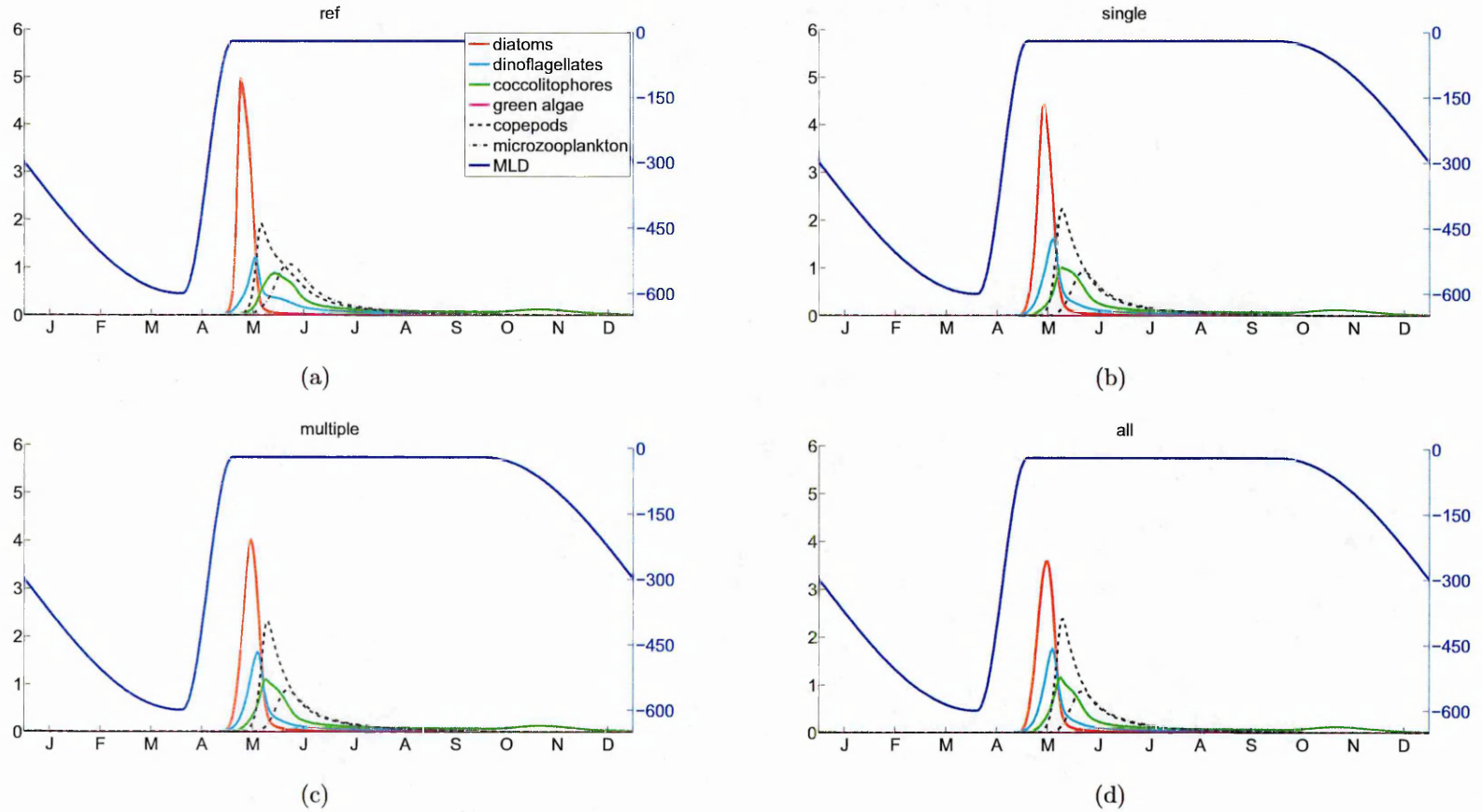

Figure 6.4: Model compartments concentrations in the (a) *reference*, (b) *single*, (c) *multiple* and (d) *all* scenario. Phytoplankton PFT were color-grouped according to the PFT, yet each line depicts single PFT concentration. In all the scenarios the last year of a simulation for the same planktonic community was depicted. Parameters used for the EGC: concentration threshold - 0.1 $[mmolC/l]$, growth rate decrease 50%)

scenario	*reference*	*single*	*multiple*	*all*
max biomass				
phytoplankton	102.18±12.79	98.61±12.73	88.43±12.05	85.65±11.51
diatoms	99.16±12.43	94.15±16.28	79.87±12.02	77.70±12.71
dinoflagellates	9.25±3.95	10.77±6.66	12.65±7.15	12.66±7.36
coccolitophores	19.73±5.99	22.30±6.80	24.41±7.23	24.31±7.23
green algae	1.74±4.33	1.12±5.08	1.01±5.69	0.97±5.75
copepods	29.71±4.32	31.09±6.92	34.09±7.13	34.17±7.22
microzooplankton	24.12±3.35	23.21±3.85	22.43±3.74	22.41±3.77
biomass peak time				
phytoplankton	128.00±15.84	130.00±16.27	133.00±16.58	133.50±16.61
diatoms	128.00±15.84	130.00±16.23	133.00±16.52	133.00±16.54
dinoflagellates	140.00±17.73	140.00±17.64	140.00±17.52	140.00±17.51
coccolitophores	152.00±18.82	151.50±18.71	151.00±18.66	150.00±18.60
green algae	159.00±19.87	158.00±19.79	158.00±19.81	158.00±19.78
copepods	140.00±17.38	143.50±17.76	144.00±17.87	143.50±17.82
microzooplankton	159.00±19.67	159.00±19.67	159.00±19.64	159.00±19.62
Median biomass	reference	single	multiple	all
phytoplankton	4.13±0.86	3.82±0.84	3.73±0.80	3.73±0.81
diatoms	0.44±0.33	0.44±0.33	0.44±0.34	0.47±0.34
dinoflagellates	1.13±0.34	1.03±0.30	0.97±0.29	0.97±0.29
coccolitophores	1.88±0.36	1.87±0.37	1.86±0.37	1.86±0.37
green algae	0.01±0.20	0.01±0.19	0.01±0.19	0.01±0.19
copepods	0.23±0.03	0.22±0.03	0.21±0.03	0.21±0.03
microzooplankton	0.27±0.04	0.25±0.03	0.24±0.03	0.24±0.03
total yearly biomass	reference	single	multiple	all
phytoplankton	3276.92±433.43	3265.94±428.93	3209.48±418.10	3196.34±417.5
diatoms	1151.75±239.17	1149.24±244.26	1105.43±224.65	1090.41±227.7
dinoflagellates	569.63±169.36	533.43±172.27	519.59±176.46	520.28±176.5(
coccolitophores	1307.30±277.18	1316.60±290.60	1329.36±297.43	1328.84±298.3
green algae	43.92±170.82	26.10±179.26	24.14±187.99	23.52±188.58
copepods	1064.13±132.72	1074.41±135.75	1091.96±138.58	1092.59±138.8
microzooplankton	846.41±110.63	754.72±108.37	732.00±100.96	728.49±101.2
maximal concentration				
phytoplankton	4.18 ± 0.27	4.05 ± 0.30	4.05 ± 0.30	3.29 ± 0.43
diatoms	4.09 ± 0.21	3.91 ± 0.31	3.91 ± 0.31	3.17 ± 0.26
dinoflagellates	1.16 ± 0.28	0.16 ± 0.05	0.16 ± 0.05	0.16 ± 0.05
coccolitophores	0.40 ± 0.03	1.45 ± 0.24	1.45 ± 0.24	1.42 ± 0.22
green algae	0.05 ± 0.05	0.11 ± 0.11	0.11 ± 0.11	0.12 ± 0.12
resources depletion time				
NO3 median	161.00±1.43	159.00±1.56	158.00±1.40	158.00±1.47
SiO2 median	128.00±4.59	131.50±5.36	135.00±4.31	136.00±4.64

Table 6.2: Phytoplankton (P) and zooplankton (Z) biomass ($[mmolC]$) in different ecological scenarios.

6.3.1.2 Change in the species diversity and community composition

This new phytoplankton biomass distribution pattern was accompanied by a change of the diversity at the level of the species and of functional groups (Fig. 6.2).

The diatoms community in the reference scenario was composed out of the species characterised with a high intrinsic growth rate ($\mu > 1.4$ Fig. 6.5a). The surviving species varied in terms of their physiological fingerprint and, consequently, in terms of the maximal concentration reached during the vegetative season (Fig. 6.5a). It was assumed in this study that the EGC mechanism was activate at a certain concentration threshold equal to 0.1 $[mmolC/m^3]$, thus only species able to reach concentrations exceeding it were considered to undergo sexual reproduction in the scenarios *single* and *multiple*. All diatoms species were considered to undergo sexual reproduction in the scenario *all*.

The EGC caused a decrease of the growth rate of the selected species when their concentration exceeds a specified threshold. That resulted in a decrease of the biomass accumulation rate and lower nutrients consumption rate, hence in the relaxation of the species' competitive interactions. The physiological characteristics of the diatoms species surviving in the ecosystem were altered, i.e. species characterised with growth rate higher than 0.8 ($0.8 \leq \mu \leq 1.4$) were able to withstand the competition in the scenarios addressing the EGC while the same species were competitively excluded in the reference case (Fig. 3.13). The maximal annual concentration of the species affected by the EGC decreased as a result of the EGC activation, and the maximal concentration of the remaining species increased in al considered scenarios. The number of species which could be characterised as rare based on their maximal concentration reached during the vegetative season increased considerably (e.g., Fig. 6.5d). The number of co-existing species increased in the scenarios *single* (Fig. 6.5b), *multiple* (Fig. 6.5c) and *all* (Fig. 6.5d) with respect to the *reference* case (Fig. 6.5a).

The introduction of the EGC mechanism into the description of diatoms affected indirectly also other phytoplankton functional types, e.g. change in their seasonal abundance or diversity described above. However, the physiological characteristics allowing dinoflagellates (Fig. 6.6), coccolitophores (Fig. 6.7) or green algae (Fig. 6.8) to survive in the virtual ecosystem did not change with respect to the characteristics

reported in the reference scenario. The concentration of the species in the ecosystem altered as a result of the change in the competitive interactions at the species but also PFTs level and the change in the grazing pressure. In particular, the median maximal concentration of green algae increased by two folds with respect to the *reference* scenario, as well as the median maximal concentration of the coccolitophores by more than 3 folds (Tab. 6.2). Conversely, the median maximal concentration of the diatoms and dinoflagellates decreased in the scenarios addressing EGC.

The restructuring of the community was observed also at the species level within the resolved PFTs. In particular, the maximal concentration reached by coccolitophores characterised with a $\mu \geq 1.1$ and $H_N \geq 0.2$ increased considerably (Fig. 6.7), and new species emerged in the diatoms group (Fig. 6.5).

In order to explain the observed increase in the diatoms species diversity it is necessary to investigate the bottom-up and top-down processes regulating species dynamics. The growth of some of the diatoms species, those which description incorporates the EGC mechanism, is decreased above a specified concentration threshold which results in a decrease of the nutrients drawdown rate. This in turn affects the temporal availability of resources and causes a delay in the occurence of the resources depletion (Tab. 6.2). The relaxation of the inter-specific species competition for resources allow some new diatoms' species to emerge (Fig. 6.5). These species emerge simultaneously with other diatoms shortly after water column restratification, hence in the period when the per capita grazing pressure is relatively low. Notably, the increase of diatoms diversity occurred in spite of the observed increase in the copepods maximal and total annual biomass in the scenarios *single, multiple* and *all* (Tab. 6.2).

Concentration based species diversity changed in a similar fashion in all explored EGC scenarios. The median species richness based on species maximal concentration decreased by 3 in *single* and *multiple*, and by 2 in the scenario *all* scenarios with respect to the reference scenario (Fig. 6.10a). The median value of the biomass based diversity remained almost at the same level in all scenarios, though the distribution of observed values was narrower in the scenarios *simple*, *multiple* and *all* with respect to the reference case (Fig. 6.9a). The change in the species richness was strongly driven by the initial community composition. This statement is supported by the observed rate

of diversity change across all ensemble members. Namely, species richness could either decrease by 1 or increase by up to 3-4 species, and such changes were observed both in the concentration and biomass based richness (Fig. 6.10 and 6.9). The introduction of EGC into a single, multiple or all diatom species physiological characteristics resulted, on average, in 1 or 2 additional diatoms species able to withstand competition in the virtual ecosystem in case of concentration (Fig. 6.10b) and biomass (Fig. 6.9b) based indices of diversity. The coccolitophores and green algae richness based on maximal concentration increased by 1 species in numerous communities in scenarios *single*, *multiple* and *all* (Fig. 6.10d, 6.10e), while the value of the index based on median species' biomass decreased in case of coccolitophores by 1 (Fig. 6.9d) and remained unchanged in case of green algae (Fig. 6.9e). The concentration and biomass based diversity of dinoflagellates decreased by up to 4 and 1 species respectively in all explored scenarios in the vast majority of communities (Fig. 6.10c, 6.9c).

The community composition in the scenarios addressing EGC was altered with respect to the *reference* case with some species undergoing extinction and some new species emerging (Fig. 6.11, 6.12, 6.13). The newly emerging diatoms species in the scenarios *single, multiple* and *all* were physiologically similar to the diatoms species observed in the *reference* scenario, though the range of physiological parameters was broader, i.e. the growth rate of some of the emerging species spanned from 0.8 to 2.9, and nutrients half-saturation spanning from 0.9 to 2.05 (Fig. 6.11). Notably, none of the diatoms species underwent extinction in the scenarios exploring EGC (Fig. 6.11a, 6.12a, 6.13a). Thus, specifically, none of the diatoms reproducing sexually underwent extinction despite the temporal decrease of the growth rate attributed to the EGC formulation and the presence of the other competitors representing all PFTs. The analysis of the concentration and biomass based diversity indices revealed that the extinction affected a large part of the dinoflagellates, while only few new species emerged (Fig. 6.11b, 6.12b, 6.13b) which resulted in an overall decrease in the diversity within this functional group. The biomass based diversity of coccolitophores decreased as well and most of the species undergoing extinction were characterised by a growth rate $\mu \leq 1.1$ and nutrients half-saturation $H_N \leq 0.2$. Conversely, the concentration based diversity increased in the scenarios investigating EGC and most of the emerging species were

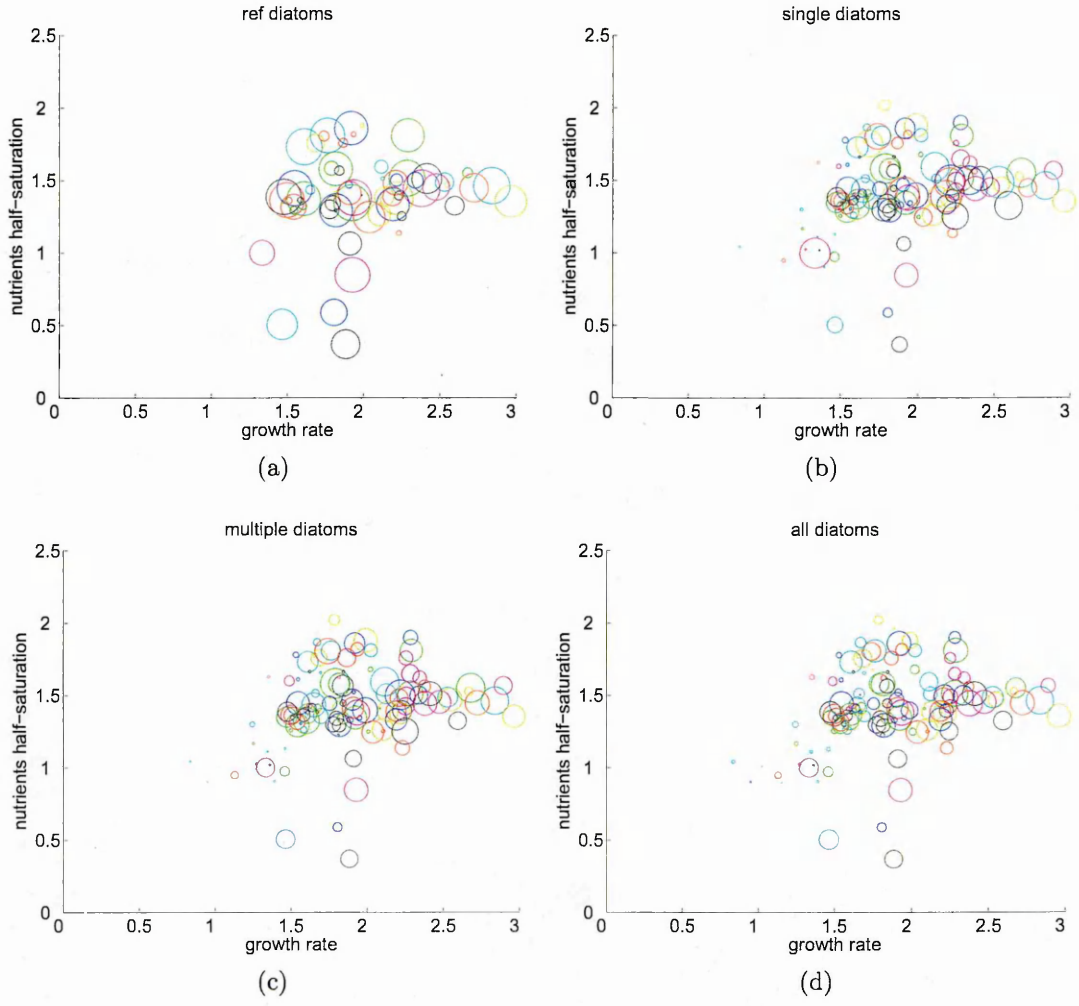

Figure 6.5: Traits distribution of the surviving diatoms species in the scenarios considering the endogenous growth control: (a) *reference*, (b) *single*, (c) *multiple* and (d) *all* case. Each circle depicts a single phytoplankton species. The size of the circle is proportional to the maximal concentration of the species reached during the year. The plot illustrates the characteristics of the species from all 30 ensemble communities, where the communities were distinguished by colours. The axis represents nitrate half-saturation constant and intrinsic growth rate.

characterised by a growth rate $\mu \geq 1.1$ and nutrients half-saturation $H_N \geq 0.2$ (Fig. 6.11c, 6.12c, 6.13c). Amongst the green algae a similar number of species undergoing extinction and emerging was observed which resulted in only a slight increase of concentration based diversity and almost unchanged biomass based diversity (Fig. 6.11d, 6.12d, 6.13d). Additional analysis are required in order to characterise the physiological properties of the species undergoing extinction and emerging, and are planned as a continuation of this study.

The survival success of the species reproducing sexually has been investigated in the Section 6.3.2. In particular, it has been tested if the species undergoing sexual re-

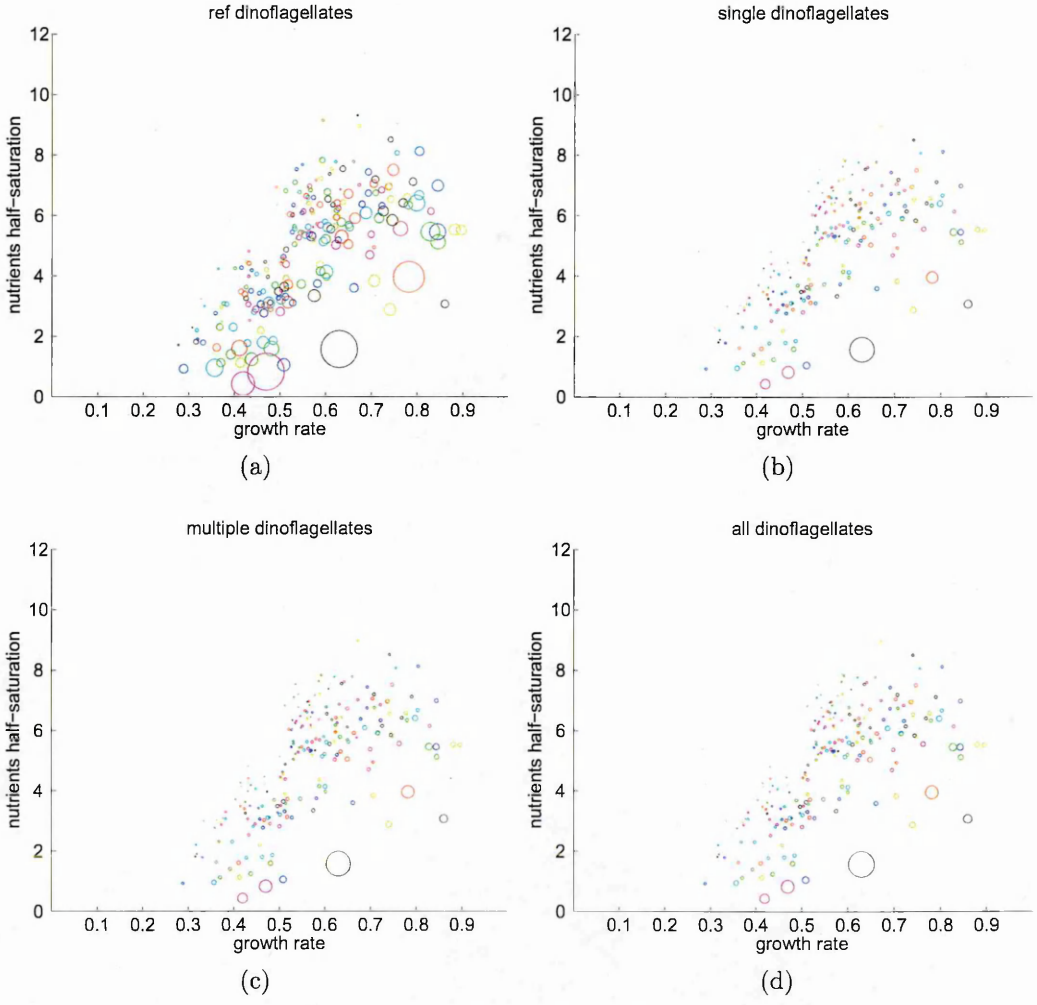

Figure 6.6: Traits distribution of the surviving dinoflagellates species in the scenarios considering the endogenous growth control: (a) *reference*, (b) *single*, (c) *multiple* and (d) *all* case. Each circle depicts a single phytoplankton species. The size of the circle is proportional to the maximal concentration of the species reached during the year. The plot illustrates the characteristics of the species from all 30 ensemble communities, where the communities were distinguished by colours. The axis represents nitrate half-saturation constant and intrinsic growth rate.

production were able to survive in the presence of the strains of the same species which did not reduce their growth rate (i.e. were reproducing asexually). The obtained results demonstrated that, in the considered framework, the species reproducing sexually would not be eliminated by the strains reproducing asexually as long as the growth rate reduction does not exceed 20-40% of the growth rate value for the fast growing species and 40-60% for the slow growing species (Fig. 6.18a). Furthermore, it has been demonstrated that, in the considered framework, diatoms species reproducing sexually and characterised by the growth rate higher than 1.6 would not be eliminated either by the strains of the same species reproducing asexually or by the other species

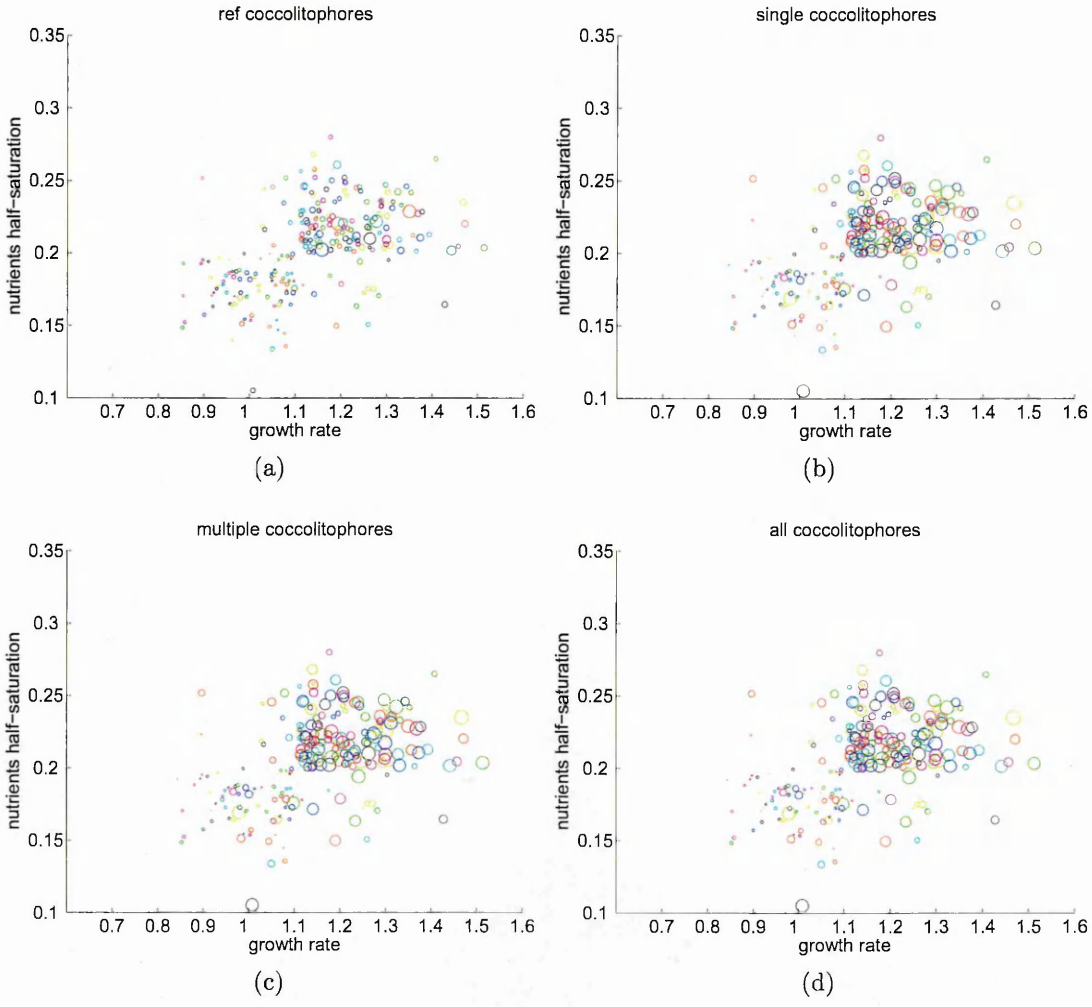

Figure 6.7: Traits distribution of the surviving coccolitophores species in the scenarios considering the endogenous growth control: (a) *reference*, (b) *single*, (c) *multiple* and (d) *all* case. Each circle depicts a single phytoplankton species. The size of the circle is proportional to the maximal concentration of the species reached during the year. The plot illustrates the characteristics of the species from all 30 ensemble communities, where the communities were distinguished by colours. The axis represents nitrate half-saturation constant and intrinsic growth rate.

reproducing asexually present in the ecosystem as long as the growth rate reduction does not exceed 20-30% for the species with $2.0 \leq \mu$ and 40-80% for the species with $1.6 \leq \mu \leq 2.0$ (Fig. 6.18b). Clearly not all the species undergoing sexual reproduction were able to survive in the virtual ecosystem where their extinction would be related either (or both) to the presence of the other diatoms being competitively superior (e.g. with higher growth rate and lower nutrients half-saturation) or to the presence of the mutants of the same species reproducing asexually which could evolve in time (Fig. 6.18).

In light of the above it is reasonable to argue that the elevated number of sur-

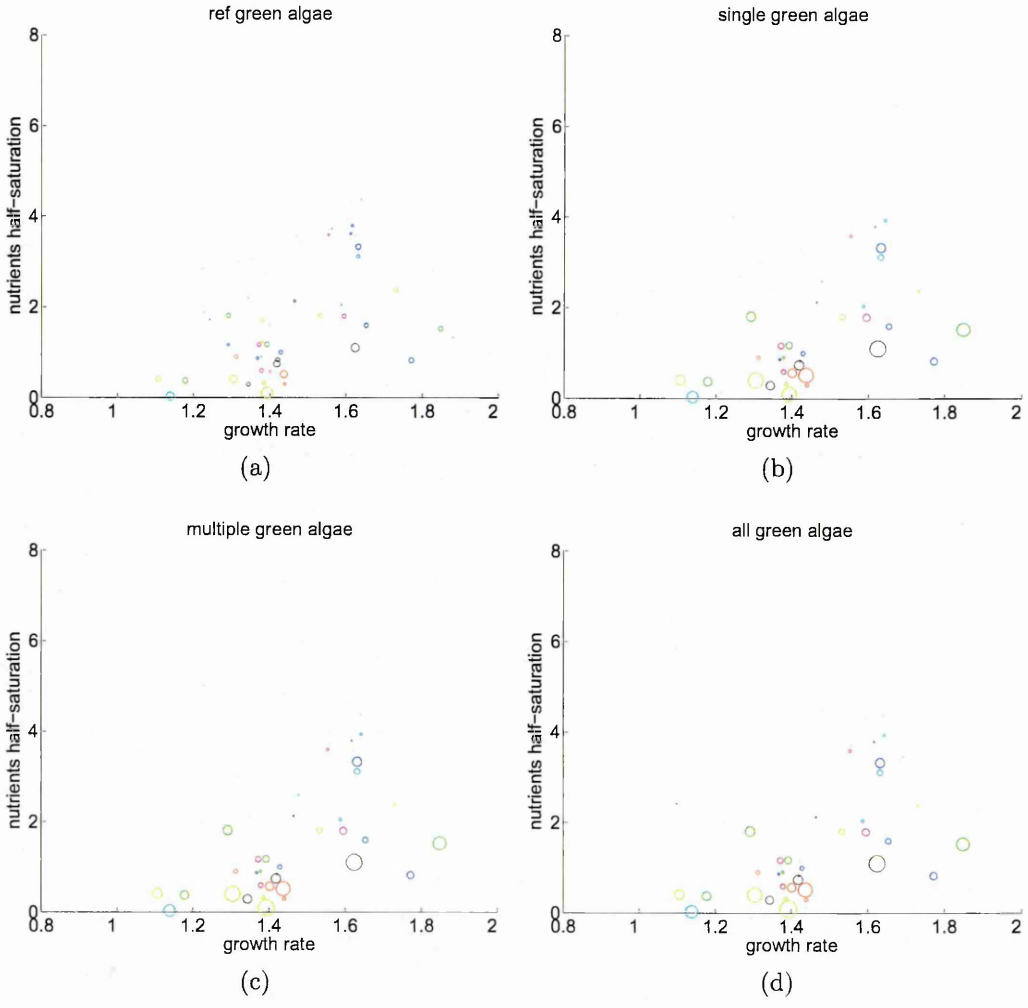

Figure 6.8: Traits distribution of the surviving green algae species in the scenarios considering the endogenous growth control: (a) *reference*, (b) *single*, (c) *multiple* and (d) *all* case. Each circle depicts a single phytoplankton species. The size of the circle is proportional to the maximal concentration of the species reached during the year. The plot illustrates the characteristics of the species from all 30 ensemble communities, where the communities were distinguished by colours. The axis represents nitrate half-saturation constant and intrinsic growth rate.

viving diatoms observed in the scenarios investigating EGC is directly related to the temporal relaxation of the species competitive interactions originating from the sexual reproduction and the growth rate reduction of some of the diatoms species, and not to the selection of the species they competed against i.e. only slow growing species.

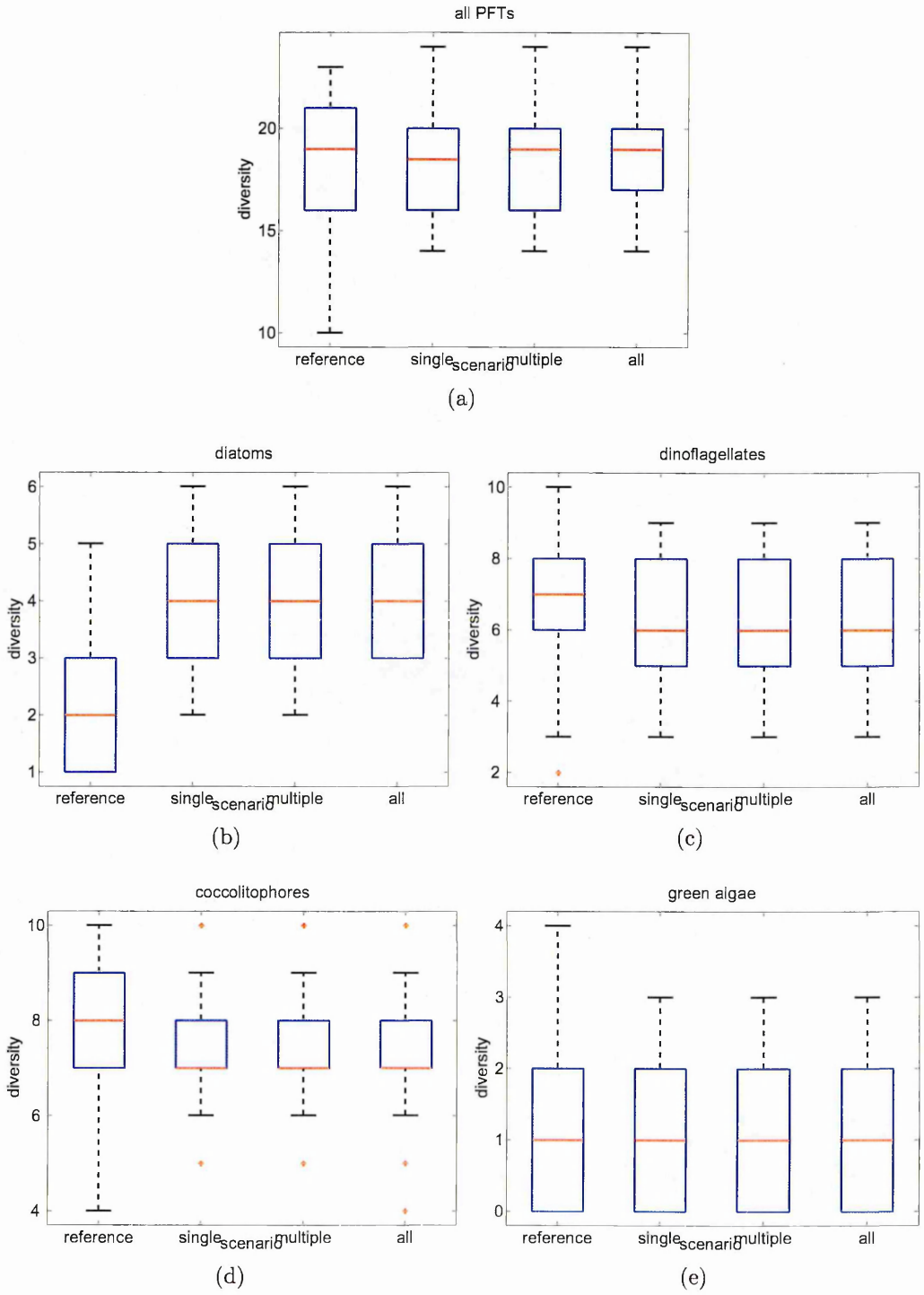

Figure 6.9: Biomass based species diversity in the scenarios exploring effects of EGC: (a) all PFTs, (b) diatoms, (c) dinoflagellates, (d) coccolitophores and (e) green algae.

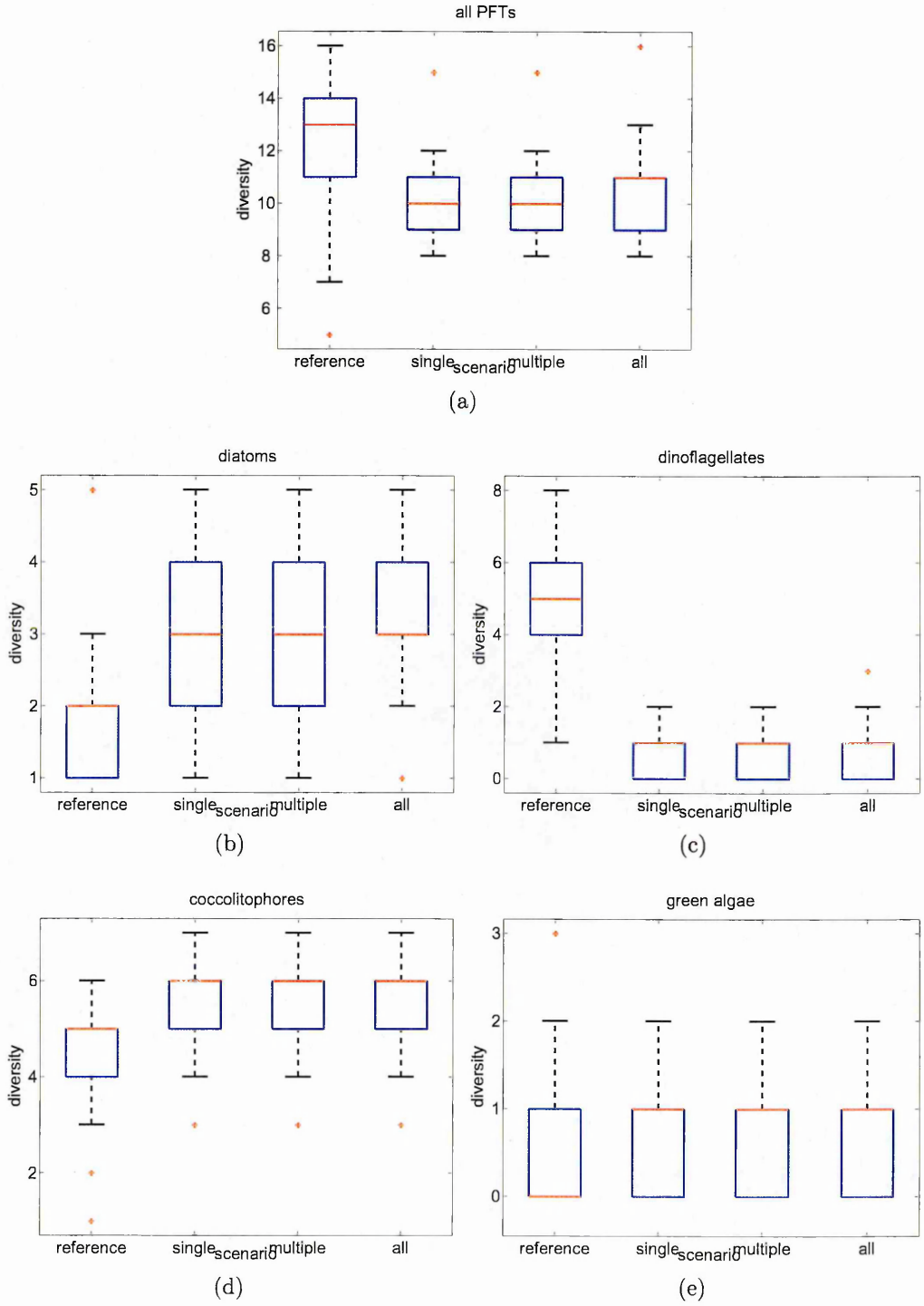

Figure 6.10: Concentration based species diversity in the scenarios exploring effects of EGC: (a) all PFTs, (b) diatoms, (c) dinoflagellates, (d) coccolitophores and (e) green algae.

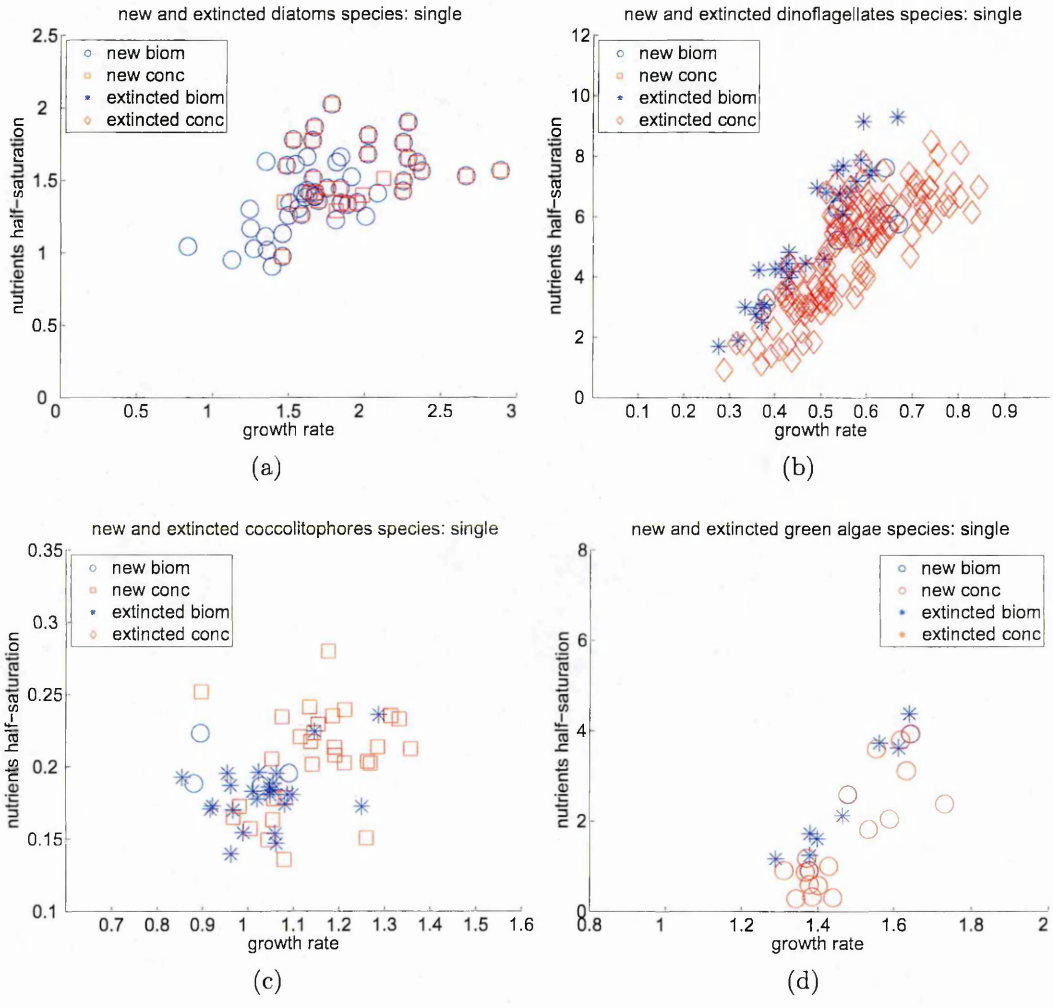

Figure 6.11: Species undergoing extinction and emerging in the *single* EGC scenario with respect to the *reference* case: (a) diatoms, (b) dinoflagellates, (c) coccolitophores and (d) green algae. The presented markers illustrate to the newly emerging species (based on the biomass *new biom* or concentration *new conc*) criterion) and the species competitively excluded (based on the biomass *extincted biom* or concentration *extincted conc*) criterion) with respect to the *reference* scenario.

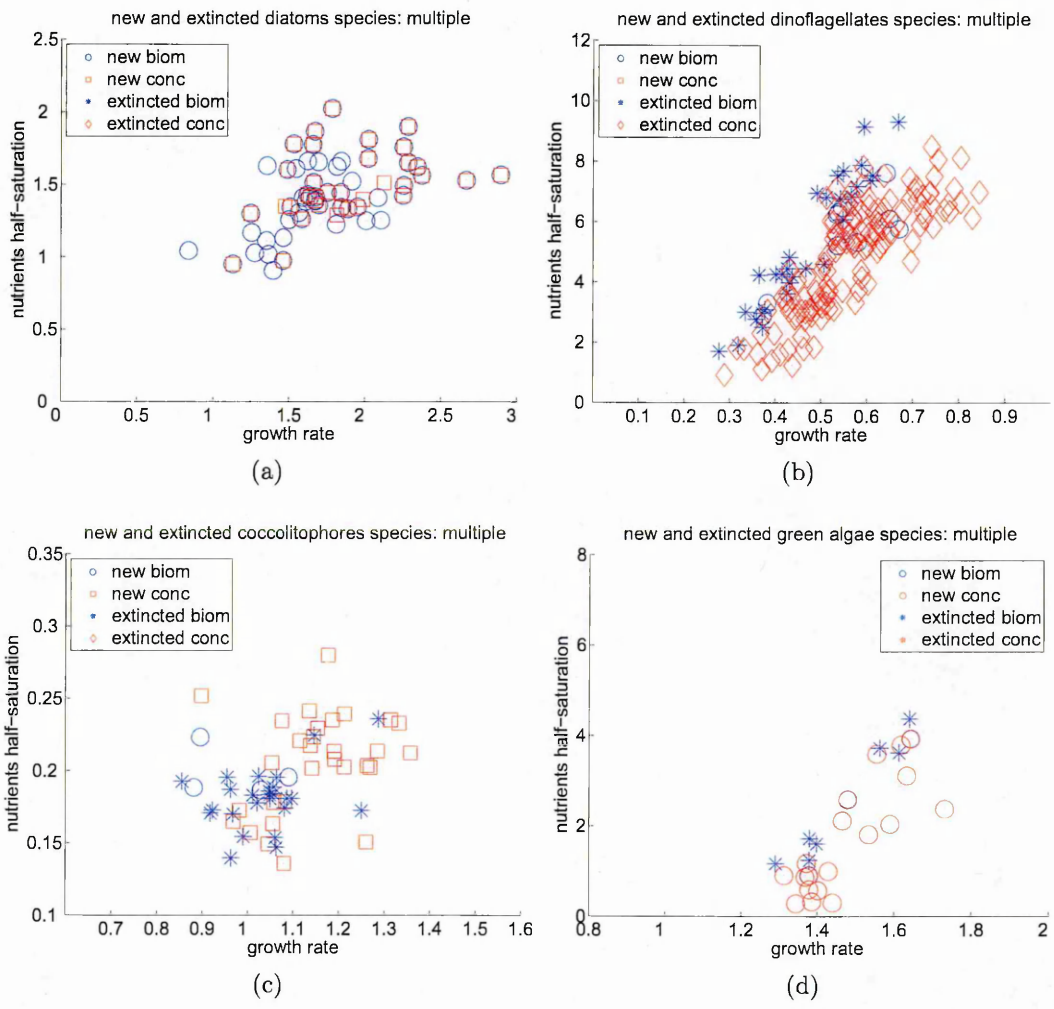

Figure 6.12: Species undergoing extinction and emerging in the *multiple* EGC scenario with respect to the *reference* case: (a) diatoms, (b) dinoflagellates, (c) coccolitophores and (d) green algae. The presented markers illustrate to the newly emerging species (based on the biomass *new biom* or concentration *new conc*) criterion) and the species competitively excluded (based on the biomass *extincted biom* or concentration *extincted conc*) criterion) with respect to the *reference* scenario.

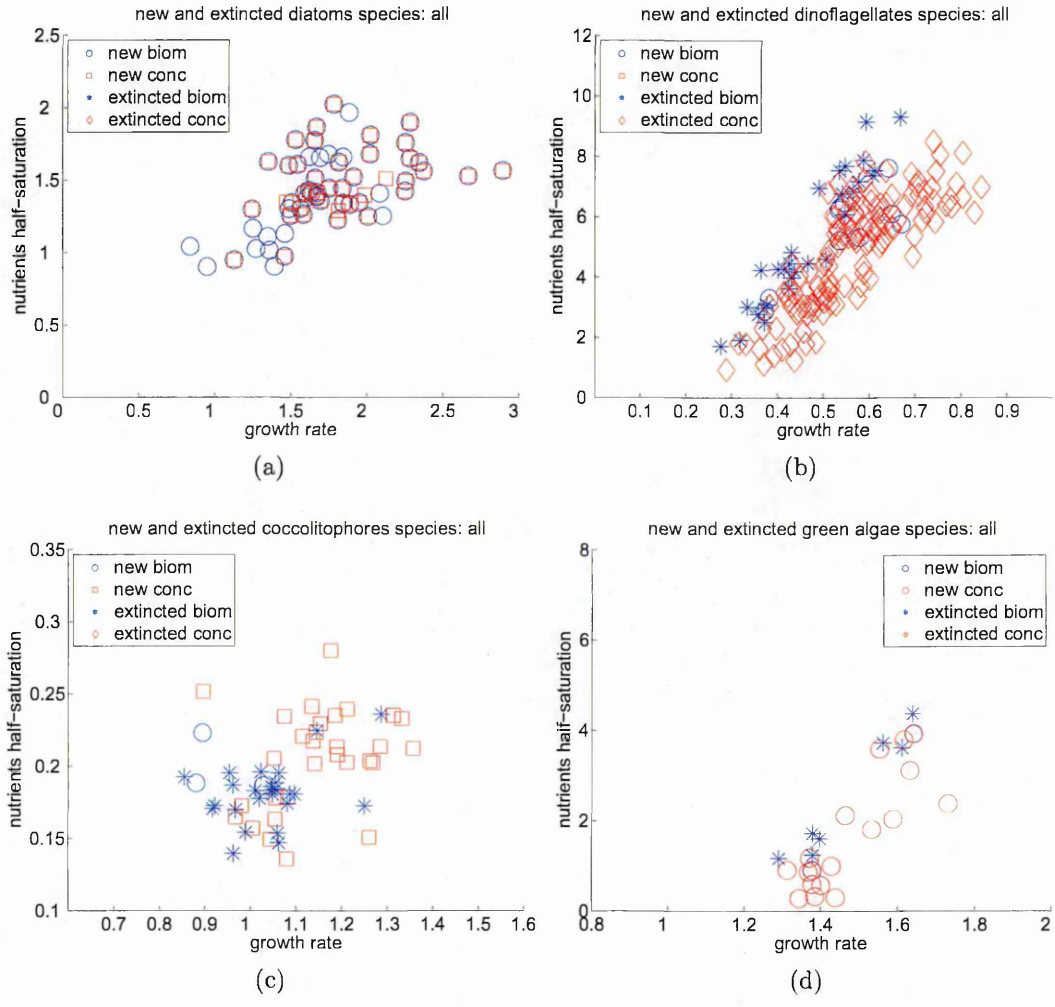

Figure 6.13: Species undergoing extinction and emerging in the *all* EGC scenario with respect to the *reference* case: (a) diatoms, (b) dinoflagellates, (c) coccolitophores and (d) green algae. The presented markers illustrate to the newly emerging species (based on the biomass *new biom* or concentration *new conc*) criterion) and the species competitively excluded (based on the biomass *extincted biom* or concentration *extincted conc*) criterion) with respect to the *reference* scenario.

6.3.1.3 Comparison with the NABE data

As indicated in the 2nd chapter, the *in situ* data originating from the North Atlantic Bloom Experiment (NABE) form an excellent base for a qualitative and quantitative estimate of model's ability to reproduce phytoplankton dynamics, in particular spring bloom formation, with the focus on mechanisms such as net primary production (NPP), nutrients consumption and phytoplankton accumulation (via chlorophyll-a concentration).

A quantitative approach based on assessment of normalized standard deviation (σ^*), correlation coefficient (R) and root-mean-square difference ($RMSD$) of appropriate model variables and the available observations was provided to evaluate model performance. Because of the ensemble approach, the appropriate indicators were computed for each ensemble member.

The augmented version of the model show better correlation with NABE *in situ* measurements of chlorophyll-a (by 26, 44 and 45%; Tab. 6.3; Fig. 6.14), net primary production (by 40, 65 and 65%; Tab. 6.3; Fig. 6.17) and particulated organic nitrogen (by 30, 63 and 66%; Tab. 6.3; Fig. 6.16) in scenarios *single, multiple* and *all* respectively. A slight decrease, by 1 and 8%, in the correlation coefficient of surface nitrate and silicate with model results was reported in considered scenarios (Tab. 6.3; Fig. 6.15). The shift in silicate consumption was further illustrated by a decrease in the normalised standard deviation - in here its lower value indicates lower uptake rate due to EGC activation.

A considerable decrease in the median R value was observed for net primary production, namely its value decreased from 1.4 in the *reference* scenario to 1.21, 1.15 and 1.12 in the *single, multiple* and *all* respectively (Tab. 6.4). This implies that the NPP standard deviation in the model with life cycle related traits was more similar to that of the *in situ* measurements (Fig. 6.17). In a similar fashion the median R values decreased in case of chlorophyll and PON (Tab. 6.4). These changes however indicated somewhat narrower spread of model values with respect to the observations (Fig. 6.14, 6.16).

The $RMSD$ median values remained at a comparable level in all scenarios for all explored indicators (Tab. 6.5).

Overall, the introduction of a sexual phase in the model increased species diversity and increased the correlation between the model data and the *in situ* North Atlantic Bloom Experiment observation. Clearly, the presented results may alter with respect to the concentration threshold used for the EGC definition. Hence, a sensitivity to the threshold value should be investigated in the continuation of this study.

Nevertheless, the data regarding the diatoms sexual reproduction in the open ocean are still scarce. Thus a skill assessment of a model which construction incorporates diatoms sexual reproduction should be approached with caution. Clearly the reliability of the parameterisation should be thoroughly investigated and a robust sensitivity analysis ought to be undertaken in order to address all the uncertainties related to this still poorly understood process. At this point it is impossible to state whether or not the model construction has been improved by considering diatoms sexual reproduction. Empirically (i.e. by comparison with the data), one cannot make the case that either model version is better than the other. It has been however illustrated that diatoms life cycles may have a profound impact on species diversity and ecosystem functioning, and hence should be a subject to future studies.

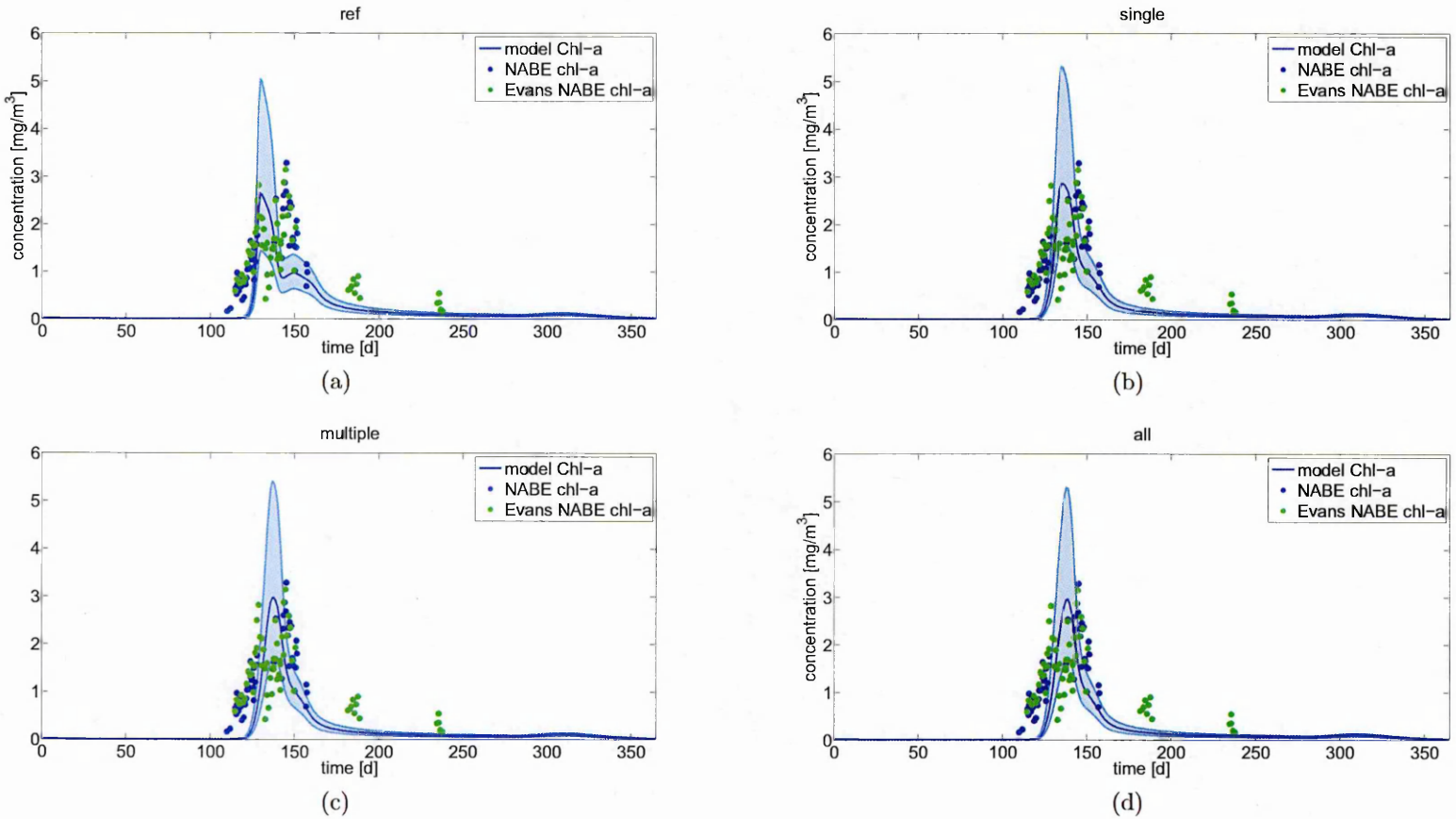

Figure 6.14: Model chlorophyll-a concentrations in the (a) *reference*, (b) *single*, (c) *multiple* and (d) *all* scenario. Chlorophyll-a concentration was calculated with a carbon-to-chlorophyll ratios (Sathyendranath et al. [2009], and the shaded area depicts the chlorophyll concentration based on min and max ratio values. In all the scenarios the last year of a simulation for the same planktonic community was depicted. Parameters used for the EGC: concentration threshold - 0.1 $[mmolC/l]$, growth rate decrease 50%)

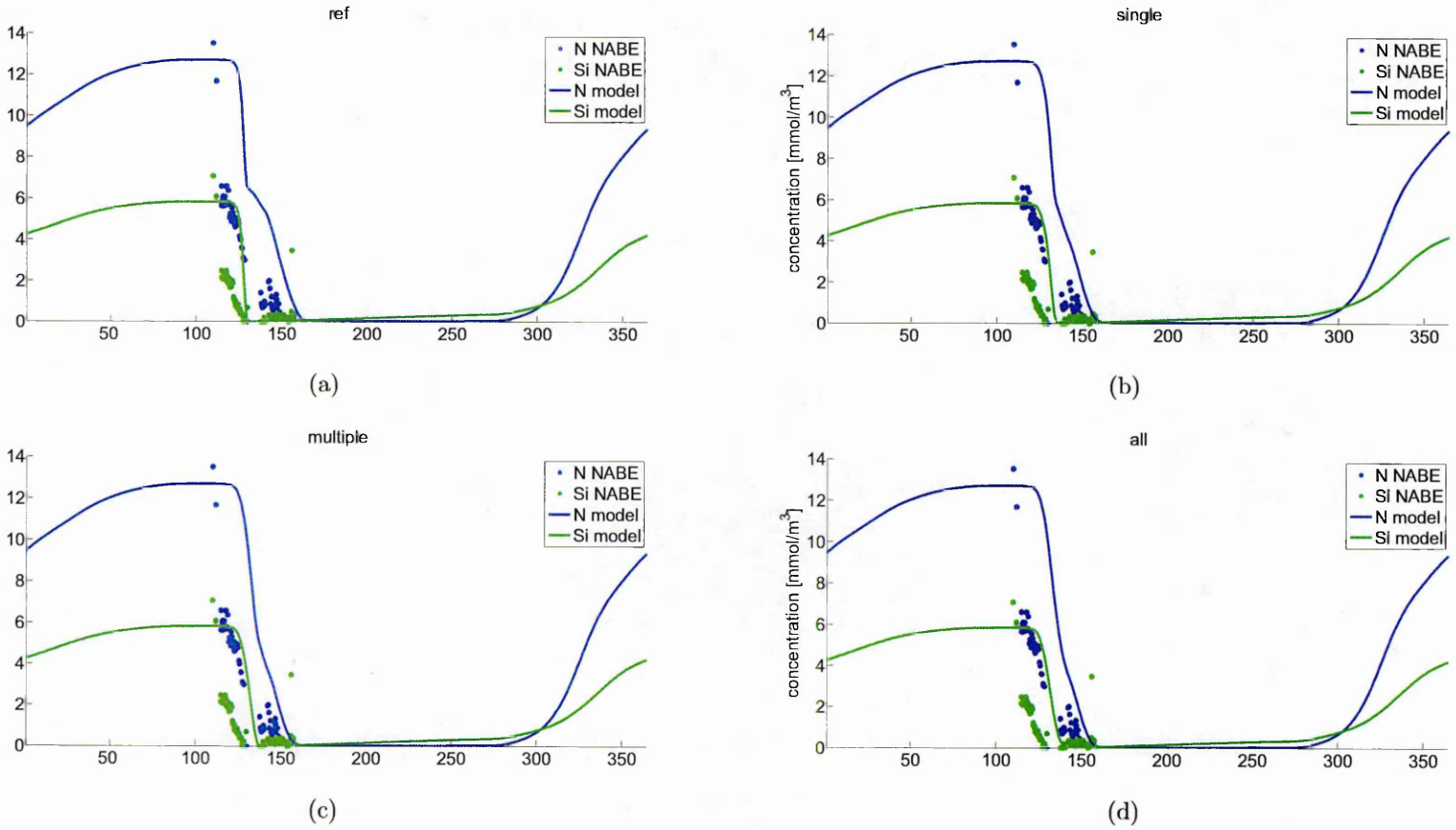

Figure 6.15: Model nutrients concentrations in the (a) *reference*, (b) *single*, (c) *multiple* and (d) *all* scenario. In all the scenarios the last year of a simulation for the same planktonic community was depicted. Parameters used for the EGC: concentration threshold - 0.1 $[mmolC/l]$, growth rate decrease 50%)

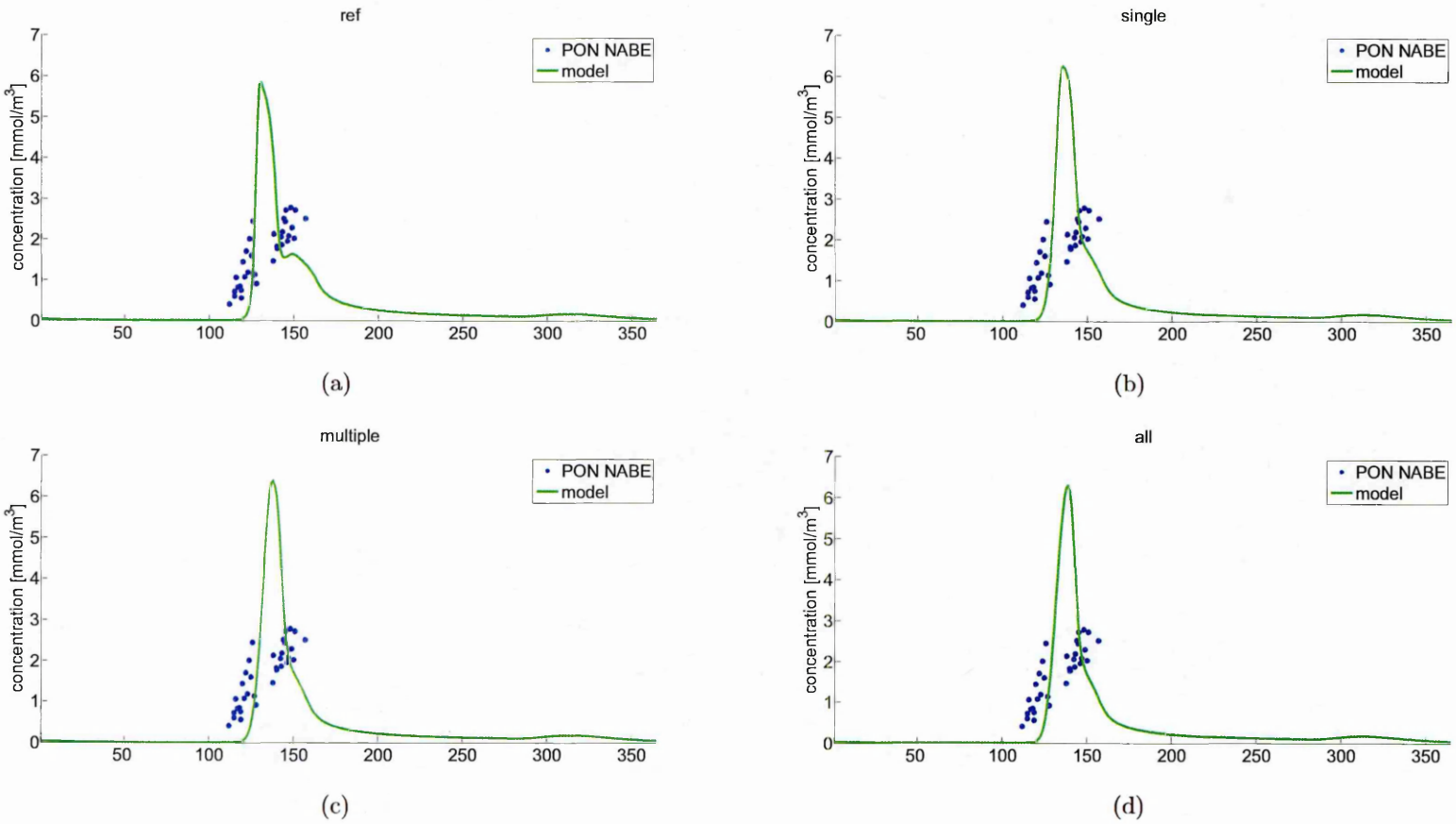

Figure 6.16: Phytoplankton functional types concentrations in the (a) *reference*, (b) *single*, (c) *multiple* and (d) *all* scenario. In all the scenarios the last year of a simulation for the same planktonic community was depicted. Parameters used for the EGC: concentration threshold - 0.1 $[mmolC/l]$, growth rate decrease 50%)

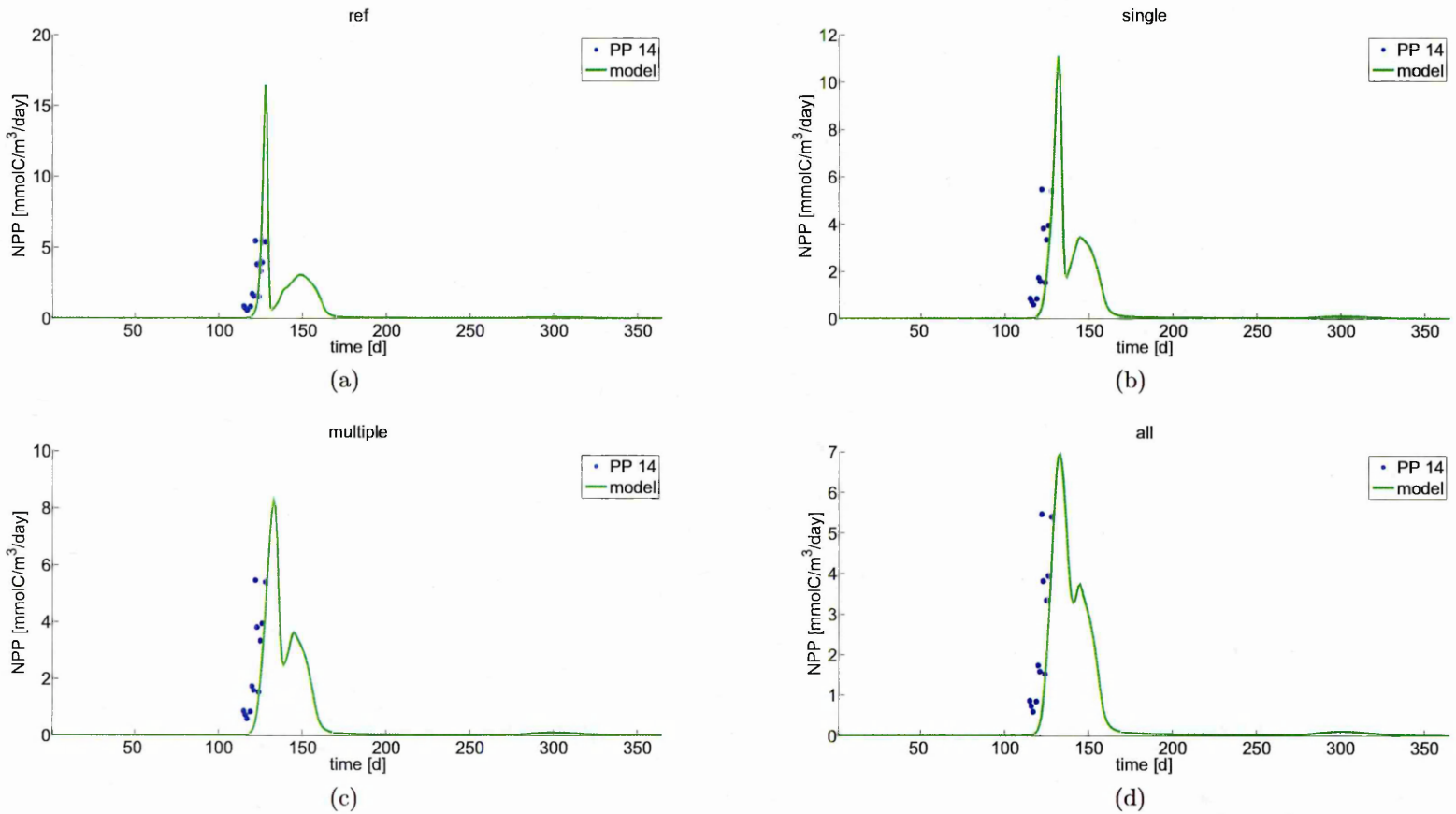

Figure 6.17: Model net primary production concentrations in the (a) *reference*, (b) *single*, (c) *multiple* and (d) *all* scenario. In all the scenarios the last year of a simulation for the same planktonic community was depicted. Parameters used for the EGC: concentration threshold - 0.1 [$mmolC/l$], growth rate decrease 50%). Note different Y-axis scale.

Table 6.3: Correlation of model compartments and North Atlantic Bloom Experiments *in situ* measurements. The values illustrate median correlation of all ensemble communities and the median absolute deviation.

scenario	Chl-a	NO3	SiO2	NPP	PON
ref	0.49 ± 0.09	0.87 ± 0.01	0.72 ± 0.05	0.44 ± 0.14	0.34 ± 0.07
single	0.65 ± 0.09	0.86 ± 0.02	0.69 ± 0.07	0.68 ± 0.10	0.46 ± 0.07
multiple	0.70 ± 0.07	0.86 ± 0.02	0.66 ± 0.06	0.70 ± 0.03	0.56 ± 0.06
all	0.70 ± 0.07	0.86 ± 0.02	0.66 ± 0.06	0.70 ± 0.03	0.56 ± 0.06

Table 6.4: Normalised standard deviation of model compartments and North Atlantic Bloom Experiments *in situ* measurements. The values illustrate median normalised standard deviation of all ensemble communities and the median absolute deviation.

scenario	Chl-a	NO3	SiO2	NPP	PON
ref	0.92 ± 0.09	0.38 ± 0.04	1.01 ± 0.10	1.40 ± 0.24	0.97 ± 0.06
single	0.86 ± 0.13	0.40 ± 0.05	0.92 ± 0.09	1.21 ± 0.23	0.90 ± 0.11
multiple	0.86 ± 0.15	0.41 ± 0.06	0.87 ± 0.05	1.14 ± 0.22	0.87 ± 0.15
all	0.86 ± 0.15	0.41 ± 0.06	0.86 ± 0.05	1.11 ± 0.22	0.87 ± 0.15

Table 6.5: Normalised root-mean square distance (RMSD) of model compartments and North Atlantic Bloom Experiments *in situ* measurements. The values illustrate median RMSD of all ensemble communities and the median absolute deviation.

scenario	Chl-a	NO3	SiO2	NPP	PON
ref	0.29 ± 0.03	0.42 ± 0.04	0.37 ± 0.05	0.32 ± 0.06	0.25 ± 0.03
single	0.28 ± 0.03	0.44 ± 0.04	0.39 ± 0.06	0.31 ± 0.06	0.26 ± 0.03
multiple	0.27 ± 0.03	0.44 ± 0.03	0.41 ± 0.05	0.30 ± 0.05	0.26 ± 0.03
all	0.27 ± 0.03	0.44 ± 0.03	0.41 ± 0.05	0.30 ± 0.05	0.26 ± 0.03

6.3.2 Linking diatom's sexual reproduction and its ecological niche.

As illustrated in section 6.2.2, sexual reproduction imposes previously overlooked constrains on the species fitness (here intended as long term organism's ability to survive and reproduce in a particular environment), since the physiological change that occurs during the sexual phase perturbs two paradigmatic terms of competitive ability, the growth rate and the nutrient assimilation rates, with the aggravating effect of giving space to other species.

Implications of this feature on the persistence of diatoms on long time scales were investigated in here by adopting an evolutionary invasibility approach (Smith [1982]). Specifically mutants, strains having various degrees of EGC, were added to numerical ecosystems at equilibrium and evaluated the rate of survival on long time scales (Section 6.2.2). The effect of growth rate reductions ranging from 10 to 100% in the absence of other phytoplankton species with a $0.25[mmolC/m^3]$ threshold value in abundance to undergo successful sexual reproduction were explored.

The analysis of a scenario with a single diatom species represented by multiple strains in an ecosystem where no other phytoplankton species were present, revealed a negative correlation between the species intrinsic growth rate and the possible maximal rate of the growth rate decrease imposed by the biological trait at which strains did not undergo extinction. Namely, the species with the lowest growth rates were capable of up to 60% growth rate reduction without being competitively excluded by strains not reducing their growth rate after mating. On a contrary, species with highest growth rate were able to reduce their growth rate only by up to 20% (Fig. 6.18a).

Similar relationship was observed in a system where additional phytoplankton species were coexisting with the test species. In particular, species with the highest growth rate could afford a 20% growth rate reduction without being competitively excluded, while species with intermediated growth rate could decrease their growth rate by up to 70%, thus 20% more than in the system without other phytoplankton species. Notably, only diatoms which growth rate higher $\mu = 1.7[d^{-1}]$ were able to

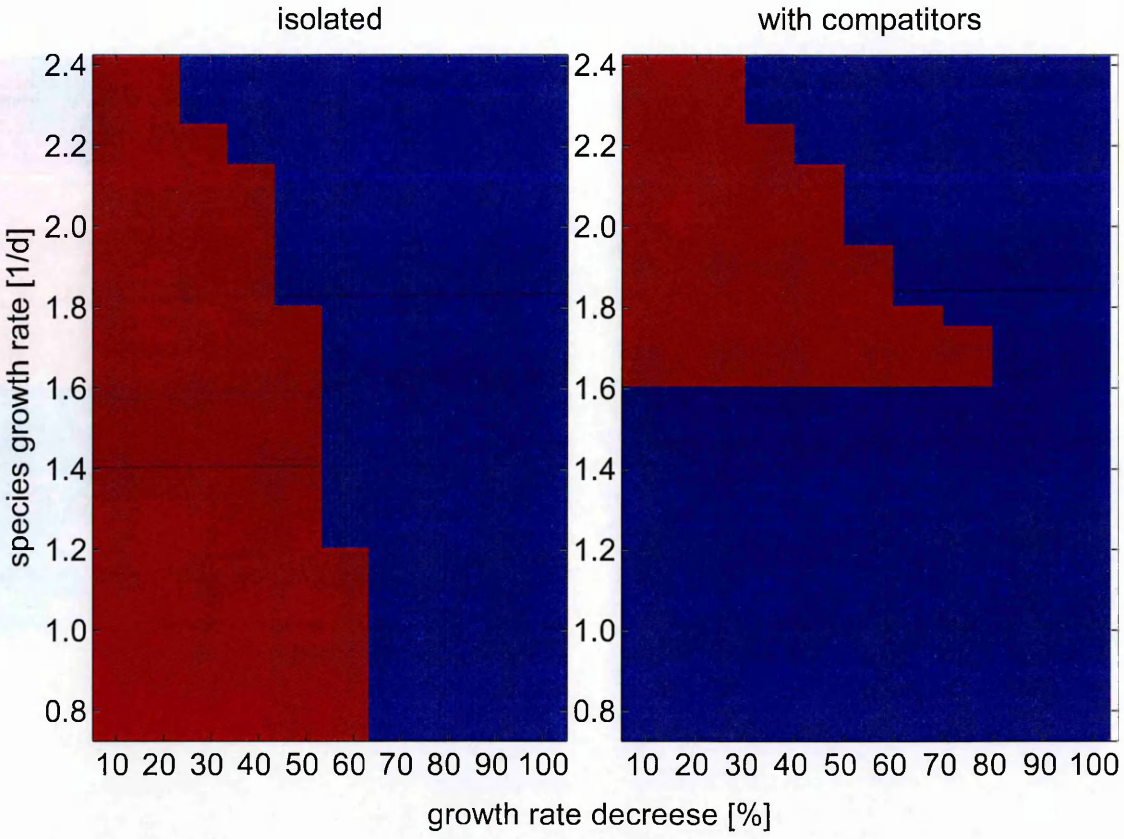

Figure 6.18: Maximal value of growth rate reduction of a diatom strain without being competitively excluded by other strains of the same species in (a) an isolated environment and (b) with other phytoplankton competitors. Strains marked with red (blue) were able (unable) to survive in the system.

form a bloom and exceed predefined abundance threshold, thus successfully undergo sexual reproduction. Species which intrinsic growth rate was lower than 1.7 were competitively excluded by other phytoplankton species (Fig. 6.18b).

6.3.3 F1 generation strain fitness function.

The maximal cell concentration reached in a vegetative period determines the species *inoculum*, and consequently the success of a sex event, in the following period. A notable feature of the diatom sexual reproduction is that only a small percent, $1-10\%$, of the cells undergo a full sexual transformation into the F1 generation (see chapter 5 and Scalco et al. [2014]). Due to the low initial concentrations to persist in the environment in presence of other competing species, including their parental strains, the F1 generation must either rapidly increase in abundance until resources area available,

or drastically reduce its mortality, eventually moving to a dormant stage.

The analysis of the former scenario focused on the maximal concentration of the F1 generation cells before nutrients depletion as a metric for the fitness; it allowed to explore to what extent the decrease in growth rate of parental strains' increased the F1 fitness. The competition between the progeny and the parental strains was simulated by implicitly assuming invariant biology in the other components of the community and considering various values of the strains' competitive abilities and various initial concentrations of the F1 generation cells α (section 6.2.3). The growth rates ratio observed in the laboratory experiments were indicated by $r_{F1} : r_P = 3.2$ and $r_{F1} : r_P = 1.13$ in SH1 and RW1 experiments respectively (chapter 5), hence the F1 generation was considered competitively advantaged ($r_{F1} : r_P > 1$).

The numerical simulations revealed an increase of the F1 generation fitness corresponding to a decrease of the parental strains growth rate equivalent to the increase of the $r_{F1} : r_P$ ratio (Figure 6.19).

For instance, the fitness of the F1 generation cells increased by 6.5 folds when $r_{F1} : r_P$ increased from 1 to 3.2, and almost doubled when $r_{F1} : r_P = 1.13$ for $\alpha = 0.1$ (Figure 6.19). This corresponded to an increase from 10% to 65% of the biomass formed by F1 generation cells for $r_{F1} : r_P = 1$ and $r_{F1} : r_P = 3.2$ respectively before nutrients depletion (Figure 6.19). Notably, $\alpha = 0.1$ refers to the highest initial concentration of F1 generation cells observed during the experiments (Chapter 5 and Scalco et al. [2014]).

The results further depicted that equivalent fitness might be achieved by the temporal parental strains growth rate decrease or by an increased initial concentration of the progeny cells. Thus, the lower is the initial F1 generation cells concentration the higher must be the compensation provided by the EGC mechanism.

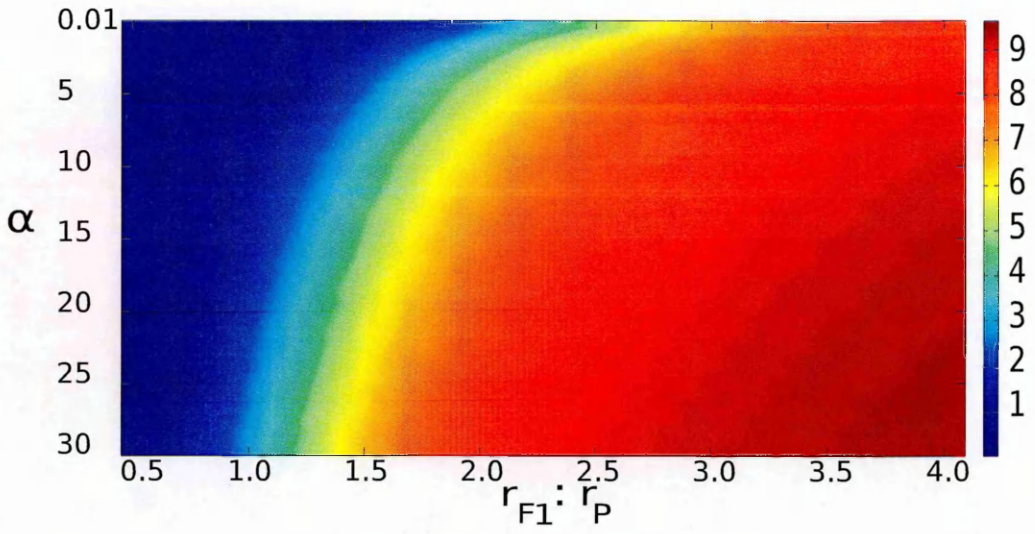

Figure 6.19: The ratio of the F1 generation cells concentration to the cumulative concentration of the F1 and parental strains at the moment of the first indications of nutrients limitations. The α represents the ratio of the F1 generation cells shortly after sexual reproduction occurred, while the $r_{F1} : r_P$ the intrinsic growth rate ratios of the F1 and the parental strains. The maximal concentration of the strain may be considered as a strains' fitness function, hence the higher ratio of the F1 to total system concentration the higher F1 generation strain fitness.

6.4 Discussion

The results of the numerical experiments exploring the ecological consequences of the resource independent growth modulation by diatoms during the phase of sexual reproduction have been presented in this chapter. The peculiar behaviour of diatom species *P. multistriata* at the time of mating reported in the course of laboratory experiments (see Chapter 5 for details) has been extended to several virtual species and investigated with an ecological model (see Chapter 2 for details).

Sexual reproduction is a costly and risky event (Lewis Jr [1983]). It requires more time to produce gametes and meiosis is more time and energy-consuming in comparison to mitosis. Meiosis and syngamy are complex cellular events and, consequently, they are more prone to errors. Cells undergoing gametogenesis are, in some way, lost, i.e. they cannot be used for increasing the population biomass through vegetative divisions. The energy allocated in the formation of gametes can be easily lost. Observations show that some gametangia and gametes abort. In the case of diatoms, where gametes are deprived of the siliceous frustule, gamets are also vulnerable for predation, grazing and infection.

Sexual reproduction represents a fundamental phase of diatoms life cycle and even-though it is highly risky and costly process, the benefits and advantages of sexual reproduction are remarkable. It is linked to both the production of genotypic diversity and the formation of large-sized initial cells(Chepurnov et al. [2005],Amato et al. [2005]). The production of new genetic combinations through meiotic recombination provides species with long-term adaptive advantages allowing not only to survive in a changing environment but also to conquer new territories. Therefore it is essential for the long term survival of a species.Because of the cost and complexity, success in sexual reproduction requires a perfect timing and the right combination of the internal cues (i.e. cell size in diatoms) and the external conditions.

The performed analysis focused on the possible hindrances of the sexual phase and did not discuss its benefits at the level of genetic/genomic variability or phytoplankton-zooplankton interactions. Instead, the analysis focused solely on the growth rate reduction following the sexual reproduction and its ecological consequences. Future studies should address both the advantages and disadvantages of the sexual reproduction in the context of species diversity and ecosystem functioning.

The presented results have shown unequivocally that the coordinated growth rate reduction in diatoms during mating, even in presence of plentiful resources, would affect the functioning of the plankton community even if shared only by a subset of species. More specifically, the numerical analysis revealed that the occurrence of a sex event in a few species would alter the phytoplankton phenology and the seasonal succession, increase the diatom diversity, while improving the model predictive skill. The biomass change of the most abundant functional groups would in turn affect the zooplankton dynamics and the biogeochemical processes because of the tight link between the community composition and elemental export to the deeper layers (e.g., coccolithophores versus non-calcifying small algae). Therefore, it is argued that the standard assumption that phytoplankton would always tend to grow at the maximum rate allowed by proximate factors, as they apparently do during the vegetative phase in the laboratory, does not hold true at least in one case, and likely, also in other phases of their life cycle or in other biological contexts. This in turn implies that to fully account for the persistence of a species in nature the traits of the whole species-specific life cycle must be

taken into account Wyatt and Zingone [2014]. As a corollary, also the paradigm that competitive exclusion is always driving the dynamics of plankton community (Grinnell [1904], Armstrong and McGehee [1980]) has to be revised. Interestingly, a similar comment was made by Hutchinson [1961] with an argument that is to some extent linked to the argument presented in here.

Indeed, even in trait-based models aimed at reconstructing the seasonal succession of phytoplankton communities, i.e., within a more biologically oriented conceptual framework, the choice of traits is generally restricted to the factors regulating phytoplankton ability to compete for resources (Reynolds [2001],Litchman and Klausmeier [2008], McGill et al. [2006], Litchman [2010]). The traits related to the life cycle, even if fully acknowledged in conceptual reviews (e.g., Litchman and Klausmeier [2008], Litchman et al. [2013]) are seldom considered. One of the reasons is certainly the present knowledge gaps on those traits which impact also on our capability to reproduce the natural phytoplankton diversity (Hood et al. [2006], Anderson [2005]). Multidisciplinary approaches, as has been shown in this chapter, may significantly help in filling those gaps.

Clearly, there are numerous limitations of this study and by any mean it should not be considered as exhaustive. Therefore, it ought to be seen rather as a proof of the concept that the inclusion of regulating mechanisms independent of proximate conditions changes the current view on plankton dynamics. In the laboratory experiments presented in chapter 5 only a single diatom species has been used and further work is needed to evaluate the relevance of the examined trait for other diatoms. This is especially true for species which do not perform their sexual reproduction during the exponential phase, using instead nutrient depletion as cue (Davis et al. [1980b]). Nevertheless, it has been shown that the diatom life cycles shape a different ecological niche from that currently perceived.

The null or relatively scarce motility of diatoms sexual stages implies that high concentrations must be reached to allow for a successful reproduction (i.e., high encounter rates). In addition, the need to have a sexualization phase (a sort of preparatory phase) before the event and the risk of possible sudden dilution events (e.g., deep mixing) that would decrease the encounter rate, impose that sexual events: 1) must occur only at

high concentrations to have a sufficient encounter rate; 2) require a highly synchronized population and 3) occur over a very short time window, as in fact it has been observed at sea (Sarno et al. [2010]).

Scalco et al. (Scalco et al. [2014]) speculated that, requiring the sexual reproduction of *P. multistriata* synchronization and a significant density for a finite chance for cell-to-cell encounters, quorum sensing might be involved in coordinating the crucial steps. The quorum sensing has not been explicitly included in the model but it has been imposed that cells would be able to finalize mating only beyond a certain concentration, thus implicitly assuming that some form of interaction favoring maturation of sexual stages and encounter was in place.

The simplified physical structure of the model used in here implies that the phytoplankton community is homogeneously distributed in the mixed layer (Chapter 2). As stated above, high concentrations must be reached to allow for a successful reproduction, thus in this modelling framework the EGC mechanism may be attributed only to the species which average concentration in the mixed layer exceeds a predefined threshold. Otherwise, sexual reproduction will not take place and the effects of the EGC will not be observed.

It has been discussed in the 5th chapter that the formation of the thin layers may facilitate cells interactions as the cell concentration inside the thin layer may be considerably higher with respect to the rest of the water column. Consequently, species may cross the considered concentration threshold within the thin layer, while its average concentration in the whole water column remains lower than that threshold.

Formation of the thin layers cannot be reproduced in the modelling framework employed in here. Thus the EGC mechanism should be explored also with the models resolving spatial structure of the water column, i.e., 1- or 3-dimensional models, in which formation of the thin layers would be possible. That would further allow for investigating the implications of the EGC mechanism for a broader set of species.

The second relevant conclusion is that only diatom species with high growth rates, and a parallel high nutrient assimilation rate, are able to reach the sufficiently high cell concentrations needed to cope with the negative impact of EGC on competitive capabilities. Extrapolating further, it is argued that the effective resource acquisi-

tion and the high growth rate of many diatoms during their vegetative phase could be the adaptive solution to cope with the requirements, and the need, of the sexual reproduction.

The experiments in chapter 5 showed also that a putative endogenous growth control acts on a time scale longer than that required for mating. Hence, the need for sex implies a cost which is different from the cost of generating mates, or that of the meiosis (Lewis Jr [1984]) or that of signaling. This additional cost seems to be huge for the population. But is it really a cost? In fact, one may ask what compensates for the cost of an endogenous growth control so as to favor the persistence of the species.

Indeed, this kind of trade-off is not limited to plankton, being a common feature of many species on both terrestrial and aquatic environments. More intriguingly, can the growth rate reduction due to the EGC be interpreted as an intergenerational mutualism and cooperation among the parental and the progeny strains? It is argued that this possibility cannot be excluded despite theoretical arguments on a parallel larger advantage for strains without an EGC in presence of EGC clones would lead to a dismissal of that hypothesis. The argument goes as follows.

Diatom sexual events produce only a small numbers of the cells undergoing a full sexual transformation into a new (F1) generation (1-10% see chapter 5 and Scalco et al. [2014]). The adaptive value of this trait may be related to the reduction of the risk that, with all the cells of a species participating to sexual reproduction, a single highly dispersive mixing event may dramatically impact on the persistence of the species. Likewise, an infection or massive grazing of auxospores (auxospores are soft and vulnerable to grazing and viral attack) may cause extinction of the whole population. On the other hand, creating new genotypes could temporarily reset the impact of viruses coevolving with the species, while solving the problem of size reduction.

To cope with the other risks of being in low numbers F1 generation should be favored in the competitions with the parents. If they reduce their consumption the F1's are able to reach high concentrations before resources are depleted (as described in chapter 5 and further supported by specific simulations in section 6.2.3). How to minimize the competition by F1's and their parental strains which may profit of the EGC without expressing it? The hypothesis is that the Deborah number, e.g., the

ratio between the time scale needed to profit of the locally lower nutrient consumption by the parents and the time of dispersal of F1's and competing strains (e.g., Jenkinson and Wyatt [1992]) is low enough to make that solution advantageous and thus kept during evolution.

In synthesis, It is not claimed that the suites of traits that were characterized and analyzed in here, in particular the switch between the high growth rate and temporary arrest during mating, is the decisive missing trait of diatom biology to understand the succession in plankton communities. Rather it is posited that it is a convincing and unequivocal example of how ultimate factors and biological interactions shaped to work on evolutionary time scales, integrate in a substantial way our view of which processes drive plankton dynamics and ask for a more systematic analysis of the biology of those, apparently simple, unicellular organisms, also exploiting the wealth of opportunities offered by the modern, integrative biology.

Chapter 7

Thesis summary and outlook

7.1 Thesis scope and main results

The general aim of my thesis was to introduce new processes in modelling plankton dynamics by gathering multidisciplinary information from biology, physics, and ecology. This asks also for a different conceptual approach on the drivers of that dynamics, among which the role of biological traits of planktonic organisms. I firstly explored the impact of the different biological profiles of planktonic organisms in sustaining biodiversity and adapting to physical variability. This led to a more in depth exploration on the factors affecting plankton succession including grazers' migration and immigration. Finally I introduced a purely biological process, i.e., the sexual reproduction in diatoms which, on the basis of the observations in the laboratory, could alter significantly the resource acquisition by algae. To be more specific, I inspected the impact of diatom sexual reproduction, on the diversity of phytoplankton using a suitably adapted community model.

In the presented thesis I have provided sufficient evidence and new information regarding the role of life cycles in shaping diatom diversity. I have shown that the coordinated growth rate reduction in diatoms during mating, occurring also under nutrients replete conditions, would affect the functioning of the plankton community and contribute to the observed diversity (Chapter 6). More specifically, I have demonstrated that the occurrence of a sex event, even if shared only by a subset of diatom species, have broad implications including change in the phytoplankton phenology and the seasonal succession, change in the zooplankton dynamics, increase of the diatom diversity, and alternation of the biogeochemical processes (due to the tight link between the community composition and elemental export to the deeper layers, e.g., coccolithophores versus noncalcifying small algae).

In the presented thesis I have integrated laboratory and numerical experiments to explore the ecological consequences of the resource independent growth modulation by diatoms during the phase of sexual reproduction. Such a peculiar behaviour has been observed in the course of laboratory experiments with batch cultures of *P. multistriata* at the time of mating (Chapter 5). Sexual reproduction represents a fundamental phase of diatoms life cycle as it is linked to both the production of genotypic diversity and the formation of large sized initial cells (Chapter 1).

I have provided also evidence that diatoms should not be perceived as passive transducers of biomass as they are capable of growth rate modulation independent of proximal conditions (Chapter 5). I have shown that the diatom life cycles shape a different ecological niche from that currently considered (Chapter 6). Finally, I have identified an important biological trait capable of driving phytoplankton life strategies along paths more sophisticated than just those driven by the short term availability of resources.

The trait-based approach is frequently invoked when the seasonal structure of planktonic communities is addressed (Chapter 1). The approach is mostly focused on factors regulating the ability to compete for resources, and in fact, traits related to the life cycle, even though recognised in conceptual reviews, are rarely considered. One of the reasons is the knowledge gap on those traits. Presented in here multidisciplinary approach may certainly help in filling this gap and consequently improve our capability of reproducing the marine ecosystems dynamics.

In this thesis I have also illustrated the implementation of a conceptual numerical model of seasonal plankton diversity in the mixed layer. Characteristics of the model include stochastic approach to phytoplankton community description, explicit representation of species diversity considering also diversity within phytoplankton functional groups, species immigration, and biological processes such as copepods overwintering and diatoms life cycles (Chapters 2, 3 and 6).

Noteworthy, despite the simplified description of the seasonal forcing and incorporated processes, the presented model successfully reproduces the wax and wane of the main features of subpolar ecosystem over the year.

A stochastic approach to the community composition simulations allowed to partially circumvent the limitations presented by scarce information on phytoplankton physiology and processes controlling phytoplankton population dynamics. Furthermore, the model has been embedded within an ensemble approach allowing to assess the impact of initial conditions, here phytoplankton community composition, on the obtained results.

Simple model construction allowed for running multiple simulations within a relatively short time, but also guaranteed transparency and ease in terms of the analysis and

interpretation of the results. Indeed it was possible to gain interesting results regarding the physical and biological processes shaping community composition in mid-latitude environments (Chapters 3, 4 and 6).

The illustrated framework incorporating a simple model embedded within a stochastic and ensemble approach proved to be useful when the impact of the model assumptions and mechanisms formulation on ecosystem functioning has been explored. Henceforth, I have demonstrated that the model is simultaneously acceptably simple to investigate ecological hypotheses and sufficiently complex to produce generic insights in dynamics of multispecies communities in seasonally forced environment. This modelling approach can naturally evolve to explore the community composition and its time course in various environment types as it is discussed in the following chapters, or to explore the relations between marine ecosystems, evolution, biogeochemical cycles, and past and future climate change.

7.2 Thesis summary

In the 1st chapter, the background information on the two main topics addressed by this study have been provided i.e. an overview of the modelling approaches currently applied to plankton dynamics, of estimates of diversity, and of diatom life cycles. It has been illustrated what is known specifically in relation to pelagic phytoplankton diversity. The mechanisms driving phytoplankton species coexistence and the relationship between species diversity and functioning of the aquatic ecosystems have also been described. In addition to that, the difficulties in reproducing species diversity in the current modelling framework have been illustrated and examples of mechanisms contributing to maintaining species diversity have been provided. Finally diatoms life cycles and factors inducing life stage transformation as a source of previously overlooked biological traits with the potential to control species diversity have been discussed .

In the 2nd chapter a detail description of a simple 0-D NPZD model inspired by the MIT Darwin Model and slab models has been provided. The presentation focused on model's components, physical and biological processes underlining incorporated

mechanisms, and their appropriate mathematical formulation. The presented model parametrisation, necessary for its implementation, was tuned to reproduce dynamics observed in mid-latitude ecosystems, in particular North Atlantic Bloom Experiment location (NABE, 47°N 20°W). A rigid qualitative and quantitative validation of the model performance with respect to available observations have been also provided. It has been also demonstrated that the model was able to successfully reproduce the multi-annual average properties of the ecosystem in the area surrounding NABE by comparing seasonal cycles of chlorophyll-a, PIC and POC (SeaWiFS data), surface nitrate and silicate (World Ocean Atlas 2013 data), and seasonal abundance of the phytoplankton functional groups (Continuous Plankton Recorder data) with their model counterparts. Model capability to reproduce specific ecosystem dynamics has also been proved by collating data regarding chlorophyll-a, PON, nitrate and silicate concentrations observed during the North Atlantic Bloom Experiment in 1989 with the data generated by the model.

The presented comparison provided a satisfactory results in terms of model predictive skill and proved that, despite the simplicity of the presented framework, it was capable of producing insightful information on ecosystem functioning. Henceforth the model may be considered as a valuable tool to explore relevant mechanisms and test hypothesis regarding processes driving phytoplankton community time course and its composition. In particular it is suitable to explore questions addressed with my thesis.

One of the advantages of the presented model is the explicit representation of multiple species representing different phytoplankton functional groups. In the 3rd chapter, species diversity in the virtual ecosystem has been explored. To be more specific, ecological indicators such as species richness and Shannon index has bee used to describe the overall number of co-existing species and their relative abundance, but also the physiological traits distribution of species surviving in the virtual ecosystem has been illustrated. Seasonal variability in species diversity has been explored. Additionally, the mechanisms driving species competition and shaping phytoplankton community composition on the ecological time scale have been investigated. Finally, a link between observed seasonal variability in the species diversity and physical conditions has

been established.

Furthermore, a structural sensitivity analysis has been performed to assess model sensitivity to the presence-absence of copepods winter diapause and phytoplankton immigration. The analyses have illustrated how these process affect both the bulk phytoplankton properties and the community composition. In fact, it has been demonstrated that introduction of copepods winter diapause into the model had almost negligible impact on phytoplankton seasonal abundance patterns and species diversity. These results however, should not be considered as exhaustive and conclusive, and further exploration is required to assess the role of copepods overwintering in shaping phytoplankton dynamics. On a contrary, the introduction of phytoplankton immigration improved the representation of phytoplankton functional groups and resulted in an elevated species diversity. This sensitivity analysis allowed to explore how model assumptions and mechanisms formulation affect processes regulating species coexistence and ecosystem functioning.

The physical forcing characteristics demonstrate strong spatial variability at the global but also at the basin scale. The analytical formulation of physical forcing used in the model allowed to account for this variability, to reproduce the main features of the MLD observed all over the open ocean environments and to explore the model dynamics in environments with markedly different seasonal cycles. In the 4th chapter the relationship between the environmental forcing characteristics and the functioning of a simplified ecosystem has been investigated. The presented analysis allowed to explore how changes in the beginning and duration of spring water column restratification, winter mixed layer depth, and duration of summer stratification affect species community composition and species diversity in the virtual ecosystems.

The obtained results have been extrapolated into particular environmental characteristics reported in the basin of the North Atlantic and contrasted with the CPR data. The qualitative agreement of model outcomes with the field observations, and the sensitivity to changes in physical forcing have illustrated model's plasticity and potential of its applicability for various types of environment. It allowed also to investigate the relevance of bottom-up and top-down processes on community composition

and, above all, on species diversity. Finally, these results have been used to indicate models limitations and to identify relevant processes, which could improve the model representation of the ecosystem.

The 5th chapter has been dedicated to the description of laboratory experiments with batch cultures of marine pennate diatom *Pseudo-nitzschia multistriata*. Experiments with the single mating type strains and the co-culture of opposite mating type strains, hence experiments in which sexual reproduction could not and could take place have been presented. This experimental set-up allowed to successfully demonstrate that sexual reproduction impairs population dynamics and nutrients consumption.

In particular it has been shown that in concomitance to the onset of the sexual phase, parental strains lowered their growth and nutrients consumption was significantly reduced. It has been also indicated that the growth rate reduction took place independently from resources availability and was observed on a time scale exceeding that required for sexual reproduction.

Furthermore, it has been demonstrated that the observed change in population dynamics was unequivocally attributed to the sexual reproduction and not to the competitive interactions between the two differing in size parental strains. It has been achieved by setting up a simple nutrient-phytoplankton model with the idea to mimic performed laboratory experiments. The obtained results have indicated that a model considering only competitive interactions was unable to reproduce population dynamics observed in laboratory experiments during the onset of sexual reproduction.

Results presented in chapter 5 provide support for the fact that growth rate of species is not a direct function of nutrient availability but can be modulated during the transition from one life stage to another. Consequently, it has been concluded that additional mechanisms, e.g., diatoms endogenous growth control related to sexual reproduction, must be included in the conceptual plankton models in order to account for the differences in population dynamics in various life cycle phases. Henceforth, the need for introduction of processes related to life cycles into ecological models has been indicated as a mean of increasing their accuracy and predictive capability.

This need has been partially satisfied in the 6th chapter. The results of the laboratory experiments have been conceptualised and coined into a mathematical formulation of the Endogenous Growth Control mechanism (EGC). This peculiar mechanisms described the growth rate of the vegetative stage (a trait) reduction in preparation for the next stage, here sexual reproduction. The impact of the EGC on phytoplankton community structure and its time course has been assessed with an ecological model (Chapter 2) in which the growth rate characteristics of some diatom species was augmented with the developed EGC formulation.

It has been shown that the introduction of the EGC mechanism resulted in a change in seasonal patterns of phytoplankton leading to a reorganization of the community even if affecting directly only a subset of diatoms species. The latter was supported with the analysis of the physiological traits distribution of the species surviving in the virtual ecosystems. This new phytoplankton biomass distribution pattern was accompanied by a change of the diversity at the level of the species and of functional groups. The introduction of EGC reshaped also spring bloom phenology, and altered duration of the vegetative period based on signatures of nutrient limitations. The restructuring of the phytoplankton community affected also the zooplankton seasonal abundance patterns. Hence, the implementation of the EGC indirectly affected bottom-up and top-down processes shaping phytoplankton community structure. The model skill was also improved when EGC was implemented as indicated by an increased agreement of the nutrients, chlorophyll-a, PON and NPP measurements obtained during NABE with their model counterparts. Overall, it has been demonstrated that the introduction of a sexual phase in the model improved the representation of the functional groups and altered the species richness in the virtual ecosystem.

In addition to the above analysis, it has been argued that the need for sexual reproduction, and the cost related to it, determines the ecological niche of diatoms as only species with high growth rate and high nutrients half-saturation were able to successfully undergo sexual reproduction and withstand the growth rate decrease. Finally it has been demonstrated that this temporal growth rate reduction increases success rate of sexual reproduction and consequently affects species fitness. In summary, some of the implications of the Endogenous Growth Control have been explored considering

both the ecological and evolutionary times scale.

7.3 General considerations and future perspectives

This study was subject to many limitations. Only a single species was considered in the laboratory experiments and only a single cue was used for inducing sexual reproduction. Further work is required to evaluate the relevance of the observed processes for other diatoms for witch additional factors triggering sexual reproduction ought to be investigated (see Chapter 1). This is particularly important for species that do not perform sexual reproduction during the exponential phase, but use instead nutrient depletion (Steele [1965], Davis et al. [1973], French and Hargraves [1985]) or light quality or quantity (Drebes [1977c], Mouget et al. [2009]) as a cue. Notably, the presented analysis focused solely on the hindrances of sexual reproduction and the benefits in form of population genetic/genomic variability providing evolutionary advantage were not discussed (Lewis Jr [1984]).

As illustrated in Chapter 1, diatoms are characterised by complex, heteromorphic life cycles going beyond the vegetative phase and the sexual reproduction considered in this study. In this sense, the work presented in here remain unfinished and the fact that no additional biological processes were investigated may be considered as a failure. A failure which can be attributed to the considerable gap in our knowledge on the diatoms biology and factors regulating life stage transformation (see Chapter 1). A lack of empirical data on species-specific phase transition impaired their implementation into the modelling framework and the evaluation of their impact on species diversity. Therefore more experimental work is needed to fully understand the complexity of phytoplankton life strategies and their interactions with the environment. Research in this direction, i.e. coupling laboratory experiments and numerical simulations on the factors that determine resting stage formation/germination, those inducing apoptosis, or changes in growth dynamics due interactions with other species, ought to be pursued.

In fact there is a growing need to organise a theoretical framework for the exploitation of insight on the basic processes derived from laboratory studies on func-

tional genomics (e.g., Falciatore and Bowler [2002]; Kooistra et al. [2007]; Coelho et al. [2013]; Mock and Kirkham [2012]) and fully exploiting the enormous quantity of data originating from recent global genomic surveys (e.g., TARA Oceans: http://www.embl.de/tara-oceans/start/). This brings a necessity of expanding the genomic predictions into specific, biologically-based life traits and introducing them into phytoplankton models. The emphasis ought to be placed on underlying mechanism of cell physiology and activity, followed by their impact on phytoplankton dynamics at a population level and subsequently foodweb interactions (Allen and Polimene [2011]).

Phytoplankton competition models could be augmented with additional state variables describing molecular and genomic data e.g., gene expression regulating physiological state of the population (Dunlop et al. [2009], Cherie [2012], Sardans et al. [2011], Satinsky et al. [2014], Veldhoen et al. [2012], Kostka et al. [2014]).

Building upon the genomic data, the models could be also enriched with reliable cell systems biology sub-models, thus assimilating processes at the intracellular level (e.g., cell physiology and response to stress) with those at the intercellular level (e.g., grazing, competition). This would result in modelling the metabolic state of the population and increase the models capability to consistently reconstruct the observed phytoplankton biodiversity and community composition in various environments (Allen and Polimene [2011], Armstrong [2006]).

The genomic information may be used also for identification of the molecular mechanisms underpinning organisms trophic modes (de Vargas et al. [2015], Hilton et al. [2013]). In addition to the phototrophic "producers" and heterotrophic "consumers", other trophic modes have been recognised, e.g., mixotrophy being a combination of phototrophic and heterotrophic metabolism (Estep et al. [1986], Hartmann et al. [2012], Hartmann et al. [2012]), osmotrophy in which cells absorb organic material from the external environment as small molecules or macromolecules (Stoecker and Gustafson [2003]), symbioses being a mutualistic relationships where one species lives within or on another species (Decelle et al. [2012]), or parasitism where one organism exists in association with another to the detriment of that partner (Guillou et al. [2008], Chambouvet et al. [2011], Bachvaroff et al. [2012]).

These modes may have profound implications in terms of the population dynamics

e.g., chain formation illustrating plasticity of morphological characteristics that highly impacts the coupling with higher trophic levels (Bergkvist et al. [2012]), or mixotrophy broadening the pool of available resources as the ingestion of prey may serve as a source of energy and carbon when photosynthesis is limited by light availability or resources are scarce (Tittel et al. [2003]). They also affect species physiological characteristics; for instance maximum specific growth rates and nutrients affinity of mixotrophic dinoflagellates are typically lower with respect to photoautotrophs (Edwards et al. [2012]), and their growth and grazing rates are slower than in similar heterotrophic specialists (Jeong et al. [2010]. Yet, despite being capable of affecting phytoplankton dynamics at the population level and restructuring microbial food web, modes other than phototrophy and heterotrophy are seldom considered in the modelling studies. Therefore future studies ought to put more emphasis on a broader representation of inter- and intra-specific phytopalntkon interactions.

Modelling approach generally resolves a few coarse phytoplankton phenotypes with highly simplified physiology (e.g., Quere et al. [2005], Litchman et al. [2006]) and diversity within those few functional types is related to cell size or temperature adaptations (Follows et al. [2007]). It has been illustrated in this thesis that in order to progress in our understanding of ecosystem functioning, the representation of phytoplankton physiology has to be improved and has to account also for the complex heteromorphic life cycles. It has been pointed out that additional trophic modes ought to be considered in the next-generation models. In a similar fashion, the representation of the microbial community has to be improved. In particular viruses which activity may potentially restructure microbial communities and interrupt nutrients cycle by affecting the microbial loop (Breitbart [2012], Lehahn et al. [2014], Short [2012], Haaber and Middelboe [2009]). Indeed, viruses can influence predator populations directly by infection and lysis or by reducing prey availability as well as serve as a food particles for them (Haaber and Middelboe [2009], Evans and Wilson [2008], Miki and Jacquet [2008], Miki and Jacquet [2010]). Viral-mediated cell lysis can be rapidly assimilated and remineralized by microbes causing increased bacterial growth. Through lysing their hosts, marine viruses may control abundance of phytoplantkon, bacteria and zooplank-

ton, affect community composition, and impact global biogeochemical cycles. Yet, the are rarely represented in ecosystem model and future studies should account for their presence and activity.

Empirical studies on community dynamics that explicitly considered evolutionary processes support the view that ecologically important traits of a population alter substantially over a period of a few generations, on the same time scale as the ecological changes that drive them (e.g.Hendry and Kinnison [1999], Hairston et al. [2005], Ellner and Becks [2011], Ellner et al. [2011]). Therefore, the evolutionary and the ecological dynamics often occur on similar time-scales. Examples of the eco-evolutionary feedbacks in nature emerged as a result of predator-prey (Becks et al. [2012], Yoshida et al. [2003]), host-parasite or host-pathogen interactions (Wolinska et al. [2008], Duffy et al. [2009], Penczykowski et al. [2011]), and could be expected also from other interactions amongst the species. These feedbacks may play an important role in the functioning of the community and the ecosystem as they co-determine the dynamical behaviour of ecological communities (Becks et al. [2012], Yoshida et al. [2003] Bell and Gonzalez [2009], Fussmann et al. [2007]). Coordinated experimental and modelling studies ought to investigate how pervasive eco-evolutionary feedback loops are for plankton and examine the role that eco-evolutionary processes play in ecosystems functioning.

Ocean dynamics (e.g., lateral advection and stirring due to planetary waves) mix organisms from different habitats e.g., in the Gulf Stream region the boundary current transports away the subtropical communities which are subsequently mixed with locally adapted organisms and eventually outcompeted. Phytoplankton dispersal is an essential element of oceanic habitats. Migration plays a major role in shaping aquatic community composition and consequently affect ecosystem functioning (Cloern and Dufford [2005]). A simplified physical structure used in the 0-dimensional models offers a compelling framework for exploring dynamics of marine ecosystems, but it is unable to reconstruct the above processes.

This issue may be circumvented by considering an explicit background reservoir of planktonic species that immigrate into the system. Such a simplified representation

was considered also in this thesis (Chapter 3) and was used for investigating the role of dispersal in species diversity and functional groups representation. The presented results were in line with those obtained by Levy et al. Lévy et al. [2014]). In their recent paper, Levy et al. suggest that dispersal of phytoplankton by oceanic transport processes increases phytoplankton diversity at the local scale of (α-diversity). They also point out that mesoscale turbulence modifies the community composition and leads to a γ-diversity decrease. Thus, the dispersal of plankton play a crucial role in controlling species diversity and community composition. In addition, immigration may be considered as a step towards realistic representation of the pelagic ecosystems and should be incorporated in the construction of ecological models.

Another inherent limitation of the 0-dimensional models is the homogeneous distributed of the ecosystem compartments within the mixed layer. Evidence has been provided for the density-dependent processes regulating life stage transformation of *P. multistriata* (Scalco et al. [2014]). It is speculated that the formation of thin layers due to physical processes such as vertical gradients of horizontal velocity due to shear, advection, or gradients in temperature and/or salinity along the water column (Durham and Stocker [2012]) in which cell concentration vastly exceed that outside the accumulation layers (Rines et al. [2002], Ryan et al. [2005], McManus et al. [2008], Velo-Suárez et al. [2008]). This could facilitate cell-to-cell signalling and induce sexual reproduction. The formation of thin layers cannot be reproduced in a simplified 0D model using a double-layer slab physics, thus the density dependent mechanisms presented in Chapters 5 and 6 ought to be explored in more complex model in order to account for dispersal and accumulation of phytoplankton cells.

The oversimplified spatial dimensions may be considered as a limitation of the model presented in this thesis. This simplification however was considered as a trade-off with the possibility of using many species over a wide range of environmental scenarios for several decades. Overall, it has been illustrated that despite its simplicity the presented model proved useful for exploring the role of physical and biological processes in ecosystem functioning.

Moreover, there is the need to improve the skill of biogeochemical models used for

the forecast of climate changes and of the impact of such changes on the ecosystems. The results presented in Chapter 4 confirms that environmental forcing determines community structure and its productivity. Aside from the shape of the diversity-productivity relationship, the nutrient supply also sets an upper limit to diversity in the model. In fact, reduced mixing due to enhanced stratification of the upper ocean and thereby lower input of nutrients into the surface layers is one of the consequences predicted under a warming climate (e.g., Sarmiento et al. [2004]; Steinacher et al. [2010]). Other studies evaluating oceanic changes due to rising atmospheric CO_2 levels predict export production to decline as much as, or more than, primary production on centennial scales, so that the ratio between export to total primary production remains nearly constant or decreases (e.g., Steinacher et al. [2010]). The negative effect of reduced nutrient supply on primary production may be counteracted by an increase in light availability and temperature in a shallower surface mixed layer (Sarmiento et al. [2004]), which may be beneficial to phytoplankton growth (Laufkötter et al. [2015], Boyd et al. [2015]) .

These processes may be investigated with the model presented in this thesis. Clearly the main focus of the analysis presented in Chapter 3,4, and 6 was on species diversity and not on bio-geochemical cycles, nevertheless the results presented in there were in concord with other modelling studies (Steinacher et al. [2010]; Taucher and Oschlies [2011]). The sudden change in nutrient supply implied by sudden change in maximal MLD value, in this setup is, however, not realistic in the sense of expected time scales of change in the ocean in a changing climate. A realistic setup would require a model configured to mimic climate change simulations, i.e., an online simulation coupled to the physical model or a decreasing trend in max MLD value. For instance, sets of simulations could be performed to address future community structure: one with a trend in physical forcing related to climate change, and the other one without climatic to provide a control simulation.

Concluding remarks While bottom-up processes related to resources availability and top-down mechanisms controlling diversity through zooplankton feeding are al-

ready captured in the ocean ecosystem model, biological processes reflecting phytoplankton life cycles have not been represented in detail to date. This thesis investigates for the first time the control of phytoplankton diversity by the processes related to diatoms life strategies, namely sexual reproduction and cost attributed to it. It thereby depicts the importance of biological mechanisms which may drive phytoplankton life strategies along paths more sophisticated than just those driven by the short term availability of resources.

The approach presented in here incorporates two compatible methodologies: laboratory experiments and numerical simulations, and generates insights much broader than from what can be learned by applying either approach alone. This multidisciplinary approach allows to investigate how processes observed in experiments, developed into concepts of competition and coexistence, and implemented into idealized models, may apply to ocean phytoplankton communities. This thesis reveals considerable effects of phytoplankton life strategies on phytoplankton diversity, succession, community structure, and mechanisms of competition and coexistence in the model. It motivates further experimental and theoretical work on phytoplankton biology and the development of mechanistic models representing changes in species physiology attributed to life stage transformation, which may improve our representation of diverse model plankton communities. Furthermore, it demonstrates that diversity has the potential to influence the functioning of the ecosystem. At the same time, it becomes evident that the mechanisms regulating the species diversity observed in the ocean are not well understood, but above all that the species diversity per se is not known.

The results presented in this outlook indicate avenues for future work which make use of the unique structure of the diversity-resolving ecosystem model employed here. The influence of resource supply to the surface ocean on phytoplankton diversity and productivity and their potential feedbacks is relevant for scenarios of the ocean and its role in biogeochemical cycling in a future climate. How the resource supply affects diversity and productivity in ocean ecosystems is not well understood.

Clearly, there is a need to assess the uncertainties inherent to simulating ocean ecosystems based on plankton functional types. In particular, the limitations imposed by the scarce knowledge on the phytoplankton biology ought to be addressed. Indeed,

the biological processes related to life cycles present the capability to drive phytoplankton dynamics on paths more sophisticated than temporal resources availability. Thus, above all, the experimental studies should further explore the diversity of complex life cycles observed among all the phytoplankton species.

Finally, human activities and environmental changes are expected to impact significantly oceanic ecosystems (Bopp et al. [2013]) but their resilience is difficult to assess and remains poorly predictable (Hoegh-Guldberg and Bruno [2010]). Ecosystems' resilience is a function of phenotypic plasticity, population diversity, and ecosystems connectivity (Côté and Darling [2010]). Evidently, addressing the issue of the diversity would allow to better understand the resilience of phytoplankton communities in light of the climate change. Observational and theoretical studies have identified lower temporal variability of production or biomass in more diverse systems (McGrady-Steed et al. [1997]; Cottingham et al. [2001]). In addition to the variability and robustness of predictions in relation to diversity, the simulations can help to identify any potential buffering effect of diversity on ecosystem functions under the influence of environmental changes.

Bibliography

Aarssen, L. W. (1997). High productivity in grassland ecosystems: effected by species diversity or productive species. *Oikos*, 80:183–184.. 11

Ainsworth, C., Samhouri, J., Busch, D., Cheung, W. W., Dunne, J., and Okey, T. A. (2011). Potential impacts of climate change on northeast pacific marine foodwebs and fisheries. *ICES Journal of Marine Science: Journal du Conseil.* 11, 108

Aksnes, D. and Egge, J. (1991). A theoretical model for nutrient uptake in phytoplankton. *Marine Ecology Progress Series. Oldendorf*, 70(1):65–72. 96, 148

Alatalo, R. V. (1981). Problems in the measurement of evenness in ecology. *Oikos*, pages 199–204. 3, 107

Allen, A. P., Gillooly, J. F., Savage, V. M., and Brown, J. H. (2006). Kinetic effects of temperature on rates of genetic divergence and speciation. *Proceedings of the National Academy of Sciences of the United States of America*, 103(24):9130–5. 5

Allen, J. and Polimene, L. (2011). Linking physiology to ecology: towards a new generation of plankton models. *Journal of plankton research*, 33(7):989–997. 310

Allen, J., Somerfield, P., and Gilbert, F. (2007). Quantifying uncertainty in high-resolution coupled hydrodynamic-ecosystem models. *Journal of Marine Systems*, 64(1):3–14. 95

Amato, A., Orsini, L., D'Alelio, D., and Montresor, M. (2005). Life cycle, size reduction patterns, and ultrastructure of the pennate planktonic diatom *Pseudo-nitzschia delicatissima* (Bacillariophyceae). *Journal of Phycology*, 41(3):542–556. 20, 21, 23, 24, 25, 34, 232, 296

Ammerman, J., Hood, R. R., Case, D. A., and Cotner, J. B. (2003). Phosphorus deficiency in the atlantic: An emerging paradigm in oceanography. *Eos*, 84(18):165. 223

Anderson, D. M., Glibert, P. M., and Burkholder, J. M. (2002). Harmful algal blooms and eutrophication: nutrient sources, composition, and consequences. *Estuaries*, 25(4):704–726. 30, 256

Anderson, D. M. and Rengefors, K. (2006). Community assembly and seasonal succession of marine dinoflagellates in a temperate estuary: The importance of life cycle events. *Limnology and Oceanography*, 51(2):860–873. 134

Anderson, T., Gentleman, W., and Yool, A. (2015). Empower-1.0: an efficient model of planktonic ecosystems written in r. *Geoscientific Model Development Discussions*, 8(1):53–140. 44, 59, 73, 94, 222

Anderson, T. R. (1993). A spectrally averaged model of light penetration and photosynthesis. *Limnology and Oceanography*, 38(7):1403–1419. 100

Anderson, T. R. (1994). Relating c: N ratios in zooplankton food and faecal pellets using a biochemical model. *Journal of Experimental Marine Biology and Ecology*, 184(2):183–199. 56

Anderson, T. R. (2005). Plankton functional type modelling: running before we can walk? *Journal of Plankton Research*, 27(3):1–1. 16, 17, 31, 39, 102, 146, 151, 156, 297

Anderson, T. R. and Hessen, D. O. (1995). Carbon or nitrogen limitation in marine copepods? *Journal of Plankton Research*, 17(2):317–331. 56

Anderson, T. R. and Pondaven, P. (2003). Non-redfield carbon and nitrogen cycling in the Sargasso Sea: pelagic imbalances and export flux. *Deep Sea Research Part I: Oceanographic Research Papers*, 50(5):573–591. 12, 147

Arhonditsis, G. B., Brett, M. T., et al. (2004). Evaluation of the current state of mechanistic aquatic biogeochemical modeling. *Marine Ecology Progress Series*, 271(2004):13–26. 95

Armstrong, R. A. (1999). An optimization-based model of iron-light-ammonium colimitation of nitrate uptake and phytoplankton growth. *Limnology and Oceanography*, 44:1436–1446. 12, 14, 148

Armstrong, R. A. (2006). Optimality-based modeling of nitrogen allocation and photoacclimation in photosynthesis. *Deep Sea Research Part II: Topical Studies in Oceanography*, 53(5):513–531. 310

Armstrong, R. A., Lee, C., Hedges, J. I., Honjo, S., and Wakeham, S. G. (2001). A new, mechanistic model for organic carbon fluxes in the ocean based on the quantitative association of poc with ballast minerals. *Deep Sea Research Part II: Topical Studies in Oceanography*, 49(1):219–236. 33

Armstrong, R. A. and McGehee, R. (1980). Competitive exclusion. *American Naturalist*, pages 151–170. 8, 148, 297

Arrigo, K. R. (2004). Marine microorganisms and global nutrient cycles. *Nature*, 437(7057):349–355. 2

Arrigo, K. R., Robinson, D. H., Worthen, D. L., Dunbar, R. B., Di Tullio, G. R., VanWoert, M., and Lizotte, M. P. (1999). Phytoplankton community structure and the drawdown of nutrients and CO2 in the Southern Ocean. *Science*, 283(5400):365–367. 11

Assmy, P. and Smetacek, V. (2009). Algal blooms. *Encyclopedia of Microbiology/Moselio Schaechter, Editor. Oxford: Elsevier (Academic Pr.)*, pages 27–41. 166

Assmy, P., Smetacek, V., Montresor, M., Klaas, C., Henjes, J., Strass, V. H., Arrieta, J. M., Bathmann, U., Berg, G. M., Breitbarth, E., et al. (2013). Thick-shelled, grazer-protected diatoms decouple ocean carbon and silicon cycles in the iron-limited Antarctic Circumpolar Current. *Proceedings of the National Academy of Sciences*, 110(51):20633–20638. 11, 107

Bachvaroff, T. R., Kim, S., Guillou, L., Delwiche, C. F., and Coats, D. W. (2012). Molecular diversity of the syndinean genus eduboscquella based on single-cell pcr analysis. *Applied and environmental microbiology*, 78(2):334–345. 310

Backhaus, J. O., Harms, I. H., Krause, M., and Heath, M. R. (1994). An hypothesis concerning the space-time succession of calanus finmarchicus in the northern north sea. *ICES Journal of Marine Science: Journal du Conseil*, 51(2):169–180. 157

Backhaus, J. O., Wehde, H., Hegseth, E. N., and Kämpf, J. (1999). 'phyto-convection': the role of oceanic convection in primary production. *Marine ecology. Progress series*, 189:77–92. 73, 222

Bagniewski, W., Fennel, K., Perry, M. J., and D'Asaro, E. a. (2011). Optimizing models of the North Atlantic spring bloom using physical, chemical and bio-optical observations from a Lagrangian float. *Biogeosciences*, 8(5):1291–1307. 49

Balmford, A., Bruner, A., Cooper, P., Costanza, R., Farber, S., Green, R. E., Jenkins, M., Jefferiss, P., Jessamy, V., Madden, J., et al. (2002). Economic reasons for conserving wild nature. *science*, 297(5583):950–953. 10, 146

Banse, K. (1982). Mass-scaled rates of respiration and intrinsic growth in very small invertebrates. *Marine Ecology Progress Series*, 9(3):281–297. 14

Bardwell, L. (2005). A walk-through of the yeast mating pheromone response pathway. *Peptides*, 26(2):339–350. 231

Barton, A. D., Dutkiewicz, S., Flierl, G., Bragg, J., and Follows, M. J. (2010). Patterns of diversity in marine phytoplankton. *Science (New York, N.Y.)*, 327(5972):1509–11. 15, 61, 110, 118, 119, 121, 150, 153, 219, 225

Bates, S. S., Garrison, D. L., and Horner, R. A. (1998). *Bloom dynamics and physiology of domoic-acid-producing Pseudo-nitzschia species*, volume 41. Citeseer. 25

Beardall, J. and Raven, J. A. (2004). The potential effects of global climate change on microalgal photosynthesis, growth and ecology. *Phycologia*, 43(1):26–40. 2

Beardall, J. and Stojkovic, S. (2006). Microalgae under global environmental change: implications for growth and productivity, populations and trophic flow. *ScienceAsia*, 32(s1):001–010. 2

Becking, L. G. M. B. (1934). *Geobiologie, of Inleiding Tot de Milieukunde: Met Literatuurlijst en Ind.* Van Stockum. 134

Becks, L., Ellner, S. P., Jones, L. E., and Hairston, N. G. (2012). The functional genomics of an eco-evolutionary feedback loop: linking gene expression, trait evolution, and community dynamics. *Ecology letters*, 15(5):492–501. 312

Becks, L., Hilker, F. M., Malchow, H., Jürgens, K., and Arndt, H. (2005). Experimental demonstration of chaos in a microbial food web. *Nature*, 435(7046):1226–9. 9

Behl, S., Donval, A., Stibor, H., et al. (2011). The relative importance of species diversity and functional group diversity on carbon uptake in phytoplankton communities. *Limnology and Oceanography*, 56(2):683–694. 4, 11

Behrenfeld, M. J. (2010). Abandoning Sverdrup's Critical Depth Hypothesis on phytoplankton blooms. *Ecology*, 91(4):977–89. 155

Behrenfeld, M. J., Randerson, J. T., McClain, C. R., Feldman, G. C., Los, S. O., Tucker, C. J., Falkowski, P. G., Field, C. B., Frouin, R., Esaias, W. E., et al. (2001). Biospheric primary production during an ENSO transition. *Science*, 291(5513):2594–2597. 2

Beijerinck, M. (1913). De infusies ende ontdekking der bacteriën. *Amsterdam, The Netherlands*. 134

Béja, O., Spudich, E. N., Spudich, J. L., Leclerc, M., and DeLong, E. F. (2001). Proteorhodopsin phototrophy in the ocean. *Nature*, 411(6839):786–789. 100

Bell, G. and Gonzalez, A. (2009). Evolutionary rescue can prevent extinction following environmental change. *Ecology Letters*, 12(9):942–948. 312

Benincà, E., Huisman, J., Heerkloss, R., Jöhnk, K. D., Branco, P., Van Nes, E. H., Scheffer, M., and Ellner, S. P. (2008). Chaos in a long-term experiment with a plankton community. *Nature*, 451(7180):822–5. 6, 9, 256

Berges, J. and Falkowski, P. (1998). Physiological stress and cell death in marine phytoplankton: induction of proteases in response to nitrogen or light limitation. *Limnology and Oceanography*, 43:129–135. 28

Bergkvist, J., Thor, P., Jakobsen, H. H., Wängberg, S.-Å., and Selander, E. (2012). Grazer-induced chain length plasticity reduces grazing risk in a marine diatom. *Limnology and Oceanography*, 57(1):318–324. 311

Bidle, K. and Falkowski, P. (2004). Cell death in planktonic, photosynthetic microorganisms. *Nature Reviews Microbiology*, 2:643–655. 28

Blackburn, S. and Parker, N. (2005). Microalgal life cycles: encystment and excystment. *Algal Culturing Techniques: A Book for All Phycologists*, pages 399–417. 231

Blackford, J., Allen, J., and Gilbert, F. (2004). Ecosystem dynamics at six contrasting sites: a generic modelling study. *Journal of Marine Systems*, 52(1):191–215. 16

Bopp, L., Aumont, O., Cadule, P., Alvain, S., and Gehlen, M. (2005). Response of diatoms distribution to global warming and potential implications: A global model study. *Geophysical Research Letters*, 32(19). 146

Bopp, L., Monfray, P., Aumont, O., Dufresne, J.-L., Le Treut, H., Madec, G., Terray, L., and Orr, J. C. (2001). Potential impact of climate change on marine export production. *Global Biogeochemical Cycles*, 15(1):81–99. 159

Bopp, L., Resplandy, L., Orr, J. C., Doney, S. C., Dunne, J. P., Gehlen, M., Halloran, P., Heinze, C., Ilyina, T., Séférian, R., Tjiputra, J., and Vichi, M. (2013). Multiple stressors of ocean ecosystems in the 21st century: projections with CMIP5 models. *Biogeosciences Discussions*, 10(2):3627–3676. 316

Boss, E. and Behrenfeld, M. (2010). *In situ* evaluation of the initiation of the North Atlantic phytoplankton bloom. *Geophysical Research Letters*, 37(18). 99

Bouman, H. A., Ulloa, O., Scanlan, D. J., Zwirglmaier, K., Li, W. K., Platt, T., Stuart, V., Barlow, R., Leth, O., Clementson, L., et al. (2006). Oceanographic basis of the global surface distribution of prochlorococcus ecotypes. *Science*, 312(5775):918–921. 100

Boyd, P. W. and Doney, S. C. (2002). Modelling regional responses by marine pelagic ecosystems to global climate change. *Geophysical Research Letters*, 29(16):53–1. 146

Boyd, P. W., Lennartz, S. T., Glover, D. M., and Doney, S. C. (2015). Biological ramifications of climate-change-mediated oceanic multi-stressors. *Nature Climate Change*, 5(1):71–79. 314

Boyer, T. P., Antonov, J. I., Baranova, O. K., Garcia, H. E., Johnson, D. R., Mishonov, A. V., O'Brien, T. D., Seidov, D., Smolyar, I., Zweng, M. M., et al. (2013). *World Ocean Database 2013*. 49, 65, 98

Bracco, A., Provenzale, A., and Scheuring, I. (2000). Mesoscale vortices and the paradox of the plankton. *Proceedings of the Royal Society of London B: Biological Sciences*, 267(1454):1795–1800. 225

Brand, L. and Guillard, R. (1981). The effects of continuous light and light intensity on the reproduction rates of twenty-two species of marine phytoplankton. *Journal of Experimental Marine Biology and Ecology*, 50(2):119–132. 49

Breitbart, M. (2012). Marine viruses: truth or dare. *Marine Science*, 4. 100, 311

Brock, T. D. (1981). Calculating solar radiation for ecological studies. *Ecological modelling*, 14(1):1–19. 59

Broerse, A. T., Ziveri, P., van Hinte, J. E., and Honjo, S. (2000). Coccolithophore export production, species composition, and coccolith-$CaCO_3$ fluxes in the NE Atlantic (34°N 21°W and 48°N 21°W). *Deep Sea Research Part II: Topical Studies in Oceanography*, 47(9):1877–1905. 71, 97

Brose, U. (2008). Complex food webs prevent competitive exclusion among producer species. *Proceedings of the Royal Society B: Biological Sciences*, 275(1650):2507–2514. 9

Bruggeman, J. and Kooijman, S. A. L. M. (2007). A biodiversity-inspired approach to aquatic ecosystem modeling. *Methods*, 52(4):1533–1544. 14, 16, 30, 103, 152, 218, 257

Brussaard, C. P., Noordeloos, A. A., and Riegman, R. (1997). Autolysis kinetics of the marine diatom *Ditylum brightwellii* (bacillariophyceae) under nitrogen and phosphorus limitation and starvation. *Journal of Phycology*, 33(6):980–987. 28

Buesseler, K. O., Bacon, M. P., Cochran, J. K., and Livingston, H. D. (1992). Carbon and nitrogen export during the jgofs north atlantic bloom experiment estimated from 234 th: 238 u disequilibria. *Deep Sea Research Part A. Oceanographic Research Papers*, 39(7):1115–1137. 97

Cadotte, M. W. (2006). Dispersal and species diversity: A meta-analysis. *The American Naturalist*, 167(6):913–924. 153

Cardinale, B. J., Duffy, J. E., Gonzalez, A., Hooper, D. U., Perrings, C., Venail, P., Narwani, A., Mace, G. M., Tilman, D., Wardle, D. A., Kinzig, A. P., Daily, G. C., Loreau, M., Grace, J. B., Larigauderie, A., Srivastava, D. S., and Naeem, S. (2012). Biodiversity loss and its impact on humanity. *Nature*, 486(7401):59–67. 2, 10, 218

Cardinale, B. J., Ives, A. R., and Inchausti, P. (2004). Effects of species diversity on the primary productivity of ecosystems: extending our spatial and temporal scales of inference. *Oikos*, 104(3):437–450. 11

Cardinale, B. J., Matulich, K. L., Hooper, D. U., Byrnes, J. E., Duffy, E., Gamfeldt, L., Balvanera, P., O'Connor, M. I., and Gonzalez, A. (2011). The functional role of producer diversity in ecosystems. *American Journal of Botany*, 98(3):572–592. 10, 11, 146

Cardinale, B. J., Palmer, M. A., and Collins, S. L. (2002). Species diversity enhances ecosystem functioning through interspecific facilitation. *Nature*, 415(6870):426–429. 11

Cardinale, B. J., Srivastava, D. S., Duffy, J. E., Wright, J. P., Downing, A. L., Sankaran, M., and Jouseau, C. (2006). Effects of biodiversity on the functioning of trophic groups and ecosystems. *Nature*, 443(7114):989–992. 146

Caron, D. and Countway, P. (2009). Hypotheses on the role of the protistan rare biosphere in a changing world. *Aquatic Microbial Ecology*, 57(3):227–238. 11, 107

Carter, C., Ross, A., Schiel, D., Howard-Williams, C., and Hayden, B. (2005). *In situ* microcosm experiments on the influence of nitrate and light on phytoplank-

ton community composition. *Journal of Experimental Marine Biology and Ecology*, 326(1):1–13. 96

Cermeño, P., De Vargas, C., Abrantes, F., and Falkowski, P. G. (2010). Phytoplankton biogeography and community stability in the ocean. *PloS ONE*, 5(4):e10037. 15

Cermeño, P., Dutkiewicz, S., Harris, R. P., Follows, M., Schofield, O., and Falkowski, P. G. (2008). The role of nutricline depth in regulating the ocean carbon cycle. *Proceedings of the National Academy of Sciences*, 105(51):20344–20349. 5, 160

Chambouvet, A., Alves-de Souza, C., Cueff, V., Marie, D., Karpov, S., and Guillou, L. (2011). Interplay between the parasite amoebophrya sp.(alveolata) and the cyst formation of the red tide dinoflagellate scrippsiella trochoidea. *Protist*, 162(4):637–649. 310

Chase, J. M. and Leibold, M. A. (2003). *Ecological niches: linking classical and contemporary approaches.* University of Chicago Press. 256

Chavez, F. P., Ryan, J., Lluch-Cota, S. E., and Ñiquen, M. (2003). From anchovies to sardines and back: multidecadal change in the pacific ocean. *Science*, 299(5604):217–221. 218

Chepurnov, V. A., Mann, D. G., Sabbe, K., Vannerum, K., Casteleyn, G., Verleyen, E., Peperzak, L., and Vyverman, W. (2005). Sexual reproduction, mating system, chloroplast dynamics and abrupt cell size reduction in *Pseudo-nitzschia pungens* from the North Sea (Bacillariophyta). *European Journal of Phycology*, 40(4):379–395. 20, 23, 34, 231, 251, 257, 296

Chepurnov, V. A., Mann, D. G., Sabbe, K., and Vyverman, W. (2004). Experimental studies on sexual reproduction in diatoms. *International review of cytology*, 237:91–154. 19, 22, 23, 24, 25, 26, 231

Cherie, M. (2012). Environmental marine metabolomics: from whole organism system biology to ecosystem management. *Journal of Marine Science Research & Development.* 310

Chesson, P. (2000). Mechanisms of maintenance of species diversity. *Annual review of Ecology and Systematics*, 31:343–366. 7, 8, 10, 148, 152

Chisholm, S. W. (1992). Phytoplankton size. In *Primary productivity and biogeochemical cycles in the sea*, pages 213–237. Springer. 96, 148

Chisholm, S. W. and Costello, J. C. (1980). Influence of environmental factors and population composition on the timing of cell division in *Thalassiosira fluviatilis* (bacillariophyceae) grown on light/dark cycles. *Journal of Phycology*, 16(3):375–383. 21

Christian, J., Verschell, M., Murtugudde, R., Busalacchi, A., and McClain, C. (2001). Biogeochemical modelling of the tropical pacific ocean. i: Seasonal and interannual variability. *Deep Sea Research Part II: Topical Studies in Oceanography*, 49(1):509–543. 99

Clayton, S., Dutkiewicz, S., Jahn, O., and Follows, M. J. (2013). Dispersal, eddies, and the diversity of marine phytoplankton. *Limnology and Oceanography: Fluids and Environments*, 3(1):182–197. 225

Cloern, J. E. and Dufford, R. (2005). Phytoplankton community ecology: principles applied in San Francisco Bay. *Marine Ecology Progress Series*, 285:11–28. 134, 312

Coelho, S. M., Simon, N., Ahmed, S., Cock, J. M., and Partensky, F. (2013). Ecological and evolutionary genomics of marine photosynthetic organisms. *Molecular ecology*, 22(3):867–907. 310

Connell, J. H. (1978). Diversity in tropical rain forests and coral reefs. *Science*, 199(4335):1302–1310. 6, 8

Côté, I. M. and Darling, E. S. (2010). Rethinking ecosystem resilience in the face of climate change. *PLoS Biology*, 8(7):e1000438. 316

Côte, P. and Whiteway, M. (2008). The role of *Candida albicans* FAR1 in regulation of pheromone-mediated mating, gene expression and cell cycle arrest. *Molecular Microbiology*, 68(2):392–404. 231

Cottingham, K., Brown, B., and Lennon, J. (2001). Biodiversity may regulate the temporal variability of ecological systems. *Ecology Letters*, 4(1):72–85. 316

Currie, D. J. (1991). Energy and large-scale patterns of animal-and plant-species richness. *American Naturalist*, pages 27–49. 4

Dahms, H. U. (1995). Dormancy in the copepoda - an overview. *Hydrobiologia*, 306(3):199–211. 231

Daily, G. (1997). Nature's services: societal dependence on natural ecosystems. 10, 146

Dakos, V., Benincà, E., van Nes, E. H., Philippart, C. J. M., Scheffer, M., and Huisman, J. (2009). Interannual variability in species composition explained as seasonally entrained chaos. *Proceedings. Biological sciences / The Royal Society*, 276(1669):2871–80. 6, 53, 135, 152, 256

Davidovich, N. A. and Bates, S. S. (1998a). Sexual reproduction in the pennate diatoms pseudo-nitzschia multiseries and p. pseudodelicatissima (bacillariophyceae). *Journal of Phycology*, 34(1):126–137. 232

Davidovich, N. A. and Bates, S. S. (1998b). Sexual reproduction in the pennate diatoms *Pseudo-nitzschia multiseries* and *P. pseudodelicatissima* (bacillariophyceae). *Journal of Phycology*, 34(1):126–137. 24

Davis, C., Harrison, P., and Dugdale, R. (1973). Continuous culture of marine diatoms under silicate limitation. I. Synchronized life cycle of *Skeletonema costatum*. *Journal of Phycology*, 9:175–180. pdf on diana. 26, 309

Davis, C., Hollibaugh, J., Seibert, D., Thomas, W., and Harrison, P. (1980a). Formation of resting spores by *Leptocylindrus danicus* (Bacillariophyceae) in a controlled experimental ecosystem. *Journal of Phycology*, 16:296–302. 27, 154

Davis, C. O., Hollibaugh, J. T., Seibert, D. L., Thomas, W. H., and Harrison, P. J. (1980b). Formation of resting spores by leptocylindrus danicus (bacillariophyceae) in a controlled experimental ecosystem1. *Journal of Phycology*, 16(2):296–302. 297

De Benedictis, P. A. (1973). On the correlations between certain diversity indices. *American Naturalist*, pages 295–302. 3

de Boyer Montegut, C., Madec, G., Fischer, A. S., Lazar, A., and Iudicone, D. (2004). Mixed layer depth over the global ocean: An examination of profile data and a profile-based climatology. *Journal of Geophysical Research: Oceans (1978–2012)*, 109(C12). 67, 159, 161, 162, 163, 164

De Groot, R. S., Wilson, M. A., and Boumans, R. M. (2002). A typology for the classification, description and valuation of ecosystem functions, goods and services. *Ecological Economics*, 41(3):393–408. 2

De Martino, A., Meichenin, A., Shi, J., Pan, K., and Bowler, C. (2007). Genetic and phenotypic characterization of *Phaeodactylum tricornutum* (Bacillariophyceae) accessions. *Journal of Phycology*, 43(5):992–1009. 21

de Vargas, C., Audic, S., Henry, N., Decelle, J., Mahé, F., Logares, R., Lara, E., Berney, C., Le Bescot, N., Probert, I., et al. (2015). Eukaryotic plankton diversity in the sunlit ocean. *Science*, 348(6237):1261605. 310

Dearman, J., Taylor, A., and Davidson, K. (2003). Influence of autotroph model complexity on simulations of microbial communities in marine mesocosms. *Marine Ecology Progress Series*, 250:13–28. 151

Decelle, J., Probert, I., Bittner, L., Desdevises, Y., Colin, S., de Vargas, C., Galí, M., Simó, R., and Not, F. (2012). An original mode of symbiosis in open ocean plankton. *Proceedings of the National Academy of Sciences*, 109(44):18000–18005. 310

Doney, S. C. (1999). Major challenges confronting marine biogeochemical modeling. *Global Biogeochemical Cycles*, 13(3):705–714. 151

Drebes, G. (1966). On the life history of the marine plankton diatom *Stephanopyxis palmeriana*. *Helgolander wissenschaftilche Meeresuntersuchungen*, 13:104–114. 23

Drebes, G. (1977a). *Sexuality. In The biology of diatoms. (Ed. by D. Werner)*. Blackwell Scientific Publications, Oxford. 20, 23, 25

Drebes, G. (1977b). *Sexuality:[The biology of diatoms: chapter 9]*. Blackwell. 19, 25

Drebes, G. (1977c). *Sexuality:[The biology of diatoms: chapter 9]*. Blackwell. 309

Duffy, J., Stachowicz, J. J., et al. (2006). Why biodiversity is important to oceanography: potential roles of genetic, species, and trophic diversity in pelagic ecosystem processes. *Marine Ecology Progress Series*, 311:179–189. 2, 11, 12, 107, 146

Duffy, M. A., Hall, S. R., Cáceres, C. E., and Ives, A. R. (2009). Rapid evolution, seasonality, and the termination of parasite epidemics. *Ecology*, 90(6):1441–1448. 312

Dunlop, E. S., Heino, M., and Dieckmann, U. (2009). Eco-genetic modeling of contemporary life-history evolution. *Ecological Applications*, 19(7):1815–1834. 310

Durbin, E. G. (1977). Studies on the autecology of the marine diatom *Thalassiosira nordenskioeldii*. Ii. The influence of cell size on growth rate, and carbon, nitrogen, chlorophyll *a* and silica content. *Journal of Phycology*, 13(2):150–155. 21

Durham, W. M. and Stocker, R. (2012). Thin phytoplankton layers: characteristics, mechanisms, and consequences. *Annual Review of Marine Science*, 4:177–207. 250, 313

Dutkiewicz, S., Follows, M., and Bragg, J. G. (2009). Modeling the coupling of ocean ecology and biogeochemistry. *Global Biogeochemical Cycles*, 23(4). 30, 31, 51, 118, 119, 153

DAlelio, D., Amato, A., Luedeking, A., and Montresor, M. (2009). Sexual and vegetative phases in the planktonic diatom *Pseudo-nitzschia multistriata*. *Harmful Algae*, 8(2):225–232. 20, 23, 24, 25

Edlund, M. B. and Stoermer, E. F. (1997). Ecological, evolutionary, and systematic significance of diatom life histories. *Journal of Phycology*, 33(6):897–918. 17, 19, 23, 30, 231

Edwards, A. M. and Yool, A. (2000). The role of higher predation in plankton population models. *Journal of Plankton Research*, 22(6):1085–1112. 47

Edwards, K. F., Thomas, M. K., Klausmeier, C. A., and Litchman, E. (2012). Allometric scaling and taxonomic variation in nutrient utilization traits and maximum

growth rate of phytoplankton. *Limnology and Oceanography*, 57(2):554–566. 224, 311

Ellner, S. P. and Becks, L. (2011). Rapid prey evolution and the dynamics of two-predator food webs. *Theoretical Ecology*, 4(2):133–152. 312

Ellner, S. P., Geber, M. A., and Hairston, N. G. (2011). Does rapid evolution matter? measuring the rate of contemporary evolution and its impacts on ecological dynamics. *Ecology Letters*, 14(6):603–614. 312

Estep, K. W., Davis, P. G., Keller, M. D., and Sieburth, J. M. (1986). How important are oceanic algal nanoflagellates in bacterivory? 1. *Limnology and oceanography*, 31(3):646–650. 310

Evans, C. and Wilson, W. H. (2008). Preferential grazing of oxyrrhis marina on virus infected emiliania huxleyi. *Limnology and Oceanography*, 53(5):2035–2040. 101, 311

Evans, G. T. and Parslow, J. S. (1985). A model of annual plankton cycles. *Biological oceanography*, 3(3):327–347. 43, 44, 45, 58, 60

Falciatore, A. and Bowler, C. (2002). Revealing the molecular secrets of marine diatoms. *Annual Review of Plant Biology*, 53(1):109–130. 310

Falkowski, P. and Wirick, C. (1981). A simulation model of the effects of vertical mixing on primary productivity. *Marine Biology*, 65(1):69–75. 44, 45

Falkowski, P. G., Barber, R. T., and Smetacek, V. (1998). Biogeochemical controls and feedbacks on ocean primary production. *Science*, 281(5374):200–206. 2, 10, 11, 107, 146

Falkowski, P. G., Katz, M. E., Knoll, A. H., Quigg, A., Raven, J. A., Schofield, O., and Taylor, F. (2004). The evolution of modern eukaryotic phytoplankton. *science*, 305(5682):354–360. 99

Falkowski, P. G. and Oliver, M. J. (2007). Mix and match: how climate selects phytoplankton. *Nature Reviews. Microbiology*, 5(10):813–819. 2

Falkowski, P. G. and Raven, J. A. (2013). *Aquatic photosynthesis.* Princeton University Press. 99

Fasham, M. (1995). Variations in the seasonal cycle of biological production in subarctic oceans: A model sensitivity analysis. *Deep Sea Research Part I: Oceanographic Research Papers*, 42(7):1111–1149. 98

Fasham, M. J. (1993). Modelling the marine biota. In *The global carbon cycle*, pages 457–504. Springer. 47, 49, 56

Fasham, M. J. R., Ducklow, H. W., and McKelvie, S. M. (1990). A nitrogen-based model of plankton dynamics in the oceanic mixed layer. *Journal of Marine Research*, 48(3):591–639. 43, 44, 45, 46, 49, 58, 60, 98, 216

Fennel, K. and Boss, E. (2003). Subsurface maxima of phytoplankton and chlorophyll: Steady-state solutions from a simple model. *Limnology and Oceanography*, 48(4):1521–1534. 98, 99

Fernandez, E., Boyd, P., Holligan, P., and Harbour, D. (1993). Production of organic and inorganic carbon within a large-scale coccolithophore bloom in the northeast atlantic ocean. *Marine Ecology Progress Series*, 97:271–285. 91, 210

Fiksen, O. (2000). The adaptive timing of diapause a search for evolutionarily robust strategies in *Calanus finmarchicus*. *ICES Journal of Marine Science*, 57(6):1825–1833. 54

Finkel, Z. V. (2001). Light absorption and size scaling of light-limited metabolism in marine diatoms. *Limnology and Oceanography*, 46(1):86–94. 12, 14

Finkel, Z. V. and Irwin, A. J. (2000). Modeling size-dependent photosynthesis: light absorption and the allometric rule. *Journal of Theoretical Biology*, 204(3):361–9. 11, 49

Flynn, K. (2005). Castles built on sand: dysfunctionality in plankton models and the inadequacy of dialogue between biologists and modellers. *Journal of Plankton Research*, 27(12):1205–1210. 95

Follows, M. J. and Dutkiewicz, S. (2011). Modeling diverse communities of marine microbes. *Annual review of marine science*, 3:427–451. 13

Follows, M. J., Dutkiewicz, S., Grant, S., and Chisholm, S. W. (2007). Emergent biogeography of microbial communities in a model ocean. *Science (New York, N.Y.)*, 315(5820):1843–6. 14, 15, 30, 31, 39, 43, 45, 49, 51, 52, 53, 56, 91, 92, 103, 147, 151, 218, 265, 311

Fox, J. W. (2013). The intermediate disturbance hypothesis should be abandoned. *Trends in ecology & evolution*, 28(2):86–92. 9

Frada, M., Probert, I., Allen, M. J., Wilson, W. H., and de Vargas, C. (2008). The cheshire cat escape strategy of the coccolithophore emiliania huxleyi in response to viral infection. *Proceedings of the National Academy of Sciences*, 105(41):15944–15949. 257

French, F. W. and Hargraves, P. E. (1985). Spore formation in the life cycles of the diatoms chaetoceros diadema and leptocylindrus danicus1. *Journal of phycology*, 21(3):477–483. 26, 309

French III, F. and Hargraves, P. (1985). Spore formation in the life cycles of the diatoms *Chaetoceros diadema* and *Leptocylindrus danicus*. *Journal of Phycology*, 21:477–483. 23, 27

Fuchs, N., Scalco, E., Kooistra, W. H., Assmy, P., and Montresor, M. (2013). Genetic characterization and life cycle of the diatom fragilariopsis kerguelensis. *European Journal of Phycology*, 48(4):411–426. 23, 232

Fuhrman, J. A., Steele, J. A., Hewson, I., Schwalbach, M. S., Brown, M. V., Green, J. L., and Brown, J. H. (2008). A latitudinal diversity gradient in planktonic marine bacteria. *Proceedings of the National Academy of Sciences*, 105(22):7774–7778. 5

Fulton, E. A., Parslow, J. S., Smith, A. D., and Johnson, C. R. (2004). Biogeochemical marine ecosystem models ii: the effect of physiological detail on model performance. *Ecological Modelling*, 173(4):371–406. 101, 224

Furnas, M. (1985). Diel synchronization of sperm formation in the diatom *Chaetoceros curvisetus Cleve*. *Journal of Phycology*, 21:667–671. 25

Fussmann, G., Loreau, M., and Abrams, P. (2007). Eco-evolutionary dynamics of communities and ecosystems. *Functional Ecology*, 21(3):465–477. 312

Gallagher, J. (1983). Cell enlargement in *Skeletonema costatum* (Bacillariophyceae). *Journal of Phycology*, 19:539–542. 26

Gamfeldt, L., Hillebrand, H., and Jonsson, P. (2005). Species richness changes across two trophic levels simultaneously affect prey and consumer biomass. *Ecology Letters*, 8(7):696–703. 12

Garside, C. and Garside, J. (1993). The f-ratio on 20 w during the north atlantic bloom experiment. *Deep Sea Research Part II: Topical Studies in Oceanography*, 40(1):75–90. 97

Gause, G. (1934). The struggle for existence. 6, 99, 148

Geider, R., MacIntyre, H., and Kana, T. (1997). Dynamic model of phytoplankton growth and acclimation: responses of the balanced growth rate and the chlorophyll a: carbon ratio to light, nutrient-limitation and temperature. *Oceanographic Literature Review*, 9(44):974. 71

Gentleman, W., Leising, A., Frost, B., Strom, S., and Murray, J. (2003). Functional responses for zooplankton feeding on multiple resources: a review of assumptions and biological dynamics. *Deep Sea Research Part II: Topical Studies in Oceanography*, 50(22):2847–2875. 46, 47

Ghilarov, A. (1996). What does biodiversitymeanscientific problem or convenient myth? *Trends in ecology & evolution*, 11(7):304–306. 3

Gillard, J., Frenkel, J., Devos, V., Sabbe, K., Paul, C., Rempt, M., Inzé, D., Pohnert, G., Vuylsteke, M., and Vyverman, W. (2013). Metabolomics enables the structure elucidation of a diatom sex pheromone. *Angewandte Chemie International Edition*, 52(3):854–857. 25, 253

Gilpin, M. E. (1975). Limit cycles in competition communities. *American Naturalist*, pages 51–60. 9

Giovagnetti, V., Cataldo, M. L., Conversano, F., and Brunet, C. (2012). Growth and photophysiological responses of two picoplanktonic minutocellus species, strains rcc967 and rcc703 (bacillariophyceae). *European Journal of Phycology*, 47(4):408–420. 257

Gismervik, I. and Andersen, T. (1997). Prey switching by acartia clausi: experimental evidence and implications of intraguild predation assessed by a model. *Marine Ecology Progress Series*, 157:247–259. 46

Gitav, H. and Noble, I. (1997). What are functional types and how should we seek them? *Plant functional types: their relevance to ecosystem properties and global change*, 1(3). 4

Godhe, A., Kremp, A., and Montresor, M. (2014). Genetic and microscopic evidence for sexual reproduction in the centric diatom *Skeletonema marinoi*. *Protist.* 22, 232

Graham, D. W., Knapp, C. W., Van Vleck, E. S., Bloor, K., Lane, T. B., and Graham, C. E. (2007). Experimental demonstration of chaotic instability in biological nitrification. *The ISME journal*, 1(5):385–393. 9

Gregg, W. W., Ginoux, P., Schopf, P. S., and Casey, N. W. (2003). Phytoplankton and iron: validation of a global three-dimensional ocean biogeochemical model. *Deep Sea Research Part II: Topical Studies in Oceanography*, 50(22):3143–3169. 39, 49, 71, 91, 102, 146, 147, 151, 265

Grinnell, J. (1904). The origin and distribution of the chest-nut-backed chickadee. *The Auk*, 21(3):364–382. 297

Große, F., Lindemann, C., Pätsch, J., and Backhaus, J. O. (2015). The influence of winter convection on primary production: A parameterisation using a hydrostatic three-dimensional biogeochemical model. *Journal of Marine Systems*, 147:138–152. 222

Grover, J. P. (1991). Resource competition in a variable environment: phytoplankton growing according to the variable-internal-stores model. *American Naturalist*, pages 811–835. 14

Guillard, R. (1980). *Division rates. In Handbook of Phycological Methods.* Cambridge Univ Press. 235

Guillou, L., Viprey, M., Chambouvet, A., Welsh, R., Kirkham, A., Massana, R., Scanlan, D. J., and Worden, A. (2008). Widespread occurrence and genetic diversity of marine parasitoids belonging to syndiniales (alveolata). *Environmental Microbiology*, 10(12):3349–3365. 310

Haaber, J. and Middelboe, M. (2009). Viral lysis of phaeocystis pouchetii: implications for algal population dynamics and heterotrophic c, n and p cycling. *The ISME journal*, 3(4):430–441. 100, 101, 311

Hairston, N. G., Ellner, S. P., Geber, M. A., Yoshida, T., and Fox, J. A. (2005). Rapid evolution and the convergence of ecological and evolutionary time. *Ecology Letters*, 8(10):1114–1127. 312

Hamm, C. and Smetacek, V. (2007). *Armor: why, when, and how.* Boston, Elsevier. 17

Hamm, C. E., Merkel, R., Springer, O., Jurkojc, P., Maier, C., Prechtel, K., and Smetacek, V. (2003). Architecture and material properties of diatom shells provide effective mechanical protection. *Nature*, 421(6925):841–843. 5

Hamm, C. E., Simson, D. A., Merkel, R., and Smetacek, V. (1999). Colonies of phaeocystis globosa are protected by a thin but tough skin. *Marine ecology. Progress series*, 187:101–111. 257

Hansen, H. and Grasshoff, K. (1983). *Automated chemical analysis. In Methods of seawater analysis.* Verlag Chemie, Weinheim. 235

Hanski, I. and Hanski, I. A. (1999). *Metapopulation ecology*, volume 232. Oxford University Press Oxford. 134

Hardin, G. et al. (1960). The competitive exclusion principle. *Science*, 131(3409):1292–1297. 6, 103, 150

Harper, J. L. and Hawksworth, D. L. (1994). Biodiversity: measurement and estimation. *Philosophical transactions of the Royal Society of London. Series B, Biological Sciences*, 345(1311):5–12. 3

Hartmann, M., Grob, C., Tarran, G. A., Martin, A. P., Burkill, P. H., Scanlan, D. J., and Zubkov, M. V. (2012). Mixotrophic basis of atlantic oligotrophic ecosystems. *Proceedings of the National Academy of Sciences*, 109(15):5756–5760. 310

Hastings, A. and Powell, T. (1991). Chaos in a three-species food chain. *Ecology*, 72:896–903. 9

Havskum, H. and Riemann, B. (1996). Ecological importance of bacterivorous, pigmented flagellates(mixotrophs) in the bay of aarhus, denmark. *Marine Ecology Progress Series*, 137(1):251–263. 224

Heerkloss, R. and Klinkenberg, G. (1998). A long-term series of a planktonic foodweb: a case of chaotic dynamics. *Verhandlungen des Internationalen Verein Limnologie*, 26:1952–1956. 9

Hendry, A. P. and Kinnison, M. T. (1999). Perspective: the pace of modern life: measuring rates of contemporary microevolution. *Evolution*, pages 1637–1653. 312

Hildebrand, M., Frigeri, L. G., and Davis, A. K. (2007). Synchronized growth of *Thalassiosira pseudonana* (Bacillariophyceae) provides novel insights into cell-wall synthesis processes in relation to the cell cycle. *Journal of Phycology*, 43(4):730–740. 21

Hill, M. O. (1973). Diversity and evenness: a unifying notation and its consequences. *Ecology*, pages 427–432. 2, 3, 107

Hillebrand, H. (2004). On the generality of the latitudinal diversity gradient. *The American Naturalist*, 163(2):192–211. 4

Hilligsøe, K. M., Richardson, K., Bendtsen, J., Sørensen, L.-L., Nielsen, T. G., and Lyngsgaard, M. M. (2011). Linking phytoplankton community size composition

with temperature, plankton food web structure and sea–air CO2. *Deep Sea Research Part I: Oceanographic Research Papers*, 58(8):826–838. 11, 108

Hilton, J. A., Foster, R. A., Tripp, H. J., Carter, B. J., Zehr, J. P., and Villareal, T. A. (2013). Genomic deletions disrupt nitrogen metabolism pathways of a cyanobacterial diatom symbiont. *Nature communications*, 4:1767. 310

Hind, A., Gurney, W. S., Heath, M., and Bryant, A. (2000). Overwintering strategies in calanus finmarchicus. *Marine ecology. Progress series*, 193:95–107. 54

Hirche, H.-J. (1996). Diapause in the marine copepod, calanus finmarchicusa review. *Ophelia*, 44(1-3):129–143. 53, 155

Hoegh-Guldberg, O. and Bruno, J. F. (2010). The impact of climate change on the worlds marine ecosystems. *Science*, 328(5985):1523–1528. 316

Holtermann, K. E., Bates, S. S., Trainer, V. L., Odell, A., and Virginia Armbrust, E. (2010). Mass Sexual Reproduction in the Toxigenic Diatoms Pseudo-Nitzschia Australis and P. Pungens (Bacillariophyceae) on the Washington Coast, Usa1. *Journal of Phycology*, 46(1):41–52. 249

Honjo, S. and Okada, H. (1974). Community structure of coccolithophores in the photic layer of the mid-pacific. *Micropaleontology*, 20(2):209–230. 5

Hood, R., Laws, E., Follows, M., and Siegel, D. (2006). Modeling and prediction of marine microbial populations in the genomic era. *Oceanography*, 20(2):155–165. 30, 94, 102, 146, 297

Hooper, D., Chapin III, F., Ewel, J., Hector, A., Inchausti, P., Lavorel, S., Lawton, J., Lodge, D., Loreau, M., Naeem, S., et al. (2005). Effects of biodiversity on ecosystem functioning: a consensus of current knowledge. *Ecological monographs*, 75(1):3–35. 4, 10, 11, 146

Hubbell, S. P. (2001). *The unified neutral theory of biodiversity and biogeography (MPB-32)*, volume 32. Princeton University Press. 10, 256

Huisman, J., Johansson, A. M., Folmer, E. O., and Weissing, F. J. (2001). Towards a solution of the plankton paradox: the importance of physiology and life history. *Ecology Letters*, 4(5):408–411. 6, 9

Huisman, J., Jonker, R. R., Zonneveld, C., and Weissing, F. J. (1999a). Competition for light between phytoplankton species: experimental Ttsts of mechanistic theory. *Ecology*, 80(1):211. 5, 6, 9

Huisman, J., Sharples, J., Stroom, J. M., Visser, P. M., Kardinaal, W. E. A., Verspagen, J. M., and Sommeijer, B. (2004). Changes in turbulent mixing shift competition for light between phytoplankton species. *Ecology*, 85(11):2960–2970. 220

Huisman, J. and Sommeijer, B. (2002). Population dynamics of sinking phytoplankton in light-limited environments: simulation techniques and critical parameters. *Journal of Sea Research*, 48(2):83–96. 97

Huisman, J., Thi, N. N. P., Karl, D. M., and Sommeijer, B. (2006). Reduced mixing generates oscillations and chaos in the oceanic deep chlorophyll maximum. *Nature*, 439(7074):322–325. 45

Huisman, J., van Oostveen, P., and Weissing, F. J. (1999b). Critical depth and critical turbulence: two different mechanisms for the development of phytoplankton blooms. *Limnology and Oceanography*, 44(7):1781–1787. 73, 97

Huisman, J., van Oostveen, P., and Weissing, F. J. (1999c). Species dynamics in phytoplankton blooms: incomplete mixing and competition for light. *The American Naturalist*, 154(1):46–68. 97

Huisman, J. and Weissing, F. J. (1999). Biodiversity of plankton by species oscillations and chaos. *Nature*, 402(6760):407–410. 9

Huisman, J. and Weissing, F. J. (2001). Fundamental unpredictability in multispecies competition. *The American naturalist*, 157(5):488–94. 256

Huisman, J. and Weissing, F. J. (2002). Oscillations and chaos generated by competition for interactively essential resources. *Ecological Research*, 17(2):175–181. 9

Hurlbert, S. H. (1971). The nonconcept of species diversity: a critique and alternative parameters. *Ecology*, 52(4):577–586. 3, 107

Huston, M. A. (1997). Hidden treatments in ecological experiments: re-evaluating the ecosystem function of biodiversity. *Oecologia*, 110(4):449–460. 11

Hutchinson, G. (1961). The paradox of the plankton. *The American Naturalist*, 95(882):137–145. 5, 6, 30, 256, 297

Hutchinson, G. E. (1957). Cold spring harbor symposium on quantitative biology. *Concluding remarks*, 22:415–427. 11, 30, 256

Iglesias-Rodríguez, M. D., Brown, C. W., Doney, S. C., Kleypas, J., Kolber, D., Kolber, Z., Hayes, P. K., and Falkowski, P. G. (2002). Representing key phytoplankton functional groups in ocean carbon cycle models: Coccolithophorids. *Global Biogeochemical Cycles*, 16(4):47–1. 160, 227, 265

Irigoien, X. (2005). Phytoplankton blooms: a 'loophole' in microzooplankton grazing impact? *Journal of Plankton Research*, 27(4):313–321. 5

Irwin, A. J., Finkel, Z. V., Schofield, O. M., and Falkowski, P. G. (2006). Scaling-up from nutrient physiology to the size-structure of phytoplankton communities. *Journal of Plankton Research*, 28(5):459–471. 2, 14

Jassby, A. D. and Platt, T. (1976). Mathematical formulation of the relationship between photosynthesis and light for phytoplankton. 45

Jenkinson, I. R. and Wyatt, T. (1992). Selection and control of deborah numbers in plankton ecology. *Journal of plankton research*, 14(12):1697–1721. 300

Jeong, H. J., Du Yoo, Y., Kim, J. S., Seong, K. A., Kang, N. S., and Kim, T. H. (2010). Growth, feeding and ecological roles of the mixotrophic and heterotrophic dinoflagellates in marine planktonic food webs. *Ocean science journal*, 45(2):65–91. 224, 311

Jewson, D. (1992a). Life cycle of a *Stephanodiscus* sp. (Bacillariophyta). *Journal of Phycology*, 28:856–866. 21

Jewson, D. (1992b). Size reduction, reproductive strategy and the life strategy of a centric diatom. *Philosophical Transactions of the Royal Society of London. Serie B*, 336:191–213. 21

Joint, I., Pomroy, A., Savidge, G., and Boyd, P. (1993). Size-fractionated primary productivity in the northeast atlantic in may–july 1989. *Deep Sea Research Part II: Topical Studies in Oceanography*, 40(1):423–440. 156

Jolliff, J. K., Kindle, J. C., Shulman, I., Penta, B., Friedrichs, M. A., Helber, R., and Arnone, R. A. (2009). Summary diagrams for coupled hydrodynamic-ecosystem model skill assessment. *Journal of Marine Systems*, 76(1):64–82. 66

Jones, S. E. and Lennon, J. T. (2010). Dormancy contributes to the maintenance of microbial diversity. *Proceedings of the National Academy of Sciences of the United States of America*, 107(13):5881–6. 18, 31

Josey, S., Pascal, R., Taylor, P., and Yelland, M. (2003). A new formula for determining the atmospheric longwave flux at the ocean surface at mid-high latitudes. *Journal of Geophysical Research: Oceans (1978–2012)*, 108(C4). 59

Kaartvedt, S. (1996). Habitat preference during overwintering and timing of seasonal vertical migration of calanus finmarchicus. *Ophelia*, 44(1-3):145–156. 53

Károlyi, G., Péntek, Á., Scheuring, I., Tél, T., and Toroczkai, Z. (2000). Chaotic flow: the physics of species coexistence. *Proceedings of the National Academy of Sciences*, 97(25):13661–13665. 6, 10, 256

Kassen, R., Buckling, A., Bell, G., and Rainey, P. B. (2000). Diversity peaks at intermediate productivity in a laboratory microcosm. *Nature*, 406(6795):508–512. 5

Kawamiya, M., Kishi, M. J., and Suginohara, N. (2000). An ecosystem model for the North Pacific embedded in a general circulation model: Part I: Model description and characteristics of spatial distributions of biological variables. *Journal of Marine Systems*, 25(2):129–157. 12, 147

Keddy, P. A. (1992). Assembly and response rules: two goals for predictive community ecology. *Journal of Vegetation Science*, 3(2):157–164. 4

Kenitz, K., Williams, R. G., Sharples, J., Selsil, Ö., and Biktashev, V. N. (2013). The paradox of the plankton: species competition and nutrient feedback sustain phytoplankton diversity. *Marine Ecology Progress Series*, 490:107–119. 9

Kershaw, H. M. and Mallik, A. U. (2013). Predicting plant diversity response to disturbance: applicability of the intermediate disturbance hypothesis and mass ratio hypothesis. *Critical Reviews in Plant Sciences*, 32(6):383–395. 8

Kilham, P. and Hecky, R. E. (1988). Comparative ecology of marine and freshwater phytoplankton. *Limnology and Oceanography*, 33(4):776–795. 13

Kiørboe, T. (1993). Turbulence, phytoplankton cell size, and the structure of pelagic food webs. *Advances in Marine Biology*, 29:1–72. 160

Kirk, J. T. O. (1994). *Light and photosynthesis in aquatic ecosystems.* Cambridge university press. 49

Koen-Alonso, M. (2007). A process-oriented approach to the multispecies functional response. In *From energetics to ecosystems: the dynamics and structure of ecological systems*, pages 1–36. Springer. 46

Koester, J. A., Brawley, S. H., Karp-Boss, L., and Mann, D. G. (2007). Sexual reproduction in the marine centric diatom *Ditylum brightwellii* (Bacillariophyta). *European Journal of Phycology*, 42(4):351–366. pdf on diana. 26

Kooijman, S. (2001). Quantitative aspects of metabolic organization: a discussion of concepts. *Philosophical Transactions of the Royal Society of London. Series B: Biological Sciences*, 356(1407):331–349. 14

Kooistra, W., Gersonde, R., Medlin, L. K., Mann, D. G., Falkowski, P., and Knoll, A. (2007). The origin and evolution of the diatoms: their adaptation to a planktonic existence. *Evolution of primary producers in the sea*, pages 207–249. 18, 310

Kostka, J. E., Teske, A. P., Joye, S. B., and Head, I. M. (2014). The metabolic pathways and environmental controls of hydrocarbon biodegradation in marine ecosystems. *Frontiers in microbiology*, 5. 310

Langdon, C. (1988). On the causes of interspecific differences in the growth-irradiance relationship for phytoplankton. ii. a general review. *Journal of Plankton Research*, 10(6):1291–1312. 49

Laufkötter, C., Vogt, M., Gruber, N., Aita-Noguchi, M., Aumont, O., Bopp, L., Buitenhuis, E., Doney, S., Dunne, J., Hashioka, T., et al. (2015). Drivers and uncertainties of future global marine primary production in marine ecosystem models. *Biogeosciences Discussions*, 12(4):3731–3824. 314

Laws, E. A. (1975). The importance of respiration losses in controlling the size distribution of marine phytoplankton. *Ecology*, 56(2):419–426. 14

Laws, E. A., Falkowski, P. G., Smith, W. O., Ducklow, H., and McCarthy, J. J. (2000). Temperature effects on export production in the open ocean. *Global Biogeochemical Cycles*, 14(4):1231–1246. 2

Lehahn, Y., Koren, I., Schatz, D., Frada, M., Sheyn, U., Boss, E., Efrati, S., Rudich, Y., Trainic, M., Sharoni, S., et al. (2014). Decoupling physical from biological processes to assess the impact of viruses on a mesoscale algal bloom. *Current Biology*, 24(17):2041–2046. 100, 311

Leibold, M. A. and Norberg, J. (2004). Biodiversity in metacommunities: Plankton as complex adaptive systems? *Limnology and Oceanography*, 49(4):1278–1289. 15, 134, 152

Lelong, A., Hégaret, H., Soudant, P., and Bates, S. S. (2012). Pseudo-nitzschia (bacillariophyceae) species, domoic acid and amnesic shellfish poisoning: revisiting previous paradigms. *Phycologia*, 51(2):168–216. 251

Lennon, J. T. and Jones, S. E. (2011). Microbial seed banks: the ecological and evolutionary implications of dormancy. *Nature Reviews Microbiology*, 9(2):119–130. 257

Leonard, C. L., McClain, C. R., Murtugudde, R., Hofmann, E. E., and Harding, L. W. (1999). An iron-based ecosystem model of the central equatorial pacific. *Journal of Geophysical Research: Oceans (1978–2012)*, 104(C1):1325–1341. 99

Levin, S. A. (1970). Community equilibria and stability, and an extension of the competitive exclusion principle. *American Naturalist*, 104(939):413–423. 7, 8

Levin, S. A. (1998). Ecosystems and the biosphere as complex adaptive systems. *Ecosystems*, 1(5):431–436. 152

Levins, R. (1966). The strategy of model building in population biology. *American scientist*, 121(6):421–431. 94, 101, 157

Lévy, M., Resplandy, L., and Lengaigne, M. (2014). Oceanic mesoscale turbulence drives large biogeochemical interannual variability at middle and high latitudes. *Geophysical Research Letters*, 41(7):2467–2474. 10, 134, 153, 225, 313

Lewis Jr, W. M. (1983). Interruption of synthesis as a cost of sex in small organisms. *American Naturalist*, 121(6):825–833. 22, 34, 232, 252, 295

Lewis Jr, W. M. (1984). The diatom sex clock and its evolutionary significance. *American Naturalist*, 123(1):73–80. 24, 34, 232, 252, 299, 309

Litchman, E. (2010). Invisible invaders: non-pathogenic invasive microbes in aquatic and terrestrial ecosystems. *Ecology letters*, 13(12):1560–72. 297

Litchman, E., Edwards, K., Klausmeier, C., and Thomas, M. (2012). Phytoplankton niches, traits and eco-evolutionary responses to global environmental change. *Marine Ecology Progress Series*, 470:235–248. 257

Litchman, E. and Klausmeier, C. a. (2008). Trait-Based Community Ecology of Phytoplankton. *Annual Review of Ecology, Evolution, and Systematics*, 39(1):615–639. 12, 13, 14, 30, 253, 256, 260, 297

Litchman, E., Klausmeier, C. A., Miller, J. R., Schofield, O. M., and Falkowski, P. G. (2006). Multi-nutrient, multi-group model of present and future oceanic phytoplankton communities. *Biogeosciences*, 3(4):585–606. 17, 30, 45, 49, 52, 58, 59, 97, 100, 102, 146, 147, 218, 223, 265, 311

Litchman, E., Klausmeier, C. a., Schofield, O. M., and Falkowski, P. G. (2007). The role of functional traits and trade-offs in structuring phytoplankton communities:

scaling from cellular to ecosystem level. *Ecology letters*, 10(12):1170–81. 12, 13, 14, 257

Litchman, E., Ohman, M. D., and Kiorboe, T. (2013). Trait-based approaches to zooplankton communities. *Journal of Plankton Research*, 35(3):473–484. 297

Lochte, K., Ducklow, H., Fasham, M., and Stienen, C. (1993). Plankton succession and carbon cycling at 47 N 20 W during the JGOFS North Atlantic Bloom Experiment. *Deep Sea Research Part II: Topical Studies in Oceanography*, 40(1):91–114. 71, 96

Longhi, M. L. and Beisner, B. E. (2010). Patterns in taxonomic and functional diversity of lake phytoplankton. *Freshwater Biology*, 55(6):1349–1366. 4

Longhurst, A. and Dandonneau, Y. (1999). Ecological geography of the sea. *Nature*, 400(6743):423–423. 218

Longhurst, A., Sathyendranath, S., Platt, T., and Caverhill, C. (1995). An estimate of global primary production in the ocean from satellite radiometer data. *Journal of Plankton Research*, 17(6):1245–1271. 160

Loreau, M. (1998). Separating sampling and other effects in biodiversity experiments. *Oikos*, pages 600–602. 11

MacArthur, R. and Levins, R. (1967). The limiting similarity, convergence, and divergence of coexisting species. *American naturalist*, pages 377–385. 99

MacArthur, R. and Wilson, E. (1967). The theory of island biogeography. *Monographs in population biology*. 5, 11, 13, 15

Macdonald, J. D. (1869). On the structure of the diatomaceous frustule, and its genetic cycle. *Journal of Natural History*, 3(13):1–8. 19

Mackey, R. L. and Currie, D. J. (2001). The diversity-disturbance relationship: is it generally strong and peaked? *Ecology*, 82(12):3479–3492. 8

Magurran, A. E. and Magurran, A. E. (1988). *Ecological diversity and its measurement*, volume 168. Springer. 3

Mahadevan, A., D'Asaro, E., Lee, C., and Perry, M. J. (2012). Eddy-driven stratification initiates North Atlantic spring phytoplankton blooms. *Science (New York, N.Y.)*, 337(6090):54–8. 97

Manabe, S., Stouffer, R., Spelman, M., and Bryan, K. (1991). Transient responses of a coupled ocean-atmosphere model to gradual changes of atmospheric co2. part i. annual mean response. *Journal of Climate*, 4(8):785–818. 160

Manizza, M., Buitenhuis, E. T., and Le Quéré, C. (2010). Sensitivity of global ocean biogeochemical dynamics to ecosystem structure in a future climate. *Geophysical Research Letters*, 37(13). 146

Mann, D. (1993). Patterns of sexual reproduction in diatoms. In *Twelfth International Diatom Symposium*, pages 11–20. Springer. 34

Mann, D. and Marchant, H. (1989). *The origins of the diatom and its life cycle.* 21

Mann, D. G. (1999). The species concept in diatoms. *Phycologia*, 38(6):437–495. 18

Mann, D. G., Chepurnov, V. A., and Droop, S. J. (1999). Sexuality, incompatibility, size variation, and preferential polyandry in natural populations and clones of sellaphora pupula (bacillariophyceae). *Journal of Phycology*, 35(1):152–170. 20

Mann, D. G. and Poulíčková, A. (2010). Mating system, auxosporulation, species taxonomy and evidence for homoploid evolution in amphora (bacillariophyta). *Phycologia*, 49(2):183–201. 232

Mann, K. and Lazier, J. (2009). *Dynamics of marine ecosystems: biological-physical interactions in the oceans.* John Wiley & Sons. 218

Marcus, N. H. (1998). Minireview: The importance of benthic-pelagic coupling and the forgotten role of life cycles in coastal aquatic systems. *Limnology and Oceanography*, 43(5):763–768. 231

Margalef, R. (1968). Perspectives in ecological theory. 159

Margalef, R. (1974). Ecología, ed. *Omega, Barcelona*, 951:0–0. 30, 256

Margalef, R. (1978). Life-forms of phytoplankton as survival alternatives in an unstable environment. *Oceanologica acta*, 1(4):493–509. 12, 13, 95, 148, 160, 256

Martiny, J. B. H., Bohannan, B. J., Brown, J. H., Colwell, R. K., Fuhrman, J. A., Green, J. L., Horner-Devine, M. C., Kane, M., Krumins, J. A., Kuske, C. R., et al. (2006). Microbial biogeography: putting microorganisms on the map. *Nature Reviews Microbiology*, 4(2):102–112. 5

May, R. M. (1975). Patterns of species abundance and diversity. *Ecology and evolution of communities*, pages 81–120. 3

May, R. M. and Leonard, W. J. (1975). Nonlinear aspects of competition between three species. *SIAM Journal on Applied Mathematics*, 29(2):243–253. 134

May, R. M. and Mac Arthur, R. H. (1972). Niche overlap as a function of environmental variability. *Proceedings of the National Academy of Sciences*, 69(5):1109–1113. 99

Maynard-Smith, J. (1978). *The evolution of sex*. Cambridge Univ Press. 232

McCann, K. S. (2000). The diversity–stability debate. *Nature*, 405(6783):228–233. 2, 10, 18

McGill, B. J., Enquist, B. J., Weiher, E., and Westoby, M. (2006). Rebuilding community ecology from functional traits. *Trends in Ecology & Evolution*, 21(4):178–85. 297

McGrady-Steed, J., Harris, P. M., and Morin, P. J. (1997). Biodiversity regulates ecosystem predictability. *Nature*, 390(6656):162–165. 316

McIntyre, S., Lavorel, S., Landsberg, J., and Forbes, T. (1999). Disturbance response in vegetation–towards a global perspective on functional traits. *Journal of Vegetation Science*, 10(5):621–630. 4

McKinney, M. L. and Drake, J. A. (2013). *Biodiversity dynamics: turnover of populations, taxa, and communities*. Columbia University Press. 3

McManus, M. a., Kudela, R. M., Silver, M. W., Steward, G. F., Donaghay, P. L., and Sullivan, J. M. (2007). Cryptic Blooms: Are Thin Layers the Missing Connection? *Estuaries and Coasts*, 31(2):396–401. 250

McManus, M. A., Kudela, R. M., Silver, M. W., Steward, G. F., Donaghay, P. L., and Sullivan, J. M. (2008). Cryptic blooms: are thin layers the missing connection? *Estuaries and Coasts*, 31(2):396–401. 313

McQuoid, M. and Hobson, L. (1996). Diatom resting stages. *Journal of Phycology*, 32:889–902. 26, 27, 154

Menden-Deuer, S. and Lessard, E. J. (2000). Carbon to volume relationships for dinoflagellates, diatoms, and other protist plankton. *Limnology and oceanography*, 45(3):569–579. 260

Michael, K., Min, C., Peter, R., Ulrich, S., and Anthony, L. (2005). A niche for cyanobacteria containing chlorophyll d. 100

Michaels, A. F. and Silver, M. W. (1988). Primary production, sinking fluxes and the microbial food web. *Deep Sea Research Part A. Oceanographic Research Papers*, 35(4):473–490. 2

Miki, T. and Jacquet, S. (2008). Complex interactions in the microbial world: underexplored key links between viruses, bacteria and protozoan grazers in aquatic environments. *Aquatic Microbial Ecology*, 51(2):195. 311

Miki, T. and Jacquet, S. (2010). Indirect interactions in the microbial world: specificities and similarities to plant–insect systems. *Population ecology*, 52(4):475–483. 311

Miller, A. D., Roxburgh, S. H., and Shea, K. (2011). How frequency and intensity shape diversity–disturbance relationships. *Proceedings of the National Academy of Sciences*, 108(14):5643–5648. 9

Mitra, A., Castellani, C., Gentleman, W. C., Jónasdóttir, S. H., Flynn, K. J., Bode, A., Halsband, C., Kuhn, P., Licandro, P., Agersted, M. D., et al. (2014). Bridging the gap

between marine biogeochemical and fisheries sciences; configuring the zooplankton link. *Progress in Oceanography*, 129:176–199. 47

Mittelbach, G. G., Schemske, D. W., Cornell, H. V., Allen, A. P., Brown, J. M., Bush, M. B., Harrison, S. P., Hurlbert, A. H., Knowlton, N., Lessios, H. A., et al. (2007). Evolution and the latitudinal diversity gradient: speciation, extinction and biogeography. *Ecology letters*, 10(4):315–331. 5

Mittelbach, G. G., Steiner, C. F., Scheiner, S. M., Gross, K. L., Reynolds, H. L., Waide, R. B., Willig, M. R., Dodson, S. I., and Gough, L. (2001). What is the observed relationship between species richness and productivity? *Ecology*, 82(9):2381–2396. 5

Mizuno, M. and Okuda, K. (1985). Seasonal change in the distribution of cell size of *Cocconeis scutellum* var. *ornata* (*Bacillariophyceae*) in relation to growth and sexual reproduction. *Journal of Phycology*, 21:547–553. 25

Mock, T. and Kirkham, A. (2012). What can we learn from genomics approaches in marine ecology? from sequences to eco-systems biology! *Marine Ecology*, 33(2):131–148. 310

Møller, E. F., Thor, P., and Nielsen, T. G. (2003). Production of doc by calanus finmarchicus, c. glacialis and c. hyperboreus through sloppy feeding and leakage from fecal pellets. *Marine Ecology Progress Series*, 262:185–191. 47

Monterey, G. and S, L. (1997). *Seasonal variability of mixed layer depth for the world ocean, NOAA Atlas NESDIS 14*. US Department of Commerce, National Oceanic and Atmospheric Administration, National Environmental Satellite, Data, and Information Service. 159

Montresor, M., Lewis, J., Subba Rao, D., et al. (2006). Phases, stages and shifts in the life cycles of marine phytoplankton. *Algal cultures, analogues of blooms and applications*, 1:91–129. 17, 30, 231

Moore, L. R., Post, A. F., Rocap, G., and Chisholm, S. W. (2002). Utilization of different nitrogen sources by the marine cyanobacteria *Prochlorococcus* and *Syne-*

chococcus. *Limnology and Oceanography*, 47(4):989–996. 39, 49, 91, 102, 146, 147, 151, 265

Morán, X. A. G., LÓPEZ-URRUTIA, Á., CALVO-DÍAZ, A., and Li, W. K. (2010). Increasing importance of small phytoplankton in a warmer ocean. *Global Change Biology*, 16(3):1137–1144. 146

Morel, A. (1988). Optical modeling of the upper ocean in relation to its biogenous matter content (case i waters). *Journal of Geophysical Research: Oceans (1978–2012)*, 93(C9):10749–10768. 100

Mouget, J. L., Gastineau, R., Davidovich, O., Gaudin, P., and Davidovich, N. A. (2009). Light is a key factor in triggering sexual reproduction in the pennate diatom *Haslea ostrearia*. *FEMS Microbiology Ecology*, 69(2):194–201. 25, 309

Mougi, a. and Kondoh, M. (2012). Diversity of interaction types and ecological community stability. *Science*, 337(6092):349–51. 6, 10

Mouquet, N. and Loreau, M. (2003). Community patterns in source-sink metacommunities. *The american naturalist*, 162(5):544–557. 153

Muhammad, I. (1983). An introduction to solar radiation. *Vancouver: Academic*. 59

Mullin, M. M. and Brooks, E. R. (1967). Laboratory culture, growth rate, and feeding behavior of a planktonic marine copepod. *Limnology Oceanogrophy*, 12(4):657–666. 231

Murphy, J. M., Sexton, D. M., Barnett, D. N., Jones, G. S., Webb, M. J., Collins, M., and Stainforth, D. A. (2004). Quantification of modelling uncertainties in a large ensemble of climate change simulations. *Nature*, 430(7001):768–772. 51, 103

Nagai, S., Hori, Y., Manabe, T., and Imai, I. (1995). Restoration of cell size by vegetative cell enlargement in *Coscinodiscus wailesii* (Bacillariophyceae). *Phycologia*, 34:533–535. 24, 26

Norberg, J. (2004). Biodiversity and ecosystem functioning: a complex adaptive systems approach. *Limnology and Oceanography*, 49(4):1269–1277. 16

Norberg, J., Swaney, D. P., Dushoff, J., Lin, J., Casagrandi, R., and Levin, S. A. (2001). Phenotypic diversity and ecosystem functioning in changing environments: a theoretical framework. *Proceedings of the National Academy of Sciences*, 98(20):11376–11381. 16, 152

Omand, M. M. and Mahadevan, A. (2014). Shape of the oceanic nitracline. *Biogeosciences Discussions*, 11(10):14729–14763. 98

Paasche, E. (1973). Silicon and the ecology of marine plankton diatoms. I. *Thalassiosira pseudonana* (Cyclotella nana) grown in a chemostat with silicate as limiting nutrient. *Marine Biology*, 19(2):117–126. 21

Painter, S., Henson, S., Forryan, A., Steigenberger, S., Klar, J., Stinchcombe, M., Rogan, N., Baker, A., Achterberg, E. P., and Moore, C. (2014). An assessment of the vertical diffusive flux of iron and other nutrients to the surface waters of the subpolar north atlantic ocean. *Biogeosciences*, 11(8):2113–2130. 71, 97, 98

Palmer, J. and Totterdell, I. (2001). Production and export in a global ocean ecosystem model. *Deep Sea Research Part I: Oceanographic Research Papers*, 48(5):1169–1198. 12, 147

Peeters, F., Kerimoglu, O., and Straile, D. (2012). Implications of seasonal mixing for phytoplankton production and bloom development. *Theoretical Ecology*, 6(2):115–129. 216

Penczykowski, R. M., Forde, S. E., and Duffy, M. A. (2011). Rapid evolution as a possible constraint on emerging infectious diseases. *Freshwater Biology*, 56(4):689–704. 312

Perruche, C., Rivière, P., Lapeyre, G., Carton, X., and Pondaven, P. (2011). Effects of surface quasi-geostrophic turbulence on phytoplankton competition and coexistence. *Journal of Marine Research*, 69(1):105–135. 225

Perruche, C., Rivière, P., Pondaven, P., and Carton, X. (2010). Phytoplankton competition and coexistence: Intrinsic ecosystem dynamics and impact of vertical mixing. *Journal of marine systems*, 81(1):99–111. 225

Petchey, O. L. and Gaston, K. J. (2006). Functional diversity: back to basics and looking forward. *Ecology letters*, 9(6):741–758. 4

Petchey, O. L., O'Gorman, E. J., and Flynn, D. F. (2009). A functional guide to functional diversity measures. *Biodiversity, ecosystem functioning, and human wellbeing An ecological and economic perspective*, pages 49–60. 4

Pfitzer, E. (1869). Uber den bau und zellteilung der diatomeen. *Botanische Zeitung*, 27:774–776. 19

Pierson, B. K., Sands, V. M., and Frederick, J. L. (1990). Spectral irradiance and distribution of pigments in a highly layered marine microbial mat. *Applied and environmental microbiology*, 56(8):2327–2340. 100

Platt, T., Gallegos, C., and Harrison, W. (1981). Photoinhibition of photosynthesis in natural assemblages of marine phytoplankton. *Journal of Marine Research*, 38:687–701. 45

Pomeroy, L. R. (2001). Caught in the food web: complexity made simple? *Scientia Marina*, 65(S2):31–40. 151

Pommier, T., Canbäck, B., Riemann, L., Boström, K. H., Simu, K., Lundberg, P., Tunlid, a., and Hagström, a. (2007). Global patterns of diversity and community structure in marine bacterioplankton. *Molecular Ecology*, 16(4):867–80. 4

Popova, E., Fasham, M., a.V. Osipov, and Ryabchenko, V. (1997). Chaotic behaviour of an ocean ecosystem model under seasonal external forcing. *Journal of Plankton Research*, 19(10):1495–1515. 45, 58, 94, 216

Poulíčková, A. and Mann, D. G. (2006). Sexual reproduction in *Navicula cryptocephala* (Bacillariophyceae). *Journal of Phycology*, 42(4):872–886. 23

Prowe, a. F., Pahlow, M., Dutkiewicz, S., Follows, M., and Oschlies, A. (2012a). Top-down control of marine phytoplankton diversity in a global ecosystem model. *Progress in Oceanography*, 101(1):1–13. 6, 7, 30, 31, 148, 223

Prowe, A. F., Pahlow, M., and Oschlies, A. (2012b). Controls on the diversity–productivity relationship in a marine ecosystem model. *Ecological Modelling*, 225:167–176. 46, 223

Ptacnik, R., Moorthi, S. D., and Hillebrand, H. (2010). Hutchinson reversed, or why there need to be so many species. *Advances in Ecological Research*, 43:1–43. 2, 11, 15, 146

Ptacnik, R., Solimini, A. G., Andersen, T., Tamminen, T., Brettum, P. l., Lepistö, L., Willén, E., and Rekolainen, S. (2008). Diversity predicts stability and resource use efficiency in natural phytoplankton communities. *Proceedings of the National Academy of Sciences of the United States of America*, 105(13):5134–8. 2, 10, 146

Quere, C. L., Harrison, S. P., Colin Prentice, I., Buitenhuis, E. T., Aumont, O., Bopp, L., Claustre, H., Cotrim Da Cunha, L., Geider, R., Giraud, X., et al. (2005). Ecosystem dynamics based on plankton functional types for global ocean biogeochemistry models. *Global Change Biology*, 11(11):2016–2040. 16, 49, 147, 151, 265, 311

Quijano-Scheggia, S., Garcès, E., Andree, K., Fortuo, J., and Camp, J. (2009). Homothallic auxosporulation in pseudo-nitzschia brasiliana (bacillariophyta). *Journal of Phycology*, 45(1):100–107. 24

Quine, W. V. (1975). On empirically equivalent systems of the world. *Erkenntnis*, 9(3):313–328. 104

Randall Hughes, A., Byrnes, J. E., Kimbro, D. L., and Stachowicz, J. J. (2007). Reciprocal relationships and potential feedbacks between biodiversity and disturbance. *Ecology letters*, 10(9):849–864. 8

Raven, J. (1998). The twelfth tansley lecture. small is beautiful: the picophytoplankton. *Functional ecology*, 12(4):503–513. 5

Redfield, A. C. (1958). The biological control of chemical factors in the environment. *American scientist*, pages 230A–221. 11, 107

Reed, R. (1977). On estimating insolation over the ocean. *Journal of Physical Oceanography*, 7(3):482–485. 60

Reynolds, C. (2001). Emergence in pelagic communities. *Scientia Marina*, 65(S2):5–30. 297

Reynolds, C. S. (1984). *The ecology of freshwater phytoplankton.* Cambridge University Press. 12, 13

Reynolds, C. S., Usher, M., Saunders, D., Dobson, A., Peet, R., Adam, P., Birks, H., Gustafsson, L., McNeely, J., Paine, R., et al. (2006). *Ecology of phytoplankton.* Cambridge University Press Cambridge. 30, 148, 256

Richardson, A. J. and Schoeman, D. S. (2004). Climate impact on plankton ecosystems in the Northeast Atlantic. *Science*, 305(5690):1609–1612. 11, 108

Richardson, K., Beardall, J., and Raven, J. (1983). Adaptation of unicellular algae to irradiance: an analysis of strategies. *New Phytologist*, 93(2):157–191. 49

Richerson, P., Armstrong, R., and Goldman, C. R. (1970). Contemporaneous disequilibrium, a new hypothesis to explain the paradox of the plankton. *Proceedings of the National Academy of Sciences*, 67(4):1710–1714. 10, 152

Ricklefs, R. E., Schluter, D., et al. (1993). *Species diversity in ecological communities: historical and geographical perspectives.* University of Chicago Press. 3

Rines, J., Donaghay, P., Dekshenieks, M., Sullivan, J., and Twardowski, M. (2002). Thin layers and camouflage: hidden *Pseudo-nitzschia* spp.(Bacillariophyceae) populations in a fjord in the San Juan Islands, Washington, USA. *Marine Ecology Progress Series*, 225:123–137. 250, 251, 313

Rocap, G., Larimer, F. W., Lamerdin, J., Malfatti, S., Chain, P., Ahlgren, N. A., Arellano, A., Coleman, M., Hauser, L., Hess, W. R., et al. (2003). Genome divergence in two prochlorococcus ecotypes reflects oceanic niche differentiation. *Nature*, 424(6952):1042–1047. 100

Rose, J. M. and Caron, D. A. (2007). Does low temperature constrain the growth rates of heterotrophic protists? evidence and implications for algal blooms in cold waters. *Limnology and Oceanography*, 52(2):886–895. 223

Rosenzweig, M. L. (1995). *Species diversity in space and time.* Cambridge University Press. 5

Round, F. (1972). problem of reduction of cell size during diatom cell division. *Nova Hedwigia.* 20

Round, F. E., Crawford, R. M., and Mann, D. G. (1990a). *The diatoms: biology & morphology of the genera.* Cambridge University Press. 34, 231

Round, F. E., Crawford, R. M., and Mann, D. G. (1990b). *The diatoms. Biology and morphology of the genera.* Cambridge University Press, Cambridge. 19, 21, 23

Roy, S. and Chattopadhyay, J. (2007). Towards a resolution of the paradox of the plankton: A brief overview of the proposed mechanisms. *Ecological Complexity*, 4(1-2):26–33. 6

Rueffler, C., Van Dooren, T. J., Leimar, O., and Abrams, P. A. (2006). Disruptive selection and then what? *Trends in Ecology & Evolution*, 21(5):238–245. 99

Russell, G. L., Miller, J. R., and Rind, D. (1995). A coupled atmosphere-ocean model for transient climate change studies. *Atmosphere-ocean*, 33(4):683–730. 160

Ryabchenko, V., Fasham, M., Kagan, B., and Popova, E. (1997). What causes short-term oscillations in ecosystem models of the ocean mixed layer? *Journal of Marine Systems*, 13(1-4):33–50. 46

Ryan, J., Chavez, F., and Bellingham, J. (2005). Physical-biological coupling in Monterey Bay, California: topographic influences on phytoplankton ecology. *Marine Ecology Progress Series*, 287:23–32. 250, 313

Sabbe, K., Chepurnov, V. A., Mann, D. G., and Vyverman, W. (2004). Sexual behaviour, auxosporulation and chloroplast dynamics in a marine *Amphora* (Bacillariophyceae) studied in culture. *Botanica Marina*, 47:53–63. 23, 26

Sabehi, G., Kirkup, B. C., Rozenberg, M., Stambler, N., Polz, M. F., and Béjà, O. (2007). Adaptation and spectral tuning in divergent marine proteorhodopsins from the eastern mediterranean and the sargasso seas. *The ISME journal*, 1(1):48–55. 100

Sardans, J., Penuelas, J., and Rivas-Ubach, A. (2011). Ecological metabolomics: overview of current developments and future challenges. *Chemoecology*, 21(4):191–225. 310

Sarmiento, J. L., Hughes, T. M., Stouffer, R. J., and Manabe, S. (1998). Simulated response of the ocean carbon cycle to anthropogenic climate warming. *Nature*, 393(6682):245–249. 159, 160

Sarmiento, J. L., Slater, R., Barber, R., Bopp, L., Doney, S. C., Hirst, A., Kleypas, J., Matear, R., Mikolajewicz, U., Monfray, P., et al. (2004). Response of ocean ecosystems to climate warming. *Global Biogeochemical Cycles*, 18(3). 160, 225, 314

Sarno, D., Zingone, A., and Montresor, M. (2010). A massive and simultaneous sex event of two *Pseudo-nitzschia* species. *Deep Sea Research Part II: Topical Studies in Oceanography*, 57(3):248–255. 249, 298

Sarthou, G., Timmermans, K. R., Blain, S., and Tréguer, P. (2005). Growth physiology and fate of diatoms in the ocean: a review. *Journal of Sea Research*, 53(1):25–42. 17, 49, 50, 52, 252, 260

Sathyendranath, S., Stuart, V., Nair, A., Oka, K., Nakane, T., Bouman, H., Forget, M.-H., Maass, H., and Platt, T. (2009). Carbon-to-chlorophyll ratio and growth rate of phytoplankton in the sea. *Mar. Ecol. Prog. Ser*, 383(7). 71, 76, 287

Satinsky, B. M., Crump, B. C., Smith, C. B., Sharma, S., Zielinski, B. L., Doherty, M., Meng, J., Sun, S., Medeiros, P. M., Paul, J. H., et al. (2014). Microspatial gene expression patterns in the amazon river plume. *Proceedings of the National Academy of Sciences*, 111(30):11085–11090. 310

Sato, S., Beakes, G., Idei, M., Nagumo, T., and Mann, D. G. (2011a). Novel sex cells and evidence for sex pheromones in diatoms. *PloS ONE*, 6(10):e26923. 25, 253

Sato, S., Vanormelingen, P., Idei, M., and Mann, D. G. (2011b). Sexual reproduction and haploid parthenogenesis in the raphid diatom amphora commutata. *European Journal of Phycology*, 46:186–187. only the abstract. 24

Savage, V. M., Webb, C. T., and Norberg, J. (2007). A general multi-trait-based framework for studying the effects of biodiversity on ecosystem functioning. *Journal of theoretical biology*, 247(2):213–229. 16

Savidge, G., Boyd, P., Pomroy, A., Harbour, D., and Joint, I. (1995). Phytoplankton production and biomass estimates in the northeast Atlantic Ocean, May–June 1990. *Deep Sea Research Part I: Oceanographic Research Papers*, 42(5):599–617. 96

Scalco, E. (2010). *Factors regulating transitions among life cycle phases in the marine pennate diatom Pseudo-nitzschia multistriata.* Open University. 21, 233, 250, 254

Scalco, E., Stec, K., Iudicone, D., Ferrante, M. I., and Montresor, M. (2014). The dynamics of sexual phase in the marine diatom *Pseudo-nitzschia multistriata* (Bacillariophyceae). *Journal of Phycology.* 25, 232, 233, 250, 251, 252, 254, 257, 259, 260, 293, 294, 298, 299, 313

Schartau, M. and Oschlies, A. (2003). Simultaneous data-based optimization of a 1D-ecosystem model at three locations in the North Atlantic: Part I - Method and parameter estimates. *Journal of Marine Research*, 61(6):765–793. 12, 97, 147

Scheffer, M., Rinaldi, S., Huisman, J., and Weissing, F. J. (2003). Why plankton communities have no equilibrium: solutions to the paradox. *Hydrobiologia*, 491(1-3):9–18. 9

Schmid, A.-M. M. (1995). Sexual reproduction in *Coscinodiscus granii* Gough in culture: a preliminary report. In *Proceedings of the 13th International Diatom Symposium*, pages 139–159. Biopress Bristol. 232

Schmidtke, A., Gaedke, U., and Weithoff, G. (2010). A mechanistic basis for underyielding in phytoplankton communities. *Ecology*, 91(1):212–221. 12

Schmittner, A., Latif, M., and Schneider, B. (2005). Model projections of the north atlantic thermohaline circulation for the 21st century assessed by observations. *Geophysical Research Letters*, 32(23). 160

Schmittner, A., Oschlies, A., Matthews, H. D., and Galbraith, E. D. (2008). Future changes in climate, ocean circulation, ecosystems, and biogeochemical cycling sim-

ulated for a business-as-usual CO2 emission scenario until year 4000 AD. *Global Biogeochemical Cycles*, 22(1). 160

Schoener, T. W. (1989). The ecological niche. 11

Schultz, M. E. and Trainor, F. R. (1968). Production of male gametes and auxospores in the centric diatoms *Cyclotella meneghiniana* and c. *Cryptica*. *Journal of Phycology*, 4(2):85–88. 232

Schulze, E. and Mooney, H. (1993). Design and execution of experiments on co2 enrichment: proceedings of a workshop held at weidenberg, germany, october 26 to 30, 1992. *Ecosystems research report series/Commission of the European Communities (*, (6). 18

Schulze, E.-D. and Mooney, H. A. (1994). Biodiversity and ecosystem function: with 22 tables. 99. 2, 10

Shannon, C. E. and Weaver, W. (1949). The mathematical theory of information. 3, 107

Shine, K. (1984). Parametrization of the shortwave flux over high albedo surfaces as a function of cloud thickness and surface albedo. *Quarterly Journal of the Royal Meteorological Society*, 110(465):747–764. 59

Short, S. M. (2012). The ecology of viruses that infect eukaryotic algae. *Environmental microbiology*, 14(9):2253–2271. 100, 311

Sieracki, M. E., Verity, P. G., and Stoecker, D. K. (1993). Plankton community response to sequential silicate and nitrate depletion during the 1989 North Atlantic spring bloom. *Deep Sea Research Part II: Topical Studies in Oceanography*, 40(1):213–225. 11, 107

Signorini, S., Häkkinen, S., Gudmundsson, K., Olsen, A., Omar, A., Olafsson, J., Reverdin, G., Henson, S., McClain, C., and Worthen, D. (2012a). The role of phytoplankton dynamics in the seasonal and interannual variability of carbon in the subpolar north atlantic–a modeling study. *Geoscientific Model Development*, 5(3):683–707. 49, 52, 64

Signorini, S. R., Häkkinen, S., Gudmundsson, K., Olsen, a., Omar, a. M., Olafsson, J., Reverdin, G., Henson, S. a., McClain, C. R., and Worthen, D. L. (2012b). The role of phytoplankton dynamics in the seasonal and interannual variability of carbon in the subpolar North Atlantic a modeling study. *Geoscientific Model Development*, 5(3):683–707. 66

Smetacek, V. (1999a). Diatoms and the ocean carbon cycle. *Protist*, 150(1):25–32. 33

Smetacek, V. (1999b). Revolution in the ocean. *Nature*, 401:647. pdf on diana. 17, 18

Smetacek, V., Assmy, P., and Henjes, J. (2004). The role of grazing in structuring southern ocean pelagic ecosystems and biogeochemical cycles. *Antarctic Science*, 16:541–558. pdf on diana. 17

Smith, B. and Wilson, J. B. (1996). A consumer's guide to evenness indices. *Oikos*, pages 70–82. 3, 107

Smith, E. L. (1936). Photosynthesis in relation to light and carbon dioxide. *Proceedings of the National Academy of Sciences of the United States of America*, 22(8):504. 43

Smith, J. M. (1982). *Evolution and the Theory of Games*. Cambridge university press. 292

Smith, S. L., Yamanaka, Y., Pahlow, M., and Oschlies, A. (2009). Optimal uptake kinetics: physiological acclimation explains the pattern of nitrate uptake by phytoplankton in the ocean. *Marine Ecology Progress Series*, 384:1–12. 14

Smout, S., Asseburg, C., Matthiopoulos, J., Fernández, C., Redpath, S., Thirgood, S., and Harwood, J. (2010). The functional response of a generalist predator. 46

Sommer, U. (1984). The paradox of the plankton: fluctuations of phosphorus availability maintain diversity of phytoplankton in flow-through cultures. *Limnology and Oceanography*, 29(3):633–636. 8

Sommer, U. (1985). Comparison between steady state and non-steady state competition: Experiments with natural phytoplankton. *Limnology and Oceanography*, 30(2):335–346. 8

Sommer, U. (1995). An experimental test of the intermediate disturbance hypothesis using cultures of marine phytoplankton. *Limnology and Oceanography*, 40:1271–1277. 8

Sommer, U. and Worm, B. (2002). *Competition and coexistence*, volume 161. Springer. 6, 8

Sournia, A. (1982). Form and function in marine phytoplankton. *Biological reviews*, 57(3):347–394. 96, 148

Speirs, D. C., Gurney, W. S., Heath, M. R., and Wood, S. N. (2005). Modelling the basin-scale demography of calanus finmarchicus in the north-east atlantic. *Fisheries Oceanography*, 14(5):333–358. 54

Sprintall, J. and Roemmich, D. (1999). Characterizing the structure of the surface layer in the pacific ocean. *Journal of Geophysical Research: Oceans (1978–2012)*, 104(C10):23297–23311. 159

Steele, J. H. (1974). The structure of marine ecosystems. *Harvard University Press Cambridge*. 12, 147

Steele, J. H. and Henderson, E. W. (1992a). The role of predation in plankton models. *Journal of Plankton Research*, 14(1):157–172. 48

Steele, J. H. and Henderson, E. W. (1992b). The role of predation in plankton models. *Journal of Plankton Research*, 14(1):157–172. 47

Steele, J. H. and Henderson, E. W. (1993). The significance of interannual variability. In *Towards a model of ocean biogeochemical processes*, pages 237–260. Springer. 98

Steele, R. (1965). Induction of sexuality in two centric diatoms. *BioScience*, 15(4):298. pdf diana. 26, 309

Steinacher, M., Joos, F., Frölicher, T., Bopp, L., Cadule, P., Cocco, V., Doney, S., Gehlen, M., Lindsay, K., Moore, J., et al. (2010). Projected 21st century decrease in marine productivity: a multi-model analysis. *Biogeosciences*, 7(3):979–1005. 314

Stenseth, N. C., Mysterud, A., Ottersen, G., Hurrell, J. W., Chan, K.-S., and Lima, M. (2002). Ecological effects of climate fluctuations. *Science*, 297(5585):1292–1296. 218

Sterner, R. W. (1989). The role of grazers in phytoplankton succession. In *Plankton ecology*, pages 107–170. Springer. 148

Sterner, R. W. and Elser, J. J. (2002). *Ecological stoichiometry: the biology of elements from molecules to the biosphere.* Princeton University Press. 2

Stewart, F. M. and Levin, B. R. (1973). Partitioning of resources and the outcome of interspecific competition: a model and some general considerations. *American Naturalist*, 107(954):171–198. 7, 148

Stirling, G. and Wilsey, B. (2001). Empirical relationships between species richness, evenness, and proportional diversity. *The American Naturalist*, 158(3):286–299. 2, 3, 107

Stoecker, D. K. and Gustafson, D. E. (2003). Cell-surface proteolytic activity of photosynthetic dinoflagellates. *Aquatic Microbial Ecology*, 30(2):175–183. 310

Striebel, M., Behl, S., Diehl, S., and Stibor, H. (2009). Spectral niche complementarity and carbon dynamics in pelagic ecosystems. *The American Naturalist*, 174(1):141–147. 12

Strom, S., Brainard, M., Holmes, J., and Olson, M. (2001). Phytoplankton blooms are strongly impacted by microzooplankton grazing in coastal north pacific waters. *Marine Biology*, 138(2):355–368. 5

Sullivan, J. M., Twardowski, M. S., Donaghay, P. L., and Freeman, S. a. (2005). Use of optical scattering to discriminate particle types in coastal waters. *Applied optics*, 44(9):1667–80. 250

Sverdrup, H. (1953). On conditions for the vernal blooming of phytoplankton. *Journal du Conseil Permanent International pour l'Exploration de la Mer*, 18(3):287–295. 96, 155, 226

Talmy, D., Blackford, J., Hardman-Mountford, N., Polimene, L., Follows, M., and Geider, R. J. (2014). Flexible c: N ratio enhances metabolism of large phytoplankton when resource supply is intermittent. *Biogeosciences*, 11(17):4881–4895. 101

Tang, E. P. (1995). The allometry of algal growth rates. *Journal of Plankton Research*, 17(6):1325–1335. 14

Taucher, J. and Oschlies, A. (2011). Can we predict the direction of marine primary production change under global warming? *Geophysical Research Letters*, 38(2). 314

Taylor, K. E. (2000). *Summarizing multiple aspects of model performance in a single diagram.* Program for Climate Model Diagnosis and Intercomparison, Lawrence Livermore National Laboratory, University of California. 66

Tesson, S. V., Legrand, C., van Oosterhout, C., Montresor, M., Kooistra, W. H., and Procaccini, G. (2013). Mendelian inheritance pattern and high mutation rates of microsatellite alleles in the diatom *Pseudo-nitzschia multistriata*. *Protist*, 164(1):89–100. 231

Thekaekara, M. P. and Drummond, A. J. (1971). Standard values for the solar constant and its spectral components. *Nature*, 229(1):6–9. 59

Thingstad, T. F. and Cuevas, L. A. (2010). Nutrient pathways through the microbial food web: principles and predictability discussed, based on five different experiments. 2, 16

Tilman, D. (1977). Resource competition between plankton algae: an experimental and theoretical approach. *Ecology*, pages 338–348. 6, 7, 148

Tilman, D. (1981). Resource competition and community structure. *Monographs in population biology*, 17:1–296. 118, 119

Tilman, D. (2001). Functional diversity. *Encyclopedia of biodiversity*, 3(1):109–120. 4

Tilman, D. and Kareiva, P. M. (1997). *Spatial ecology: the role of space in population dynamics and interspecific interactions*, volume 30. Princeton University Press. 152

Tilman, D., Kilham, S. S., and Kilham, P. (1982). Phytoplankton community ecology: the role of limiting nutrients. *Annual Review of Ecology and Systematics*, pages 349–372. 6, 13, 152

Tilman, D., Knops, J., Wedin, D., Reich, P., Ritchie, M., and Siemann, E. (1997a). The influence of functional diversity and composition on ecosystem processes. *Science*, 277(5330):1300–1302. 10, 11

Tilman, D., Lehman, C. L., and Thomson, K. T. (1997b). Plant diversity and ecosystem productivity: theoretical considerations. *Proceedings of the National Academy of Sciences*, 94(5):1857–1861. 218

Tittel, J., Bissinger, V., Zippel, B., Gaedke, U., Bell, E., Lorke, A., and Kamjunke, N. (2003). Mixotrophs combine resource use to outcompete specialists: implications for aquatic food webs. *Proceedings of the National Academy of Sciences*, 100(22):12776–12781. 224, 311

Tittensor, D. P., Mora, C., Jetz, W., Lotze, H. K., Ricard, D., Berghe, E. V., and Worm, B. (2010). Global patterns and predictors of marine biodiversity across taxa. *Nature*, 466(7310):1098–1101. 10

Totterdell, I. J., Armstrong, R., Drange, H., Parslow, J., Powell, T., and Taylor, A. (1993). Trophic resolution. *Towards a Model of Ocean Biogeochemical Processes. NATO ASI*, 1:10. 16, 39, 91, 102, 146

Tozzi, S., Schofield, O., and Falkowski, P. (2004). Historical climate change and ocean turbulence as selective agents for two key phytoplankton functional groups. *Marine Ecology Progress Series*, 274:123–132. 159

Tréguer, P. J. and De La Rocha, C. L. (2013). The world ocean silica cycle. *Annual Review of Marine Science*, 5:477–501. 17

Vallina, S. M., Ward, B., Dutkiewicz, S., and Follows, M. (2014). Maximal feeding with active prey-switching: A kill-the-winner functional response and its effect on global diversity and biogeography. *Progress in Oceanography*, 120:93–109. 7

van Nes, E. H. and Scheffer, M. (2004). Large species shifts triggered by small forces. *The American Naturalist*, 164(2):255–266. 9

Vandermeer, J. (1993). Loose coupling of predator-prey cycles: entrainment, chaos, and intermittency in the classic MacArthur consumer-resource equations. *American Naturalist*, pages 687–716. 9

Veldhoen, N., Ikonomou, M. G., and Helbing, C. C. (2012). Molecular profiling of marine fauna: Integration of omics with environmental assessment of the world's oceans. *Ecotoxicology and environmental safety*, 76:23–38. 310

Velo-Suárez, L., González-Gil, S., Gentien, P., Lunven, M., Bechemin, C., Fernand, L., Raine, R., and Reguera, B. (2008). Thin layers of *Pseudo-nitzschia* spp. and the fate of *Dinophysis acuminata* during an upwelling–downwelling cycle in a Galician Ria. *Limnology and oceanography*, 53(5):1816. 250, 251, 313

Vila, X. and Abella, C. A. (2001). Light-harvesting adaptations of planktonic phototrophic micro-organisms to different light quality conditions. *Hydrobiologia*, 452(1-3):15–30. 100

Villareal, T. A., Pilskaln, C., Brzezinski, M., Lipschultz, F., Dennett, M., and Gardner, G. B. (1999). Upward transport of oceanic nitrate by migrating diatom mats. *Nature*, 397(6718):423–425. 250

Von Dassow, P., Chepurnov, V. A., and Armbrust, E. (2006). Relationships between growth rate, cell size, and induction of spermatogenesis in the centric diatom thalassiosira weissflogii (bacillariophyta) 1. *Journal of phycology*, 42(4):887–899. 21, 24

von Dassow, P., John, U., Ogata, H., Probert, I., Bendif, E. M., Kegel, J. U., Audic, S., Wincker, P., Da Silva, C., Claverie, J.-M., et al. (2015). Life-cycle modification in open oceans accounts for genome variability in a cosmopolitan phytoplankton. *The ISME journal*, 9(6):1365–1377. 257

von Dassow, P. and Montresor, M. (2010a). Unveiling the mysteries of phytoplank-

ton life cycles: patterns and opportunities behind complexity. *Journal of Plankton Research*, 33(1):3–12. 20, 231

von Dassow, P. and Montresor, M. (2010b). Unveiling the mysteries of phytoplankton life cycles: patterns and opportunities behind complexity. *Journal of Plankton Research*, page fbq137. 28

von Stosch, H. (1965). Manipulierung der zellgrsse von diatomeen in experiment. *Phycologia*, 5:21–44. 26

Waide, R., Willig, M., Steiner, C., Mittelbach, G., Gough, L., Dodson, S., Juday, G., and Parmenter, R. (1999). The relationship between productivity and species richness. *Annual review of Ecology and Systematics*, pages 257–300. 5

Walker, B., Kinzig, A., and Langridge, J. (1999). Original articles: plant attribute diversity, resilience, and ecosystem function: the nature and significance of dominant and minor species. *Ecosystems*, 2(2):95–113. 4

Walsh, J. J. (1981). A carbon budget for overfishing off Peru. *Nature*, 290:300–304. 2

Waniek, J. J. (2003). The role of physical forcing in initiation of spring blooms in the Northeast Atlantic. *Journal of Marine Systems*, 39(1-2):57–82. 216

Ward, B. A., Dutkiewicz, S., Barton, A. D., and Follows, M. J. (2011). Biophysical aspects of resource acquisition and competition in algal mixotrophs. *The American Naturalist*, 178(1):98–112. 224

Weis, J. J., Cardinale, B. J., Forshay, K. J., and Ives, A. R. (2007). Effects of species diversity on community biomass production change over the course of succession. *Ecology*, 88(4):929–939. 11, 12

Whittaker, R. H. (1965). Dominance and diversity in land plant communities numerical relations of species express the importance of competition in community function and evolution. *Science*, 147(3655):250–260. 2, 107

Williams, G. C. (1975). *Sex and evolution.* Number 8. Princeton University Press. 232

Wirtz, K.-W. and Eckhardt, B. (1996). Effective variables in ecosystem models with an application to phytoplankton succession. *Ecological Modelling*, 92(1):33–53. 152

Wolinska, J., Lively, C. M., and Spaak, P. (2008). Parasites in hybridizing communities: the red queen again? *Trends in parasitology*, 24(3):121–126. 312

Wood, A. M., Phinney, D. A., and Yentsch, C. S. (1998). Water column transparency and the distribution of spectrally distinct forms of phycoerythrin-containing organisms. *Marine Ecology Progress Series*, 162:25–31. 100

Worm, B., Lotze, H. K., Hillebrand, H., and Sommer, U. (2002). Consumer versus resource control of species diversity and ecosystem functioning. *Nature*, 417(6891):848–851. 146

Wroblewski, J. S., Sarmiento, J. L., and Flierl, G. R. (1988). An Ocean Basin Scale Model of plankton dynamics in the North Atlantic: 1. Solutions For the climatological oceanographic conditions in May. *Global Biogeochemical Cycles*, 2:199–218. 12, 147

Wyatt, T. (2014). Margalef's mandala and phytoplankton bloom strategies. *Deep Sea Research Part II: Topical Studies in Oceanography*, 101:32–49. 256

Wyatt, T. and Jenkinson, I. R. (1997). Notes on Alexandrium population dynamics. *Journal of Plankton Research*, 19(5):551–575. 231

Wyatt, T. and Zingone, A. (2014). Population dynamics of red tide dinoflagellates. *Deep Sea Research Part II: Topical Studies in Oceanography*, 101:231–236. 297

Yachi, S. and Loreau, M. (1999). Biodiversity and ecosystem productivity in a fluctuating environment: the insurance hypothesis. *Proceedings of the National Academy of Sciences*, 96(4):1463–1468. 10

Yool, A., Popova, E., et al. (2011). Medusa-1.0: a new intermediate complexity plankton ecosystem model for the global domain. *Geoscientific Model Development*, 4(2):381. 47

Yoshida, T., Jones, L. E., Ellner, S. P., Fussmann, G. F., and Hairston, N. G. (2003). Rapid evolution drives ecological dynamics in a predator–prey system. *Nature*, 424(6946):303–306. 312

Zubkov, M. V. and Tarran, G. A. (2008). High bacterivory by the smallest phytoplankton in the north atlantic ocean. *Nature*, 455(7210):224–226. 224